An Exploratory Analysis of Trends in Shallow Lakes Water Chemistry Time Series Data from Arctic Network and Central Alaska Network Parks



An Exploratory Analysis of Trends in Shallow Lakes Water Chemistry Time Series Data from Arctic Network and Central Alaska Network Parks

Leigh Ann Starcevich,[1] Jared Studyvin,[2] and Diem Pham[3]

[1]Western Ecosystems Technology, Inc.
2725 NW Walnut Boulevard
Corvallis, Oregin 97330

[2]Western Ecosystems Technology, Inc.
200 South Second Street
Laramie, Wyoming 82070

[3]Western Ecosystems Technology, Inc.
2121 Midpoint Drive, Suite 201
Fort Collins, Colorado 80525

February 2021

U.S. Department of the Interior
National Park Service
Central Alaska Network
Fairbanks, Alaska

Views, statements, findings, conclusions, recommendations, and data in this report do not necessarily reflect views and policies of the National Park Service, U.S. Department of the Interior. Mention of trade names or commercial products does not constitute endorsement or recommendation for use by the U.S. Government.

This report is available in digital format from irma@nps.gov.

Please cite this publication as:

Starcevich, L.A., J. Studyvin, and D. Pham. 2021. Analysis of Trends in Shallow Lakes Water Chemistry at Arctic Network and Central Alaska Network Parks. National Park Service, Fairbanks, Alaska.

Point of contact: Amy Larsen, Amy_Larsen@nps.gov

Contents

Page

Figures....iv

Tables....v

Executive Summary....vi

Acknowledgments....vi

Introduction....1

Methods....1

Data Formatting....2

Analysis Methods....3

Results....6

Dissolved Oxygen....6

pH....8

Specific Conductance....10

Sonde Temperature....12

Sediment Temperature....14

Thermistor Chain Temperature....16

Comparison of Temperature Outcomes....18

Case Study....19

Preparing for Analysis....19

Preparing R....19

Accessing the R scripts....19

Preparing for the Analysis....19

Case Study: Specific Conductance at YUCH-004....22

Discussion....47

Literature Cited....50

Appendix A: Trend Analysis Results by Outcome and Lake....52

Appendix B: Temperature Correlation Plots by Lake....414

Figures

Page

Figure 1. Survey years used for all analyses of dissolved oxygen and truncation within each year (truncated analyses only) by lake. 6

Figure 2. Survey years used for all analyses of pH and truncation within each year (truncated analyses only) by lake. 8

Figure 3. Survey years used for all analyses of specific conductance and truncation within each year (truncated analyses only) by lake. 10

Figure 4. Survey years used for all analyses of sonde temperature and truncation within each year (truncated analyses only) by lake. 12

Figure 5. Survey years used for all analyses of sediment temperature and truncation within each year (truncated analyses only) by lake. 14

Figure 6. Survey years used for all analyses of water temperature and truncation within each year (truncated analyses only) by lake. 16

Figure 7. Correlation plot of temperature metrics by depth across all lakes and dates. 18

Figure 8. Time series plot of the untransformed complete data set of YUCH-004 specific conductance. 23

Figure 9. Residual diagnostic plots for the untransformed complete data model. 25

Figure 10. Additive outliers plot for YUCH-004 specific conductance. 25

Figure 11. Residual diagnostics plot for the untransformed additive outliers model. 26

Figure 12. Time series plot of the untransformed truncated data set of YUCH-004 specific conductance. 27

Figure 13. Residual diagnostic plots for the untransformed truncated model. 28

Figure 14. Time series decomposition plot for YUCH-004 specific conductance. 29

Figure 15. Residual diagnostic plots for the untransformed truncated seasonally adjusted model. 30

Figure 16. Observed (blue) and imputed (red) relative humidity values plotted by time. 32

Figure 17. Residual diagnostic plots for the full covariate model assuming independent error for YUCH-004 specific conductance. 33

Figure 18. Residual diagnostic plots for the full covariate ARIMA model for YUCH-004 specific conductance 34

Figure 19. Residual diagnostic plots for the untransformed monthly complete data model....36

Figure 20. Additive outliers plot for monthly YUCH-004 specific conductance means....36

Figure 21. Residual diagnostic plots for the untransformed monthly additive outliers model....37

Figure 22. Residual diagnostic plots for the untransformed monthly truncated data model....38

Figure 23. Time series decomposition plot of monthly YUCH-004 specific conductance means....39

Figure 24. Residual diagnostic plots for the untransformed monthly truncated seasonally adjusted model....40

Figure 25. Residual diagnostic plots for the log-transformed monthly complete data model....41

Figure 26. Residual diagnostic plots for the log-transformed monthly mean covariate model assuming independent errors....43

Figure 27. Residual diagnostic plots for the log-transformed monthly mean full covariate ARIMA model....44

Figure 28. Residual diagnostic plots for the log-transformed monthly mean final covariate model assuming independent errors....46

Tables

Page

Table 1. Monitoring start date by lake....2

Table 2. Environmental covariates used for modeling....5

Table 3. Modeling results for Dissolved Oxygen....7

Table 4. Modeling results for pH....9

Table 5. Modeling results for Specific Conductance....11

Table 6. Modeling results for Sonde Temperature....13

Table 7. Modeling results for Sediment Temperature....15

Table 8. Modeling results for Water Temperature....17

Executive Summary

The Central Alaska Network and Arctic Network shallow lakes protocol monitors water chemistry and physical characteristics of several of the tens of thousands of lakes distributed across the parks in these two networks. In this report, we address three primary goals: (1) identify the best trend model for the outcome and lake, (2) evaluate the environmental covariates that were most highly associated with the outcome at that lake, and (3) provide analysis tools in R for analyzing water chemistry data downloaded from Aquarius. We focus on the four core shallow lakes metrics: temperature, dissolved oxygen, pH, and specific conductivity. We apply four trend models to the daily data as well as two data transformations for data collected at 12 lakes over time. Covariate modeling is conducted to determine if relationships exist with other environmental covariates. This analysis is exploratory and serves to examine approaches to model shallow lakes water chemistry monitoring data as a function of time and/or fine scale (e.g. daily, weekly) covariate data. As such, these results are preliminary and should not be used to make inference on lake condition.

Acknowledgments

Western EcoSystems Technology, Inc. conducted this work under task order RFQ 140P9719F0038.

Introduction

The Central Alaska Network (CAKN) and Arctic Network (ARCN) monitor shallow lakes as part of the National Park Service Inventory and Monitoring (I&M) Vital Signs Program. The shallow lakes protocol was selected as a Vital Signs resource because the tens of thousands of lakes distributed across the parks in these two networks are critical to ecological functions that support wildlife and human population and are sensitive to the impacts of global climate change (Larsen et al. 2011). The shallow lakes protocol is conducted at all CAKN parks, including Wrangell-St. Elias National Park and Preserve (WRST), Denali National Park and Preserve (DENA), and Yukon-Charley Rivers National Preserve (YUCH), and three ARCN parks, including Noatak National Preserve (NOAT), Kobuk Valley National Park (KOVA), and Bering Land Bridge National Preserve (BELA). Each park contains shallow lakes and ponds of depths less than five meters (m) and areas between one and 50 hectares where water quantity, water chemistry, vegetation structure and composition, and invertebrate communities are monitored. In this report, we focus on the four core water chemistry metrics: temperature, dissolved oxygen, pH, and specific conductivity.

The sampling frame of lakes was obtained through remote sensing imagery (Larsen et al. 2011). The sampling design incorporated an unequal probability sample with design weights inversely proportional to distance from navigable water to minimize time travel on foot. Spatially balanced sampling via general randomized tessellation stratified sampling (Stevens and Olsen 2003, 2004) was applied within each park to obtain a sample of lakes allocated across the diverse and variable extent of the shallow lake distribution. Two lakes were randomly selected for monitoring at each of the three parks within each network for 12 total lakes.

Primary objectives of the Vital Signs Program are to monitor status and trends in the condition of the park resources. Western EcoSystems Technology, Inc. was tasked with conducting a trend analysis for six water quality and water chemistry metrics at each of the 12 lakes. In this report, we address three primary goals: (1) identify the best trend model for the outcome and lake, (2) evaluate the environmental covariates that were most highly associated with the outcome at that lake, and (3) provide analysis tools in R for analyzing water chemistry data downloaded from Aquarius. We outline the data formatting and trend analysis methods used, describe the results of the trend analysis for 12 shallow lakes in ARCN and CAKN, and discuss the implications of the analysis on future monitoring efforts. This exploratory analysis exercise serves to investigate the utility of the selected analysis methods for estimating trends and identifying associated environmental covariates. Given the exploratory nature of this work, the results of this analysis will not be used for inference on lake condition.

Methods

In this section, we describe the methods used to format and analyze the data in order to satisfy the three primary goals. The data were initially obtained from ARCN/CAKN personnel who downloaded the data from Aquarius and provided for analysis. We assume that any future data that will be analyzed will be in the same format with the same column names. Data formatting functions were

developed in R (2020) and summarized in the **NPSH2OAK** package (Studyvin et al. 2021). Modeling trends and covariate relationships was conducted with daily means, but aggregated to weekly or monthly means if models of daily means with acceptable fit could not be obtained. Model fit was assessed with residual diagnostics and tests of independence, and methods to conform data to necessary standards (e.g., consecutive years) and to improve model fit included data truncation of survey years, data truncation within a year, defining additive outliers, and removing the seasonal effect from the time series. The analysis scripts used to format the data and to conduct trend and covariate modeling were archived in the **NPSH2OAK** package to document the analysis steps used in this exploratory modeling exercise and to serve as templates for future analysis.

Data Formatting

Every year in the spring, three instruments (sonde, thermistor chain, and barometric pressure logger) were placed at the lake to measure the outcomes of interest. Measurements were collected hourly (sonde) to every 12 hours (sediment temperature). The outcomes of interest were summarized to a common time scale, usually daily, by taking the mean of all measurements within the time scale. Other time scales, such as weekly or monthly, were also considered when necessary. The thermistor chain water temperature measurements were taken at various depths.

Lake monitoring began for each lake in years ranging from 2005-2015 (Table 1) and continue to the present. Occasionally, surveys were not conducted for a year or two during the monitoring period. Most time series analysis methods require consecutive time periods (Moritz and Bartz-Beielstein 2017). Rather than imputing entire years of missing data and risk introducing erroneous estimates that impact the trend estimate, the longest continuous time series available was used for analysis for each lake. Climate variables from nearby weather stations were examined as model predictors to assess relationships among monitoring outcomes and environmental covariates. Trend and covariate relationships were modeled independently by lake and outcome of interest.

Table 1. Monitoring start date by lake.

Lake	Start date
BELA-088	7/6/2012
BELA-108	6/15/2015
DENA-018	6/25/2007
DENA-023	6/20/2007
KOVA-085	6/3/2010
KOVA-086	7/8/2009
NOAT-052	6/15/2015
NOAT-107	6/10/2014
WRST-005	5/26/2010
WRST-016	5/26/2009
YUCH-004	6/7/2005

Lake	Start date
YUCH-005	5/26/2009

Analysis Methods

Trend analyses and covariate analyses were conducted for six outcomes of interest: pH, dissolved oxygen, specific conductance, surface temperature, sediment temperature, and water temperature. For each analysis, the goal was to estimate the effects of time (trend) and/or covariates while accounting for the correlated nature of the time series. I&M ecologists requested daily data be modeled because daily covariate data were available for modeling. Therefore, by using daily data, fine-scale relationships between the outcomes of interest and environmental covariates could be examined. The second goal of the trend analysis is to estimate the standard error of the annual trend estimate. Only with a reliable standard error can the magnitude and significance of trend and covariate effects be assessed. Failure to account for temporal correlation in outcomes of interest may result in underestimation of fixed effects standard errors. Standard errors that are too small due to autocorrelation, lead to erroneous trend inference from narrow confidence intervals and tests of trend and covariate effects that inaccurately imply a significant effect (Zuur et al. 2007). Preliminary modeling indicated that daily data exhibited considerable autocorrelation, so modeling methods that could account for a variety of correlation structures were considered.

An autoregressive moving average (ARMA) model was used to estimate the annual trend in the context of a time series analysis. The ARMA model is a species case of an integrated autoregressive moving average (ARIMA) which is an ARMA that employs differencing by some lag amount. An ARIMA model is usually denoted with three parameters as ARIMA(p, d, q), where p is the number of autoregressive terms, d is the lag differencing, and q is the number of moving average terms. Because differencing is generally used to remove the trend from a time series (Chatfield 2003), models of the form ARIMA(p, 0, q) were considered. Time series models are appropriately interpreted when the assumption of stationarity is met. A time series is stationary when its mean, variance, and autocorrelation structure do not change over time and when the time series exhibits no systematic patterns such as trend or cyclical effects (Yaffee and McGee 2000). These assumptions are necessary for forecasting and for assumptions of convergence to the true mean and variance.

Modeling was conducted with the *auto.arima* function in the **forecast** package (Hyndman 2008, Hyndman et al. 2020,). The *auto.arima* function uses an iterative approach incorporating maximum likelihood estimation and information criteria to obtain the model that minimizes the Akaike Information Criterion that is corrected for small samples, AICc (Burnham and Anderson 2002). Differencing was not used to remove trend, but temporal or environmental covariates were included in the model as fixed effects for evaluation. Note that the *auto.arima* function includes an intercept term in the model only when the AICc is reduced if the intercept is added. In these cases, model results report an “NA” for the intercept.

Residual diagnostics from the **forecast** package were used to assess stationarity and included autocorrelation function plots, residual histograms, and the Ljung-Box test to assess the

autocorrelation in the model residuals. Models generating Ljung-Box tests with p-values greater than the assumed Type I error rate of 0.05 were assumed to have adequately modeled the autocorrelation in the time series so that the assumption of independent residuals could be met. For more detailed information on ARIMA models, stationarity, and the Ljung-Box test, refer to a time series textbook such as Chatfield (2003) or Cryer and Chan (2008).

Differencing is a critical tool in most time series analyses for obtaining a stationary time series by removing the trend over time. Because trend estimation was a primary analysis goal, differencing could not be applied. Preliminary modeling identified four main trend modeling approaches that were applied to the shallow lakes data so that a stationary model could be identified for every outcome and lake. The four approaches included modeling the:

1) Complete data set
2) Complete data set with fixed effects for additive outliers to account for seasons
3) Truncated data set with defined seasons of equal length
4) Truncated data set with seasonal adjustment

The first approach included all of the data where first date of measurement in a year is assumed to come directly after the last date of measure of the previous year. This assumption is making the time series a "regular" time series, meaning there are no gaps are missing points in the time interval. However, the number of days that lake outcomes were monitored varied by year. To differentiate among seasons, but use the full time series, the second approach included additional covariates in the form of additive outliers (Battaglia et al. 2019). These fixed effects denoted the beginning of a new year so that changes in the time series from the end of one season (year) and the beginning of the next season (year) were modeled.

The third approach involved truncating the data so that every season (year) was of equal length. The year with the shortest measurement window was used and all other years were truncated to match. This allows for the time series modeling to account for period changes across seasonal effects. This expands the ARIMA model to ARIMA(p, d, q, P, D, Q) where the capital letters are on the seasonal scale with the same meaning as the lower case letters. As before, no differencing was considered, thus models of the form ARIMA($p, 0, q, P, 0, Q$). However, a within-season correlation structure was only included in the *auto.arima* modeling process when its effect was to lower the AICc value. The fourth approach used the truncated data from Approach 3, but the time series was decomposed (using the *decompose* function R Core Team [2020]) into three components: trend, seasonal, and random. The estimated seasonal component was subtracted from the original time series prior to modeling. The four approaches were applied to the original data and to logarithmically transformed data. The final trend model was selected as the first model in the order of modeling that demonstrated acceptable residuals with the order defined as the four models for untransformed data followed by the four models for untransformed data. This ordering starts with the simplest sets of assumptions (no transformation, no data truncation, no seasonal adjustment) and ends with the most complex set of assumptions (transformation, data truncation, and seasonal adjustment).

Covariate modeling was conducted to determine if one or more of five selected environmental covariates (Table 2) were associated with the time series of interest. Additionally, a fixed effect for year to detect trends and a fixed effect for month to account for within-season effects were also considered for seven possible covariates. The variance inflation factor (VIF; Neter et al. 1996) was calculated for covariate models with two or more predictors, models with a VIF greater than 1.14 (approximately corresponding to pairwise correlation of 0.35) were not considered. This criterion reduced the potential for multicollinearity issues that would impact interpretation of modeling results. The model within two units of the lowest AICc value and with the fewest parameters was selected as the final covariate model. The complete data set (the same set of years and all available days used in the complete data analysis for trend) was used for covariate modeling, but the truncated data (same years, but truncated to the common set of days within each year) were used if an acceptable covariate model could not be obtained with the complete data set.

Table 2. Environmental covariates used for modeling.

Regression predictor	Data type	Units
Air temperature	Continuous	Degree C
Daily precipitation	Continuous	mm
Relative humidity	Percentage	Percent
Solar radiation	Continuous	W
Wind speed	Continuous	m/s

If the four approaches did not produce a model with stationary residuals for either of the data transformations, then the covariate model containing a year term for trend with the lowest AICc value and an acceptable Ljung-Box test was used for trend detection. If no trend model was obtained in the covariate modeling process and/or if no acceptable covariate model could be obtained, then the data were aggregated by computing weekly means of the outcomes of interest and related covariates. If acceptable models could not be obtained from weekly means, then trends and covariate relationships were examined with monthly means.

Water temperature was measured with a thermistor chain at various depths. The depths at which water temperature was measured varied by lake and year. Temperatures were often highly correlated among depths. For a given lake and year, this relationship was used to impute missing temperatures with multivariate normal imputation in the **mtsdi** package (Junger and Ponce de Leon 2018). Water temperatures were highly correlated at different depths, suggesting very similar trends among temperatures measured at different depths at the same lake. Therefore, the trends and covariate relationships were assessed for a single depth, preferably one m when completely measured. If water temperatures were not measured at one m for all years, then the closest depth with complete measurements was used. In the case studies included later in this report, we will demonstrate how the missing data are imputed and how to apply the selected model to water temperatures measured at other depths.

Results

The results of the modeling exercise are provided by outcome and summarized by lake. Detailed analysis results, including tables and figures, are provided in Appendix A.

Dissolved Oxygen

When modeling trends in dissolved oxygen at the 12 lakes, data were included from the years 2009-2019, when possible, but were restricted to as few as four years for NOAT-107 (Figure 1). Within each year, data were collected during May-October, but restricting to the common survey dates for all years at a lake resulted in a wide range of truncated dates, and no dates were common for all years at WRST-005 (Figure 1). We were able to fit trend models with stationary residuals for all 12 lakes (Table 3). The final approach varied across the lakes with the majority requiring the data be truncated to the shortest season within a year. Only three lakes (NOAT-052, WRST-005, and YUCH-004) used the complete data, but additive outliers were also used for NOAT-052. The trend results varied from positive to negative to no significant trend (p-value < 0.05). The number of autoregressive terms ranged from zero to two with two lags as the most common form, indicating that dissolved oxygen values are related to the dissolved oxygen values from one and two days prior. The number of moving average parameters was typically one and ranged from zero to two. This indicates that residual of the previous day's dissolved oxygen is related to the current dissolved oxygen. The most common covariate to be included in the top-ranked AICc model was relative humidity, which was present in seven of the 12 models. Relative humidity was always estimated to have a negative relationship with dissolved oxygen. Month was present in six of 12 models and always estimated to have a positive relationship with dissolved oxygen. Wind speed was present in two models and estimated to have negative relationship with dissolved oxygen. The remaining covariates appeared in two or fewer lakes for the selected model.

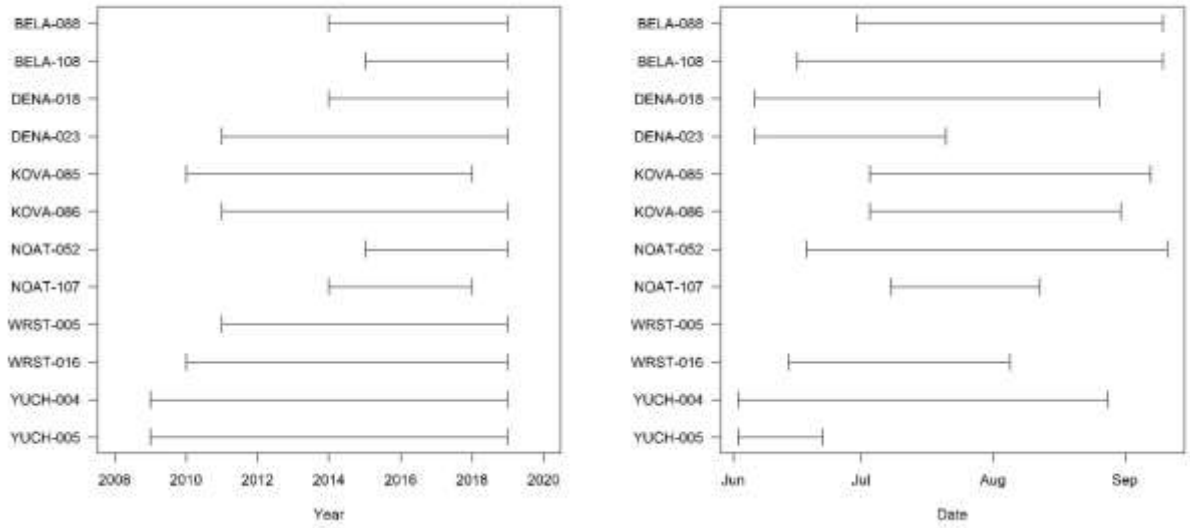


Figure 1. Survey years used for all analyses of dissolved oxygen and truncation within each year (truncated analyses only) by lake.

Table 3. Modeling results for Dissolved Oxygen.

Lake	Data	Logged	Final Approach	Intercept	Trend Coefficient	Trend SE	Trend p-value	AR	MA	LB stat	LB p-value	Covariate Model
BELA-088	Daily	FALSE	truncSA	9.6725	0.0520	0.0543	0.3379	1	1	77.44	0.6221	Relative Humidity + Month
BELA-108	Daily	FALSE	trunc	19.3994	-0.7223	0.0719	< 0.0001	2	1	89.45	0.1977	DailyPrecip+month
DENA-018	Daily	FALSE	trunc	8.3985	0.0607	0.0514	0.2372	1	1	94.78	0.4292	Solar Radiation
DENA-023	Daily	FALSE	trunc	11.7577	-0.1253	0.0608	0.0391	2	0	98.63	0.8468	Relative Humidity
KOVA-085	Daily	FALSE	trunc	11.7577	-0.1253	0.0608	0.0391	2	0	98.63	0.8468	Relative Humidity + Month
KOVA-086	Daily	FALSE	truncSA	9.6687	0.0239	0.0152	0.1155	2	2	119.52	0.0892	Daily Precipitation + Month
NOAT-052	Daily	FALSE	trunc	32.5426	-1.4900	0.1006	< 0.0001	1	1	98.53	0.0783	Wind Speed + Relative Humidity + Month
NOAT-107	Daily	FALSE	completeAO	11.9199	-0.1253	0.0749	0.0943	2	1	7.46	0.0587	Relative Humidity + Month
WRST-005	Daily	FALSE	complete	8.4524	0.0250	0.0906	0.7822	0	1	6.26	0.1808	Relative Humidity
WRST-016	Daily	FALSE	truncSA	8.4424	-0.0278	0.0329	0.3979	2	2	114.12	0.1270	Air Temperature
YUCH-004	Daily	FALSE	complete	9.0742	-0.0049	0.0290	0.8663	2	0	8.64	0.1950	Wind Speed + Relative Humidity
YUCH-005	Daily	FALSE	trunc	2.6290	0.3878	0.2377	0.1028	1	0	40.65	0.2355	Air Temperature

pH

Survey data for pH were included from the years 2009-2019, when possible, but were restricted to as few as four years for NOAT-107 (Figure 2). Truncating each annual data set to the subset of common dates across years resulted in datasets with over three months of data for YUCH-005, but as only a month of monitoring data each year for NOAT-107 (Figure 2). We were able to fit trend models with stationary residuals for all 12 lakes (Table 4). The final approach varied across the lakes with the majority using the complete data set. Three lakes required truncation and, of those three, two applied the seasonal adjustment. The trend result varied from positive (four lakes) to negative (three lakes) to no significant trend (five lakes). The number of autoregressive terms ranged from one to three, with one lag as the most common. The number of moving average parameters ranged from zero to three. This indicates that residual of the previous few day's pH is related to the current pH.

The most common covariate to be included in the top-ranked AICc model was wind speed, which was present in four lakes. Wind speed was estimated to be negatively associated with pH at three lakes, but a positive relationship was observed at one lake. Relative humidity and air temperature were in the top models for three lakes, each. Relative humidity was always estimated to have a negative relationship with pH, and air temperature exhibited a positive relationship with pH. The remaining covariates appeared in two or fewer lakes for the selected model.

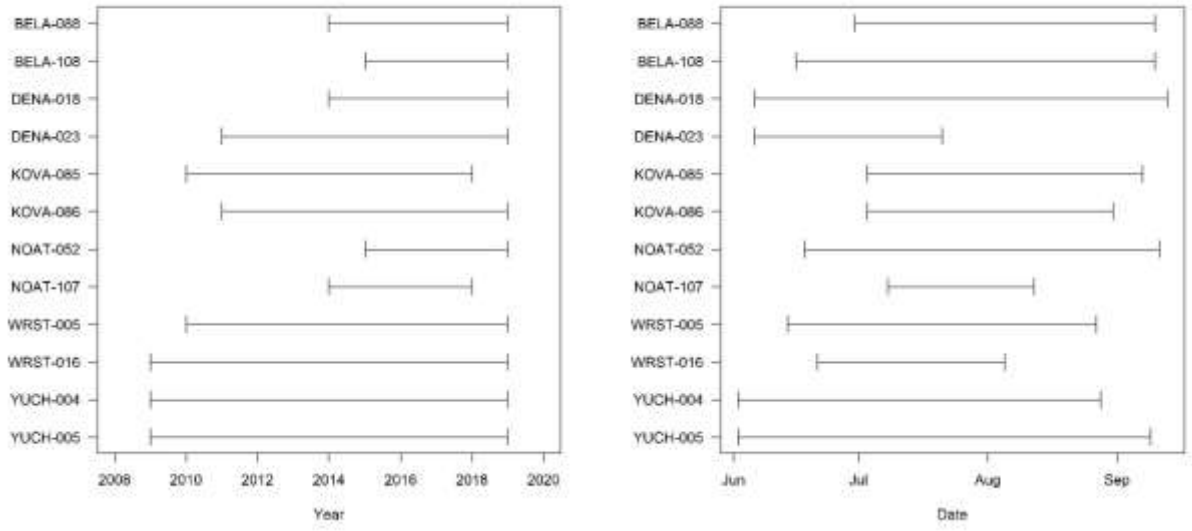


Figure 2. Survey years used for all analyses of pH and truncation within each year (truncated analyses only) by lake.

Table 4. Modeling results for pH.

Lake	Data	Logged	Final Approach	Intercept	Trend Coefficient	Trend SE	Trend p-value	AR	MA	LB stat	LB p-value	Covariate Model
BELA-088	Daily	FALSE	truncSA	7.4133	0.0543	0.0239	0.0229	3	2	71.54	0.7123	Relative Humidity
BELA-108	Daily	FALSE	complete	8.5765	-0.0853	0.0201	< 0.0001	1	2	3.58	0.6114	Daily Precipitation + Month
DENA-018	Daily	FALSE	complete	3.7081	0.2807	0.0515	< 0.0001	1	3	4.31	0.3651	Solar Radiation + Year
DENA-023	Daily	FALSE	complete	9.3459	-0.1022	0.0367	0.0053	3	1	3.91	0.4178	Air Temperature + Wind Speed + Daily Precipitation
KOVA-085	Daily	FALSE	truncSA	8.5630	-0.0298	0.0243	0.2210	2	2	109.83	0.5669	Relative Humidity + Month
KOVA-086	Daily	FALSE	complete	7.5025	0.0180	0.0201	0.3686	1	2	2.56	0.7669	Wind Speed + Relative Humidity + Year
NOAT-052	Daily	FALSE	trunc	6.3580	0.1025	0.0335	0.0022	2	1	95.18	0.0904	Wind Speed + Relative Humidity
NOAT-107	Daily	FALSE	complete	12.7919	-0.3135	0.0719	< 0.0001	1	1	8.41	0.2099	Air Temperature + Year
WRST-005	Daily	FALSE	complete	5.5434	0.0993	0.0266	0.0002	1	2	6.51	0.2600	Relative Humidity
WRST-016	Daily	FALSE	complete	7.3331	-0.0174	0.0130	0.1835	1	2	2.56	0.7677	Air Temperature + Wind Speed + Year
YUCH-004	Daily	FALSE	complete	7.3265	-0.0030	0.0132	0.8198	1	0	2.48	0.9283	Air Temperature + Wind Speed
YUCH-005	Daily	FALSE	complete	8.0744	-0.0636	0.0679	0.3495	3	3	5.27	0.1534	Relative Humidity + Year

Specific Conductance

Survey data for specific conductance were included from the years 2009-2019, when possible, but were restricted to as few as four years for several lakes (Figure 3). Truncating each annual data set to the subset of common dates across years resulted in datasets with as few as one month and as many as three months of monitoring data each year (Figure 3). We were able to fit trend models with stationary residuals for all 12 lakes (Table 5). The final approach varied across the lakes with the majority using truncated data with most of these also requiring seasonal adjustments. The trend result for most lakes (eight) indicated a positive trend with the rest having no significant trend (large p-value). The number of autoregressive terms was generally one, but ranged from zero to five. This indicates that specific conductance today is related to the specific conductance from the day before and, occasionally, more past days. The number of moving average parameters was typically zero or one, but ranged from zero to five. This indicates that residual of the previous day's specific conductance is related to the current specific conductance.

The most common covariate to be included in the top-ranked AICc model was month, which was present in nine lakes. Month most often estimated a positive relationship with specific conductance and only two lakes with a negative relationship. Daily precipitation was in the top model at five lakes, with only one lake estimated to have a positive relationship. The remaining covariates appeared in two or fewer lakes for the selected model.

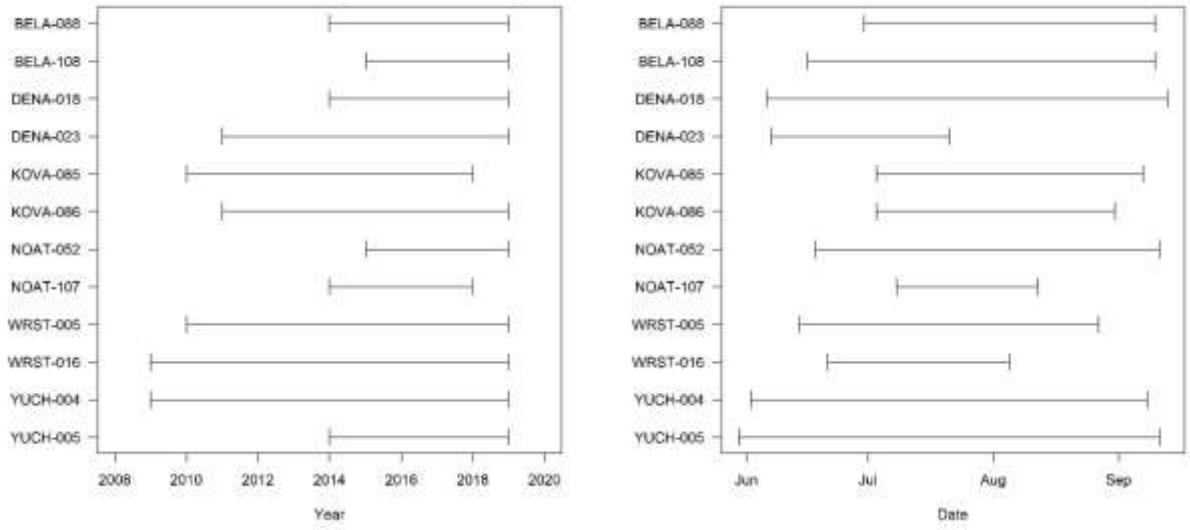


Figure 3. Survey years used for all analyses of specific conductance and truncation within each year (truncated analyses only) by lake.

Table 5. Modeling results for Specific Conductance.

Lake	Data	Logged	Final Approach	Intercept	Trend Coefficient	Trend SE	Trend p-value	AR	MA	LB stat	LB p-value	Covariate Model
BELA-088	Daily	FALSE	truncSA	167.36	0.2300	0.82	0.7812	1	1	87.48	0.3191	Daily Precipitation + Month
BELA-108	Weekly	FALSE	truncSA	78.66	1.2400	0.41	0.0024	0	5	7.15	0.2098	Relative Humidity + Month
DENA-018	Daily	FALSE	completeAO	57.89	2.2400	0.83	0.0072	5	3	5.45	0.1417	Air Temperature + Year
DENA-023	Daily	FALSE	truncSA	74.7	0.5300	0.42	0.2091	1	0	53.02	0.9793	Daily Precipitation + Month
KOVA-085	Daily	FALSE	truncSA	94.46	0.5100	0.98	0.6	1	0	95.09	0.9223	Year + Month
KOVA-086	Daily	FALSE	trunc	44.92	1.1200	0.15	< 0.0001	1	0	127.74	0.0497	Air temperature + Wind Speed + year
NOAT-052	Daily	FALSE	complete + covariates	19.88	5.4000	0.52	< 0.0001	2	1	6.95	0.1385	Year + Month
NOAT-107	Daily	FALSE	trunc	29.19	3.6000	0.29	< 0.0001	3	1	29.80	0.3231	Daily Precipitation + Month
WRST-005	Weekly	FALSE	truncSA	45.5966	-0.0895	0.3301	0.7862	2	1	21.71	0.1527	Daily Precipitation + Month
WRST-016	Daily	FALSE	trunc	44.83	1.9800	0.34	< 0.0001	1	0	74.32	0.7411	Wind Speed + Month
YUCH-004	Monthly	TRUE	complete	4.5378	0.0520	0.0167	0.0019	0	3	9.29	0.0980	Year + Month
YUCH-005	Daily	FALSE	complete + covariates	75.8959	7.0489	3.8523	0.06728	2	2	6.36	0.0954	Wind Speed + Month

Sonde Temperature

Survey data for sonde temperature were included from the years 2009-2019, when possible, but were restricted to as few as four years for several lakes (Figure 4). Truncating each annual data set to the subset of common dates across years resulted in datasets with as few as one month and as many as three months of monitoring data each year (Figure 4). We were able to fit trend models with stationary residuals at 10 lakes using daily data, and two lakes required using weekly data (Table 6). The final approach varied across the lakes with the majority using truncated data with most of these also requiring seasonal adjustments. Only lake BELA-108 used the complete data with additive outliers. The trend result for most lakes (six) indicated a positive trend with the rest having no significant trend (large p-value). The number of autoregressive terms was a mix of values ranging from one to four. This indicates that sonde temperature today is related to the sonde temperature from one or more days before. The number of moving average parameters was typically zero or one, but ranged from zero to three. This indicates that residual of the previous day's sonde temperature is related to the current sonde temperature.

The most common covariate to be included in the top-ranked AICc model was wind speed, which was present in six lakes. Wind speed most often estimated a negative relationship with sonde temperature; only two lakes demonstrated a positive relationship. Air Temperature was in the top model at five lakes, with positive relationships with sonde temperature estimated in every case. Month was in the top model at four lakes, and all relationships were negatively associated with sonde temperature. The remaining covariates appeared in two or fewer lakes for the selected model.

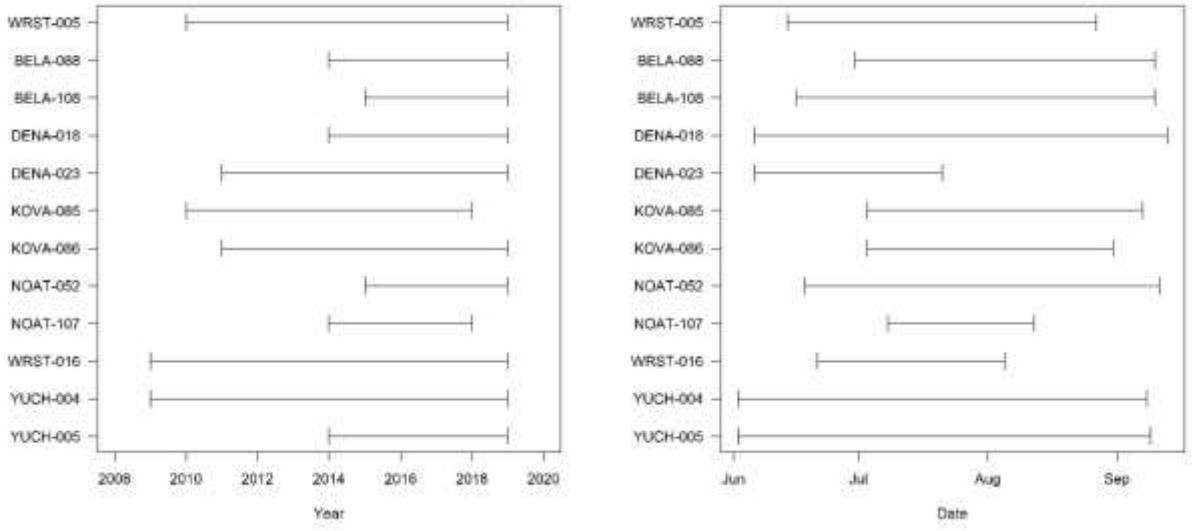


Figure 4. Survey years used for all analyses of sonde temperature and truncation within each year (truncated analyses only) by lake.

Table 6. Modeling results for Sonde Temperature.

Lake	Data	Logged	Final Approach	Intercept	Trend Coefficient	Trend SE	Trend p-value	AR	MA	LB stat	LB p-value	Covariate Model
BELA-088	Weekly	FALSE	trunc	12.5229	0.2661	0.2616	0.3091	2	0	11.53	0.0733	Relative Humidity + Month
BELA-108	Daily	FALSE	completeAO	NA	1.2405	0.0802	< 0.0001	1	3	3.05	0.3846	Wind Speed + Relative Humidity + Year + Month
DENA-018	Weekly	FALSE	trunc	NA	1.9868	0.3309	< 0.0001	1	0	11.75	0.5480	Air Temperature + Wind Speed
DENA-023	Daily	FALSE	trunc	17.6210	0.1242	0.1239	0.3161	1	2	69.14	0.6984	Air temperature + Wind Speed
KOVA-085	Daily	FALSE	truncSA	15.6620	-0.0075	0.1076	0.9446	4	2	92.22	0.9022	Air Temperature + Wind Speed
KOVA-086	Daily	FALSE	truncSA	14.7521	0.1194	0.0940	0.2038	2	0	126.12	0.0529	Wind Speed + Month
NOAT-052	Daily	FALSE	truncSA	12.7018	0.1081	0.1338	0.4194	4	0	84.04	0.3279	Solar Radiation + year
NOAT-107	Daily	FALSE	trunc	-13.5904	2.1636	0.5120	< 0.0001	4	1	19.84	0.7990	Air Temperature + Year
WRST-005	Daily	FALSE	truncSA	15.3177	0.1394	0.0731	0.0566	2	1	156.73	0.2043	Air Temperature
WRST-016	Daily	FALSE	trunc	14.3041	0.1898	0.0635	0.0028	1	2	67.42	0.8928	Air Temperature + Year
YUCH-004	Daily	FALSE	truncSA	18.4247	-0.0017	0.0569	0.9768	3	0	210.03	0.1643	Air Temperature
YUCH-005	Daily	FALSE	truncSA	12.6001	0.3769	0.1080	0.0005	2	3	111.21	0.5034	Wind Speed + Month

Sediment Temperature

Survey data for sediment temperature were included from as early as 2007 and as late as 2019, but were restricted to as few as four years for several lakes (Figure 5). NOAT-107 monitoring data were insufficient for trend analysis. Truncating each annual data set to the subset of common dates across years resulted in datasets with two to nearly four months of monitoring data each year (Figure 5). We were able to fit trend models with stationary residuals at nine lakes using daily data, one lake required using weekly data, and one lake only had a single year of data available (Table 7). The final trend modeling approach varied across the lakes with the majority using truncated data with most of these also requiring seasonal adjustments. Only lake YUCH-005 used the complete data. The trend result for three lakes indicated a positive trend, one indicated a negative trend, with the rest having no significant trend (large p-value). The number of autoregressive terms was generally two with a one and a three also. This indicates that sediment temperature today is related to the sediment temperature from typically one and two days before. The number of moving average parameters was typically zero, but ranged from zero to two. This indicates that residual of the previous day's sediment temperature is typically not related to the current sediment temperature.

The most common covariate to be included in the top-ranked AICc model was wind speed and month, which was present in five lakes, each. Wind speed most often estimated a positive relationship with sediment temperature and only one lake with a negative relationship. Month was negatively related to sediment temperature at three lake and positive at the other two. Air Temperature was in the top model at three lakes, with all estimating a positive relationship with sediment temperature. The remaining covariates appeared in two or fewer lakes for the selected model.

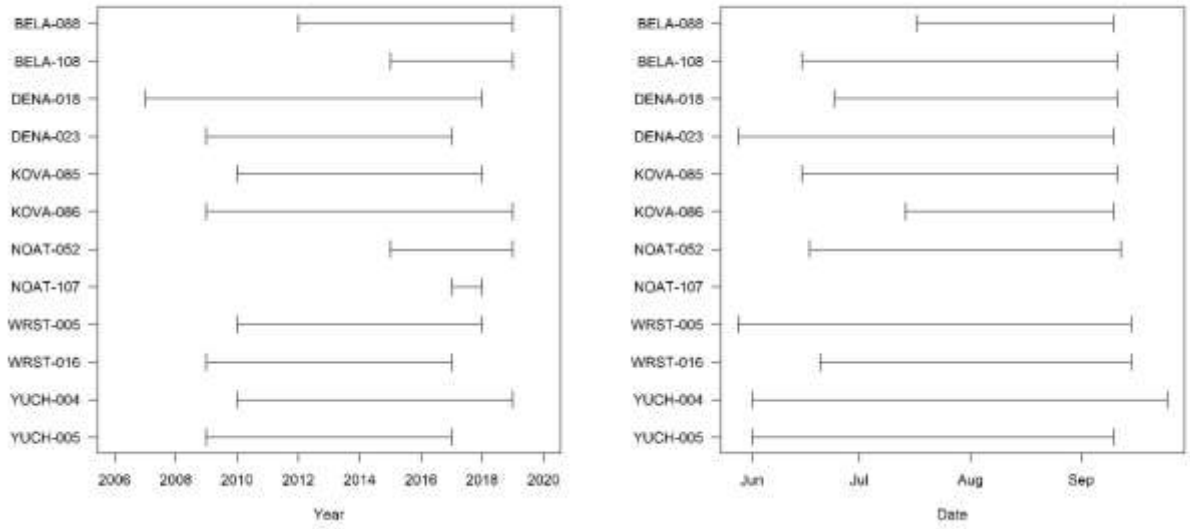


Figure 5. Survey years used for all analyses of sediment temperature and truncation within each year (truncated analyses only) by lake.

Table 7. Modeling results for Sediment Temperature.

Lake	Data	Logged	Final Approach	Intercept	Trend Coefficient	Trend SE	Trend p-value	AR	MA	LB stat	LB p-value	Covariate Model
BELA-088	Daily	FALSE	truncSA	10.2470	0.1936	0.1276	0.1292	2	1	89.96	0.2818	Air Temperature
BELA-108	Daily	FALSE	truncSA	13.3096	-0.0130	0.1988	0.9479	3	0	79.43	0.5907	Air temperature
DENA-018	Daily	FALSE	truncSA	14.3819	0.0567	0.0562	0.3132	2	0	168.87	0.1951	Daily Precipitation + Month
DENA-023	Daily	FALSE	truncSA	13.9933	0.1263	0.1088	0.2457	2	0	180.17	0.5865	Daily Precipitation + Year
KOVA-085	Daily	FALSE	truncSA	15.2505	-0.0082	0.0883	0.9264	2	0	145.90	0.6670	Wind Speed + Month
KOVA-086	Weekly	FALSE	trunc	11.8894	0.1004	0.1680	0.5501	2	0	10.07	0.6098	Air Temperature + Wind Speed + Relative Humidity
NOAT-052	Daily	FALSE	trunc	25.2099	-1.1118	0.1392	< 0.0001	2	2	66.79	0.8721	Air Temperature + Month
NOAT-107						Insufficient data						
WRST-005	Daily	FALSE	trunc	5.1212	0.7942	0.1457	< 0.0001	2	1	187.45	0.1846	Wind Speed + Solar Radiation
WRST-016	Weekly	FALSE	trunc	NA	0.9490	0.1842	< 0.0001	1	0	12.77	0.9568	Relative Humidity + Month
YUCH-004	Daily	FALSE	truncSA	10.3991	-0.0100	0.0538	0.8522	2	1	238.54	0.2865	Wind Speed + Month
YUCH-005	Weekly	FALSE	complete	4.5855	-0.0305	0.0679	0.6533	2	1	1.75	0.8823	Solar Radiation

Thermistor Chain Temperature

Survey data for water temperature were included from as early as 2009 and as late as 2019, but were restricted to as few as four years for several lakes (Figure 6). Truncating each annual data set to the subset of common dates across years resulted in datasets with 2.0 to 3.5 months of monitoring data each year (Figure 6). We were able to fit trend models with stationary residuals at all 10 lakes using daily data at five lakes and weekly data at five lakes (Table 8). The final trend modeling approach varied across the lakes with four lakes modeled from complete data and six lakes modeled from the truncated data, with three of these lakes applying seasonal adjustments. Five lakes indicated a positive trend over time, and five lakes exhibited no significant trend (large p-value). The number of autoregressive terms ranged from zero to four, and the number of moving average parameters ranged from zero to three.

The most common covariates for modeling thermistor chain water temperature data were relative humidity, month, wind speed, and air temperature. Relative humidity and month were both included in models for four lakes and were both negatively associated with water temperature. Air Temperature had a positive relationship with water temperature at three lakes. Wind speed was positively related to water temperature at YUCH-004, but indicated a negative relationship at DENA-018 and DENA-023.

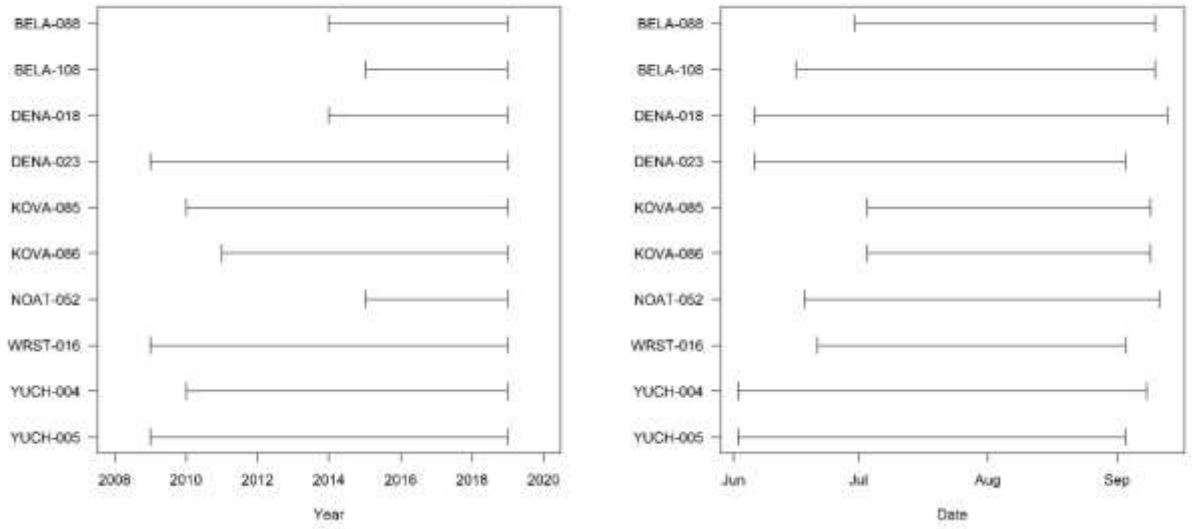


Figure 6. Survey years used for all analyses of water temperature and truncation within each year (truncated analyses only) by lake.

Table 8. Modeling results for Water Temperature.

Lake	Data	Depth	Logged	Final Approach	Intercept	Trend Coefficient	Trend SE	Trend p-value	AR	MA	LB stat	LB p-value	Covariate Model
BELA-088	Weekly	1.00m	FALSE	complete	7.8276	1.2019	0.5366	0.0251	1	0	13.98	0.0516	Relative Humidity + Month
BELA-108	Daily	1.50m	FALSE	complete + covariates	NA	2.3667	0.1208		1	3	3.75	0.2895	Relative Humidity + Year + Month
DENA-018	Weekly	1.00m	FALSE	trunc	NA	2.2710	0.3361	< 0.0001	1	0	4.73	0.9082	Wind Speed + Solar Radiation
DENA-023	Weekly	1.00m	FALSE	trunc	16.8055	0.0734	0.1188	0.5364	0	1	28.34	0.2031	Air Temperature + Wind Speed
KOVA-085	Daily	1.00m	FALSE	truncSA	15.3813	0.0215	0.0863	0.8036	2	0	128.09	0.5800	Air Temperature
KOVA-086	Daily	0.25m	FALSE	truncSA	14.3884	0.1155	0.0934	0.2163	2	0	97.44	0.9164	Relative Humidity + Month
NOAT-052	Daily	1.50m	FALSE	truncSA	12.3256	0.1403	0.1355	0.3005	3	3	96.70	0.0640	Relative Humidity + Month
NOAT-107						Insufficient data							
WRST-005						Insufficient data							
WRST-016	Weekly	1.00m	FALSE	complete	12.5542	0.0991	0.0432	0.0218	4	1	4.97	0.1739	Air Temperature + Year
YUCH-004	Weekly	1.00m	FALSE	trunc	17.4337	0.0540	0.1284	0.6743	0	2	25.02	0.2960	Wind Speed + Month
YUCH-005	Daily	1.50m	FALSE	complete	37.2627	-2.3868	0.1049	< 0.0001	2	2	5.23	0.2648	Daily Precipitation + Year

Comparison of Temperature Outcomes

Three classes of lake temperature data are collected in this protocol, and many of the metrics are correlated. The correlation between water temperature metrics (Figure 7) exceeds 0.8 in many cases (large dark blue circles) and that correlation decreases as a function of the difference in depth at which the measurement is collected. However, even measurements taken at very different depths are still positively correlated. This summary many provide information on reducing the number of metrics collected at a lake for this protocol, particularly if any metrics are costly to collect. Correlation among temperature metrics is provided by lake in Appendix B.

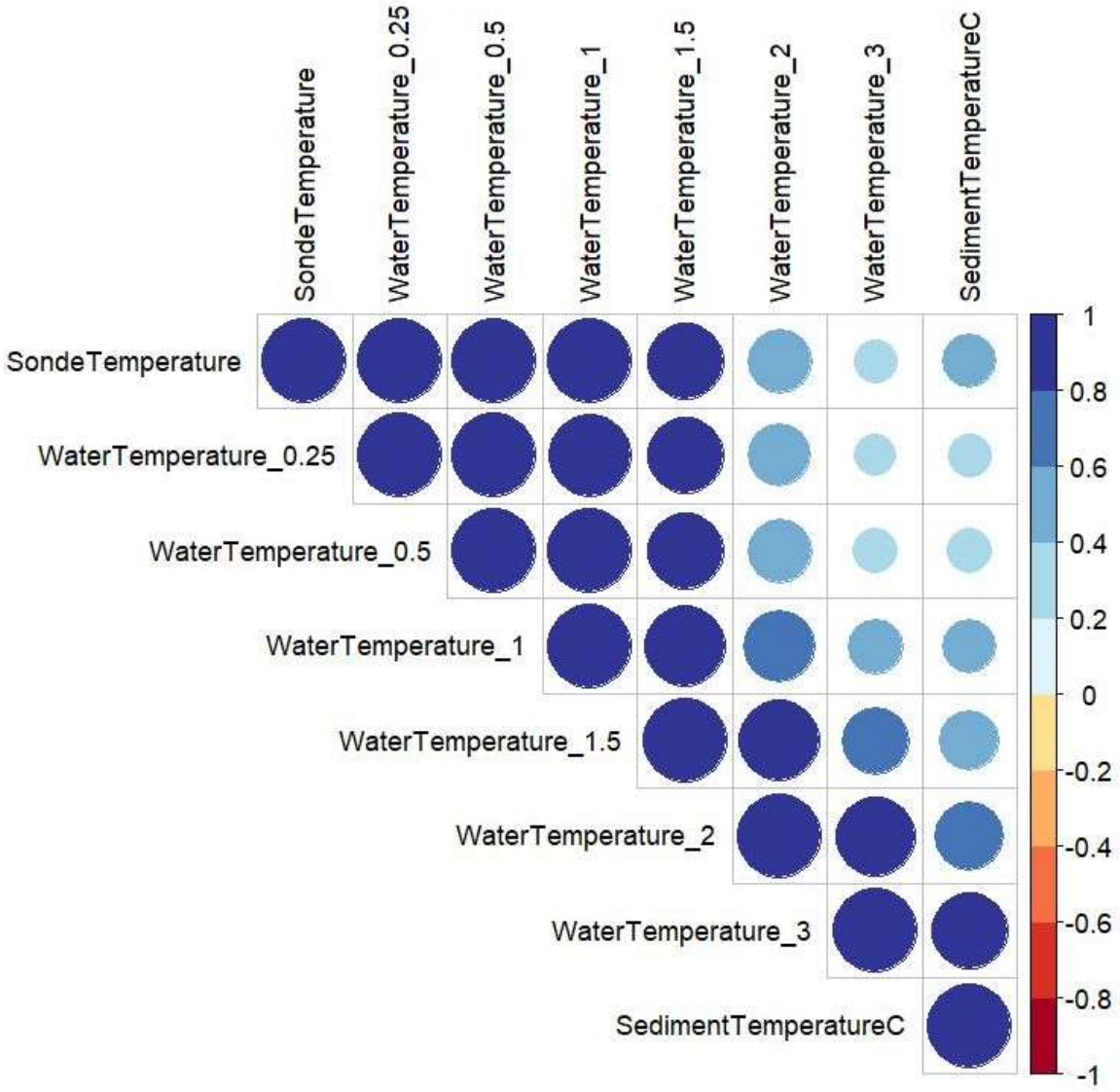


Figure 7. Correlation plot of temperature metrics by depth across all lakes and dates.

Case Study

Preparing for Analysis

The following steps provide guidance on installing and using the R package for the ARCN/CAKN shallow lakes trend analysis package, *NPSH2OAK*.

Preparing R

The R package **NPSH2OAK** depends on other R packages to function. In order for *NPSH2OAK* to work on your local machine, it is necessary to first obtain these external packages. The Rtools package must be downloaded and installed, and this step will not be needed again until package updates are needed.

Download and install Rtools: https://cran.r-project.org/bin/windows/Rtools/

The following code installs the packages needed for the **NPSH2OAK** package and installs the package.

```
## install needed packages

packageList <- c('plyr','lubridate', 'dplyr',  'tidyr', 'imputeTS',
'stringr', 'stats', 'tidyr', 'forecast', 'lmtest', 'broom')

lapply(packageList,install.packages)

## install NPSH2OAK package
packagePath <- 'C:/…' # change to the location of the NPSH2OAK_1.0.4.tar.gz
file
install.packages(file.path(packagePath,'NPSH2OAK_1.0.4.tar.gz'),repos=NULL)
```

Accessing the R scripts

The R scripts are stored with the package. It is recommended that the R scripts be copied to a new location for use and making changes.

The R command: `.libPaths()` will tell you the location of the R packages you have installed. Inside the *NPSH2OAK* folder is the folder called *Rscripts*. This folder has subfolder containing all of the R scripts to do the analyses.

Preparing for the Analysis

The following code prepares the data for the analysis for YUCH-004 lake and specific conductance as the response variable. For other analyses, these would need to be updated in the code below.

```
### Loading packages
library(scales); library(ggplot2); library(forecast); library(tidyverse);
library(imputeTS); library(snakecase); library(gridExtra); library(lmtest);
require(usdm); library(corrplot); library(RColorBrewer);
library(flextable);library(NPSH2OAK)
packageVersion("NPSH2OAK") # '1.0.5'
```

```
### Setting file path
### Set the working directory as the appropriate top level for your analysis
localPath <- getwd()
workspacePath <- file.path(localPath, "workspace")
figurePath <- file.path(localPath, "trendResults/figures")
modelSelectionPath <- file.path(localPath, "trendResults/modelSelection")
regSummaryPath <- file.path(localPath, "trendResults/regSummary")

lapply(list(workspacePath,figurePath,modelSelectionPath,regSummaryPath),funct
ion(f){
    if(!dir.exists(f)){
        dir.create(f,recursive=TRUE)
    }#end if
    return(NULL)
})#end lapply



### Load example data, from the package
data("continuousLakeClimateData")
data("metricRef")


### Setting parameteres
#### Lake name
subsetLake <- "YUCH-004"


#### Covariates
allCov <- c(
  "AirTemp", "WindSpeed", "SolarRadiation", "RelativeHumidity",
  "DailyPrecip"
)

#### response variable
responseVar_orig <- "SpecificConductance(SpCond)"
responseVar <- "SpecificConductanceSpCond"

#### Confidence alpha limit
alfa <- 0.05

#### Cut-off for imputing missing data
cutoff <- 0.4

#### Cutoff for VIF among covariates
vif.max <- 1.14

#### Get the formal name for the reponse variable to use in plotting figures
```

```
(formalResVar <- metricRef$inReportName[metricRef$currentMetric ==
responseVar_orig])
(yLabText <- paste0(
  formalResVar, " (",
  metricRef$unit[metricRef$currentMetric == responseVar_orig], ")"
))

### File name to save image
(fileName <- paste0("trend-Modeling_", subsetLake, "_", responseVar,
".RData"))




#################################################################
# Formatting and exploring data
#################################################################

### Formatting raw data in long format
formattedData <- FormatData(
  df = continuousLakeClimateData,
  lake = subsetLake,
  metric = c(allCov, responseVar_orig)
)
head(formattedData)

### Providing summary output, specifically average for each metric
## all analyses will be done on the day scale
dailyDf_long <- SummarizeData(
  df = formattedData,
  timeInterval = "yday",
  includeYear = TRUE,
  c("lake", "metric", "depth")
)

### Format summary data from long to wide format for data analysis
dailyDf <- ReshapeWideFormat(
  summarizedDf = dailyDf_long,
  dateTimeCol = "datetime",
  valueCol = "summary",
  depthCol = "depth",
  metricCol = "metric",
  lakeCol = "lake",
  subsetLake = NULL,
  metric = c(responseVar_orig, allCov),
  toDrop = c("grade", "interpolation", "approval"),
  bottomTemp = FALSE
)
```

```
## rename
names(dailyDf)[which(names(dailyDf)==responseVar_orig)] <- responseVar

## order by date
dailyDf <- dailyDf[order(dailyDf$datetime), ]

### Create date related covariates for trending modeling
dailyDf$Date <- as.POSIXct(as.character(as.Date(dailyDf$datetime)),format =
"%Y-%m-%d")
dailyDf$jDay <- as.numeric(strftime(dailyDf$Date, format = "%j"))
dailyDf$month <- as.numeric(strftime(dailyDf$datetime, format = "%m"))
dailyDf$month2 <- dailyDf$month^2
dailyDf$year <- lubridate::year(dailyDf$datetime)
dailyDf$wyear <- dailyDf$year - min(dailyDf$year)
```

Case Study: Specific Conductance at YUCH-004

We begin the analysis by opening the analysis template script, formatting the data for analysis as described in the previous section, and defining the *subsetLake* and *responseVar* objects. Set up the paths for the directories where the workspaces and modeling output will be written. Next, examine missingness in the time series across years.

```
> propYearMissing <- aggregate(list(propYear=is.na(dailyDf[, responseVar])),list(year=dailyDf$year),mean)
> propYearMissing <- propYearMissing[propYearMissing$year<2020,]
> propYearMissing
   year  propYear
1  2004 1.0000000
2  2005 0.9260274
3  2006 1.0000000
4  2007 0.7150685
5  2008 1.0000000
6  2009 0.6849315
7  2010 0.7315068
8  2011 0.6849315
9  2012 0.6584699
10 2013 0.7095890
11 2014 0.6958904
12 2015 0.7068493
13 2016 0.6912568
14 2017 0.7123288
15 2018 0.6657534
16 2019 0.5274725
```

We see that the proportion of missingness is 100% for years 2004, 2006, and 2008. Note that proportions of missingness are inflated because we have not yet removed dates where covariate data are available, but surveys were not conducted. We see that the longest consecutive set of years with surveys begin in 2009, so we remove data for years through 2008. We observe also that surveys began in May or June each year and ended in September.

```
> minYear <- max(propYearMissing$year[propYearMissing$propYear==1])+1
> minYear
[1] 2009
> dailyDf_orig <- dailyDf
> dim(dailyDf_orig)
[1] 5493   14
> dailyDf <- dailyDf[!is.na(dailyDf[, responseVar]) & dailyDf$year >= minYear, ]
>
> (MinMaxMonth <- aggregate(dailyDf$month,list(dailyDf$year), function(x){
+   return(c(min(x),max(x)))
+ }))
   Group.1 x.1 x.2
1     2009   5   9
2     2010   6   9
3     2011   5   9
4     2012   5   9
5     2013   6   9
6     2014   5   9
```

An initial plot of the data indicates an extreme increasing trend, possibly exponential (Figure 8).

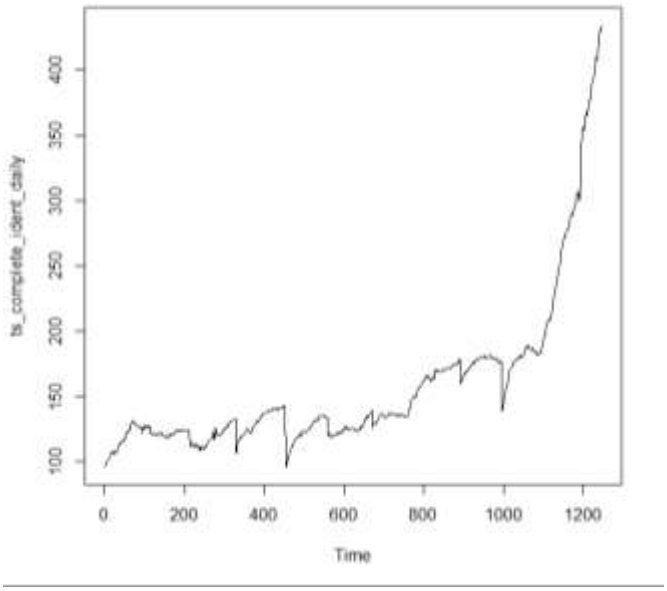


Figure 8. Time series plot of the untransformed complete data set of YUCH-004 specific conductance.

Now we begin the modeling process with the complete data model and untransformed data. First, a time series is created with the *ts* function in the **forecast** package. The trend model is fit with the *auto.arima function*, a fixed effect for year (*wyear*) is specified for trend estimation, and the *max.d* option is set to zero to suppress differencing. The model results indicate that the time series correlation structure is an ARIMA(0,0,5) structure.

```
>  trendModel_complete_ident_daily
Series: ts_complete_ident_daily
Regression with ARIMA(0,0,5) errors

Coefficients:
         ma1     ma2    ma3     ma4     ma5  intercept    xreg
      1.9438  2.4597  2.230  1.4219  0.5349    61.8981  9.6202
s.e.  0.0407  0.0710  0.062  0.0371  0.0232     6.5837  0.6278

sigma^2 estimated as 43.79:  log likelihood=-4121.87
AIC=8259.74   AICc=8259.85   BIC=8300.76
```

The *checkresiduals* function provides residual diagnostics for the complete data model. As with most linear models, the residuals must demonstrate independent residuals that are normally distributed with a mean of zero and constant variance. The Ljung-Box test tests to see if autocorrelations of residuals among a number of lag times are all zero, i.e., the residuals are independently distributed. The Ljung-Box test indicates that significant autocorrelation is still present in the residuals from the complete model ($p < 0.0001$).

```
        Ljung-Box test

data:  Residuals from Regression with ARIMA(0,0,5) errors
Q* = 3062.8, df = 3, p-value < 2.2e-16

Model df: 7.   Total lags used: 10
```

Three figures are provided by the *checkresiduals* function for the complete data model (Figure 9). The top figure plots the residuals across time. We use this plot to identify outliers, assess the assumption of residuals with a mean of zero, and examine any non-constant variance. The mean of the residuals appears to be near zero until the most recent dates, and the variance is roughly constant over time with the exception of several large outliers at roughly regular intervals. These occur at the beginning of each new survey season and indicate that the model does not account for the breaks in seasons. The autocorrelation figure indicates substantial autocorrelation at numerous lags as indicated by the vertical lines that extend beyond the blue dashed lines within which autocorrelation is considered relatively small. This pattern of autocorrelation decreasing over lags suggests that an autoregressive term be included in the model. The last figure is a histogram of residuals, and this figure is used to evaluate the normality assumption for model residuals. This figure indicates that the residuals are light-tailed, or leptokurtic. Given the substantial autocorrelation in the residuals, we reject this model for trend inference. Unmodeled autocorrelation causes standard errors to be underestimated, which results in narrow confidence intervals and hypothesis tests that suggest a significant trend when none exists (Type I error).

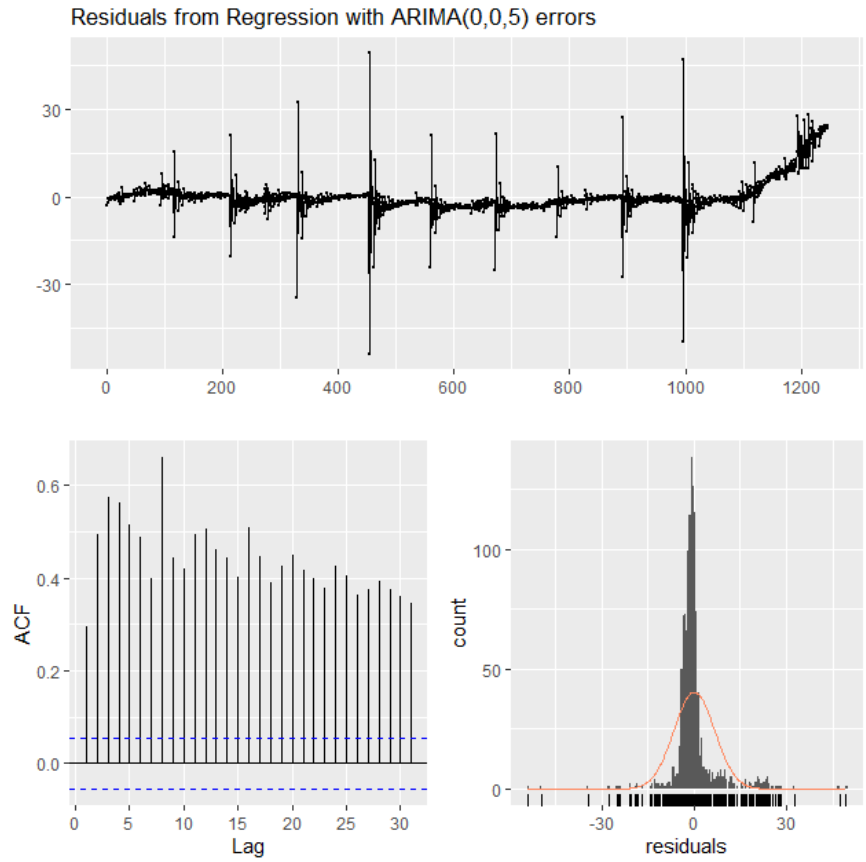


Figure 9. Residual diagnostic plots for the untransformed complete data model.

Now we fit the additive outliers model. For this model, we create fixed effects for the first date of each year to account for the new season. These effects are located at the blue dotted lines in the figure below (Figure 10).

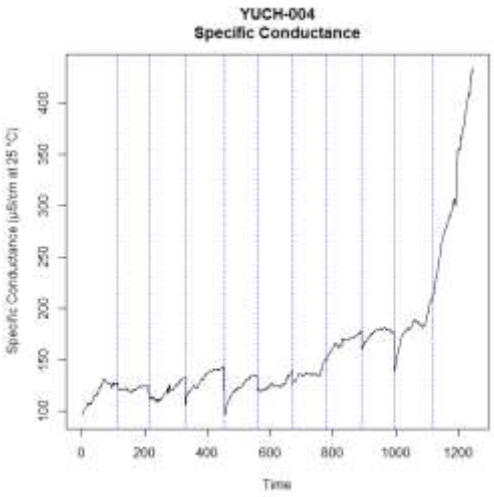


Figure 10. Additive outliers plot for YUCH-004 specific conductance.

Fitting the model to the data, we obtain estimates of the intercept, trend slope (unlabeled in the output for reasons unknown), and the 10 additive outliers for the 10 years of data. In this model, no autoregressive or moving-average parameters are modeled, so independent residuals are assumed. However, the Ljung-Box test indicates that the residuals are not independent ($p < 0.0001$).

```
> trendModel_completeAO_ident_daily
Series: ts_complete_ident_daily
Regression with ARIMA(0,0,0) errors

Coefficients:
      intercept                AO1      AO2       AO3       AO4       AO5       AO6       AO7       AO8
        15.7736  14.1776  20.5776  -3.2375  -21.3505  -44.9051  -37.7161  -45.6436  -37.1546  -40.0821
s.e.     4.0685   0.3844  43.3183  43.3061   43.2972   43.2918   43.2898   43.2912   43.2960   43.3043
            AO9       AO10
      -75.8497  -18.3457
s.e.   43.3159   43.3310

sigma^2 estimated as 1891:  log likelihood=-6462.32
AIC=12950.64   AICc=12950.93   BIC=13017.3
```

```
> checkresiduals(trendModel_completeAO_ident_daily)

        Ljung-Box test

data:  Residuals from Regression with ARIMA(0,0,0) errors
Q* = 15411, df = 3, p-value < 2.2e-16

Model df: 12.   Total lags used: 15
```

The residual plots indicate that the mean residual value diverges from zero over time (Figure 11). Significant autocorrelation still exists in the residuals, and their distribution is slightly skewed right in this model. We reject this model for these reasons.

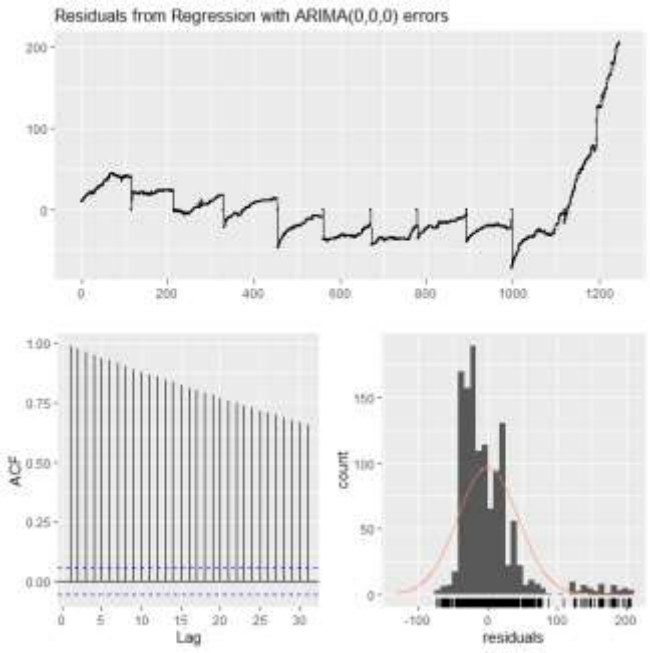


Figure 11. Residual diagnostics plot for the untransformed additive outliers model.

Now we truncate the data to the set of dates that are common to all years and define seasons by year. We identify the set of Julian days from the data set surveyed in all years as follows:

```
> # Truncated time series data
> (MinMax <- aggregate(dailyDf$jDay, list(dailyDf$year), function(x) {
+   return(c(min(x), max(x)))
+ }))
   Group.1 x.1 x.2
1     2009 151 265
2     2010 154 251
3     2011 149 263
4     2012 147 271
5     2013 154 259
6     2014 146 256
7     2015 152 258
8     2016 151 263
9     2017 149 253
10    2018 147 268
11    2019 139 267
>
> c(max(MinMax[, 2][, 1]), min(MinMax[, 2][, 2]))
[1] 154 251
```

We check the dates and make sure that each set of dates is the same length (here, 98 days). Then we can create a time series of the truncated data set and plot the new truncated time series (Figure 12).

```
> start.yr.mo <- c(2009, 6) # <--- Change this for the appropriate data
> ts_trunc_ident_daily <- ts(dailyDf_trunc[, responseVar],
+                       start = start.yr.mo,
+                       frequency = freq.num_daily)
> plot(ts_trunc_ident_daily)
```

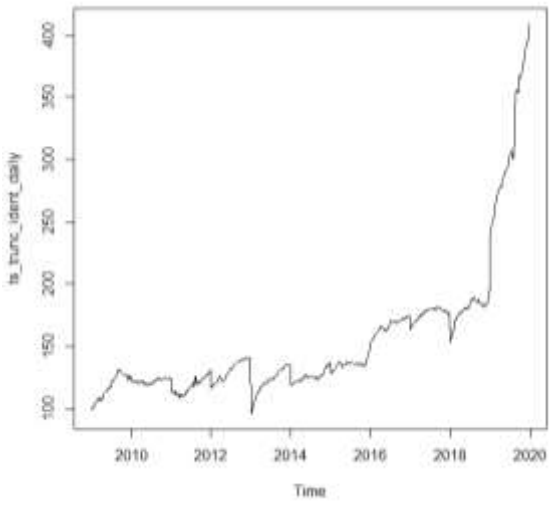


Figure 12. Time series plot of the untransformed truncated data set of YUCH-004 specific conductance.

Now we model the truncated data set, adding to the code options to suppress the differencing among seasons (*max.D* = 0) and allowing seasonal effects to be modeled if useful (*seasonal* = TRUE). The resulting model has an ARIMA(0,0,5) structure, but the Ljung-Box test indicates that the residuals are not independent ($p < 0.0001$). The residual plots also demonstrate substantial autocorrelation, so this model is rejected also (Figure 13).

```
Series: ts_trunc_ident_daily
Regression with ARIMA(0,0,5) errors

Coefficients:
         ma1     ma2     ma3     ma4     ma5  intercept     xreg
      1.8757  2.3435  2.1218  1.3618  0.5236     52.606  10.3159
s.e.  0.0396  0.0664  0.0564  0.0380  0.0261      5.779   0.5518

sigma^2 estimated as 37.52:  log likelihood=-3482.52
AIC=6981.04   AICc=6981.17   BIC=7020.9
>
>
> checkresiduals(trendModel_trunc_ident_daily)

        Ljung-Box test

data:  Residuals from Regression with ARIMA(0,0,5) errors
Q* = 8656.9, df = 189, p-value < 2.2e-16

Model df: 7.   Total lags used: 196
```

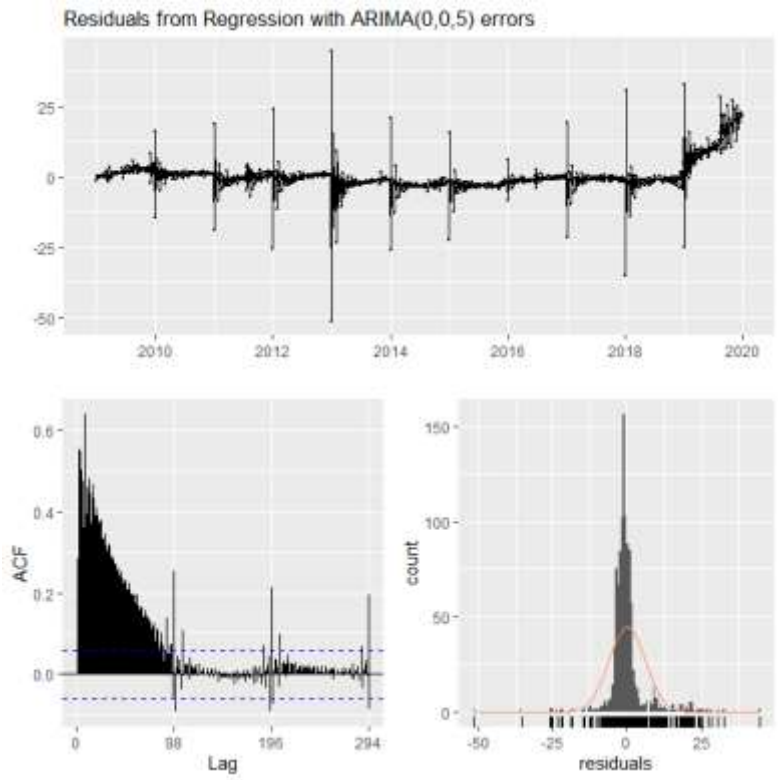


Figure 13. Residual diagnostic plots for the untransformed truncated model.

Now the seasonally adjusted truncated model is applied. First, the truncated time series is decomposed into trend effects, seasonal effects, and random error (Figure 14).

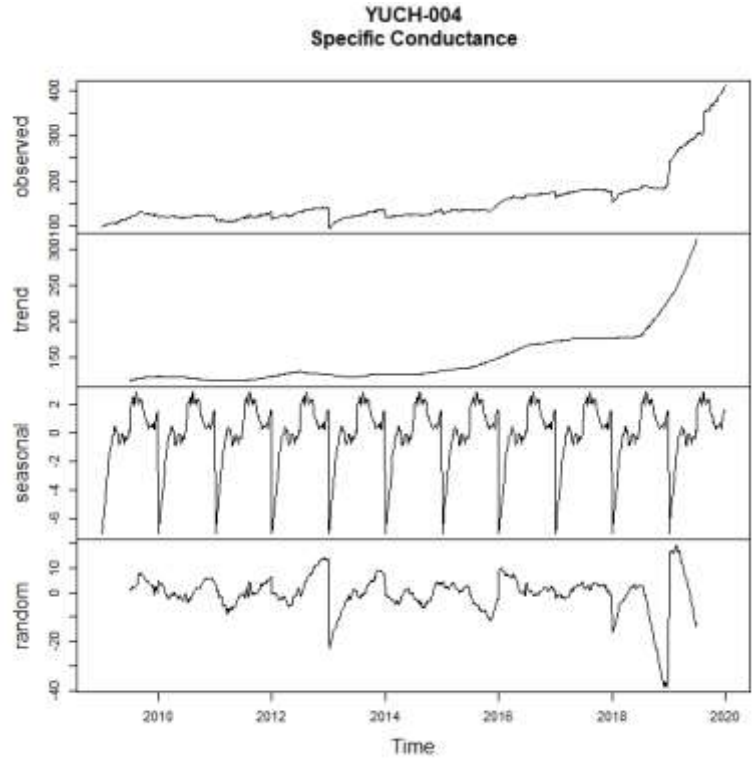


Figure 14. Time series decomposition plot for YUCH-004 specific conductance.

Then the estimated seasonal effect is subtracted from the time series. If the seasonal effect is estimated well, then the resulting time series should be a combination of trend and random error that may exhibit less autocorrelation. The model is estimated to have an ARIMA(0,0,5) structure, but the Ljung-Box test does not suggest independent residuals ($p < 0.0001$). Similarly, the autocorrelation plot indicates substantial autocorrelation (Figure 15).

```
> trendModel_trunc_ident_daily
Series: ts_trunc_ident_daily
Regression with ARIMA(0,0,5) errors

Coefficients:
         ma1     ma2     ma3     ma4     ma5  intercept     xreg
      1.8757  2.3435  2.1218  1.3618  0.5236     52.606  10.3159
s.e.  0.0396  0.0664  0.0564  0.0380  0.0261      5.779   0.5518

sigma^2 estimated as 37.52:  log likelihood=-3482.52
AIC=6981.04   AICc=6981.17   BIC=7020.9
> checkresiduals(trendModel_trunc_ident_daily)

        Ljung-Box test

data:  Residuals from Regression with ARIMA(0,0,5) errors
Q* = 8656.9, df = 189, p-value < 2.2e-16

Model df: 7.   Total lags used: 196
```

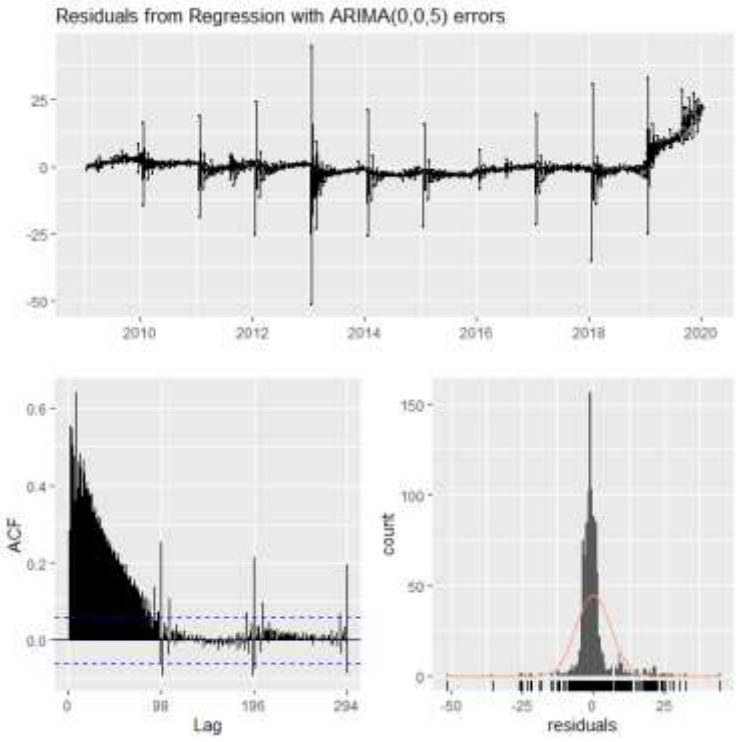


Figure 15. Residual diagnostic plots for the untransformed truncated seasonally adjusted model.

The next portion of the analysis script applies the same four models, but to the logarithmically transformed specific conductance measurements. The results of this analysis were very similar and did not result in a model with stationary residuals, so the details of the analysis are omitted here. Now, we examine covariates to determine if any associations exist with specific conductance at YUCH-004. The covariate data may be useful in explaining correlation in the residuals over time, providing the basis for trend analysis as well.

Before we begin modeling the covariate data, we examine the covariates for missingness. We apply a cutoff of 40% for missing data, omitting years for which more than 40% of the covariate is missing. Here, four covariates have missing data for 2019, and 100% of the data are missing for that year. We omit the 2019 data from the covariate analysis.

```
> ### check covariates for missing values
> covPropMissing <- plyr::ddply(dailyDf, ~year, function(d, allCov) {
+   out <- NULL
+   for (p in allCov) {
+     out <- rbind(out, data.frame(covar = p, propMiss = sum(is.na(d[, p])) / nrow(d)))
+   } # end for p
+   return(out)
+ }, allCov = allCov)
>
>
> covPropMissing[which(covPropMissing$propMiss > cutoff), ]
   year            covar propMiss
51 2019          AirTemp        1
52 2019        WindSpeed        1
53 2019   SolarRadiation        1
54 2019 RelativeHumidity        1
```

```
## Since we have missing covariates for the entire year, we should drop this
## year
##  - use only if necessary for appropriate covariates
covarSelDf_daily <- dailyDf[dailyDf$year < 2019, ]
```

An examination of the entire *covPropMissing* object shows that the only other non-zero missingness is less than 1%, and moving-average imputation will be used to fill in these missing values.

```
> covPropMissing[which(covPropMissing$propMiss > 0), ]
   year            covar    propMiss
11 2011          AirTemp 0.008695652
12 2011        WindSpeed 0.008695652
13 2011   SolarRadiation 0.008695652
14 2011 RelativeHumidity 0.008695652
16 2012          AirTemp 0.008000000
17 2012        WindSpeed 0.008000000
18 2012   SolarRadiation 0.008000000
19 2012 RelativeHumidity 0.008000000
21 2013          AirTemp 0.009433962
22 2013        WindSpeed 0.009433962
23 2013   SolarRadiation 0.009433962
24 2013 RelativeHumidity 0.009433962
45 2017      DailyPrecip 0.009523810
51 2019          AirTemp 1.000000000
52 2019        WindSpeed 1.000000000
53 2019   SolarRadiation 1.000000000
54 2019 RelativeHumidity 1.000000000
55 2019      DailyPrecip 0.015503876
```

The covariate data sets are plotted with the original data in blue and imputed data in red (Figure 16). Imputations for the relative humidity covariate fall within the range of the data set and seem appropriate.

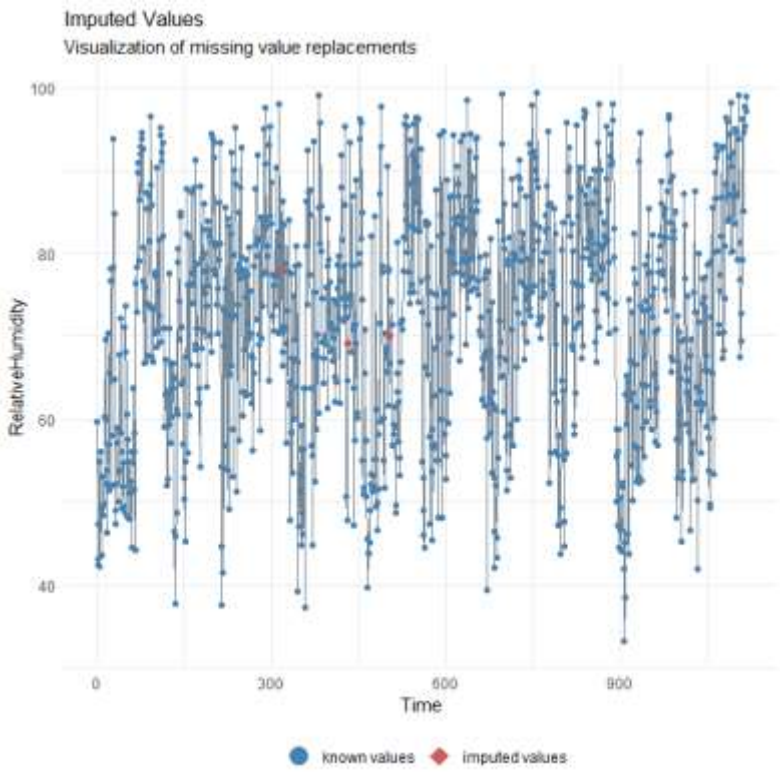


Figure 16. Observed (blue) and imputed (red) relative humidity values plotted by time.

After running the imputation code, continue to the linear model section. The first model uses the *tslm* function, which fits a linear model that can accommodate some seasonal effects, if defined. The model results show a reasonable R^2 value of 0.79 and several covariates with low p-values, but residual diagnostics do not suggest that residuals are independent, so these model results are not clearly interpretable. The Breusch-Godfrey test, which tests for serial correlation at various lags, suggests substantial correlation remains in the residuals ($p < 0.0001$). The autocorrelation plot supports this conclusion also (Figure 17).

```
> summary(fullModel_tslm)

Call:
forecast::tslm(formula = formula(paste0(responseVar, "~", paste0(allCov,
    collapse = "+"), "+year+month")), data = tsImpDf)

Residuals:
    Min      1Q  Median      3Q     Max
-28.438 -10.834   2.955   8.387  26.940

Coefficients:
                  Estimate Std. Error t value Pr(>|t|)
(Intercept)      -1.488e+04  2.667e+02 -55.797  < 2e-16 ***
AirTemp           3.065e-01  1.029e-01   2.978  0.00297 **
WindSpeed        -8.666e-01  7.200e-01  -1.204  0.22897
SolarRadiation    1.021e-02  6.718e-03   1.520  0.12872
RelativeHumidity -7.912e-03  4.301e-02  -0.184  0.85406
DailyPrecip       2.045e+00  2.373e+00   0.862  0.38904
year              7.430e+00  1.315e-01  56.509  < 2e-16 ***
month             7.522e+00  4.241e-01  17.738  < 2e-16 ***
---
Signif. codes:  0 '***' 0.001 '**' 0.01 '*' 0.05 '.' 0.1 ' ' 1

Residual standard error: 11.58 on 1109 degrees of freedom
Multiple R-squared:  0.7881,    Adjusted R-squared:  0.7868
F-statistic: 589.2 on 7 and 1109 DF,  p-value: < 2.2e-16
```

```
> checkresiduals(fullModel_tslm)

        Breusch-Godfrey test for serial correlation of order up to 11

data:  Residuals from Linear regression model
LM test = 1074, df = 11, p-value < 2.2e-16
```

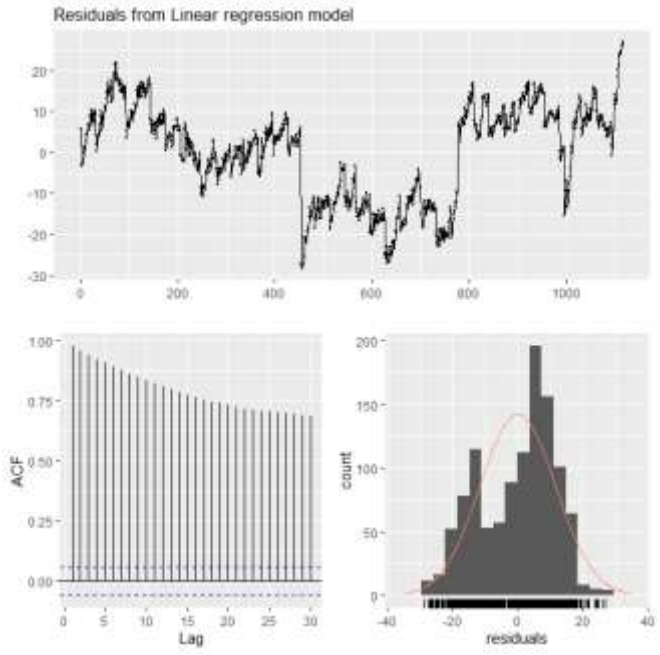


Figure 17. Residual diagnostic plots for the full covariate model assuming independent error for YUCH-004 specific conductance.

The full suite of covariates are then included in an ARMA model with the *auto.arima* function. An ARIMA(0,0,5) structure is estimated along with fixed effects for the intercept and all covariates. However, the Ljung-Box test indicates dependence in the residuals ($p < 0.0001$) and the diagnostic plots suggest autocorrelated residuals. The residuals plotted against time in the top figure and the plot of the residuals against fitted values on the right demonstrate large residual values (Figure 18).

```
> fullModel_ARIMA
Series: tsImpDf[, responseVar]
Regression with ARIMA(0,0,5) errors

Coefficients:
         ma1     ma2     ma3     ma4     ma5  intercept  AirTemp  WindSpeed  SolarRadiation
      1.4877  1.6329  1.4175  0.9344  0.4028    37.0079  -0.0915    -0.1994         -0.0005
s.e.  0.0335  0.0504  0.0439  0.0348  0.0257     2.8952   0.0355     0.1036          0.0013
      RelativeHumidity  DailyPrecip   wyear   month
                -0.0211      -0.4115  6.9931  5.4682
s.e.             0.0096       0.3105  0.1906  0.1868

sigma^2 estimated as 7.263:  log likelihood=-2687.42
AIC=5402.84   AICc=5403.22   BIC=5473.09
```

```
> checkresiduals(fullModel_ARIMA)

        Ljung-Box test

data:  Residuals from Regression with ARIMA(0,0,5) errors
Q* = 2241.2, df = 3, p-value < 2.2e-16

Model df: 13.   Total lags used: 16
```

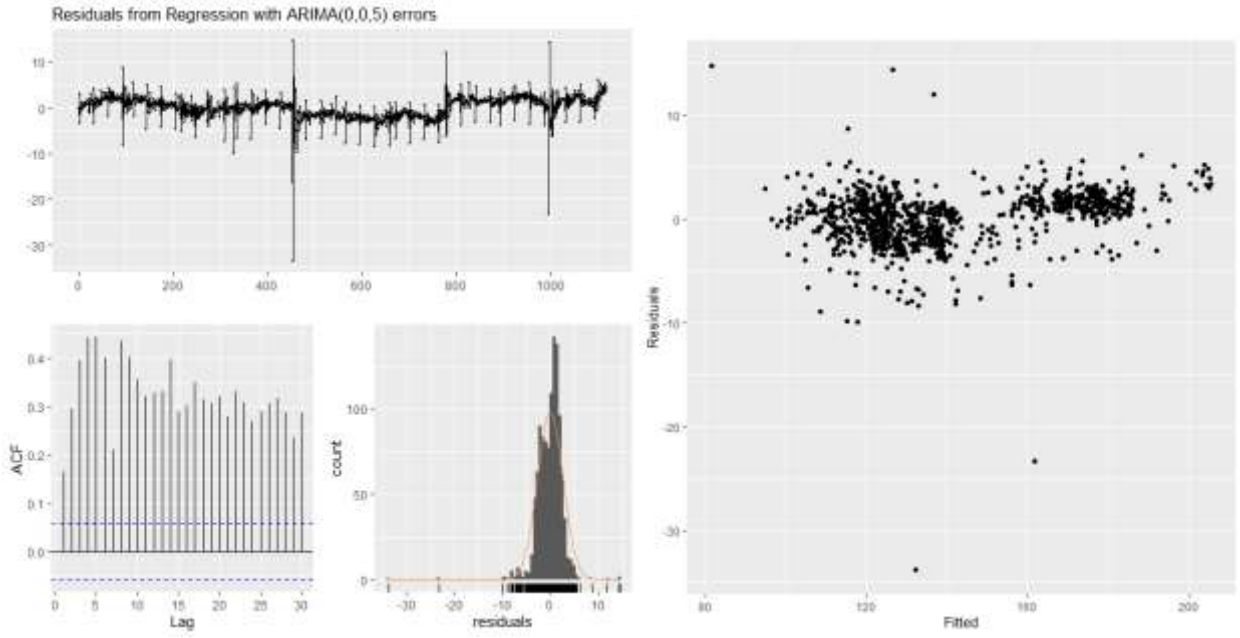


Figure 18. Residual diagnostic plots for the full covariate ARIMA model for YUCH-004 specific conductance

The results of the full covariate ARIMA model do not suggest that an acceptable covariate model will be obtained from the daily data, and model selection among covariates did not improve model fit. No model with stationary residuals could be obtained from the daily data. We skip to the sections called “Save outputs” and “Creating appendix table” to save the data plots and trend modeling result tables. The specific conductance data were then summarized to the week level, and all trend and covariate modeling was conducted on the weekly means. No model with acceptable residuals could be identified from the weekly data either. We continue with the analysis using monthly data. The data summary function *SummarizeData* is called with *timeInterval* = "month" and the *ReshapeWideFormat* function finalizes the monthly data for analysis. The same subset of years beginning in 2009 is used for the analysis of monthly means.

The model of the complete monthly data set is fit and the fit is much improved for means at the monthly level. The Ljung-Box test still indicates dependence in the residuals, and the autocorrelation function demonstrates some substantial autocorrelation at lags one through three, so we reject this model due to correlation in the residuals. The mean of the residuals is near zero for the entire time series with the exception of the end of the time series (Figure 19).

```
Series: ts_complete_ident_month
Regression with ARIMA(0,0,2) errors

Coefficients:
         ma1     ma2  intercept     xreg
      0.9469  0.7481    47.0024  12.2598
s.e.  0.1094  0.0851    26.0872   2.7124

sigma^2 estimated as 603.4:  log likelihood=-243.79
AIC=497.57   AICc=498.85   BIC=507.43
>
> checkresiduals(trendModel_complete_ident_month)

        Ljung-Box test

data:  Residuals from Regression with ARIMA(0,0,2) errors
Q* = 18.143, df = 6, p-value = 0.005884

Model df: 4.   Total lags used: 10
```

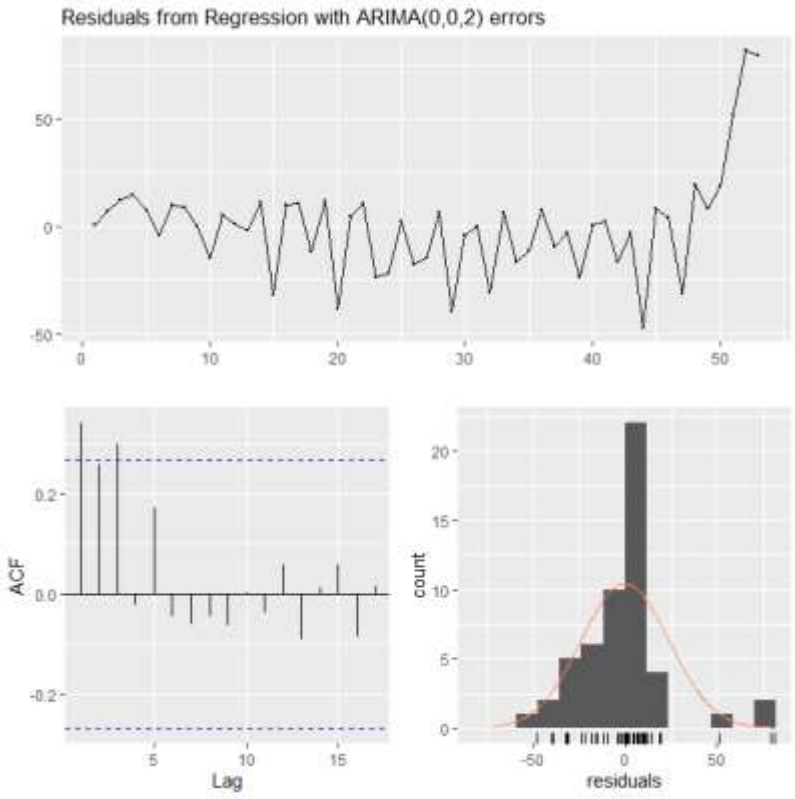


Figure 19. Residual diagnostic plots for the untransformed monthly complete data model.

The additive outliers model is now fit to the monthly means by defining the beginning of each year with fixed effects (Figure 20).

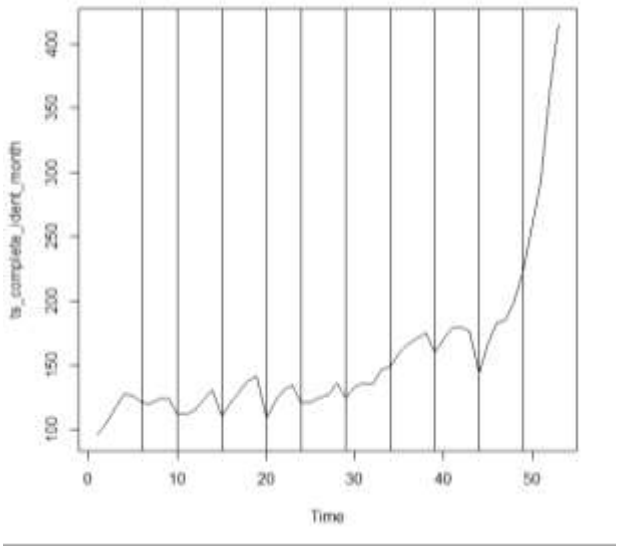


Figure 20. Additive outliers plot for monthly YUCH-004 specific conductance means.

The additive outlier model for the monthly data did not improve the fit, with evidence of substantial correlation among residuals from the Ljung-Box test ($p < 0.0001$) and autocorrelation plot. The residuals exhibit a trend in the plot against time and are skewed right in the histogram. We reject this model for correlated residuals and poor fit (Figure 21).

```
Series: ts_complete_ident_month
Regression with ARIMA(0,0,0) errors

Coefficients:
                AO1      AO2       AO3       AO4       AO5       AO6       AO7       AO8       AO9
      17.2796  34.8606   8.4027  -10.7713  -29.6409  -34.7697  -47.7962  -41.5838  -47.0941  -81.2566
s.e.   0.6446  40.5422  40.5985   40.6650   40.7415   40.8281   40.9247   41.0311   41.1474   41.2735
         AO10
      -20.1914
s.e.   41.4091

sigma^2 estimated as 2061:  log likelihood=-271.26
AIC=566.52   AICc=574.32   BIC=590.16
>
> checkresiduals(trendModel_completeAO_identmonth)

        Ljung-Box test

data:  Residuals from Regression with ARIMA(0,0,0) errors
Q* = 43.218, df = 3, p-value = 2.212e-09

Model df: 11.   Total lags used: 14
```

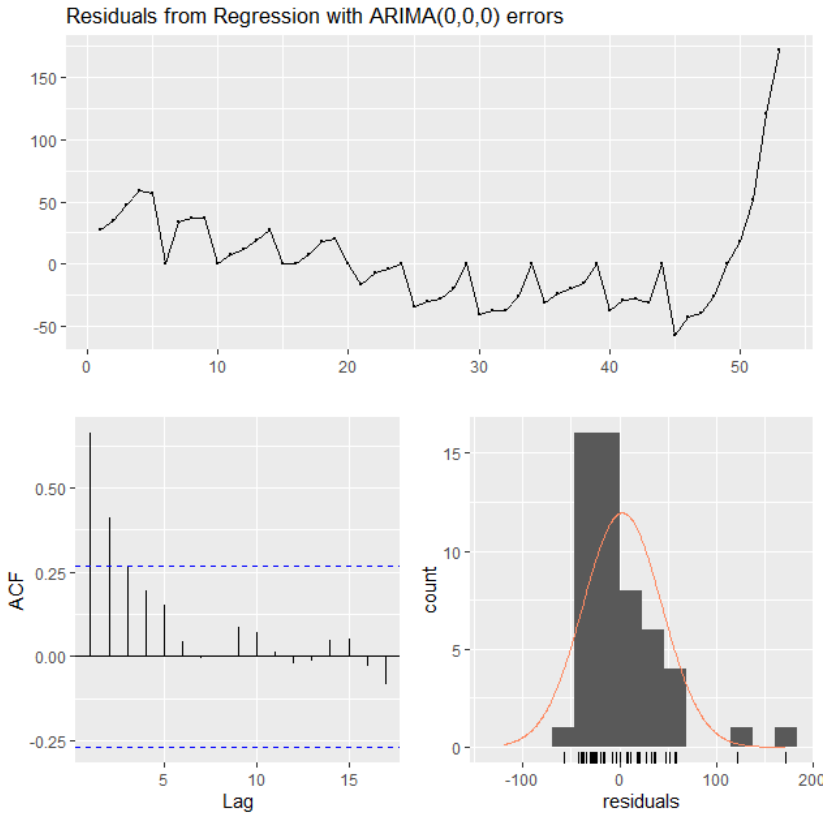


Figure 21. Residual diagnostic plots for the untransformed monthly additive outliers model.

The truncated monthly data are obtained by restricting the monthly data to the months of June through September. Modeling the truncated monthly data, we obtain a seasonal ARIMA model with MA(1) structure among years, but also an AR(1) model within seasons. However, this model also exhibits correlated residuals as evidenced by the Ljung-Box test ($p < 0.0001$) and the autocorrelation plot (Figure 22).

```
Series: ts_trunc_ident_month
Regression with ARIMA(0,0,1)(1,0,0)[4] errors

Coefficients:
         ma1     sar1      xreg
      0.8399  0.7219  19.9920
s.e.  0.0693  0.1553   2.5197

sigma^2 estimated as 785.4:  log likelihood=-209.17
AIC=426.35   AICc=427.38   BIC=433.49
>
> checkresiduals(trendModel_trunc_ident_month)

        Ljung-Box test

data:  Residuals from Regression with ARIMA(0,0,1)(1,0,0)[4] errors
Q* = 26.095, df = 5, p-value = 8.553e-05

Model df: 3.   Total lags used: 8
```

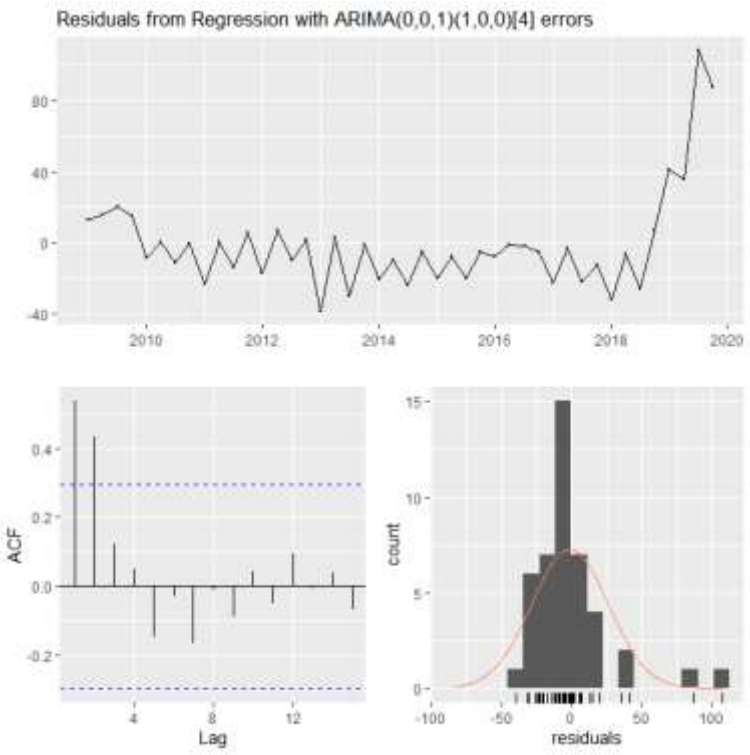


Figure 22. Residual diagnostic plots for the untransformed monthly truncated data model.

The time-series decomposition of the monthly data indicates a strong seasonal component with an exponential trend (Figure 23).

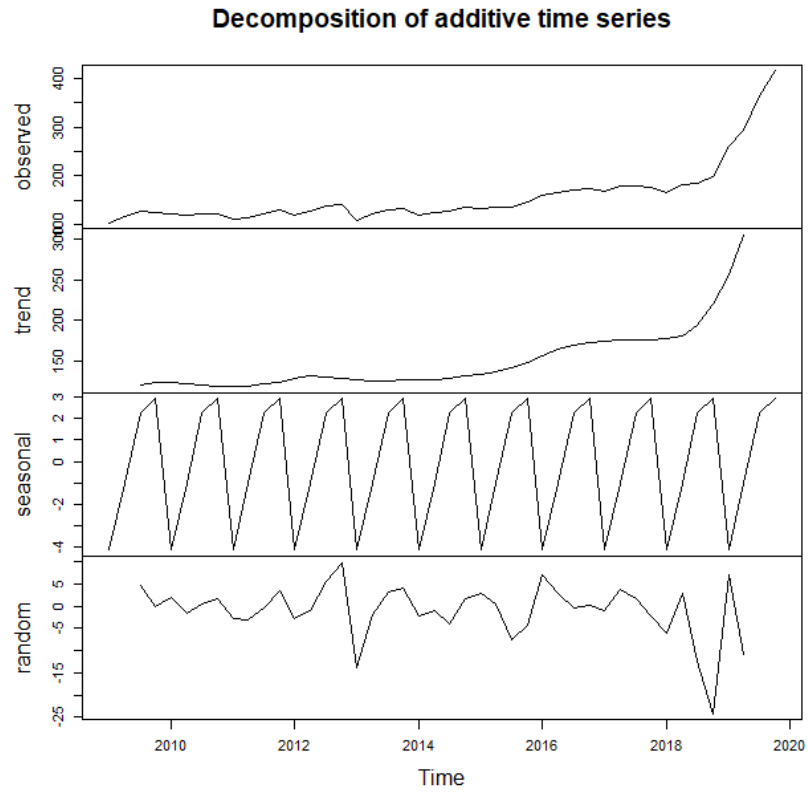


Figure 23. Time series decomposition plot of monthly YUCH-004 specific conductance means.

Removing the seasonal component from the truncated time series and fitting the trend model produces a similar model to the truncated model, with an annual MA(1) and a seasonal MA(1). However, the Ljung-Box test ($p < 0.0001$) and the autocorrelation function still indicate that the residuals are not independent (Figure 24).

```
Series: ts_truncSA_ident_month
Regression with ARIMA(0,0,1)(0,0,1)[4] errors

Coefficients:
         ma1     sma1     xreg
      0.8104   0.8869  18.6832
s.e.  0.0590   0.2832   1.3120

sigma^2 estimated as 689.5:  log likelihood=-207.86
AIC=423.72   AICc=424.74   BIC=430.86
>
> checkresiduals(trendModel_truncSA_ident_month)

        Ljung-Box test

data:  Residuals from Regression with ARIMA(0,0,1)(0,0,1)[4] errors
Q* = 26.719, df = 5, p-value = 6.471e-05

Model df: 3.   Total lags used: 8
```

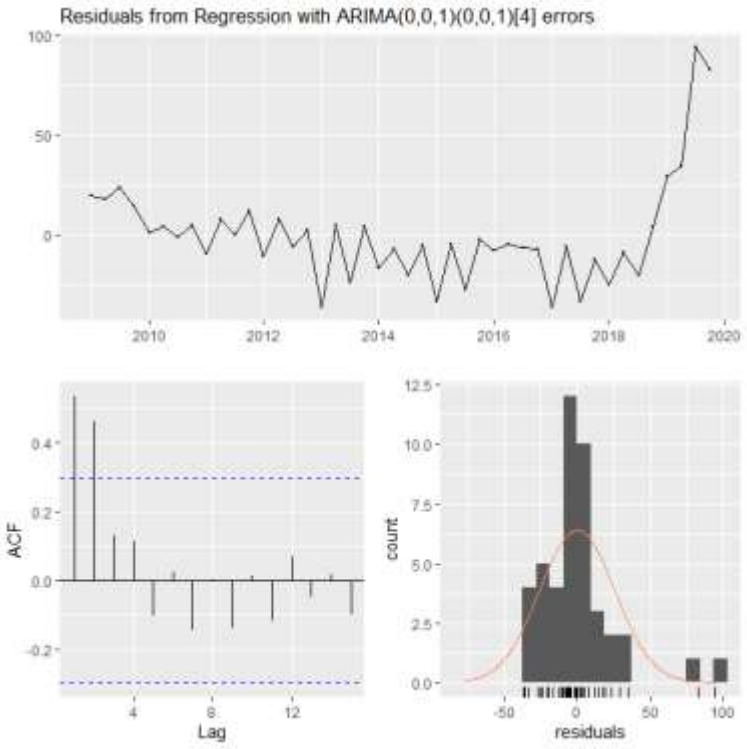


Figure 24. Residual diagnostic plots for the untransformed monthly truncated seasonally adjusted model.

Now we examine the logarithmically transformed specific conductance data. The complete data model has an ARIMA(0,0,3) structure and both the Ljung-Box test ($p = 0.0980$) and the autocorrelation function plot provide evidence for independent residuals. This will serve as the final model for trend inference (Figure 25).

```
Series: ts_complete_log_month
Regression with ARIMA(0,0,3) errors

Coefficients:
         ma1     ma2     ma3  intercept    xreg
      1.3017  1.1096  0.6529     4.5378  0.0520
s.e.  0.1346  0.1802  0.1146     0.1619  0.0167

sigma^2 estimated as 0.01136:  log likelihood=44.68
AIC=-77.37   AICc=-75.54   BIC=-65.54
>
> checkresiduals(trendModel_complete_log_month)

        Ljung-Box test

data:  Residuals from Regression with ARIMA(0,0,3) errors
Q* = 9.2915, df = 5, p-value = 0.09799

Model df: 5.   Total lags used: 10
```

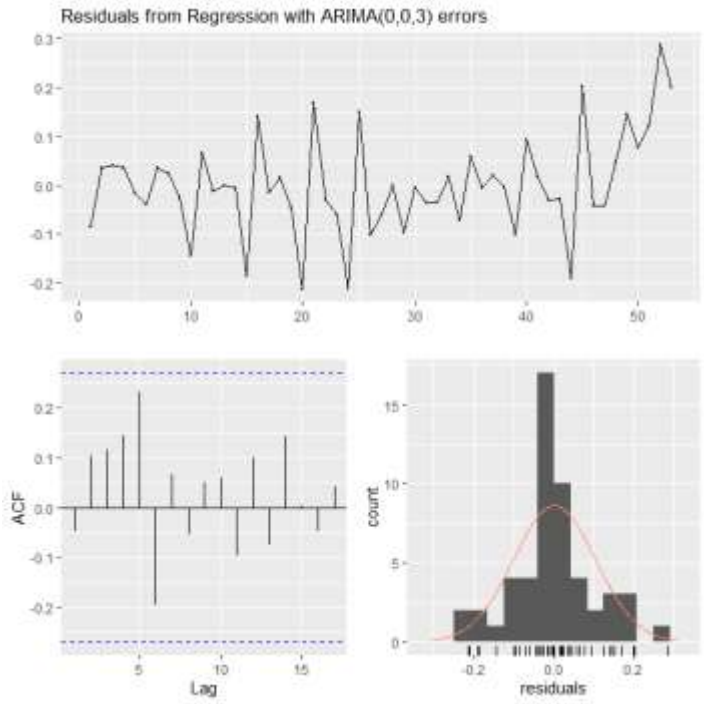


Figure 25. Residual diagnostic plots for the log-transformed monthly complete data model.

Note that, for untransformed data, trend estimates are the amount that the outcome of interest increase or decrease each year. Because the metric is log-transformed in this model, trend inference is interpreted as exponential growth. We back-transform the trend coefficient and use the standard error to construct a 95% confidence interval (CI). We estimate a mean annual increase of 5.34% (95% CI: 1.95%, 8.84%) in the median specific conductance metric at YUCH-004 since 2009.

```
> 100*(exp(c(0.0520, 0.0520-1.96*0.0167, 0.0520+1.96*0.0167))-1)
[1] 5.337574 1.945483 8.842533
```

Subsequent modeling obtains acceptable residuals for the truncated and seasonally adjusted truncated models, but not for the additive outliers model. The final model results for the daily and monthly data are provided in Appendix A.

We then proceed with the covariate modeling exercise using the monthly mean data. First, we check the missingness of covariates by year. We see that 80% of the measurements for four covariates are missing for 2019, so we omit this year for the covariate analysis. Examining the object *covPropMissing_month*, we see that other than the 2019 missingness, the monthly covariate means are complete for 2009-2018. Note that aggregating data in time can remove some of the missingness that occurs at the daily level. This is useful for metrics that do not vary much from day to day and are approximated well by means at coarser time intervals.

```
> ### check covariates for missing values
> covPropMissing_month <- plyr::ddply(monthDf, ~year, function(d, allCov) {
+   out <- NULL
+   for (p in allCov) {
+     out <- rbind(out, data.frame(covar = p, propMiss = sum(is.na(d[, p])) / nrow(d)))
+   } # end for p
+   return(out)
+ }, allCov = allCov)
>
>
> covPropMissing_month[which(covPropMissing_month$propMiss > cutoff), ]
   year            covar propMiss
51 2019          airTemp      0.8
52 2019        windSpeed      0.8
53 2019   solarRadiation      0.8
54 2019 relativeHumidity      0.8

> covarSelDf_month <- monthDf[monthDf$year < 2019,]
```

There is no missingness to impute in the monthly mean covariate values, but we run the imputation code nevertheless because the subsequent analysis code depends on those objects. The imputation code returns the original data sets, but under the new object names when imputation is not needed.

As with the daily data analysis, we first examine the linear model assuming no temporal correlation for the full suite of covariates. The Breusch-Godfrey test suggested temporal correlation exists in the residuals ($p = 0.0007$), and the autocorrelation function plot indicates significant autocorrelation to lag five (Figure 26).

```
> summary(fullModel_tslm_month)

Call:
forecast::tslm(formula = formula(paste0(responseVar, "~", paste0(allCov,
    collapse = "+"), "+year")), data = tsImpDf_month)

Residuals:
    Min      1Q  Median      3Q     Max
-27.890  -8.928   2.403   9.192  21.063

Coefficients:
                   Estimate Std. Error t value Pr(>|t|)
(Intercept)      -1.281e+04  1.770e+03  -7.235 7.70e-09 ***
airTemp          -3.159e-01  8.052e-01  -0.392    0.697
windSpeed        -2.106e+01  1.482e+01  -1.421    0.163
solarRadiation    2.422e-02  5.802e-02   0.417    0.679
relativeHumidity  3.798e-01  6.176e-01   0.615    0.542
dailyPrecip      -2.439e+01  6.873e+01  -0.355    0.724
year              6.432e+00  8.579e-01   7.498 3.29e-09 ***
---
Signif. codes:  0 '***' 0.001 '**' 0.01 '*' 0.05 '.' 0.1 ' ' 1

Residual standard error: 12.44 on 41 degrees of freedom
Multiple R-squared:  0.782,     Adjusted R-squared:  0.7501
F-statistic: 24.51 on 6 and 41 DF,  p-value: 4.166e-12
```

```
> checkresiduals(fullModel_tslm_month)

        Breusch-Godfrey test for serial correlation of order up to 10

data:  Residuals from Linear regression model
LM test = 30.72, df = 10, p-value = 0.0006526
```

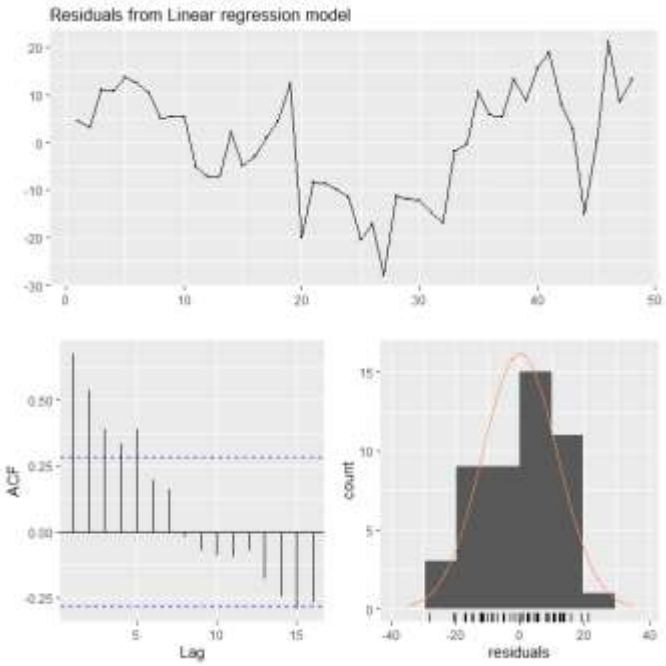


Figure 26. Residual diagnostic plots for the log-transformed monthly mean covariate model assuming independent errors.

We then apply the model for correlated time series with the *auto.arima* function for the full suite of covariates. The Ljung-Box test (p = 0.0014) and autocorrelation function plot provide evidence that temporal autocorrelation still exists in the residuals. We commence with the covariate model selection process to determine if a model with acceptable residuals can be identified for inference (Figure 27).

```
> # Fitting models with trend
> (fullModel_ARIMA_month <- forecast::auto.arima(
+   tsImpDf_month[, responseVar],
+   xreg = tsImpDf_month[, c(allCov, "year", "month")],
+   max.d = 0,
+   max.D = 0,
+   seasonal = FALSE
+ ))
Series: tsImpDf_month[, responseVar]
Regression with ARIMA(1,0,0) errors

Coefficients:
         ar1   intercept  airTemp  windSpeed  solarRadiation  relativeHumidity
      0.8837  -12473.557   1.1799    -2.8179         -0.1007           -0.1337
s.e.  0.0719    3669.247   0.4317     5.9796          0.0423            0.2750
      dailyPrecip    year   month
         -62.8722  6.2595  4.8288
s.e.      27.6526  1.8173  1.3520

sigma^2 estimated as 43.61:  log likelihood=-154.49
AIC=328.98   AICc=334.93   BIC=347.69

> checkresiduals(fullModel_ARIMA_month)

        Ljung-Box test

data:  Residuals from Regression with ARIMA(1,0,0) errors
Q* = 15.498, df = 3, p-value = 0.001437

Model df: 9.   Total lags used: 12
```

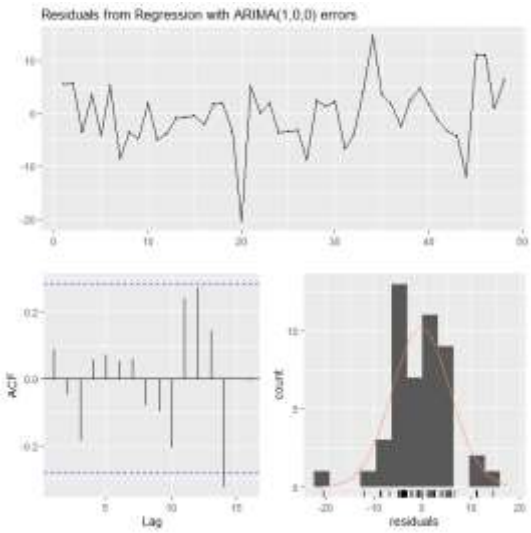


Figure 27. Residual diagnostic plots for the log-transformed monthly mean full covariate ARIMA model.

The next section of code creates the set of covariate models for evaluation, creating all combinations of available covariates and calculating the VIF to identify and omit models with highly correlated covariates. Run the model selection code, calculate the AICc and change in AICc, and then subset the models for which the Ljung-Box test with p-value ≥ 0.05. We then find that the model with the lowest AICc for which the Ljung-Box test indicates independent residuals contains fixed effects for the year and the month. Therefore, for specific conductance at YUCH-004, none of the environmental covariates explains the observed trend better than time.

```
> summaryModelSubset_month[modelSelected_month,-(3:4)]
          model nCovar     AICc LjungBoxPvalue deltaAICc
10 Year + Month      2 331.4538      0.2362344         0
```

We now evaluate the model fit. The Ljung-Box test and the autocorrelation plot provide evidence to assume that residuals may be treated as independent, and the residuals appear to be approximately normal with mean zero. There is some variance heterogeneity over time, which may increase standard errors of fixed effects estimates. However, we can use this model to make inference on trend in specific conductance, noting that mean specific conductance is estimated to increase by 7.5675 (SE = 1.2773) each year over the period 2009-2018 (Figure 28).

```
> summary(topModel_month)
Series: tsImpDf_month[, responseVar]
Regression with ARIMA(1,0,0) errors

Coefficients:
         ar1  intercept   wyear   month
      0.7864    31.4042  7.5675  6.1708
s.e.  0.0878    13.7889  1.2773  0.6143

sigma^2 estimated as 49.22:  log likelihood=-160.01
AIC=330.03   AICc=331.45   BIC=339.38

Training set error measures:
                     ME     RMSE      MAE        MPE     MAPE      MASE       ACF1
Training set -0.0950205 6.716853 5.038045 -0.2891713 3.726037 0.5885136 0.09799941
```

```
> chkResid_topModel_month <- checkresiduals(topModel_month)

        Ljung-Box test

data:  Residuals from Regression with ARIMA(1,0,0) errors
Q* = 8.0256, df = 6, p-value = 0.2362

Model df: 4.   Total lags used: 10
```

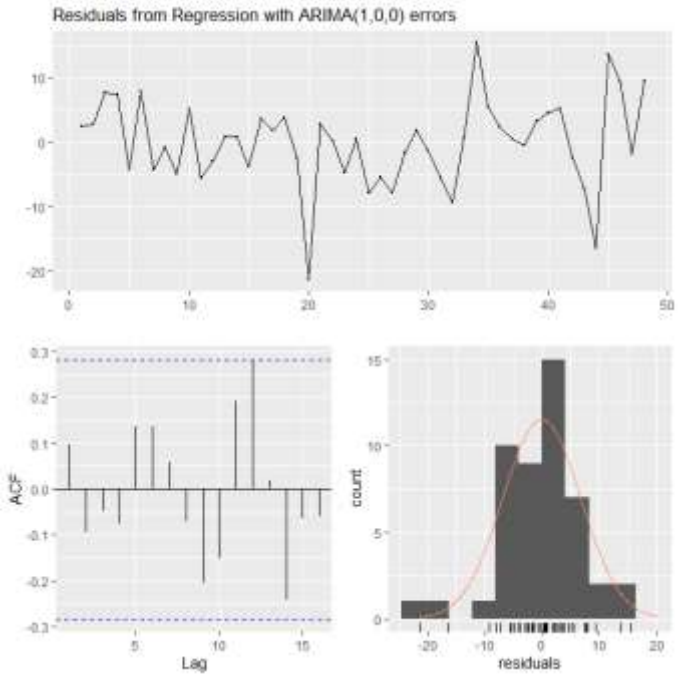


Figure 28. Residual diagnostic plots for the log-transformed monthly mean final covariate model assuming independent errors.

Noting the exponential trend pattern in the data and recalling that the best trend model for monthly means incorporated a log transform, we could also conduct the covariate model selection exercise for the logged outcome. The analysis script for specific conductance at YUCH-004 also contains the code for model selection of logged specific conductance. The model selection process selected the same model as for unlogged specific conductance, an ARIMA(1,0,0) model with fixed effects for year and month. The trend estimate from this model is interpreted as an annual percent change by back-transforming the point estimate of the year fixed effect as well as its 95% CI to obtain an estimated 5.39% change (95% CI: 3.81%, 6.99%) per year. This is very similar to the estimate from the trend model without the month term (5.34%; 95% CI: 1.95%, 8.84%), but the month fixed effect in the updated model improves precision of the trend estimate substantially.

```
> topModel_month_log
Series: log(tsImpDf_month[, responseVar])
Regression with ARIMA(1,0,0) errors

Coefficients:
         ar1  intercept   wyear   month
      0.7334     4.1511  0.0525  0.0449
s.e.  0.0946     0.0842  0.0077  0.0044

sigma^2 estimated as 0.002513:  log likelihood=77.27
AIC=-144.53   AICc=-143.11   BIC=-135.18

> 100*(exp(c(0.0525,0.0525-1.96*0.0077,0.0525+1.96*0.0077)) - 1)
[1] 5.390256 3.811649 6.992869
```

Discussion

Three primary goals were addressed in this report: (1) identify the best trend model for each outcome and lake, (2) identify the covariates that were most highly associated with the outcome at that lake, and (3) provide analysis tools in R for analyzing water chemistry data downloaded from Aquarius. ARCN/CAKN ecologists requested that daily outcome means be analyzed so that daily covariate data reflected fine-scale drivers of the outcomes over time. Because daily data were highly correlated in time, trend and covariate modeling was conducted with the *auto.arima* function in the **forecast** (Hyndman 2008, Hyndman et al. 2020) package. This modeling tool automates model selection of ARIMA structures to find the structure that best explains the autoregressive and moving average processes in the data. A limitation of this approach is that missing years of data cannot be accommodated, so the monitoring data used in the trend and covariate modeling exercises were truncated to the subset of recent consecutive years.

This initial exploratory data analysis demonstrated several trend and covariate modeling methods for the shallow lakes water chemistry monitoring data. Some modeling required truncating the data to a set of common days within each year or shortening the time series to accommodate the availability of covariate data. Inference of these results should take into consideration the sampling windows and monitoring periods used as these factors may reflect different target populations and affect trend inference. These results are preliminary and should not be used to make inference on lake condition.

The first goal was to identify the best trend model for each outcome and lake combination. The trend models reported in the results section were selected to reflect the simplest approach (i.e., least amount of truncation and/or data manipulation such as additive outlier modeling, transformations, and seasonal adjustments) for which model assumptions (independent and normally-distributed residuals) were met. The analysis of pH data was more frequently conducted with the complete data set, indicating that seasonal effects were relatively small for pH than for other outcomes. The truncated data and seasonally adjusted truncated approaches were selected in a majority of analyses and most frequently with the temperature outcomes. The additive outliers approach was selected in three cases (NOAT-107 dissolved oxygen, DENA-018 specific conductance, and BELA-108 temperature), but in only one of those cases (BELA-108 temperature) would either the truncated and seasonally adjusted truncated approaches not have also provided a valid trend model. Therefore, we do not anticipate that the additive outliers approach will be an effective modeling approach for this project. In almost every case, applying a logarithmic transformation did not improve model fit. Only when extreme exponential trend was observed (e.g., specific conductance at YUCH-004) was a log transformation effective in obtaining acceptable model residuals.

Nearly all of the significant water temperature trends (sonde, sediment, and thermistor chain) were positive, as were the trends in specific conductance. Significant trends in dissolved oxygen were always negative, and significant negative and positive trends in pH were observed among the 12 lakes. In some cases, trends from different models for the same outcome and lake differed considerably. Sometimes this was due to differences in the data sets used, such as comparing trend estimates from complete data to those from the truncated data set, which may reflect a different

inferential population. Sometimes trends of very different magnitudes were observed for the two models that employed the truncated data set. In these cases, attention to analysis details, examination of model assumptions, and additional plotting and modeling may provide clarity as to which trend estimate is more accurate. For example, if seasonal patterns are variable by year, then estimating and removing a single seasonal effect across all years, as is done in the seasonally adjusted truncated model, may introduce more error and obscure the trend signal. Because consecutive years were required for use with the *auto.arima* function in the **forecast** (Hyndman 2008, Hyndman et al. 2020) package and within-year data sometimes needed to be truncated to common dates across years, inference to lake condition from the obtained models is considered preliminary. This analysis will serve as a template for ARCN/CAKN personnel to apply their ecological expertise to determine how to organize the data to obtain unbiased inference on lake condition.

The second goal of this project was to identify covariates associated with each outcome, by lake. Because covariates were also summarized at the daily level, covariate models were obtained with the *auto.arima* function in the **forecast** (Hyndman 2008, Hyndman et al. 2020) package to account for correlation in the outcome over time. Final covariate models were generally obtained from the complete daily data set, with the exception of a few cases where the truncated, weekly, or monthly data sets were needed to obtain independent residuals. We do not anticipate that the covariate analysis is as impacted by truncation of years and days within years because we are looking for associations between the outcomes of interest and environmental covariates that should exist regardless of the time frames examined. However, if the association between outcomes and covariates is strongest at the beginning or end of a survey season, then the magnitude of the covariate effects may be muted by seasonal truncation. We might also expect that aggregating both outcomes and covariates to coarser time frames might reduce their observed association, especially for covariates that exhibit dramatic spikes that impact the outcome of interest at finer time scales.

The ability to use the complete data set for covariate modeling in most cases indicates that environmental covariates can be useful in explaining temporal correlation in daily data. However, when covariates exhibit similar trends as the outcome of interest, trends in the outcomes of interest may be entirely, or partially, explained by including the covariate in the trend model. Trend in the outcome may be associated with the change in the covariate over time, but causation cannot necessarily be inferred. In these cases, trend estimation for the outcome of interest would need to be conducted without covariates so that trend is accurately estimated over time. Note that in several cases, trend was estimated from the final covariate model because the final covariate model included a significant year effect despite the presence of environmental covariates. Aggregating to a coarser time period provides a method to reduce autocorrelation in the outcome without relying on associated covariates.

The third goal was to provide analysis tools in R for analyzing water chemistry data downloaded from Aquarius. We provided functions to aggregate data by day, week, month, or year for trend and covariates analyses in the **NPSH2OAK** R package (Studyvin et al. 2021). Furthermore, the analysis scripts used for each trend and covariate analysis were archived in the package for future use and modification.

We provide several recommendations on possible future work for this program. First, data truncation to the same set of calendar days each year at a lake may be ecologically arbitrary. Truncating to the same set of days that reflect the same seasonal characteristics (e.g., ice-free days, days since last freeze) may provide a subset of data with a more reasonable ecological interpretation for comparisons over time.

Second, many of the temperature metrics are highly correlated (Figure 7, Appendix B). If any of these metrics are excessively expensive or difficult to obtain, then monitoring a subset of these metrics may be sufficient for management needs. Sonde and sediment temperatures appear to be the least correlated among all temperature metrics, with positive correlation decreasing as a function of the difference in water depth for some lakes (Appendix B). Measuring temperature with the thermistor chain at the same depth each year improves the ability to use these metrics for trend analysis, and the high correlation among temperatures measured at different depths can be used to impute missing temperatures.

Finally, we consider the use of fine-scale data for large-scale trend inference. This analysis focused on daily data to match the grain of the covariate data available for modeling. Data aggregated at coarser time scales are not as highly correlated through time as daily data. Reducing the autocorrelation in data aggregated to coarser time scales provides additional modeling options such as generalized linear mixed models (GLMMs). GLMMs do not require consecutive survey years for trend estimation, which is a limitation of the analysis of daily data. GLMMs can accommodate simple autocorrelation structures and data from multiple lakes for trend inference at larger spatial scales. GLMMs can provide additional trend inference for comparison to trend estimates from *auto.arima* models of daily data. Then the full data set can be analyzed so that trends over the entire monitoring period can be estimated.

The extensive data sets collected for the ARCN/CAKN shallow lakes protocol provide a rich basis for a number of different analyses. Examining data at multiple temporal and spatial scales will provide inference on trends and covariate relationships at both more detailed and broader levels. Additional metrics may be developed from the outcomes of interest examined here (e.g., number of ice-free days, number of days with sediment temperature greater than a threshold, proportion of days with dissolved oxygen greater than a threshold) to determine shifts over time that are not identified in a standard trend or covariate analysis. We expect that fine-scale relationships between outcomes and covariates can be adequately modeled from daily data. Examining this wealth of data at multiple scales with multiple tools will provide a broad basis for management decisions and inference on ARCN/CAKN shallow lakes.

Literature Cited

Battaglia, F., D. Cucina, and M. Rizzo. 2019. Detection and estimation of additive outliers in seasonal time series. Computational Statistics, pp. 1-17.

Burnham, K. P. and D. R. Anderson. 2002. Model Selection and Multimodel Inference: A Practical Information-Theoretic Approach. Second Edition. Springer, New York, New York.

Chatfield, C., 2003. *The Analysis of Time Series: An Introduction*. Chapman and Hall: Washington, D.C.

Cryer, J.D. and Chan, K.S., 2008. *Time Series Analysis: With Applications in R*. Springer Science & Business Media.

Hyndman R., G. Athanasopoulos, C. Bergmeir, G. Caceres, L. Chhay, M. O'Hara-Wild, F. Petropoulos, S. Razbash, E. Wang, and F. Yasmeen. 2020. forecast: Forecasting functions for time series and linear models. R package version 8.12, Available at: http://pkg.robjhyndman.com/forecast

Hyndman, R.J. and Y. Khandakar. 2008. "Automatic time series forecasting: the forecast package for R." Journal of Statistical Software, 26 (3): 1-22. Available at: http://www.jstatsoft.org/article/view/v027i03

Junger, W. and A. Ponce de Leon. 2018. mtsdi: Multivariate Time Series Data Imputation. R package version 0.3.5. Available at: https://CRAN.R-project.org/package=mtsdi

Larsen, A., J. Houghton, J. Black, D. Verbyla, C. Ruedebusch, R. McGinnis, H. Kristenson. 2011. Shallow lake limnology monitoring protocol: Central Alaska Network (CAKN) and Arctic Network (ARCN), Version 2.0. Natural Resource Report NPS/AKRO/NRR—2011/347. National Park Service, Fort Collins, Colorado.

Moritz, S. and T. Bartz-Beielstein. 2017. imputeTS: time series missing value imputation in R. *The R Journal* 9(1): 207.

Neter, J., M.H. Kutner, C.J. Nachtsheim, and W. Wasserman. 1996. Applied Linear Statistical Models, 4th edition. McGraw-Hill.

R Core Team (2020). R: A language and environment for statistical computing. R Foundation for Statistical Computing, Vienna, Austria. Available at: https://www.R-project.org

Stevens, D. L., and A. R. Olsen. 2003. Variance estimation for spatially balanced samples of environmental resources. Environmetrics 14:594-610.

Stevens, D. L., and A. R. Olsen. 2004. Spatially balanced sampling of natural resources. Journal of the American Statistical Association 99(465):262-278.

Studyvin, J., D. Pham, L. McManus, and L.A. Starcevich. 2021. NPSH2OAK: National Parks Service Water Chemistry Data Manipulation. R package version 1.0.5.

Yaffee, R.A. and M. McGee, 2000. An Introduction to Time Series Analysis and Forecasting: with Applications of SAS® and SPSS®. Elsevier.

Zuur, A., Ieno, E.N. and Smith, G.M., 2007. *Analyzing Ecological Data*. Springer, New York, New York.

Appendix A: Trend Analysis Results by Outcome and Lake

Dissolved Oxygen

BELA-088

Data

For BELA-088, dissolved oxygen was recorded from 2012 through 2019. However, no data were recorded in 2013, so the analysis included data from 2014-2019. Over this period, 543 records were collected between June and September, with 72 days represented in all years. Truncated to the common set of days per year, the dataset contained 432 observations.

Model Selection

Stationary residuals were obtained only for the truncated seasonally adjusted model for both the unlogged and logged dissolved oxygen metrics. Trend estimates were positive, but with large standard errors indicating the trend was not significantly different from zero. For ARIMA models fitting all possible covariate combinations at lake BELA-088, AICc-based model selection yielded a final model with an ARIMA(2,0,0) structure and fixed effects for relative humidity and month. Dissolved oxygen decreases as relative humidity increases, but increases over the course of the summer. Residual diagnostics indicate one large outlier, but no substantial autocorrelation.

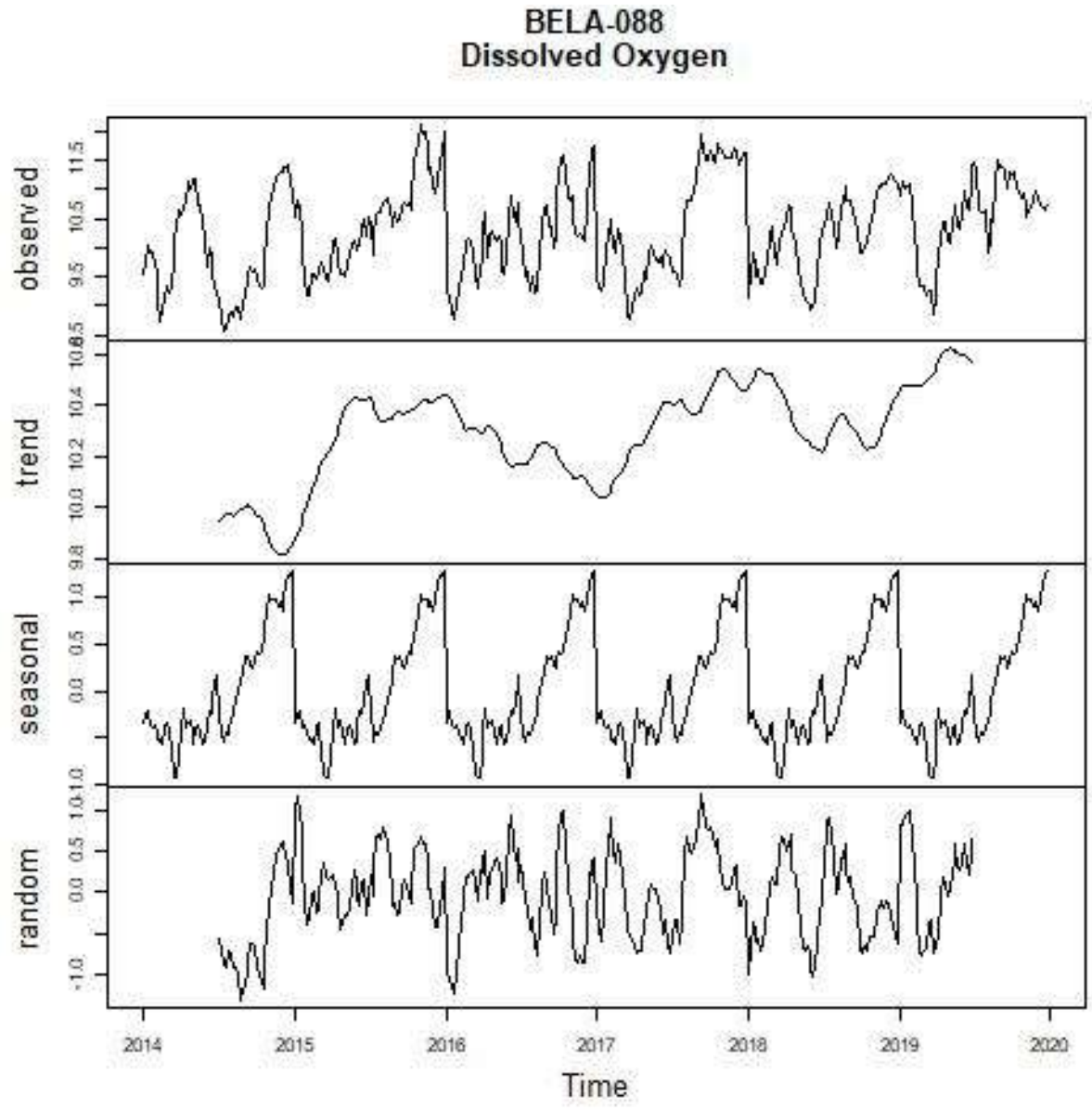


Figure A.1. Time series decomposition of truncated BELA-088 by year.

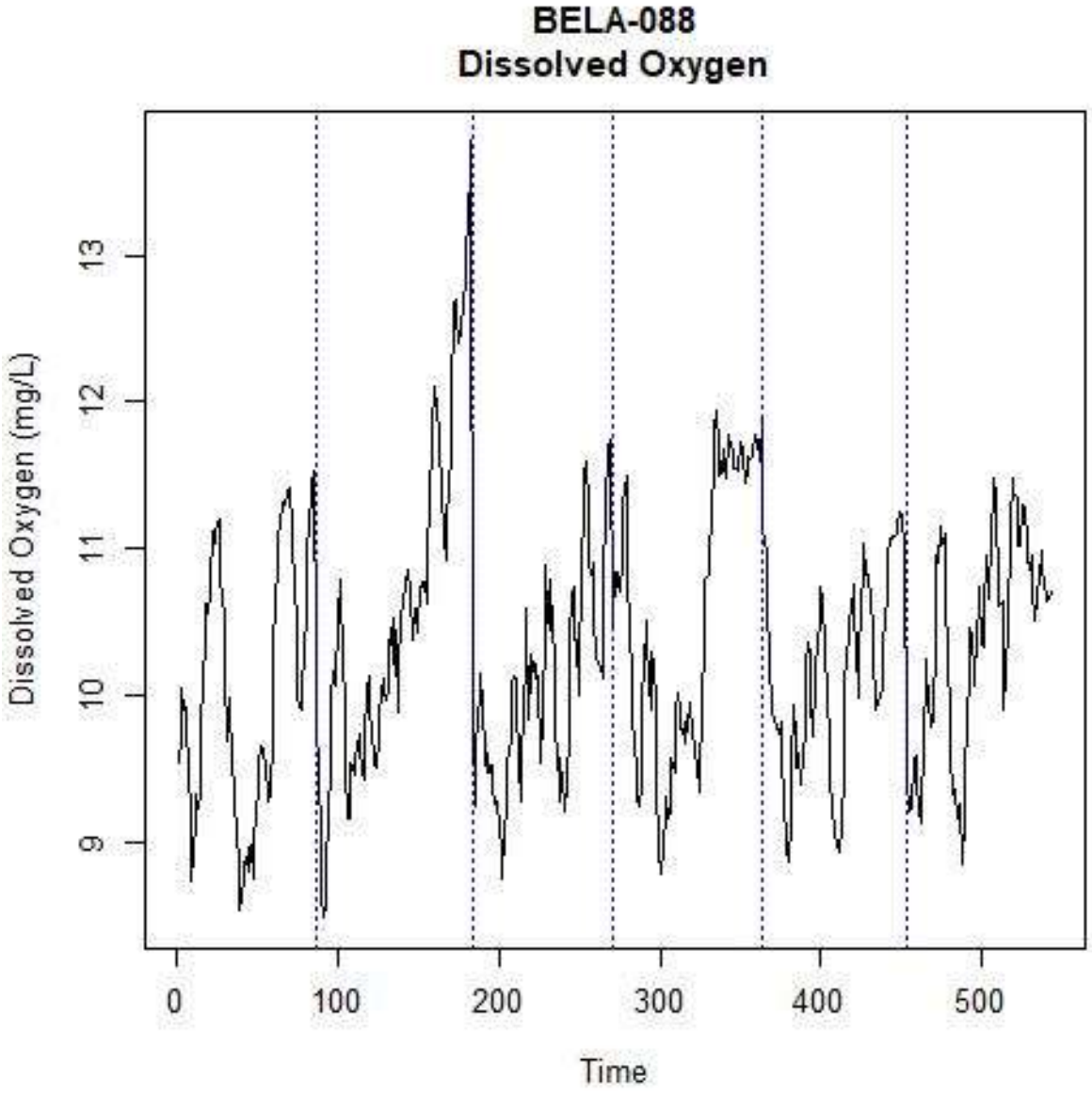


Figure A.2. Time series of BELA-088 dissolved oxygen by time point with vertical lines for additive outliers.

Table A.1. Trend modeling results for daily dissolved oxygen data at BELA-088.

			Trend			ARMA order		Ljung-Box Test	
Logged	**Method**	**Intercept**	**Coefficient**	**SE**	**p-value**	**AR**	**MA**	**Statistic**	**p-value**
FALSE	complete	11.8051	-0.1300	0.0449	0.0038	0	5	125.20	< 0.0001
FALSE	completeAO	10.7435	-0.0372	0.0422	0.3774	0	5	123.28	< 0.0001
FALSE	trunc	10.0867	0.0169	0.0430	0.6947	0	4	180.59	< 0.0001
FALSE	truncSA	9.6725	0.0520	0.0543	0.3379	1	1	77.44	0.6221
TRUE	complete	2.3755	-0.0040	0.0031	0.2020	0	3	392.98	< 0.0001
TRUE	completeAO	2.3611	-0.0027	0.0040	0.5012	0	5	118.34	< 0.0001
TRUE	trunc	2.2360	0.0080	0.0026	0.0025	0	1	1102.10	< 0.0001
TRUE	truncSA	2.2656	0.0053	0.0053	0.3213	1	1	79.28	0.5647

Table A.2. Top covariate models for daily dissolved oxygen data at BELA-088.

Model	**AICc**	**ΔAICc**	**Ljung-Box Test p-value**
Relative Humidity + Month	48.99	0.00	0.5293
Year + Month	56.77	7.78	0.0813
Daily Precipitation + Month	59.26	10.27	0.5330
Relative Humidity + Year + Month	103.09	54.10	0.3004
Air Temperature + Daily Precipitation	186.97	137.99	0.4096
Relative Humidity	188.83	139.84	0.8884
Air Temperature	194.87	145.88	0.5691
Daily Precipitation	195.08	146.09	0.6279
Intercept Only	199.98	150.99	0.7671

Table A.3. Coefficients and variance components estimates for the top covariate model for daily dissolved oxygen data at BELA-088.

Parameter	**Coefficient**	**SE**	**p-value**
ar1	1.30	0.04	< 0.0001
ar2	-0.39	0.04	< 0.0001
intercept	7.38	0.30	< 0.0001
Relative Humidity	-0.01	0.00	< 0.0001

Parameter	Coefficient	SE	p-value
Month	0.44	0.03	<0.0001

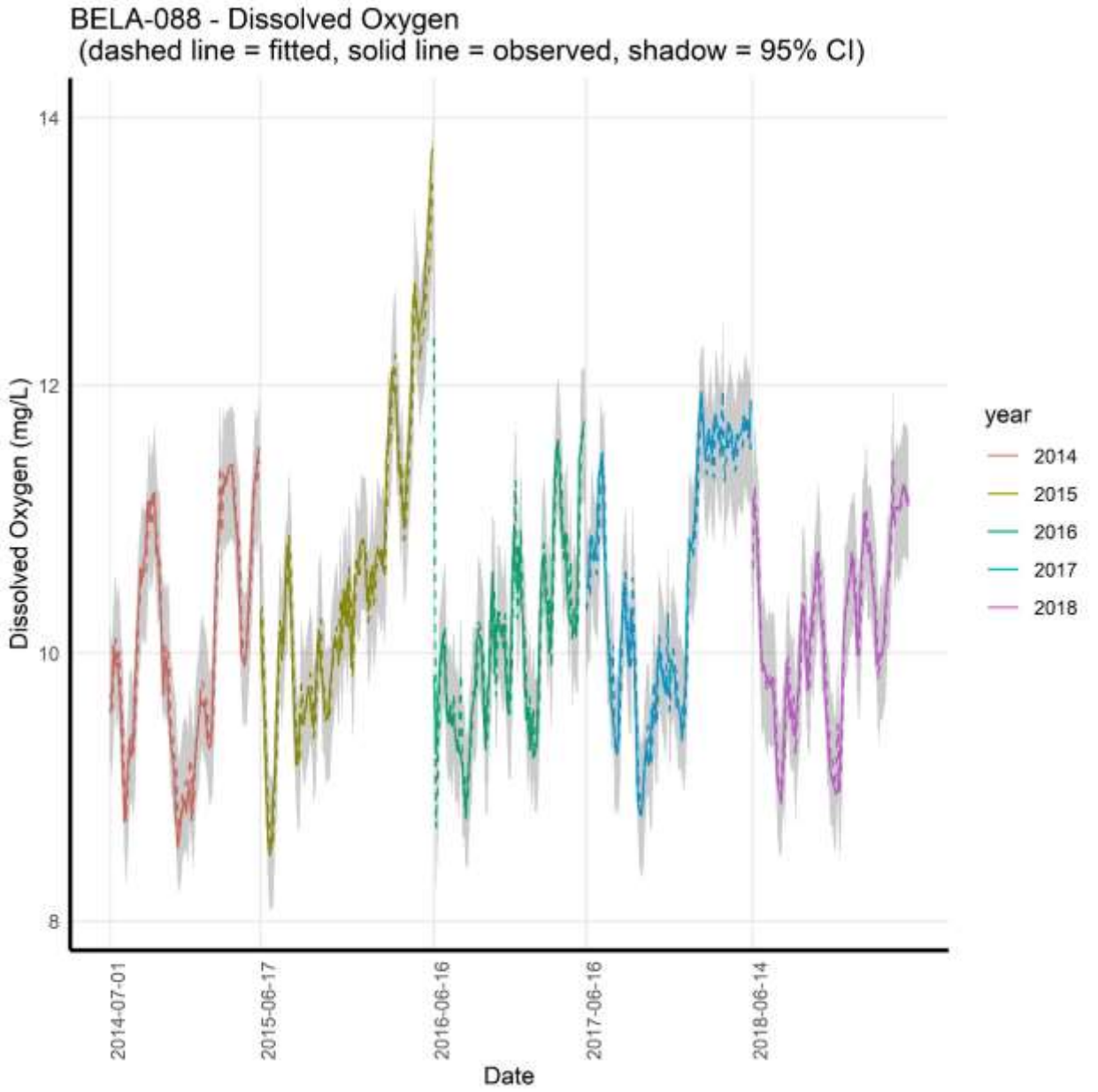


Figure A.3. Model predictions of BELA-088 dissolved oxygen by date.

BELA-108

Data

For BELA-108, dissolved oxygen was recorded from 2015 through 2019. Over this period, 456 records were collected from June to September. When truncating the data set to the subset of 86 days visited every year, the dataset had 430 observations. Covariate coverage was poor in 2019, so covariate models only considered 2013-2018, but wind speed and solar radiation were omitted from the model selection process due to missingness in 2018. This left 365 records for covariate modeling.

Model Selection

The truncated and seasonally adjusted truncated models for unlogged and logged dissolved oxygen yielded stationary residuals. Dissolved oxygen was estimated to decline over the course of the monitoring period. For ARIMA models fitting all possible covariate combinations at lake BELA-108, AICc-based model selection resulted in a model with ARIMA(2,0,0) structure and fixed effects for daily precipitation and month. Dissolved oxygen decreased as daily precipitation increased, but was estimated to increase between June and September.

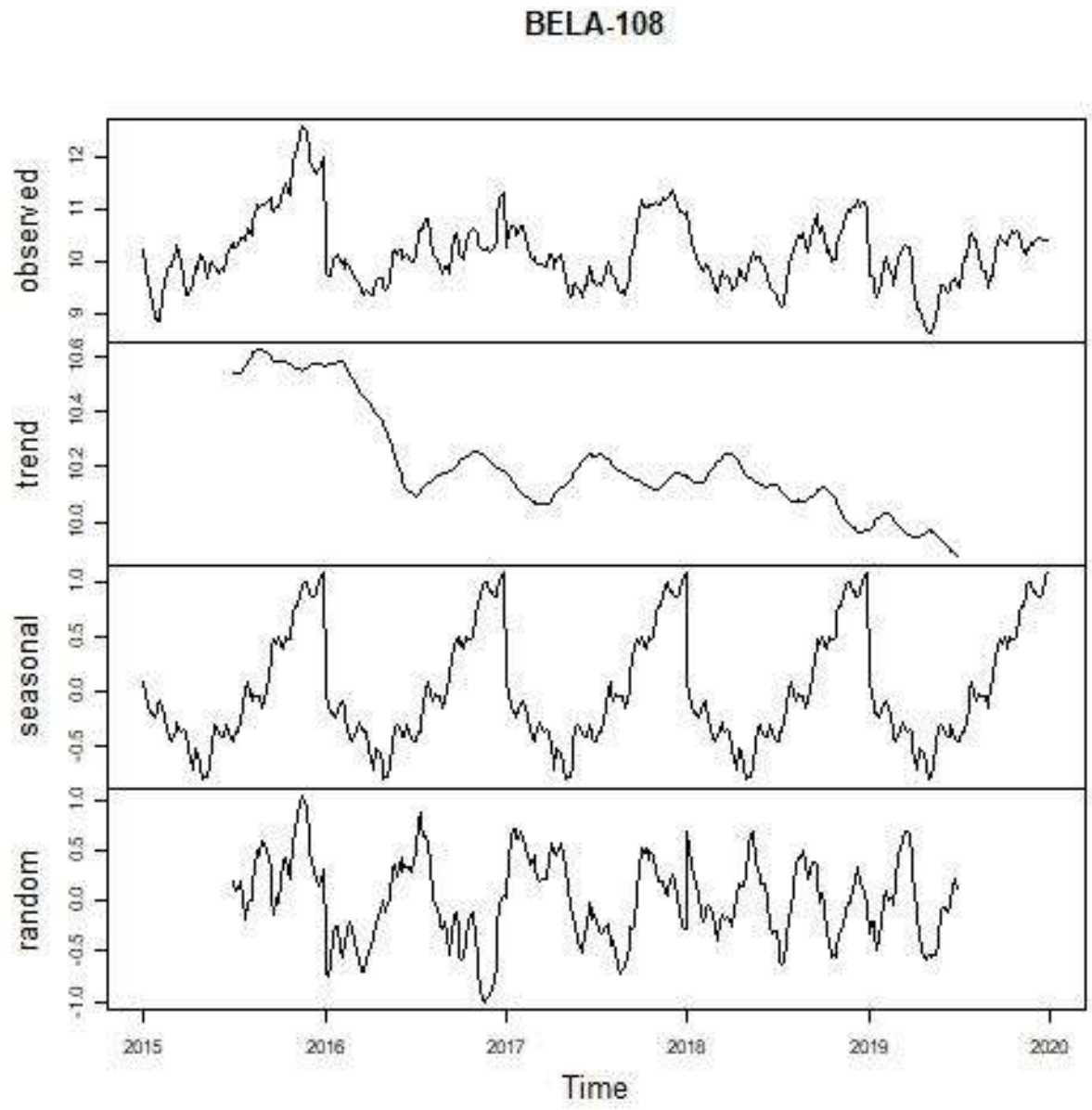


Figure A.4. Time series decomposition of truncated BELA-108 by year.

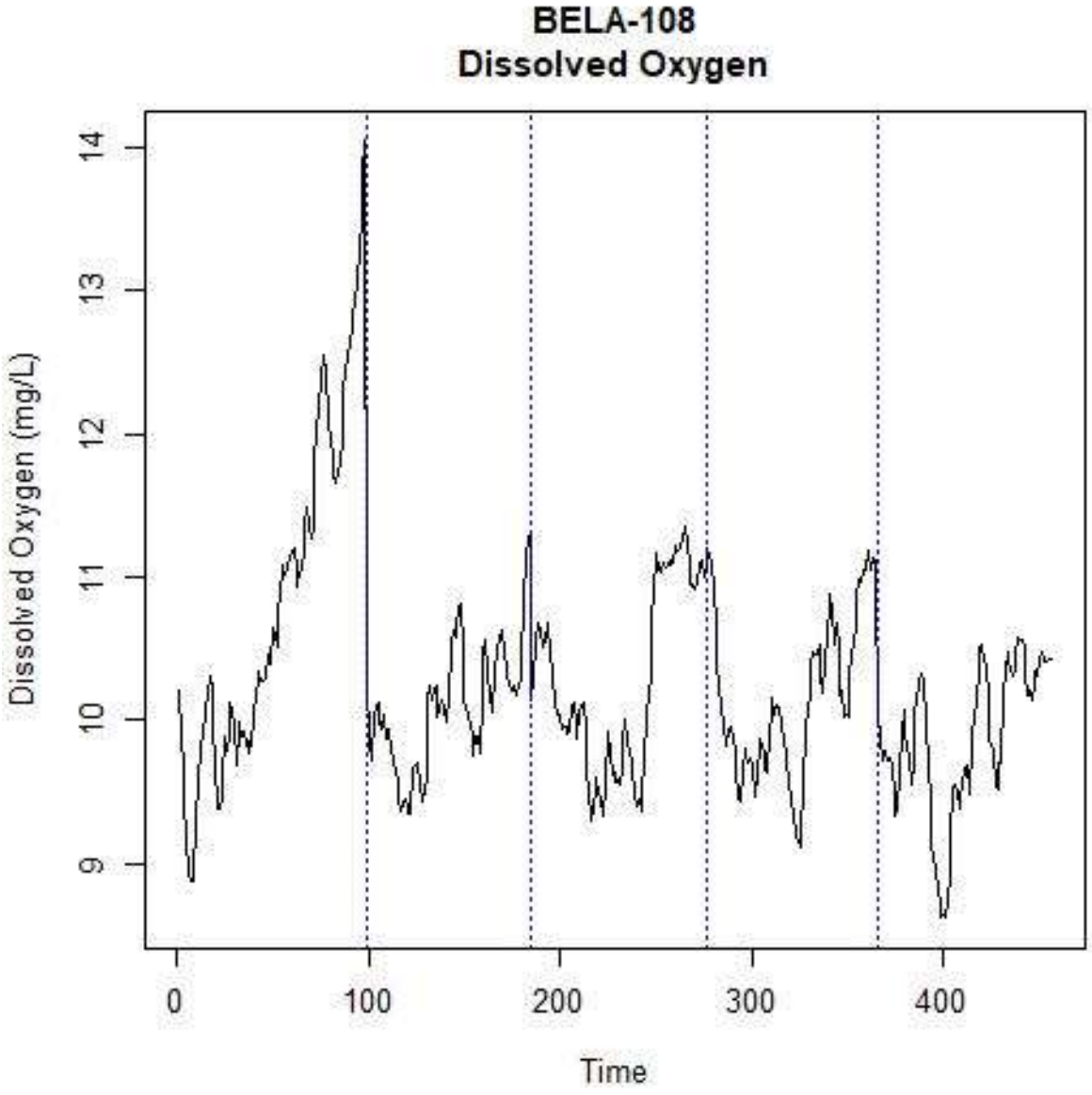


Figure A.5. Time series of BELA-108 dissolved oxygen by time point with vertical lines for additive outliers.

Table A.4. Trend modeling results for daily dissolved oxygen data at BELA-108.

			Trend			ARMA order		Ljung-Box Test	
Logged	**Method**	**Intercept**	**Coefficient**	**SE**	**p-value**	**AR**	**MA**	**Statistic**	**p-value**
FALSE	complete	13.8659	-0.3007	0.0405	< 0.0001	0	4	284.29	< 0.0001
FALSE	completeAO	13.3739	-0.2592	0.0431	< 0.0001	0	5	225.76	< 0.0001
FALSE	trunc	19.3994	-0.7223	0.0719	< 0.0001	2	1	89.45	0.1977
FALSE	truncSA	11.2849	-0.0927	0.0394	0.0187	2	2	69.15	0.8013
TRUE	complete	3.7882	-0.1199	0.0087	< 0.0001	2	0	15.45	0.0170
TRUE	completeAO	2.5394	-0.0178	0.0025	< 0.0001	0	1	1,791.75	< 0.0001
TRUE	trunc	3.4246	-0.0906	0.0076	< 0.0001	1	1	87.69	0.2864
TRUE	truncSA	2.4264	-0.0091	0.0037	0.0142	2	2	69.71	0.7876

Table A.5. Top covariate models for daily dissolved oxygen data at BELA-108.

Model	**AICc**	**ΔAICc**	**Ljung-Box Test p-value**
DailyPrecip+month	-80.30	0.00	0.5832
RelativeHumidity+month	-70.02	10.28	0.8650
AirTemp+DailyPrecip	9.72	90.01	0.1740
AirTemp	17.02	97.32	0.2850
DailyPrecip	25.48	105.77	0.6713
Intercept only	29.34	109.64	0.7893
RelativeHumidity	29.73	110.02	0.8196

Table A.6. Coefficients and variance components estimates for the top covariate model for daily dissolved oxygen data at BELA-108.

Parameter	**Coefficient**	**SE**	**p-value**
ar1	1.19	0.05	< 0.0001
ar2	-0.26	0.05	< 0.0001
intercept	7.54	0.30	< 0.0001
Daily Precipitation	-0.20	0.05	0.0002
Month	0.38	0.03	< 0.0001

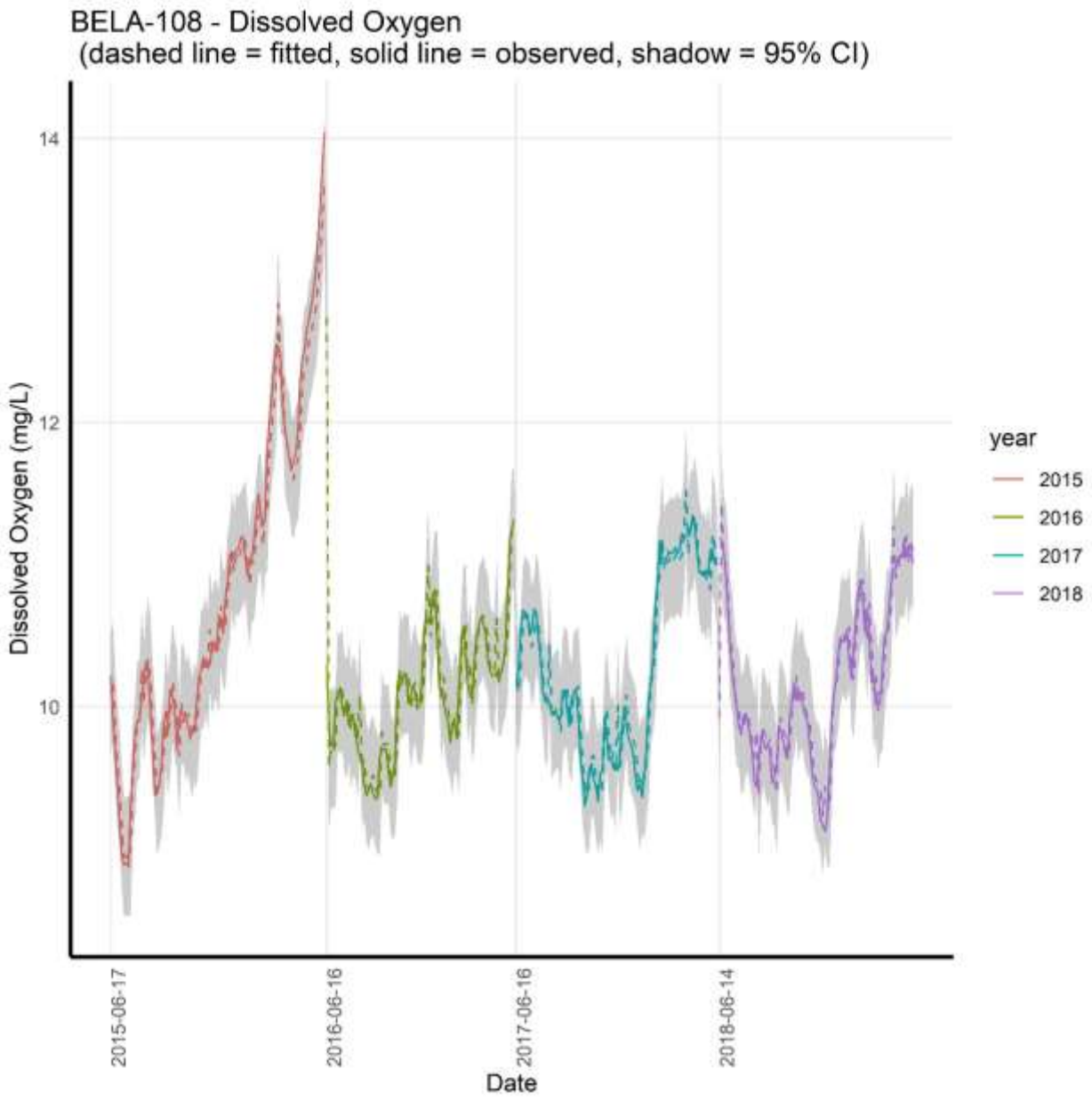


Figure A.6. Model predictions of BELA-108 dissolved oxygen by date.

DENA-018

Data

For DENA-018, dissolved oxygen was recorded from 2009 through 2019. However, no data were collected in 2013, so this analysis includes the monitoring period from 2014 through 2019. Over this period, 668 records were collected between May and September. When truncating the data set to the subset of 81 days visited every year, the dataset was reduced to 486 observations. Covariate data were complete for the 2014-2019 period, so no covariates or years of data were omitted from the model selection process.

Model Selection

The truncated and seasonally adjusted truncated models for unlogged and logged dissolved oxygen yielded stationary residuals. Estimated trends in dissolved oxygen were positive over the course of the monitoring period, but standard errors were relatively large indicating trends were not significantly different from zero. For ARIMA models fitting all possible covariate combinations at lake DENA-018, AICc-based model selection resulted in a model with ARIMA(1,0,1) structure and a fixed effect for solar radiation that indicated a positive association with dissolved oxygen.

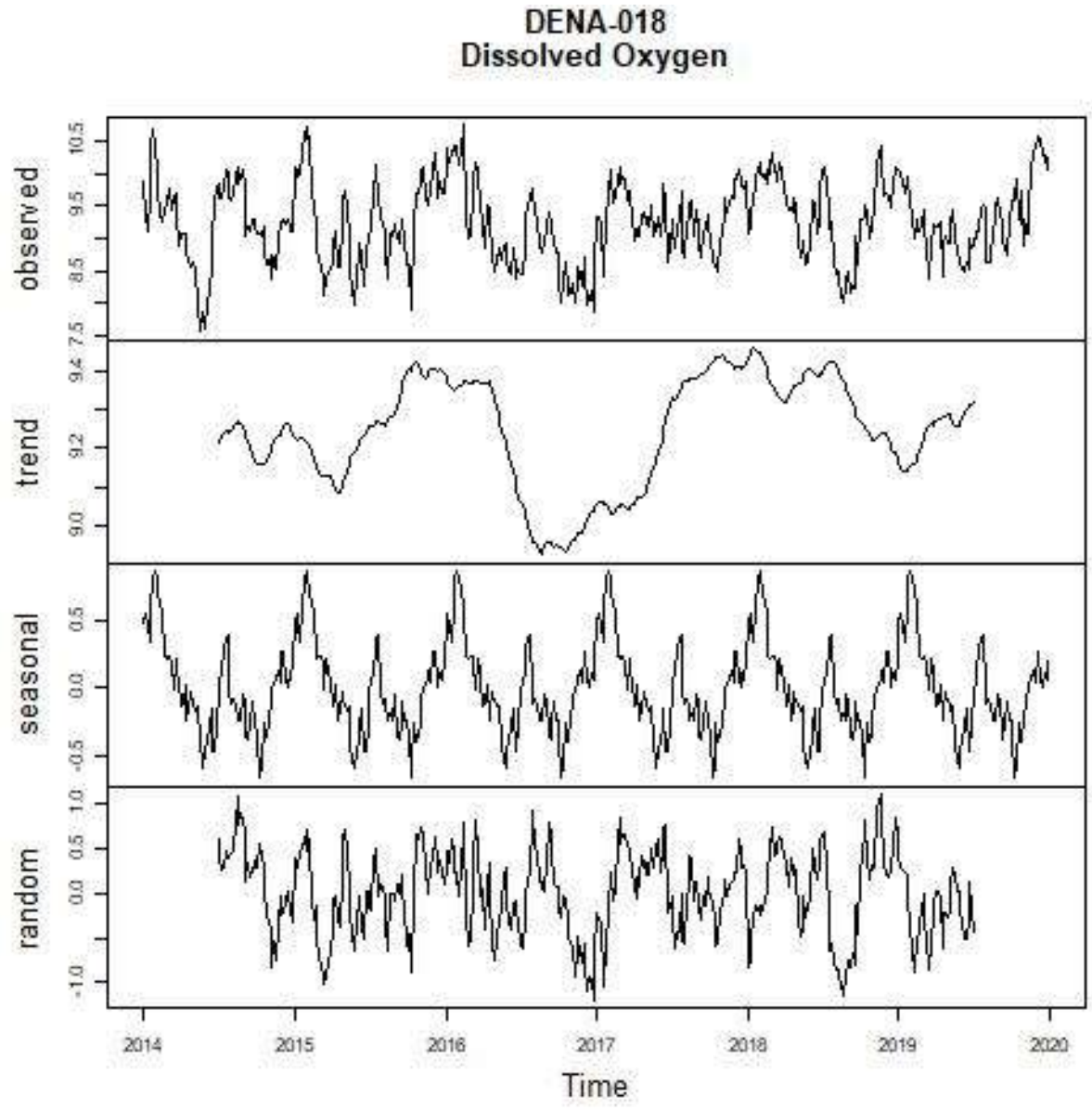


Figure A.7. Time series decomposition of truncated DENA-018 dissolved oxygen by year.

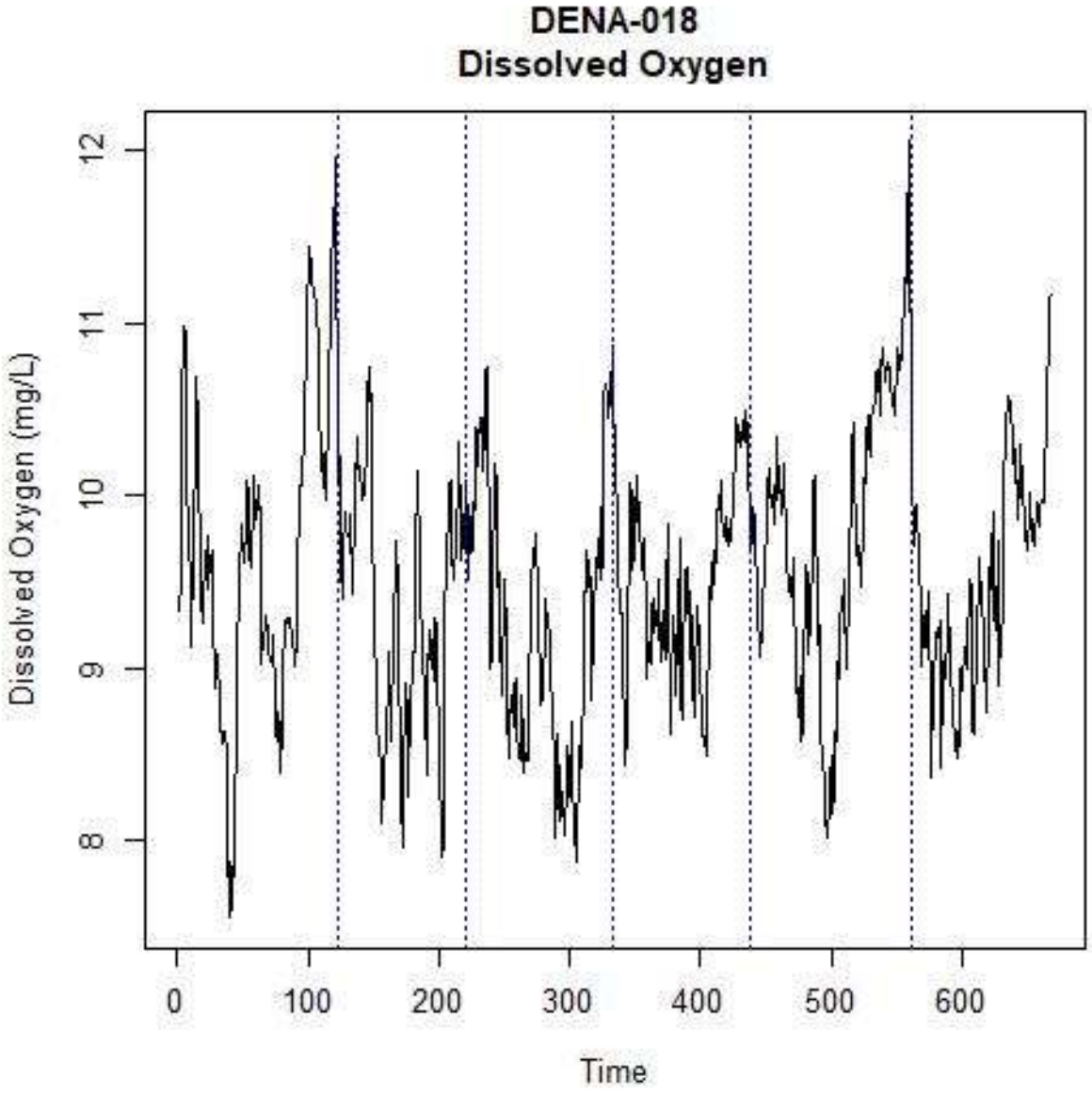


Figure A.8. Time series of DENA-018 dissolved oxygen by time point with vertical lines for additive outliers.

Table A.7. Trend modeling results for daily dissolved oxygen data at DENA-018.

			Trend			ARMA order		Ljung-Box Test	
Logged	Method	Intercept	Coefficient	SE	p-value	AR	MA	Statistic	p-value
FALSE	complete	18.6705	-0.6208	0.1765	0.0004	1	3	13.68	0.0084
FALSE	completeAO	10.5072	-0.0665	0.0791	0.4007	1	1	11.00	0.0117
FALSE	trunc	8.3985	0.0607	0.0514	0.2372	1	1	94.78	0.4292
FALSE	truncSA	8.7943	0.0328	0.0376	0.3823	2	0	108.40	0.1313
TRUE	complete	2.4649	-0.0147	0.0100	0.1421	1	1	12.41	0.0534
TRUE	completeAO	2.3226	-0.0048	0.0078	0.5366	1	1	11.53	0.0092
TRUE	trunc	2.1297	0.0066	0.0056	0.2354	1	1	95.01	0.4225
TRUE	truncSA	2.1706	0.0037	0.0041	0.3686	2	0	108.86	0.1249

Table A.8. Top covariate models for daily dissolved oxygen data at DENA-018.

Model	AICc	ΔAICc	Ljung-Box Test p-value
Solar Radiation	214.84	0.00	0.1571
Solar Radiation + Daily Precipitation	214.87	0.03	0.0885
Relative Humidity	218.51	3.67	0.1095
Wind Speed + Relative Humidity	220.21	5.37	0.0579
Daily Precipitation	283.25	68.41	0.0930
Air Temperature	290.12	75.28	0.0785
Intercept Only	296.89	82.05	0.1273
Wind Speed	297.18	82.34	0.0687

Table A.9. Coefficients and variance components estimates for the top covariate model for daily dissolved oxygen data at DENA-018.

Parameter	Coefficient	SE	p-value
ar1	0.91	0.02	< 0.0001
ma1	0.16	0.04	0.0002
intercept	9.31	0.14	< 0.0001
Solar Radiation	0.00	0.00	< 0.0001

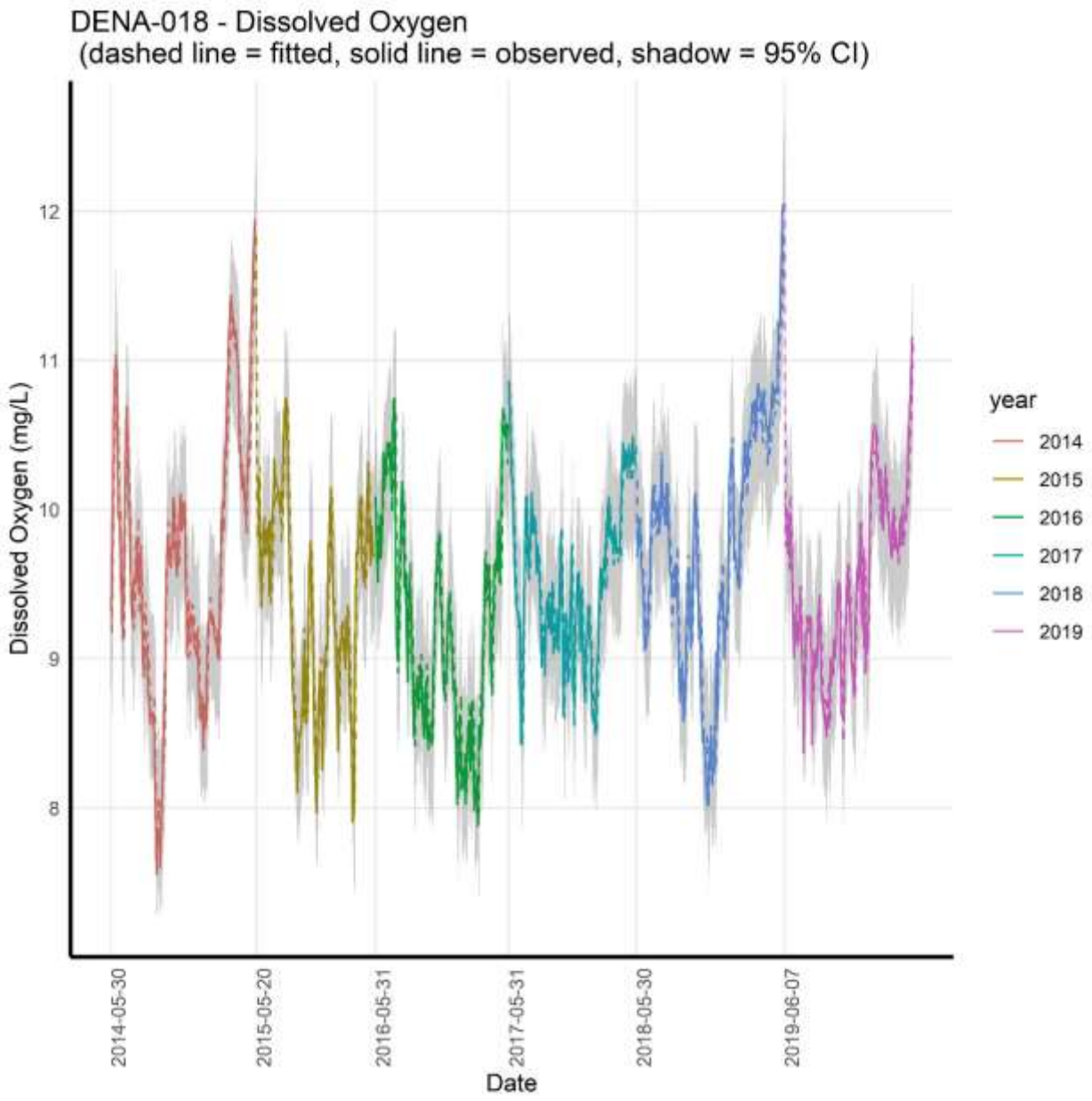


Figure A.9. Model predictions of DENA-018 dissolved oxygen by date.

DENA-023

Data

For DENA-023, dissolved oxygen was recorded from 2011-2019 and data were present for all years during this period. In total, there were 1000 records collected between May and October for this period. When truncating the data to the subset of 44 days visited in every year, the dataset was reduced to 405 observations. Data for covariates and response data were sufficiently complete that none of the covariates nor model years were omitted from the model selection process.

Model Selection

The truncated and seasonally adjusted truncated models for unlogged and logged dissolved oxygen yielded stationary residuals. Estimates for trend coefficients were negative with small standard errors and p-values < 0.0001, providing evidence for a negative trend in dissolved oxygen at DENA-023 from 2011-2019. For ARIMA models fitting all possible combinations of covariates, only one model yielded stationary residuals. This model had an ARIMA(1,0,3) structure and relative humidity as a fixed effect. Dissolved oxygen was negatively related to relative humidity, though the model tended to over-predict dissolved oxygen at low values of relative humidity.

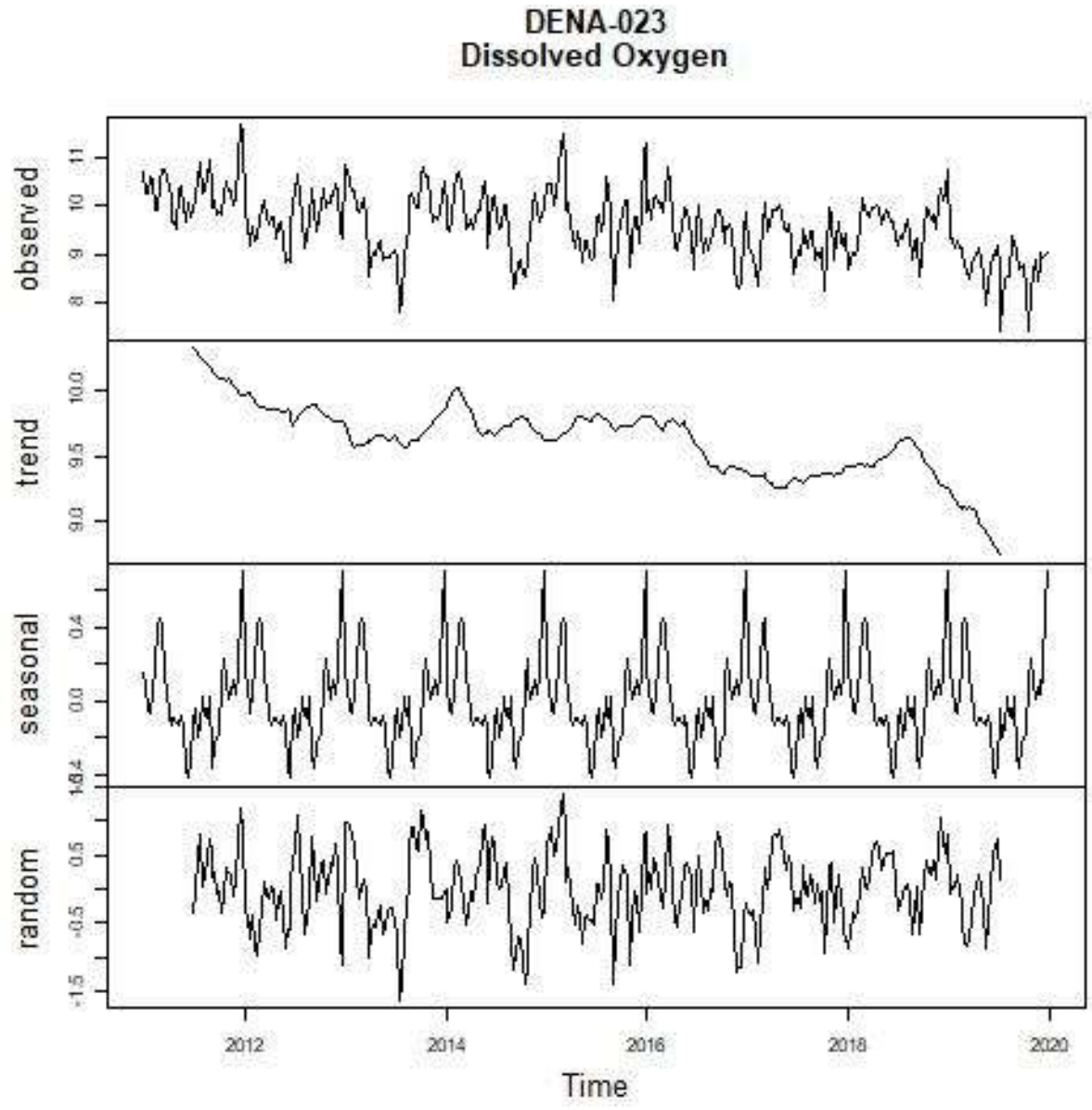


Figure A.10. Time series decomposition of truncated DENA-023 dissolved oxygen by year.

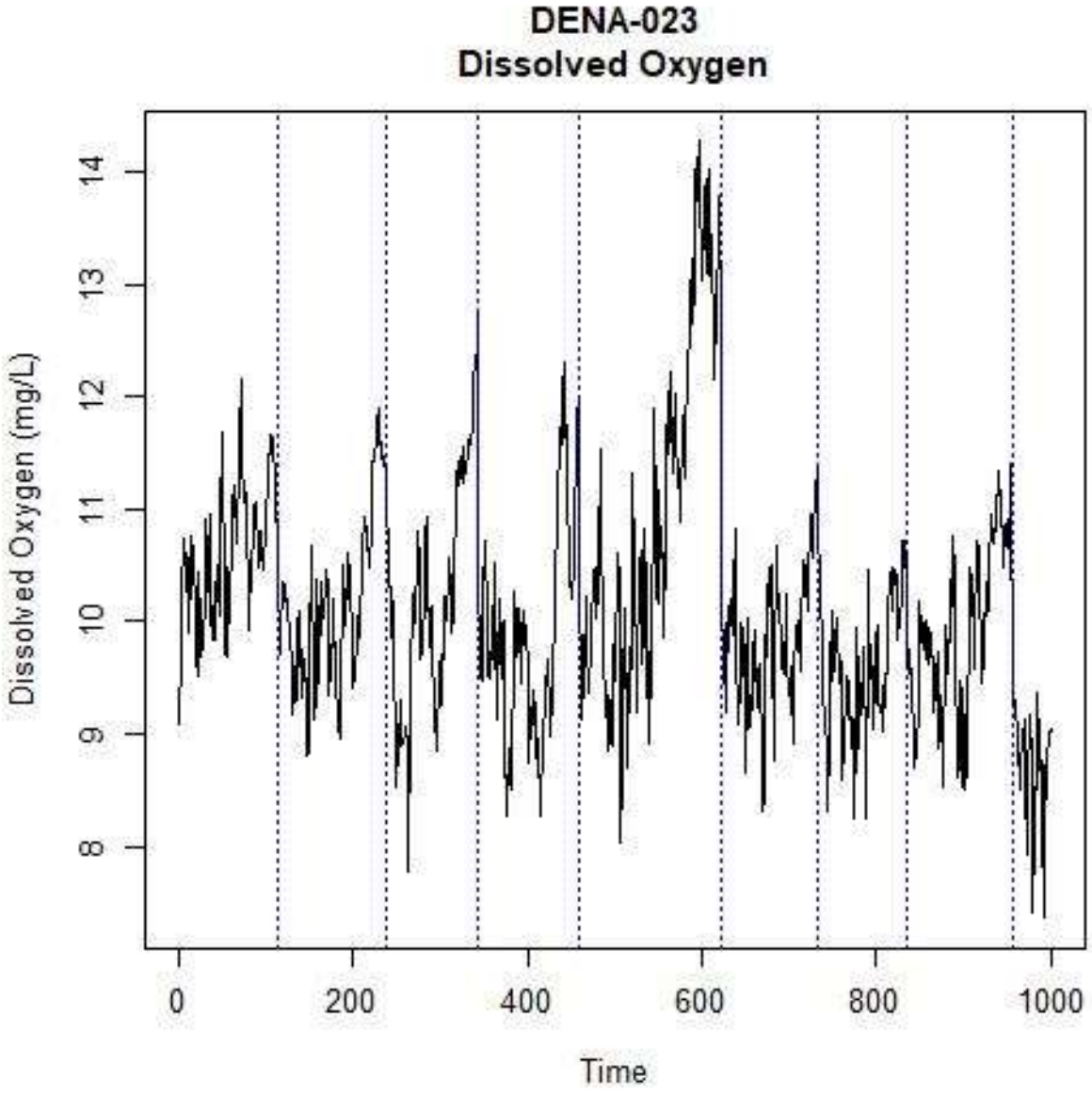


Figure A.11. Time series of DENA-023 dissolved oxygen by time point with vertical lines for additive outliers.

Table A.10. Trend modeling results for daily dissolved oxygen data at DENA-023.

			Trend			ARMA order		Ljung-Box Test	
Logged	**Method**	**Intercept**	**Coefficient**	**SE**	**p-value**	**AR**	**MA**	**Statistic**	**p-value**
FALSE	complete	11.7690	-0.1283	0.0176	< 0.0001	0	2	1,514.25	< 0.0001
FALSE	completeAO	13.2438	-0.2455	0.0795	0.0020	2	1	40.07	< 0.0001
FALSE	trunc	11.3810	-0.1364	0.0239	< 0.0001	2	2	83.30	0.2394
FALSE	truncSA	11.2222	-0.1245	0.0229	< 0.0001	1	1	84.89	0.2519
TRUE	complete	3.8225	-0.1174	0.0149	< 0.0001	1	1	68.43	< 0.0001
TRUE	completeAO	2.6266	-0.0250	0.0086	0.0037	3	0	32.12	< 0.0001
TRUE	trunc	2.4455	-0.0143	0.0027	< 0.0001	1	1	81.68	0.3362
TRUE	truncSA	2.4288	-0.0130	0.0026	< 0.0001	3	0	78.16	0.4099

Table A.11. Top covariate models for daily dissolved oxygen data at DENA-023.

Model	**AICc**	**ΔAICc**	**Ljung-Box Test p-value**
Relative Humidity	812.5	0	0.1506

Table A.12. Coefficients and variance components estimates for the top covariate model for daily dissolved oxygen data at DENA-023.

Parameter	**Coefficient**	**SE**	**p-value**
ar1	0.95	0.01	< 0.0001
ma1	0.10	0.03	0.0028
ma2	-0.09	0.04	0.0116
ma3	-0.12	0.04	0.0011
intercept	10.82	0.22	< 0.0001
Relative Humidity	-0.01	0.00	< 0.0001

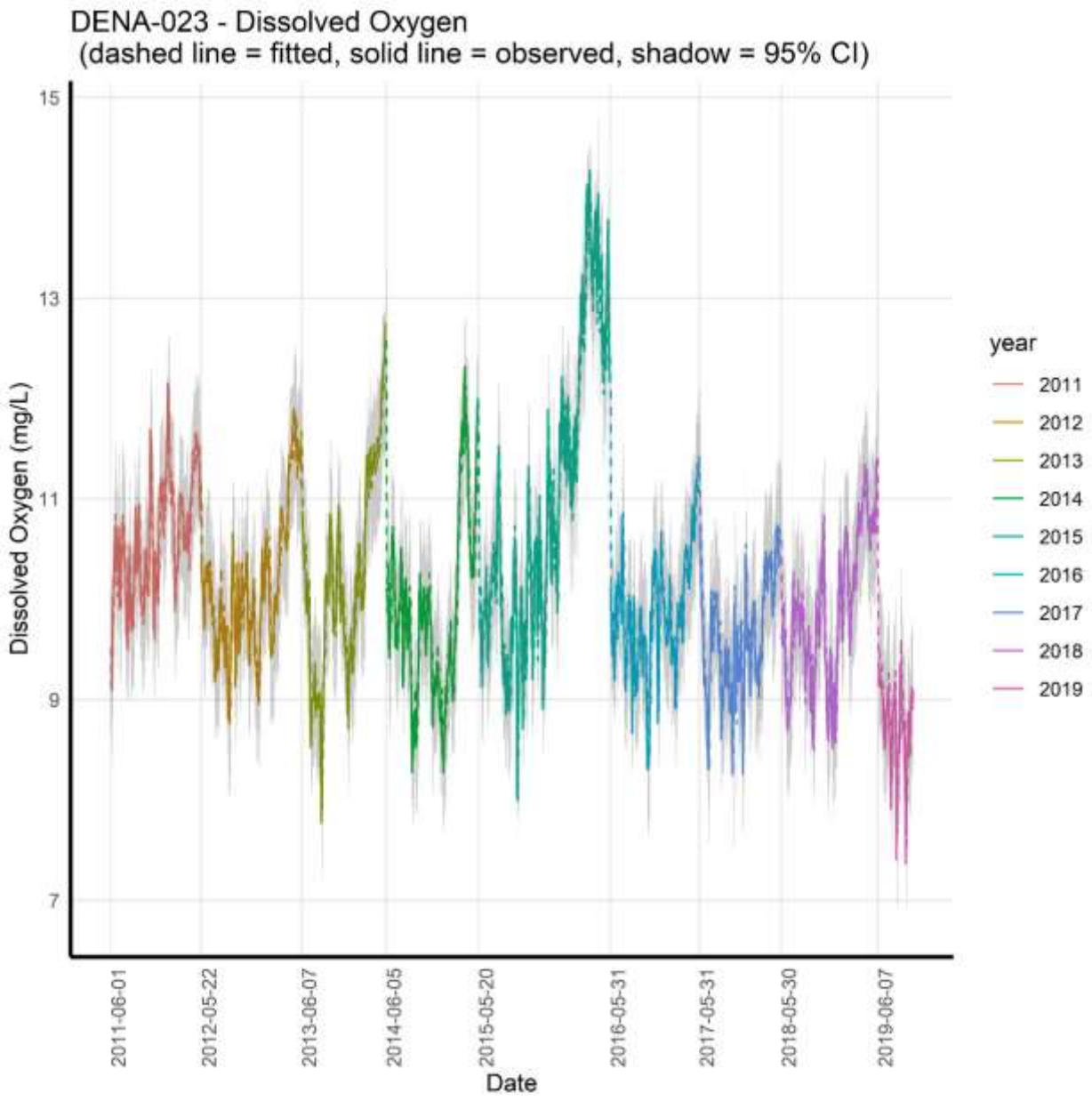


Figure A.12. Model predictions of DENA-023 dissolved oxygen by date.

KOVA-085

Data

For KOVA-085, dissolved oxygen was recorded from 2010-2018 and data were present for all years during this period. In total, there were 801 records collected between June and September for this period. When truncating the data to the subset of 45 days visited in every year, the dataset was reduced to 594 observations. Data for covariates and response data were sufficiently complete that none of the covariates nor model years were omitted from the model selection process.

Model Selection

The truncated and seasonally adjusted truncated models for unlogged and logged dissolved oxygen yielded stationary residuals. The residual distribution appeared normal for the seasonally adjusted truncated models, but the distribution was skewed negatively for the truncated-only models. The truncated model with unlogged data including a negative trend coefficient ($p = 0.391$), but none of the other three models with stationary residuals had trend coefficients that were significantly different from zero. Overall, there is little evidence for a decreasing trend in dissolved oxygen at KOVA-085. None of the ARIMA models fitting all possible combinations of covariates yielded stationary residuals when fit with daily data, so the truncated data set was used for covariate model selection.

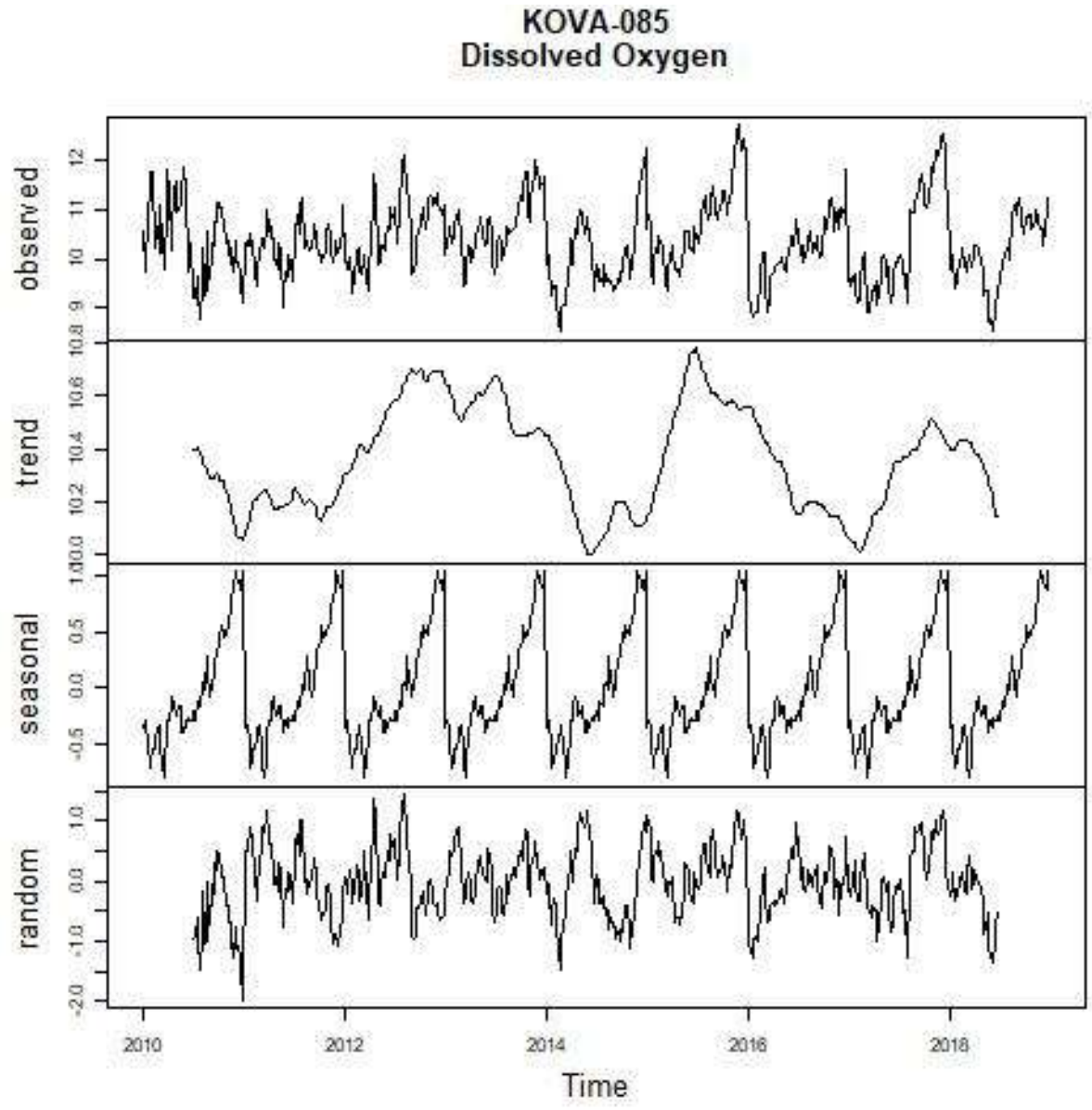


Figure A.13. Time series decomposition of truncated KOVA-085 dissolved oxygen by year.

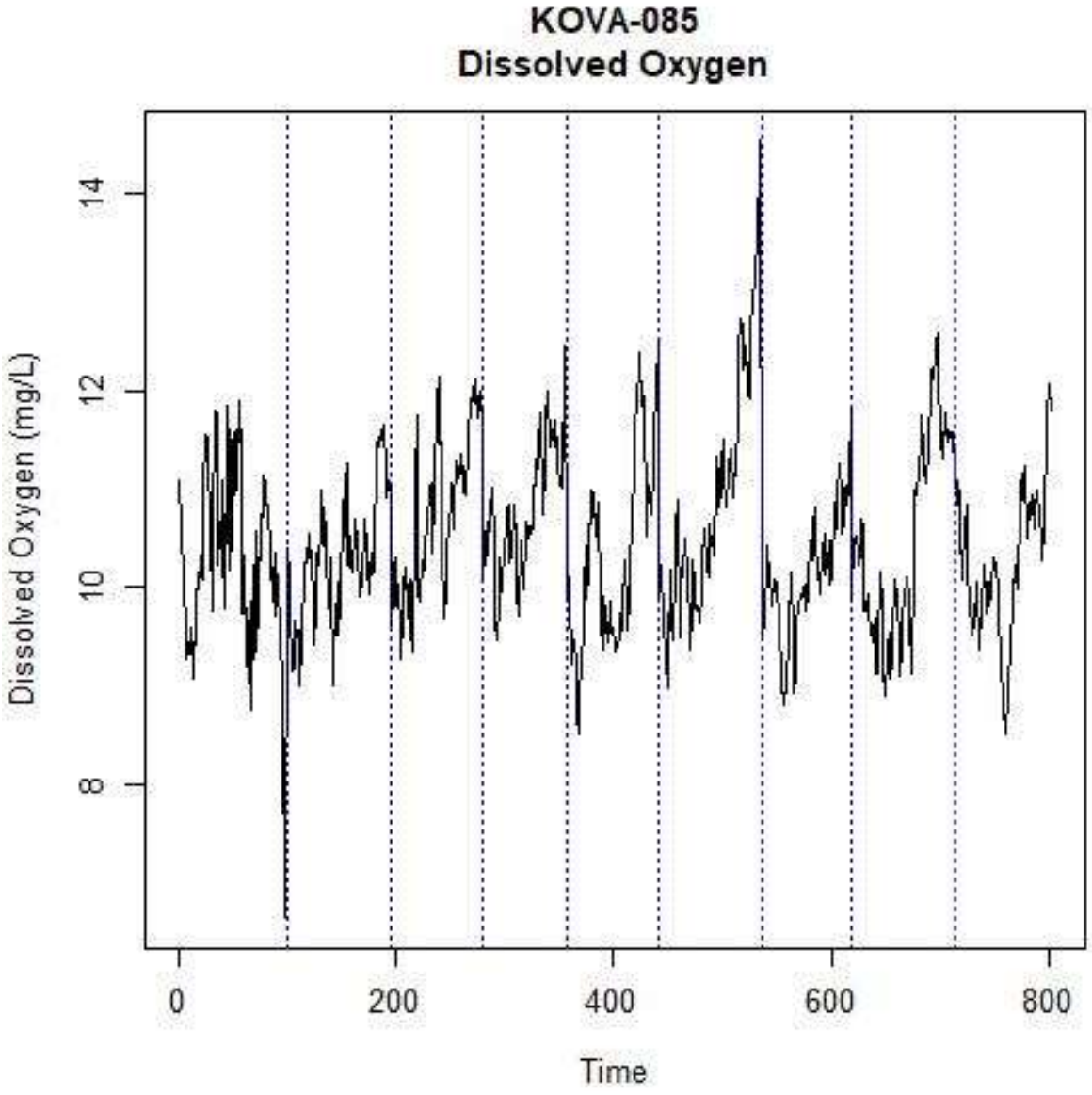


Figure A.14. Time series of KOVA-085 dissolved oxygen by time point with vertical lines for additive outliers.

Table A.13. Trend modeling results for daily dissolved oxygen data at KOVA-085.

			Trend			ARMA order		Ljung-Box Test	
Logged	**Method**	**Intercept**	**Coefficient**	**SE**	**p-value**	**AR**	**MA**	**Statistic**	**p-value**
FALSE	complete	12.1632	-0.1536	0.0914	0.0929	1	1	21.40	0.0016
FALSE	completeAO	11.2674	-0.0713	0.0564	0.2061	2	1	18.78	0.0003
FALSE	trunc	11.7577	-0.1253	0.0608	0.0391	2	0	98.63	0.8468
FALSE	truncSA	10.6823	-0.0280	0.0349	0.4231	5	0	96.16	0.8572
TRUE	complete	2.4537	-0.0099	0.0056	0.0782	2	1	16.42	0.0057
TRUE	completeAO	2.3989	-0.0048	0.0049	0.3205	2	1	18.39	0.0004
TRUE	trunc	2.4501	-0.0103	0.0053	0.0513	2	1	100.72	0.7691
TRUE	truncSA	2.3682	-0.0029	0.0033	0.3894	5	0	96.16	0.8572

Table A.14. Top covariate models for daily dissolved oxygen data at KOVA-085.

Model	**AICc**	**ΔAICc**	**Ljung-Box Test p-value**
Relative Humidity + Year + Month	446.14	0.00	0.0657
Relative Humidity + Month	447.66	1.52	0.1331
Relative Humidity + Daily Precipitation + Month	448.74	2.61	0.0613
Wind Speed + Year + Month	505.99	59.85	0.0596
Wind Speed + Month	506.48	60.34	0.1206
Daily Precipitation + Year + Month	508.13	61.99	0.0609
Daily Precipitation + Month	508.61	62.47	0.1204
Year + Month	511.59	65.45	0.1442
Wind Speed + Relative Humidity	533.38	87.24	0.0939
Wind Speed + Relative Humidity + Daily Precipitation	534.67	88.54	0.0510

Table A.15. Coefficients and variance components estimates for the top covariate model for daily dissolved oxygen data at KOVA-085.

Parameter	**Coefficient**	**SE**	**p-value**
ar1	0.10	0.13	0.4304
ar2	0.63	0.11	< 0.0001
ma1	0.81	0.11	< 0.0001
intercept	7.26	0.40	< 0.0001
Relative Humidity	-0.01	0.00	< 0.0001
Month	0.52	0.05	< 0.0001

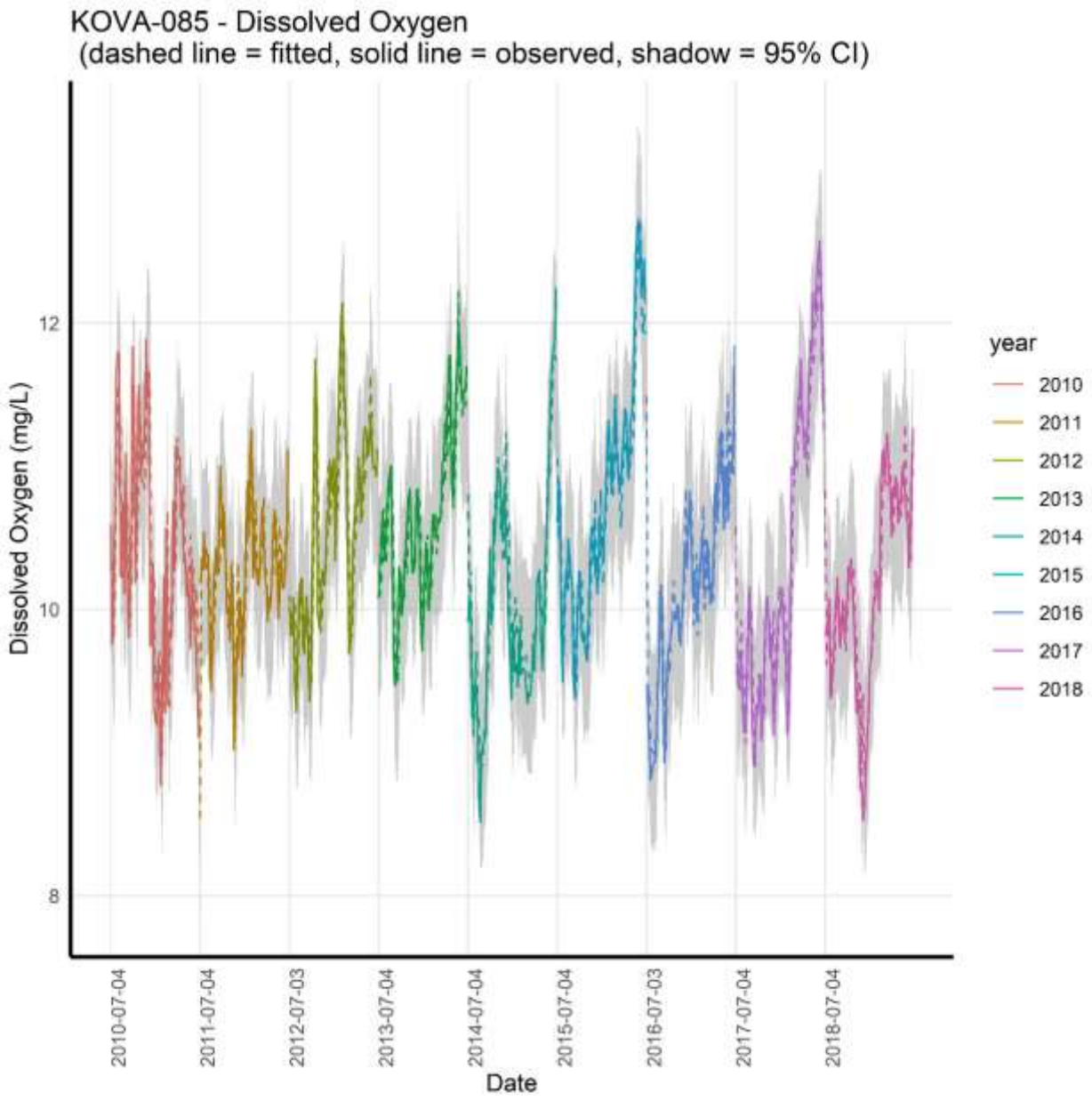


Figure A.15. Model predictions of KOVA-085 dissolved oxygen by date.

KOVA-086

Data

For KOVA-086, dissolved oxygen was recorded from 2009-2019, however data were absent for 2010, so only years 2011-2019 were included in the analysis. For this period (2011-2019), 783 dissolved oxygen records were collected during the months June through September. When truncating the data to the subset of 59 days visited in every year, the dataset was reduced to 531 observations. Data for covariates and response data were sufficiently complete that none of the covariates nor model years were omitted from the model selection process.

Model Selection

The seasonally adjusted truncated models for unlogged and logged dissolved oxygen yielded stationary residuals. Neither model included a trend coefficient that was significantly different from zero, and, overall, there is little evidence for an increasing or decreasing trend in dissolved oxygen at KOVA-086. For ARIMA models fitting all possible covariate combinations, AICc based model selection identified a final model with ARIMA(2,0,2) structure and fixed effects for daily precipitation and month. Daily precipitation was estimated to have a negative effect on dissolved oxygen whereas month of year had a positive effect. Residual diagnostics for the top covariate model indicated one large outlier, but were otherwise normally distributed with no evidence of substantial autocorrelation.

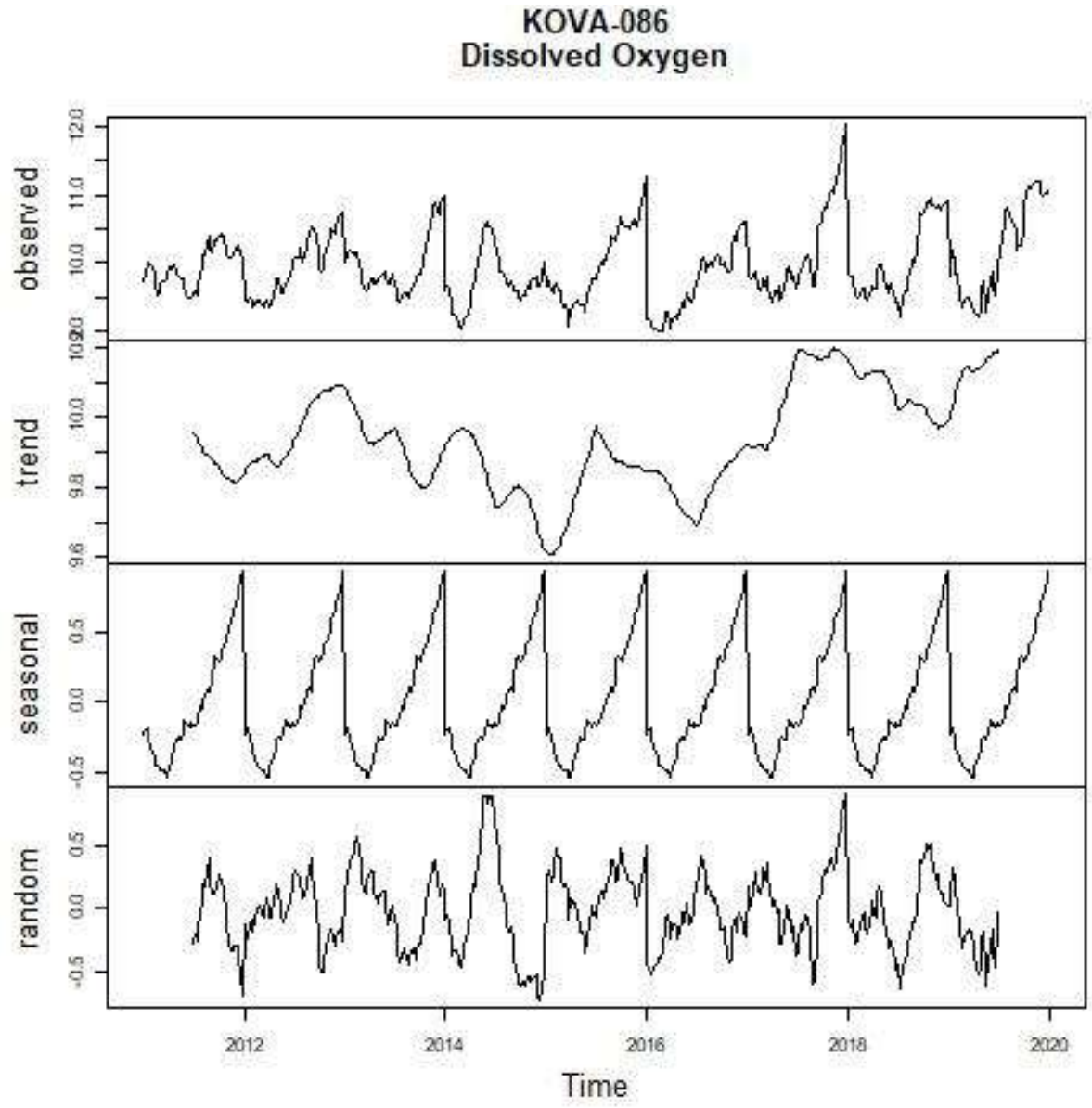


Figure A.16. Time series decomposition of truncated KOVA-086 dissolved oxygen by year.

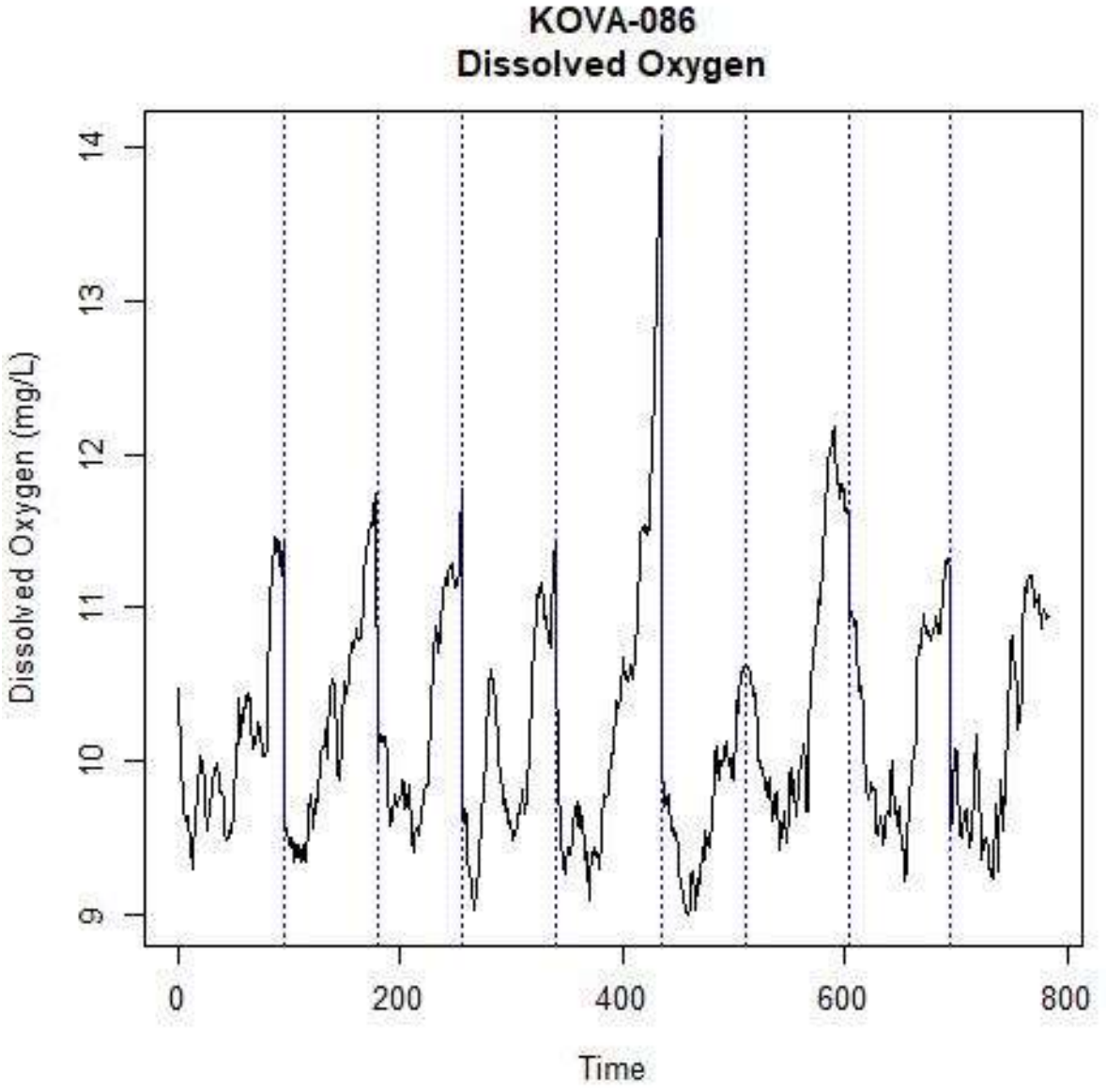


Figure A.17. Time series of KOVA-086 dissolved oxygen by time point with vertical lines for additive outliers.

Table A.16. Trend modeling results for daily dissolved oxygen data at KOVA-086.

			Trend			ARMA order		Ljung-Box Test	
Logged	**Method**	**Intercept**	**Coefficient**	**SE**	**p-value**	**AR**	**MA**	**Statistic**	**p-value**
FALSE	complete	10.8470	-0.0539	0.0190	0.0045	0	5	407.43	< 0.0001
FALSE	completeAO	10.5044	-0.0247	0.0177	0.1621	0	5	568.06	< 0.0001
FALSE	trunc	10.1461	-0.0143	0.0190	0.4496	0	5	308.46	< 0.0001
FALSE	truncSA	9.6687	0.0239	0.0152	0.1155	2	2	119.52	0.0892
TRUE	complete	2.3826	-0.0052	0.0018	0.0033	0	5	442.98	< 0.0001
TRUE	completeAO	2.3481	-0.0023	0.0017	0.1668	0	5	595.16	< 0.0001
TRUE	trunc	2.2836	0.0012	0.0013	0.3451	0	2	1196.15	< 0.0001
TRUE	truncSA	2.2703	0.0022	0.0015	0.1434	2	2	123.59	0.0550

Table A.17. Top covariate models for daily dissolved oxygen data at KOVA-086.

Model	**AICc**	**ΔAICc**	**Ljung-Box Test p-value**
Wind Speed + Daily Precipitation + Month	-501.49	0.00	0.2866
Daily Precipitation + Month	-499.75	1.74	0.3654
Wind Speed + Month	-496.32	5.17	0.3993
Air Temperature + Daily Precipitation	-203.59	297.90	0.4066
Air Temperature + Wind Speed + Daily Precipitation	-203.51	297.98	0.2471
Air Temperature + Wind Speed	-197.00	304.49	0.4701
Air Temperature	-196.23	305.26	0.6338
Wind Speed + Daily Precipitation	-115.34	386.16	0.2073
Wind Speed + Relative Humidity + Daily Precipitation	-114.58	386.91	0.1475
Wind Speed + Relative Humidity	-113.67	387.82	0.3016

Table A.18. Coefficients and variance components estimates for the top covariate model for daily dissolved oxygen data at KOVA-086.

Parameter	**Coefficient**	**SE**	**p-value**
ar1	1.92	0.02	< 0.0001
ar2	-0.93	0.02	< 0.0001
ma1	-0.83	0.04	< 0.0001
ma2	-0.14	0.04	0.0002
intercept	6.86	0.16	< 0.0001
Daily Precipitation	-0.08	0.03	0.0042
Month	0.44	0.02	< 0.0001

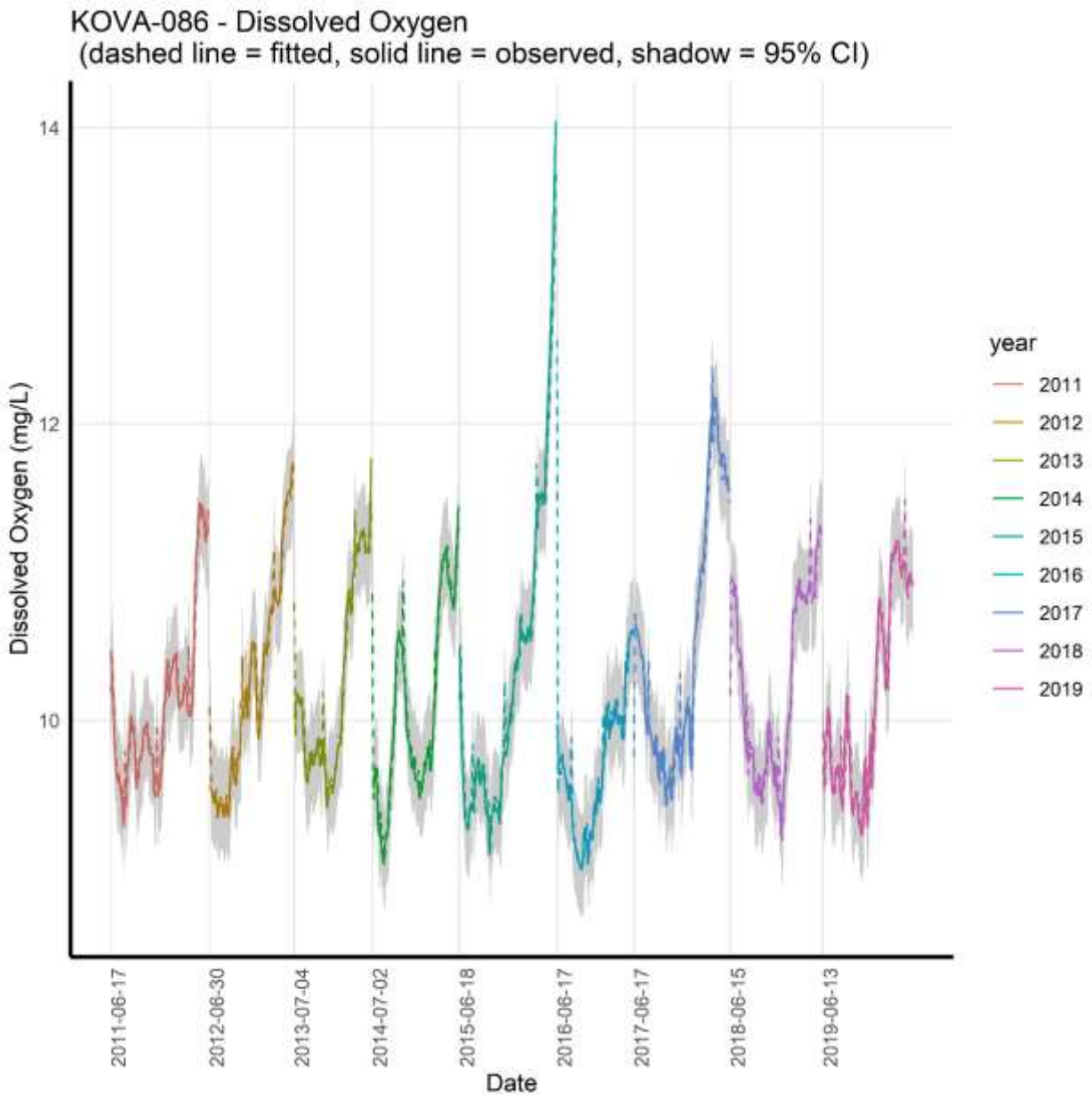


Figure A.18. Model predictions of KOVA-086 dissolved oxygen by date.

NOAT-052

Data

For lake NOAT-052, dissolved oxygen was recorded from 2015-2019. The months data were recorded varied by year and were collected from June-December in 2015, January-September in 2016, and June-September in years 2017-2019. In total, 723 dissolved oxygen observations were recorded during the 2015-2019 period analyzed. When truncating the data to the subset of 85 days that were visited in every year, the dataset was reduced to 425 observations. Data for covariates and response data were sufficiently complete that none of the covariates nor model years were omitted from the model selection process.

Model Selection

The truncated models for unlogged and logged data were the only models that yielded stationary residuals with no evidence of substantial autocorrelation, but the residual distribution appeared to be skewed slightly negative. Both models included negative trend coefficients that were significantly different from zero, suggesting a negative trend in dissolved oxygen at NOAT-052, but data plots suggest no net trend over the monitoring period. None of the ARIMA models fitting all possible combinations of covariates yielded stationary residuals when fit with daily data.

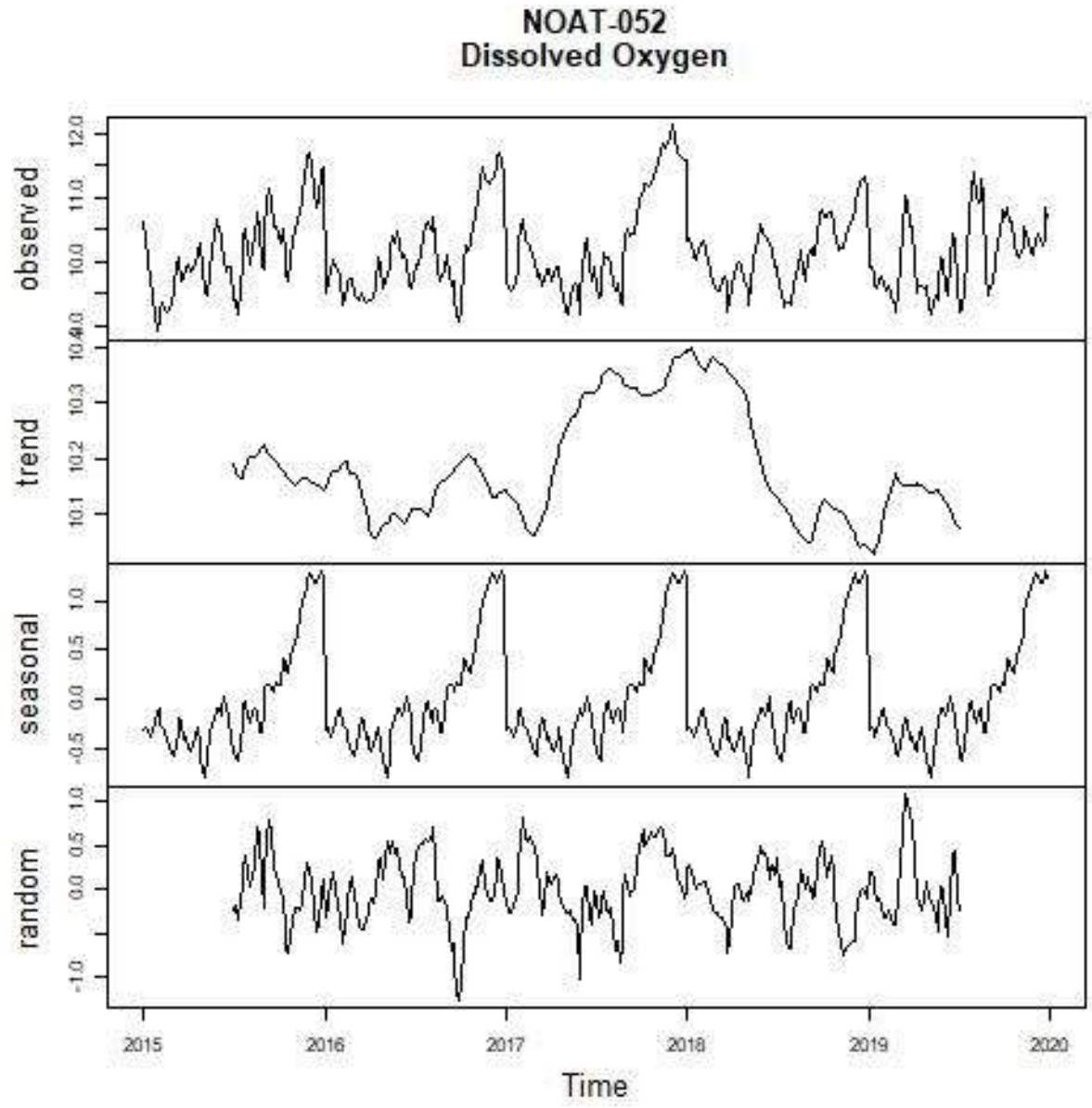


Figure A.19. Time series decomposition of truncated NOAT-052 dissolved oxygen by year.

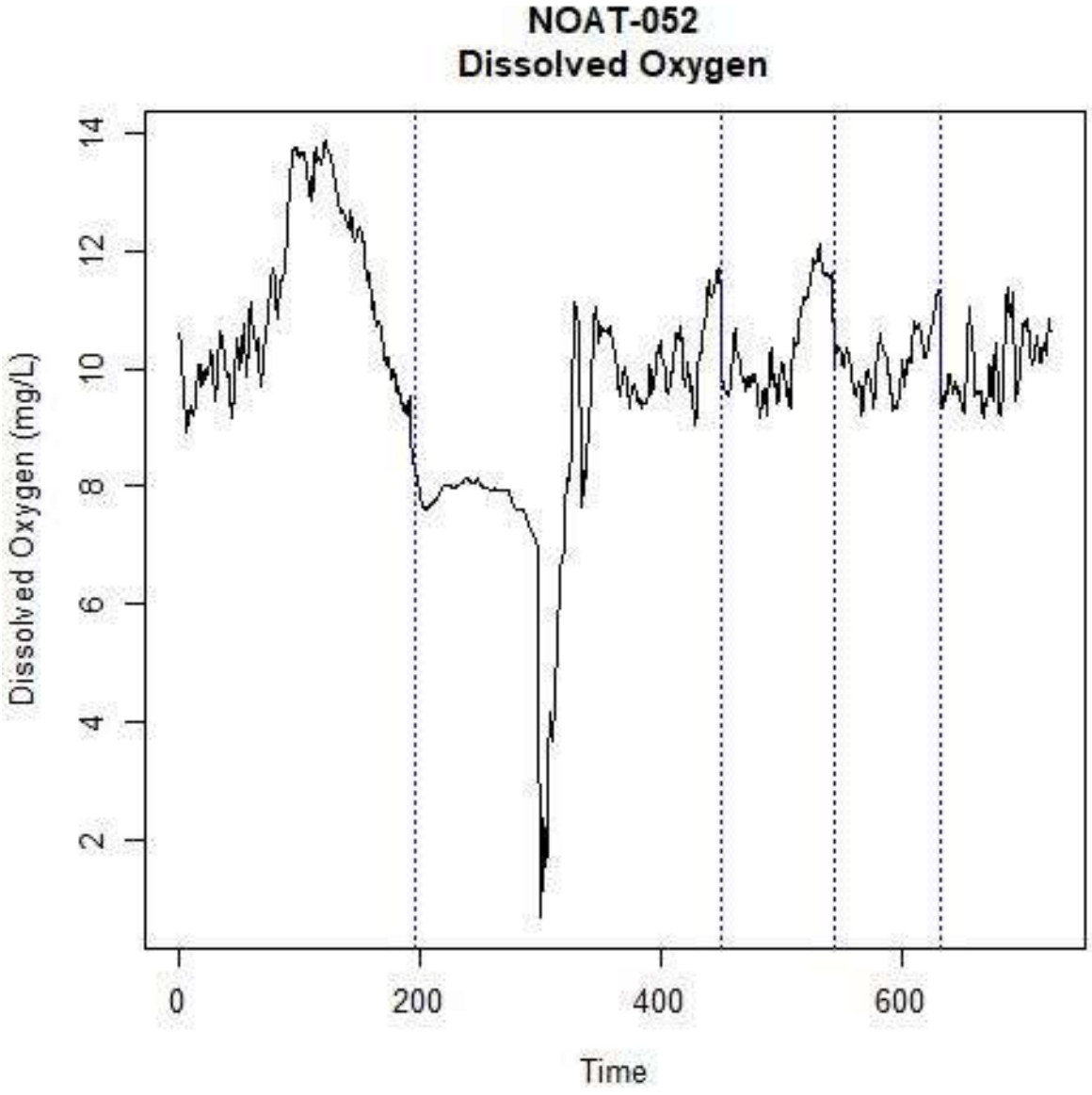


Figure A.20. Time series of NOAT-052 dissolved oxygen by time point with vertical lines for additive outliers.

Table A.19. Trend modeling results for daily dissolved oxygen data at NOAT-052.

			Trend			ARMA order		Ljung-Box Test	
Logged	**Method**	**Intercept**	**Coefficient**	**SE**	**p-value**	**AR**	**MA**	**Statistic**	**p-value**
FALSE	complete	27.2931	-1.1899	0.1116	< 0.0001	1	4	16.68	0.0008
FALSE	completeAO	25.7073	-1.0791	0.2294	< 0.0001	1	3	24.14	< 0.0001
FALSE	trunc	32.5426	-1.4900	0.1006	< 0.0001	1	1	98.53	0.0783
FALSE	truncSA	10.5674	-0.0268	0.0398	0.5004	1	2	108.85	0.0177
TRUE	complete	3.8328	-0.1070	0.0171	< 0.0001	3	3	13.63	0.0034
TRUE	completeAO	3.0718	-0.0550	0.0367	0.1338	3	3	14.85	0.0019
TRUE	trunc	4.4335	-0.1410	0.0100	< 0.0001	1	1	99.16	0.0721
TRUE	truncSA	2.3542	-0.0025	0.0038	0.5167	1	2	109.60	0.0157

Table A.20. Top covariate models for daily dissolved oxygen data at NOAT-052.

Model	**AICc**	**ΔAICc**	**Ljung-Box Test p-value**
Wind Speed + Relative Humidity + Month	-120.41	0.00	0.1171
Relative Humidity + Month	-103.06	17.35	0.1793
Wind Speed + Relative Humidity	27.40	147.82	0.3980
Wind Speed + Daily Precipitation	29.30	149.71	0.3260
Wind Speed + Solar Radiation	30.90	151.31	0.3600
Air Temperature + Wind Speed + Daily Precipitation	30.93	151.34	0.2341
Wind Speed	34.63	155.04	0.3901
Air Temperature + Wind Speed	35.18	155.60	0.3665
Daily Precipitation	39.83	160.25	0.3411
Air Temperature + Daily Precipitation	40.97	161.39	0.2862

Table A.21. Coefficients and variance components estimates for the top covariate model for daily dissolved oxygen data at NOAT-052.

Parameter	**Coefficient**	**SE**	**p-value**
ar1	0.80	0.04	< 0.0001
ma1	0.49	0.06	< 0.0001
ma2	0.09	0.06	0.1431
intercept	7.82	0.22	< 0.0001
Wind Speed	-0.04	0.01	< 0.0001
Relative Humidity	0.00	0.00	< 0.0001
Month	0.38	0.03	< 0.0001

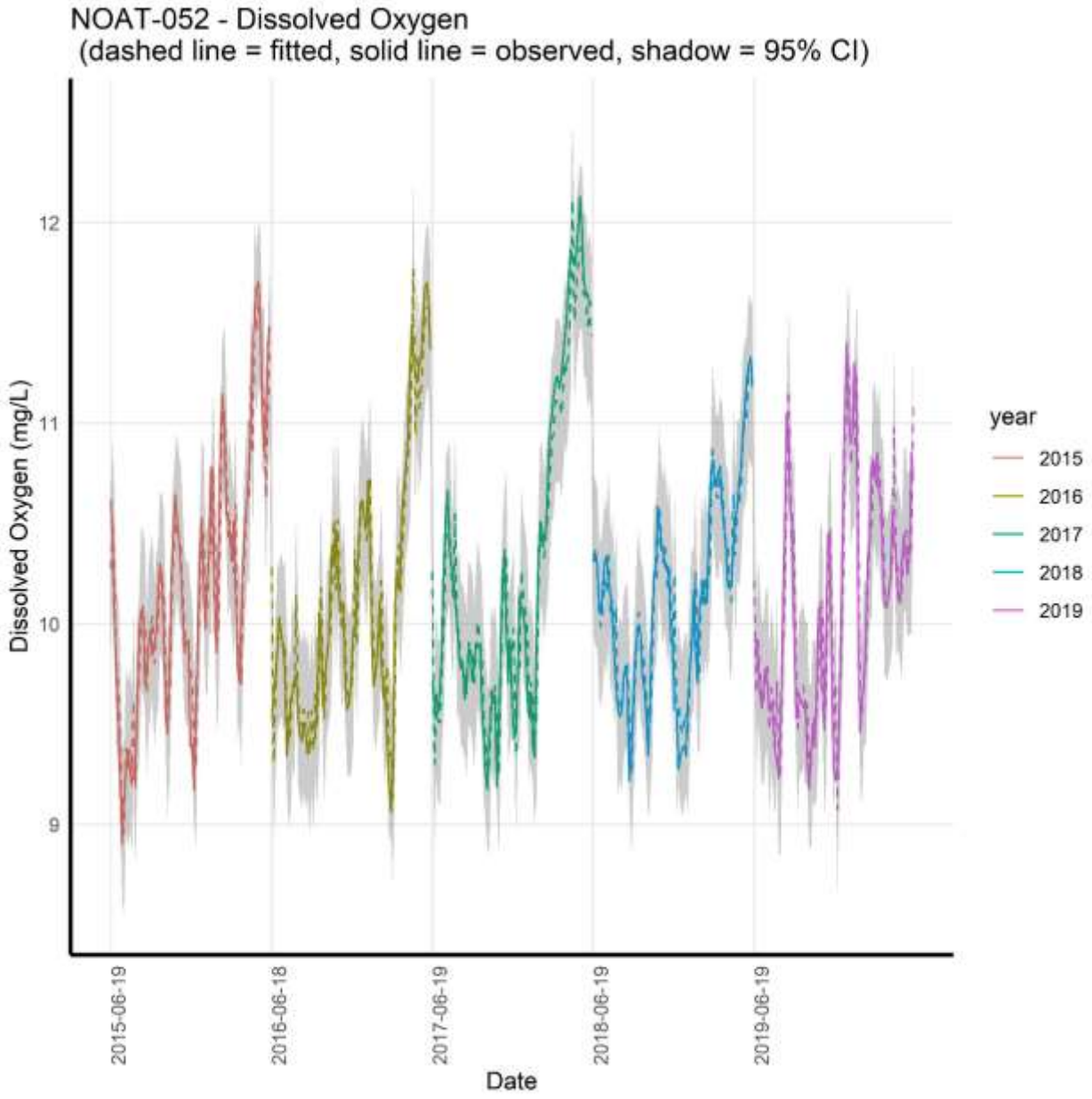


Figure A.21. Model predictions of NOAT-052 dissolved oxygen by date.

NOAT-107

Data

For lake NOAT-107, dissolved oxygen was recorded from 2014-2018. For this period, 385 dissolved oxygen observations were collected during the months June-September. When truncating the data to the subset of 35 days that were visited in every year, the dataset was reduced to 175 observations. Data for covariates and response data were sufficiently complete that none of the covariates nor model years were omitted from the model selection process.

Model Selection

Three models yielded stationary residuals for the unlogged and logged dissolved oxygen data (complete data with additive outliers, truncated data, and seasonally adjusted truncated data). The trend coefficient estimates were negative for these six models, but none of them were significantly different from zero. For ARIMA models fitting all possible combinations of covariate combinations, AICc based model selection identified a final model with ARIMA(2,0,0) structure and relative humidity and month as fixed effects. Relative humidity was estimated to have a negative effect on dissolved oxygen, whereas month (June-September) was estimated to have a positive effect. Residuals for the top covariate model were stationary with no evidence of substantial autocorrelation.

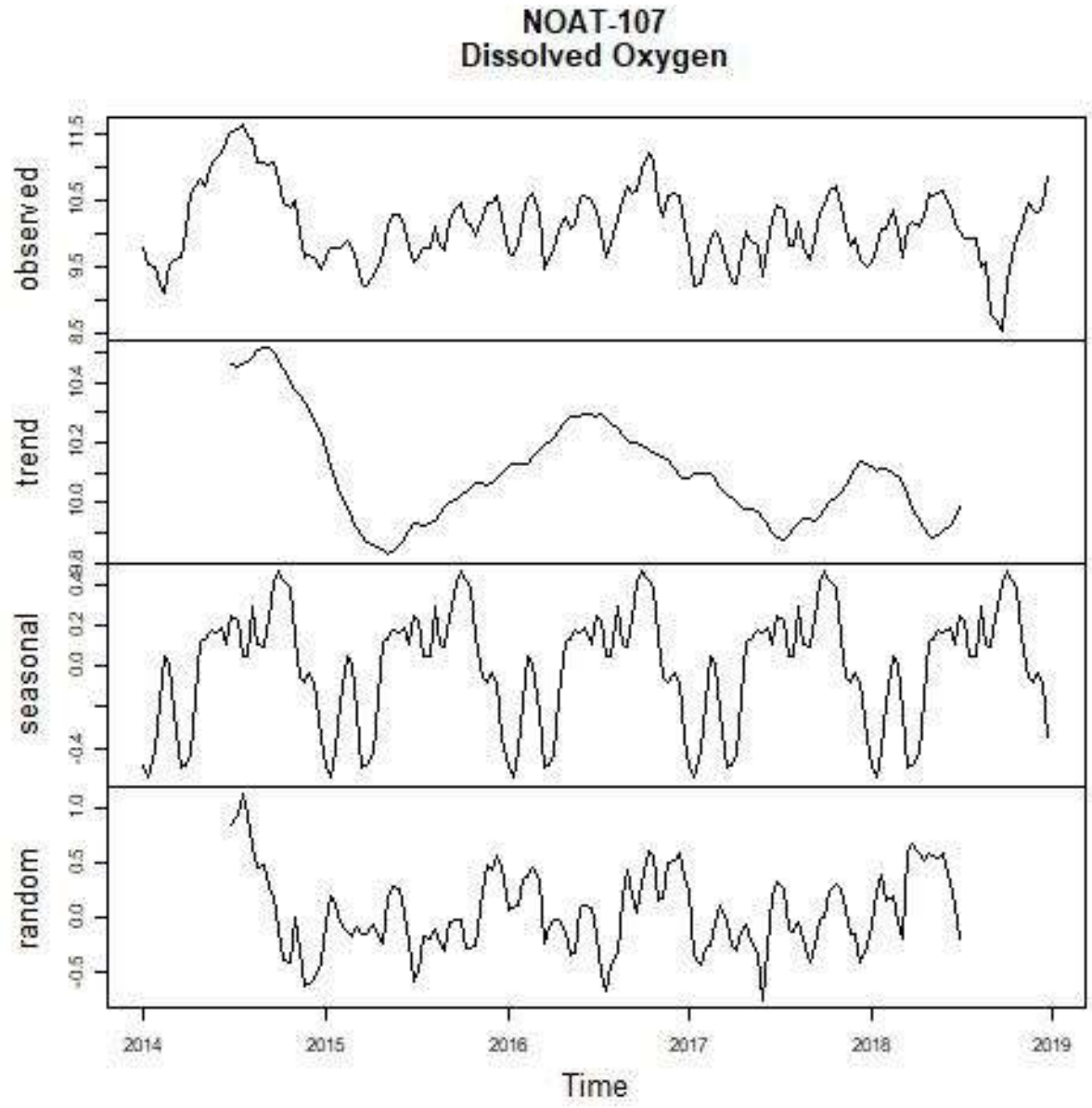


Figure A.22. Time series decomposition of truncated NOAT-107 dissolved oxygen by year.

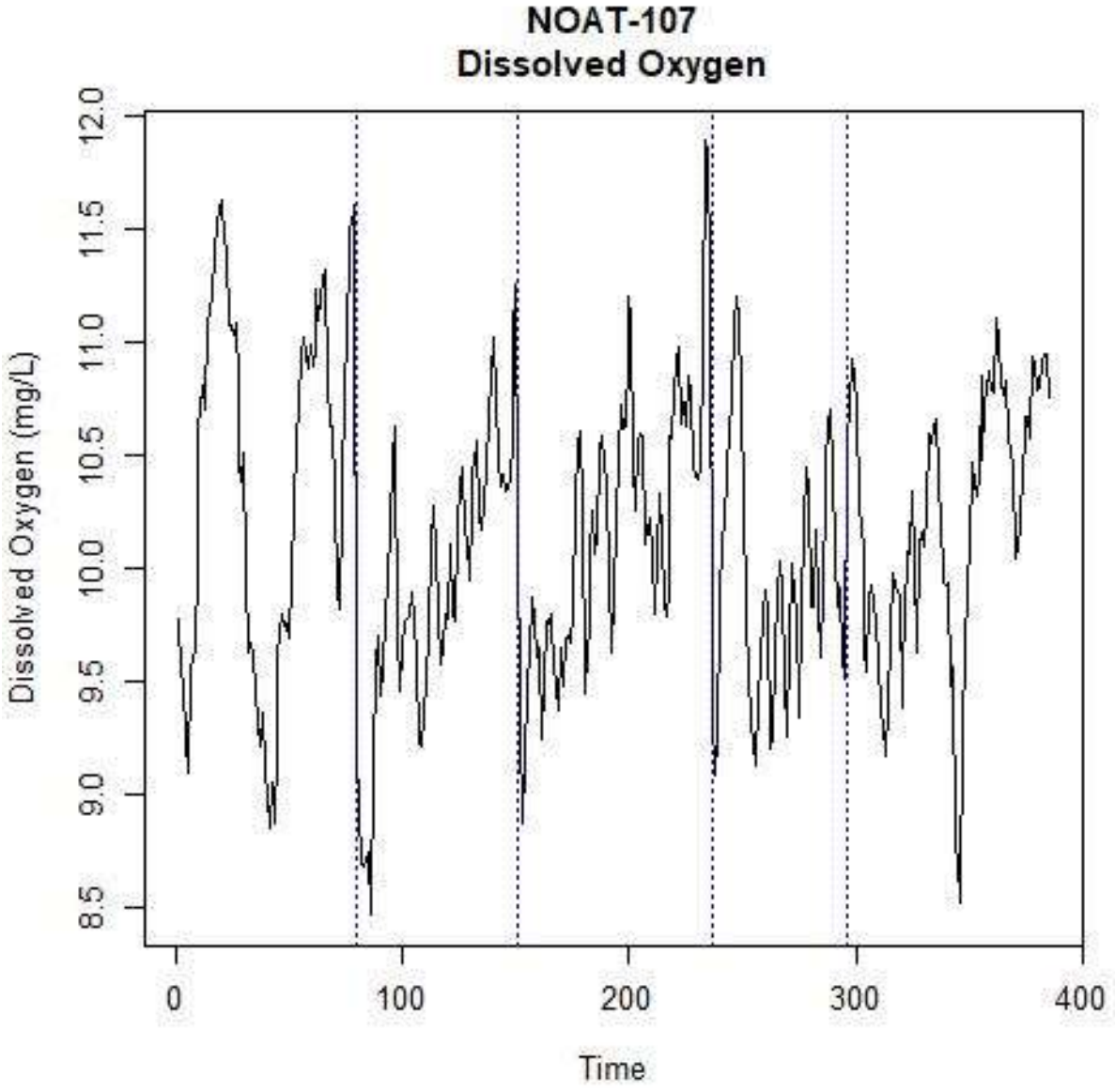


Figure A.23. Time series of NOAT-107 dissolved oxygen by time point with vertical lines for additive outliers.

Table A.22. Trend modeling results for daily dissolved oxygen data at NOAT-107.

			Trend			ARMA order		Ljung-Box Test	
Logged	**Method**	**Intercept**	**Coefficient**	**SE**	**p-value**	**AR**	**MA**	**Statistic**	**p-value**
FALSE	complete	23.3031	-0.9365	0.1622	< 0.0001	4	1	11.31	0.0101
FALSE	completeAO	11.9199	-0.1253	0.0749	0.0943	2	1	7.46	0.0587
FALSE	trunc	10.8681	-0.0531	0.0698	0.4469	1	2	33.89	0.2853
FALSE	truncSA	10.8456	-0.0502	0.0678	0.4589	1	2	37.86	0.1533

			Trend			ARMA order		Ljung-Box Test	
Logged	**Method**	**Intercept**	**Coefficient**	**SE**	**p-value**	**AR**	**MA**	**Statistic**	**p-value**
TRUE	complete	3.4999	-0.0840	0.0177	< 0.0001	1	1	12.93	0.0442
TRUE	completeAO	2.4851	-0.0120	0.0074	0.1057	1	2	6.50	0.0895
TRUE	trunc	2.3868	-0.0053	0.0068	0.4423	1	2	34.01	0.2806
TRUE	truncSA	2.3852	-0.0050	0.0066	0.4486	1	2	38.78	0.1308

Table A.23. Top covariate models for daily dissolved oxygen data at NOAT-107.

Model	**AICc**	**ΔAICc**	**Ljung-Box Test p-value**
Wind Speed + Relative Humidity + Month	66.46	0.00	0.4238
Relative Humidity + Month	66.98	0.53	0.5942
Wind Speed + Relative Humidity + Year + Month	68.07	1.61	0.2689
Relative Humidity + Year + Month	68.68	2.22	0.4398
Daily Precipitation + Month	87.88	21.42	0.7592
Daily Precipitation + Year + Month	89.75	23.29	0.6160
Wind Speed + Daily Precipitation + Month	89.92	23.46	0.6205
Wind Speed + Daily Precipitation + Year + Month	91.79	25.33	0.4429
Wind Speed + Month	104.91	38.46	0.8915
Year + Month	105.44	38.98	0.8894

Table A.24. Coefficients and variance components estimates for the top covariate model for daily dissolved oxygen data at NOAT-107.

Parameter	**Coefficient**	**SE**	**p-value**
ar1	1.14	0.05	< 0.0001
ar2	-0.31	0.05	< 0.0001
intercept	8.02	0.31	< 0.0001
Relative Humidity	-0.01	0.00	< 0.0001
Month	0.36	0.04	< 0.0001

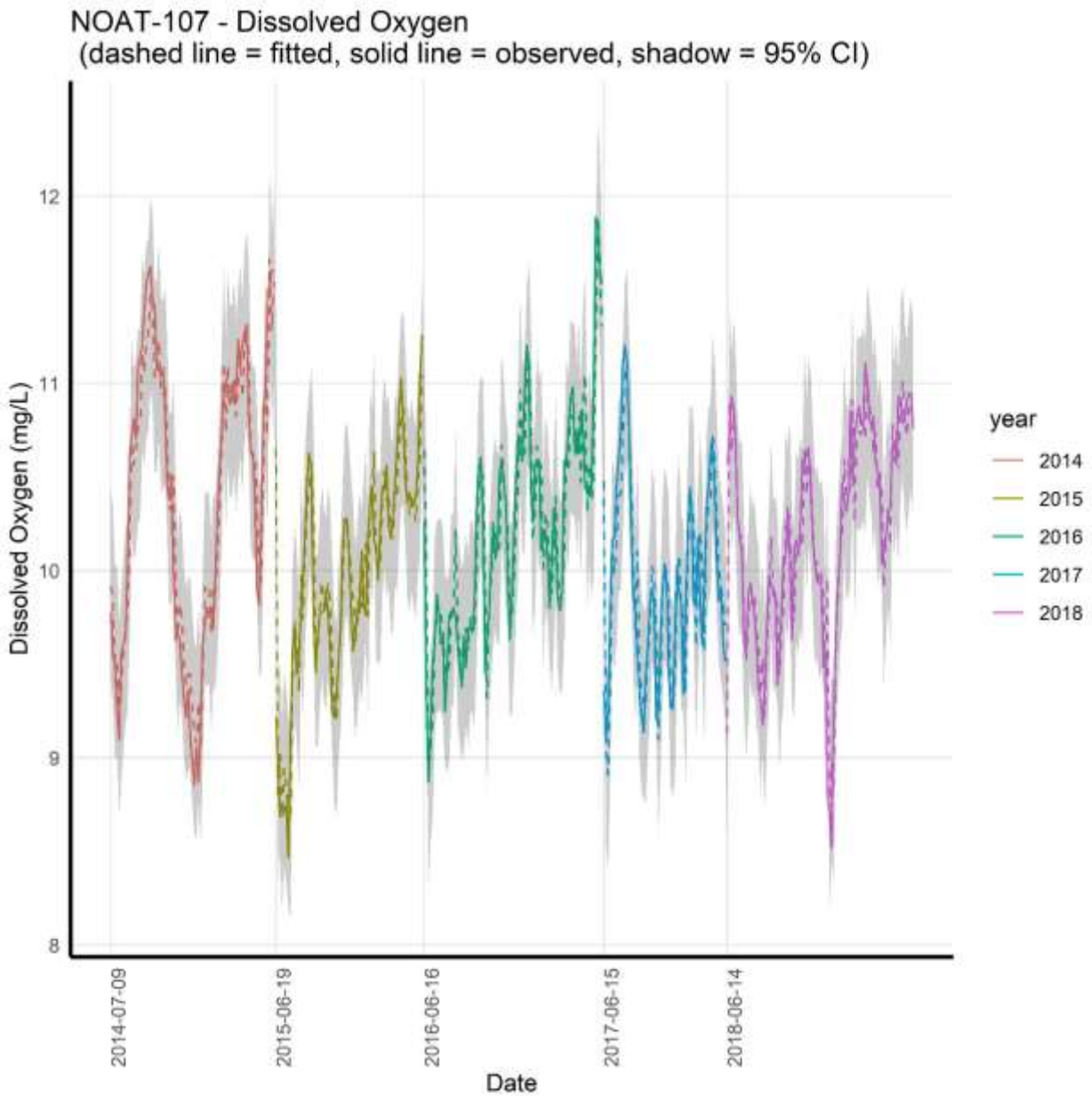


Figure A.24. Model predictions of NOAT-107 dissolved oxygen by date.

WRST-005

Data

For lake WRST-005, dissolved oxygen was recorded from 2010-2019, however only 4 observations were collected in 2010, thus only years 2011-2019 were included in this analysis. For this period (2010-2019), 636 dissolved oxygen observations were collected during the months May-September. No subset of days that were visited in every year, thus we did not consider truncated models for WRST-005. Data for covariates and response data were sufficiently complete that none of the covariates nor model years were omitted from the model selection process. There was however a 24-day period from August 27, 2018 to September 19, 2018 where data were absent for air temperature, relative humidity, solar radiation, and wind speed.

Model Selection

No trend models for daily dissolved oxygen yielded stationary residuals or ARIMA models fitting all possible combinations of covariate combinations, AICc based model selection identified a final model with ARIMA(1,0,1) structure and relative humidity as a fixed effect. Relative humidity was estimated to have a negative effect on dissolved oxygen. Residuals for the top covariate model were stationary with no evidence of substantial autocorrelation, but the residuals appeared to have a slight positive correlated with relative humidity. None of the covariate models including year as a covariate yielded stationary residuals. Weak evidence of autocorrelation was observed for the residuals of trend models of weekly means. Monthly means provided no evidence for trend.

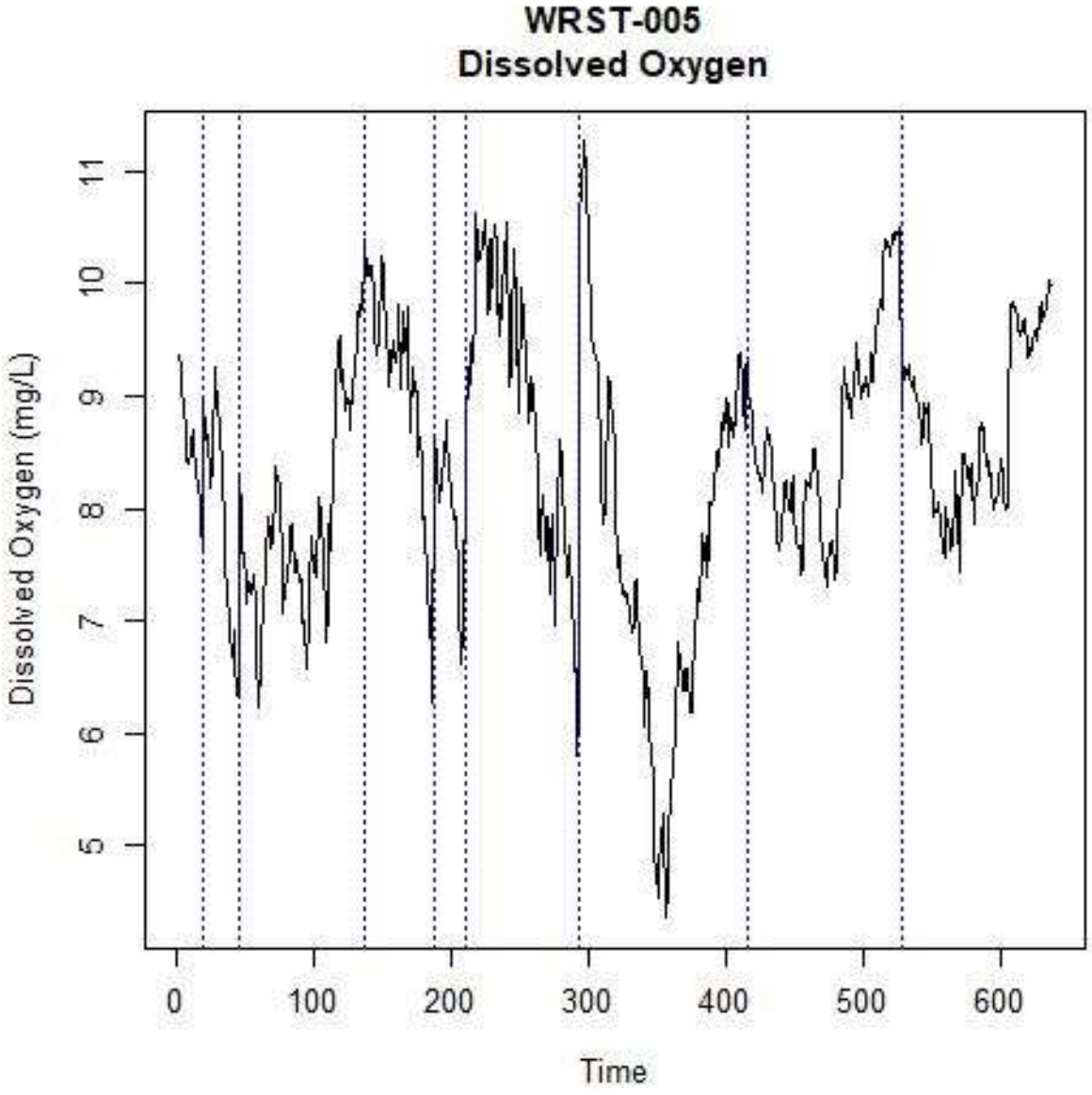


Figure A.25. Time series of WRST-005 dissolved oxygen by time point with vertical lines for additive outliers.

Table A.25. Trend modeling results for daily dissolved oxygen data at WRST-005.

			Trend			ARMA order		Ljung-Box Test	
Logged	**Method**	**Intercept**	**Coefficient**	**SE**	**p-value**	**AR**	**MA**	**Statistic**	**p-value**
FALSE	complete	7.1695	0.0859	0.0288	0.0028	0	3	786.17	< 0.0001
FALSE	completeAO	7.5710	0.0568	0.0243	0.0193	0	2	2097.73	< 0.0001
TRUE	complete	1.9909	0.0088	0.0032	0.0060	0	2	1453.59	< 0.0001
TRUE	completeAO	2.0152	0.0070	0.0036	0.0486	0	3	1208.34	< 0.0001

Table A.26. Trend modeling results for monthly dissolved oxygen means at WRST-005.

			Trend			ARMA order		Ljung-Box Test	
Logged	**Method**	**Intercept**	**Coefficient**	**SE**	**p-value**	**AR**	**MA**	**Statistic**	**p-value**
FALSE	complete	8.4524	0.0250	0.0906	0.7822	0	1	6.26	0.1808
FALSE	completeAO	8.4403	-0.0122	0.0686	0.8593	0	0	7.21	0.0656
TRUE	complete	2.1219	0.0035	0.0111	0.7498	0	1	5.57	0.2335
TRUE	completeAO	2.1202	-0.0009	0.0086	0.9180	0	0	8.30	0.0403

Table A.27. Top covariate models for daily dissolved oxygen data at WRST-005.

Model	**AICc**	**ΔAICc**	**Ljung-Box Test p-value**
Relative Humidity	421.66	0.00	0.2339
Solar Radiation	427.43	5.77	0.1378
Wind Speed + Solar Radiation	429.21	7.55	0.0791
Air Temperature + Month	464.63	42.98	0.1200
Air Temperature + Wind Speed	480.55	58.89	0.1562
Air Temperature	481.34	59.69	0.3288
Wind Speed	486.23	64.57	0.0903
Intercept Only	489.78	68.13	0.1854

Table A.28. Coefficients and variance components estimates for the top covariate model for daily dissolved oxygen data at WRST-005.

Parameter	**Coefficient**	**SE**	**p-value**
ar1	0.95	0.01	< 0.0001
ma1	0.11	0.04	0.0076
intercept	9.13	0.30	< 0.0001
Relative Humidity	-0.01	0.00	< 0.0001

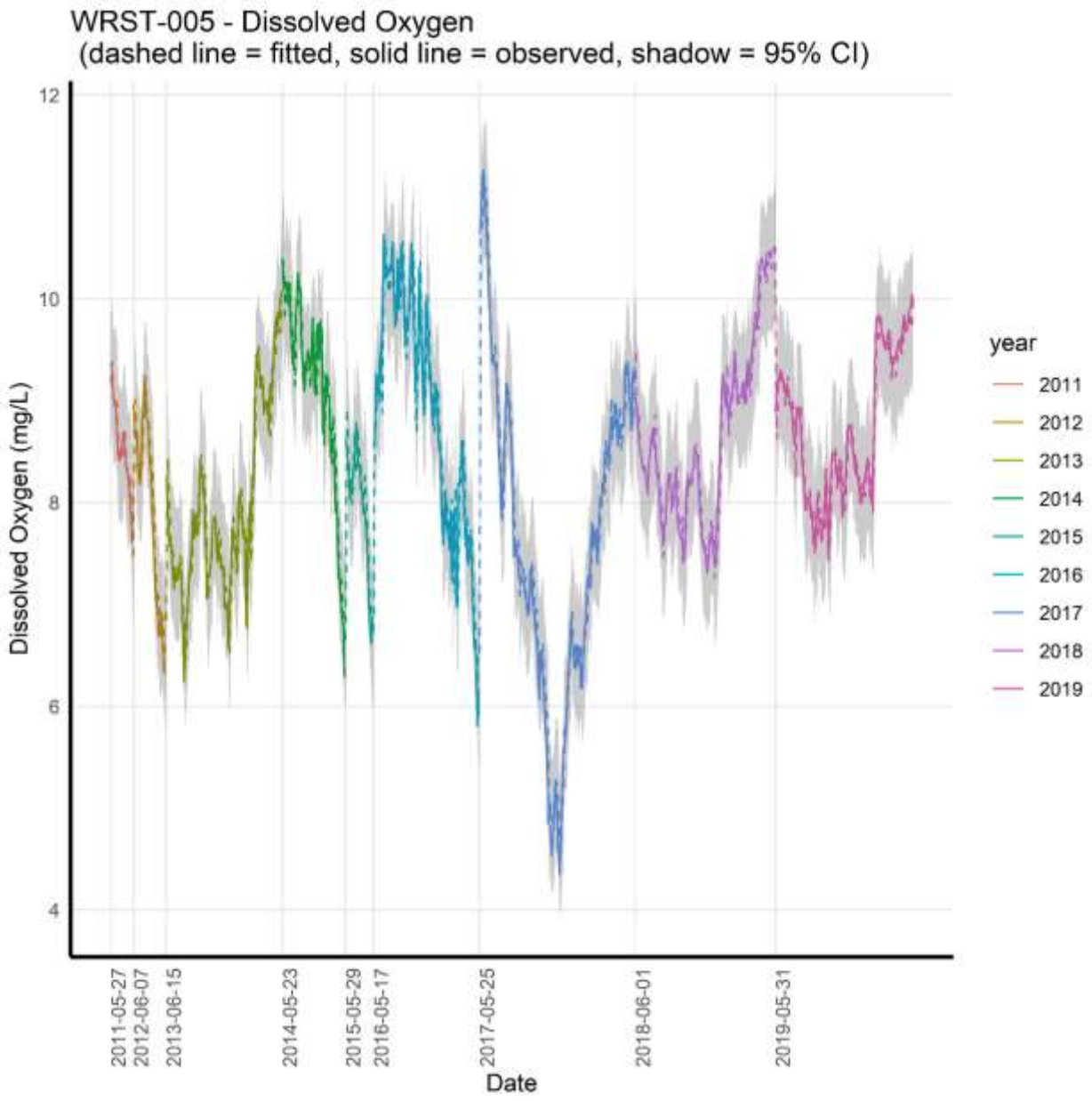


Figure A.26. Model predictions of WRST-005 dissolved oxygen by date.

WRST-016

Data

For lake WRST-016, dissolved oxygen was recorded from 2009-2019, however only 7 observations were collected in 2009, thus only years 2010-2019 were included in this analysis. For this period (2010-2019), 987 dissolved oxygen observations were collected during the months May-September. When truncating the data to the subset of 52 days that were visited in every year, the dataset was reduced to 502 observations. Data for covariates and response data were sufficiently complete that none of the covariates nor model years were omitted from the model selection process. There was, however, a 24-day period from August 27, 2018-September 19, 2018 where data were absent for air temperature, relative humidity, solar radiation, and wind speed.

Model Selection

The complete and the seasonally adjusted truncated data models for unlogged and logged dissolved oxygen yielded stationary residuals. The estimated trend coefficients were negative for these models, but none of the coefficients were significantly different from zero. For ARIMA models fitting all possible combinations of covariate combinations, AICc based model selection identified a final model with ARIMA(1,0,1) structure and air temperature as a fixed effect. Air temperature was estimated to have a positive effect on dissolved oxygen. There was no evidence for substantial autocorrelation in the residuals for the top model, but there appeared to be a slight positive correlation with air temperature.

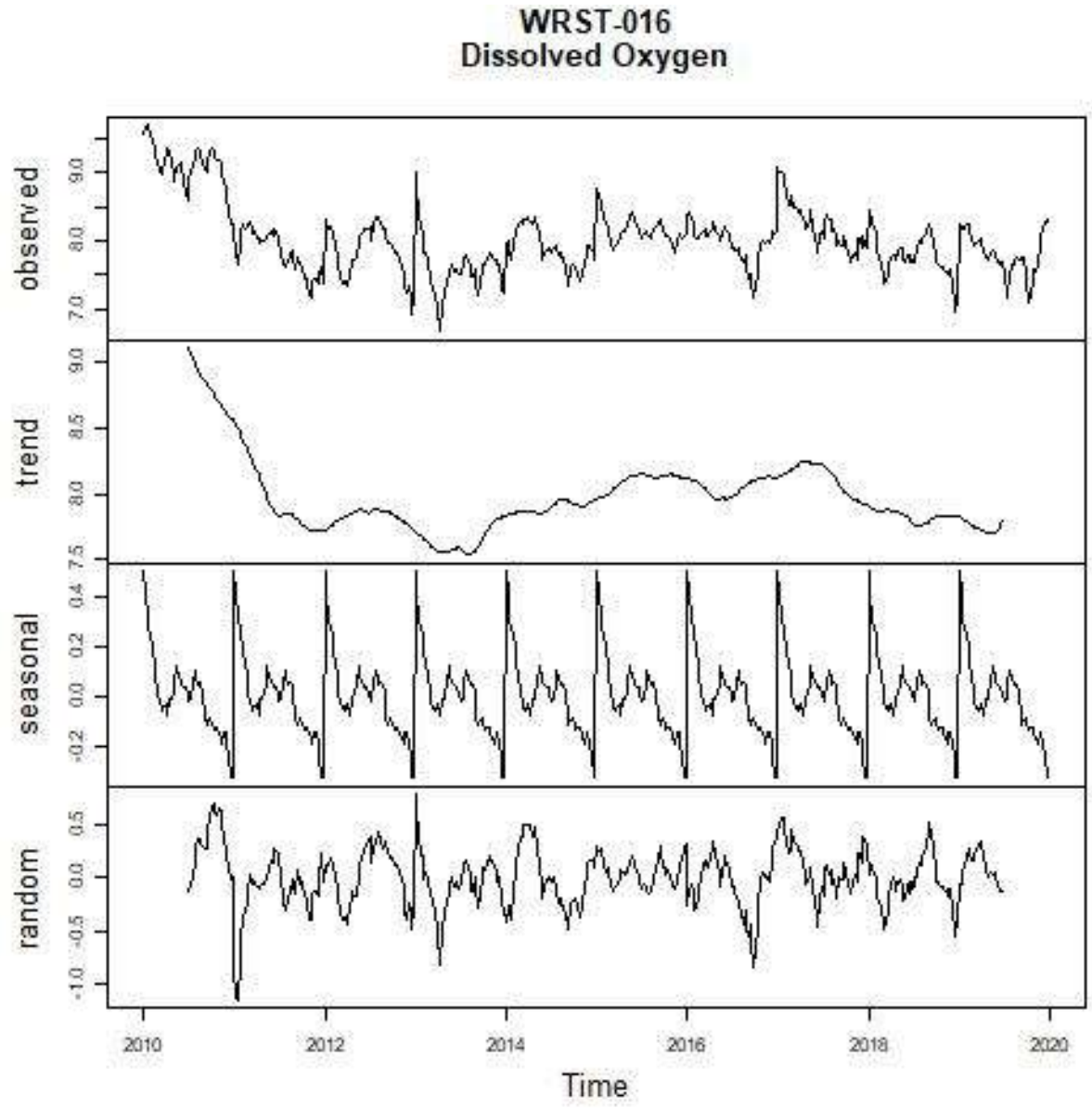


Figure A.27. Time series decomposition of truncated WRST-016 dissolved oxygen by year.

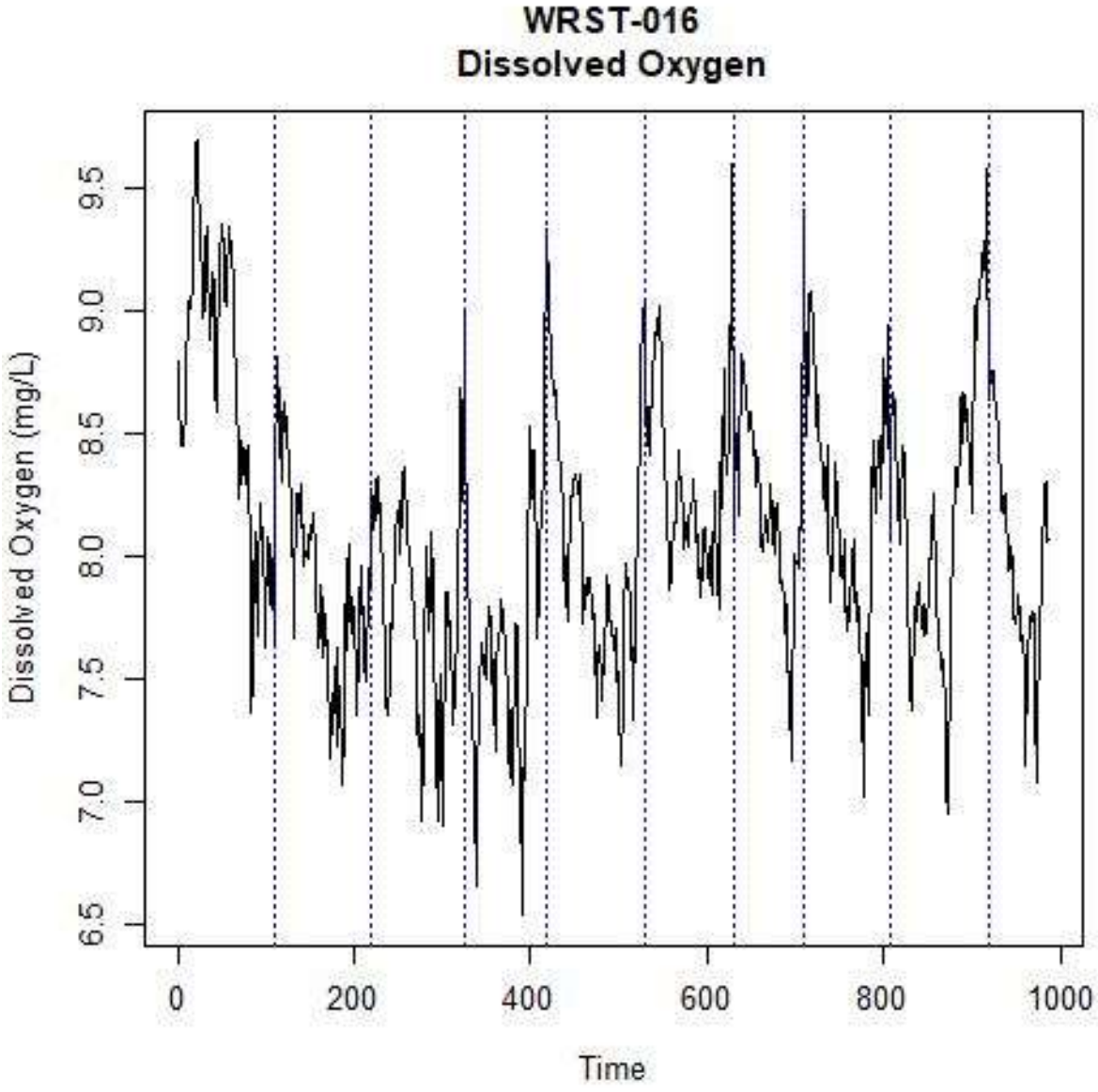


Figure A.28. Time series of WRST-016 dissolved oxygen by time point with vertical lines for additive outliers.

Table A.29. Trend modeling results for daily dissolved oxygen data at WRST-016.

			Trend			ARMA order		Ljung-Box Test	
Logged	**Method**	**Intercept**	**Coefficient**	**SE**	**p-value**	**AR**	**MA**	**Statistic**	**p-value**
FALSE	complete	8.5027	-0.0325	0.0294	0.2684	1	1	12.28	0.0559
FALSE	completeAO	8.2538	-0.0121	0.0309	0.6956	1	1	20.59	0.0001
FALSE	trunc	8.8357	-0.0622	0.0128	< 0.0001	0	2	1248.81	< 0.0001
FALSE	truncSA	8.4424	-0.0278	0.0329	0.3979	2	2	114.12	0.1270
TRUE	complete	2.1332	-0.0035	0.0036	0.3230	1	1	13.63	0.0340

			Trend			ARMA order		Ljung-Box Test	
Logged	**Method**	**Intercept**	**Coefficient**	**SE**	**p-value**	**AR**	**MA**	**Statistic**	**p-value**
TRUE	completeAO	2.1017	-0.0009	0.0037	0.8045	1	1	22.37	< 0.0001
TRUE	trunc	2.1737	-0.0072	0.0016	< 0.0001	0	2	1163.35	< 0.0001
TRUE	truncSA	2.1282	-0.0032	0.0040	0.4271	2	2	113.72	0.1325

Table A.30. Top covariate models for daily dissolved oxygen data at WRST-016.

Model	**AICc**	**ΔAICc**	**Ljung-Box Test p-value**
Wind Speed + Month	-832.71	0.00	0.0530
Air Temperature	-832.27	0.43	0.0708
Relative Humidity	-824.77	7.94	0.0531
Wind Speed	-818.15	14.56	0.0702
Intercept Only	-808.26	24.45	0.0907
Daily Precipitation	-808.12	24.59	0.0505

Table A.31. Coefficients and variance components estimates for the top covariate model for daily dissolved oxygen data at WRST-016.

Parameter	**Coefficient**	**SE**	**p-value**
ar1	0.94	0.01	< 0.0001
ma1	0.19	0.03	< 0.0001
intercept	7.94	0.11	< 0.0001
Air Temperature	0.01	0.00	< 0.0001

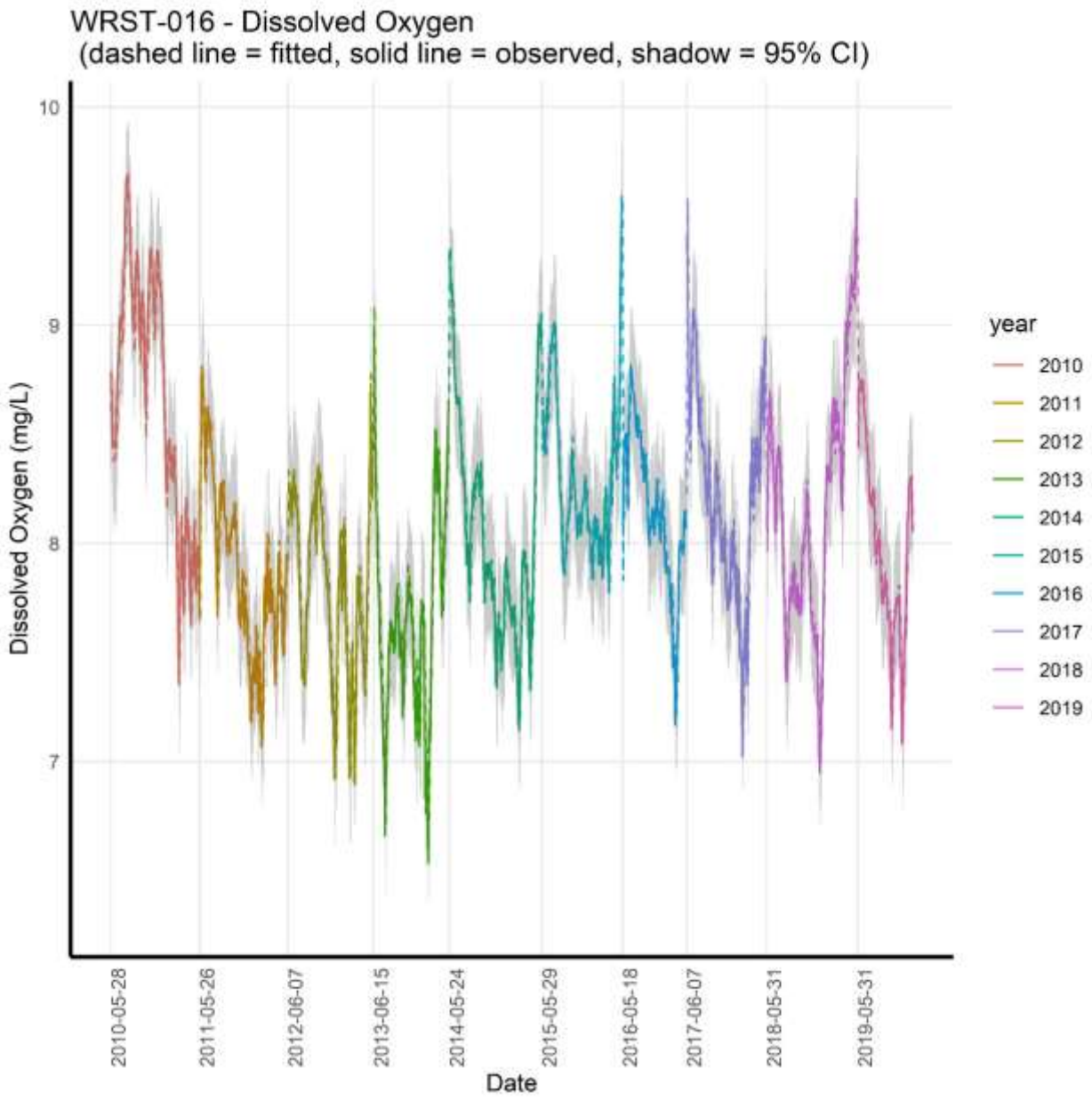


Figure A.29. Model predictions of WRST-016 dissolved oxygen by date.

YUCH-004

Data

For lake YUCH-004, dissolved oxygen was recorded from 2005-2019, however data were absent for years 2006 and 2008, thus only years 2009-2019 were included in this analysis. For this period (2009-2019), 1221 dissolved oxygen observations were collected during the months May through September. When truncating the data to the subset of 87 days that were visited in every year, the dataset was reduced to 957 observations. Data for covariates were absent in 2019, thus this year was excluded from the ARIMA covariate models.

When aggregated to mean weekly values the dissolved oxygen dataset contained 186 observations. When truncating to the subset of 14 common weeks sampled in every year the number of observations was reduced to 154.

Model Selection

None of the trend models for the daily unlogged or logged dissolved oxygen data yielded stationary residuals. For ARIMA models fitting all possible combinations of covariate combinations, AICc based model selection identified a final model with ARIMA(1,0,1) structure with wind speed and relative humidity as fixed effects. Both wind speed and relative humidity were estimated to have a negative effect on dissolved oxygen. There was no evidence for substantial autocorrelation in the residuals for the top model, but there appeared to be a slight positive correlation with air temperature. None of the covariate models that included year as a covariate yielded stationary residuals.

When fitting trend models to the weekly unlogged and logged dissolved oxygen data both the complete dataset and truncated dataset yielded stationary residuals. However, neither of these models included a trend coefficient that was significantly different from zero, thus there is no evidence for a trend in dissolved oxygen at lake YUCH-004.

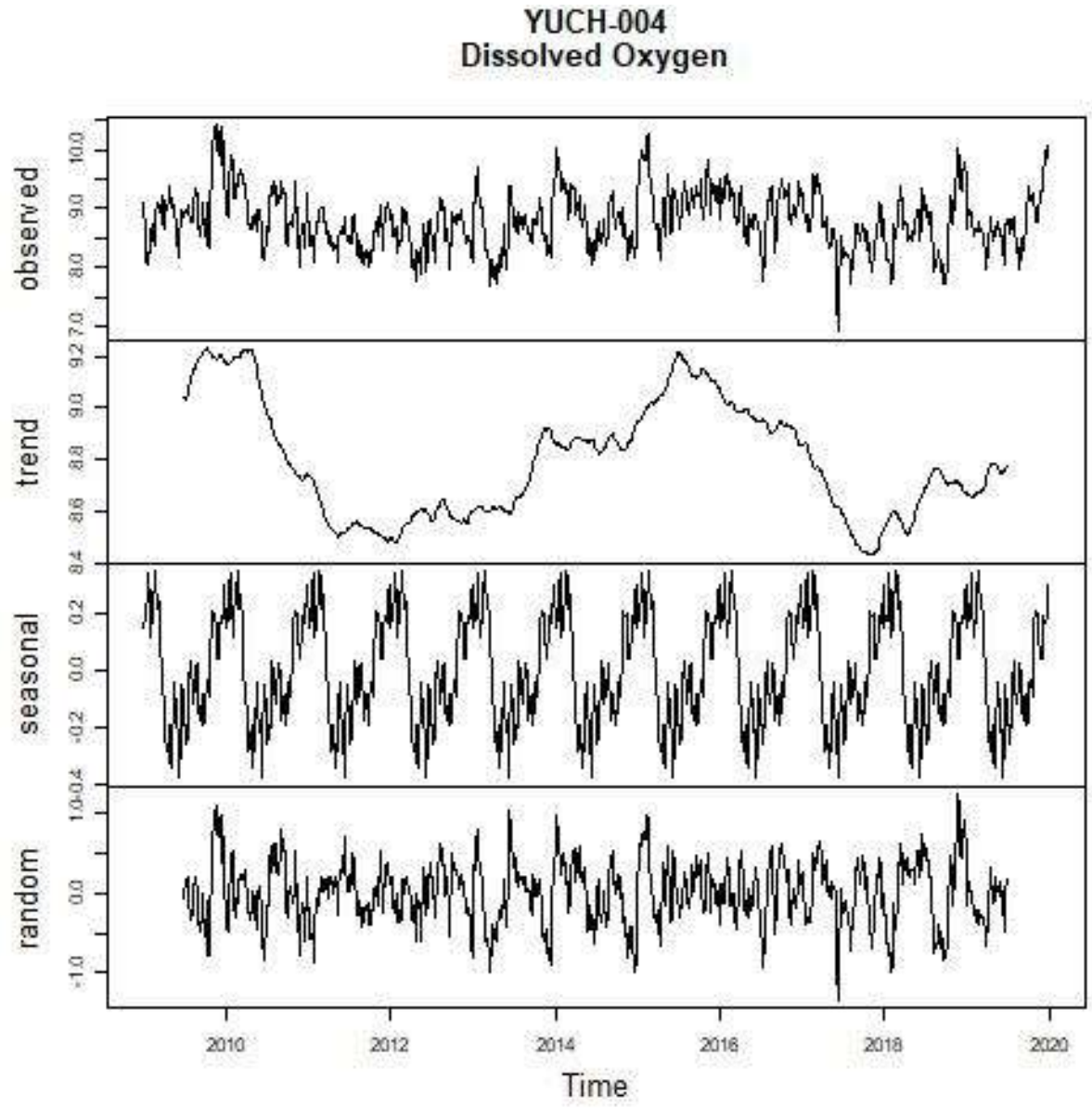


Figure A.30: Time series decomposition of truncated YUCH-004 dissolved oxygen by year.

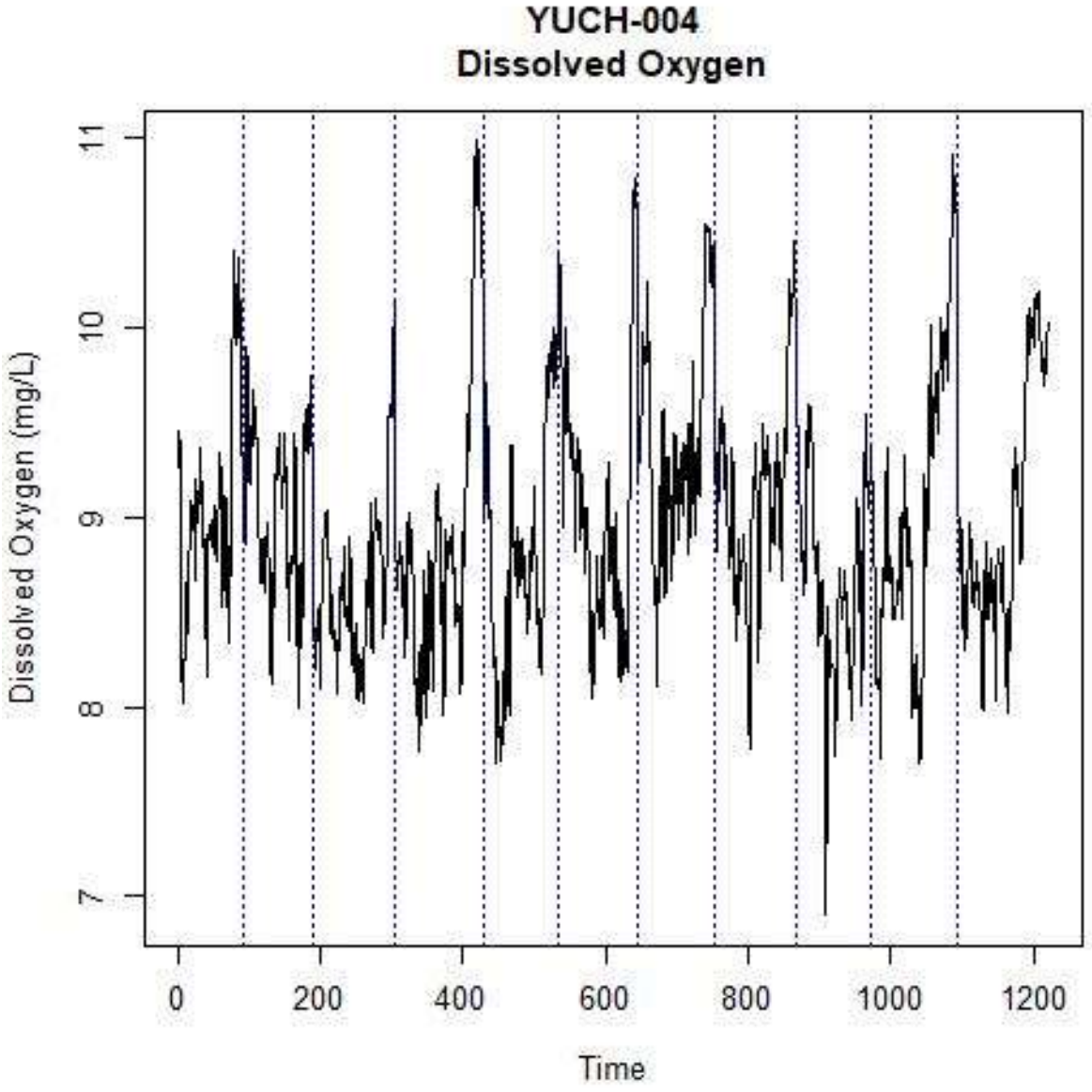


Figure A.31. Time series of YUCH-004 dissolved oxygen by time point with vertical lines for additive outliers.

Table A.32. Trend modeling results for daily dissolved oxygen data at YUCH-004.

			Trend			ARMA order		Ljung-Box Test	
Logged	**Method**	**Intercept**	**Coefficient**	**SE**	**p-value**	**AR**	**MA**	**Statistic**	**p-value**
FALSE	complete	9.0166	-0.0036	0.0108	0.7374	0	5	324.24	< 0.0001
FALSE	completeAO	9.3409	-0.0346	0.0303	0.2540	1	1	19.82	0.0002
FALSE	trunc	8.9751	-0.0166	0.0171	0.3311	2	0	217.72	0.0059

			Trend			ARMA order		Ljung-Box Test	
Logged	**Method**	**Intercept**	**Coefficient**	**SE**	**p-value**	**AR**	**MA**	**Statistic**	**p-value**
FALSE	truncSA	8.8667	-0.0061	0.0163	0.7091	3	0	226.91	0.0020
TRUE	complete	2.1958	-0.0003	0.0012	0.7868	0	5	306.50	< 0.0001
TRUE	completeAO	2.2219	-0.0028	0.0030	0.3568	1	1	20.53	0.0001
TRUE	trunc	2.1939	-0.0019	0.0020	0.3318	1	1	205.29	0.0264
TRUE	truncSA	2.1809	-0.0007	0.0018	0.6990	3	0	223.85	0.0030

Table A.33. Trend modeling results for weekly dissolved oxygen data at YUCH-004.

			Trend			ARMA order		Ljung-Box Test	
Logged	**Method**	**Intercept**	**Coefficient**	**SE**	**p-value**	**AR**	**MA**	**Statistic**	**p-value**
FALSE	complete	9.0742	-0.0049	0.0290	0.8663	2	0	8.64	0.1950
FALSE	completeAO	9.0567	-0.0010	0.0301	0.9743	2	0	21.63	< 0.0001
FALSE	trunc	9.0317	-0.0179	0.0240	0.4549	1	0	29.42	0.1666
FALSE	truncSA	8.8999	-0.0057	0.0153	0.7125	1	0	50.02	0.0009
TRUE	complete	2.2030	-0.0005	0.0032	0.8706	2	0	9.01	0.1730
TRUE	completeAO	2.2015	-0.0002	0.0033	0.9625	2	0	21.55	< 0.0001
TRUE	trunc	2.1989	-0.0020	0.0026	0.4572	1	0	30.01	0.1490
TRUE	truncSA	2.1847	-0.0006	0.0017	0.7055	1	0	51.53	0.0006

Table A.34. Top covariate models for daily dissolved oxygen data at YUCH-004.

Model	**AICc**	**ΔAICc**	**Ljung-Box Test p-value**
Wind Speed + Relative Humidity	-450.95	0.00	0.0825
Air Temperature + Wind Speed + Daily Precipitation	-406.64	44.32	0.1348
Air Temperature + Wind Speed	-405.00	45.96	0.2043
Wind Speed + Solar Radiation + Daily Precipitation	-394.13	56.83	0.0968
Relative Humidity	-388.24	62.71	0.0708
Air Temperature + Daily Precipitation	-379.76	71.19	0.1290
Air Temperature	-378.09	72.87	0.1963
Wind Speed + Solar Radiation	-375.22	75.74	0.1018
Solar Radiation + Daily Precipitation	-360.10	90.85	0.0601
Solar Radiation	-341.64	109.32	0.0647

Table A.35. Coefficients and variance components estimates for the top covariate model for daily dissolved oxygen data at YUCH-004.

Parameter	Coefficient	SE	p-value
ar1	0.93	0.01	< 0.0001
ma1	0.24	0.03	< 0.0001
intercept	9.64	0.11	< 0.0001
Wind Speed	-0.08	0.01	< 0.0001
Relative Humidity	-0.01	0.00	< 0.0001

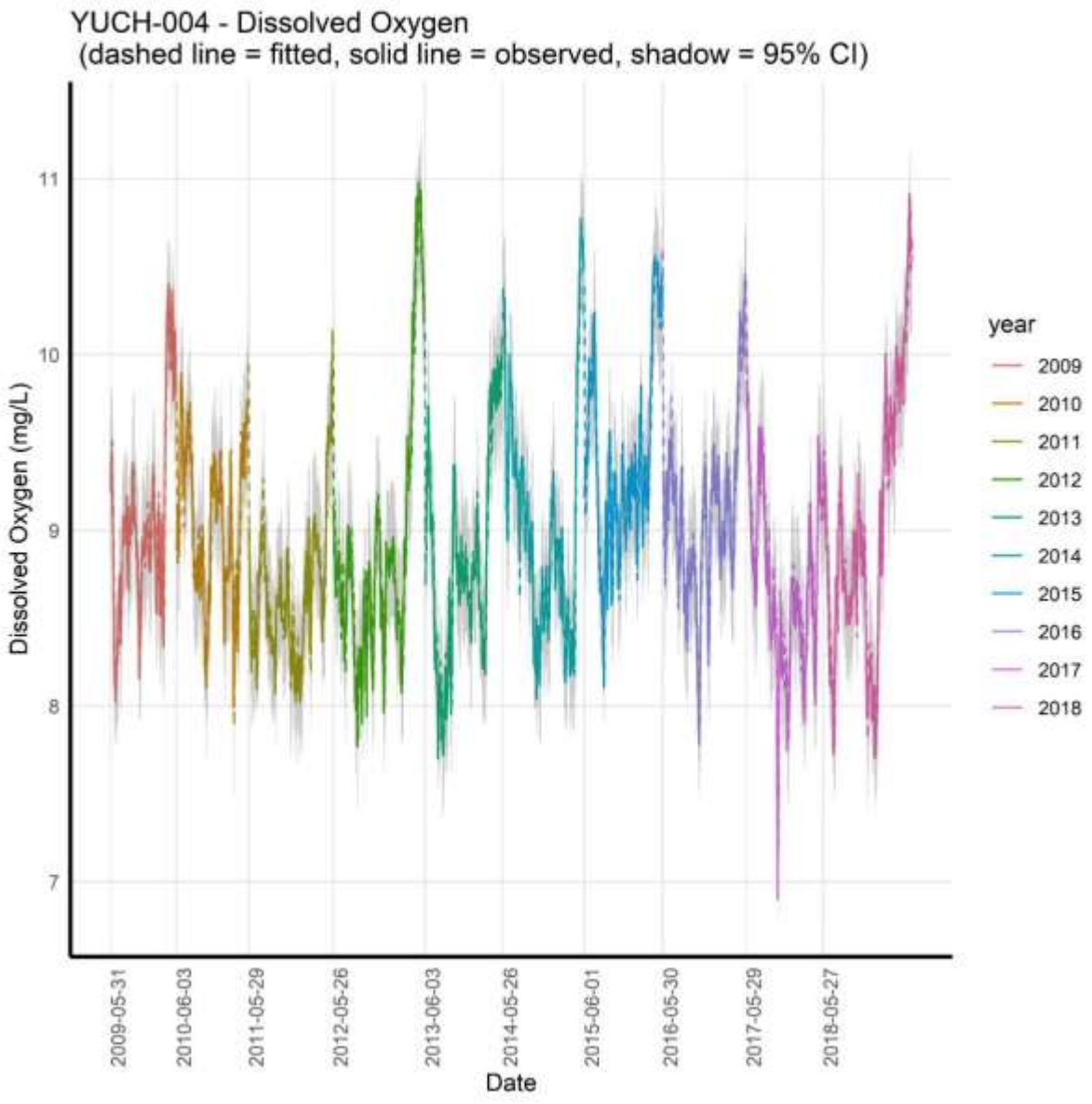


Figure A.32. Model predictions of YUCH-004 dissolved oxygen by date.

YUCH-005

Data

For lake YUCH-005, dissolved oxygen was recorded from 2009-2019 and 1019 dissolved oxygen observations were collected in the months May through September. When truncating the data to the subset of 20 days that were visited in every year, the dataset was reduced to 220 observations. Covariate data for air temperature, wind speed, solar radiation, and relative humidity were absent for 2019, thus this year was not included in the ARIMA covariate models. Additionally, there were three observations for dissolved oxygen that were less than zero.

Model Selection

The truncated data model with unlogged data was the only trend model that yielded stationary residuals. The trend coefficient for this model was positive, but it was not significantly different from zero. For ARIMA models fitting all possible combinations of covariate combinations, none of the models yielded stationary residuals when modeling the daily dissolved oxygen data.

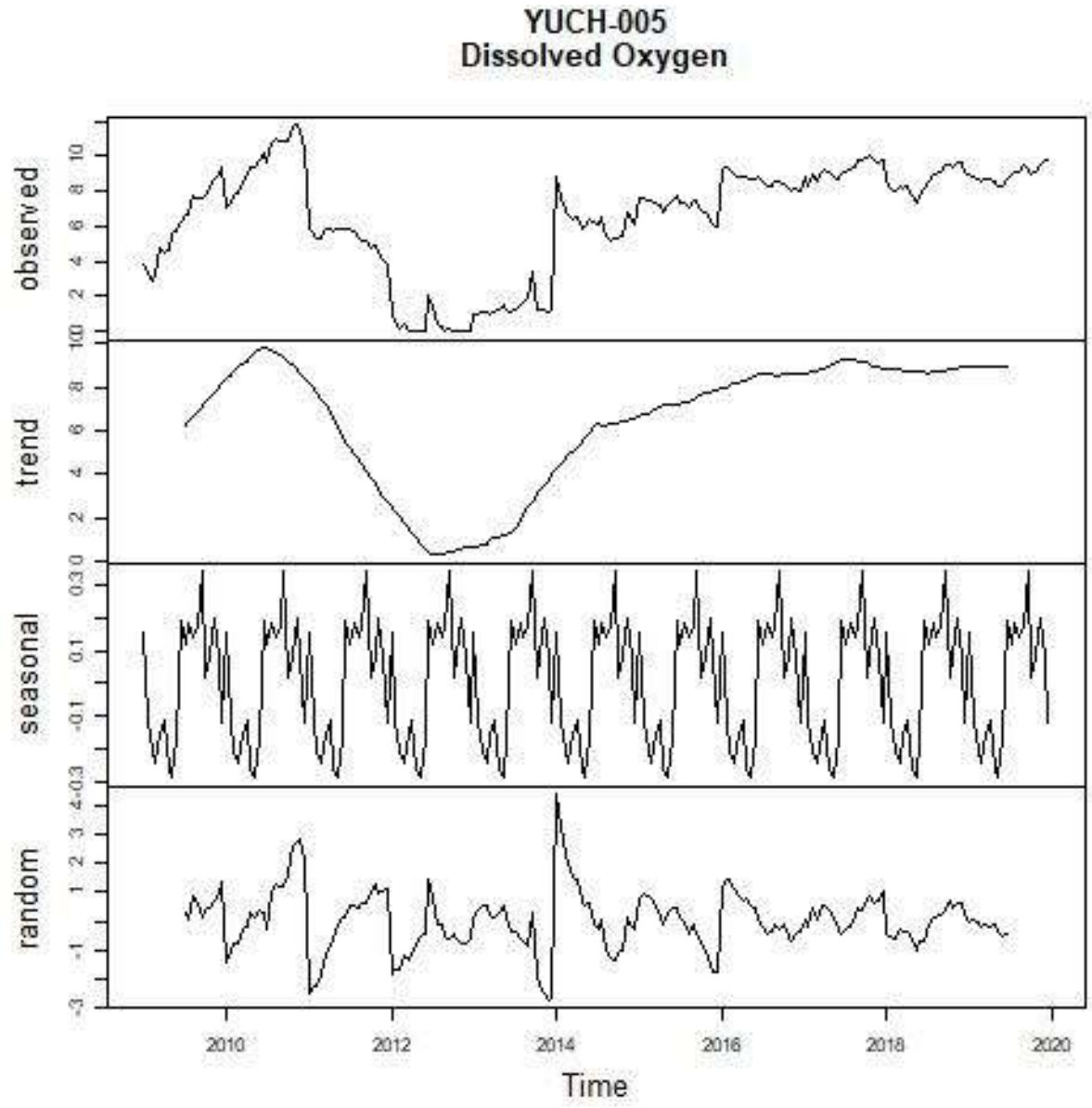


Figure A.33. Time series decomposition of truncated YUCH-005 dissolved oxygen by year.

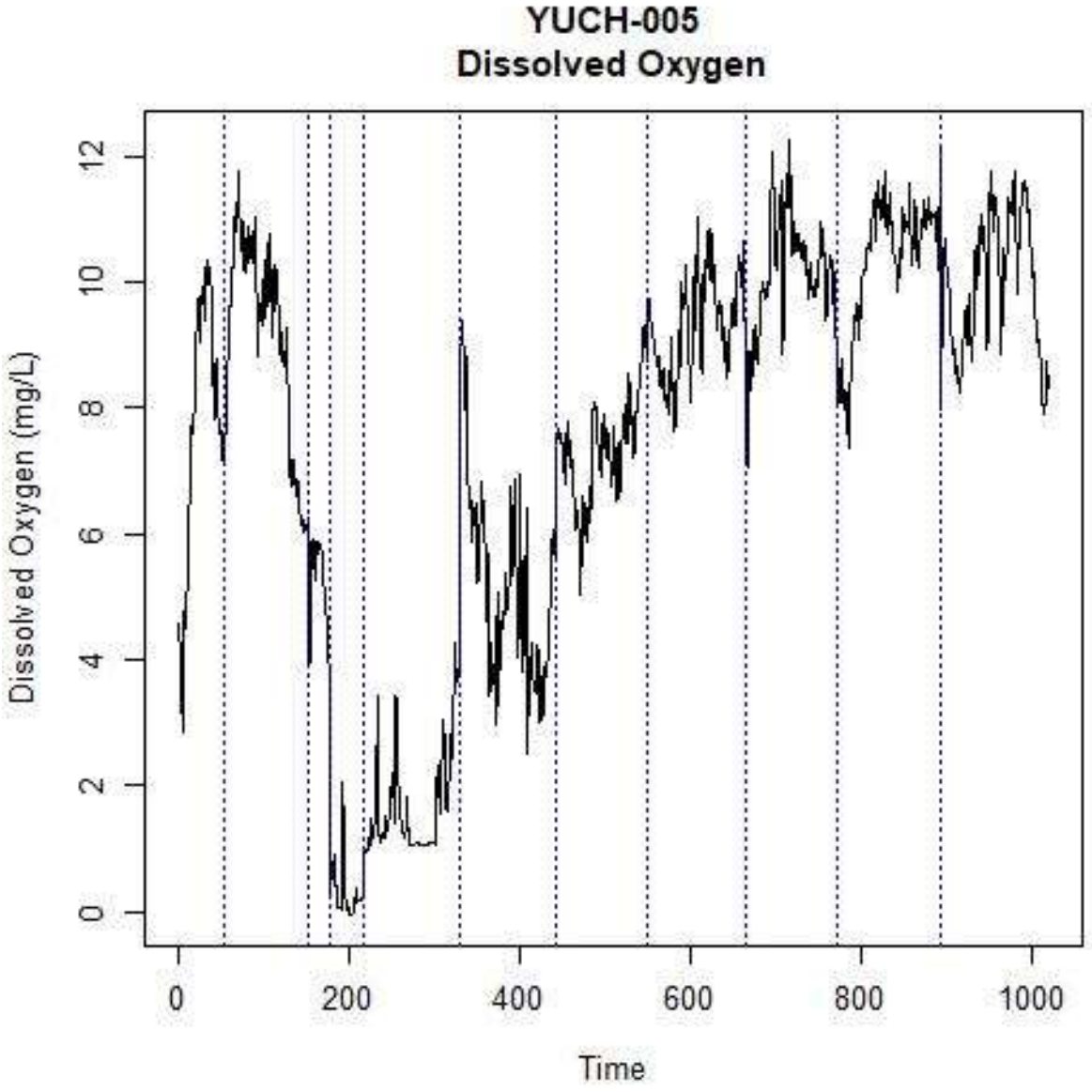


Figure A.34. Time series of YUCH-005 dissolved oxygen by time point with vertical lines for additive outliers.

Table A.36. Trend modeling results for daily dissolved oxygen data at YUCH-005.

			Trend			ARMA order		Ljung-Box Test	
Logged	**Method**	**Intercept**	**Coefficient**	**SE**	**p-value**	**AR**	**MA**	**Statistic**	**p-value**
FALSE	complete	2.5010	0.4635	0.0475	< 0.0001	0	5	1158.72	< 0.0001
FALSE	completeAO	2.1640	0.4951	0.0479	< 0.0001	0	5	2198.51	< 0.0001
FALSE	trunc	2.6290	0.3878	0.2377	0.1028	1	0	40.65	0.2355

			Trend			ARMA order		Ljung-Box Test	
Logged	**Method**	**Intercept**	**Coefficient**	**SE**	**p-value**	**AR**	**MA**	**Statistic**	**p-value**
FALSE	truncSA	4.8727	0.1723	0.2207	0.4349	1	0	53.74	0.0370
TRUE	complete	2.0919	-0.0295	0.0729	0.6856	3	0	80.49	< 0.0001
TRUE	completeAO	1.3570	0.0390	0.0685	0.5686	3	0	137.76	< 0.0001
TRUE	trunc	NA	0.1495	0.0380	< 0.0001	2	0	66.56	0.0020
TRUE	truncSA								

Table A.37. Top covariate models for daily dissolved oxygen data at YUCH-005.

Model	**AICc**	**ΔAICc**	**Ljung-Box Test p-value**
Air Temperature	507.33	0.00	0.5242
Air Temperature + Wind Speed	507.97	0.64	0.4601
Wind Speed + Year	508.60	1.26	0.5478
Air Temperature + Year	508.69	1.36	0.3990
Air Temperature + Daily Precipitation	509.13	1.80	0.3860
Air Temperature + Wind Speed + Year	509.34	2.01	0.3234
Wind Speed	509.63	2.29	0.5716
Intercept Only	509.66	2.32	0.6448
Air Temperature + Wind Speed + Daily Precipitation	509.78	2.45	0.3199
Wind Speed + Solar Radiation	510.18	2.85	0.4105

Table A.38. Coefficients and variance components estimates for the top covariate model for daily dissolved oxygen data at YUCH-005.

Parameter	**Coefficient**	**SE**	**p-value**
ar1	0.96	0.02	< 0.0001
intercept	6.97	1.47	< 0.0001
Air Temperature	-0.04	0.02	0.0348

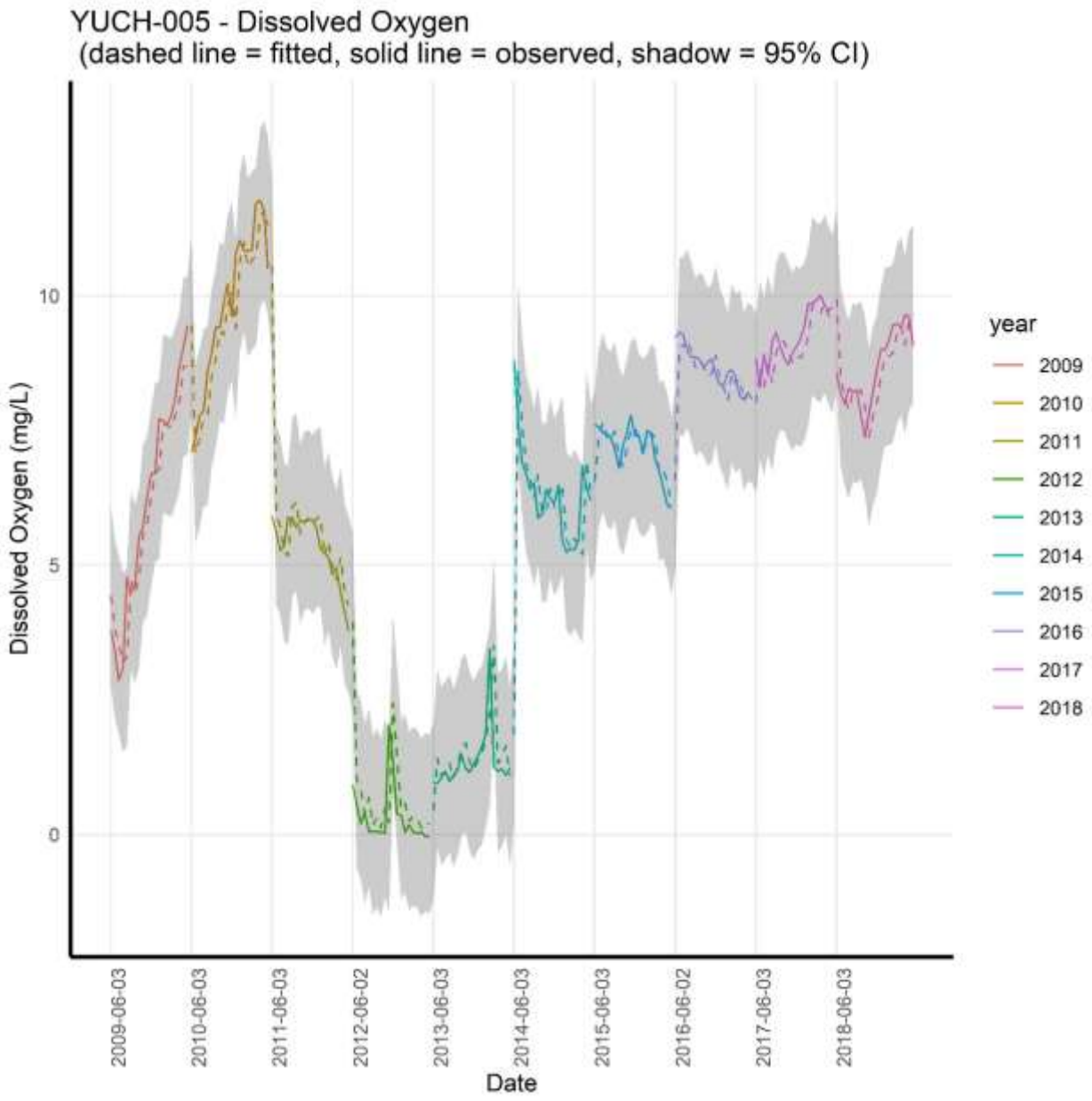


Figure A.35 Model predictions of YUCH-005 dissolved oxygen by date.

pH

BELA-088

Data

For the BELA-088 lake, pH was recorded from 2012 through 2019. However, 2013 was missing. Hence, analysis addressed 2014 through 2019. Over this period, there were 543 records of pH. Though data were generally collected from June to September, records started late in 2014 and ended early in 2018 and 2019. If truncated to the 72 days that were sampled every year, the dataset had 432 observations. Covariate coverage was poor in 2018 and 2019, so covariate models only considered 2014-2017. This left 363 records for covariate modeling.

Model Selection

For ARIMA models fitting all possible covariate combinations at lake BELA-088 with pH as the response variable, AICc-based model selection resulted in ARIMA(1,0,5) with relative humidity as the main covariate in the best model. Two trend models yielded independent residuals as assessed by the Ljung-Box test, but the models indicated trends in opposite directions. An assessment of the best covariate model containing a year term found a small precise positive trend (0.0039, SE = 0.0001). The overall evidence is inconclusive for a trend in pH at BELA-088.

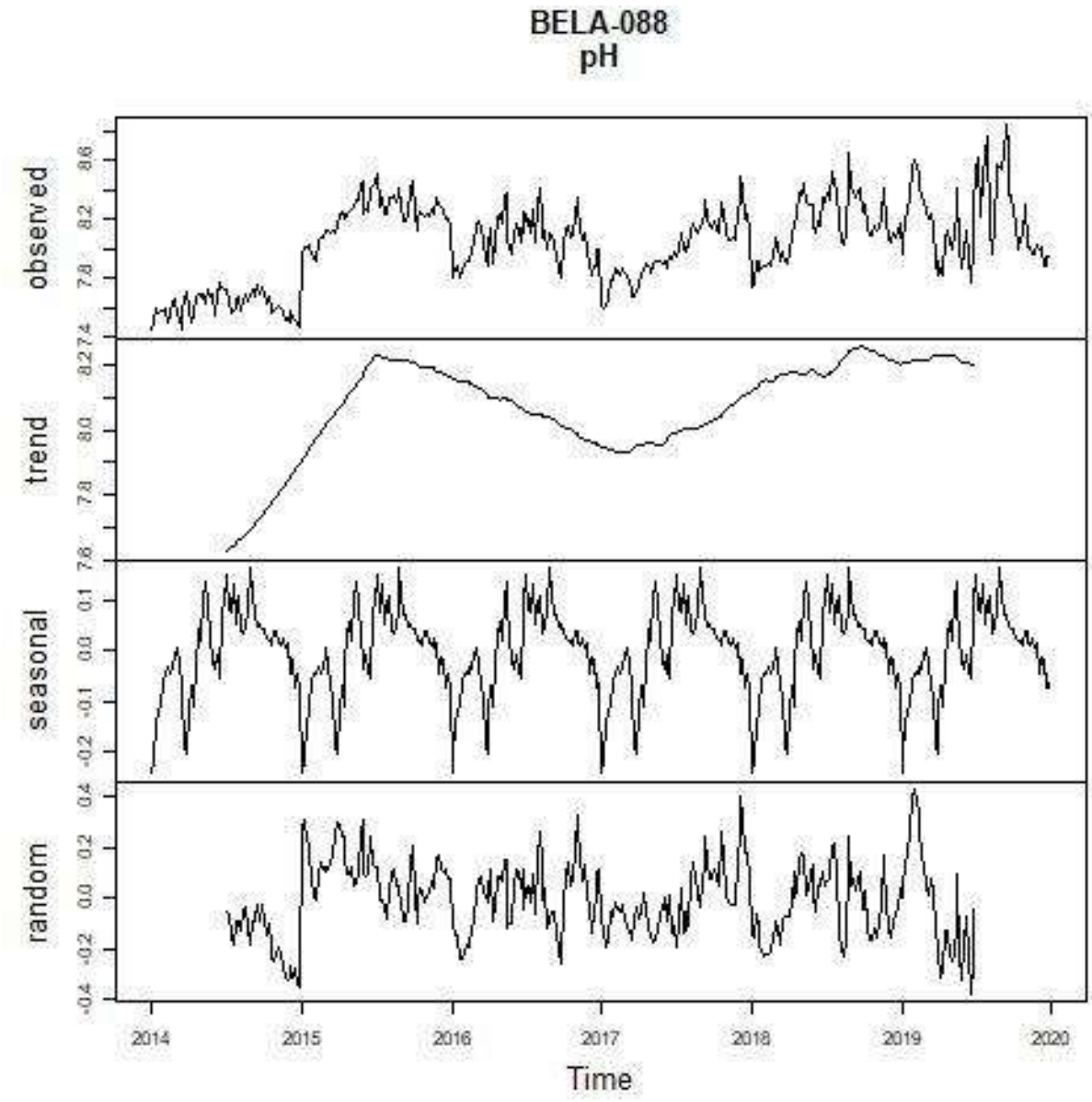


Figure A.36. Time series decomposition of truncated BELA-088 pH by year.

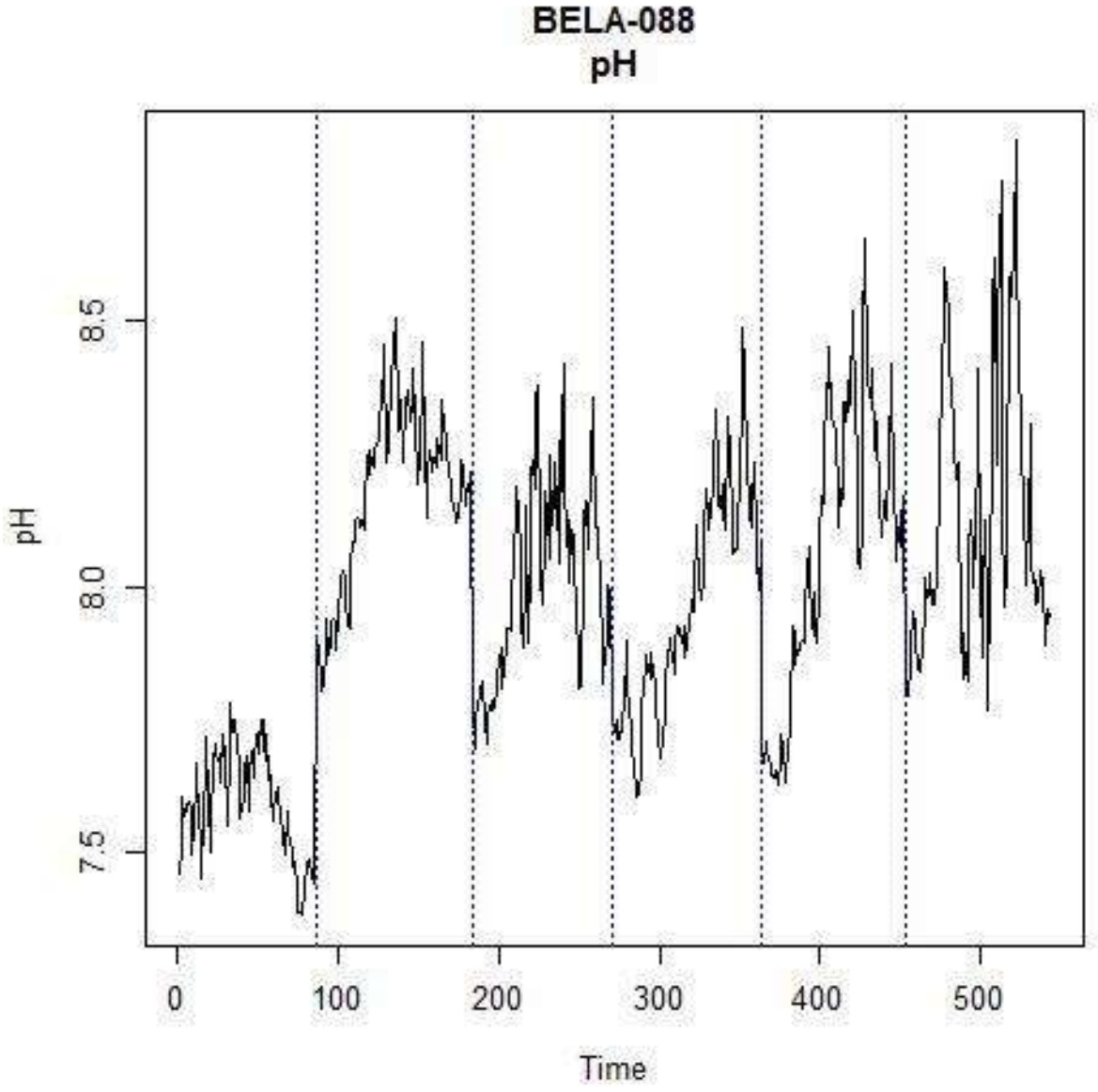


Figure A.37. Time series of BELA-088 pH by time point with vertical lines for additive outliers.

Table A.39. Trend modeling results for daily pH data at BELA-088.

			Trend			ARMA order		Ljung-Box Test	
Logged	**Method**	**Intercept**	**Coefficient**	**SE**	**p-value**	**AR**	**MA**	**Statistic**	**p-value**
FALSE	complete	9.8174	-0.1621	0.0475	0.0006	4	0	19.61	0.0006
FALSE	completeAO	9.6666	-0.1488	0.0814	0.0674	4	0	28.16	< 0.0001
FALSE	trunc	9.2468	-0.1104	0.0531	0.0375	1	3	82.51	0.4017

			Trend			ARMA order		Ljung-Box Test	
Logged	**Method**	**Intercept**	**Coefficient**	**SE**	**p-value**	**AR**	**MA**	**Statistic**	**p-value**
FALSE	truncSA	7.4133	0.0543	0.0239	0.0229	3	2	71.54	0.7123

Table A.40. Top covariate models for daily pH data at BELA-088.

Model	**AICc**	**ΔAICc**	**Ljung-Box Test p-value**
Relative Humidity	-808.60	0.00	0.2766
Relative Humidity + Year + Month	-807.23	1.37	0.0679
Wind Speed + Daily Precipitation	-805.76	2.83	0.1348
Air Temperature + Daily Precipitation	-805.13	3.47	0.0816
Daily Precipitation + Month	-800.45	8.15	0.1496
Daily Precipitation	-799.79	8.80	0.2539
Daily Precipitation + Year	-798.74	9.86	0.1592
Air Temperature	-796.92	11.68	0.4175

Table A.41. Coefficients and variance components estimates for the top covariate model for daily pH data at BELA-088.

Parameter	**Coefficient**	**SE**	**p-value**
ar1	0.98	0.01	< 0.0001
ma1	-0.06	0.05	0.2319
ma2	-0.18	0.05	0.0012
ma3	-0.09	0.05	0.1003
ma4	-0.12	0.06	0.0351
ma5	0.09	0.06	0.1137
intercept	8.09	0.14	< 0.0001
Relative Humidity	0.00	0.00	< 0.0001

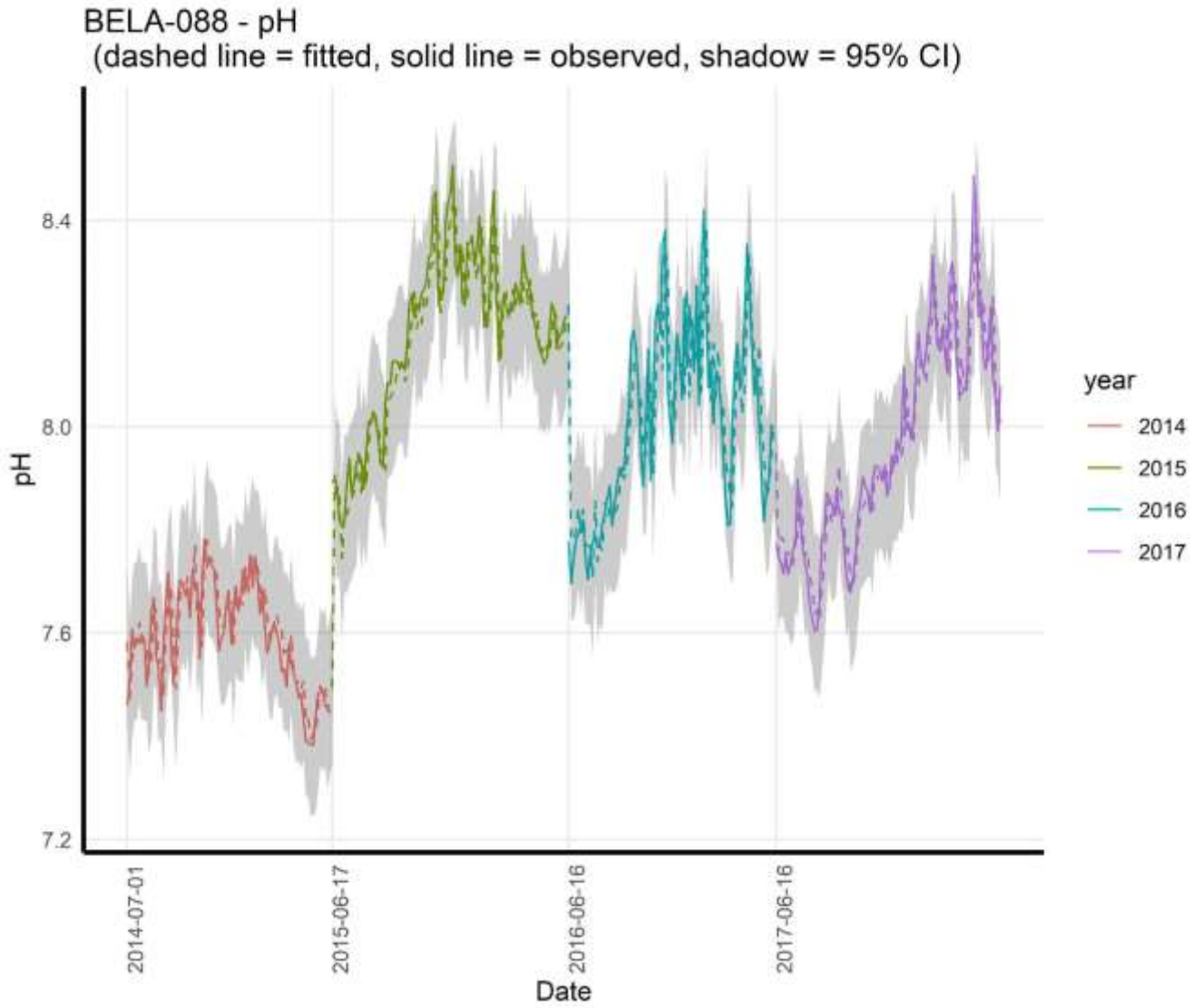


Figure A.38. Model predictions of BELA-088 pH by date.

BELA-108

Data

For the BELA-018 lake, pH was recorded from 2015 through 2019. Over this period, there were 456 records of pH. Data were collected from as early as mid-June to early September, with 86 days represented in all years. Truncated to the common set of days per year, the dataset had 430 observations. Covariate information was missing in 2018 for wind speed and solar radiation, so this year was removed for the covariate analysis.

Model Selection

The truncated trend model was unable to complete its fitting process and therefore could not be considered in model comparisons. For ARIMA models fitting all possible covariate combinations at lake BELA-018 with pH as the response variable, AICc-based model selection resulted in ARIMA(1,0,2) with solar radiation as the main covariate in the best model. Residuals showed higher variance at higher predicted values. The best trend model came from the complete data, an ARIMA(1,0,2) with no covariates, in which the trend was negative.

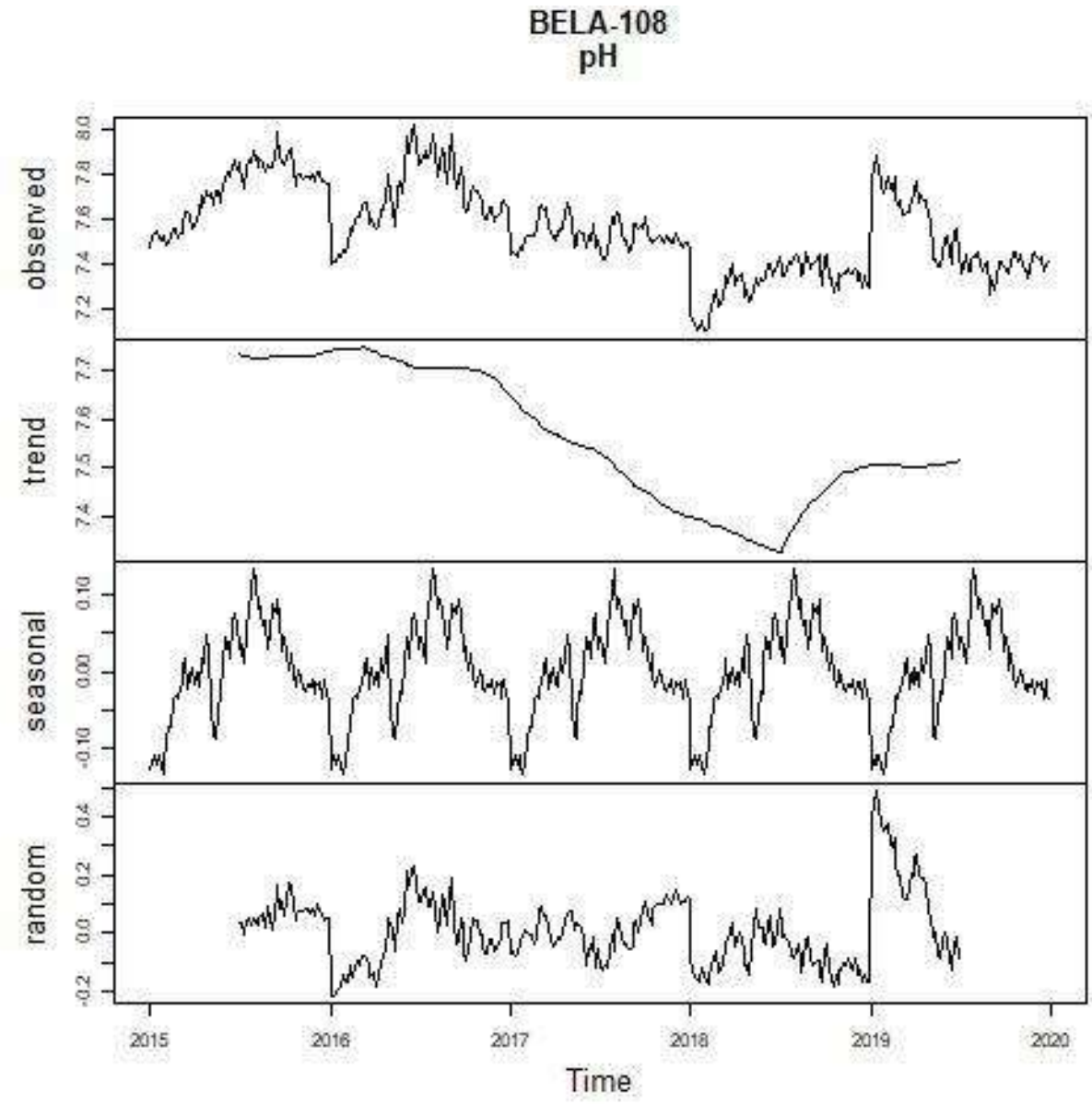


Figure A.39. Time series decomposition of truncated BELA-108 pH by year.

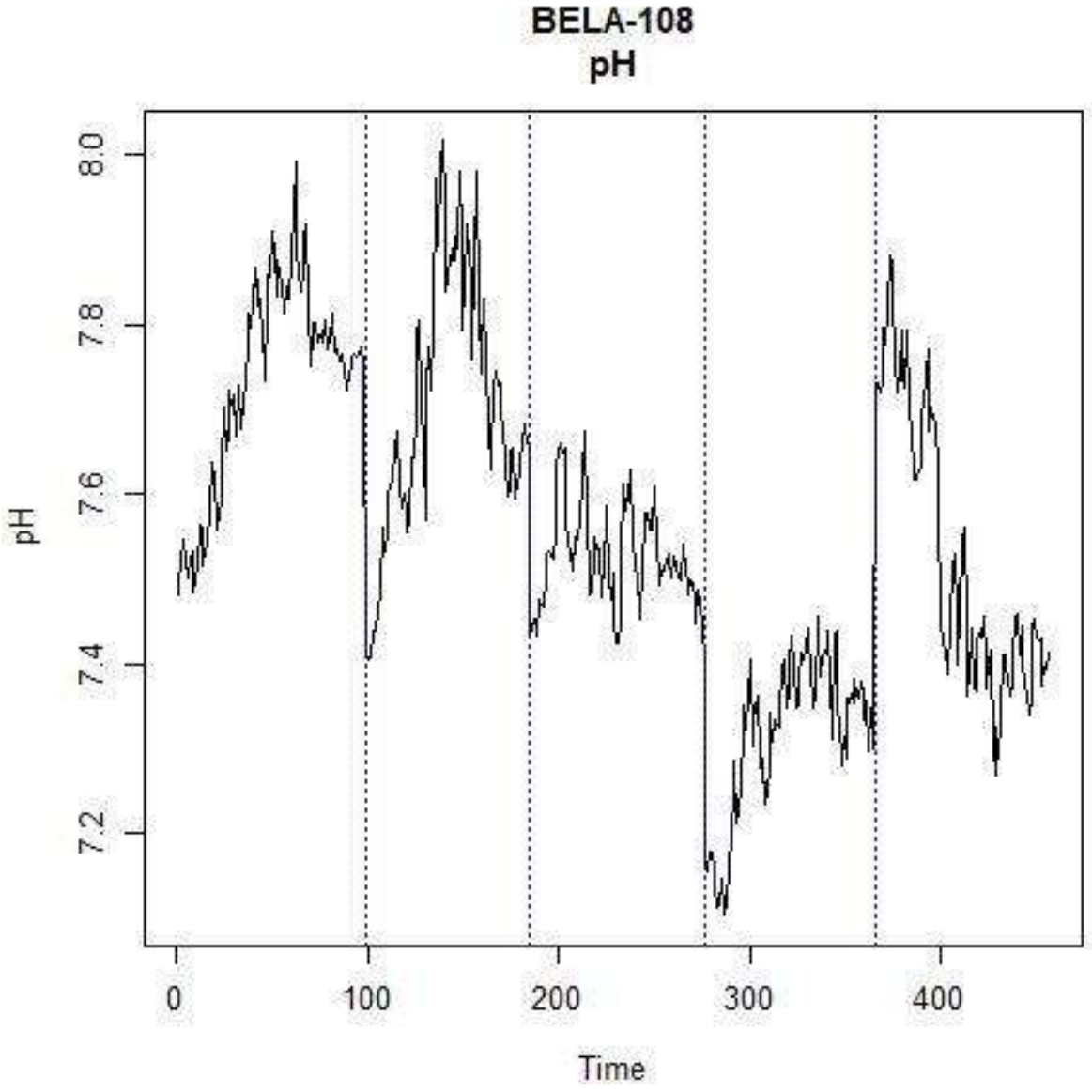


Figure A.40. Time series of BELA-108 pH by time point with vertical lines for additive outliers.

Table A.42. Trend modeling results for daily pH data at BELA-108.

			Trend			ARMA order		Ljung-Box Test	
Logged	**Method**	**Intercept**	**Coefficient**	**SE**	**p-value**	**AR**	**MA**	**Statistic**	**p-value**
FALSE	complete	8.5765	-0.0853	0.0201	< 0.0001	1	2	3.58	0.6114
FALSE	completeAO	8.5641	-0.0843	0.0239	0.0004	1	2	7.70	0.0526
FALSE	trunc	8.5811	-0.0856	0.0199	< 0.0001	1	2	66.02	0.8859
FALSE	truncSA	7.8862	-0.0274	0.0241	0.2556	1	2	79.43	0.5285

Table A.43. Top covariate models for daily pH data at BELA-108.

Model	**AICc**	**ΔAICc**	**Ljung-Box Test p-value**
Daily Precipitation + Month	-941.01	0.00	0.1217
Wind Speed + Month	-919.28	21.73	0.1442
Daily Precipitation	-880.27	60.74	0.1247
Air Temperature + Daily Precipitation	-880.13	60.88	0.0750
Wind Speed + Daily Precipitation	-878.31	62.70	0.0572
Relative Humidity	-869.63	71.38	0.0961
Intercept Only	-866.40	74.61	0.1873
Air Temperature	-865.57	75.44	0.1195

Table A.44. Coefficients and variance components estimates for the top covariate model for daily pH data at BELA-108.

Parameter	**Coefficient**	**SE**	**p-value**
ar1	1.21	0.10	< 0.0001
ar2	-1.02	0.15	< 0.0001
ar3	0.76	0.11	< 0.0001
ma1	-0.20	0.13	0.1155
ma2	0.58	0.15	0.0001
intercept	7.10	0.09	< 0.0001
dailyprecipitation	-0.07	0.01	< 0.0001
Month	0.07	0.01	< 0.0001

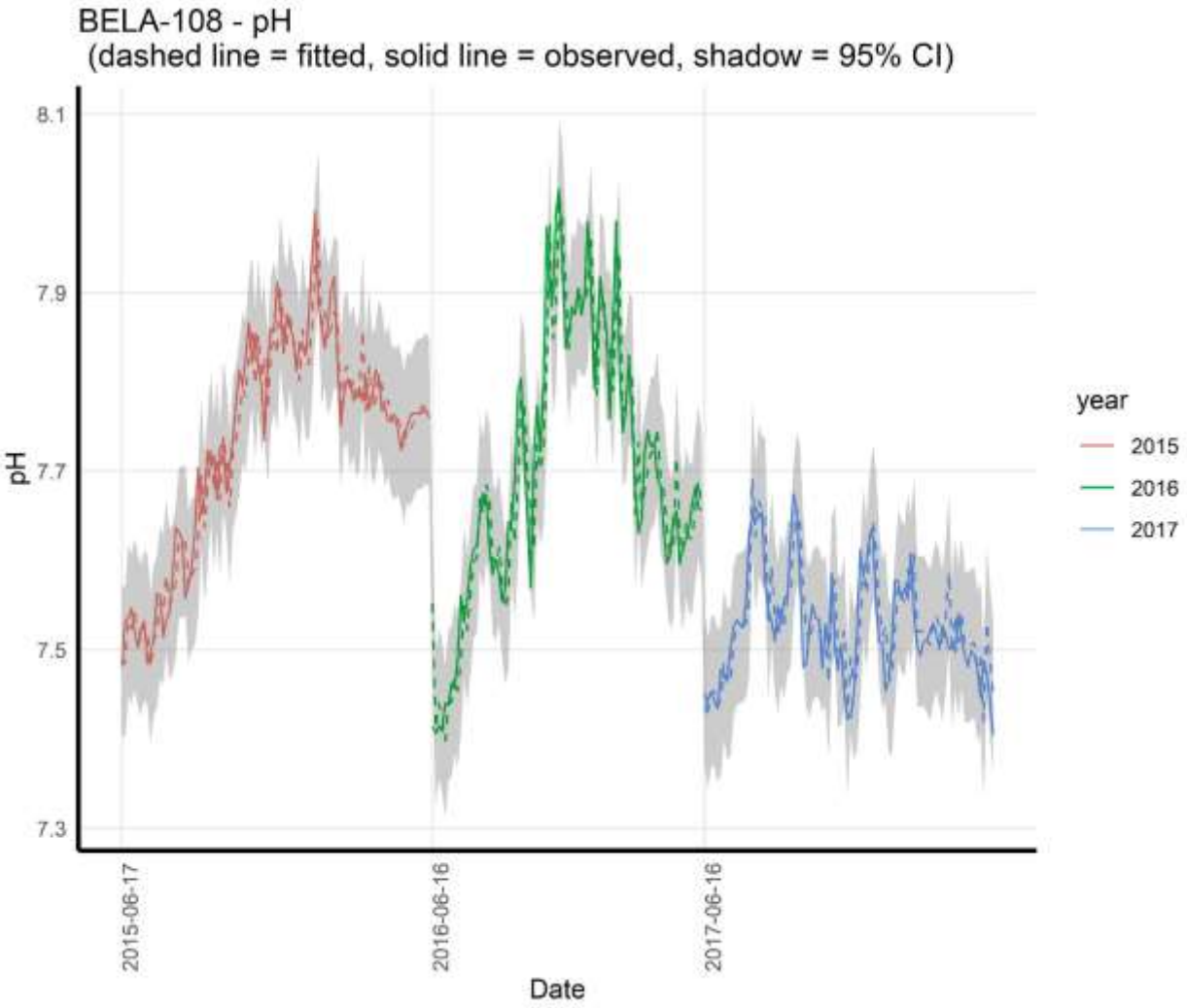


Figure A.41. Model predictions of BELA-108 pH by date.

DENA-018

Data

For the DENA-018 lake, pH was recorded from 2009 through 2019. However, no data was recorded in 2013, so the analysis only addressed 2014-2019. Over this period, there were 696 records of pH. Data were collected from as early as late May to September, with 99 days represented in all years. Truncated to the common set of days per year, the dataset had 594 observations.

Model Selection

The truncated trend model was unable to complete its fitting process and therefore could not be considered in model comparisons. For ARIMA models fitting all possible covariate combinations at lake BELA-018 with pH as the response variable, AICc-based model selection resulted in ARIMA(1,0,2) with solar radiation as the main covariate in the best model. Residuals showed higher variance at higher predicted values. The best trend model came from the complete data, an ARIMA(1,0,2) with no covariates, in which the trend was negative.

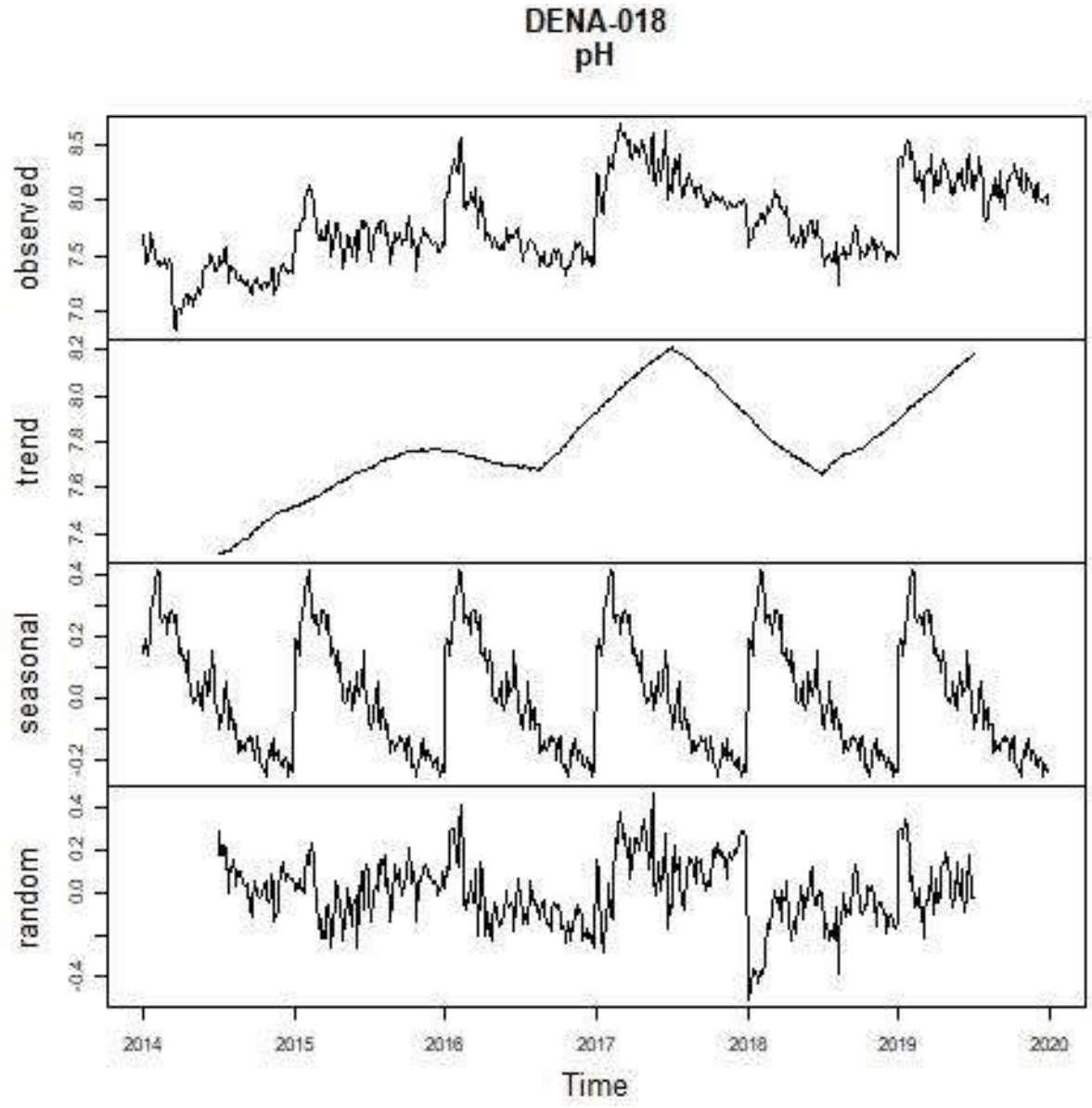


Figure A.42. Time series decomposition of truncated DENA-018 pH by year.

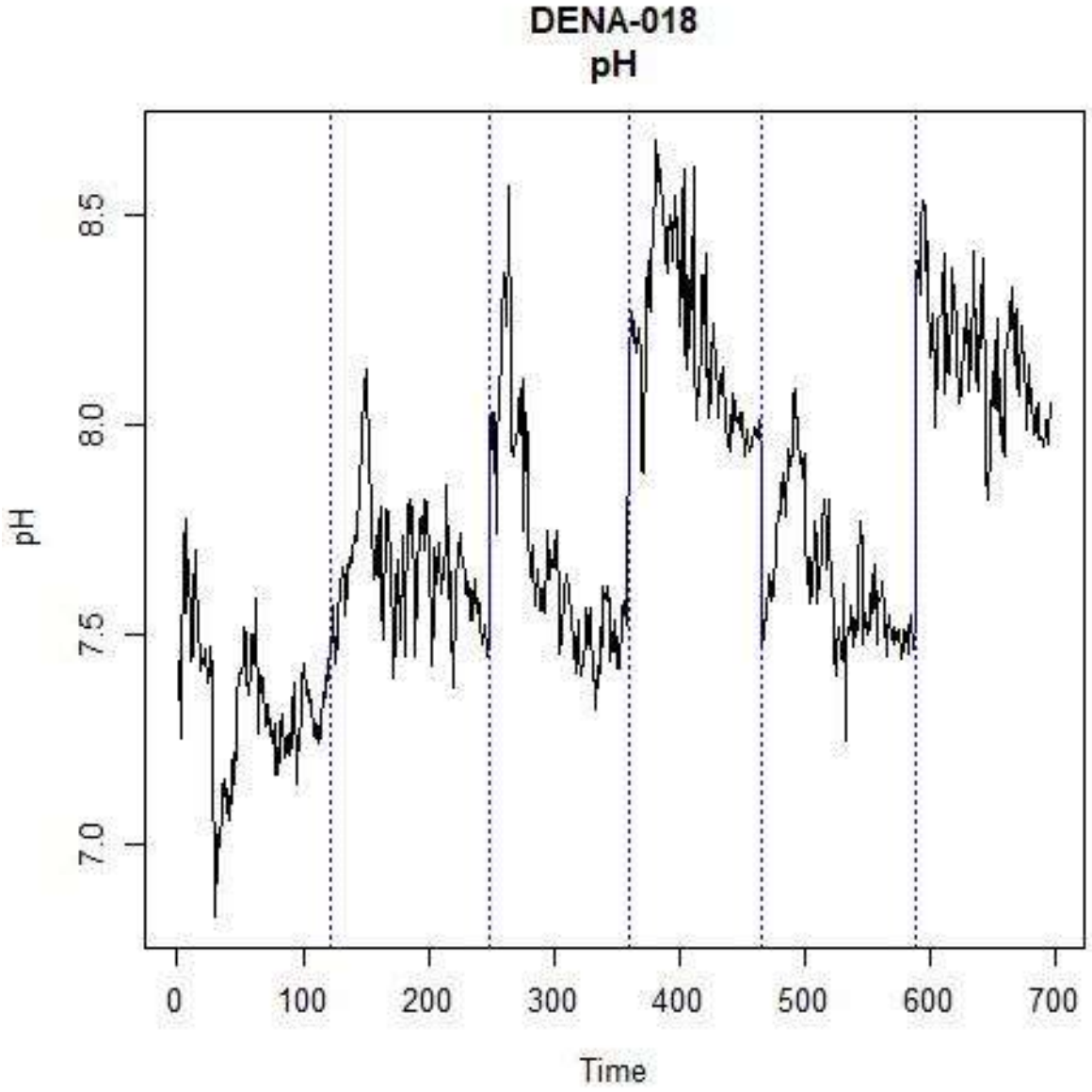


Figure A.43. Time series of DENA-018 pH by time point with vertical lines for additive outliers.

Table A.45. Trend modeling results for daily pH data at DENA-018.

			Trend			ARMA order		Ljung-Box Test	
Logged	**Method**	**Intercept**	**Coefficient**	**SE**	**p-value**	**AR**	**MA**	**Statistic**	**p-value**
FALSE	complete	3.7081	0.2807	0.0515	< 0.0001	1	3	4.31	0.3651
FALSE	completeAO	4.0475	0.2566	0.0795	0.0012	1	3	9.41	0.0243
FALSE	truncSA	7.1546	0.0441	0.0434	0.3091	2	2	172.75	0.0003

Table A.46. Top covariate models for daily pH data at DENA-018.

Model	AICc	ΔAICc	Ljung-Box Test p-value
Solar Radiation + Year	-952.83	0.00	0.5174
Solar Radiation + Daily Precipitation + Year	-950.76	2.07	0.3566
Relative Humidity + Year	-946.27	6.56	0.4501
Air Temperature + Daily Precipitation + Year	-917.35	35.48	0.1871
Air Temperature + Year	-913.81	39.02	0.2024
Wind Speed + Relative Humidity	-909.38	43.45	0.3583
Relative Humidity	-896.44	56.39	0.5037
Air Temperature + Wind Speed	-890.01	62.81	0.3483
Air Temperature + Daily Precipitation	-889.33	63.49	0.3346
Air Temperature	-886.54	66.29	0.2953

Table A.47. Coefficients and variance components estimates for the top covariate model for daily pH data at DENA-018.

Parameter	Coefficient	SE	p-value
ar1	0.95	0.02	< 0.0001
ma1	-0.11	0.05	0.0424
ma2	-0.14	0.05	0.0050
intercept	3.70	0.48	< 0.0001
Solar Radiation	0.00	0.00	< 0.0001
Year	0.29	0.03	< 0.0001

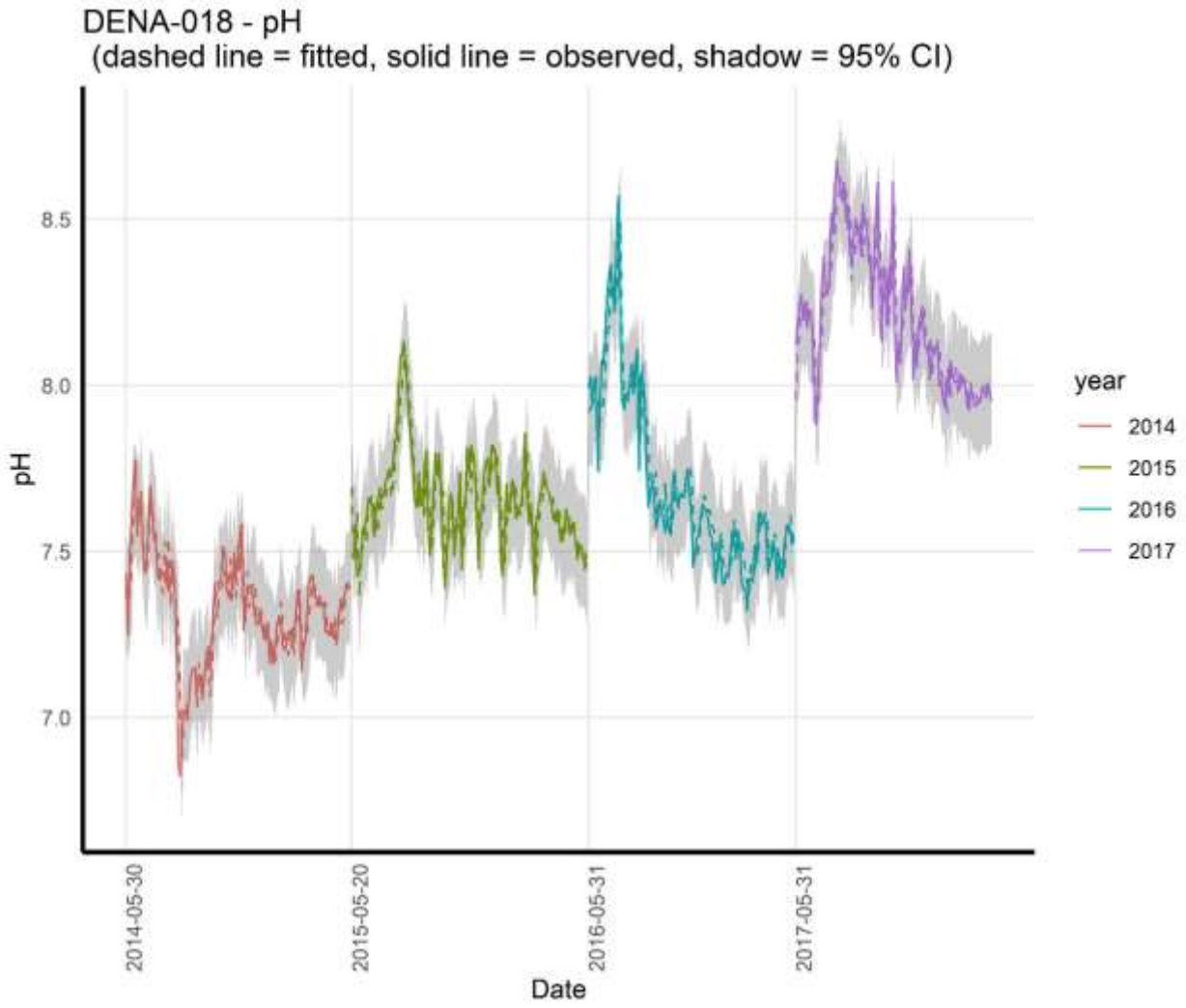


Figure A.44. Model predictions of DENA-018 pH by date.

DENA-023

Data

For DENA-023, pH was recorded from 2011 through 2019. Over this period, there were 969 records of pH. Data were collected from as early as late May to September. Sampling appears to have ended in July in 2019, making that year short. Truncated to the common set of days per year, the dataset had 405 observations. An alternate analysis discarded 2019 to maximize within-year coverage and total record count, but reached similar conclusions.

Model Selection

For ARIMA models fitting all possible covariate combinations at lake DENA-023 with pH as the response variable, AICc-based model selection resulted in ARIMA(3,0,1) with air temperature, wind speed, and daily precipitation as the main covariates in the best model. The best trend model came from the complete data, an ARIMA(3,0,1) with no covariates, in which the trend was negative.

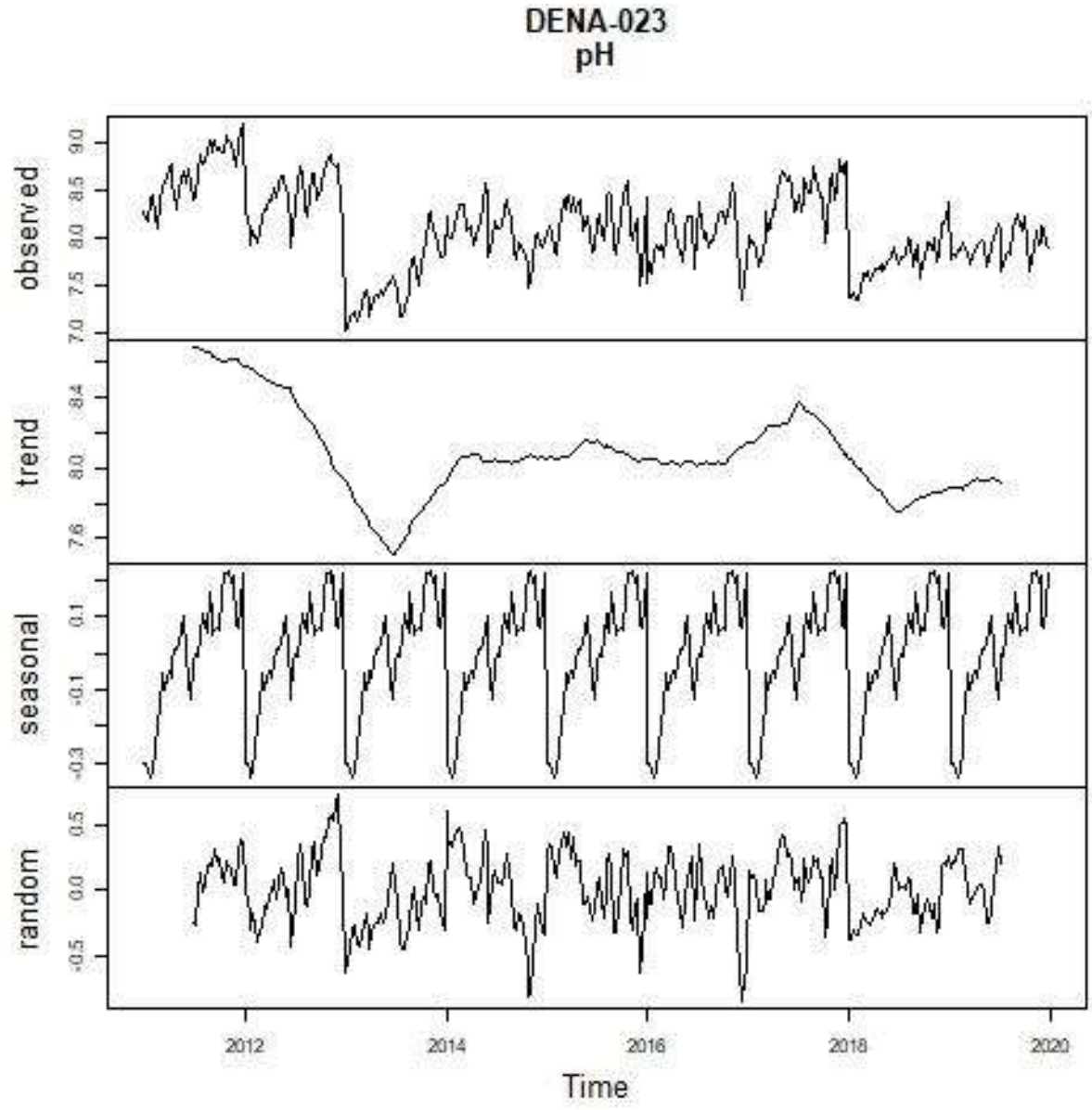


Figure A.45. Time series decomposition of truncated DENA-023 pH by year.

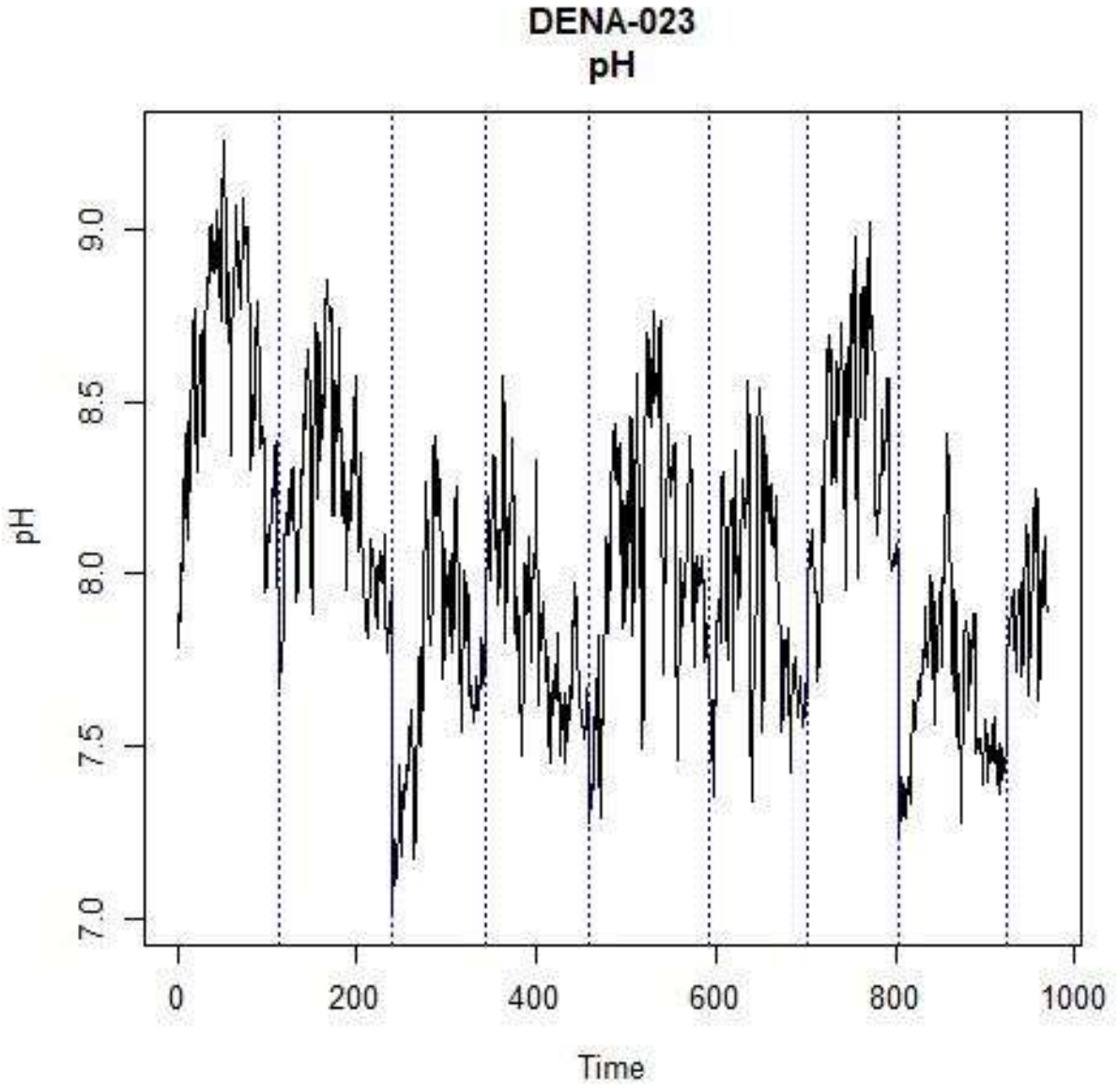


Figure A.46. Time series of DENA-023 pH by time point with vertical lines for additive outliers.

Table A.48. Trend modeling results for daily pH data at DENA-023.

			Trend			ARMA order		Ljung-Box Test	
Logged	**Method**	**Intercept**	**Coefficient**	**SE**	**p-value**	**AR**	**MA**	**Statistic**	**p-value**
FALSE	complete	9.3459	-0.1022	0.0367	0.0053	3	1	3.91	0.4178
FALSE	completeAO	8.9066	-0.0680	0.0332	0.0405	3	1	12.11	0.0070
FALSE	trunc	14.4123	-0.4861	0.0715	< 0.0001	2	1	124.73	0.0004

			Trend			ARMA order		Ljung-Box Test	
Logged	**Method**	**Intercept**	**Coefficient**	**SE**	**p-value**	**AR**	**MA**	**Statistic**	**p-value**
FALSE	truncSA	8.7117	-0.0472	0.0306	0.1237	1	3	118.47	0.0010

Table A.49. Top covariate models for daily pH data at DENA-023.

Model	**AICc**	**ΔAICc**	**Ljung-Box Test p-value**
Air Temperature + Wind Speed + Daily Precipitation	-839.63	0.00	0.0913
Air Temperature + Wind Speed	-833.25	6.38	0.0615
Wind Speed + Relative Humidity	-819.21	20.42	0.2930
Air Temperature + Daily Precipitation	-812.23	27.40	0.1914
Air Temperature	-803.98	35.64	0.2808
Relative Humidity + Year	-783.39	56.24	0.1419
Solar Radiation + Daily Precipitation	-780.79	58.83	0.1978
Solar Radiation	-777.46	62.17	0.1535
Relative Humidity	-773.96	65.67	0.3741
Wind Speed + Daily Precipitation	-769.00	70.62	0.2940

Table A.50. Coefficients and variance components estimates for the top covariate model for daily pH data at DENA-023.

Parameter	**Coefficient**	**SE**	**p-value**
ar1	1.73	0.07	< 0.0001
ar2	-0.92	0.08	< 0.0001
ar3	0.17	0.04	< 0.0001
ma1	-0.77	0.06	< 0.0001
intercept	7.85	0.12	< 0.0001
Air Temperature	0.02	0.00	< 0.0001
Wind Speed	-0.06	0.01	< 0.0001
Daily Precipitation	-0.04	0.02	0.0099

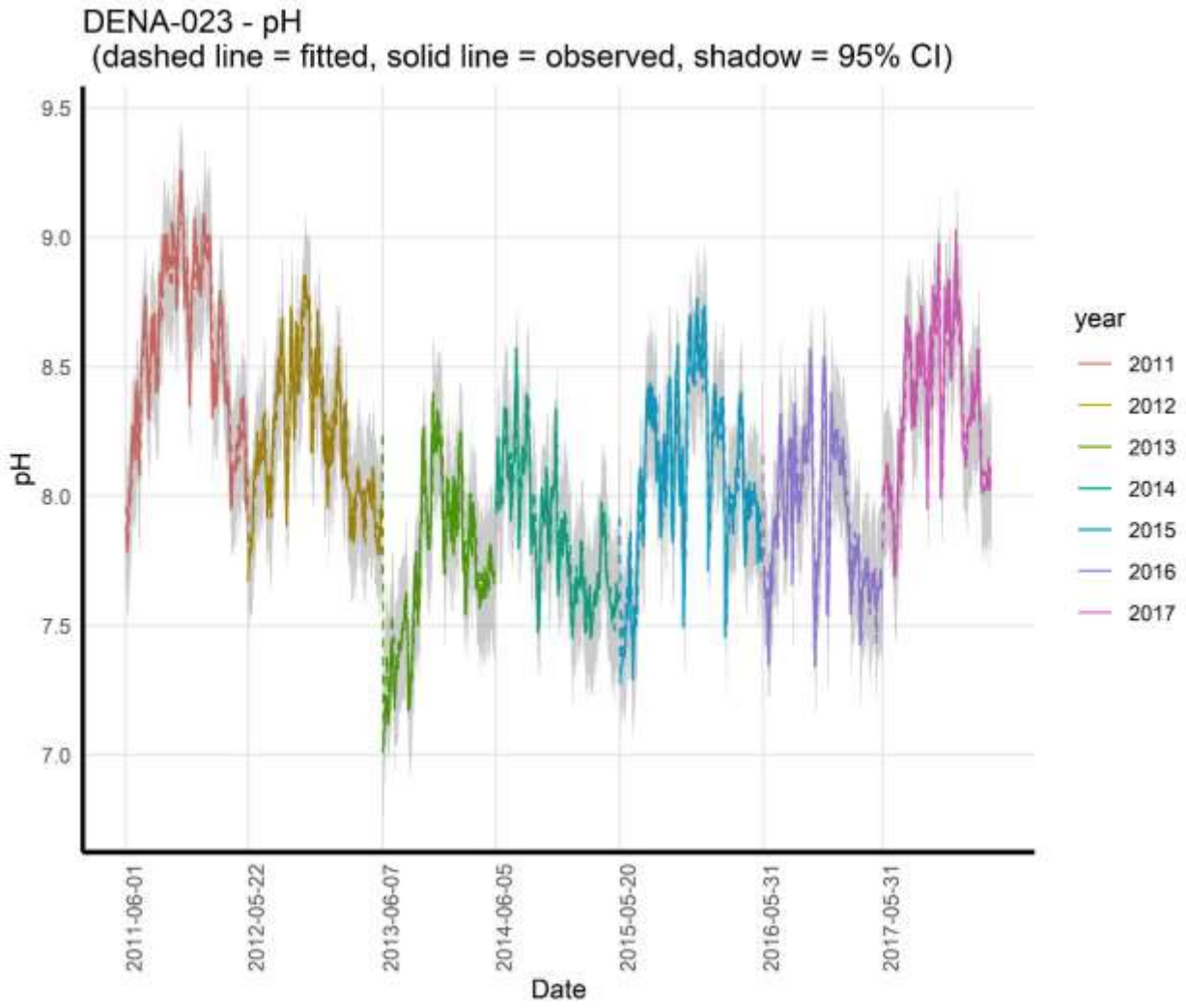


Figure A.47. Model predictions of DENA-023 pH by date.

KOVA-085

Data

For KOVA-085, pH was recorded from 2010 through 2018. Over this period, there were 801 records of pH. Data were collected from June to September. Sampling appears to have started later in 2012-2014. Truncated to the common set of days per year, the dataset had 594 observations.

Model Selection

The best trend model came from the truncated, seasonally adjusted data, an ARIMA(2,0,2) with no covariates, and the trend was negative. For ARIMA models fitting all possible covariate combinations at lake KOVA-085 with pH as the response variable, AICc-based model selection resulted in ARIMA(1,0,2) with relative humidity and month as the main covariates in the best model.

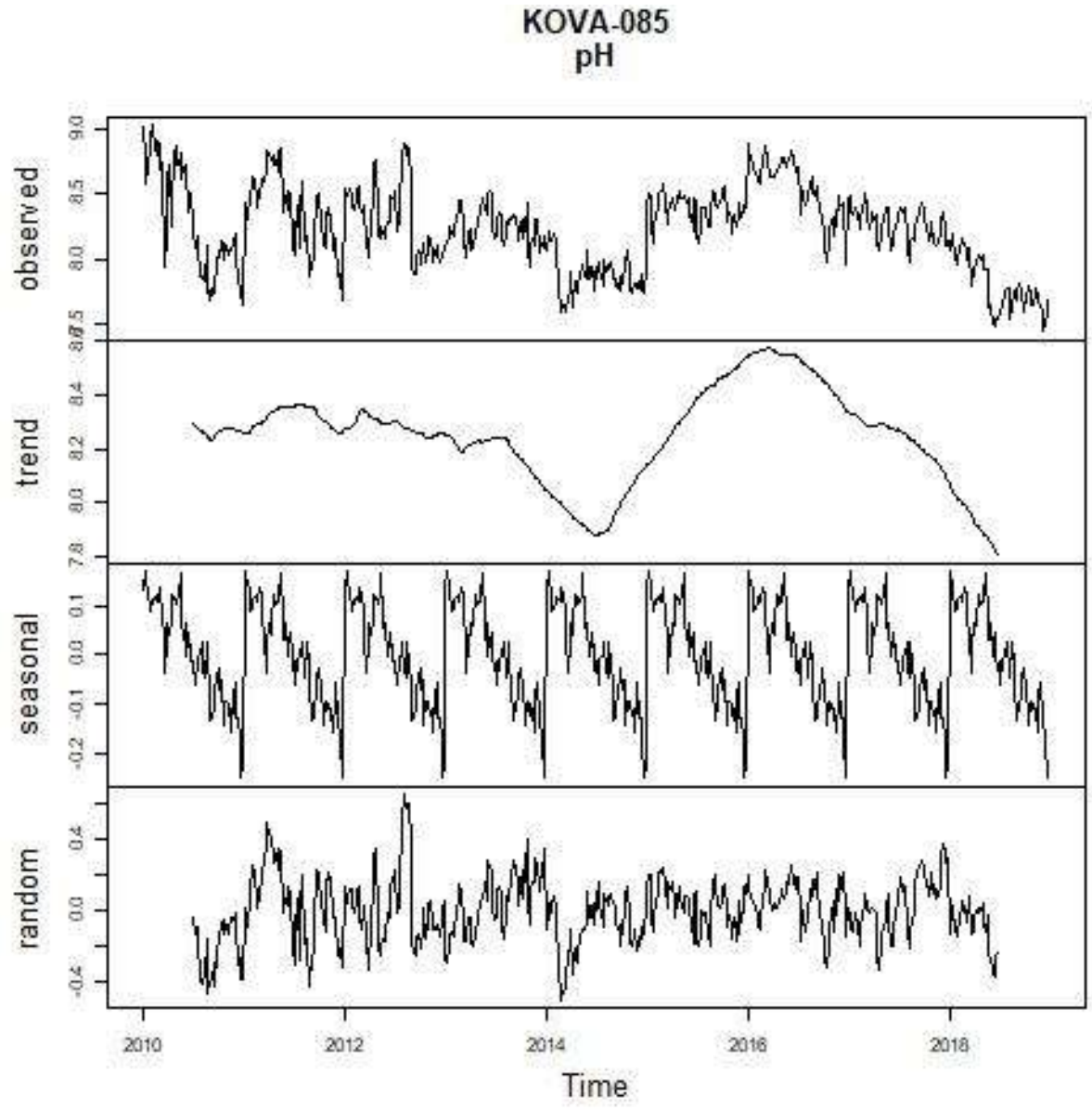


Figure A.48. Time series decomposition of truncated KOVA-085 pH by year.

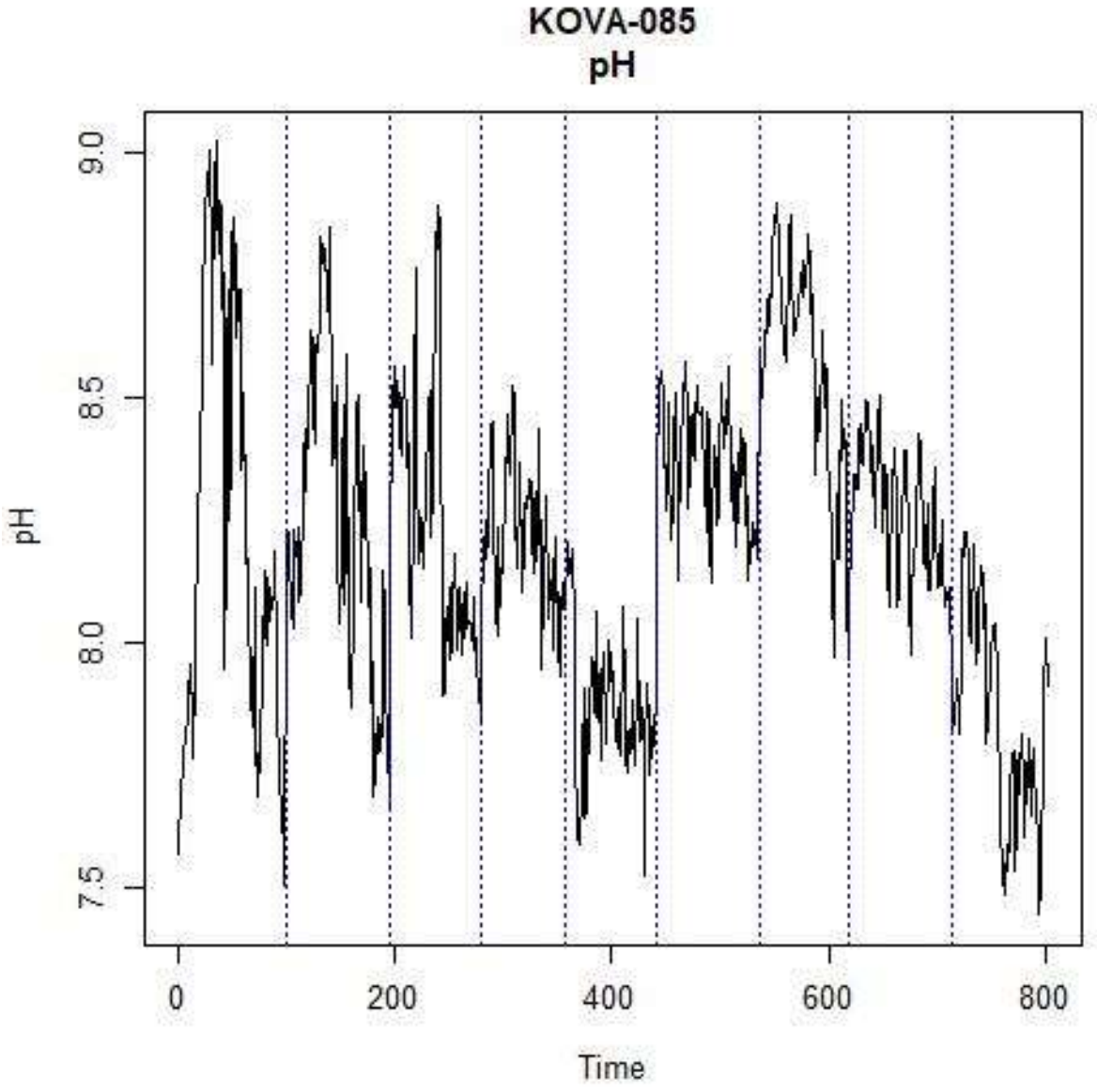


Figure A.49. Time series of KOVA-085 pH by time point with vertical lines for additive outliers.

Table A.51. Trend modeling results for daily pH data at KOVA-085.

			Trend			ARMA order		Ljung-Box Test	
Logged	**Method**	**Intercept**	**Coefficient**	**SE**	**p-value**	**AR**	**MA**	**Statistic**	**p-value**
FALSE	complete	8.2429	-0.0033	0.0079	0.6761	0	5	271.09	< 0.0001
FALSE	completeAO	7.7340	0.0414	0.0374	0.2686	3	1	17.51	0.0006
FALSE	trunc	8.5696	-0.0317	0.0066	< 0.0001	0	1	2730.15	< 0.0001

			Trend			ARMA order		Ljung-Box Test	
Logged	Method	Intercept	Coefficient	SE	p-value	AR	MA	Statistic	p-value
FALSE	truncSA	8.5630	-0.0298	0.0243	0.2210	2	2	109.83	0.5669

Table A.52. Top covariate models for daily pH data at KOVA-085.

Model	AICc	ΔAICc	Ljung-Box Test p-value
Relative Humidity + Month	-1079.42	0.00	0.0967
Year + Month	-1044.45	34.97	0.0646
Daily Precipitation + Month	-1041.76	37.67	0.0785
Wind Speed + Month	-1039.50	39.92	0.0624
Relative Humidity	-1029.44	49.98	0.3446
Relative Humidity + Daily Precipitation	-1027.93	51.49	0.2530
Wind Speed + Relative Humidity	-1027.58	51.84	0.2366
Solar Radiation	-1026.59	52.83	0.0525
Wind Speed + Relative Humidity + Daily Precipitation	-1026.12	53.30	0.1541
Daily Precipitation	-988.65	90.77	0.2958

Table A.53. Coefficients and variance components estimates for the top covariate model for daily pH data at KOVA-085.

Parameter	Coefficient	SE	p-value
ar1	0.95	0.02	< 0.0001
ma1	0.04	0.04	0.3559
ma2	-0.23	0.04	< 0.0001
intercept	9.14	0.12	< 0.0001
Relative Humidity	0.00	0.00	< 0.0001
Month	-0.09	0.01	< 0.0001

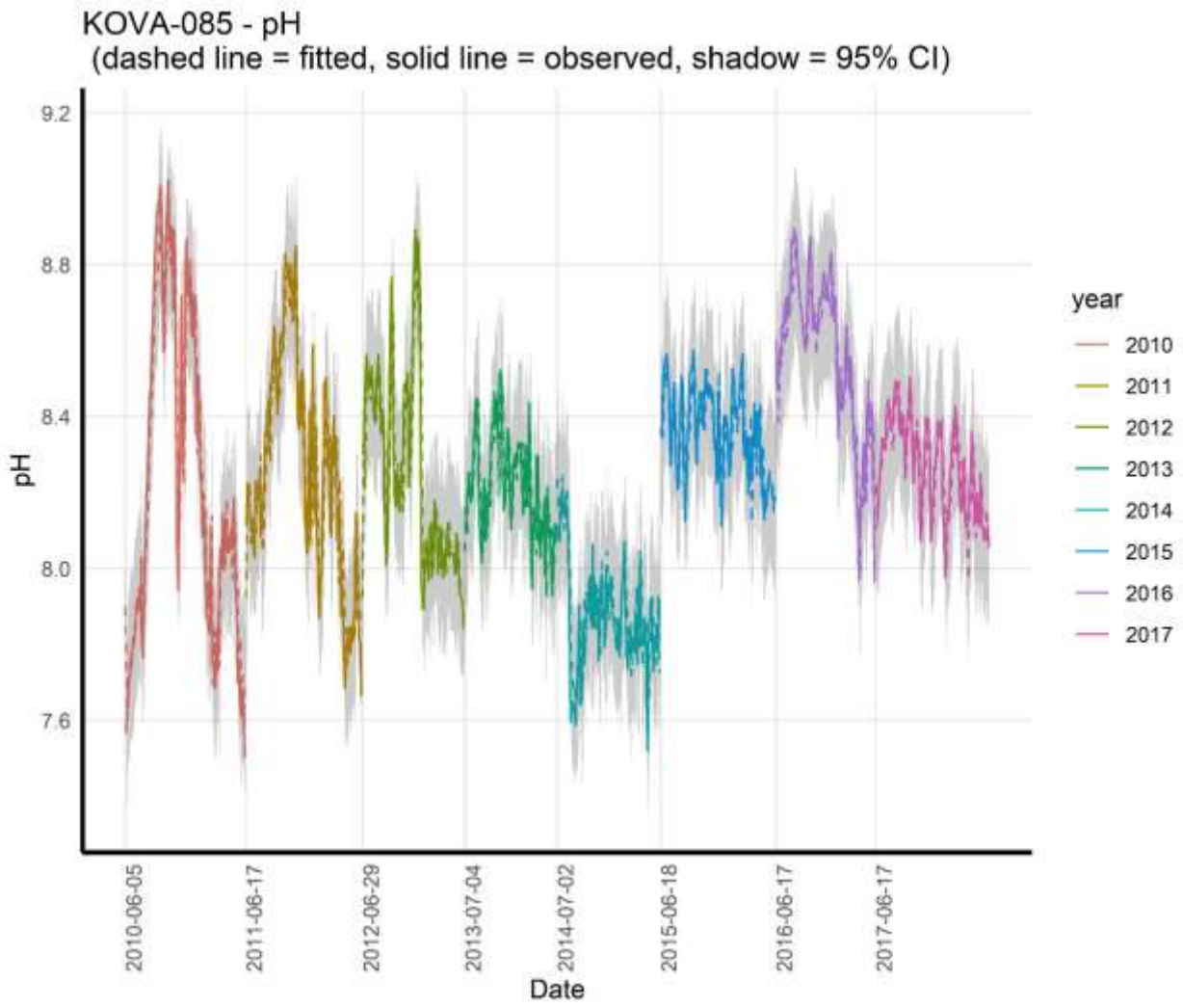


Figure A.50. Model predictions of KOVA-085 pH by date.

KOVA-086

Data

For the KOVA-086 lake, pH was recorded from 2009 through 2019. However, 2010 was missing so the analysis addressed 2011-2019. Over this period, there were 783 records of pH. Data were collected from a variable start date in June or July to a variable end date in August or September. Truncated to the common set of 59 days per year starting in July, the dataset had 531 observations.

Model Selection

For ARIMA models fitting all possible covariate combinations at lake KOVA-086 with pH as the response variable, AICc-based model selection resulted in ARIMA(1,0,3) with wind speed, relative humidity, and year as the main covariates in the best model. The environmental covariates were significant and year was marginally significant.

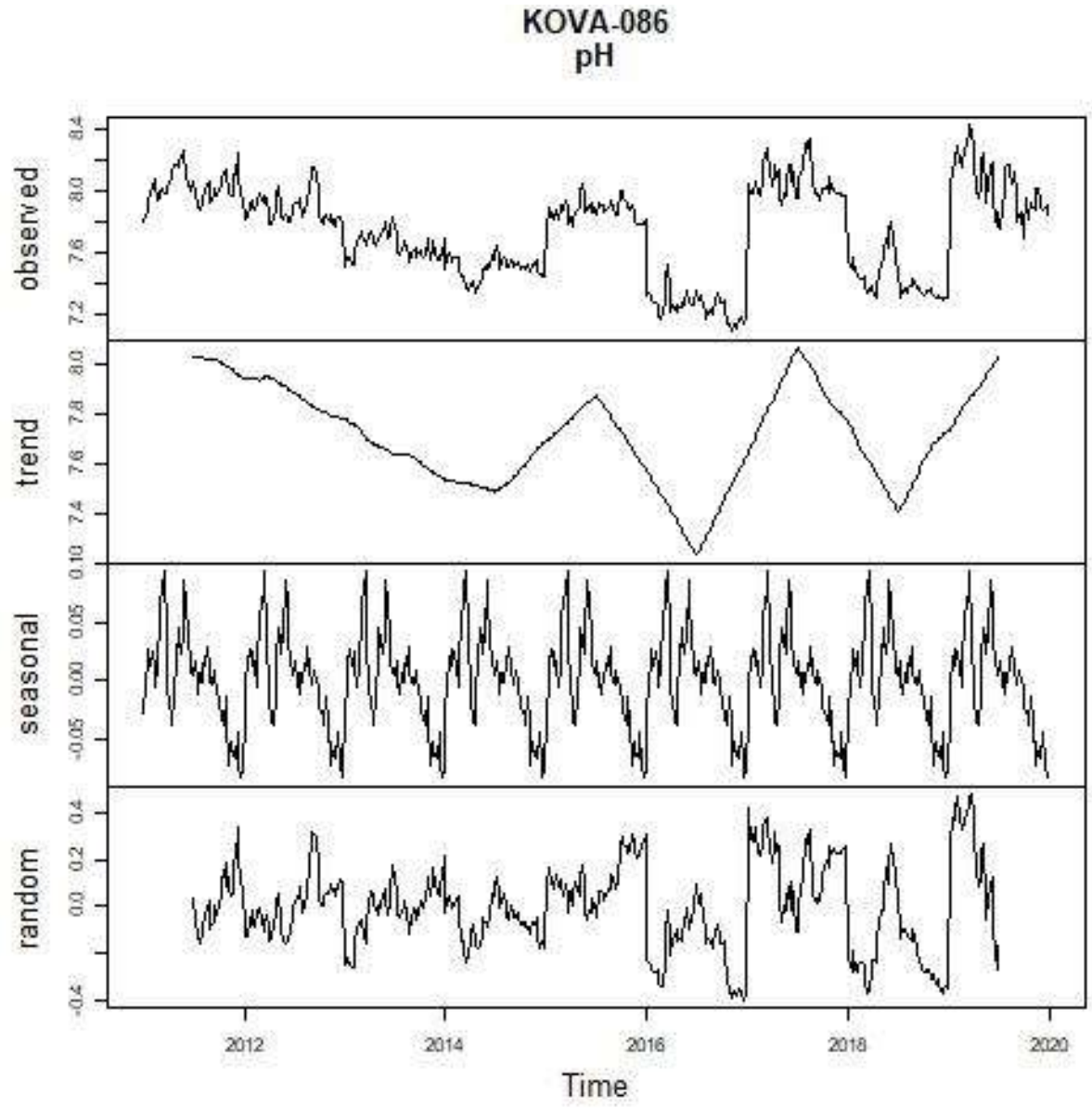


Figure A.51. Time series decomposition of truncated KOVA-086 pH by year.

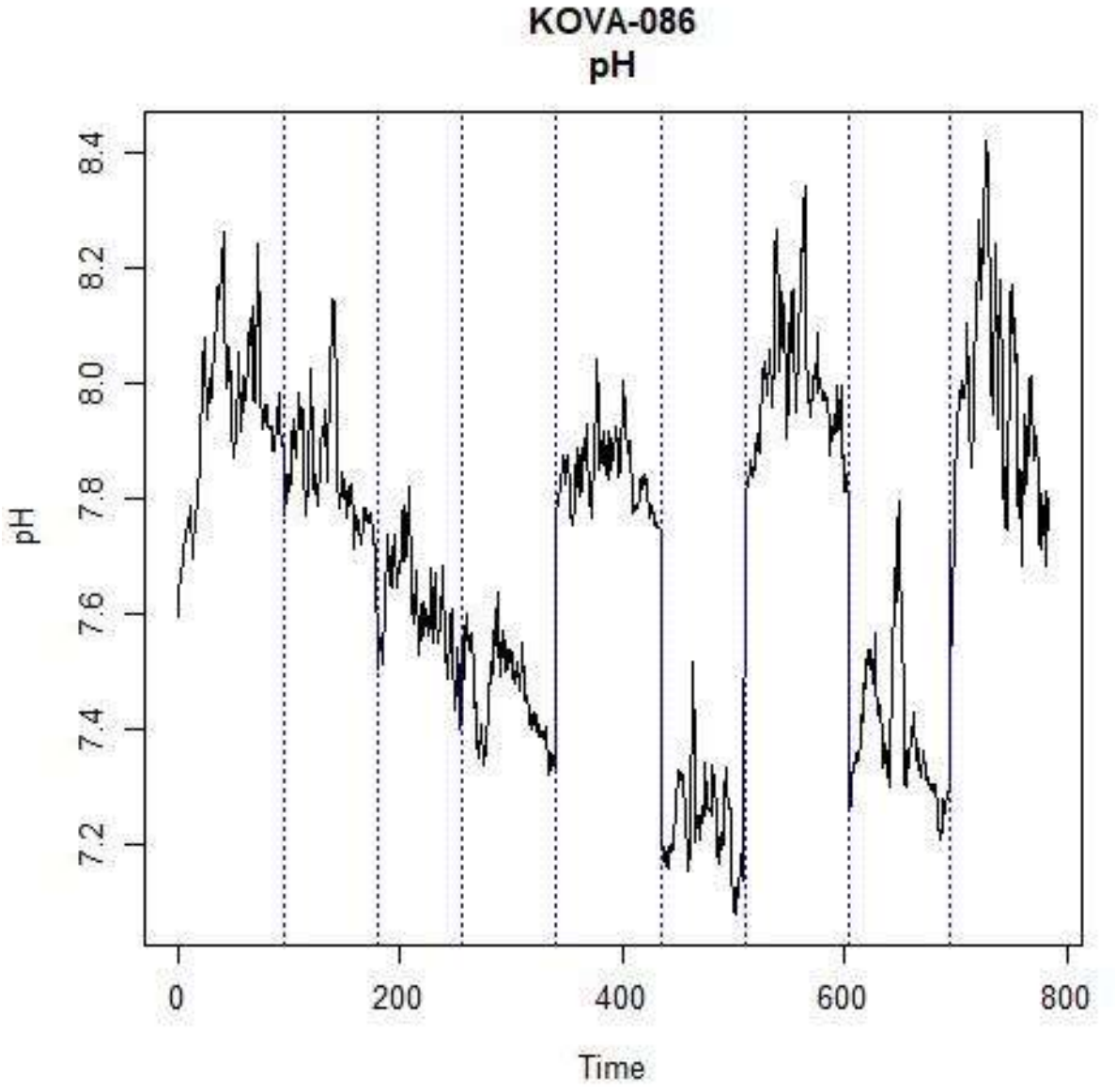


Figure A.52. Time series of KOVA-086 pH by time point with vertical lines for additive outliers.

Table A.54. Trend modeling results for daily pH data at KOVA-086.

			Trend			ARMA order		Ljung-Box Test	
Logged	**Method**	**Intercept**	**Coefficient**	**SE**	**p-value**	**AR**	**MA**	**Statistic**	**p-value**
FALSE	complete	7.5025	0.0180	0.0201	0.3686	1	2	2.56	0.7669
FALSE	completeAO	7.5696	0.0122	0.0232	0.5994	1	2	17.04	0.0007
FALSE	trunc	7.6727	0.0041	0.0154	0.7924	2	1	77.28	0.9554

			Trend			ARMA order		Ljung-Box Test	
Logged	Method	Intercept	Coefficient	SE	p-value	AR	MA	Statistic	p-value
FALSE	truncSA	7.8094	-0.0053	0.0209	0.8001	1	1	158.21	0.0003

Table A.55. Top covariate models for daily pH data at KOVA-086.

Model	AICc	ΔAICc	Ljung-Box Test p-value
Wind Speed + Relative Humidity + Year	-1631.29	0.00	0.1898
Wind Speed + Relative Humidity + Year + Month	-1624.43	6.86	0.1376
Wind Speed + Relative Humidity	-1623.60	7.69	0.3700
Wind Speed + Relative Humidity + Month	-1621.88	9.41	0.2563
Wind Speed + Solar Radiation + Year	-1620.80	10.48	0.3279
Relative Humidity + Year	-1620.60	10.69	0.3104
Relative Humidity + Year + Month	-1620.13	11.16	0.1977
Relative Humidity	-1620.04	11.25	0.4311
Wind Speed + Solar Radiation + Daily Precipitation + Year	-1618.98	12.31	0.1190
Relative Humidity + Daily Precipitation + Year	-1618.61	12.68	0.2178

Table A.56. Coefficients and variance components estimates for the top covariate model for daily pH data at KOVA-086.

Parameter	Coefficient	SE	p-value
ar1	-0.67	0.04	< 0.0001
ar2	0.70	0.02	< 0.0001
ar3	0.89	0.03	< 0.0001
ma1	1.71	0.02	< 0.0001
ma2	0.98	0.02	< 0.0001
intercept	7.34	0.28	< 0.0001
Wind Speed	-0.01	0.00	0.0430
Relative Humidity	0.00	0.00	0.0001
Year	0.04	0.02	0.0790

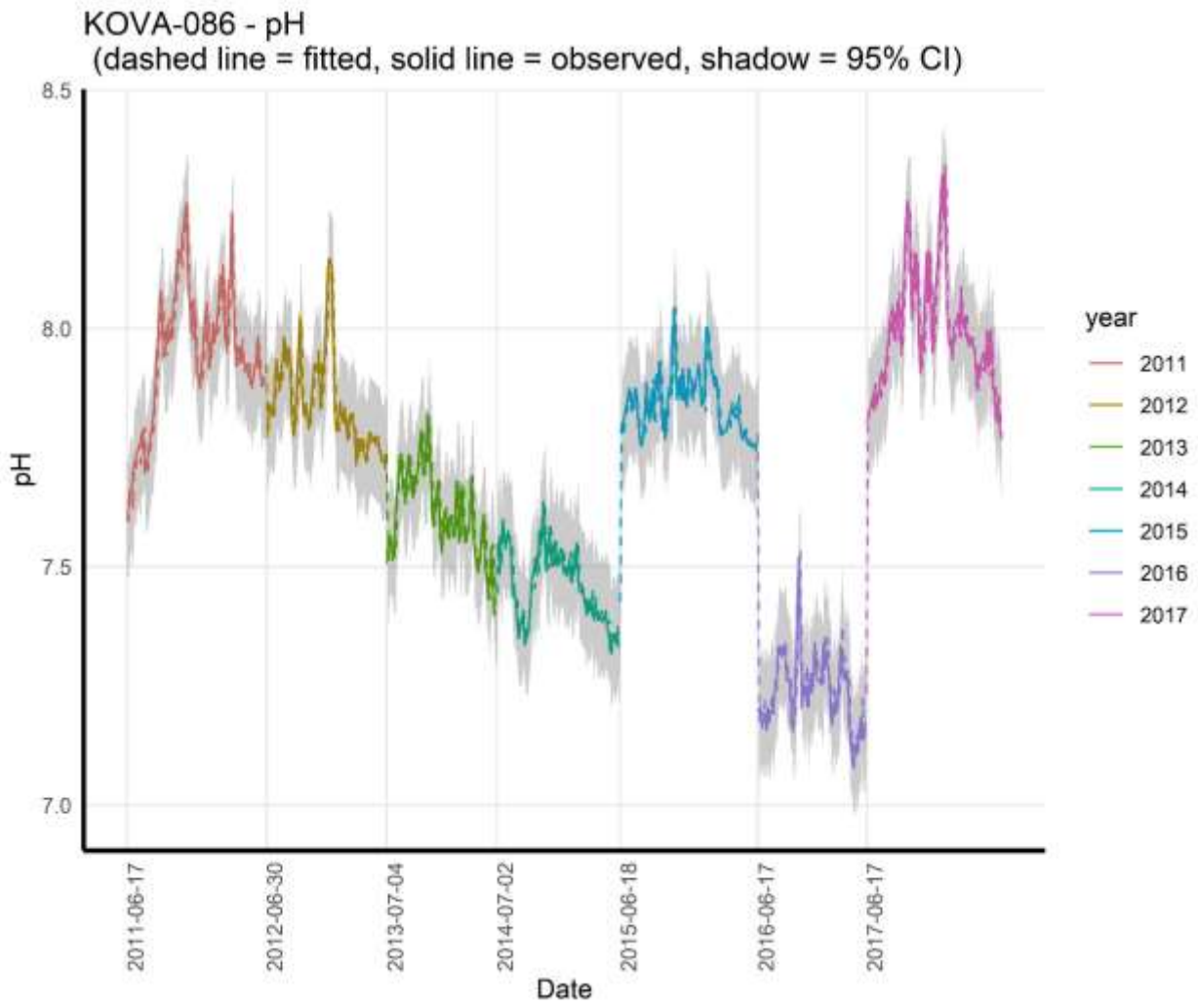


Figure A.53. Model predictions of KOVA-086 pH by date.

NOAT-052

Data

For the NOAT-052 lake, pH was recorded from 2015 through 2019. Over this period, there were 723 records of pH. Data were generally collected from June-September, but included winter and spring of 2016, as well. Therefore, we focus on the truncated analyses only for trend and covariate inference. Truncated to the common set of 85 days per year starting in July, the dataset had 425 observations.

Model Selection

For ARIMA models fitting all possible covariate combinations at lake KOVA-052 with pH as the response variable, AICc-based model selection resulted in ARIMA(1,0,1) with relative humidity and wind speed as the main covariates in the best model. The two truncated trend models yielded stationary results as assessed by the Ljung-Box test, but the trend estimates had very different magnitudes. The truncated model indicated a large positive trend, but the truncated seasonally adjusted model found no evidence of a significant trend. An assessment of the best covariate model that contained a year term found a small precise positive trend (0.0040, SE = 0.0001). The overall evidence is inconclusive for a trend in pH at NAOT-052.

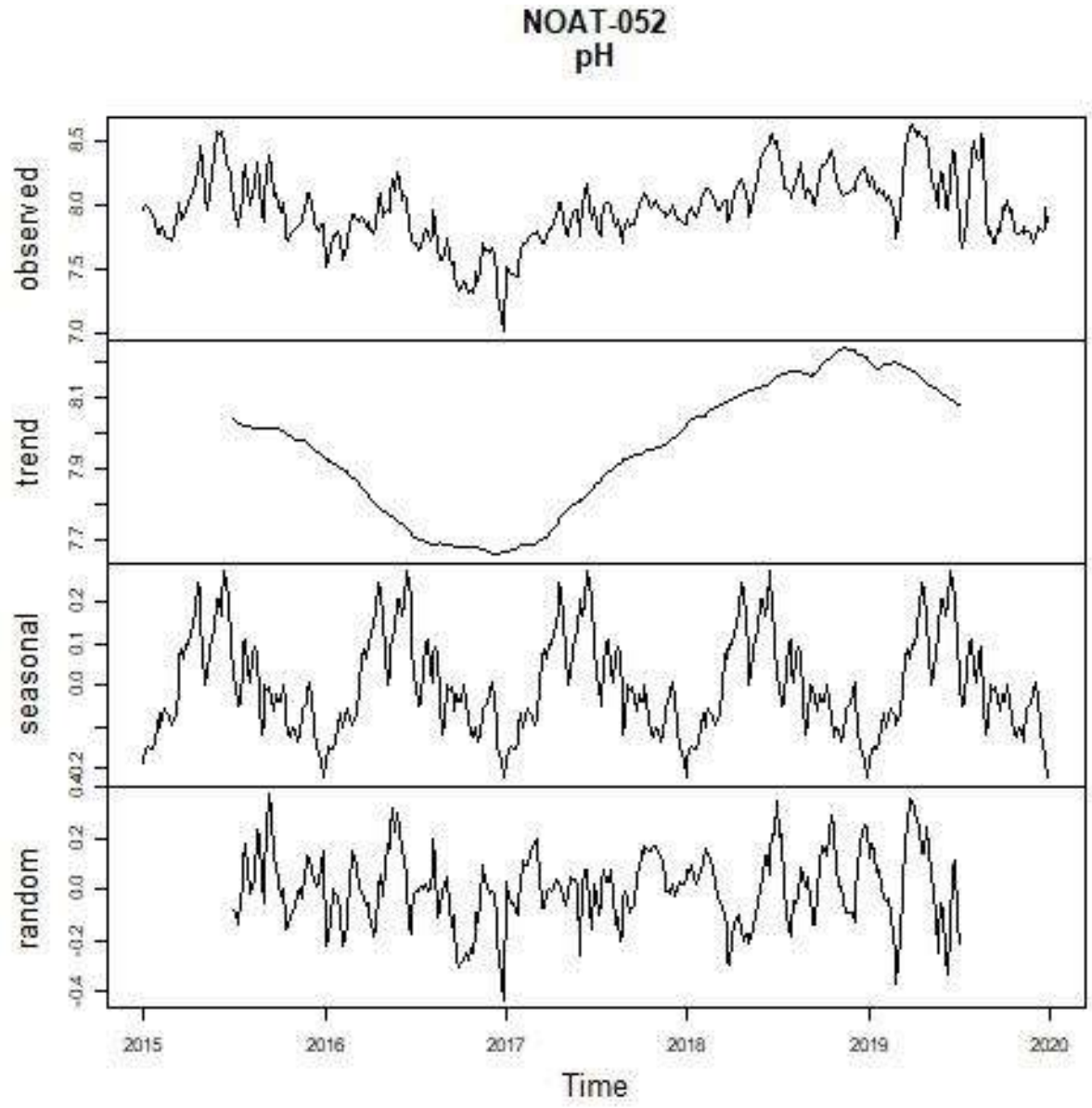


Figure A.54. Time series decomposition of truncated NOAT-052 pH by year.

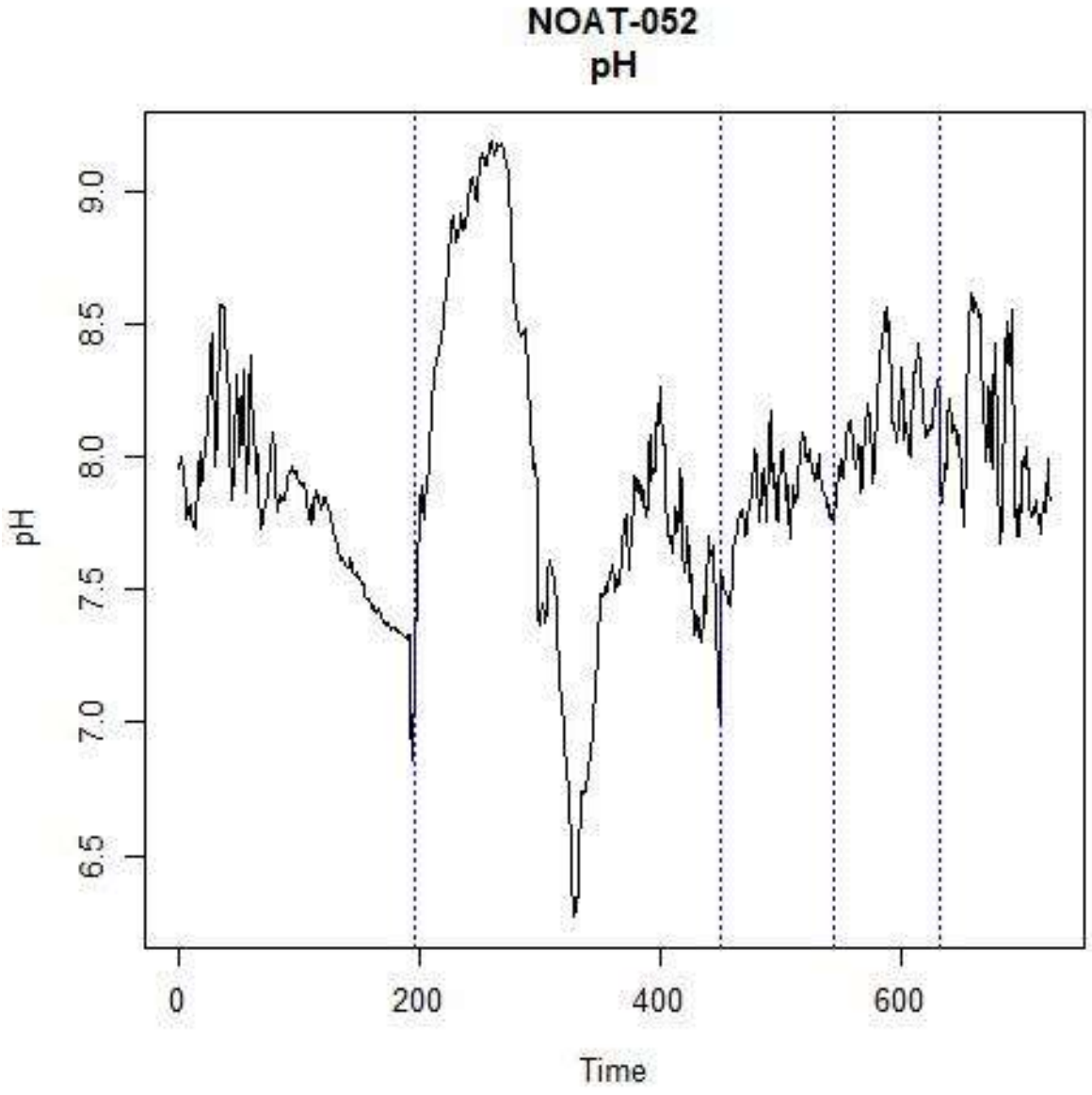


Figure A.55. Time series of NOAT-052 pH by time point with vertical lines for additive outliers.

Table A.57. Trend modeling results for daily pH data at NOAT-052.

			Trend			ARMA order		Ljung-Box Test	
Logged	**Method**	**Intercept**	**Coefficient**	**SE**	**p-value**	**AR**	**MA**	**Statistic**	**p-value**
FALSE	complete	6.7851	0.0784	0.0348	0.0242	1	1	7.31	0.2931
FALSE	completeAO	6.4933	0.0983	0.0558	0.0780	1	1	8.71	0.0333
FALSE	trunc	6.3580	0.1025	0.0335	0.0022	2	1	95.18	0.0904
FALSE	truncSA	7.8610	0.0073	0.0326	0.8221	2	3	98.44	0.0589

Table A.58. Top covariate models for daily pH data at NOAT-052.

Model	AICc	ΔAICc	Ljung-Box Test p-value
Wind Speed + Relative Humidity	-533.48	0.00	0.1907
Wind Speed + Relative Humidity + year	-531.40	2.08	0.1177
Relative Humidity	-530.58	2.90	0.2269
Relative Humidity + Month	-528.57	4.91	0.1521
Relative Humidity + year	-528.50	4.97	0.1516
Air temperature	-527.70	5.77	0.0585
Relative Humidity + year + Month	-526.65	6.83	0.0998
Daily precipitation	-501.54	31.94	0.0574
Intercept only	-496.03	37.45	0.0722
Wind Speed + Relative Humidity	-533.48	0.00	0.1907

Table A.59. Coefficients and variance components estimates for the top covariate model for daily pH data at NOAT-052.

Parameter	Coefficient	SE	p-value
ar1	0.90	0.03	< 0.0001
ma1	0.33	0.07	< 0.0001
intercept	8.10	0.07	< 0.0001
Wind Speed	-0.01	0.00	0.0247
Relative Humidity	0.00	0.00	< 0.0001

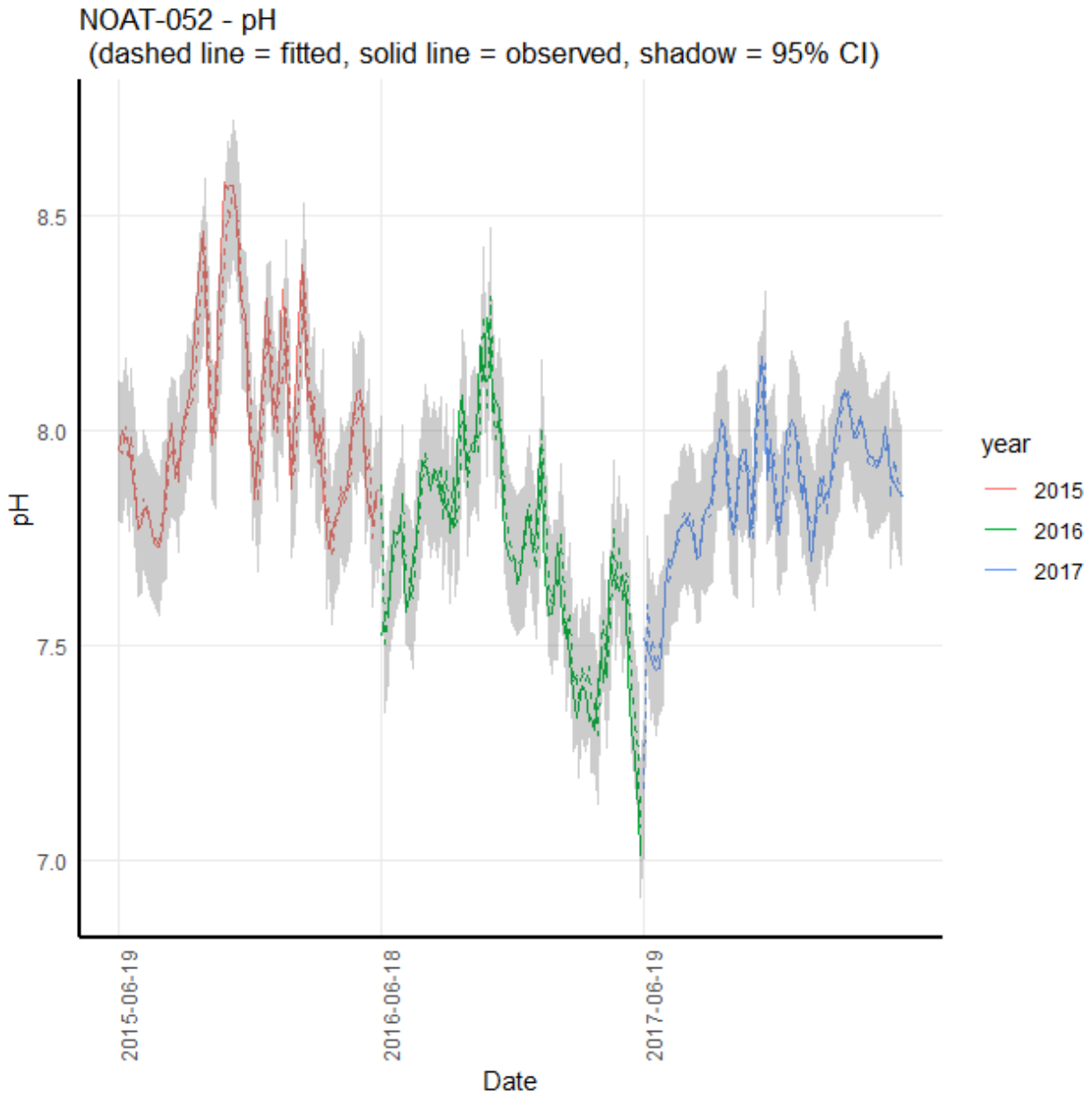


Figure A.56. Model predictions of NOAT-052 pH by date.

NOAT-107

Data

For NOAT-107, pH was recorded from 2014 through 2018. Over this period, there were 385 records of pH. Data were generally collected from a variable start data in June or July to August or September. Truncated to the common set of 35 days per year starting in July, the dataset had 175 observations.

Model Selection

For ARIMA models fitting all possible covariate combinations at lake NOAT-107 with pH as the response variable, AICc-based model selection resulted in ARIMA(1,0,1) with air temperature and year as the main covariates in the best model. The model detected a negative annual trend in pH. The three trend models with stationary residuals as assessed by the Ljung-Box test provide negative trend estimates had very different magnitudes. The complete and truncated models indicated large negative trends, but the truncated seasonally adjusted model found no evidence of a significant trend. The best covariate model indicated a large negative trend in pH at NOAT-107. Some evidence was found for a negative trend in pH at NAOT-052, but the results should be interpreted with caution.

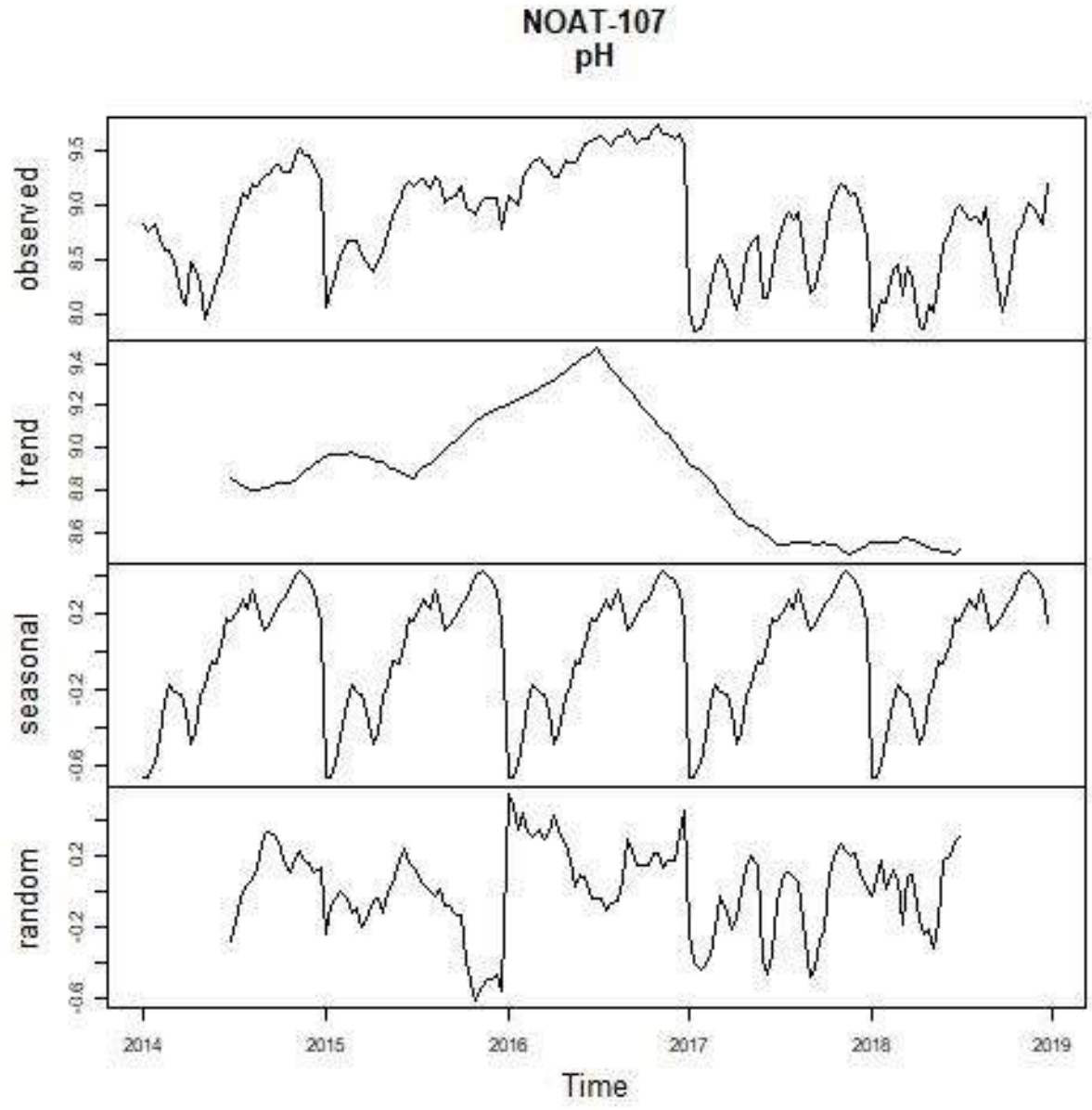


Figure A.57. Time series decomposition of truncated NOAT-107 pH by year.

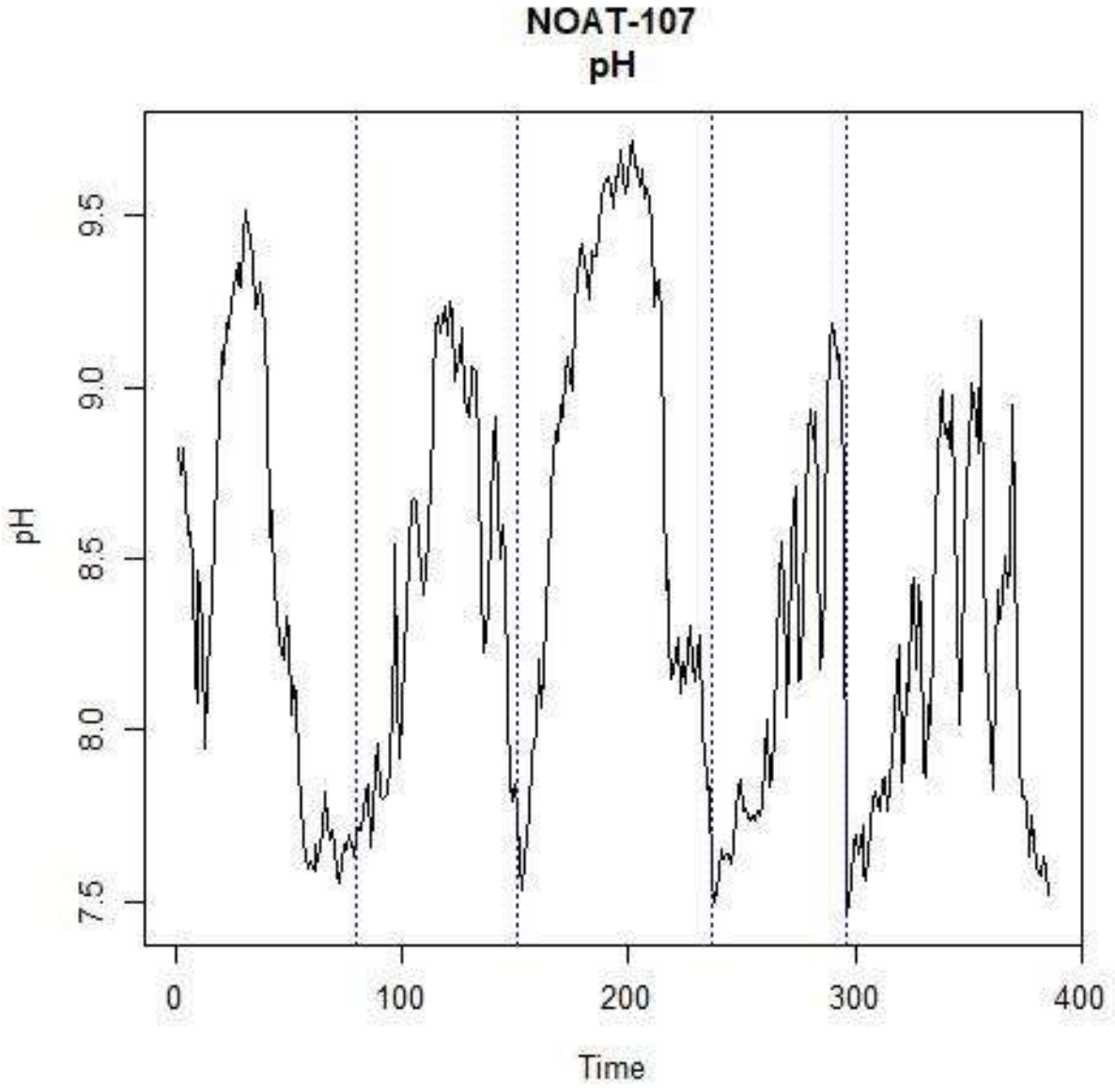


Figure A.58. Time series of NOAT-107 pH by time point with vertical lines for additive outliers.

Table A.60. Trend modeling results for daily pH data at NOAT-107.

			Trend			ARMA order		Ljung-Box Test	
Logged	**Method**	**Intercept**	**Coefficient**	**SE**	**p-value**	**AR**	**MA**	**Statistic**	**p-value**
FALSE	complete	12.7919	-0.3135	0.0719	< 0.0001	1	1	8.41	0.2099
FALSE	completeAO	12.4224	-0.2874	0.1096	0.0087	1	1	9.21	0.0266
FALSE	trunc	19.4730	-0.7382	0.0821	< 0.0001	1	1	27.19	0.6135
FALSE	truncSA	9.7015	-0.0587	0.0592	0.3216	1	1	36.63	0.2239

Table A.61. Top covariate models for daily pH data at NOAT-107.

Model	AICc	ΔAICc	Ljung-Box Test p-value
Air Temperature + Year	-372.48	0.00	0.0954
Relative Humidity + Year	-361.07	11.41	0.0829
Daily Precipitation + Year	-351.66	20.82	0.0933
Year + Month	-345.96	26.52	0.0717
Wind Speed + Year	-342.94	29.54	0.0962
Relative Humidity + Month	-338.74	33.74	0.2793
Wind Speed + Relative Humidity + Month	-337.99	34.49	0.1176
Air Temperature + Daily Precipitation	-337.86	34.62	0.4371
Air Temperature + Wind Speed + Daily Precipitation	-335.81	36.66	0.2921
Daily Precipitation + Month	-334.80	37.68	0.2710

Table A.62. Coefficients and variance components estimates for the top covariate model for daily pH data at NOAT-107.

Parameter	Coefficient	SE	p-value
ar1	0.97	0.01	< 0.0001
ma1	0.25	0.05	< 0.0001
intercept	15.11	1.18	< 0.0001
Air Temperature	0.02	0.00	< 0.0001
Year	-0.49	0.08	< 0.0001

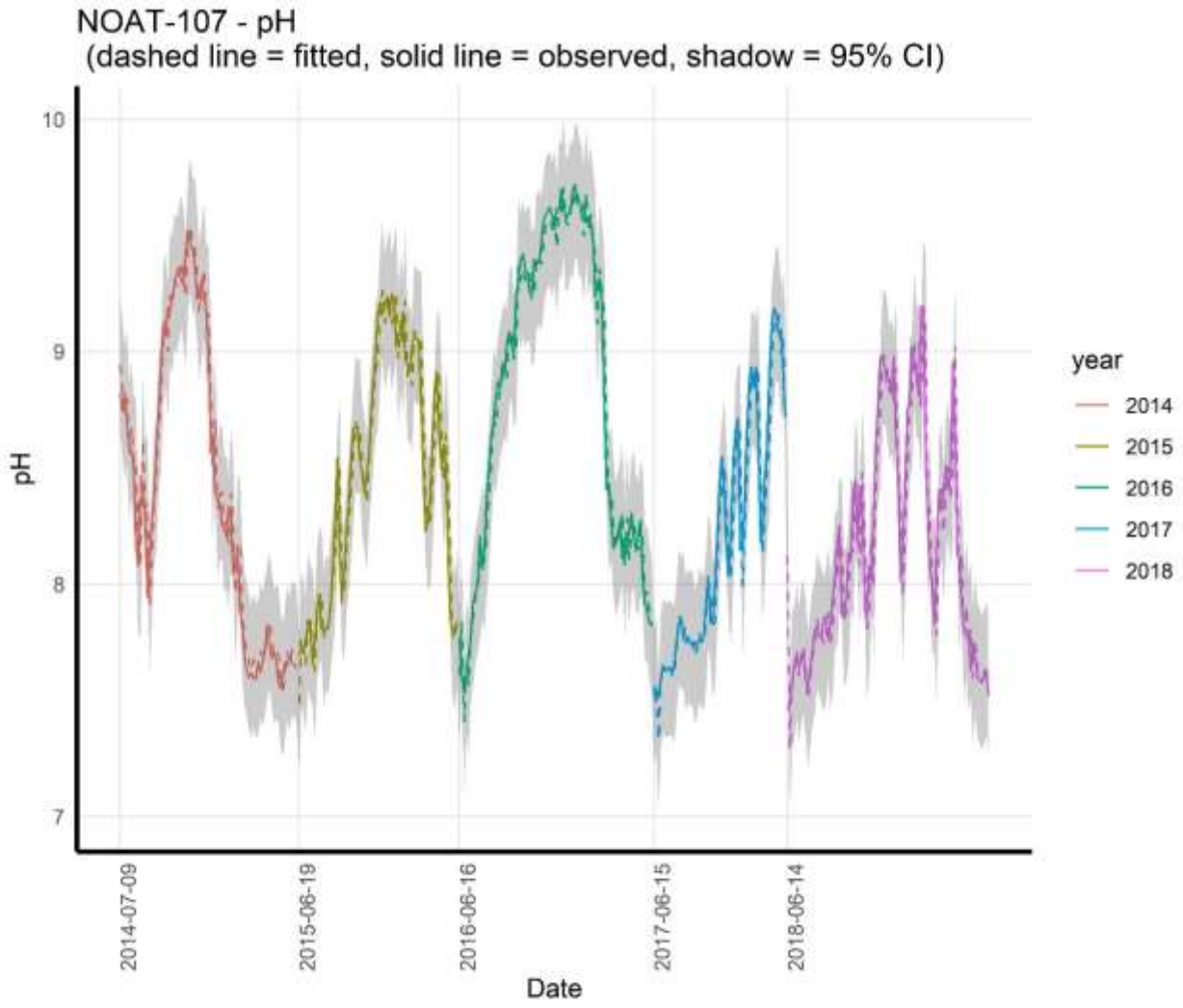


Figure A.59. Model predictions of NOAT-107 by date.

WRST-005

Data

For WRST-005, pH was recorded from 2010 through 2019. Over this period, there were 1073 records of pH. Data were generally collected from a variable start data in May or June to August or September. Truncated to the common set of 74 days per year starting in July, the dataset had 740 observations.

Model Selection

For ARIMA models fitting all possible covariate combinations at lake WRST-005 with pH as the response variable, AICc-based model selection resulted in ARIMA(1,0,0) with relative humidity as the main covariate in the best model. Both the complete data model and the seasonally adjusted truncated model yielded stationary residuals. The complete data model was chosen as the best trend model and generated a positive mean annual trend in pH.

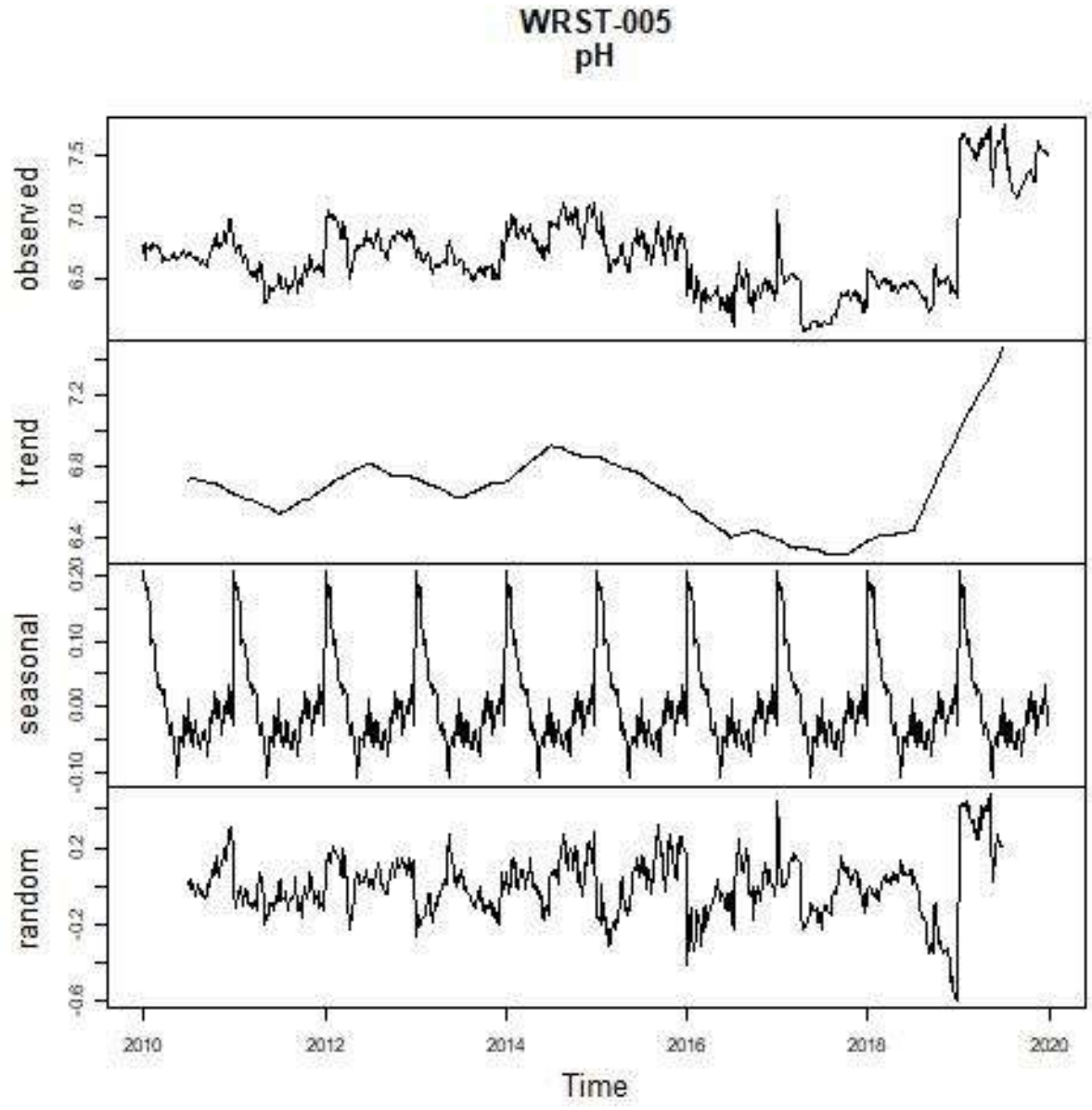


Figure A.60. Time series decomposition of truncated WRST-005 pH by year.

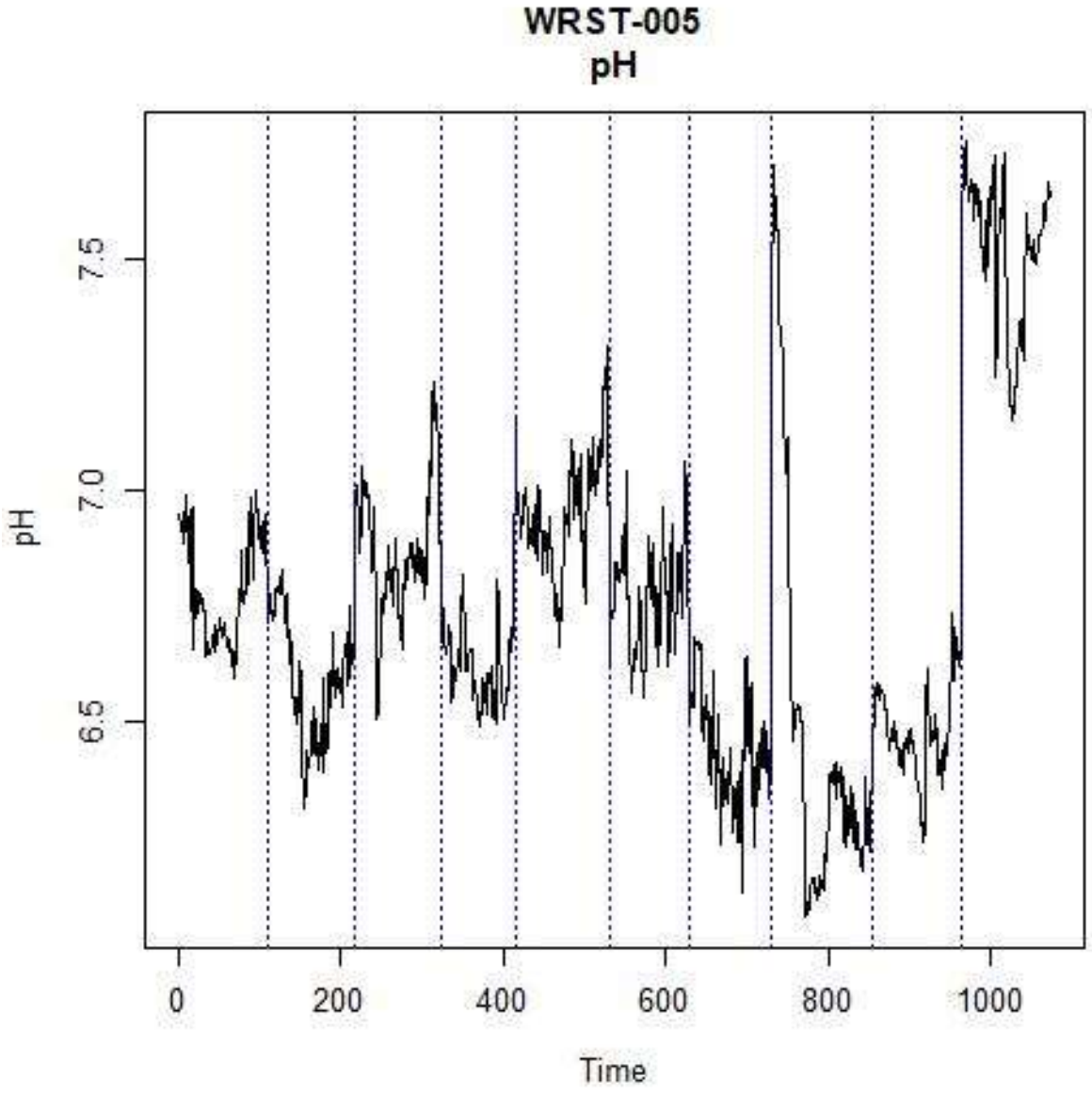


Figure A.61. Time series of WRST-005 pH by time point with vertical lines for additive outliers.

Table A.63. Trend modeling results for daily pH data at WRST-005.

			Trend			ARMA order		Ljung-Box Test	
Logged	**Method**	**Intercept**	**Coefficient**	**SE**	**p-value**	**AR**	**MA**	**Statistic**	**p-value**
FALSE	complete	5.5434	0.0993	0.0266	0.0002	1	2	6.51	0.2600
FALSE	completeAO	5.7540	0.0828	0.0329	0.0119	1	2	9.86	0.0198
FALSE	trunc	6.3723	0.0266	0.0073	0.0003	0	5	1696.42	< 0.0001
FALSE	truncSA	6.5823	0.0127	0.0218	0.5617	1	2	112.65	0.9713

Table A.64. Top covariate models for daily pH data at WRST-005.

Model	AICc	ΔAICc	Ljung-Box Test p-value
Relative Humidity	-2453.72	0.00	0.1009
Solar Radiation + Year	-2422.53	31.19	0.1530
Wind Speed + Daily Precipitation + Year	-2414.04	39.68	0.0506
Air Temperature + Wind Speed + Year	-2409.49	44.23	0.0714
Air Temperature + Daily Precipitation + Year	-2407.28	46.44	0.1132
Air Temperature + Wind Speed + Daily Precipitation	-2406.50	47.22	0.1083
Wind Speed + Daily Precipitation + Month	-2405.76	47.96	0.0735
Wind Speed + Year	-2402.57	51.15	0.1191
Wind Speed + Year + Month	-2400.66	53.07	0.0509
Wind Speed + Daily Precipitation	-2400.62	53.10	0.1301

Table A.65. Coefficients and variance components estimates for the top covariate model for daily pH data at WRST-005.

Parameter	Coefficient	SE	p-value
ar1	0.98	0.01	< 0.0001
intercept	6.92	0.11	< 0.0001
Relative Humidity	0.00	0.00	< 0.0001

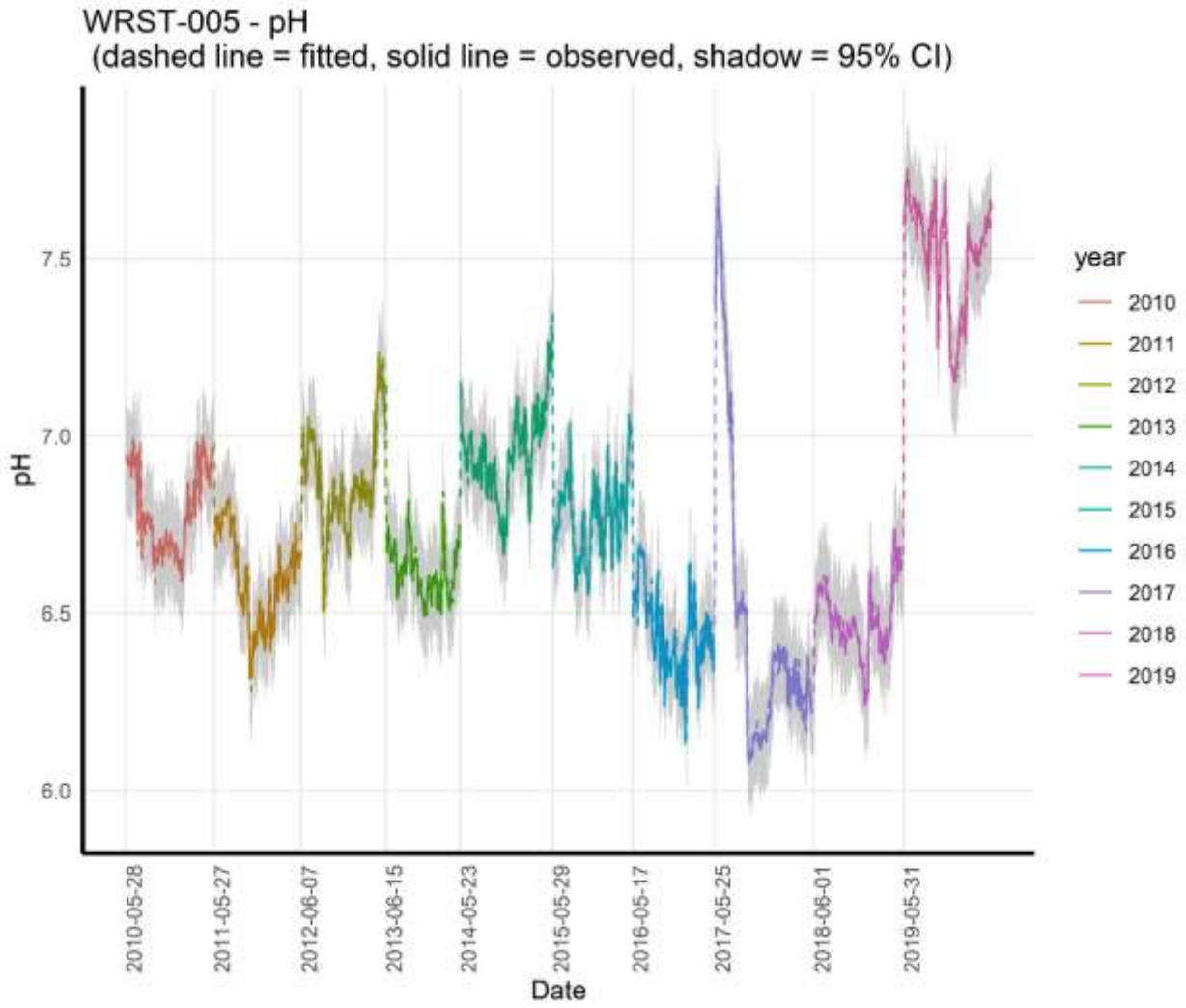


Figure A.62. Model predictions of WRST-005 pH by date.

WRST-016

Data

For the WRST-016 lake, pH was recorded from 2009 through 2019. Over this period, there were 1073 records of pH. Data were collected from a variable start data in May or June to August or September. Truncated to the common set of 45 days per year starting in June, the dataset had 496 observations.

Model Selection

For ARIMA models fitting all possible covariate combinations at lake WRST-016 with pH as the response variable, AICc-based model selection resulted in ARIMA(1,0,0) with air temperature, wind speed, and year as the main covariates in the best model. The covariate model detected a significant negative annual trend in pH, but the trend models with stationary residuals found a trend not significantly different from 0 in the complete-data model and the truncated seasonally adjusted model and a significant increasing trend in the truncated model. Trend inference is inconclusive for pH at WRST-016.

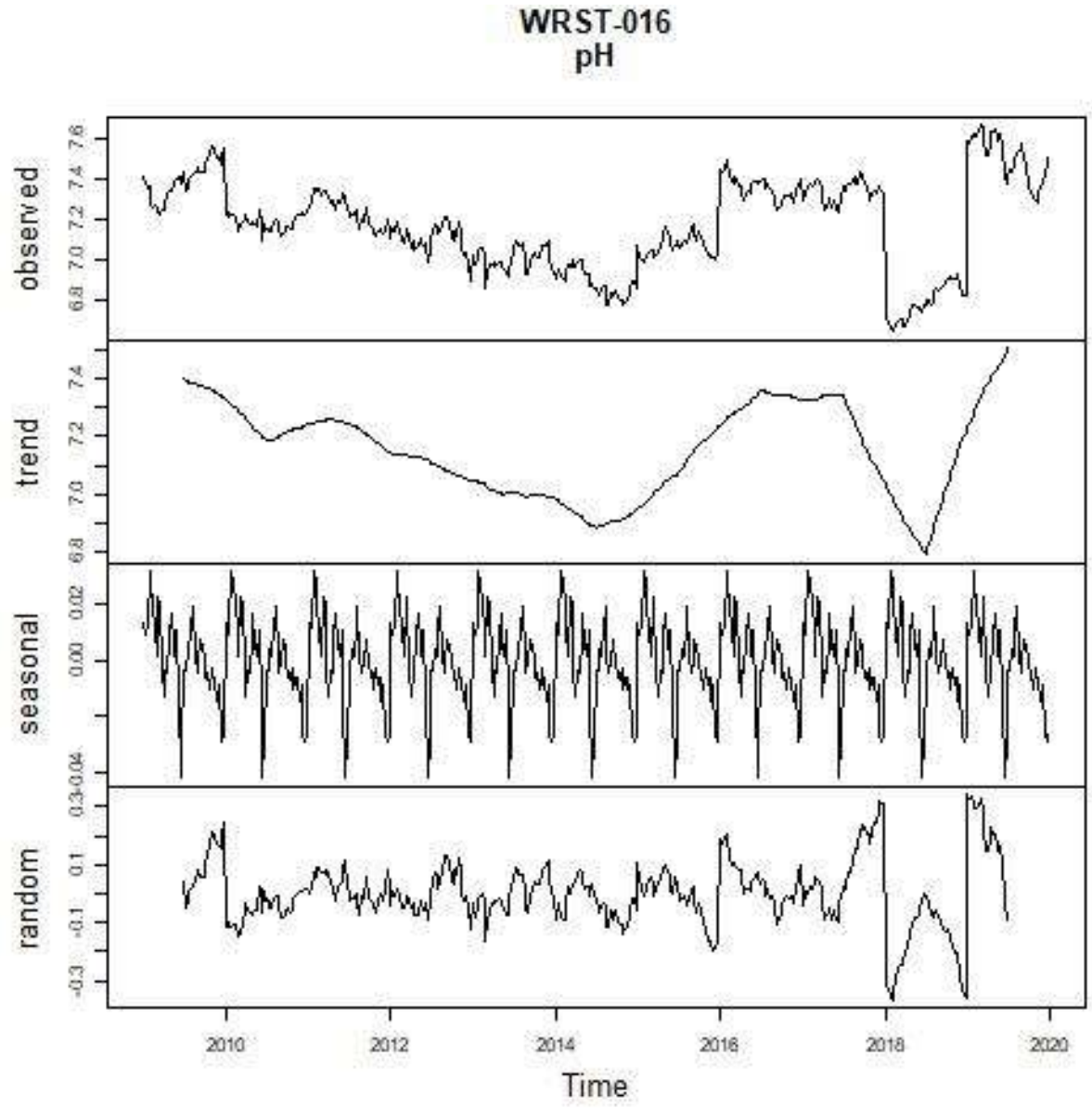


Figure A.63. Time series decomposition of truncated WRST-016 pH by year.

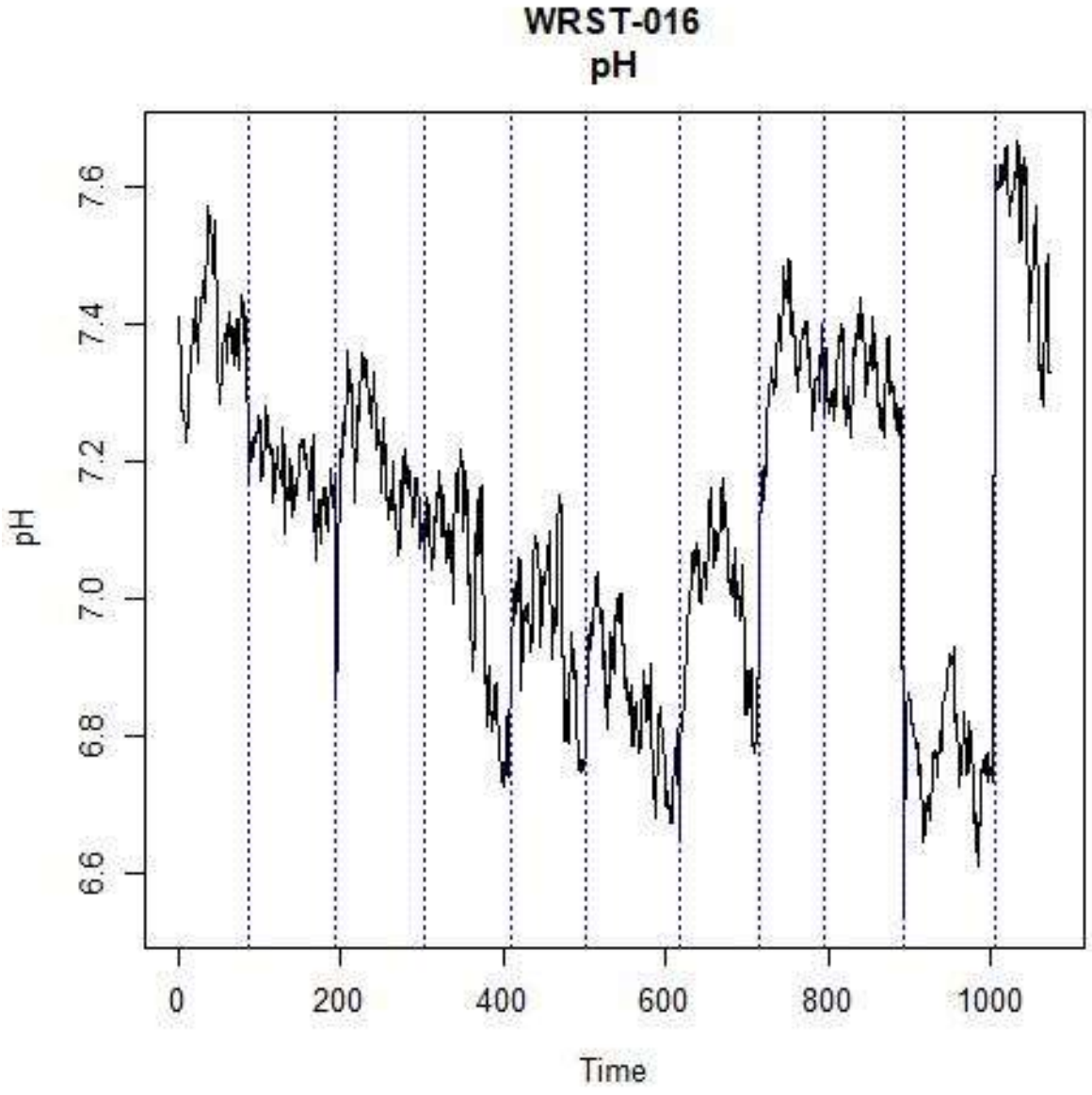


Figure A.64. Time series of WRST-016 pH by time point with vertical lines for additive outliers.

Table A.66. Trend modeling results for daily pH data at WRST-016.

			Trend			ARMA order		Ljung-Box Test	
Logged	**Method**	**Intercept**	**Coefficient**	**SE**	**p-value**	**AR**	**MA**	**Statistic**	**p-value**
FALSE	complete	7.3331	-0.0174	0.0130	0.1835	1	2	2.56	0.7677
FALSE	completeAO	7.1126	0.0015	0.0149	0.9184	1	2	11.03	0.0115
FALSE	trunc	6.8234	0.0297	0.0114	0.0092	1	0	45.19	0.9999
FALSE	truncSA	7.1951	0.0005	0.0142	0.9724	1	0	96.96	0.2182

Table A.67. Top covariate models for daily pH data at WRST-016.

Model	AICc	ΔAICc	Ljung-Box Test p-value
Air Temperature + Wind Speed + Year	-3378.74	0.00	0.2380
Air Temperature + Wind Speed + Daily Precipitation + Year	-3377.68	1.05	0.1652
Air Temperature + Wind Speed	-3375.72	3.01	0.2807
Air Temperature + Wind Speed + Daily Precipitation	-3374.49	4.24	0.2061
Air Temperature + Year	-3373.03	5.70	0.6022
Air Temperature + Daily Precipitation + Year	-3370.93	7.81	0.2487
Wind Speed + Solar Radiation + Year	-3370.64	8.09	0.3902
Air Temperature	-3369.51	9.22	0.3635
Air Temperature + Daily Precipitation	-3369.20	9.54	0.5263
Wind Speed + Month	-3368.10	10.64	0.5287

Table A.68. Coefficients and variance components estimates for the top covariate model for daily pH data at WRST-016.

Parameter	Coefficient	SE	p-value
ar1	0.98	0.01	< 0.0001
intercept	7.44	0.18	< 0.0001
Air Temperature	0.00	0.00	0.0001
Wind Speed	0.01	0.00	0.0032
Year	-0.03	0.01	0.0312

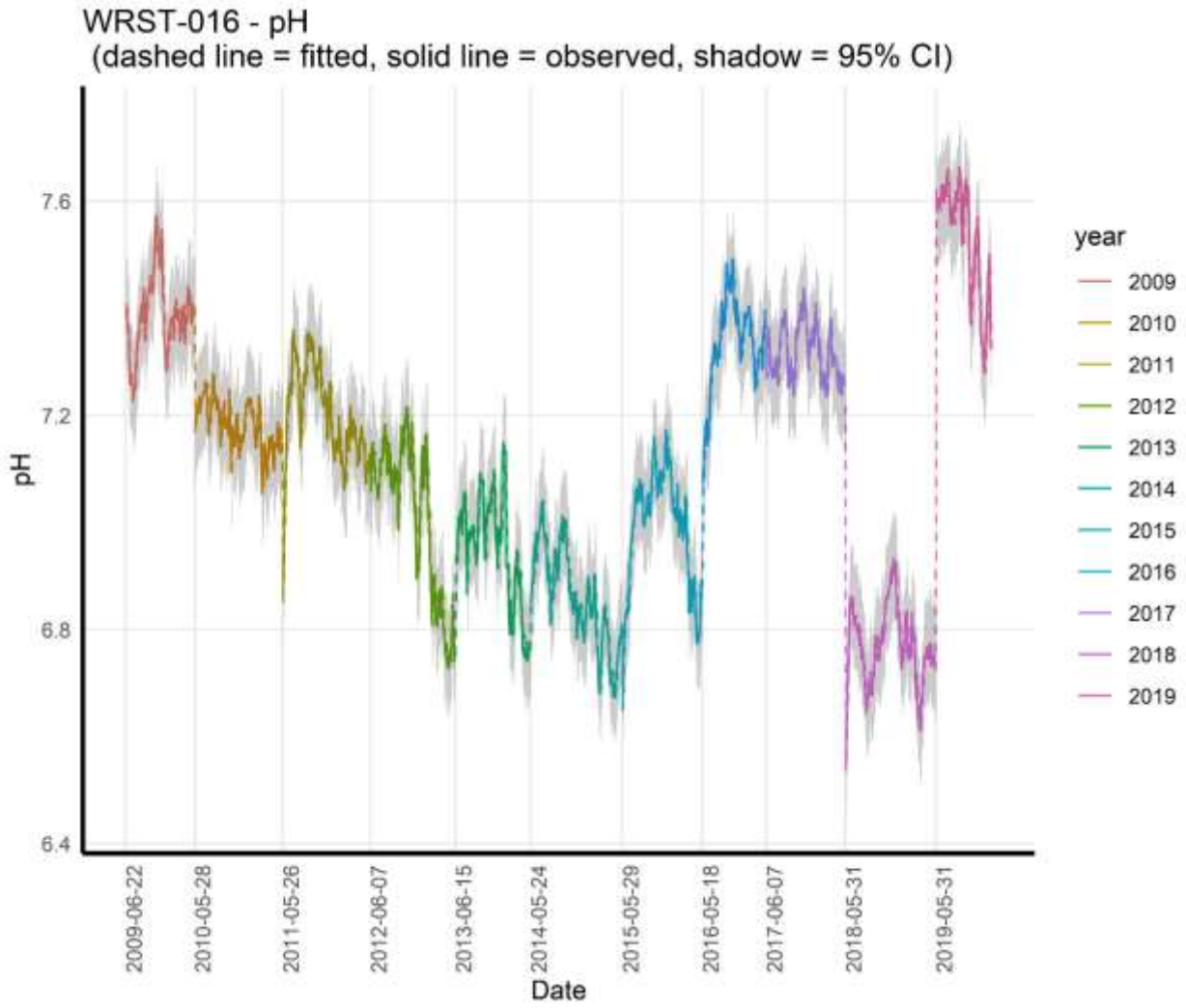


Figure A.65. Model predictions of WRST-016 pH by date.

YUCH-004

Data

For the YUCH-004 lake, pH was recorded from 2009 through 2019. Over this period, there were 1221 records of pH. Data were collected from a variable start data in May or June to August or September. Truncated to the common set of 87 days per year starting in July, the dataset had 957 observations. Covariate coverage was poor in 2019. Covariate analysis therefore excluded 2019 and used 1092 records.

When aggregate to weekly mean pH values the dataset included 207 observations for the full period and when truncated to the common set of 14 weeks the number of observations was reduced to 154.

Model Selection

No daily models exhibited stationary residuals for YUCH-004 pH. An ARIMA(2,0,3) model fit to the complete dataset suggested a significant decline in pH over time. No autocorrelation was evident when inspecting the model residuals by eye, but a Ljung-Box test indicated non-stationarity.

When fit with weekly data, all models of logged and unlogged pH yielded stationary residuals except for the additive outliers model. However, none of the models with stationary residuals included a trend estimate that was significantly different from zero, thus there is no evidence for an increasing or decreasing trend in pH at YUCH-004. For ARIMA models fitting all possible covariate combinations, AICc-based model selection resulted in a model with ARIMA(1,0,0) structure and air temperature and wind speed as fixed effects. Air temperature is estimated to have a positive effect on pH whereas wind speed is estimated to have a negative effect.

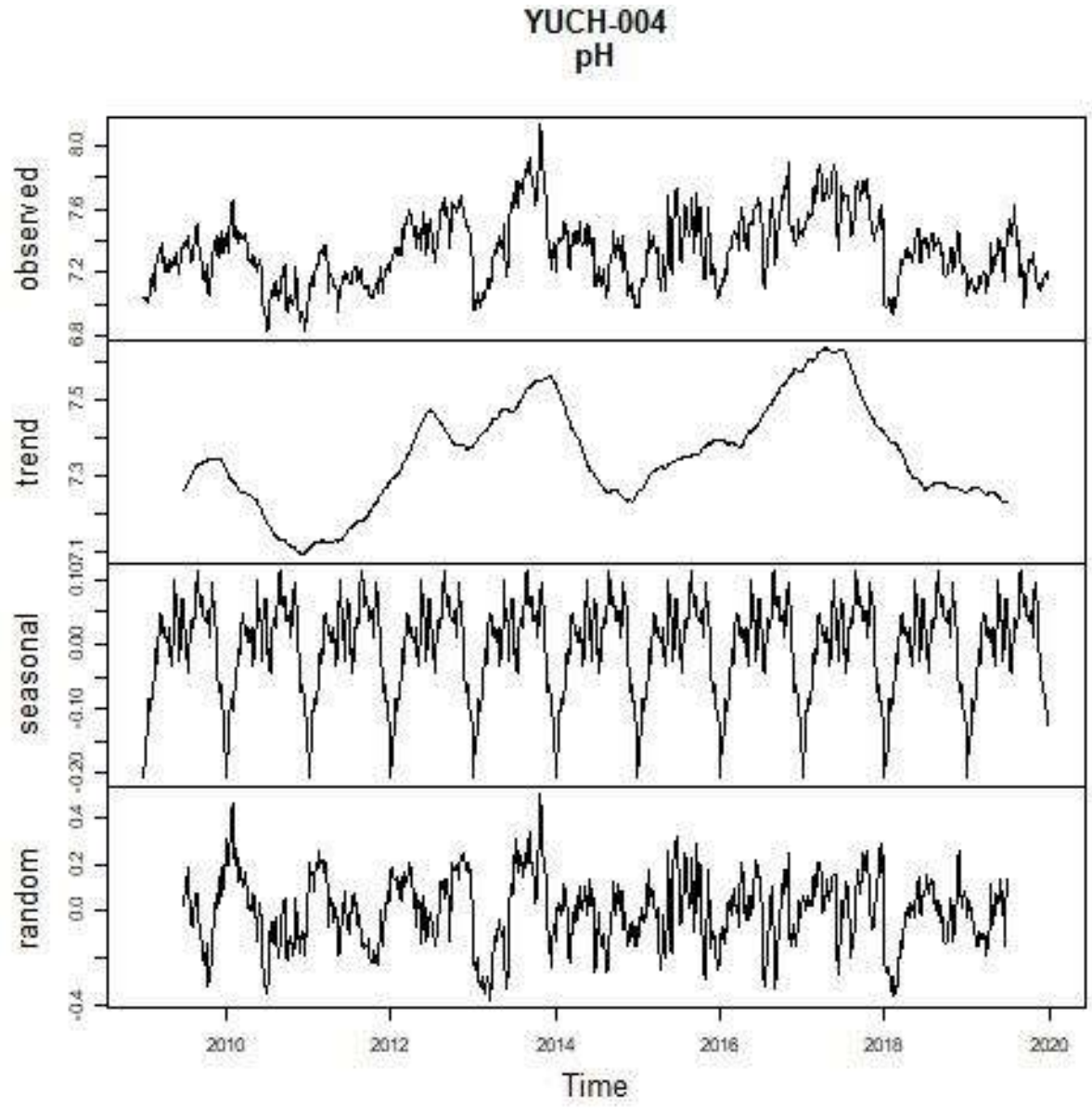


Figure A.66. Time series decomposition of truncated YUCH-004 pH by year.

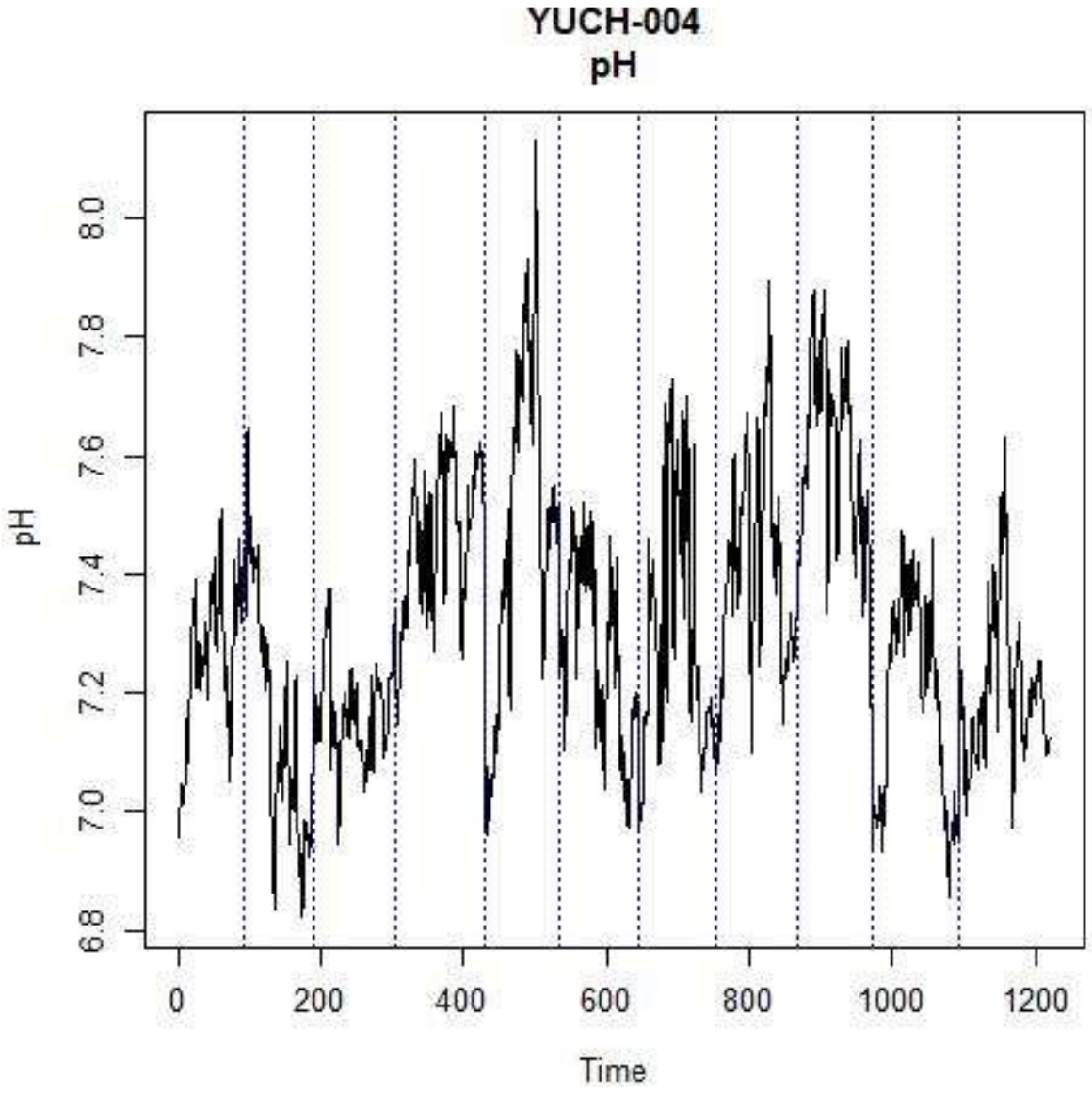


Figure A.67. Time series of YUCH-004 pH by time point with vertical lines for additive outliers.

Table A.69. Trend modeling results for daily pH data at YUCH-004.

			Trend			ARMA order		Ljung-Box Test	
Logged	**Method**	**Intercept**	**Coefficient**	**SE**	**p-value**	**AR**	**MA**	**Statistic**	**p-value**
FALSE	complete	7.9896	-0.0661	0.0297	0.0259	2	3	13.25	0.0041
FALSE	completeAO	7.3067	0.0005	0.0098	0.9609	1	1	39.87	< 0.0001
FALSE	trunc	7.3887	-0.0053	0.0115	0.6447	1	1	236.22	0.0005
FALSE	truncSA	7.2538	0.0085	0.0113	0.4484	2	3	221.32	0.0031

Table A.70. Trend modeling results for weekly pH data at YUCH-004.

			Trend			ARMA order		Ljung-Box Test	
Logged	**Method**	**Intercept**	**Coefficient**	**SE**	**p-value**	**AR**	**MA**	**Statistic**	**p-value**
FALSE	complete	7.3265	-0.0030	0.0132	0.8198	1	0	2.48	0.9283
FALSE	completeAO	7.2871	0.0014	0.0139	0.9183	1	0	10.88	0.0124
FALSE	trunc	7.2325	0.0094	0.0119	0.4310	1	2	18.69	0.7193
FALSE	truncSA	7.2038	0.0140	0.0089	0.1150	1	2	12.74	0.9173

Table A.71. Top covariate models for weekly pH data at YUCH-004.

Parameter	**AICc**	**ΔAICc**	**Ljung-Box Test p-value**
Air Temperature + Wind Speed	-213.70	0.00	0.6990
Air Temperature + Wind Speed + Daily Precipitation	-213.19	0.51	0.5590
Air Temperature	-209.61	4.10	0.7084
Air Temperature + Wind Speed + Year	-209.17	4.54	0.2524
Air Temperature + Daily Precipitation	-208.68	5.02	0.6034
Air Temperature + Wind Speed + Daily Precipitation + Year	-208.44	5.26	0.1952
Wind Speed + Relative Humidity	-206.68	7.02	0.6659
Air Temperature + Year	-206.49	7.21	0.4070

Table A.72. Coefficients and variance components estimates for the top covariate model for weekly pH data at YUCH-004.

Parameter	**Coefficient**	**SE**	**p-value**
ar1	0.79	0.05	< 0.0001
intercept	7.25	0.07	< 0.0001
Air Temperature	0.01	0.00	< 0.0001
Wind Speed	-0.09	0.03	0.0119

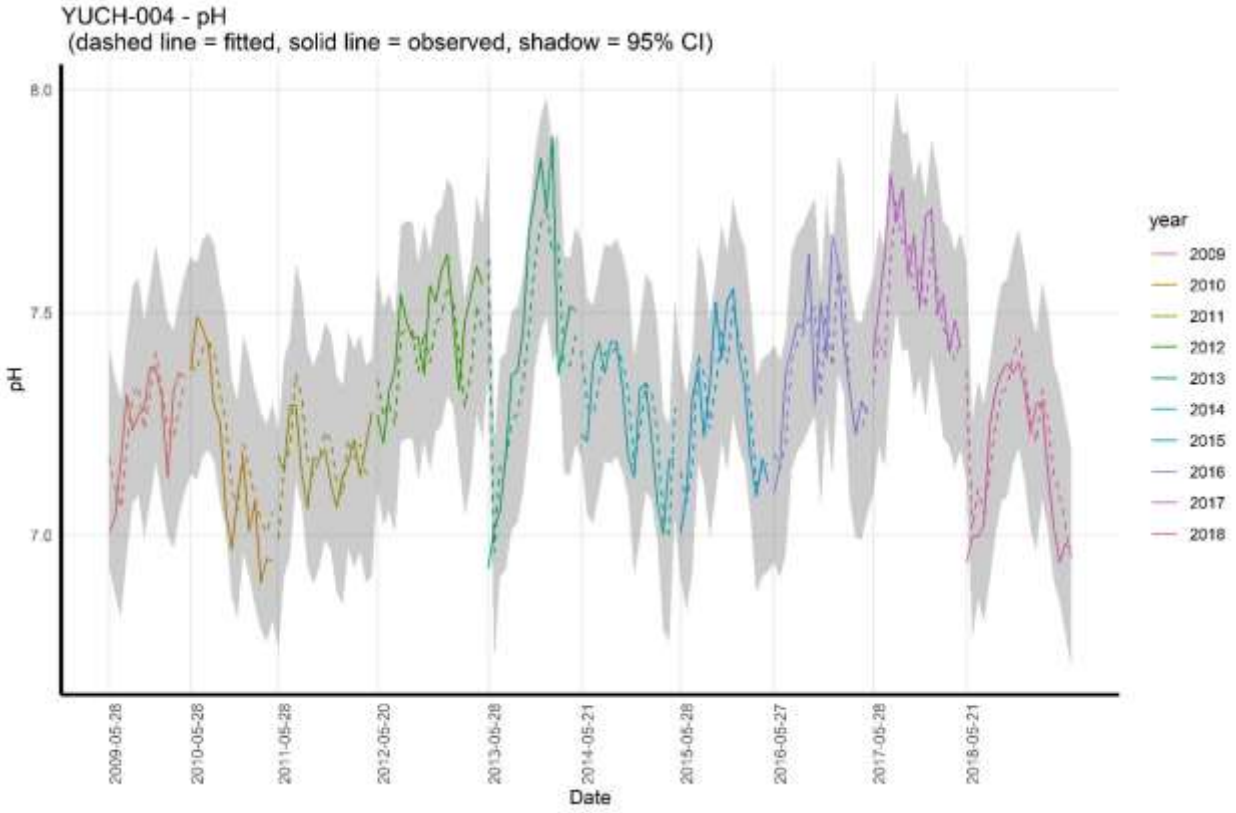


Figure A.68. Model predictions of YUCH-004 pH by week.

YUCH-005

Data

For the YUCH-005 lake, pH was recorded from 2009 through 2019. Over this period, there were 1253 records of pH. Data were collected beginning on a variable date in May or June and ending in September. Truncated to the common set of 99 days per year starting in June, the dataset had 1089 observations. When aggregating to weekly mean pH values the dataset included 190 observations for the full period and when truncated to the common set of 15 weeks the number of observations was reduced to 165.

Model Selection

No trend model of daily pH data YUCH-005 exhibited stationary in residual diagnostics. When fitting models to weekly pH data, both models for the logged and unlogged complete dataset yielded stationary residuals. However, none of these two models with stationary residuals included a trend estimate that was significantly different from zero. For ARIMA models fitting all possible covariate combinations, AICc-based model selection resulted in a model with ARIMA(1,0,4) structure and relative humidity and year as fixed effects. Both relative humidity and year were estimated to have negative effects on pH. Overall, the evidence for a trend in pH at lake YUCH-005 is weak.

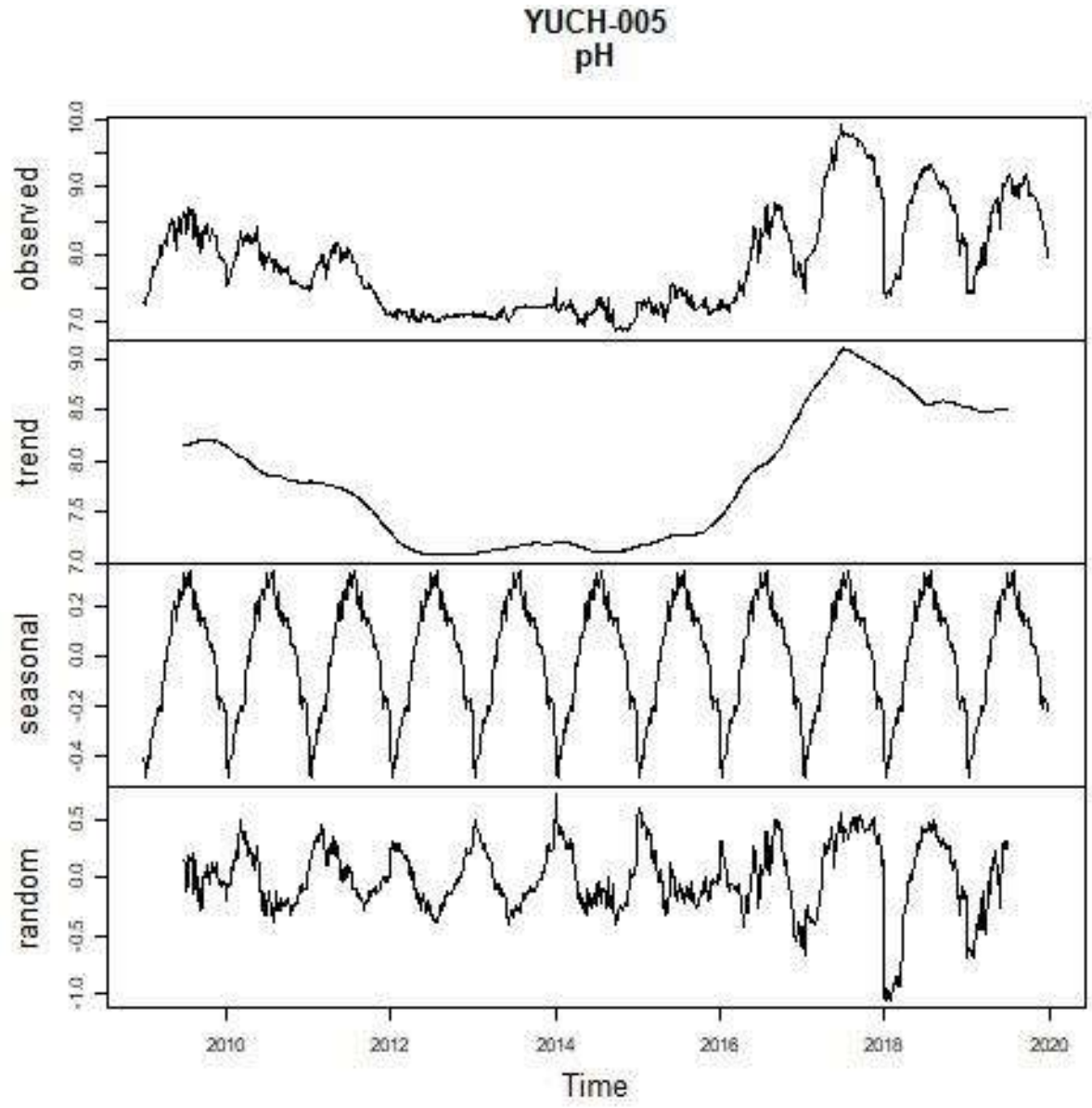


Figure A.69. Time series decomposition of truncated YUCH-005 pH by year.

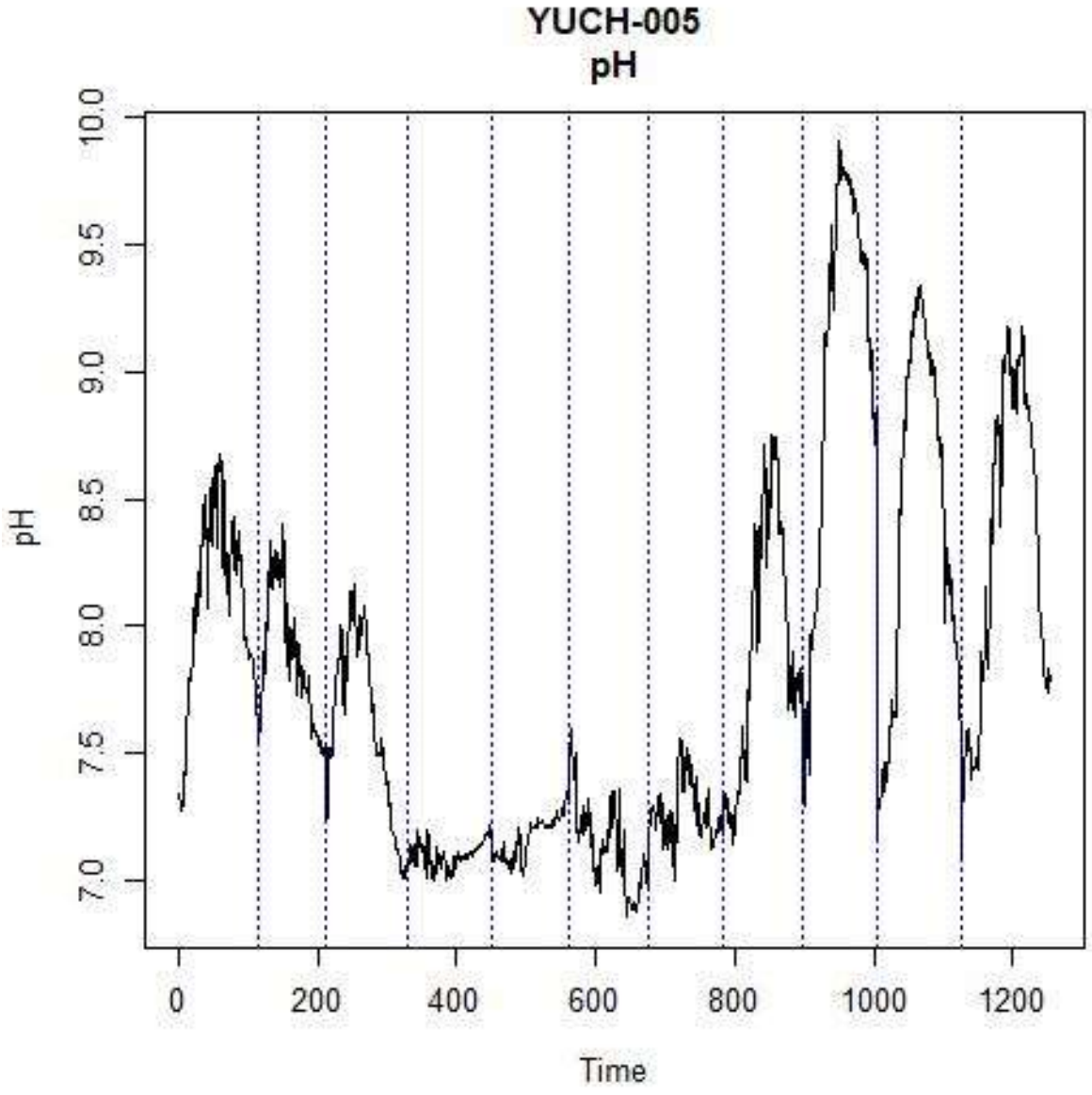


Figure A.70. Time series of YUCH-005 pH by time point with vertical lines for additive outliers.

Table A.73. Trend modeling results for daily pH data at YUCH-005.

			Trend			ARMA order		Ljung-Box Test	
Logged	**Method**	**Intercept**	**Coefficient**	**SE**	**p-value**	**AR**	**MA**	**Statistic**	**p-value**
FALSE	complete	7.0961	0.0705	0.0087	< 0.0001	0	5	2227.14	< 0.0001
FALSE	completeAO	6.9968	0.0804	0.0087	< 0.0001	0	5	4248.29	< 0.0001
FALSE	trunc	7.0658	0.0795	0.0095	< 0.0001	0	5	10393.07	< 0.0001
FALSE	truncSA	6.9579	0.0905	0.0088	< 0.0001	0	5	12439.65	< 0.0001

Table A.74. Trend modeling results for weekly pH data at YUCH-005.

			Trend			ARMA order		Ljung-Box Test	
Logged	**Method**	**Intercept**	**Coefficient**	**SE**	**p-value**	**AR**	**MA**	**Statistic**	**p-value**
FALSE	complete	8.0744	-0.0636	0.0679	0.3495	3	3	5.27	0.1534
FALSE	completeAO	7.5438	0.0444	0.0407	0.2752	5	3	37.38	< 0.0001
FALSE	trunc	8.2784	-0.0878	0.0927	0.3435	1	3	45.46	0.0035
FALSE	truncSA	7.6902	0.0348	0.0501	0.4874	2	2	39.19	0.0189

Table A.75. Top covariate models for daily pH data at YUCH-005.

Model	**AICc**	**ΔAICc**	**Ljung-Box Test p-value**
Relative Humidity + Year	-77.19	0.00	0.1062
Daily Precipitation + Month	-76.55	0.65	0.0771
Wind Speed + Month	-76.31	0.88	0.0808
Year + Month	-75.83	1.37	0.0936
Wind Speed + Year	-75.62	1.57	0.1722
Air Temperature + Year	-74.38	2.81	0.1340
Wind Speed	-73.70	3.49	0.2837
Wind Speed + Daily Precipitation	-71.29	5.90	0.1691
Wind Speed + Relative Humidity	-69.79	7.41	0.1218
Air Temperature + Wind Speed	-68.94	8.25	0.1024

Table A.76. Coefficients and variance components estimates for the top covariate model for daily pH data at YUCH-005.

Parameter	**Coefficient**	**SE**	**p-value**
ar1	0.94	0.03	< 0.0001
ma1	0.28	0.08	0.0003
ma2	0.33	0.07	< 0.0001
ma3	0.28	0.08	0.0008
ma4	0.33	0.08	< 0.0001
intercept	8.91	0.61	< 0.0001

Parameter	Coefficient	SE	p-value
Relative Humidity	0.00	0.00	0.0308
Year	-0.24	0.07	0.0011

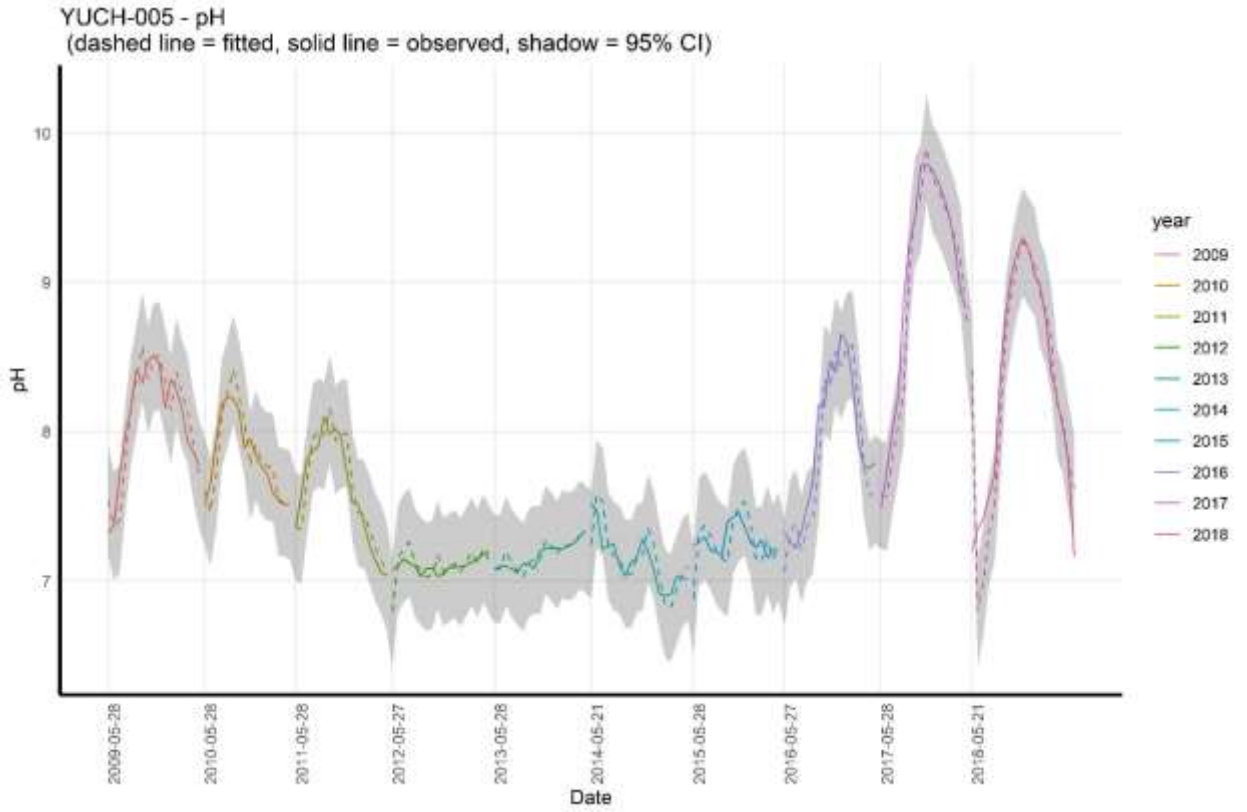


Figure A.71. Model predictions of YUCH-005 pH by week.

Specific Conductance

BELA-088

Data

For BELA-088, specific conductance was recorded from 2015 through 2019. Over this period, 543 records were collected from June to September. When truncating the data set to the subset of 72 days visited every year, the dataset had 432 observations. Covariate coverage was poor in 2019, so covariate models only considered 2015-2018, but wind speed and solar radiation were omitted from the model selection process due to missingness in 2018.

Model Selection

For BELA-088, the truncated seasonally adjusted trend models for logged and unlogged observations yielded stationary residuals. Neither of these two models included a trend coefficient that was significantly different from zero, thus there is no evidence for an increasing or decreasing trend in specific conductance at lake BELA-088. For ARIMA models fitting all possible covariate combinations, AICc-based model selection resulted in a model with ARIMA(1,0,1) structure and fixed effects for daily precipitation and month. Specific conductance was estimated to increase with month (June-September). The coefficient for daily precipitation was not significantly less than zero.

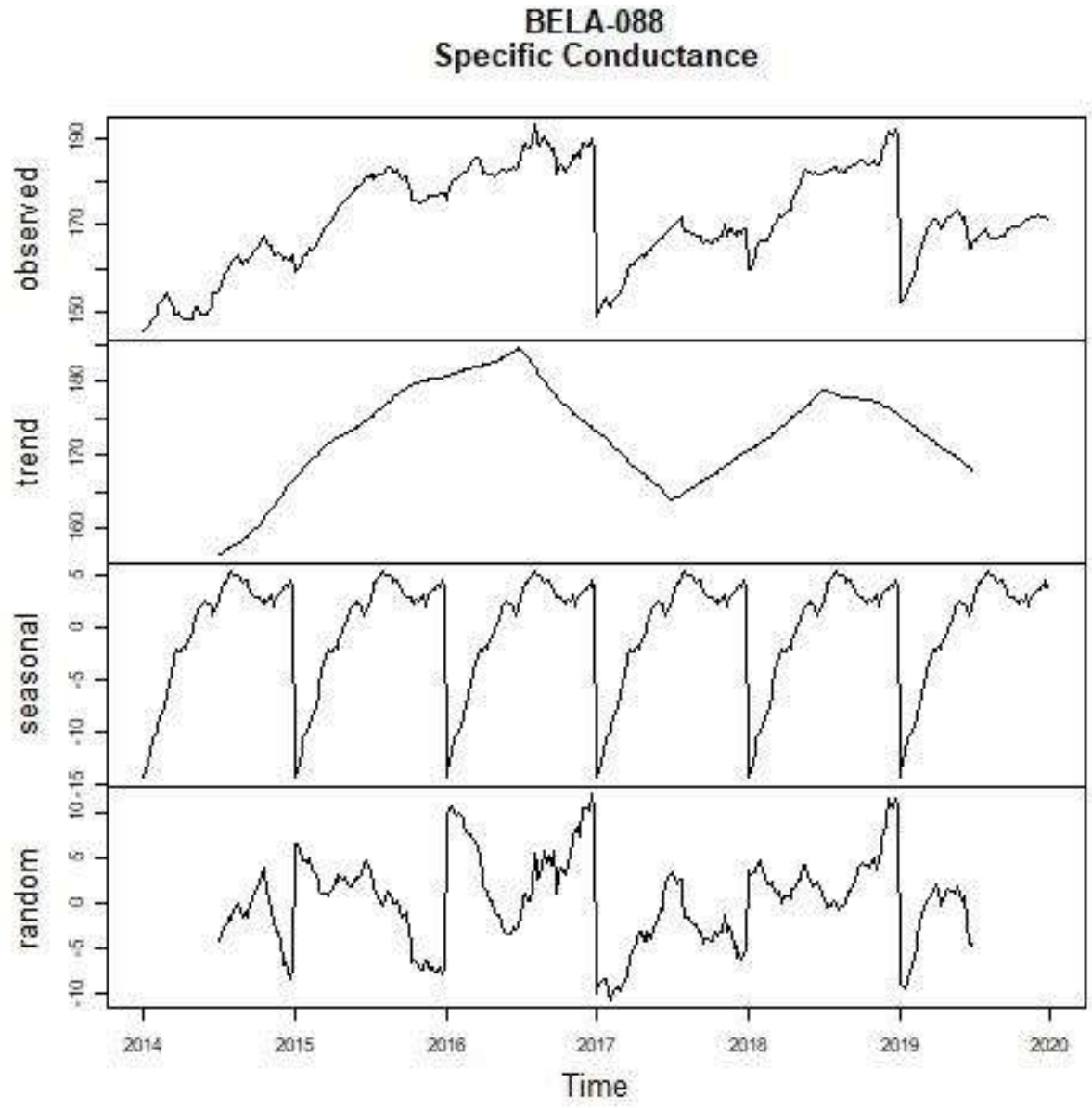


Figure A.72: Time series decomposition of truncated BELA-088 specific conductance by year.

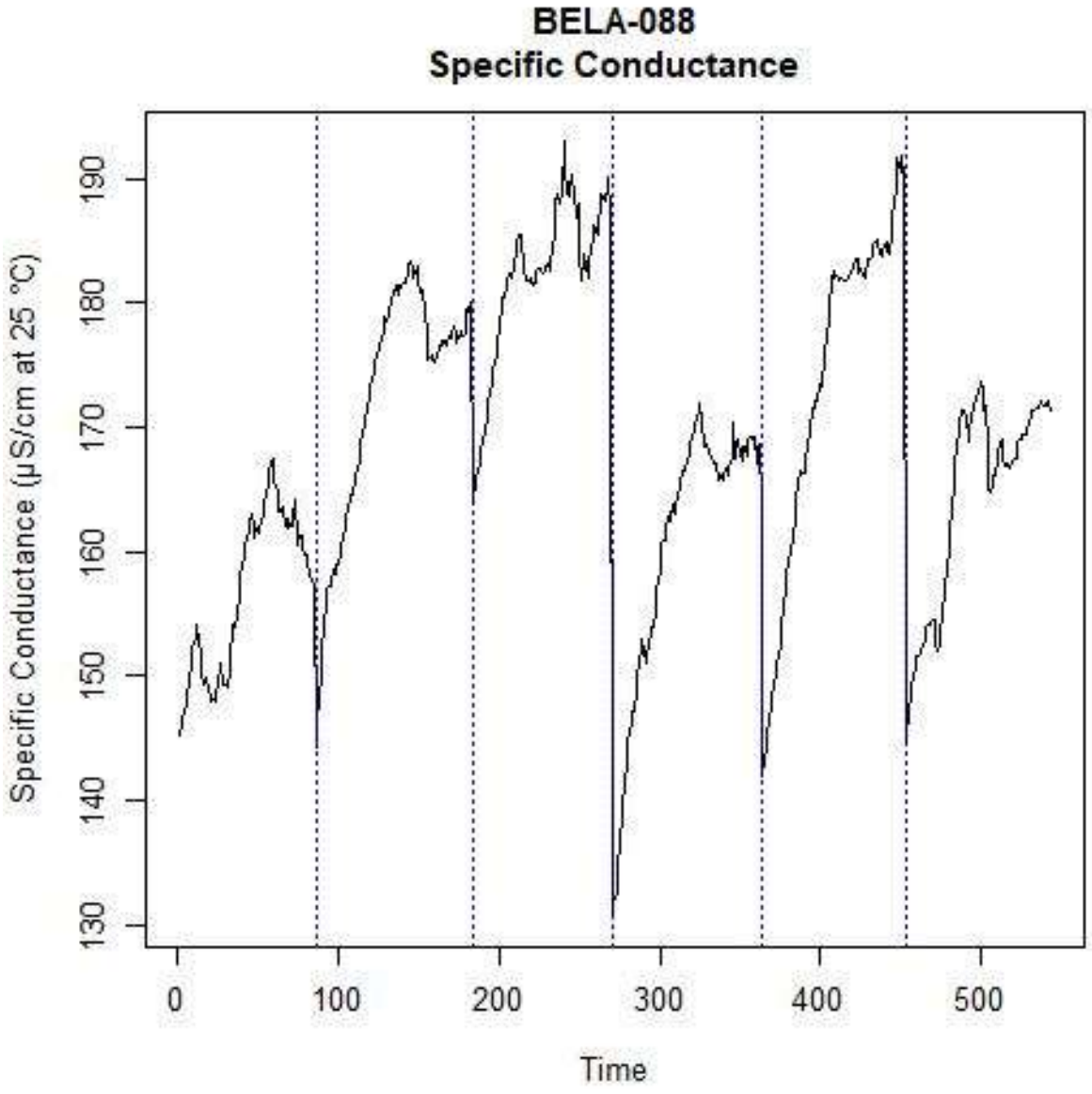


Figure A.73: Time series of BELA-088 specific conductance by time point with vertical lines for additive outliers.

Table A.77. Trend modeling results for daily specific conductance data at BELA-088.

			Trend			ARMA order		Ljung-Box Test	
Logged	**Method**	**Intercept**	**Coefficient**	**SE**	**p-value**	**AR**	**MA**	**Statistic**	**p-value**
FALSE	complete	195.37	-2.37	0.64	0.0002	0	5	386.48	< 0.0001
FALSE	completeAO	179.59	-0.98	0.53	0.0617	0	5	592.33	< 0.0001
FALSE	trunc	161.43	0.82	0.40	0.0424	0	2	2230.75	< 0.0001

			Trend			ARMA order		Ljung-Box Test	
Logged	**Method**	**Intercept**	**Coefficient**	**SE**	**p-value**	**AR**	**MA**	**Statistic**	**p-value**
FALSE	truncSA	167.36	0.23	0.82	0.7812	1	1	87.48	0.3191
TRUE	complete	5.28	-0.01	0.00	0.0003	0	5	365.28	< 0.0001
TRUE	completeAO	5.19	-0.01	0.00	0.0600	0	5	564.52	< 0.0001
TRUE	trunc	5.19	0.00	0.00	0.2143	0	5	659.27	< 0.0001
TRUE	truncSA	5.12	0.00	0.00	0.7714	1	1	86.68	0.3406

Table A.78. Top covariate models for daily specific conductance data at BELA-088.

Model	**AICc**	**ΔAICc**	**Ljung-Box Test p-value**
Daily Precipitation + Month	2065.18	0.00	0.4615
Relative Humidity + Month	2067.83	2.65	0.3758
Intercept Only	2339.10	273.92	0.9908
Air Temperature	2340.40	275.22	0.9755
Daily Precipitation	2340.93	275.75	0.9771
Relative Humidity	2341.00	275.82	0.9763
Air Temperature + Daily Precipitation	2342.11	276.93	0.9436

Table A.79. Coefficients and variance components estimates for the top covariate model for daily specific conductance data at BELA-088.

Parameter	**Coefficient**	**SE**	**p-value**
ar1	0.98	0.01	< 0.0001
ma1	0.08	0.05	0.1199
intercept	119.03	5.78	< 0.0001
Daily Precipitation	-1.04	0.60	0.0822
Month	6.53	0.33	< 0.0001

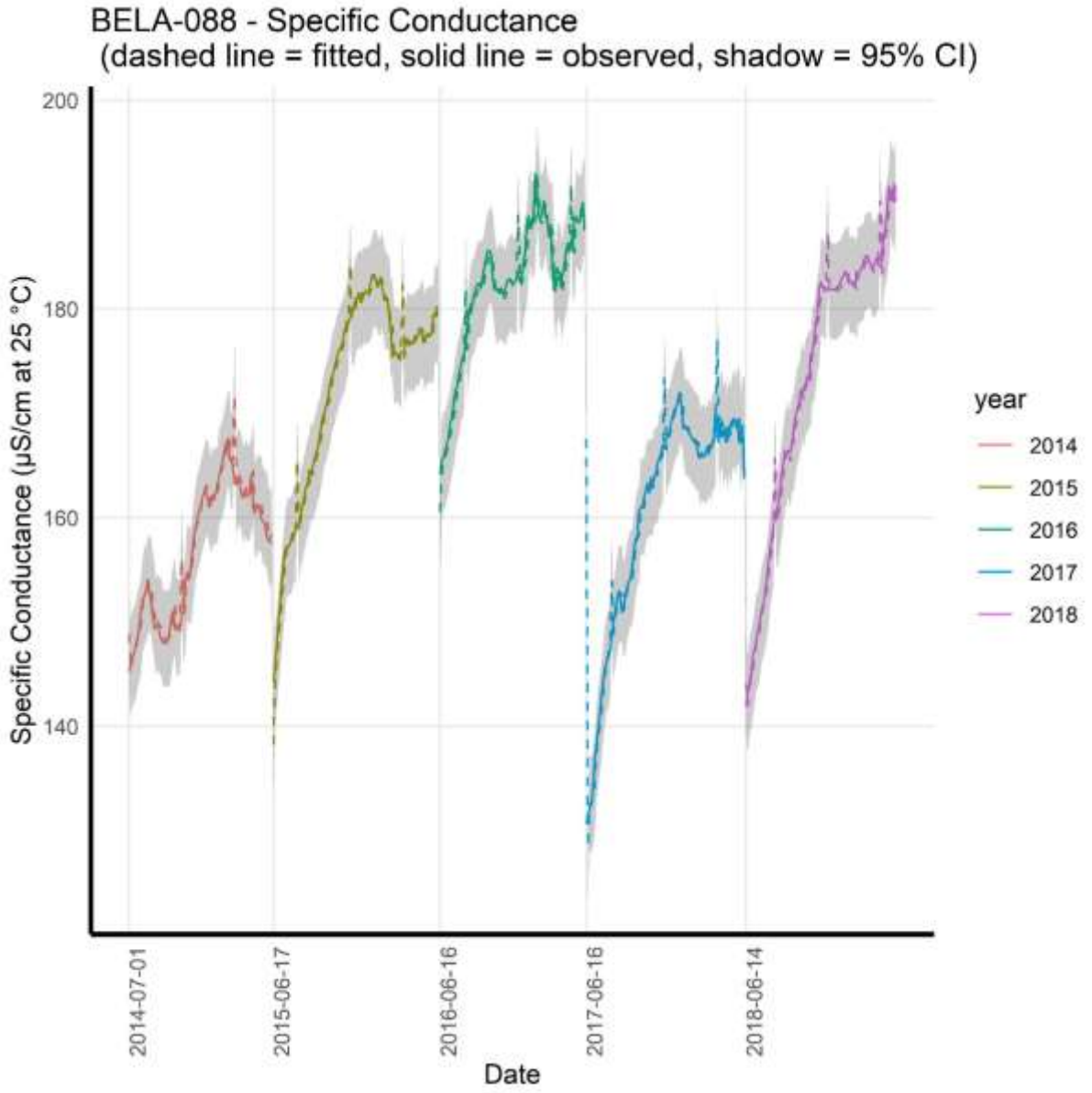


Figure A.74. Model predictions of BELA-088 specific conductance by date.

BELA-108

Data

For BELA-108, specific conductance was recorded from 2015 through 2019. Over this period, 456 records were collected from June to September. When truncating the data set to the subset of 86 days visited every year, the dataset had 430 observations. Covariate coverage was poor in 2019, so covariate models only considered 2015-2018, but wind speed and solar radiation were omitted from the model selection process due to missingness in 2018. This left 365 records for covariate modeling.

When aggregating specific conductance data to weekly mean values the number of observations was reduced to 71. When truncated the weekly data to the common set of 13 weeks sampled in every year the number of observation was further reduced to 65.

Model Selection

None of the trend models yielded stationary residuals when fit to daily specific conductance data. When fit to the weekly specific conductance data, the truncated seasonally adjusted models for logged and unlogged observations yielded stationary residuals, as well as the model for the complete logged dataset. The unlogged truncated seasonally adjusted model included a trend coefficient that was positive and significantly greater than zero, but the other two models did not include a significant trend coefficient. Overall, there is weak evidence for an increasing trend in specific conductance at lake BELA-108.

For ARIMA models fitting all possible covariate combinations fit to daily data at lake BELA-108, AICc-based model selection resulted in a model with ARIMA(1,0,0) structure and fixed effects for relative humidity and month. Specific conductance was estimated to increase with month (June-September). The coefficient for relative humidity was not significantly greater than zero.

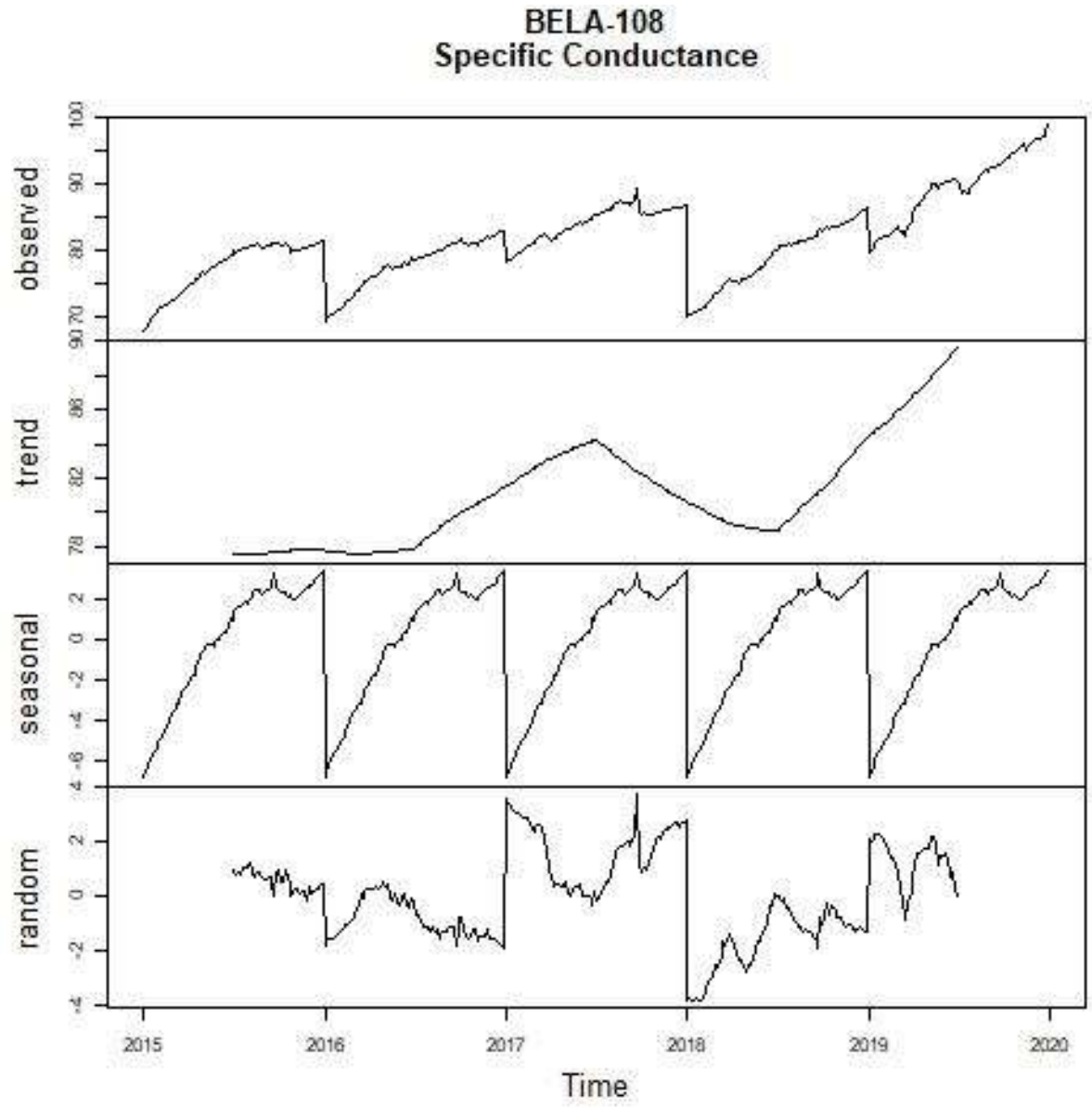


Figure A.75. Time series decomposition of truncated BELA-108 specific conductance by year.

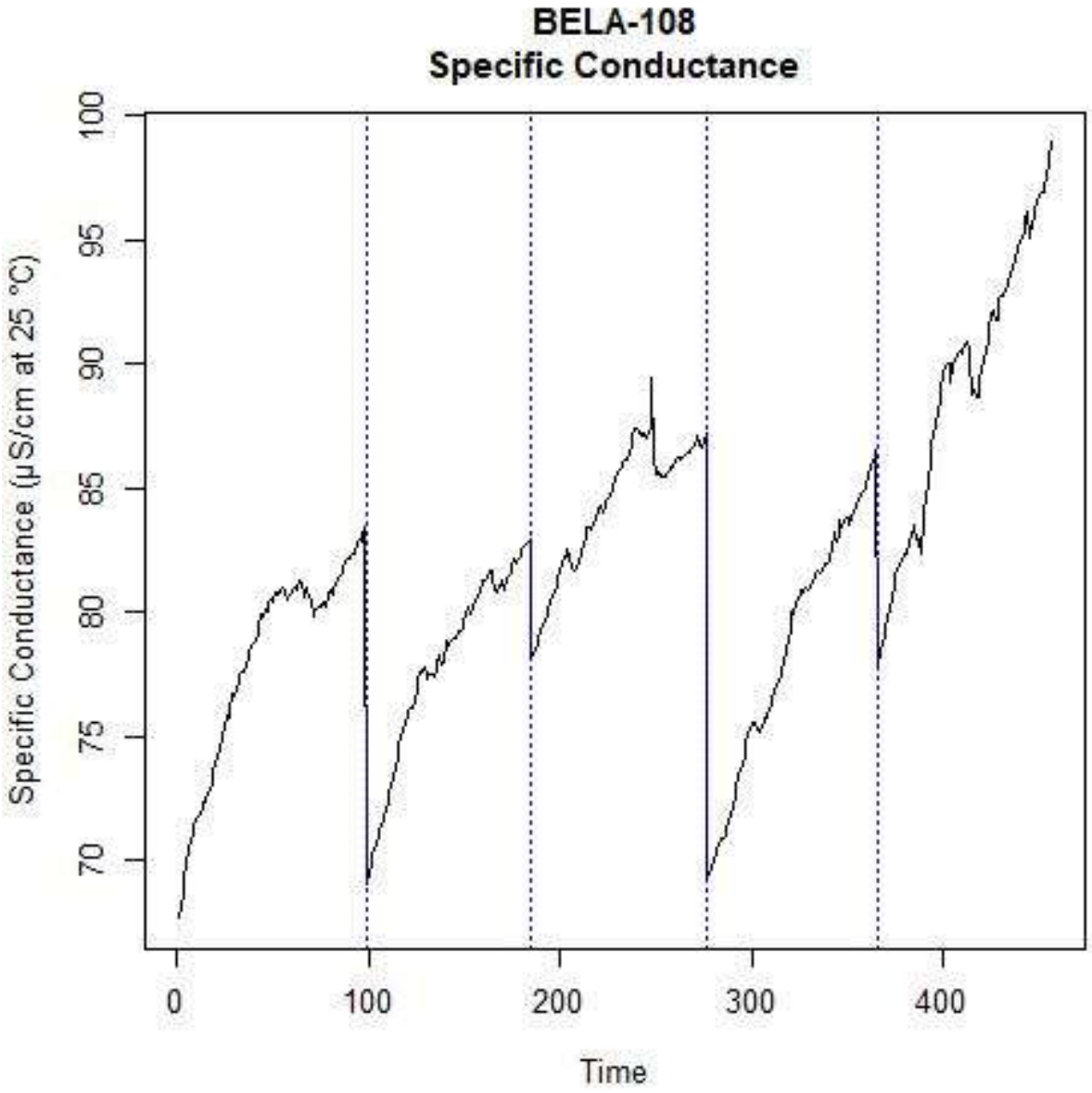


Figure A.76. Time series of BELA-108 specific conductance by time point with vertical lines for additive outliers.

Table A.80. Trend modeling results for daily specific conductance data at BELA-108.

			Trend			ARMA order		Ljung-Box Test	
Logged	**Method**	**Intercept**	**Coefficient**	**SE**	**p-value**	**AR**	**MA**	**Statistic**	**p-value**
FALSE	complete	75.65	0.50	0.37	0.1773	0	5	385.57	< 0.0001
FALSE	completeAO	64.73	1.41	0.29	< 0.0001	0	5	514.36	< 0.0001

			Trend			ARMA order		Ljung-Box Test	
Logged	**Method**	**Intercept**	**Coefficient**	**SE**	**p-value**	**AR**	**MA**	**Statistic**	**p-value**
FALSE	trunc	54.42	2.29	0.23	< 0.0001	0	2	2248.88	< 0.0001
FALSE	truncSA	56.22	2.12	0.17	< 0.0001	0	5	1565.87	< 0.0001
TRUE	complete	4.33	0.01	0.00	0.2198	0	5	361.92	< 0.0001
TRUE	completeAO	4.20	0.02	0.00	< 0.0001	0	5	489.65	< 0.0001
TRUE	trunc	4.03	0.03	0.00	< 0.0001	0	1	4179.22	< 0.0001
TRUE	truncSA	4.09	0.03	0.00	< 0.0001	0	5	1490.67	< 0.0001

Table A.81. Trend modeling results for weekly specific conductance data at BELA-108.

			Trend			ARMA order		Ljung-Box Test	
Logged	**Method**	**Intercept**	**Coefficient**	**SE**	**p-value**	**AR**	**MA**	**Statistic**	**p-value**
FALSE	complete	82.28	-0.39	1.710	0.8200	0	4	10.18	0.0375
FALSE	completeAO	76.74	2.66	0.430	< 0.0001	0	0	100.52	< 0.0001
FALSE	trunc	79.52	1.30	1.320	0.3230	0	5	12.07	0.0338
FALSE	truncSA	78.66	1.24	0.410	0.0024	0	5	7.15	0.2098
TRUE	complete	4.40	-0.00	0.020	0.8581	0	4	7.99	0.0920
TRUE	completeAO	4.34	0.03	0.010	< 0.0001	0	0	100.00	< 0.0001
TRUE	trunc	4.65	-0.14	0.000	< 0.0001	2	0	22.02	0.0049
TRUE	truncSA	4.40	0.00	0.009	0.9715	1	1	12.10	0.1467

Table A.82. Top covariate models for daily specific conductance data at BELA-108.

Model	**AICc**	**ΔAICc**	**Ljung-Box Test p-value**
Relative Humidity + Month	915.51	0.00	0.8859
Daily Precipitation + Month	916.79	1.28	0.8964
Air Temperature	1212.80	297.29	0.9997
Relative Humidity	1214.54	299.03	0.9994
Air Temperature + Daily Precipitation	1214.81	299.31	0.9987
Intercept Only	1214.88	299.37	> 0.9999
Daily Precipitation	1216.92	301.42	0.9999

Table A.83. Coefficients and variance components estimates for the top covariate model for daily specific conductance data at BELA-108.

Parameter	Coefficient	SE	p-value
ar1	0.97	0.01	< 0.0001
intercept	56.88	1.77	< 0.0001
Relative Humidity	0.01	0.00	0.0672
Month	2.91	0.14	< 0.0001

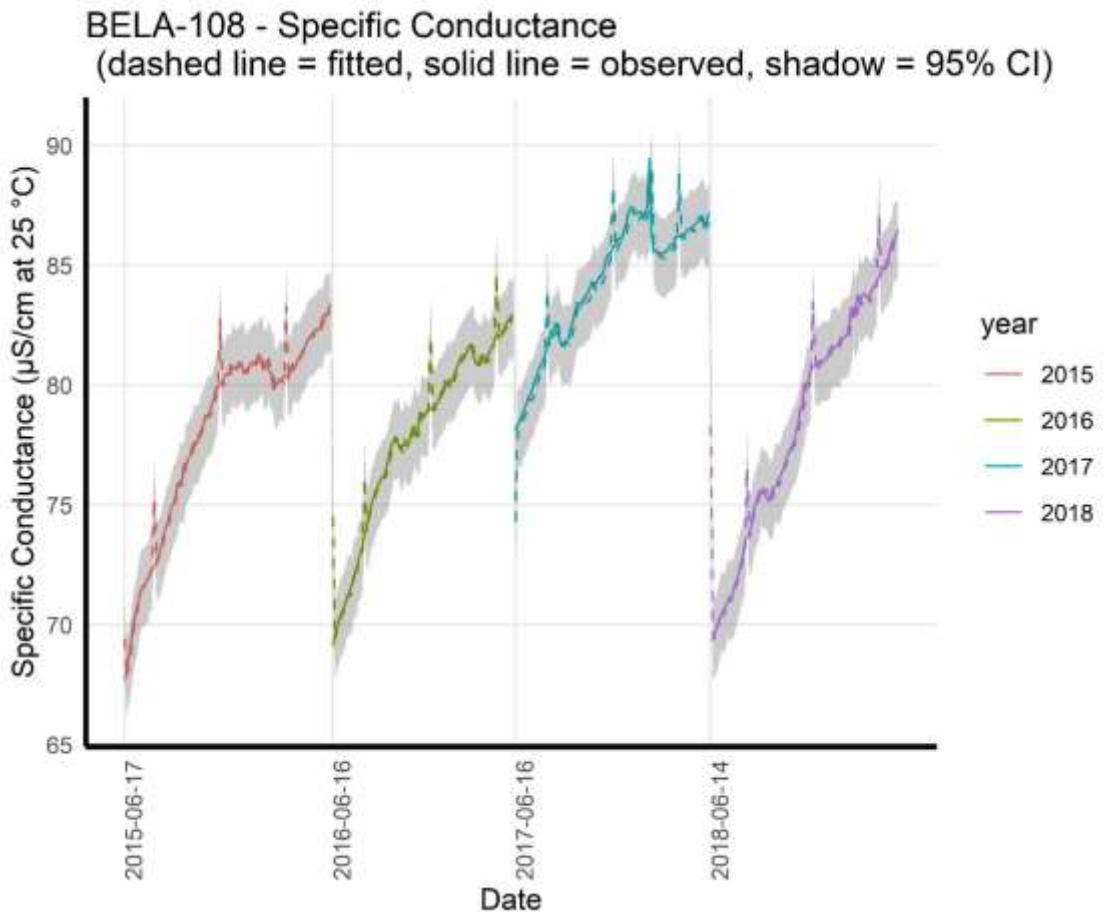


Figure A.77. Model predictions of BELA-108 specific conductance by date.

DENA-018

Data

For DENA-018, specific conductance was recorded from 2014 through 2019. Over this period, 696 records were collected from June to September. When truncating the data set to the subset of 99 days visited every year, the dataset had 594 observations. Covariate coverage was poor in 2019, so covariate models only considered data from 2014-2018.

Model Selection

For DENA-018, the following trends models yielded stationary residuals when fit to the unlogged data: complete with additive outliers, truncated, and truncated seasonally adjusted. Of these three models, two included trend coefficients that were significantly greater than zero, indicating there is evidence for an increasing trend in specific conductance at lake DENA-018. For ARIMA models fitting all possible covariate combinations, AICc-based model selection resulted in a model with ARIMA(1,0,2) structure and fixed effects for air temperature, daily precipitation, and year. Air temperature and year were estimated to have a positive effect on specific conductance, whereas the effect for daily precipitation was estimated to be negative, but was not significantly less than zero.

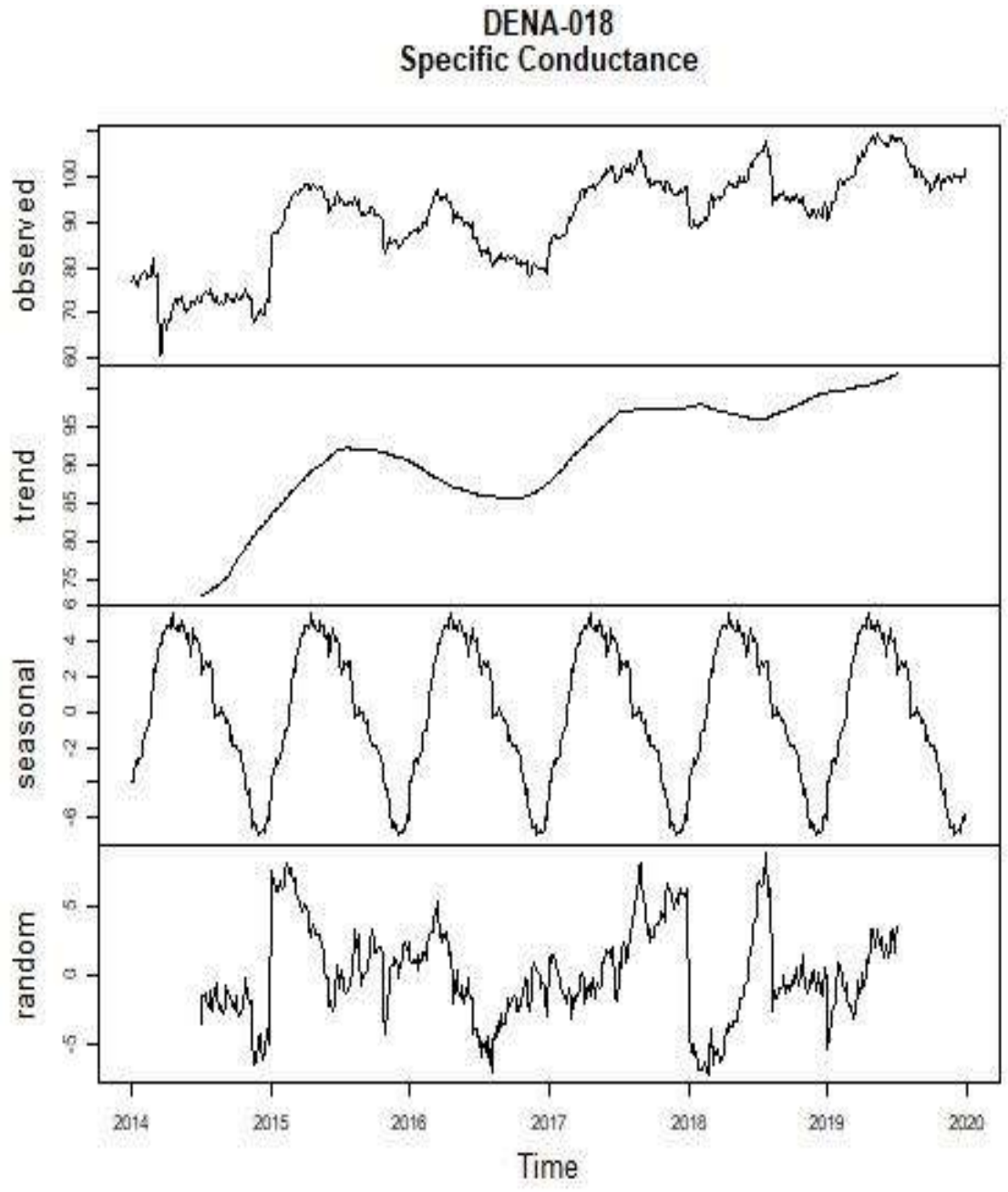


Figure A.78. Time series decomposition of truncated DENA-018 specific conductance by year.

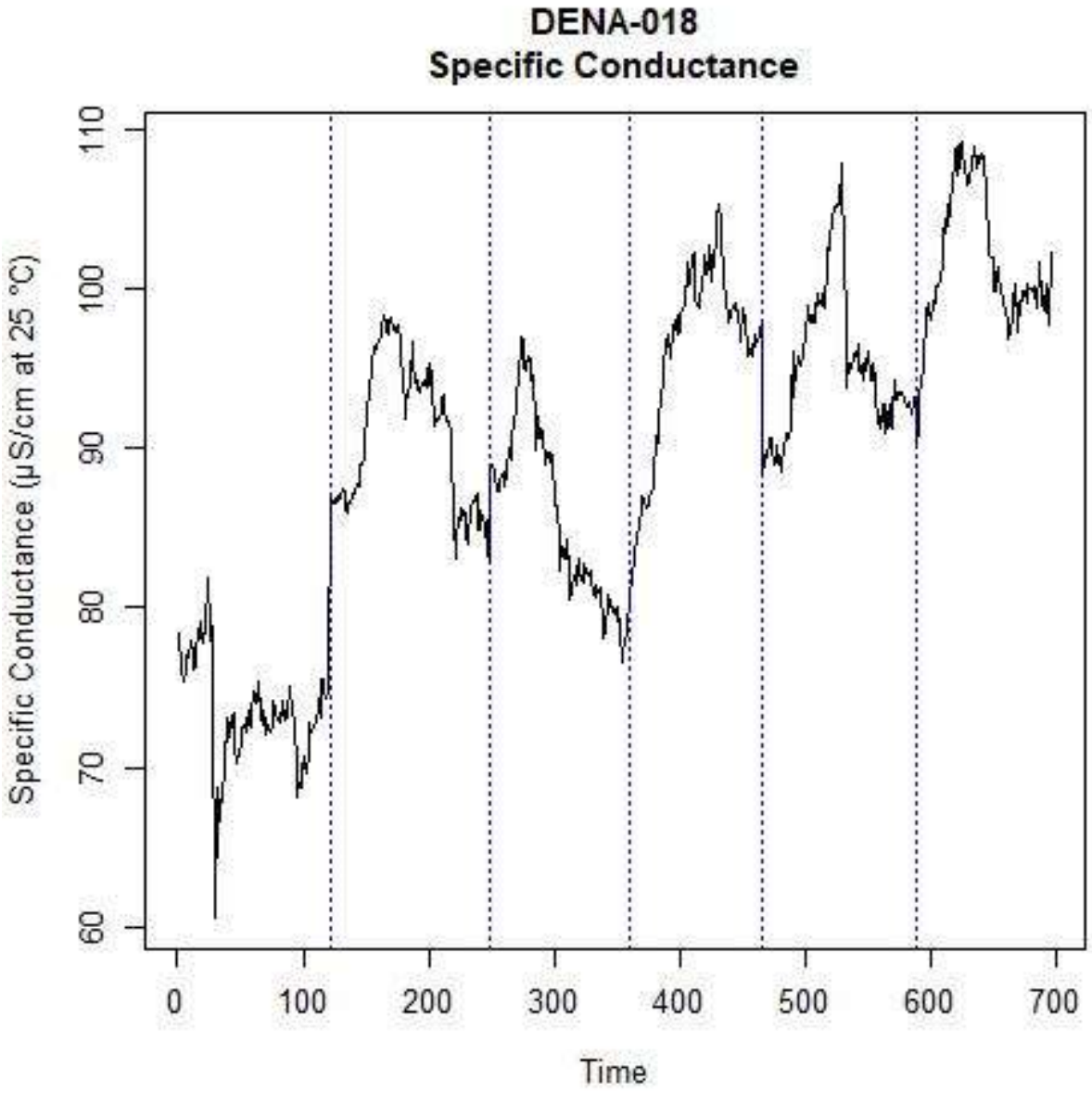


Figure A.79. Time series of DENA-018 specific conductance by time point with vertical lines for additive outliers.

Table A.84. Trend modeling results for daily specific conductance data at DENA-018.

			Trend			ARMA order		Ljung-Box Test	
Logged	**Method**	**Intercept**	**Coefficient**	**SE**	**p-value**	**AR**	**MA**	**Statistic**	**p-value**
FALSE	complete	70.28	1.38	0.60	0.0219	2	2	12.52	0.0139
FALSE	completeAO	57.89	2.24	0.83	0.0072	5	3	5.45	0.1417

			Trend			ARMA order		Ljung-Box Test	
Logged	**Method**	**Intercept**	**Coefficient**	**SE**	**p-value**	**AR**	**MA**	**Statistic**	**p-value**
FALSE	trunc	52.23	2.67	0.63	< 0.0001	1	1	90.46	0.9559
FALSE	truncSA	86.81	0.31	0.64	0.6216	1	1	106.65	0.6986
TRUE	complete	4.20	0.02	0.01	0.0039	5	2	2.62	0.4533
TRUE	completeAO	4.06	0.03	0.01	0.0016	5	3	6.54	0.0882
TRUE	trunc	3.99	0.04	0.01	< 0.0001	1	0	104.47	0.7493
TRUE	truncSA	4.44	0.00	0.01	0.5861	2	1	101.77	0.7870

Table A.85. Top covariate models for daily specific conductance data at DENA-018.

Model	**AICc**	**ΔAICc**	**Ljung-Box Test p-value**
Air Temperature + Daily Precipitation + Year	2017.97	0.00	0.0637
Air Temperature + Year	2020.24	2.28	0.0702
Air Temperature + Daily Precipitation	2020.29	2.32	0.3880
Air Temperature	2020.49	2.52	0.4163
Wind Speed + Year	2020.51	2.54	0.0714
Daily Precipitation + Year	2024.94	6.98	0.1128
Daily Precipitation + Year + Month	2026.48	8.52	0.0508
Solar Radiation + Daily Precipitation + Year	2026.86	8.89	0.0585
Solar Radiation + Year	2027.84	9.87	0.1211
Wind Speed + Solar Radiation + Daily Precipitation	2028.35	10.38	0.2670

Table A.86. Coefficients and variance components estimates for the top covariate model for daily specific conductance data at DENA-018.

Parameter	**Coefficient**	**SE**	**p-value**
ar1	0.99	0.01	< 0.0001
ma1	0.05	0.04	0.2076
ma2	-0.13	0.04	0.0015
intercept	64.17	10.28	< 0.0001
Air Temperature	0.08	0.03	0.0026
Daily Precipitation	-0.25	0.16	0.1300
Year	1.61	0.70	0.0219

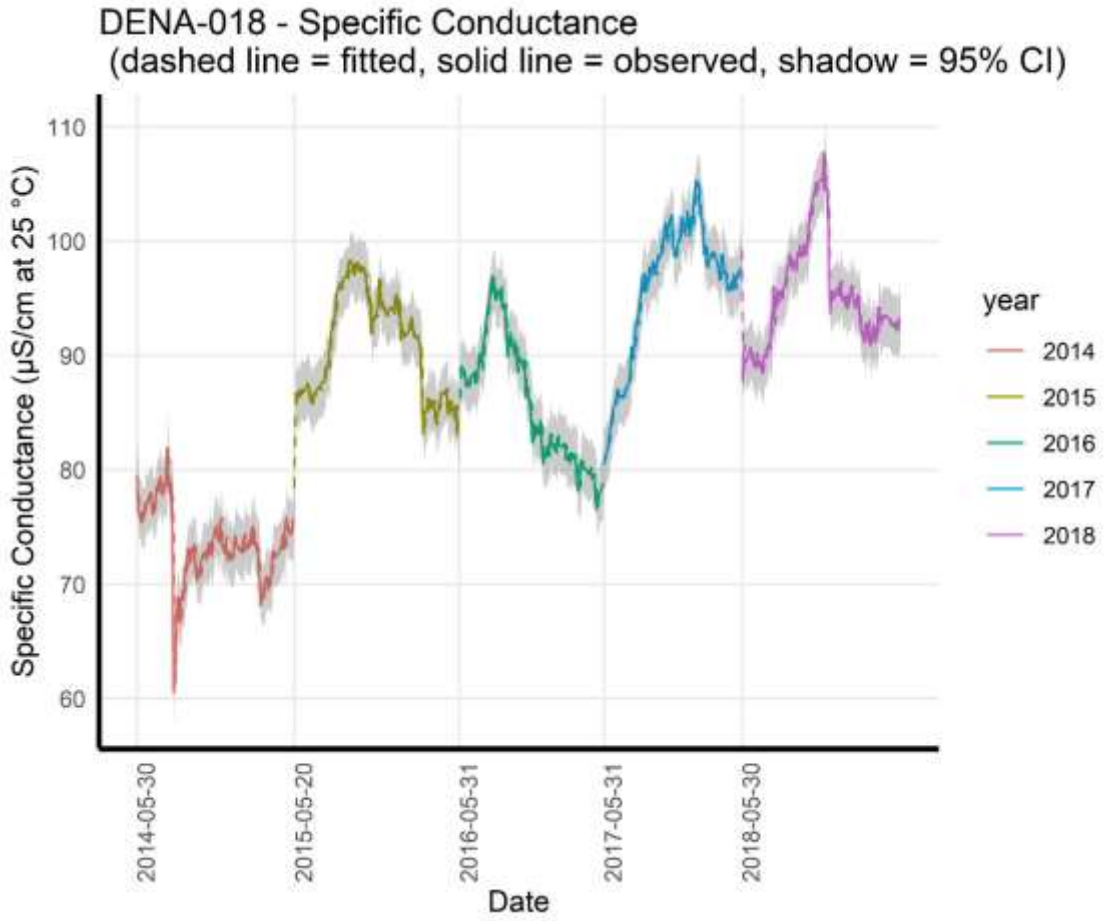


Figure A.80. Model predictions of DENA-018 specific conductance by date.

DENA-023

Data

For DENA-023, specific conductance was recorded from 2011 through 2019, during the months May-November. The complete dataset included 1017 specific conductance observations, however when truncated to the common set of 44 days visited every year, the number of observations was reduced to 396. Data coverage for covariates were sufficient such that no covariates nor years were excluded from the analysis.

Model Selection

For DENA-023, the truncated seasonally adjusted trend models fit to logged and unlogged specific conductance data yielded stationary residuals. Neither of these two models included a trend coefficient that was significantly different from zero, indicating there is no evidence for an increasing or decreasing trend in specific conductance at lake DENA-023. For ARIMA models fitting all possible covariate combinations, AICc-based model selection resulted in a model with ARIMA(1,0,1) structure and fixed effects for daily precipitation and month. Specific conductance was estimated to increase with month (May-November). The coefficient for daily precipitation was not significantly less than zero.

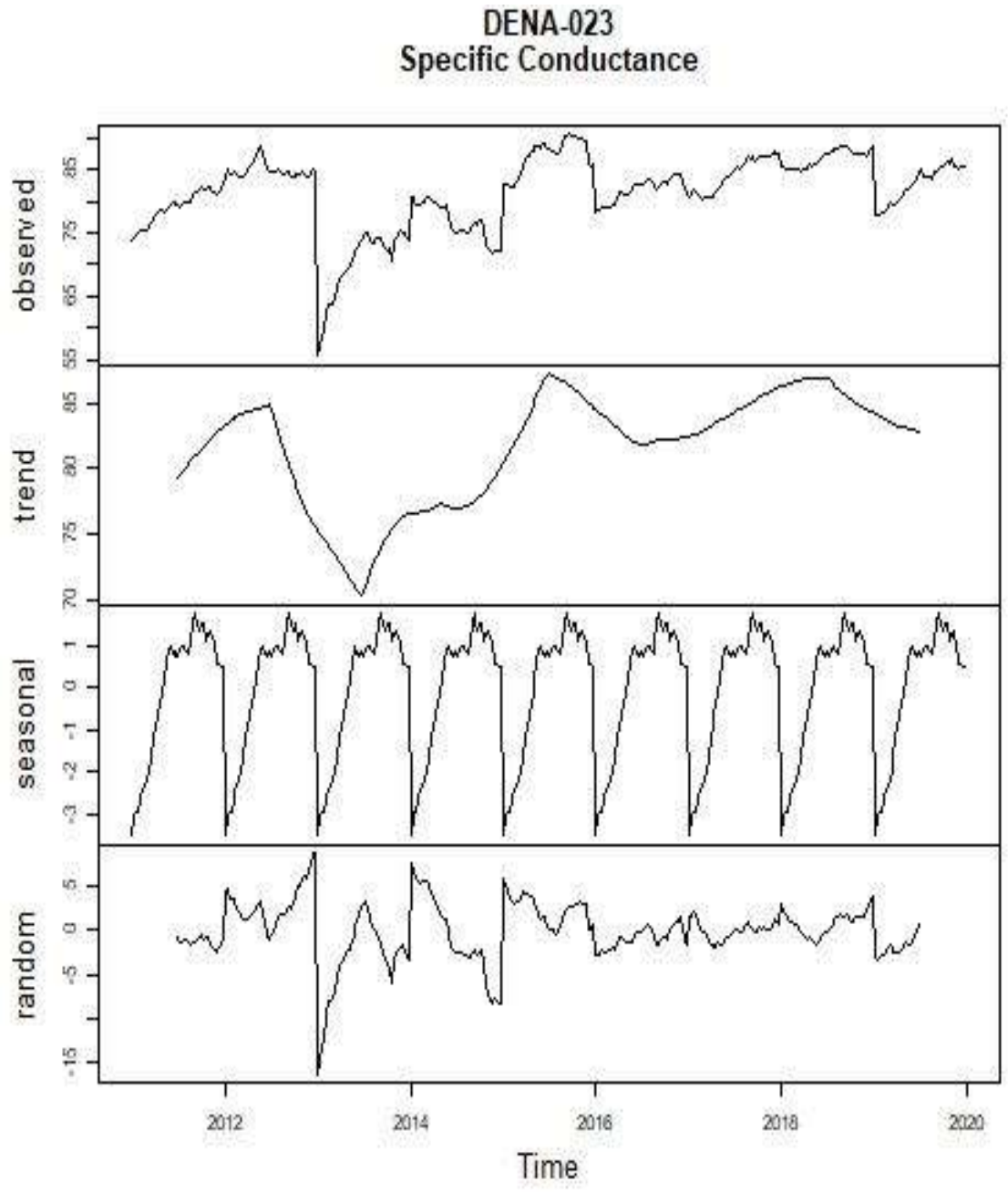


Figure A.81. Time series decomposition plot of DENA-023 specific conductance by year.

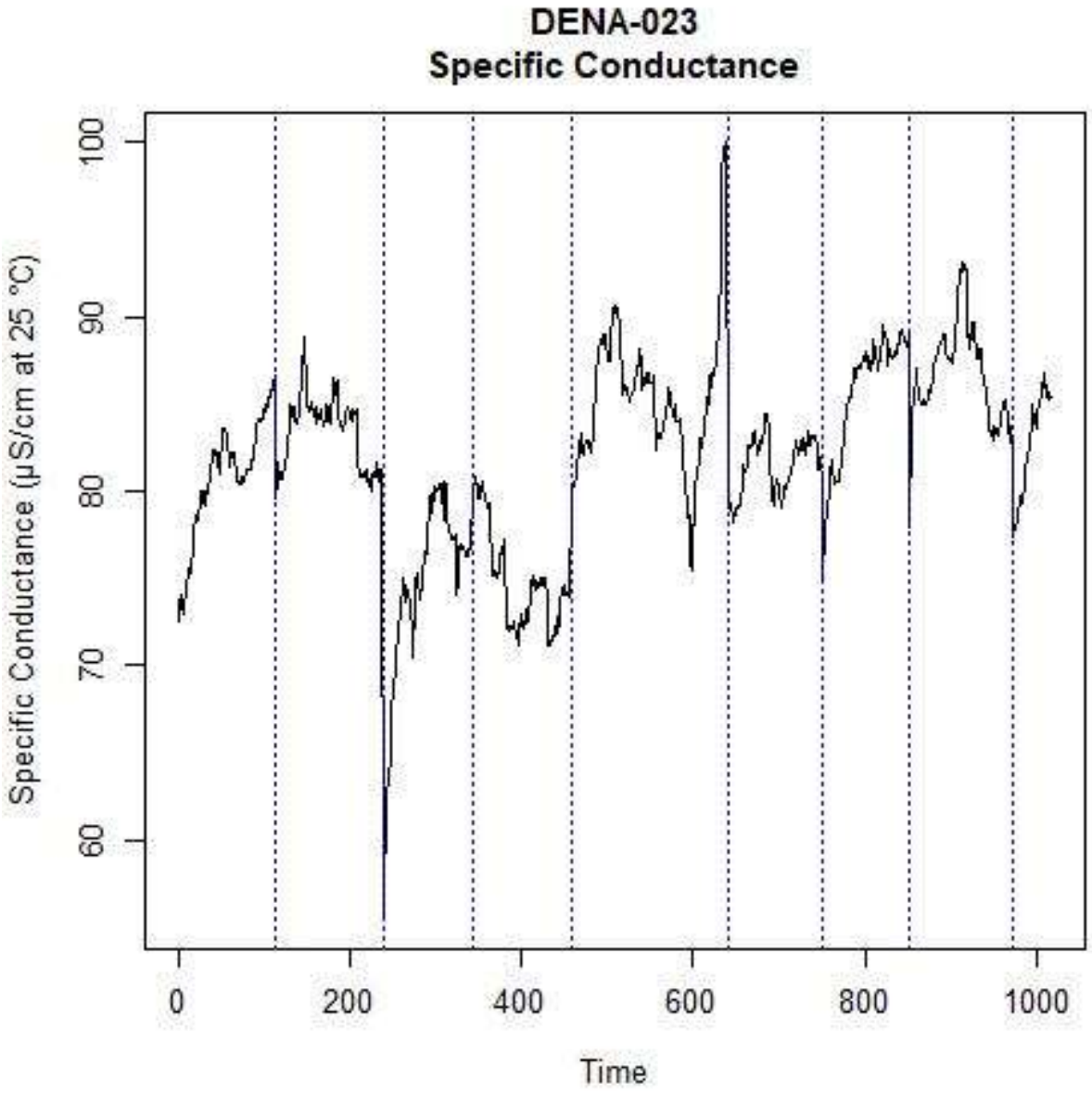


Figure A.82. Time series of DENA-023 specific conductance by time point with vertical lines for additive outliers.

Table A.87. Trend modeling results for daily specific conductance data at DENA-023.

			Trend			ARMA order		Ljung-Box Test	
Logged	**Method**	**Intercept**	**Coefficient**	**SE**	**p-value**	**AR**	**MA**	**Statistic**	**p-value**
FALSE	complete	75.68	0.49	0.12	< 0.0001	0	5	705.04	< 0.0001
FALSE	completeAO	72.99	0.71	0.11	< 0.0001	0	5	1377.65	< 0.0001

			Trend			ARMA order		Ljung-Box Test	
Logged	**Method**	**Intercept**	**Coefficient**	**SE**	**p-value**	**AR**	**MA**	**Statistic**	**p-value**
FALSE	trunc	71.03	0.80	0.15	< 0.0001	0	4	297.45	< 0.0001
FALSE	truncSA	74.70	0.53	0.42	0.2091	1	0	53.02	0.9793
TRUE	complete	4.33	0.01	0.00	< 0.0001	0	5	652.58	< 0.0001
TRUE	completeAO	4.29	0.01	0.00	< 0.0001	0	5	1313.14	< 0.0001
TRUE	trunc	4.28	0.01	0.00	< 0.0001	0	5	159.14	< 0.0001
TRUE	truncSA	4.30	0.01	0.01	0.1672	1	0	50.62	0.9890

Table A.88. Top covariate models for daily specific conductance data at DENA-023.

Model	**AICc**	**ΔAICc**	**Ljung-Box Test p-value**
Daily Precipitation + Month	3064.83	0.00	0.5170
Wind Speed + Month	3064.92	0.09	0.4976
Wind Speed + Daily Precipitation + Month	3065.87	1.04	0.3715
Air Temperature + Daily Precipitation	3302.83	237.99	0.6801
Air Temperature	3303.38	238.55	0.7979
Air Temperature + Wind Speed + Daily Precipitation	3304.21	239.37	0.5540
Air Temperature + Wind Speed	3305.09	240.26	0.7021
Solar Radiation + Daily Precipitation	3367.83	303.00	0.7956
Wind Speed + Solar Radiation + Daily Precipitation	3369.78	304.94	0.6948
Solar Radiation	3370.94	306.11	0.8567

Table A.89. Coefficients and variance components estimates for the top covariate model for daily specific conductance data at DENA-023.

Parameter	**Coefficient**	**SE**	**p-value**
ar1	0.98	0.01	< 0.0001
ma1	0.08	0.03	0.0077
intercept	69.00	1.69	< 0.0001
Daily Precipitation	-0.12	0.11	0.2406
Month	1.74	0.09	< 0.0001

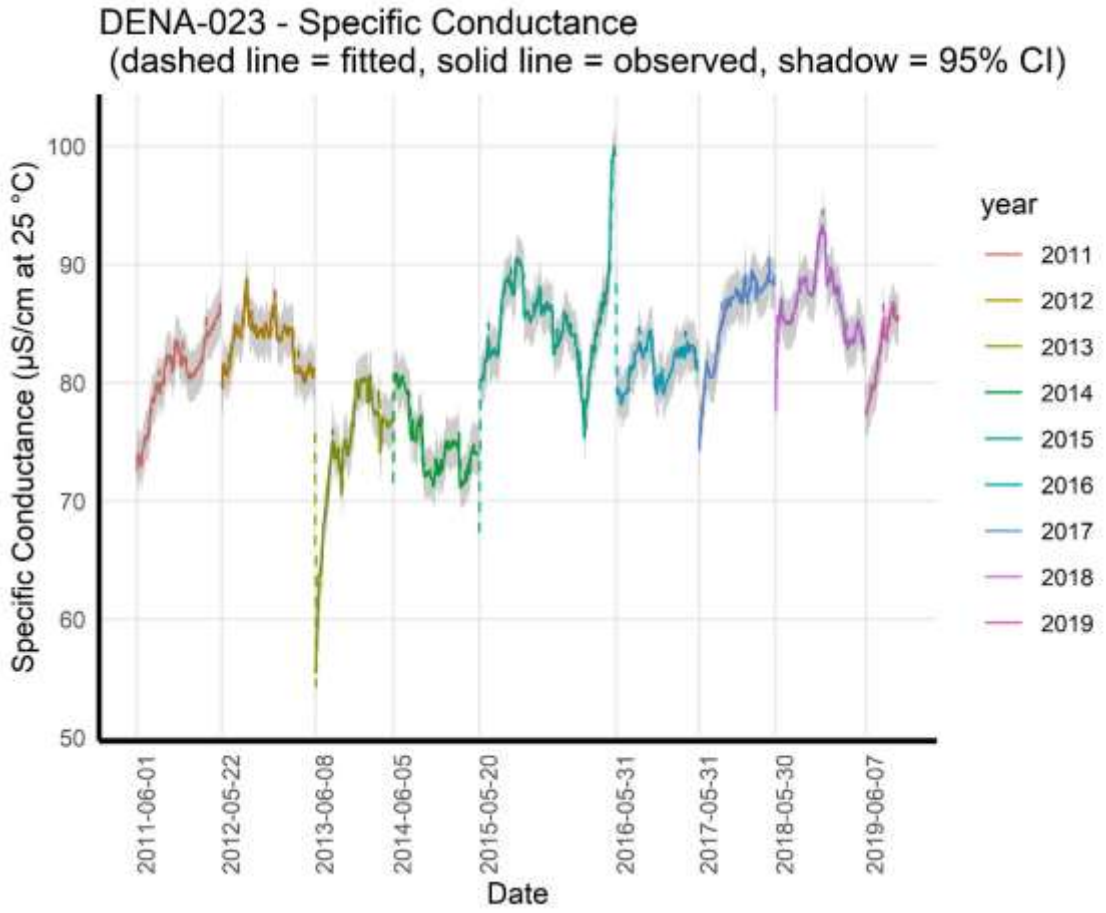


Figure A.83. Model predictions of DENA-023 specific conductance by date.

KOVA-085

Data

For KOVA-085, specific conductance was recorded from 2010 through 2018, during the months June-September. The complete dataset included 801 specific conductance observations, however when truncated to the common set of 66 days visited every year, the number of observations was reduced to 594. Data coverage for covariates were sufficient such that no covariates nor years were excluded from the analysis.

Model Selection

For KOVA-085, the complete and truncated seasonally adjusted trend models fit to logged and unlogged specific conductance data yielded stationary residuals. Of these four models, the two models fit to the complete dataset included positive trend coefficients that were significantly greater than zero, indicated there is some evidence for an increasing trend in specific conductance at lake KOVA-085. For ARIMA models fitting all possible covariate combinations, AICc-based model selection resulted in a model with ARIMA(2,0,1) structure and fixed effects for month and year. Specific conductance was estimated to increase with month (June-September) and study year (2010-2018).

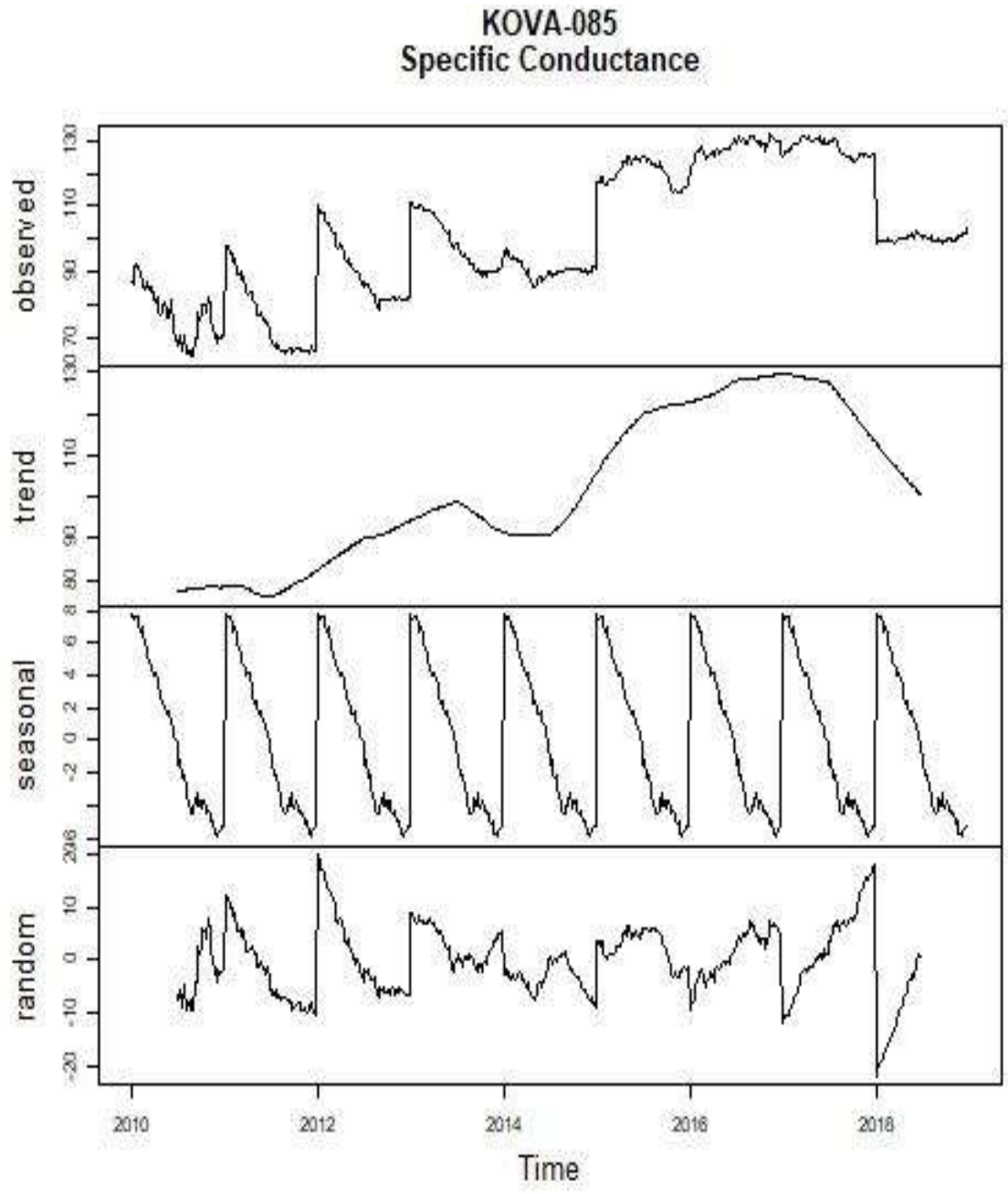


Figure A.84. Time series decomposition of truncated KOVA-085 specific conductance by year.

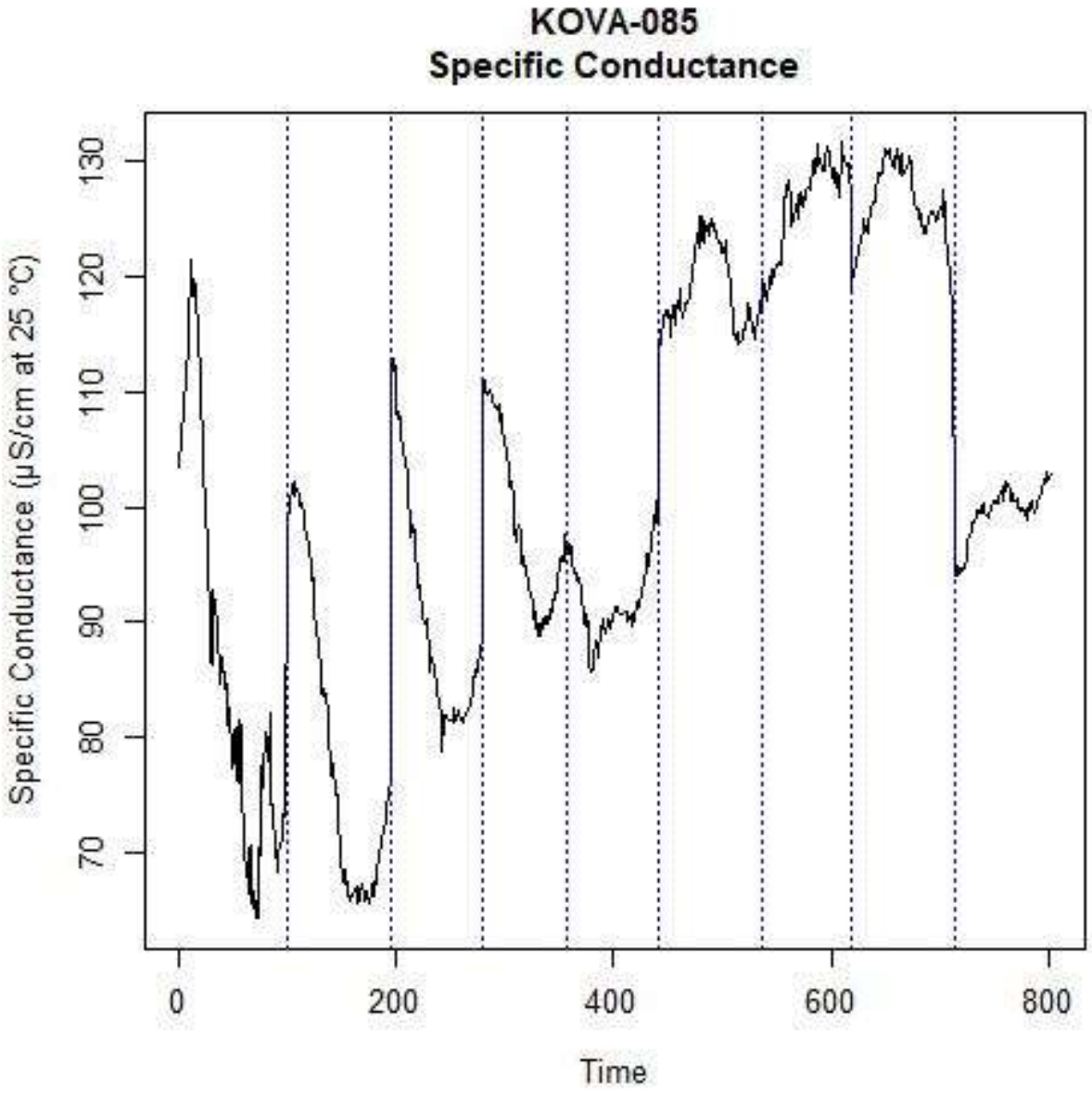


Figure A.85. Time series of KOVA-085 specific conductance by time point with vertical lines for additive outliers.

Table A.90. Trend modeling results for daily specific conductance data at KOVA-085.

			Trend			ARMA order		Ljung-Box Test	
Logged	**Method**	**Intercept**	**Coefficient**	**SE**	**p-value**	**AR**	**MA**	**Statistic**	**p-value**
FALSE	complete	NA	8.34	0.65	< 0.0001	2	1	3.70	0.7178
FALSE	completeAO	NA	8.79	0.60	< 0.0001	2	2	22.32	< 0.0001

			Trend			ARMA order		Ljung-Box Test	
Logged	Method	Intercept	Coefficient	SE	p-value	AR	MA	Statistic	p-value
FALSE	trunc	43.16	5.19	0.26	< 0.0001	0	0	10658.27	< 0.0001
FALSE	truncSA	94.46	0.51	0.98	0.6000	1	0	95.09	0.9223
TRUE	complete	3.69	0.08	0.01	< 0.0001	2	3	1.06	0.7870
TRUE	completeAO	3.65	0.09	0.01	< 0.0001	2	3	31.96	< 0.0001
TRUE	trunc	3.98	0.05	0.00	< 0.0001	0	3	2956.86	< 0.0001
TRUE	truncSA	4.52	0.01	0.01	0.5435	1	0	121.89	0.3358

Table A.91. Top covariate models for daily specific conductance data at KOVA-085.

Model	AICc	ΔAICc	Ljung-Box Test p-value
Air Temperature + Wind Speed + Year	3551.44	0.00	0.3609
Year + Month	3552.43	0.99	0.4956
Wind Speed + Year	3552.89	1.45	0.6995
Wind Speed + Relative Humidity + Year	3553.35	1.91	0.4106
Wind Speed + Daily Precipitation + Year + Month	3553.41	1.97	0.4078
Air Temperature + Year	3553.61	2.17	0.3141
Daily Precipitation + Year + Month	3553.97	2.53	0.3526
Relative Humidity + Year + Month	3553.98	2.54	0.3379
Air Temperature + Wind Speed + Daily Precipitation + Year	3554.08	2.64	0.3942
Wind Speed + Year + Month	3554.39	2.95	0.5601

Table A.92. Coefficients and variance components estimates for the top covariate model for daily specific conductance data at KOVA-085.

Parameter	Coefficient	SE	p-value
ar1	1.91	0.05	< 0.0001
ar2	-0.92	0.05	< 0.0001
ma1	-0.88	0.06	< 0.0001
intercept	40.58	15.15	0.0074
Year	5.92	1.12	< 0.0001
Month	-0.51	0.37	0.1651

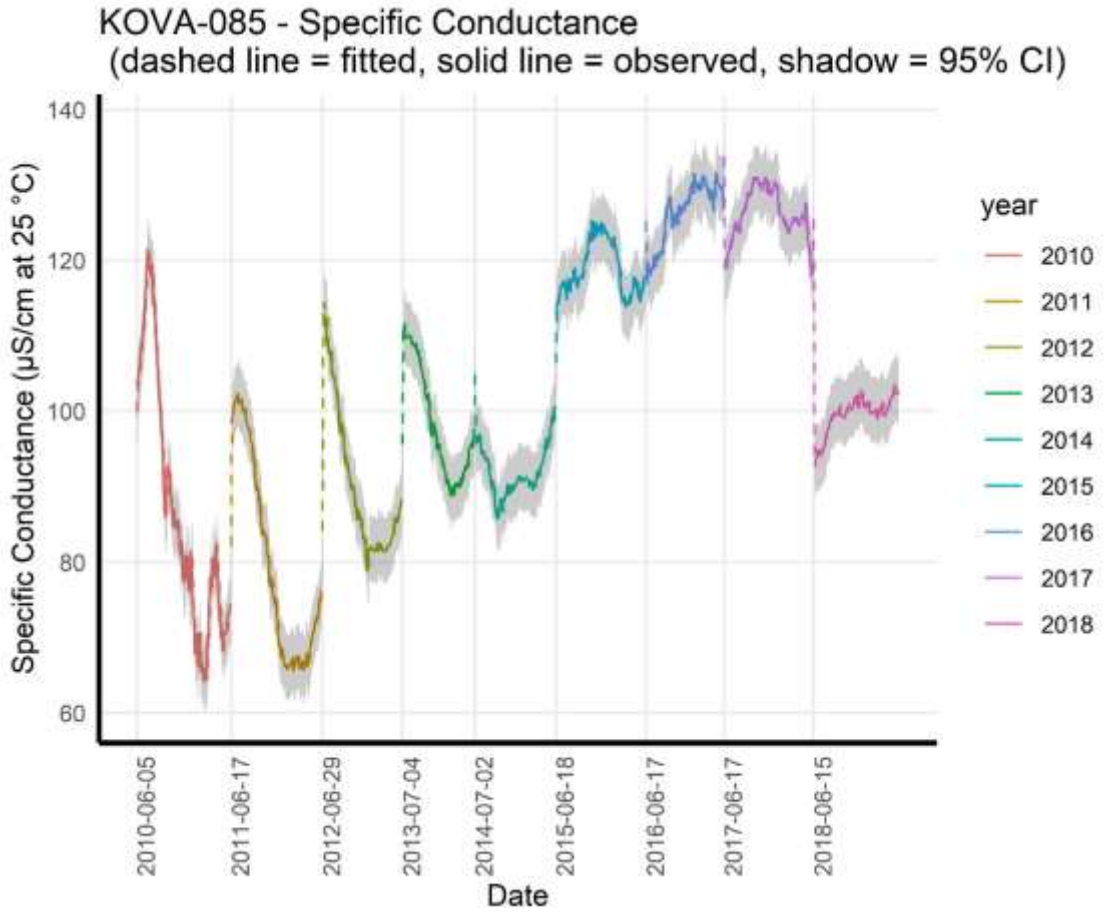


Figure A.86. Model predictions of KOVA-085 specific conductance by date.

KOVA-086

Data

For KOVA-086, specific conductance was recorded from 2011 through 2019, during the months June-September. The complete dataset included 783 specific conductance observations, however when truncated to the common set of 59 days visited every year, the number of observations was reduced to 531. Data coverage for covariates were sufficient such that no covariates nor years were excluded from the analysis.

Model Selection

For KOVA-086, only the truncated trend model fit to logged specific conductance data yielded stationary residuals. This model included a positive trend coefficient that was significantly greater than zero, indicated there is evidence for an increasing trend in specific conductance at lake KOVA-086. None of the ARIMA models fitting all possible covariate combinations yielded stationary residuals when fit to daily data for lake KOVA-086.

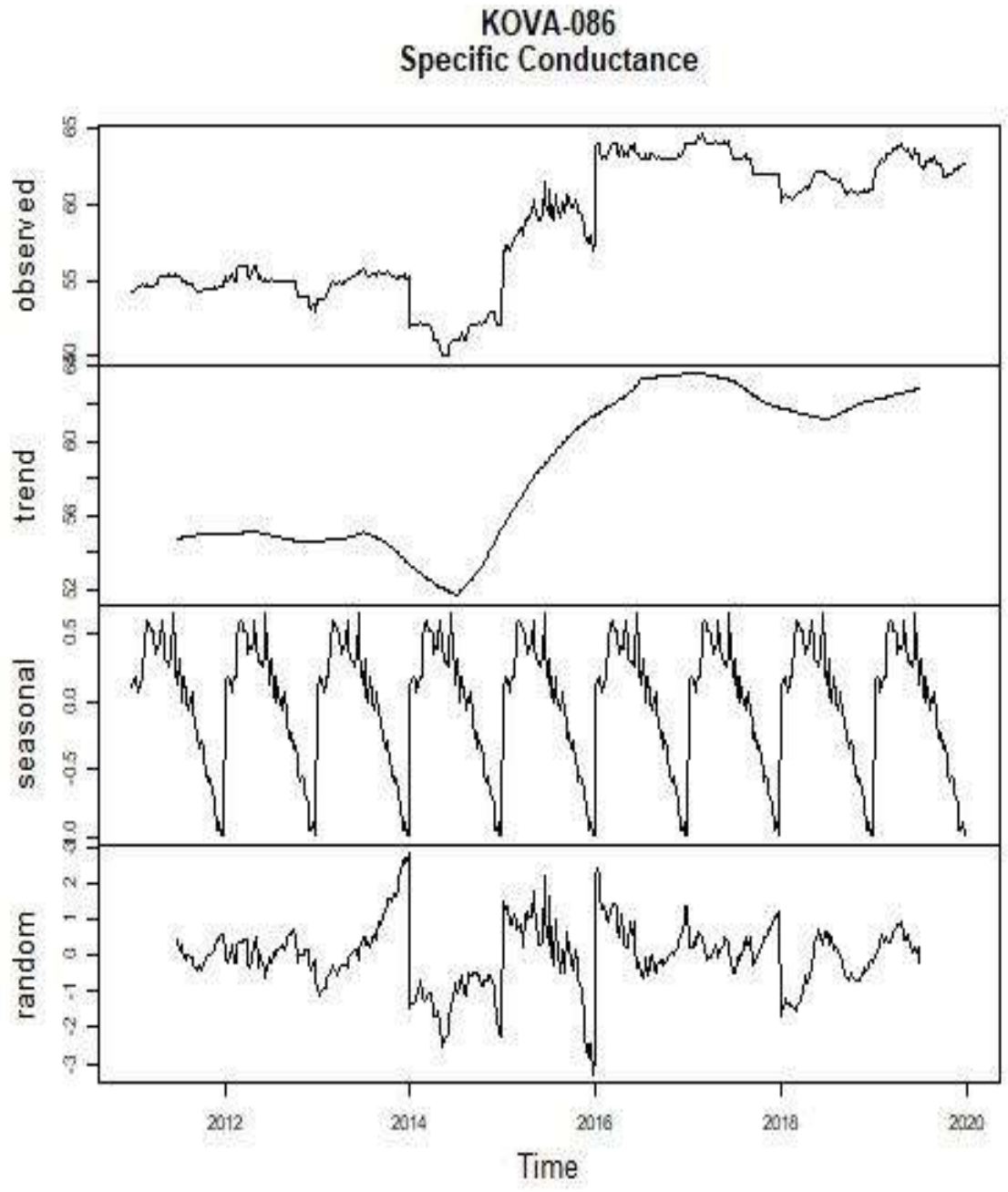


Figure A.87: Time series decomposition of truncated KOVA-086 specific conductance by year.

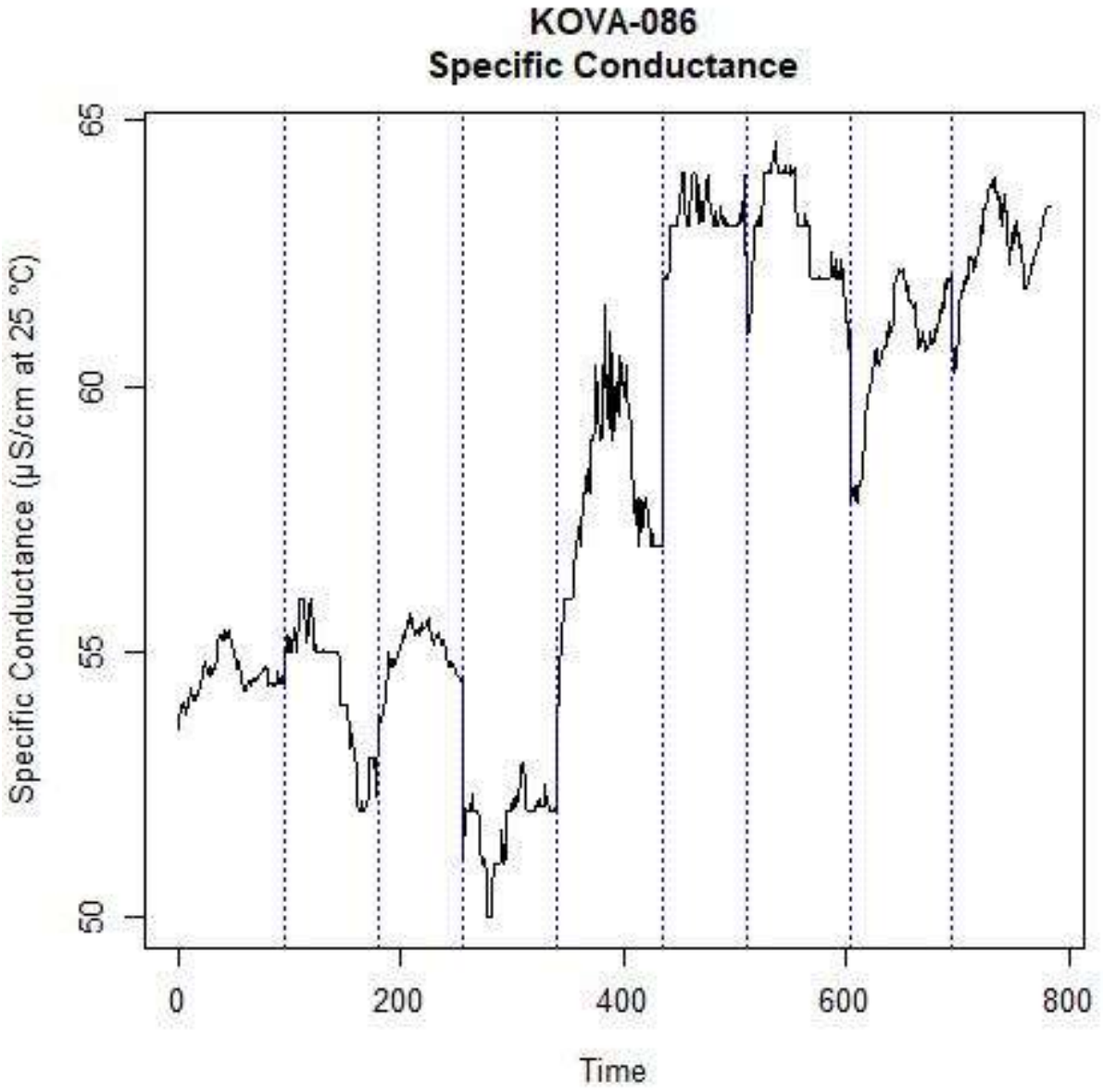


Figure A.88. Time series of KOVA-086 specific conductance by time point with vertical lines for additive outliers.

Table A.93. Trend modeling results for daily specific conductance data at KOVA-086.

			Trend			ARMA order		Ljung-Box Test	
Logged	**Method**	**Intercept**	**Coefficient**	**SE**	**p-value**	**AR**	**MA**	**Statistic**	**p-value**
FALSE	complete	43.99	1.18	0.05	< 0.0001	0	5	1049.10	< 0.0001
FALSE	completeAO	43.23	1.24	0.05	< 0.0001	0	5	2087.17	< 0.0001

			Trend			ARMA order		Ljung-Box Test	
Logged	**Method**	**Intercept**	**Coefficient**	**SE**	**p-value**	**AR**	**MA**	**Statistic**	**p-value**
FALSE	trunc	44.92	1.12	0.15	< 0.0001	1	0	127.74	0.0497
FALSE	truncSA	44.07	1.20	0.07	< 0.0001	0	5	1995.87	< 0.0001
TRUE	complete	3.82	0.02	0.00	< 0.0001	0	5	1065.75	< 0.0001
TRUE	completeAO	3.80	0.02	0.00	< 0.0001	0	5	2132.52	< 0.0001
TRUE	trunc	3.83	0.02	0.00	< 0.0001	1	0	124.72	0.0716
TRUE	truncSA	3.82	0.02	0.00	< 0.0001	0	5	1964.31	< 0.0001

Table A.94. Top covariate models for daily specific conductance data at KOVA-086.

Model	**AICc**	**ΔAICc**	**Ljung-Box Test p-value**
Air temperature + Wind Speed + year	685.32	0.00	0.1146
Air temperature + Wind Speed + daily precipitation + year	687.36	2.04	0.0652
Air temperature + year	690.52	5.20	0.1497
Air temperature + daily precipitation + year	692.39	7.07	0.0979
Wind Speed + Relative Humidity + year	695.39	10.07	0.1290
Wind Speed + year	695.43	10.11	0.1626
Wind Speed + Solar Radiation + year	696.37	11.05	0.0966
Wind Speed + year + Month	696.85	11.53	0.1044
Wind Speed + Relative Humidity + year + Month	696.99	11.67	0.0755
Wind Speed + daily precipitation + year	697.27	11.95	0.1040

Table A.95. Coefficients and variance components estimates for the top covariate model for daily specific conductance data at KOVA-086.

Parameter	**Coefficient**	**SE**	**p-value**
ar1	0.99	0.01	< 0.0001
intercept	47.80	2.37	< 0.0001
Air Temperature	0.03	0.01	0.0005
Wind Speed	-0.06	0.02	0.0069
Year	0.86	0.18	< 0.0001

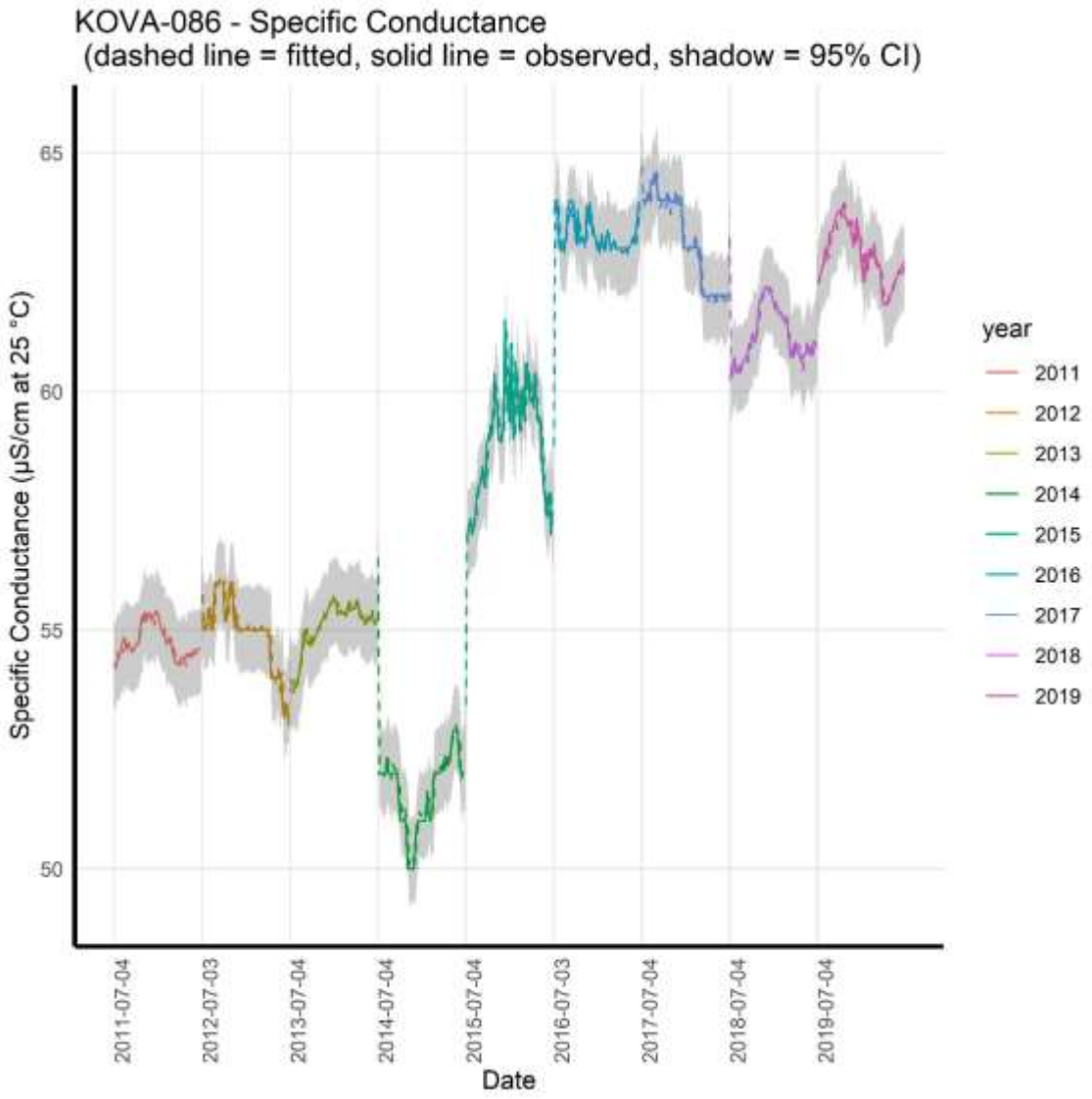


Figure A.89. Model predictions of KOVA-086 specific conductance by date.

NOAT-052

Data

For NOAT-052, specific conductance was recorded from 2015 through 2019, during the months May-September. The complete dataset included 491 specific conductance observations, however when truncated to the common set of 85 days visited every year, the number of observations was reduced to 425. Data coverage for covariates were sufficient such that no covariates nor years were excluded from the analysis.

Model Selection

For NOAT-052, none of the trend models fit to the daily specific conductance data yielded stationary residuals. For ARIMA models fitting all possible covariate combinations, AICc-based model selection resulted in a model with ARIMA(2,0,1) structure and fixed effects for month and year. Specific conductance was estimated to increase with month (June-September) and study year (2010-2018), indicating there is evidence for an increasing trend in specific conductance at lake NOAT-052 during years 2015-2019.

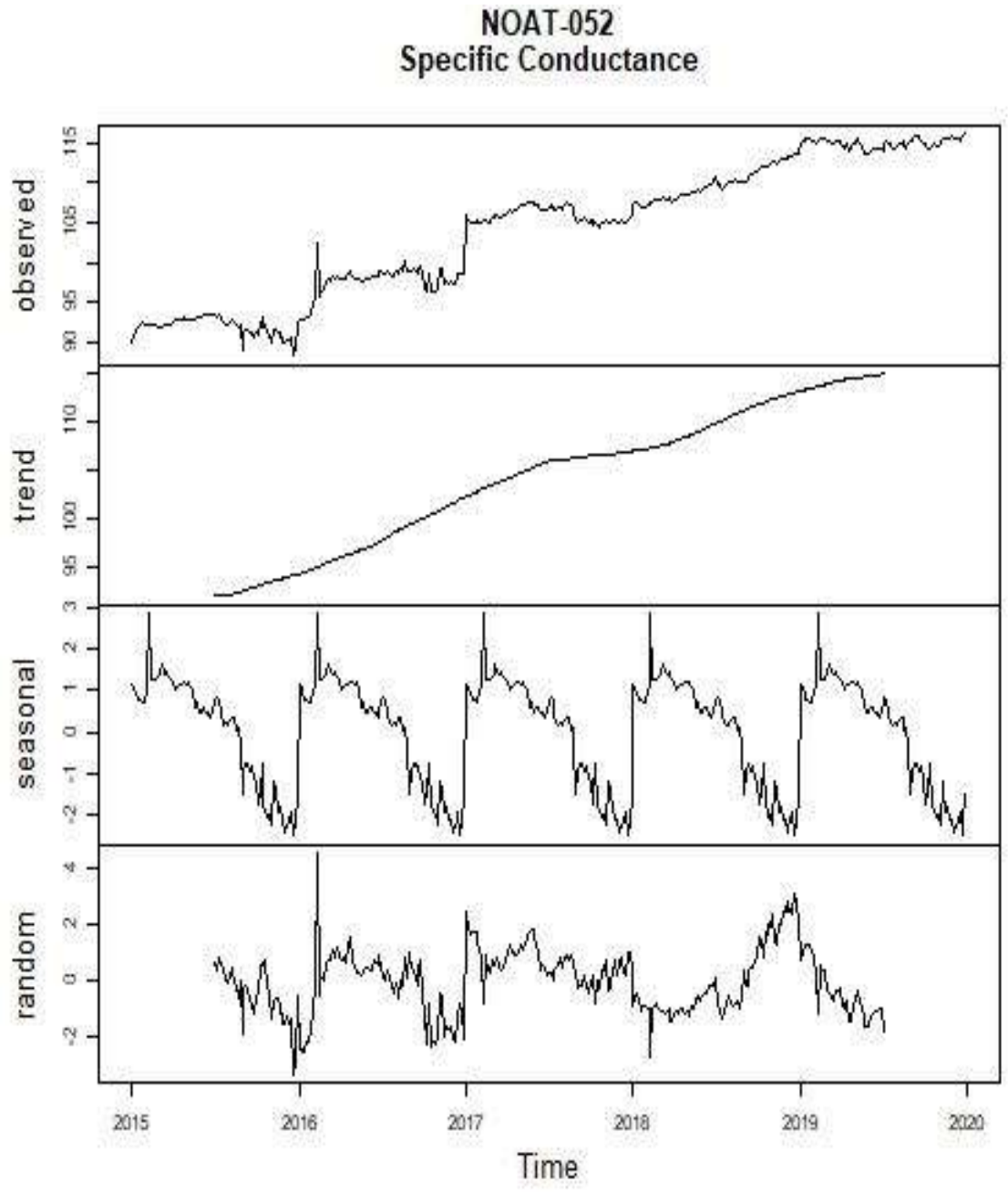


Figure A.90. Time series decomposition of truncated NOAT-052 specific conductance by year.

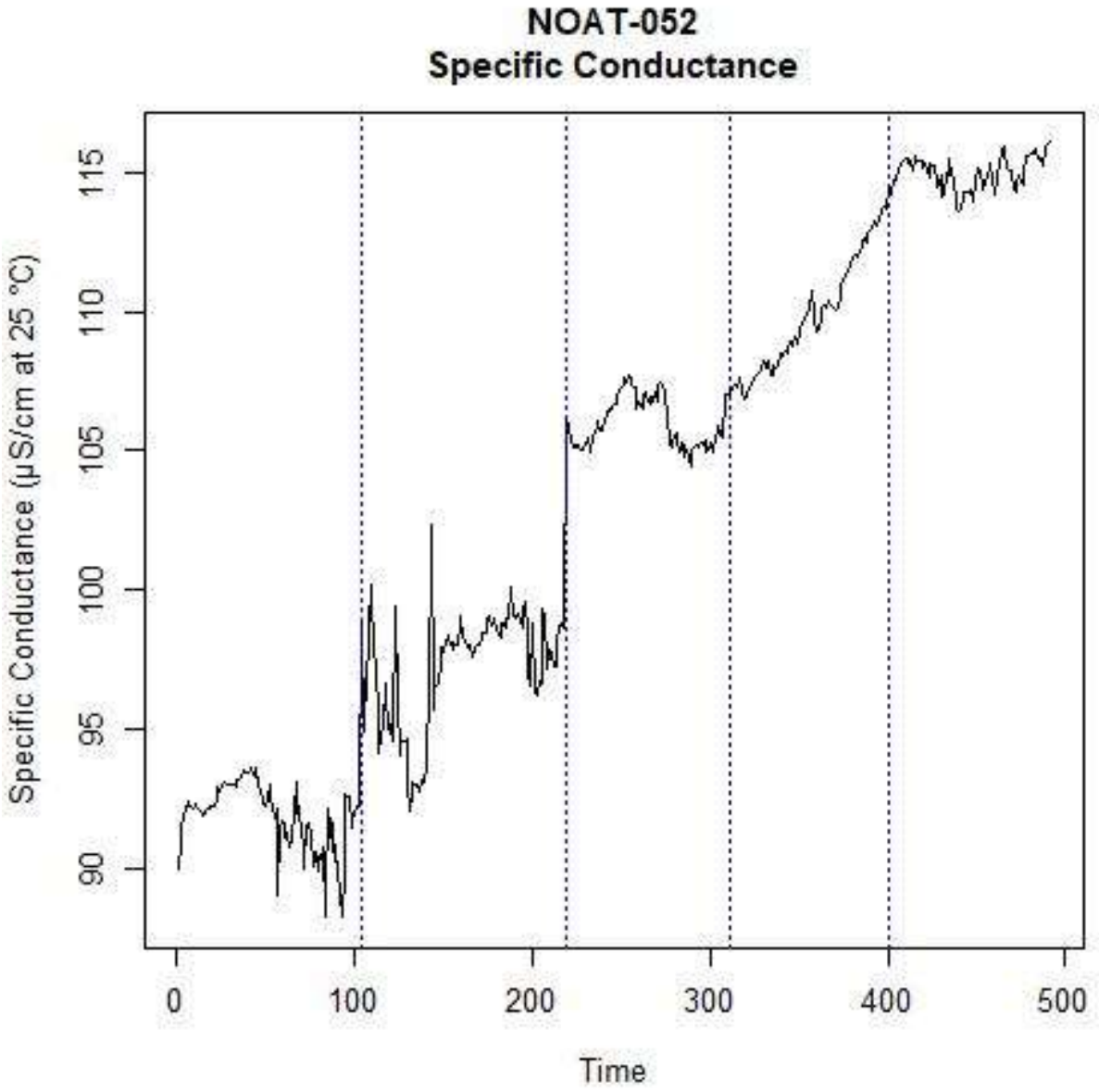


Figure A.91. Time series of NOAT-052 specific conductance by time point with vertical lines for additive outliers.

Table A.96. Trend modeling results for daily specific conductance data at NOAT-052.

			Trend			ARMA order		Ljung-Box Test	
Logged	**Method**	**Intercept**	**Coefficient**	**SE**	**p-value**	**AR**	**MA**	**Statistic**	**p-value**
FALSE	complete	48.56	3.68	0.44	< 0.0001	3	0	19.22	0.0018
FALSE	completeAO	54.91	3.23	0.72	< 0.0001	1	0	29.83	< 0.0001

			Trend			ARMA order		Ljung-Box Test	
Logged	**Method**	**Intercept**	**Coefficient**	**SE**	**p-value**	**AR**	**MA**	**Statistic**	**p-value**
FALSE	trunc	18.98	5.68	0.11	< 0.0001	0	5	404.05	< 0.0001
FALSE	truncSA	22.34	5.45	0.14	< 0.0001	0	5	422.90	< 0.0001
TRUE	complete	4.08	0.04	0.00	< 0.0001	4	0	11.19	0.0245
TRUE	completeAO	4.12	0.03	0.01	0.0002	1	0	29.78	< 0.0001
TRUE	trunc	4.23	0.03	0.00	< 0.0001	1	0	195.29	< 0.0001
TRUE	truncSA	3.85	0.05	0.00	< 0.0001	0	5	414.59	< 0.0001

Table A.97. Top covariate models for daily specific conductance data at NOAT-052.

Model	**AICc**	**ΔAICc**	**Ljung-Box Test p-value**
Year + Month	1191.99	0.00	0.1385
Daily Precipitation + Year + Month	1194.01	2.02	0.0707

Table A.98. Coefficients and variance components estimates for the top covariate model for daily specific conductance data at NOAT-052.

Parameter	**Coefficient**	**SE**	**p-value**
ar1	1.32	0.13	< 0.0001
ar2	-0.34	0.12	0.0039
ma1	-0.64	0.11	< 0.0001
intercept	19.88	8.64	0.0214
Year	5.40	0.52	< 0.0001
Month	0.40	0.15	0.0077

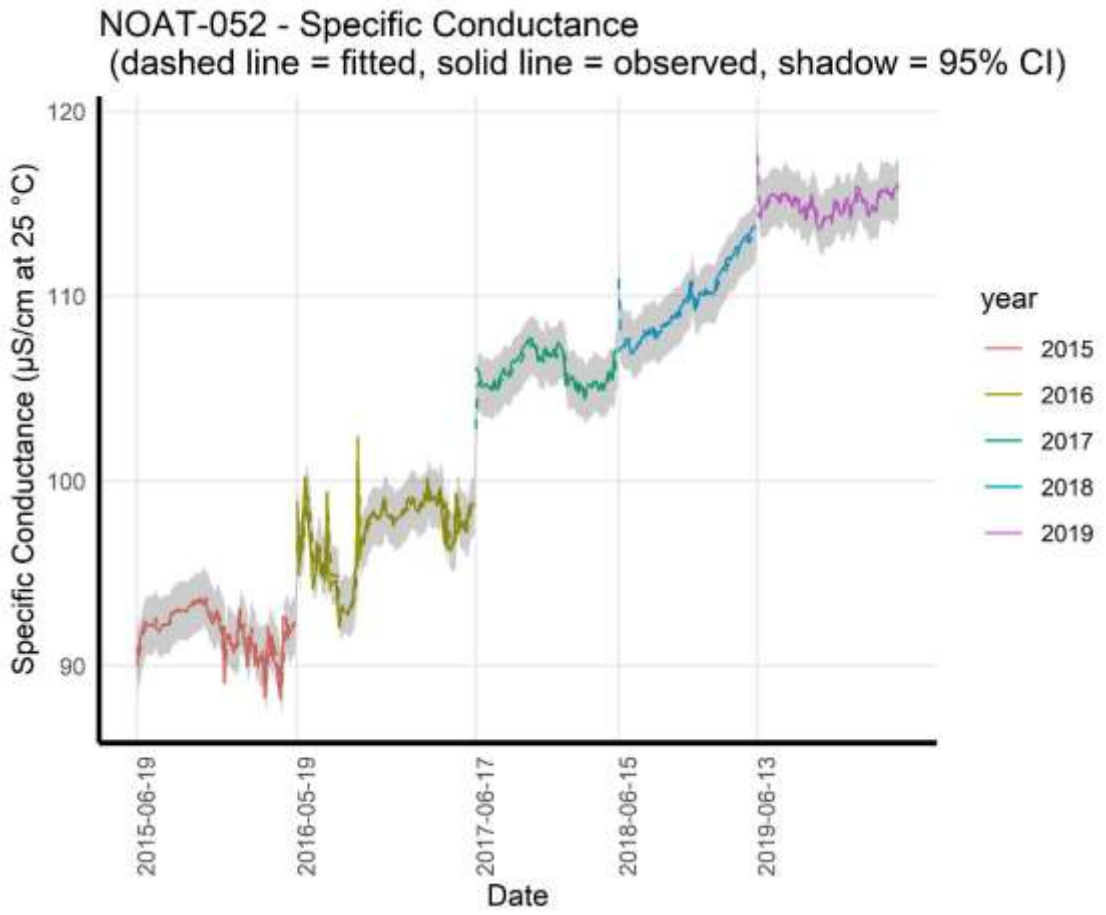


Figure A.92: Model predictions of NOAT-052 specific conductance by date.

NOAT-107

Data

For NOAT-107, specific conductance was recorded from 2014 through 2018, during the months June-September. The complete dataset included 385 specific conductance observations, however when truncated to the common set of 35 days visited every year, the number of observations was reduced to 175. Data coverage for covariates were sufficient such that no covariates nor years were excluded from the analysis.

Model Selection

For NOAT-107, the truncated trend models fit to logged and unlogged specific conductance data yielded stationary residuals. These two models both included positive trend coefficients that were significantly greater than zero, indicating there is evidence for an increasing trend in specific conductance at lake NOAT-107. For ARIMA models fitting all possible covariate combinations, AICc-based model selection resulted in a model with ARIMA(1,0,0) structure and fixed effects for daily precipitation and month. Specific conductance was estimated to increase with month (June-September). The estimated coefficient for daily precipitation was not significantly different from zero.

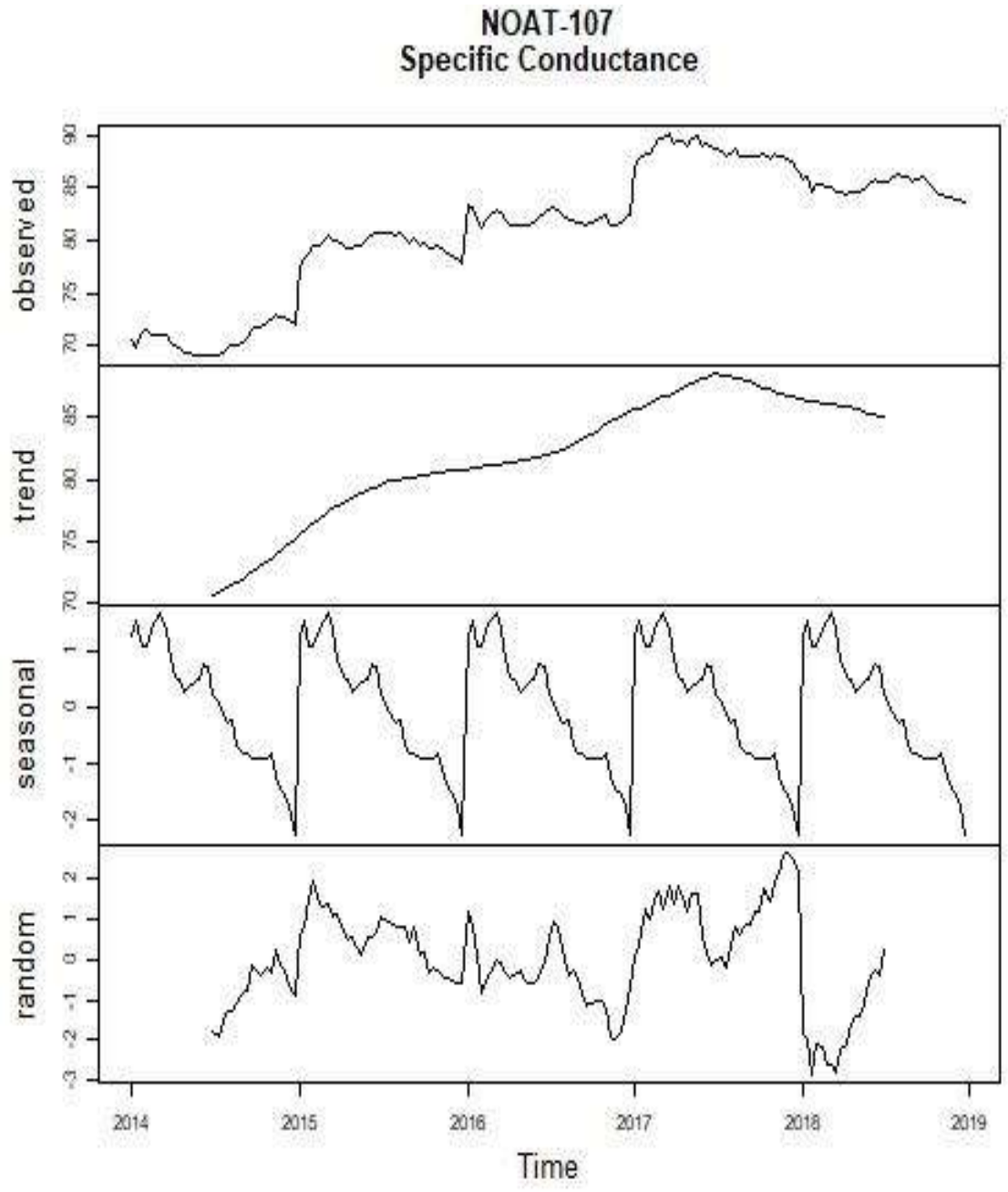


Figure A.93. Time series decomposition of truncated NOAT-107 specific conductance by year.

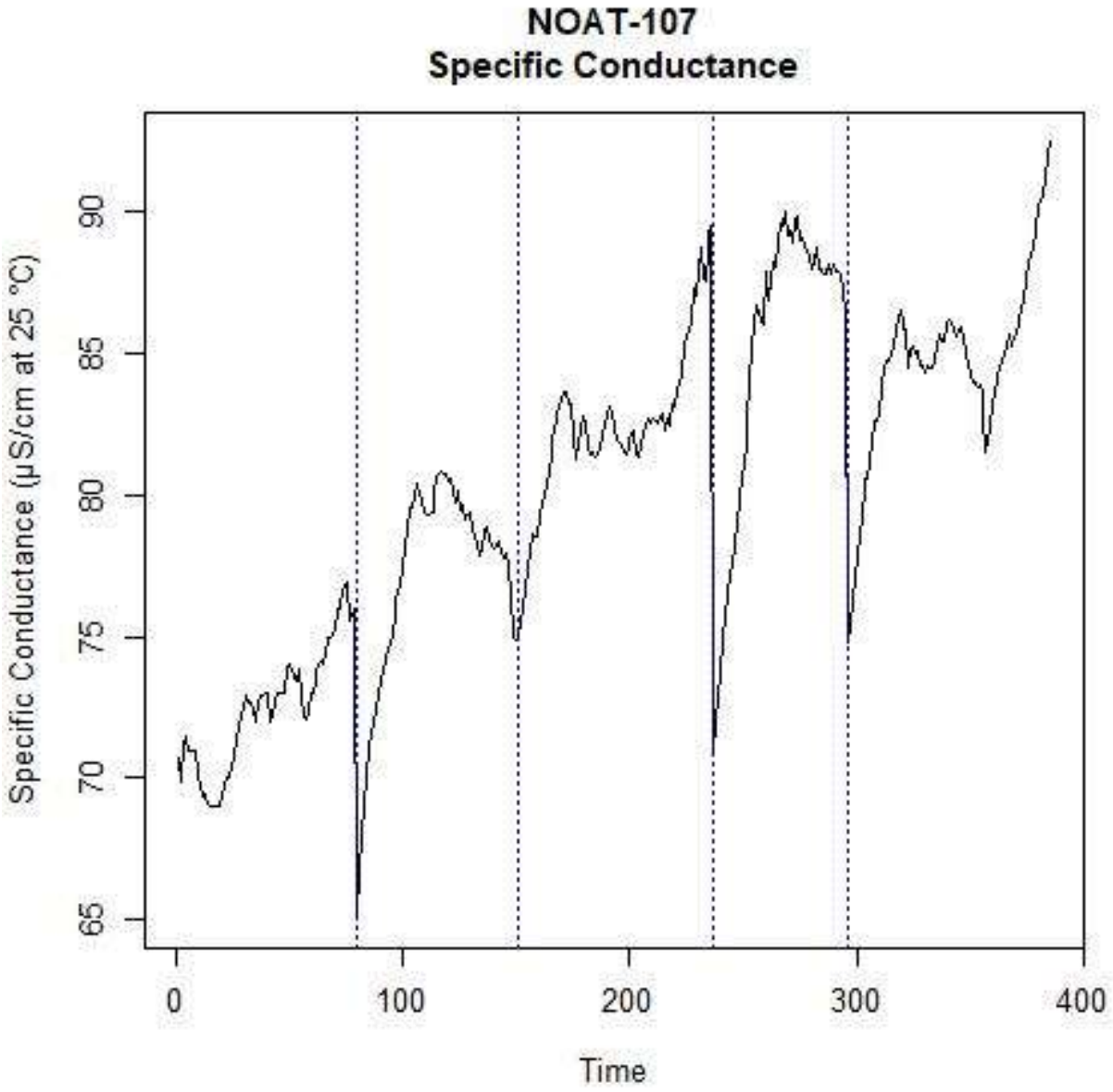


Figure A.94: Time series of NOAT-107 specific conductance by time point with vertical lines for additive outliers.

Table A.99. Trend modeling results for daily specific conductance data at NOAT-107.

			Trend			ARMA order		Ljung-Box Test	
Logged	**Method**	**Intercept**	**Coefficient**	**SE**	**p-value**	**AR**	**MA**	**Statistic**	**p-value**
FALSE	complete	50.68	2.12	0.29	< 0.0001	0	5	107.25	< 0.0001
FALSE	completeAO	43.60	2.63	0.24	< 0.0001	0	5	138.57	< 0.0001

			Trend			ARMA order		Ljung-Box Test	
Logged	**Method**	**Intercept**	**Coefficient**	**SE**	**p-value**	**AR**	**MA**	**Statistic**	**p-value**
FALSE	trunc	29.19	3.60	0.29	< 0.0001	3	1	29.80	0.3231
FALSE	truncSA	30.36	3.63	0.18	< 0.0001	0	1	972.45	< 0.0001
TRUE	complete	4.01	0.03	0.00	< 0.0001	0	5	105.11	< 0.0001
TRUE	completeAO	3.92	0.03	0.00	< 0.0001	0	5	138.15	< 0.0001
TRUE	trunc	3.72	0.05	0.00	< 0.0001	2	2	24.51	0.6022
TRUE	truncSA	3.75	0.05	0.00	< 0.0001	0	1	996.84	< 0.0001

Table A.100. Top covariate models for daily specific conductance data at NOAT-107.

Model	**AICc**	**ΔAICc**	**Ljung-Box Test p-value**
Daily Precipitation + Month	1077.51	0.00	0.5724
Wind Speed + Month	1077.63	0.13	0.6090
Wind Speed + Daily Precipitation + Month	1078.58	1.08	0.4690
Relative Humidity + Month	1078.93	1.43	0.5503
Wind Speed + Relative Humidity + Month	1079.68	2.17	0.4682
Air Temperature	1319.12	241.62	0.8147
Air Temperature + Daily Precipitation	1320.41	242.91	0.7437
Air Temperature + Wind Speed	1320.80	243.30	0.7351
Air Temperature + Wind Speed + Daily Precipitation	1322.24	244.73	0.6350
Solar Radiation	1326.83	249.33	0.8724

Table A.101. Coefficients and variance components estimates for the top covariate model for daily specific conductance data at NOAT-107.

Parameter	**Coefficient**	**SE**	**p-value**
ar1	0.99	0.01	< 0.0001
intercept	57.53	3.89	< 0.0001
Daily Precipitation	-0.24	0.19	0.2217
Month	3.05	0.16	< 0.0001

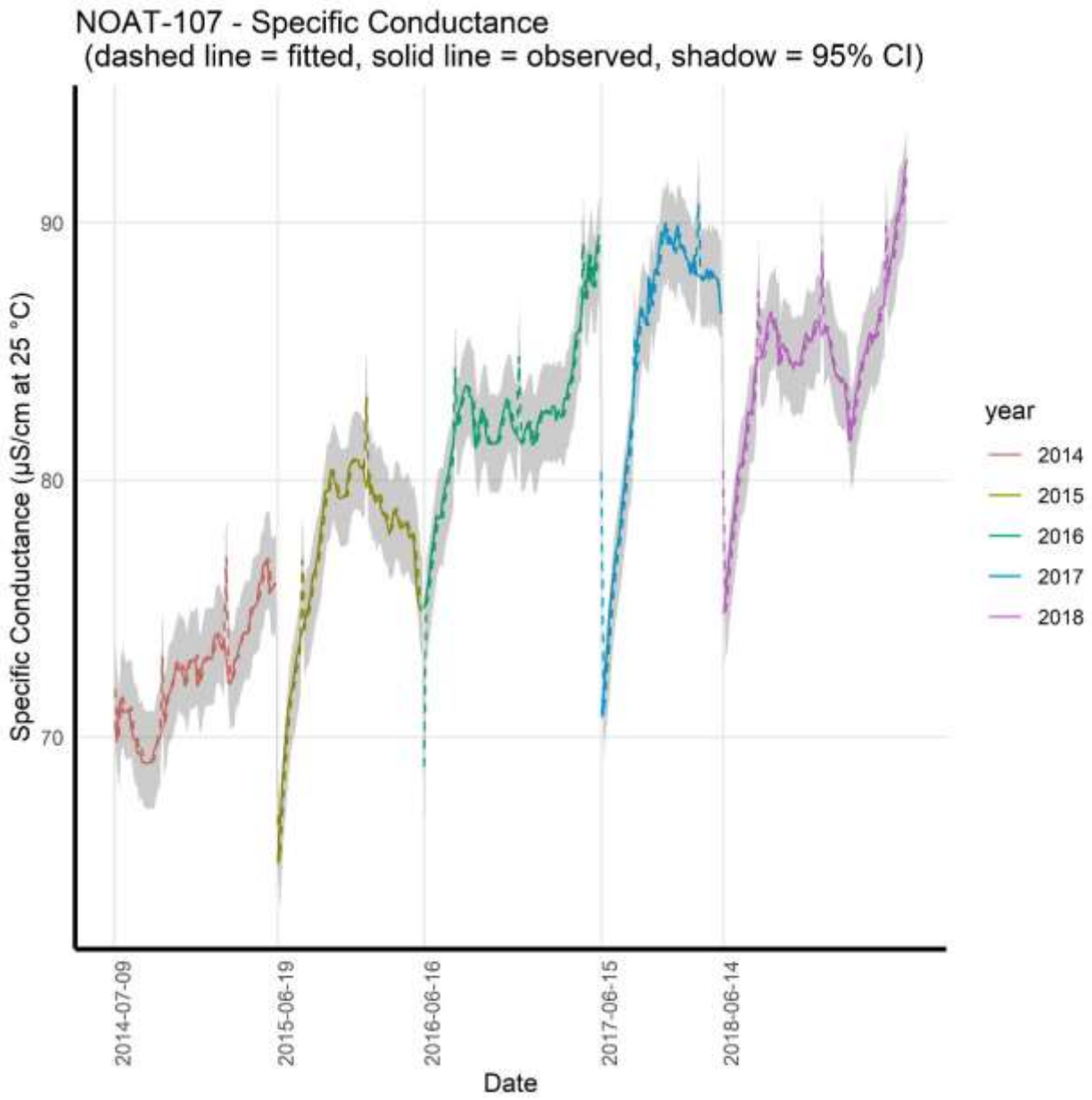


Figure A.95. Model predictions of NOAT-107 specific conductance by date.

WRST-005

Data

For WRST-005, specific conductance was recorded from 2010 through 2019, during the months May through September. The complete dataset included 1074 observations, and when truncating the data to the common set of 74 days visited in every year, the number of observations was reduced to 740. Data coverage for covariates were sufficient such that no covariates nor years were excluded from the analysis.

When aggregating specific conductance data to weekly mean values the number of observations was reduced to 165. When truncated the weekly data to the common set of 11 weeks sampled in every year the number of observation was further reduced to 110.

Model Selection

None of the trend models yielded stationary residuals when fit to daily specific conductance data. When fit to the weekly specific conductance data, the truncated seasonally adjusted models for logged and unlogged observations yielded stationary residuals. Neither of these two models included a trend coefficient that was significantly different from zero, indicating there is no evidence for an increasing or decreasing trend in specific conductance at lake WRST-005.

For ARIMA models fitting all possible covariate combinations fit to daily data at lake WRST-005, AICc-based model selection resulted in a model with ARIMA(1,0,1) structure and fixed effects for daily precipitation and month. Specific conductance was estimated to increase with daily precipitation and month (May-September).

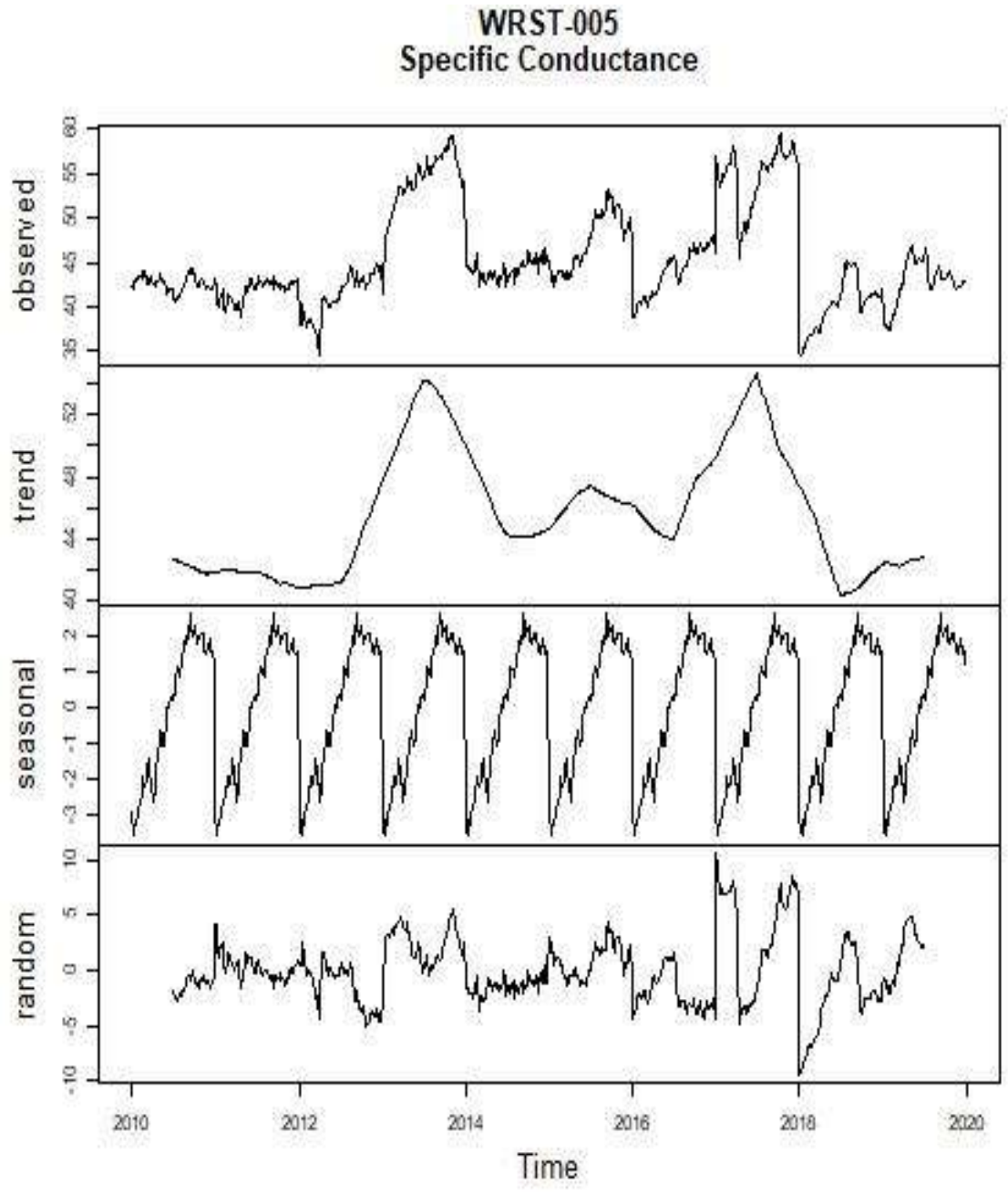


Figure A.96. Time series decomposition of truncated WRST-005 specific conductance by year.

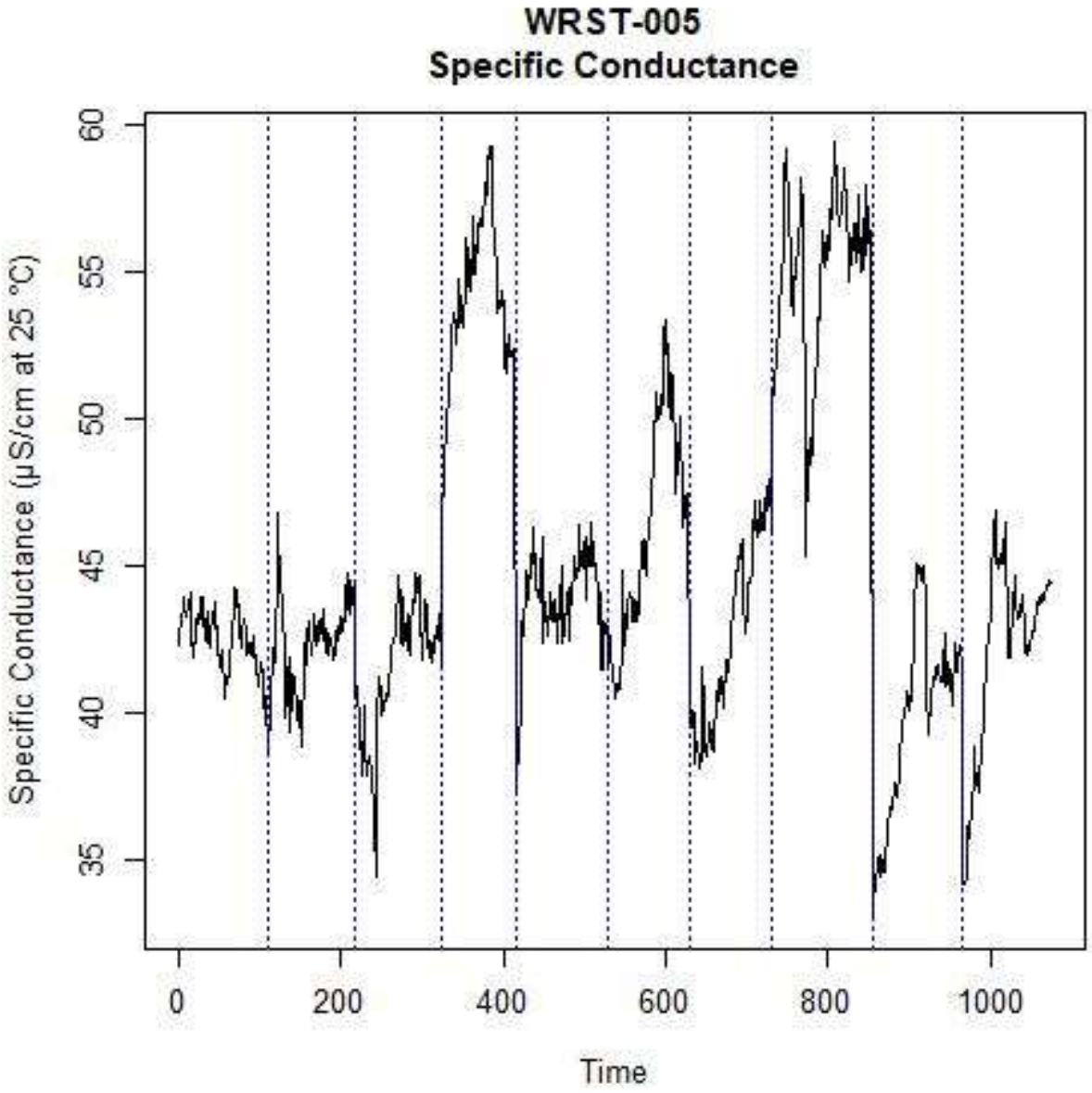


Figure A.97. Time series of WRST-005 specific conductance by time point with vertical lines for additive outliers.

Table A.102. Trend modeling results for daily specific conductance data at WRST-005.

			Trend			ARMA order		Ljung-Box Test	
Logged	**Method**	**Intercept**	**Coefficient**	**SE**	**p-value**	**AR**	**MA**	**Statistic**	**p-value**
FALSE	complete	46.20	-0.10	0.10	0.3030	0	5	1135.61	< 0.0001
FALSE	completeAO	44.26	0.06	0.09	0.5465	0	5	2085.78	< 0.0001

			Trend			ARMA order		Ljung-Box Test	
Logged	**Method**	**Intercept**	**Coefficient**	**SE**	**p-value**	**AR**	**MA**	**Statistic**	**p-value**
FALSE	trunc	43.23	0.17	0.07	0.0104	0	1	8865.15	< 0.0001
FALSE	truncSA	44.81	0.03	0.30	0.9299	1	1	268.45	< 0.0001
TRUE	complete	3.84	0.00	0.00	0.1530	0	5	1052.45	< 0.0001
TRUE	completeAO	3.79	0.00	0.00	0.8577	0	5	1939.36	< 0.0001
TRUE	trunc	3.78	0.00	0.00	0.0920	0	2	5021.60	< 0.0001
TRUE	truncSA	3.80	0.00	0.01	0.9387	1	1	252.23	< 0.0001

Table A.103. Trend modeling results for weekly specific conductance data at WRST-005.

			Trend			ARMA order		Ljung-Box Test	
Logged	**Method**	**Intercept**	**Coefficient**	**SE**	**p-value**	**AR**	**MA**	**Statistic**	**p-value**
FALSE	complete	44.4243	0.0890	0.1739	0.6089	0	1	207.23	< 0.0001
FALSE	completeAO	65.9001	-4.8956	1.0990	< 0.0001	1	2	10.38	0.0156
FALSE	trunc	68.0285	-4.6732	0.8983	< 0.0001	2	1	43.80	0.0004
FALSE	truncSA	45.5966	-0.0895	0.3301	0.7862	2	1	21.71	0.1527
TRUE	complete	3.7906	0.0010	0.0038	0.7841	0	1	184.35	< 0.0001
TRUE	completeAO	4.3221	-0.1155	0.0228	< 0.0001	2	0	12.40	0.0061
TRUE	trunc	4.2714	-0.1083	0.0195	< 0.0001	2	1	45.68	0.0002
TRUE	truncSA	3.8134	-0.0020	0.0071	0.7797	2	1	21.95	0.1449

Table A.104. Top covariate models for daily specific conductance data at WRST-005.

Model	**AICc**	**ΔAICc**	**Ljung-Box Test p-value**
Daily Precipitation + Month	3145.35	0.00	0.7328
Wind Speed + Daily Precipitation + Month	3147.37	2.02	0.5954
Wind Speed + Month	3149.41	4.06	0.7773
Solar Radiation	3300.50	155.15	0.9010
Wind Speed + Solar Radiation	3302.52	157.17	0.8203
Relative Humidity	3321.37	176.01	0.9445
Air Temperature	3334.54	189.19	0.9216
Air Temperature + Daily Precipitation	3335.39	190.04	0.8243
Air Temperature + Wind Speed	3335.93	190.58	0.8622
Air Temperature + Wind Speed + Daily Precipitation	3336.78	191.43	0.7158

Table A.105. Coefficients and variance components estimates for the top covariate model for daily specific conductance data at WRST-005.

Parameter	Coefficient	SE	p-value
ar1	0.98	0.01	< 0.0001
ma1	0.05	0.03	0.1299
intercept	35.82	1.67	< 0.0001
Daily Precipitation	0.37	0.18	0.0429
Month	1.25	0.08	< 0.0001

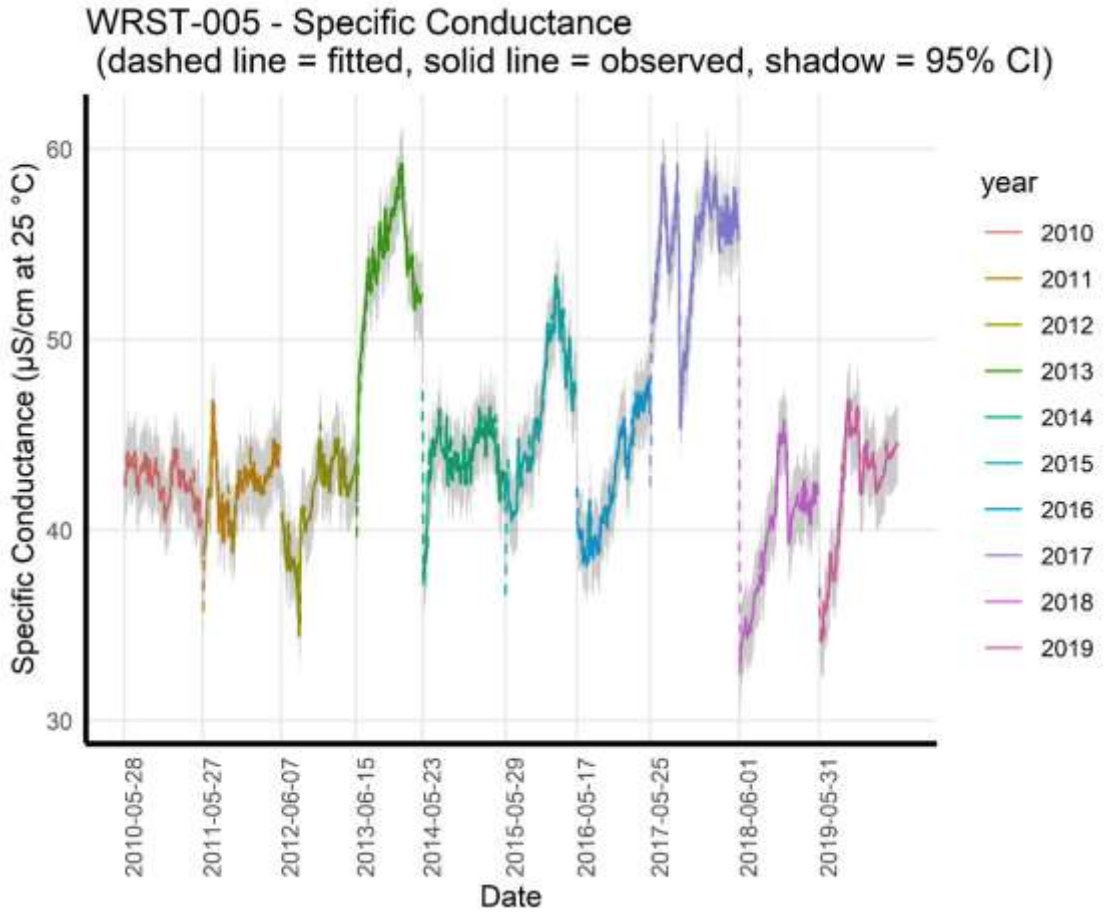


Figure A.98. Model predictions of WRST-005 specific conductance by date.

WRST-016

Data

For WRST-016, specific conductance was recorded from 2009 through 2019, during the months May-September. The complete dataset included 1073 specific conductance observations, however when truncated to the common set of 45 days visited every year, the number of observations was reduced to 495. Data coverage for covariates were sufficient such that no covariates nor years were excluded from the analysis.

Model Selection

For WRST-016, the truncated and truncated seasonally adjusted trend models for logged and unlogged daily specific conductance data yielded stationary residuals. Of these four models, two included positive trend coefficients that were significantly greater than zero, providing some evidence for an increasing trend in specific conductance at lake WRST-016. For ARIMA models fitting all possible covariate combinations, only one covariate model yielded stationary residuals. This covariate model had an ARIMA(2,0,1) structure and fixed effects for wind speed and month. Specific conductance was estimated to increase with month (May-September). The estimated coefficient for wind speed was not significantly different from zero.

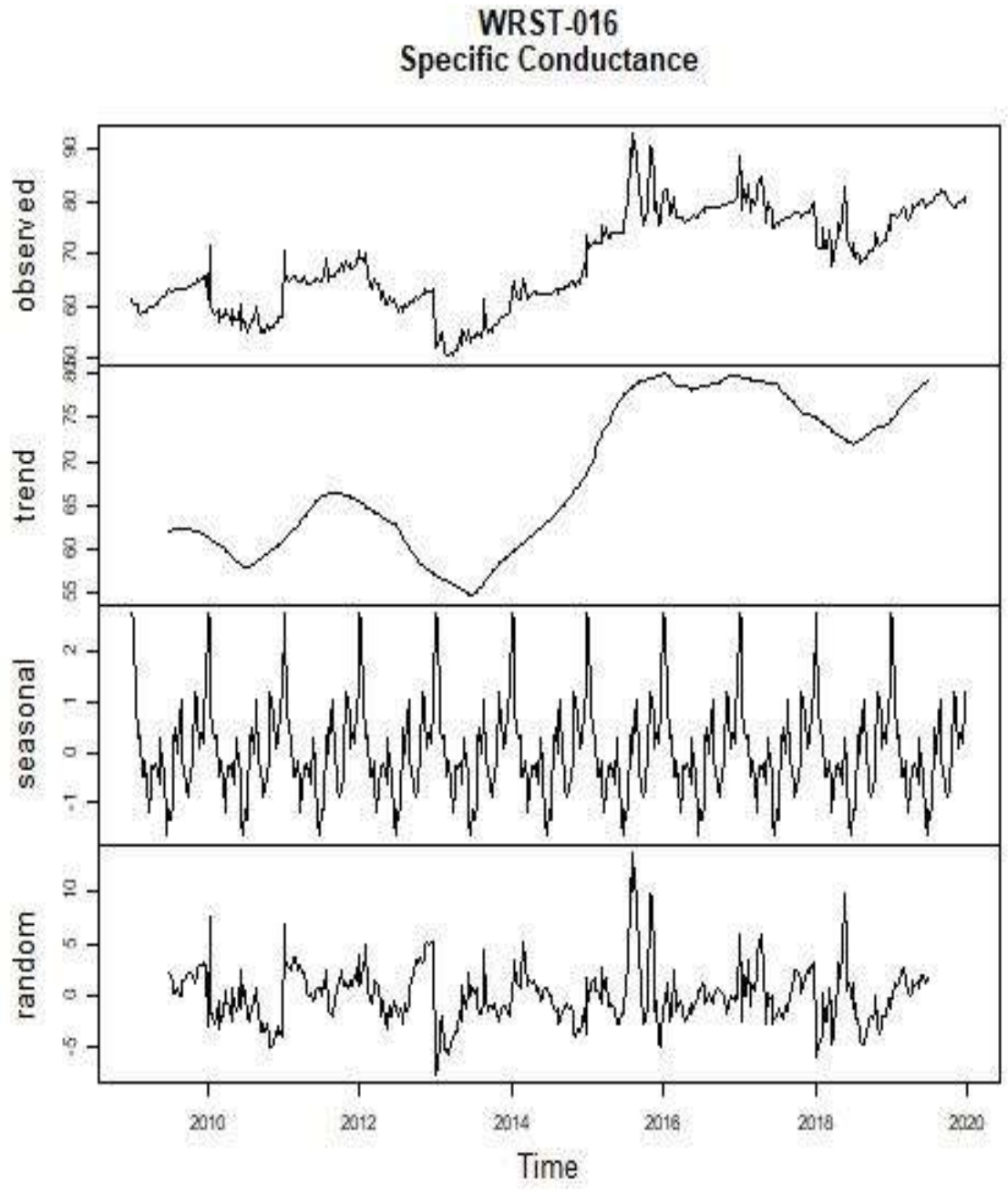


Figure A.99: Time series decomposition of truncated WRST-016 specific conductance by year.

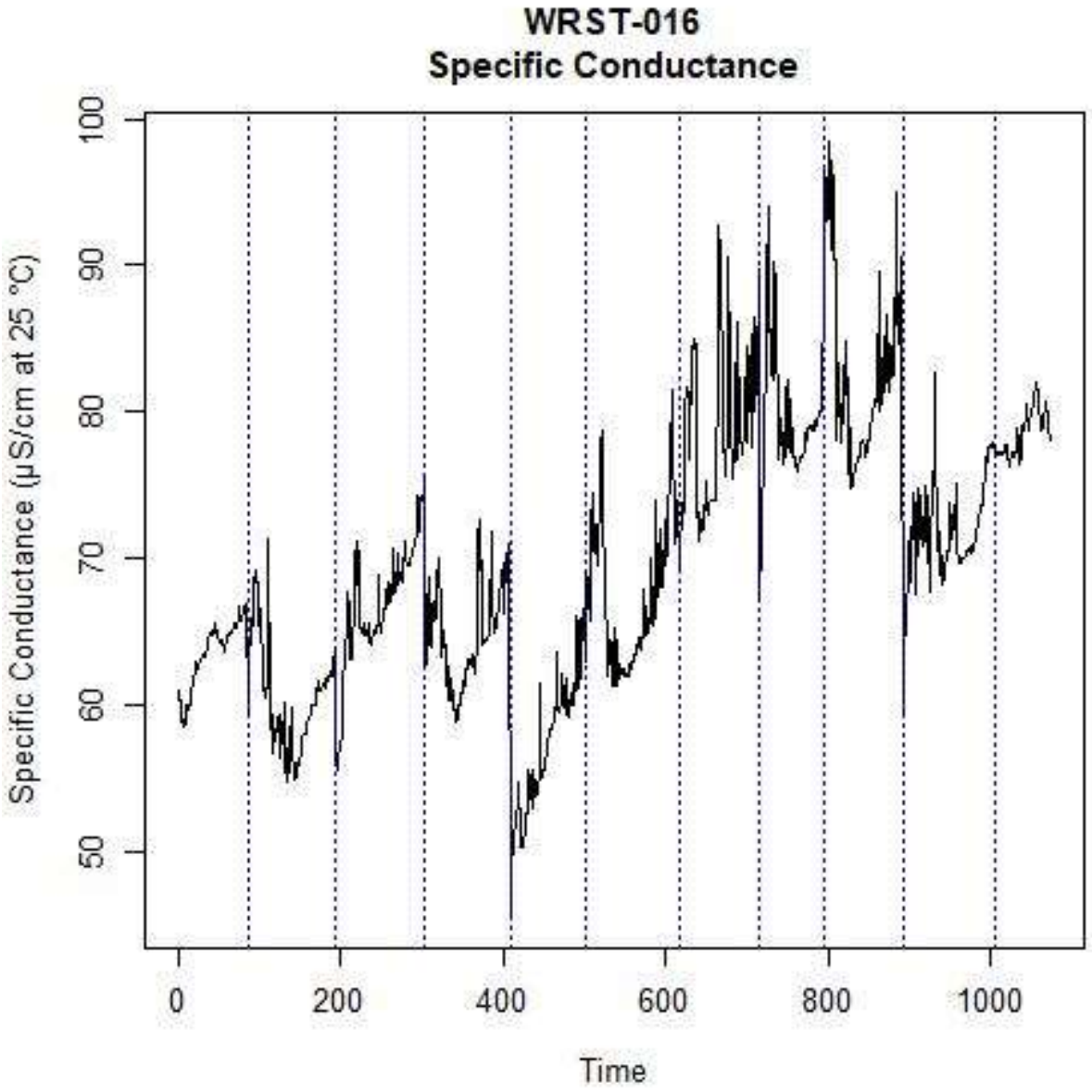


Figure A.100. Time series of WRST-016 specific conductance by time point with vertical lines for additive outliers.

Table A.106. Trend modeling results for daily specific conductance data at WRST-016.

			Trend			ARMA order		Ljung-Box Test	
Logged	**Method**	**Intercept**	**Coefficient**	**SE**	**p-value**	**AR**	**MA**	**Statistic**	**p-value**
FALSE	complete	48.55	1.79	0.12	< 0.0001	0	5	445.12	< 0.0001
FALSE	completeAO	47.13	1.91	0.12	< 0.0001	0	5	885.97	< 0.0001

			Trend			ARMA order		Ljung-Box Test	
Logged	Method	Intercept	Coefficient	SE	p-value	AR	MA	Statistic	p-value
FALSE	trunc	44.83	1.98	0.34	< 0.0001	1	0	74.32	0.7411
FALSE	truncSA	59.18	0.77	0.66	0.2386	1	1	100.08	0.1423
TRUE	complete	3.94	0.03	0.00	< 0.0001	0	5	477.39	< 0.0001
TRUE	completeAO	3.92	0.03	0.00	< 0.0001	0	5	968.96	< 0.0001
TRUE	trunc	3.93	0.02	0.01	< 0.0001	1	2	63.35	0.9466
TRUE	truncSA	4.11	0.01	0.01	0.3209	1	1	100.67	0.1333

Table A.107. Top covariate models for daily specific conductance data at WRST-016.

Model	AICc	ΔAICc	Ljung-Box Test p-value
Wind Speed + Month	4873.79	0	0.0659

Table A.108. Coefficients and variance components estimates for the top covariate model for daily specific conductance data at WRST-016.

Parameter	Coefficient	SE	p-value
ar1	1.60	0.10	< 0.0001
ar2	-0.61	0.10	< 0.0001
ma1	-0.77	0.09	< 0.0001
intercept	55.05	3.56	< 0.0001
Wind Speed	0.08	0.17	0.6239
Month	2.08	0.18	< 0.0001

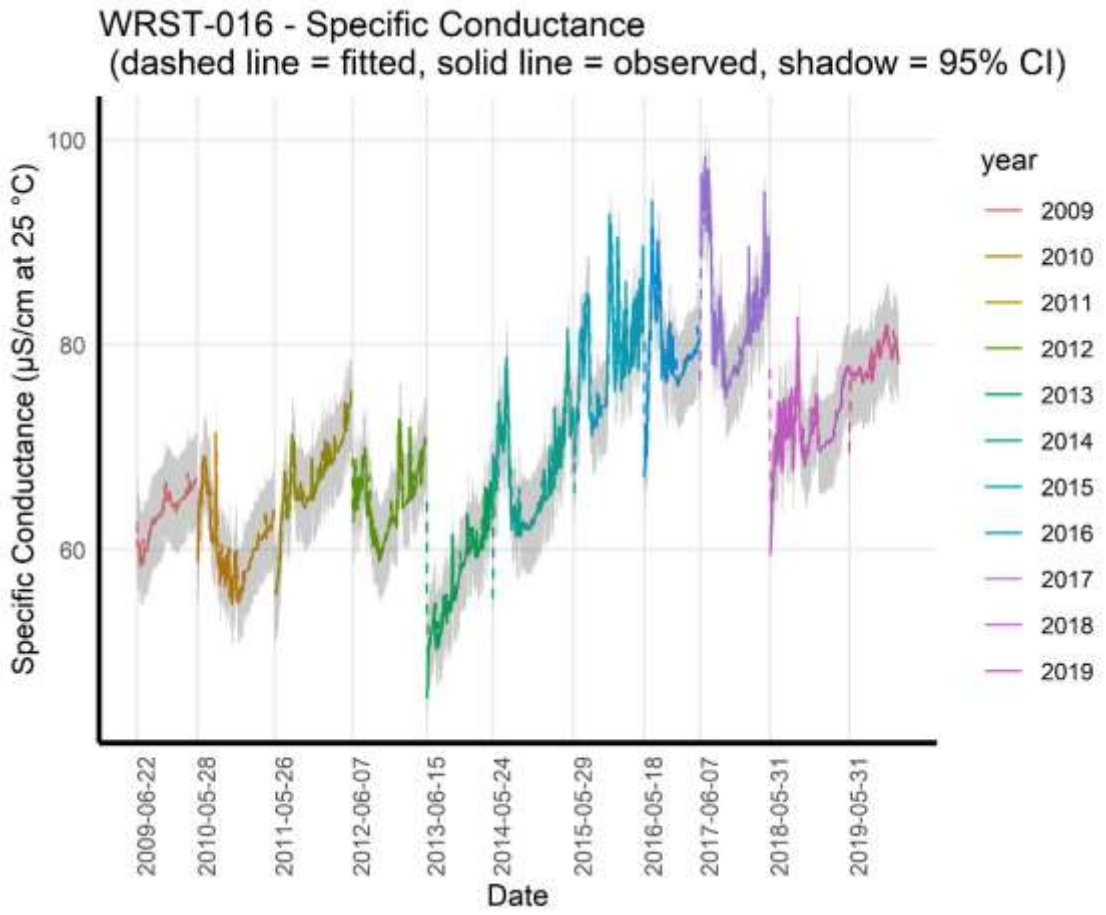


Figure A.101. Model predictions of WRST-016 specific conductance by date.

YUCH-004

Data

For YUCH-004, specific conductance was recorded from 2009 through 2019, during the months May through September. The complete dataset included 1246 observations, and when truncating the data to the common set of 93 days visited in every year, the number of observations was reduced to 1078. Covariate data were lacking for year 2019, thus this year was excluded from covariate models.

When aggregating specific conductance data to weekly mean values the number of observations was reduced to 189. When truncated the weekly data to the common set of 14 weeks sampled in every year the number of observations was further reduced to 154.

When aggregating specific conductance data to monthly mean values the number of observations was reduced to 53. When truncated the weekly data to the common set of 4 months sampled in every year the number of observations was further reduced to 44.

Model Selection

None of the trend models yielded stationary residuals when fit to daily or weekly specific conductance data. When fit to the monthly specific conductance data, three trend models (complete data with additive outliers, truncated, and truncated seasonally adjusted) fit to the logged specific conductance data yielded stationary residuals. Of these three models, two included positive trend coefficients significantly greater than zero indicating there is evidence for an increasing trend in specific conductance at lake YUCH-004. Visually, it appears that specific conductance has rapidly increased over the last four years of the time series (2015-2019).

For ARIMA models fitting all possible covariate combinations to weekly specific conductance data at lake YUCH-004, AICc-based model selection resulted in a model with ARIMA(1,0,0) structure and fixed effects for wind speed, solar radiation, and daily precipitation. Wind speed, solar radiation and daily precipitation were all estimated to have a negative effect on specific conductance.

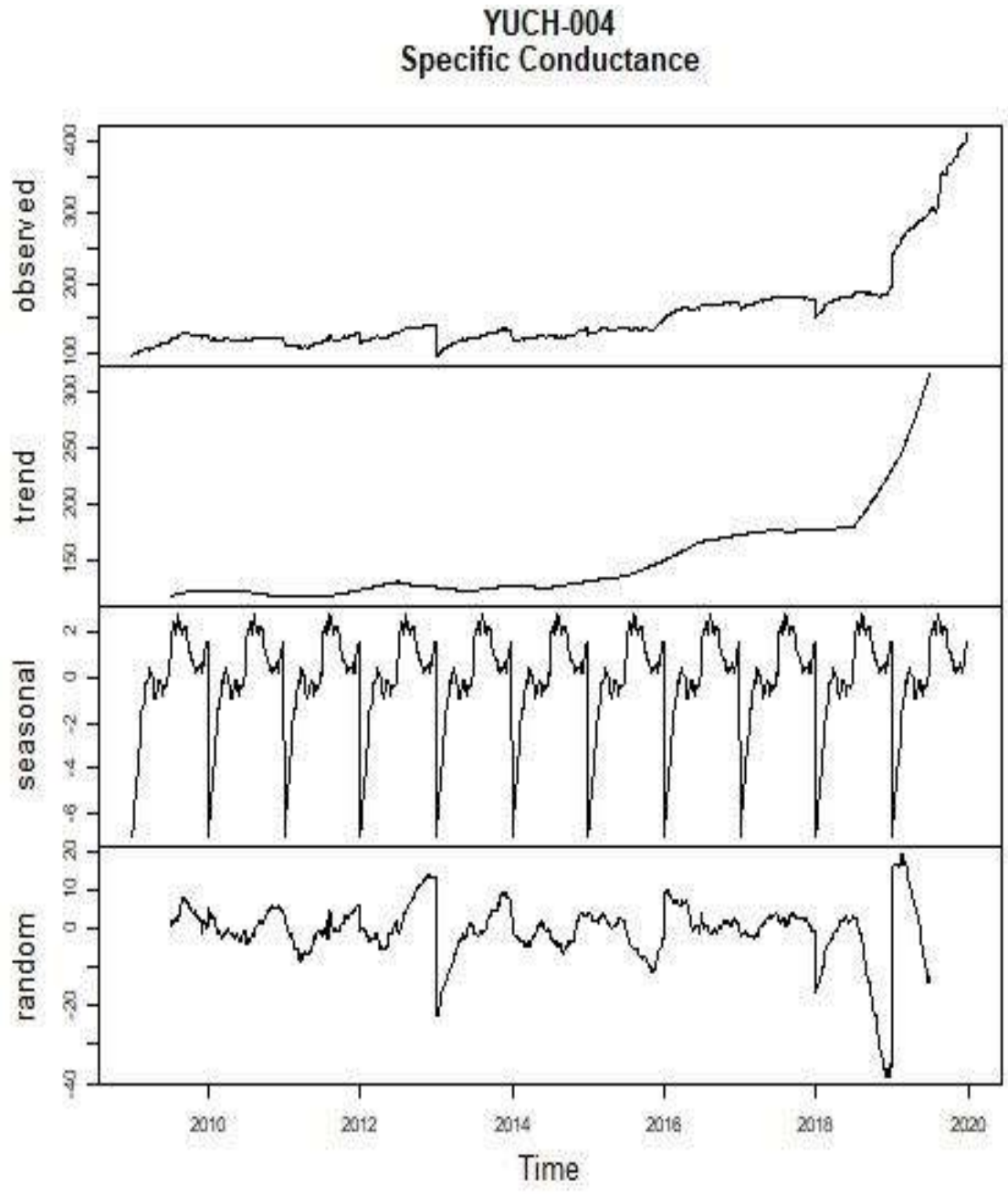


Figure A.102. Time series decomposition of truncated YUCH-004 specific conductance by year.

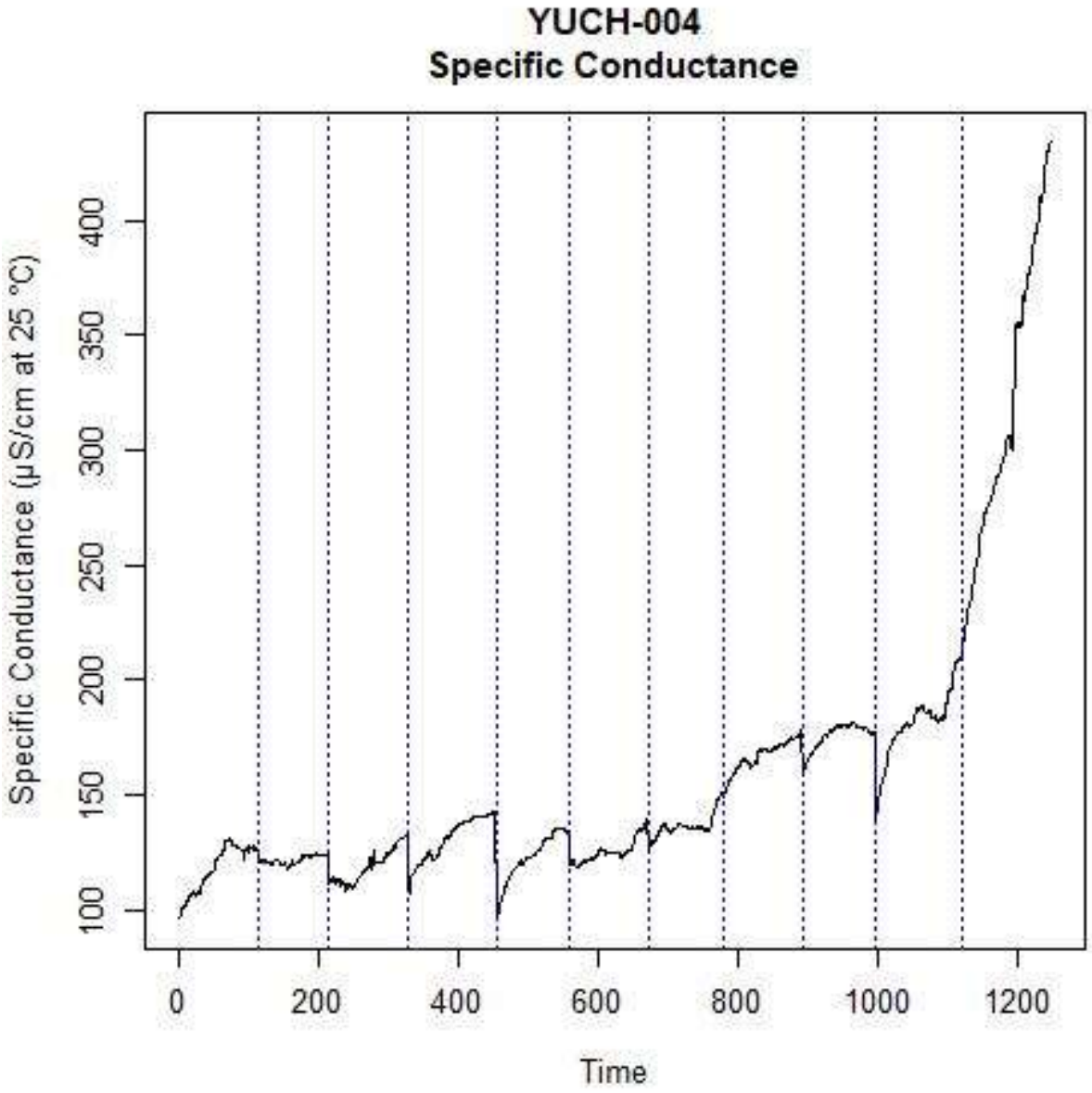


Figure A.103. Time series of YUCH-004 specific conductance by time point with vertical lines for additive outliers.

Table A.109. Trend modeling results for daily specific conductance data at YUCH-004.

			Trend			ARMA order		Ljung-Box Test	
Logged	**Method**	**Intercept**	**Coefficient**	**SE**	**p-value**	**AR**	**MA**	**Statistic**	**p-value**
FALSE	complete	61.90	9.62	0.63	< 0.0001	0	5	3062.75	< 0.0001
FALSE	completeAO	15.77	14.18	0.38	< 0.0001	0	0	15410.65	< 0.0001

			Trend			ARMA order		Ljung-Box Test	
Logged	**Method**	**Intercept**	**Coefficient**	**SE**	**p-value**	**AR**	**MA**	**Statistic**	**p-value**
FALSE	trunc	52.61	10.32	0.55	< 0.0001	0	5	8656.85	< 0.0001
FALSE	truncSA	45.16	11.06	0.51	< 0.0001	0	5	8812.93	< 0.0001
TRUE	complete	4.38	0.06	0.00	< 0.0001	0	5	2209.63	< 0.0001
TRUE	completeAO	4.24	0.08	0.00	< 0.0001	0	0	15221.61	< 0.0001
TRUE	trunc	4.37	0.06	0.00	< 0.0001	0	5	6931.60	< 0.0001
TRUE	truncSA	4.33	0.07	0.00	< 0.0001	0	5	8005.39	< 0.0001

Table A.110. Trend modeling results for monthly specific conductance data at YUCH-004.

			Trend			ARMA order		Ljung-Box Test	
Logged	**Method**	**Intercept**	**Coefficient**	**SE**	**p-value**	**AR**	**MA**	**Statistic**	**p-value**
FALSE	complete	47.0024	12.2598	2.7124	< 0.0001	0	2	18.14	0.0059
FALSE	completeAO	NA	17.2796	0.6446	< 0.0001	0	0	43.22	< 0.0001
FALSE	trunc	NA	19.9920	2.5197	< 0.0001	0	1	26.10	< 0.0001
FALSE	truncSA	NA	18.6832	1.3120	< 0.0001	0	1	26.72	< 0.0001
TRUE	complete	4.5378	0.0520	0.0167	0.0019	0	3	9.29	0.0980
TRUE	completeAO	4.3168	0.0775	0.0074	< 0.0001	0	0	40.72	< 0.0001
TRUE	trunc	5.6930	-0.0410	0.0349	0.2402	1	2	3.13	0.3718
TRUE	truncSA	4.2839	0.0863	0.0254	0.0007	2	1	1.37	0.7120

Table A.111. Top covariate models for monthly specific conductance means at YUCH-004.

Model	**AICc**	**ΔAICc**	**Ljung-Box Test p-value**
Year + Month	331.45	0.00	0.2362
Daily Precipitation + Year + Month	332.68	1.23	0.1303
Wind Speed + Year + Month	332.87	1.42	0.1657
Wind Speed + Daily Precipitation + Year + Month	333.12	1.67	0.0595
Wind Speed + Daily Precipitation + Month	338.84	7.38	0.0701
Wind Speed + Month	339.07	7.61	0.1937
Daily Precipitation + Month	339.36	7.91	0.1357
Wind Speed + Solar Radiation + Daily Precipitation	344.56	13.11	0.1167
Wind Speed + Solar Radiation	347.35	15.90	0.2449
Wind Speed + Solar Radiation + Year	348.11	16.66	0.1936

Table A.112. Coefficients and variance components estimates for the top covariate model for monthly specific conductance means at YUCH-004.

Parameter	Coefficient	SE	p-value
ar1	0.79	0.09	< 0.0001
intercept	31.40	13.79	0.0228
Year	7.57	1.28	< 0.0001
Month	6.17	0.61	< 0.0001

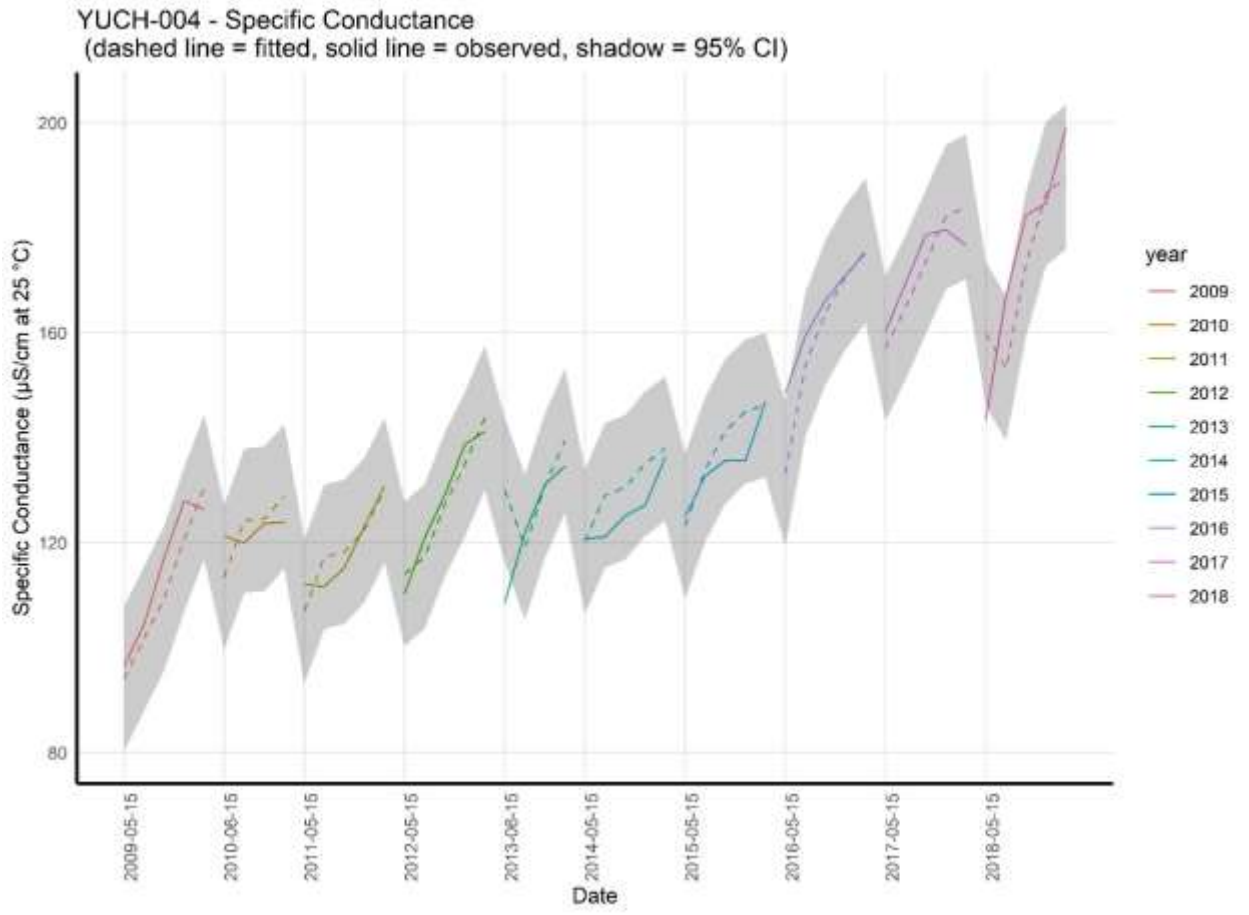


Figure A.104. Model predictions of YUCH-004 specific conductance by month.

YUCH-005

Data

For YUCH-005, specific conductance was recorded from 2014 through 2019, during the months May through September. The complete dataset included 686 observations, and when truncating the data to the common set of 104 days visited in every year, the number of observations was reduced to 624. Covariate data were lacking for year 2019, thus this year was excluded from covariate models.

When aggregating specific conductance data to weekly mean values the number of observations was reduced to 186. When truncated the weekly data to the common set of 15 weeks sampled in every year the number of observations was further reduced to 161.

Model Selection

None of the trend models yielded stationary residuals when fit to daily specific conductance data. When fit to the weekly specific conductance data, the truncated and truncated seasonally adjusted trend models for the logged and unlogged specific conductance data yielded stationary residuals. Neither of these two trend models included a trend coefficient that was significantly different from zero. For ARIMA models fitting all possible covariate combinations to daily specific conductance data, AICc-based model selection resulted in a model with ARIMA(1,0,0) structure and fixed effects for daily precipitation and year. In contrast to the trend models, there was a significant negative effect for year in the top covariate model. Overall, there is weak evidence for a decreasing trend in specific conductance at lake YUCH-005. The effect of daily precipitation was not significant.

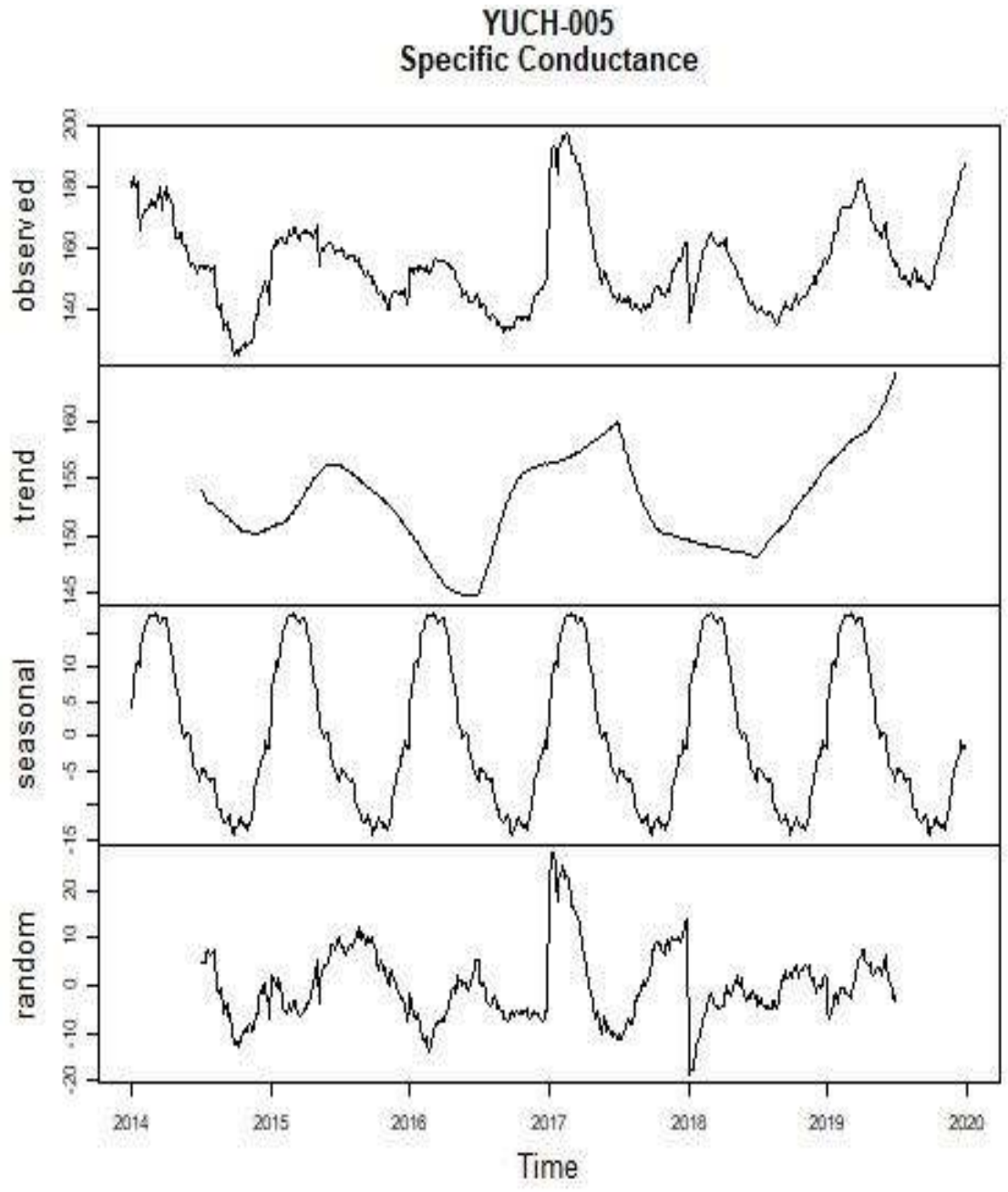


Figure A.105. Time series decomposition of truncated YUCH-005 specific conductance by year.

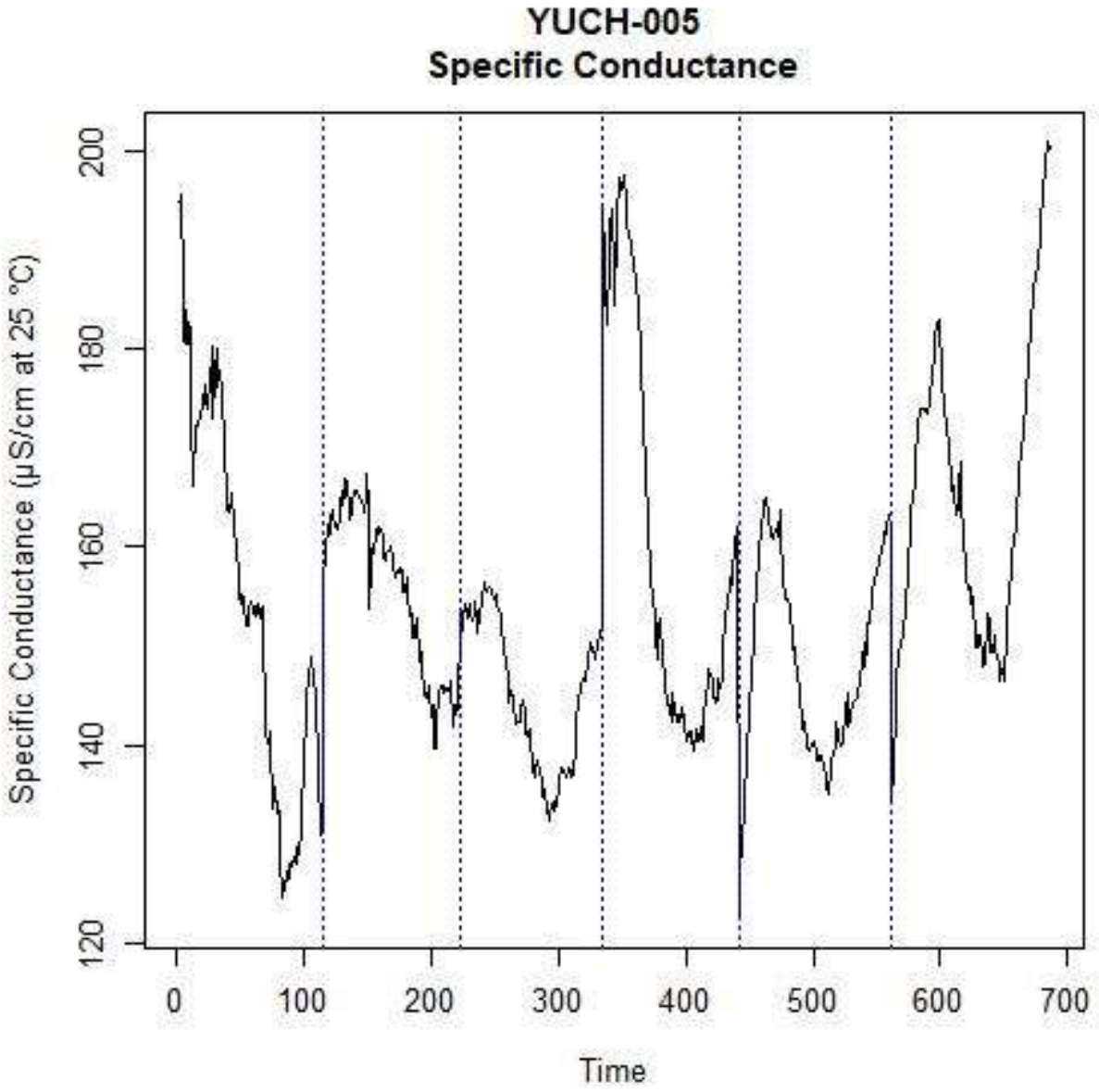


Figure A.106. Time series of YUCH-005 specific conductance by time point with vertical lines for additive outliers.

Table A.113. Trend modeling results for daily specific conductance data at YUCH-005.

			Trend			ARMA order		Ljung-Box Test	
Logged	**Method**	**Intercept**	**Coefficient**	**SE**	**p-value**	**AR**	**MA**	**Statistic**	**p-value**
FALSE	complete	46.20	-0.10	0.10	0.3030	0	5	1135.61	< 0.0001
FALSE	completeAO	44.26	0.06	0.09	0.5465	0	5	2085.78	< 0.0001

			Trend			ARMA order		Ljung-Box Test	
Logged	**Method**	**Intercept**	**Coefficient**	**SE**	**p-value**	**AR**	**MA**	**Statistic**	**p-value**
FALSE	trunc	43.23	0.17	0.07	0.0104	0	1	8865.15	< 0.0001
FALSE	truncSA	44.81	0.03	0.30	0.9299	1	1	268.45	< 0.0001
TRUE	complete	3.84	0.00	0.00	0.1530	0	5	1052.45	< 0.0001
TRUE	completeAO	3.79	0.00	0.00	0.8577	0	5	1939.36	< 0.0001
TRUE	trunc	3.78	0.00	0.00	0.0920	0	2	5021.60	< 0.0001
TRUE	truncSA	3.80	0.00	0.01	0.9387	1	1	252.23	< 0.0001

Table A.114. Top covariate models for daily specific conductance data at YUCH-005.

Model	**AICc**	**ΔAICc**	**Ljung-Box Test p-value**
Wind Speed + Month	2891.49	0.00	0.1280
Wind Speed + Daily Precipitation + Month	2893.40	1.91	0.0736
Year + Month	2897.67	6.18	0.0954
Daily Precipitation + Month	2899.25	7.77	0.1314
Wind Speed + Solar Radiation	2913.00	21.52	0.0757
Air Temperature + Wind Speed	2914.66	23.17	0.1028
Wind Speed + Relative Humidity	2914.77	23.29	0.0832
Wind Speed	2916.05	24.56	0.1807
Solar Radiation	2916.34	24.86	0.1254
Air Temperature + Wind Speed + Daily Precipitation	2916.70	25.22	0.0606

Table A.115. Coefficients and variance components estimates for the top covariate model for daily specific conductance data at YUCH-005.

Parameter	**Coefficient**	**SE**	**p-value**
ar1	0.98	0.01	< 0.0001
intercept	169.97	6.49	< 0.0001
Wind Speed	-0.58	0.21	0.0050
Month	-1.82	0.35	< 0.0001

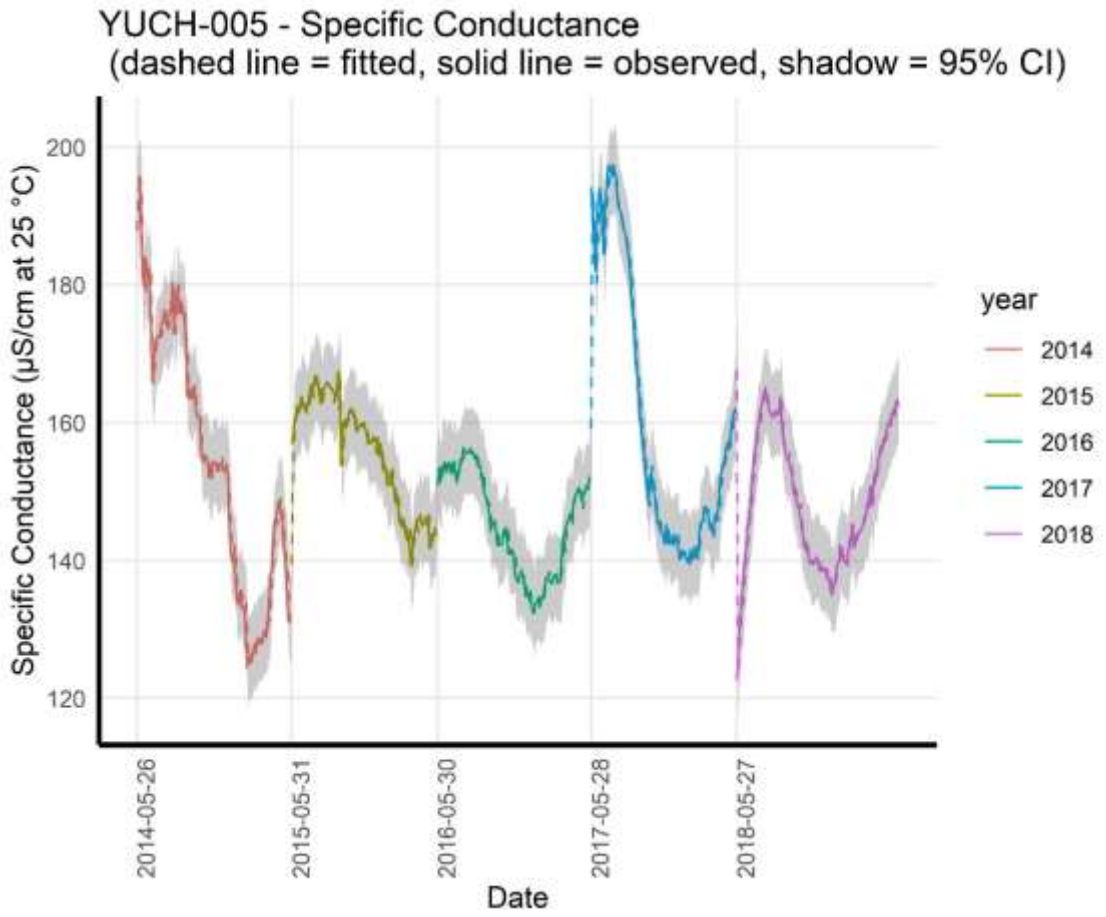


Figure A.107. Model predictions of YUCH-005 specific conductance by date.

Sonde Temperature

BELA-088

Data

Temperature was recorded from 2012 through 2019 at BELA-088. However, 2013 was missing so this analysis addressed 2014 through 2019. Over this period, there were 543 records of temperature. Though data were generally collected from June to September, records started in July in 2014 and ended early in 2018 and 2019. Truncated to the 72 days that were sampled every year, the dataset had 432 observations. Covariate coverage was poor in 2018 and 2019, so covariate models only considered 2014-2017. This left 363 records for covariate modeling.

Model Selection

For ARIMA models fitting all possible covariate combinations at lake BELA-088 with temperature as the response variable, AICc-based model selection resulted in ARIMA(2,0,0) with relative humidity and month as the main covariates in the best model. No annual trend models exhibited stationary residuals in the analysis of daily data, but residuals of truncated and seasonally adjusted models for weekly data were essentially independent. No evidence of trend in temperature was suggested for any of the valid models.

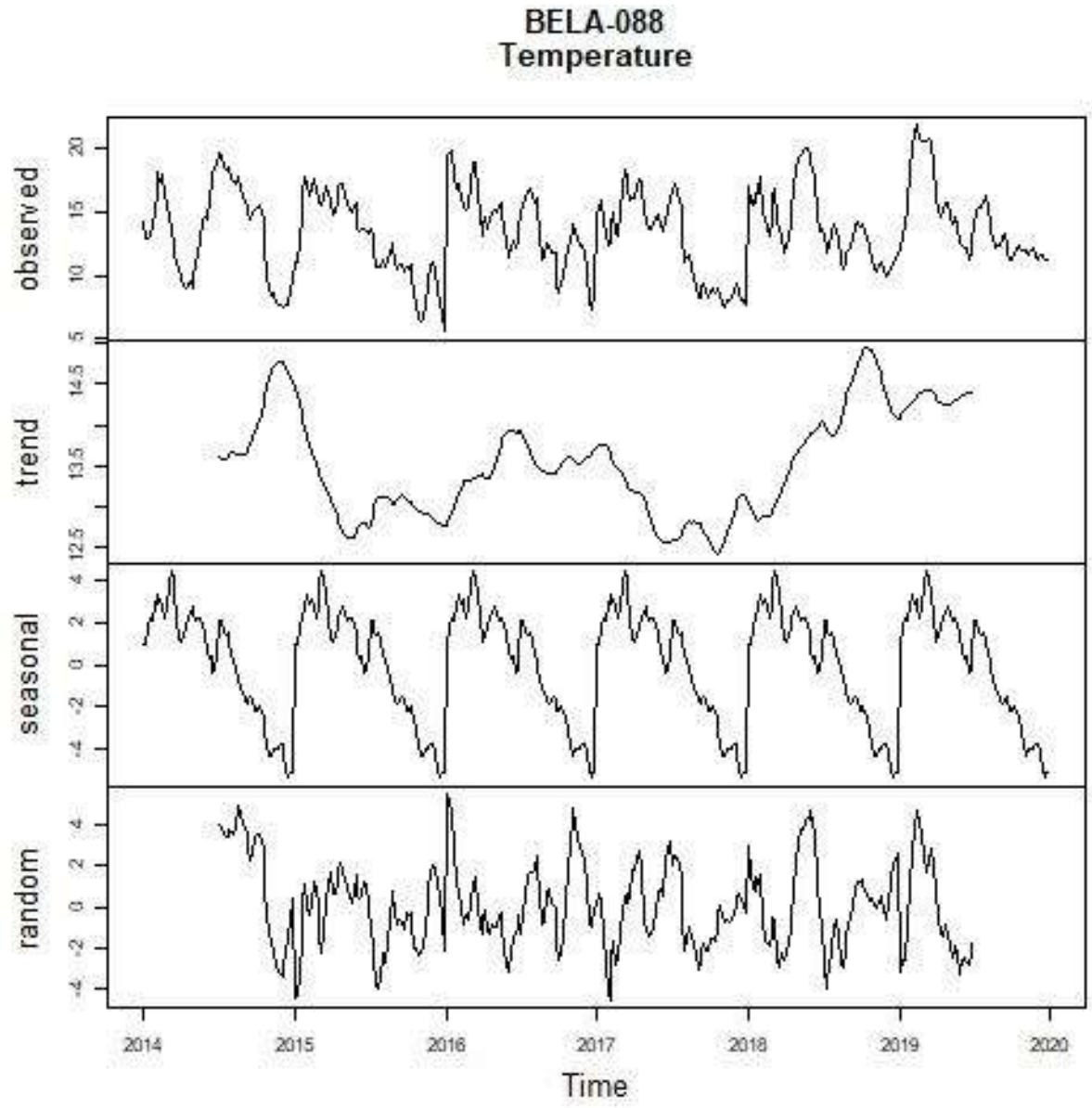


Figure A.108. Time series decomposition of truncated BELA-088 sonde temperature by year.

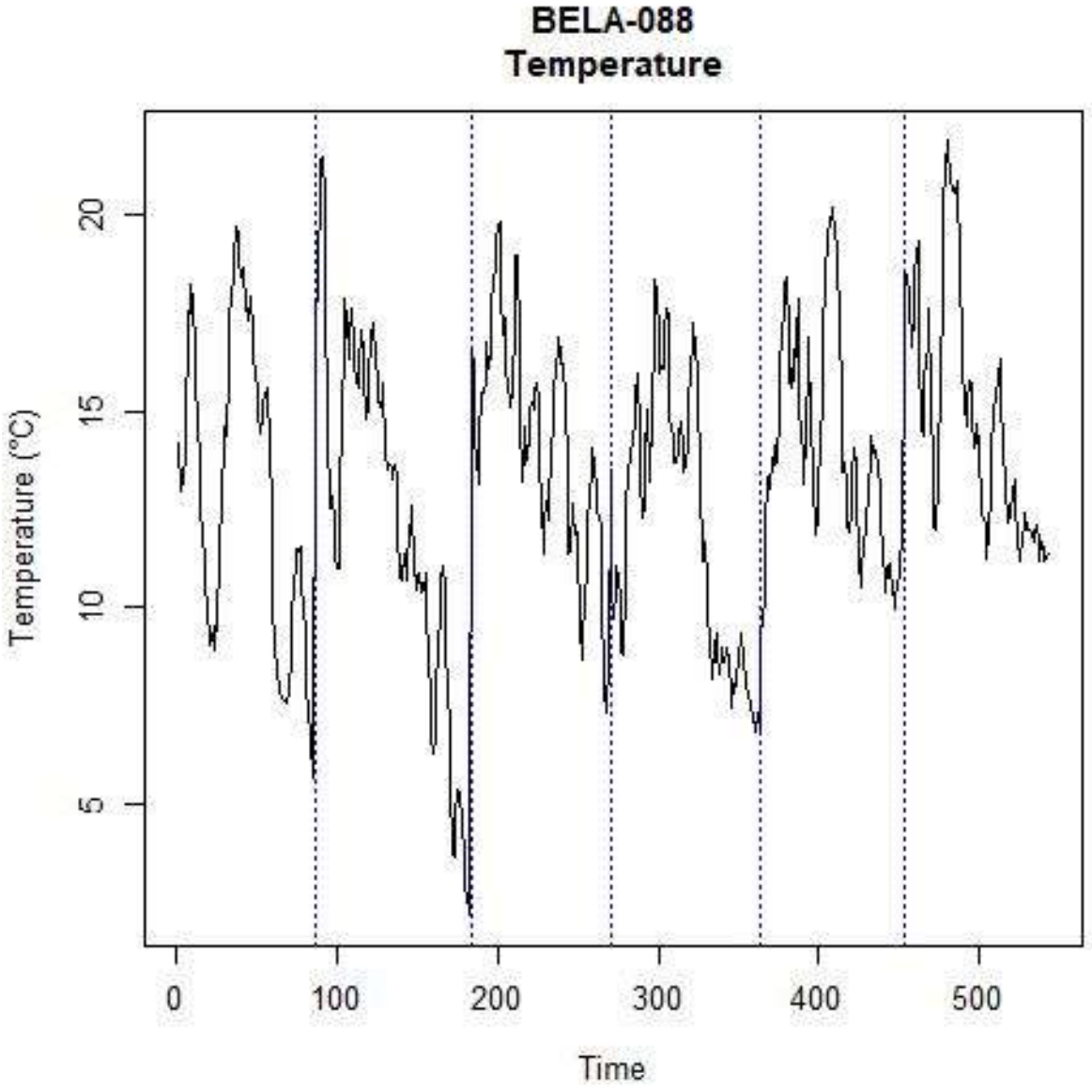


Figure A.109. Time series of BELA-088 sonde temperature by time point with vertical lines for additive outliers.

Table A.116. Trend modeling results for daily sonde temperature data at BELA-088.

			Trend			ARMA order		Ljung-Box Test	
Logged	**Method**	**Intercept**	**Coefficient**	**SE**	**p-value**	**AR**	**MA**	**Statistic**	**p-value**
FALSE	complete	0.9084	1.0817	0.1840	< 0.0001	0	5	156.43	< 0.0001
FALSE	completeAO	8.8613	0.3900	0.0906	< 0.0001	0	0	2094.08	< 0.0001

			Trend			ARMA order		Ljung-Box Test	
Logged	**Method**	**Intercept**	**Coefficient**	**SE**	**p-value**	**AR**	**MA**	**Statistic**	**p-value**
FALSE	trunc	6.6324	0.6044	0.1872	0.0012	0	5	190.80	< 0.0001
FALSE	truncSA	11.8121	0.1547	0.1886	0.4120	2	0	141.69	< 0.0001
TRUE	complete	1.4626	0.0942	0.0166	< 0.0001	0	5	134.76	< 0.0001
TRUE	completeAO	1.8124	0.0635	0.0148	< 0.0001	0	5	159.91	< 0.0001
TRUE	trunc	2.3606	0.0190	0.0087	0.0291	0	1	1231.40	< 0.0001
TRUE	truncSA	2.4012	0.0155	0.0148	0.2935	2	0	135.12	0.0002

Table A.117. Trend modeling results for weekly sonde temperature data at BELA-088.

			Trend			ARMA order		Ljung-Box Test	
Logged	**Method**	**Intercept**	**Coefficient**	**SE**	**p-value**	**AR**	**MA**	**Statistic**	**p-value**
FALSE	complete	9.4853	0.8091	0.5093	0.1122	1	0	16.29	0.0226
FALSE	completeAO	10.8172	0.4778	0.3946	0.2259	1	1	15.39	0.0015
FALSE	trunc	12.5229	0.2661	0.2616	0.3091	2	0	11.53	0.0733
FALSE	truncSA	12.3300	0.2397	0.1748	0.1704	0	2	6.62	0.5786
TRUE	complete	2.2939	0.0524	0.0268	0.0503	0	1	23.65	0.0013
TRUE	completeAO	2.2813	0.0510	0.0362	0.1586	1	1	14.00	0.0029
TRUE	trunc	2.5006	0.0193	0.0247	0.4338	2	0	9.05	0.3384
TRUE	truncSA	2.4794	0.0197	0.0134	0.1422	0	2	4.12	0.8457

Table A.118. Top covariate models for daily sonde temperature data at BELA-088.

Model	**AICc**	**ΔAICc**	**Ljung-Box Test p-value**
Relative Humidity + Month	1013.75	0.00	0.2105
Wind Speed + Relative Humidity + Month	1015.69	1.94	0.1213
Wind Speed + Month	1045.40	31.65	0.1699
dailyprecipitation + Month	1045.55	31.80	0.1759
Wind Speed + dailyprecipitation + Month	1047.45	33.70	0.1004
airtemperature	1070.80	57.04	0.4483
airtemperature + Wind Speed	1071.41	57.66	0.3145
airtemperature + dailyprecipitation	1072.67	58.92	0.3316
airtemperature + Wind Speed + dailyprecipitation	1073.40	59.64	0.2087
Solar Radiation	1155.67	141.92	0.3235

Table A.119. Coefficients and variance components estimates for the top covariate model for daily sonde temperature data at BELA-088.

Parameter	Coefficient	SE	p-value
ar1	1.32	0.05	< 0.0001
ar2	-0.40	0.05	< 0.0001
intercept	32.50	1.31	< 0.0001
Relative Humidity	-0.02	0.00	< 0.0001
Month	-2.31	0.15	< 0.0001

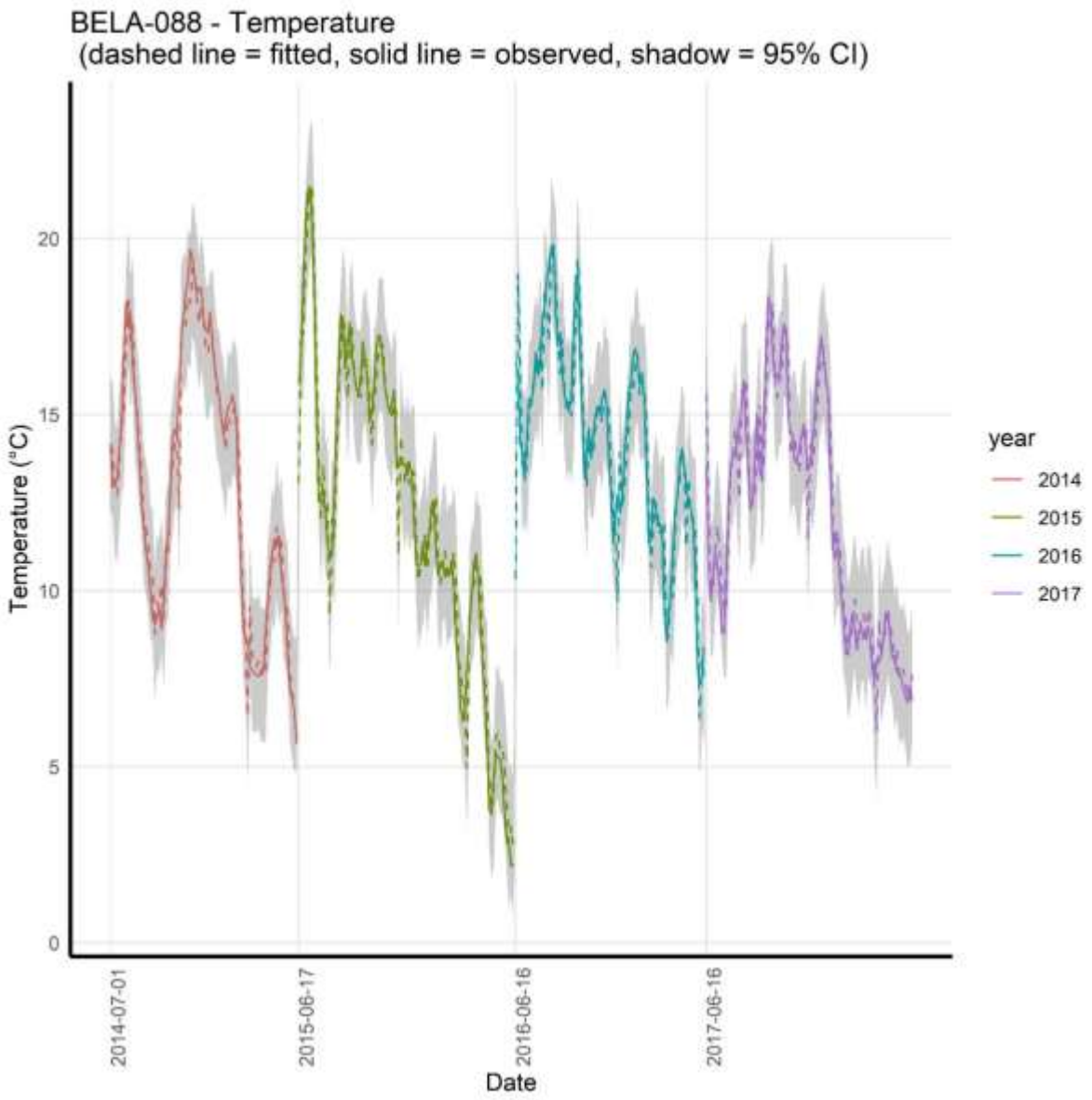


Figure A.110: Model predictions of BELA-088 sonde temperature by date.

BELA-108

Data

For BELA-108, temperature was recorded from 2015 through 2019. Over this period, there were 456 records of temperature consistently recorded from June to September. Truncated to the 86 days that were sampled every year, the dataset had 430 observations. Covariate coverage was poor in 2018 and 2019, so covariate models only considered 2015-2017. This left 276 records for covariate modeling.

Model Selection

For ARIMA models fitting all possible covariate combinations at lake BELA-108 with temperature as the response variable, AICc-based model selection resulted in ARIMA(1,0,2) with wind speed, relative humidity, month, and year as the main covariates in the best model. The wind speed coefficient was not significantly different from zero. The model detected a positive trend in temperature over the three years.

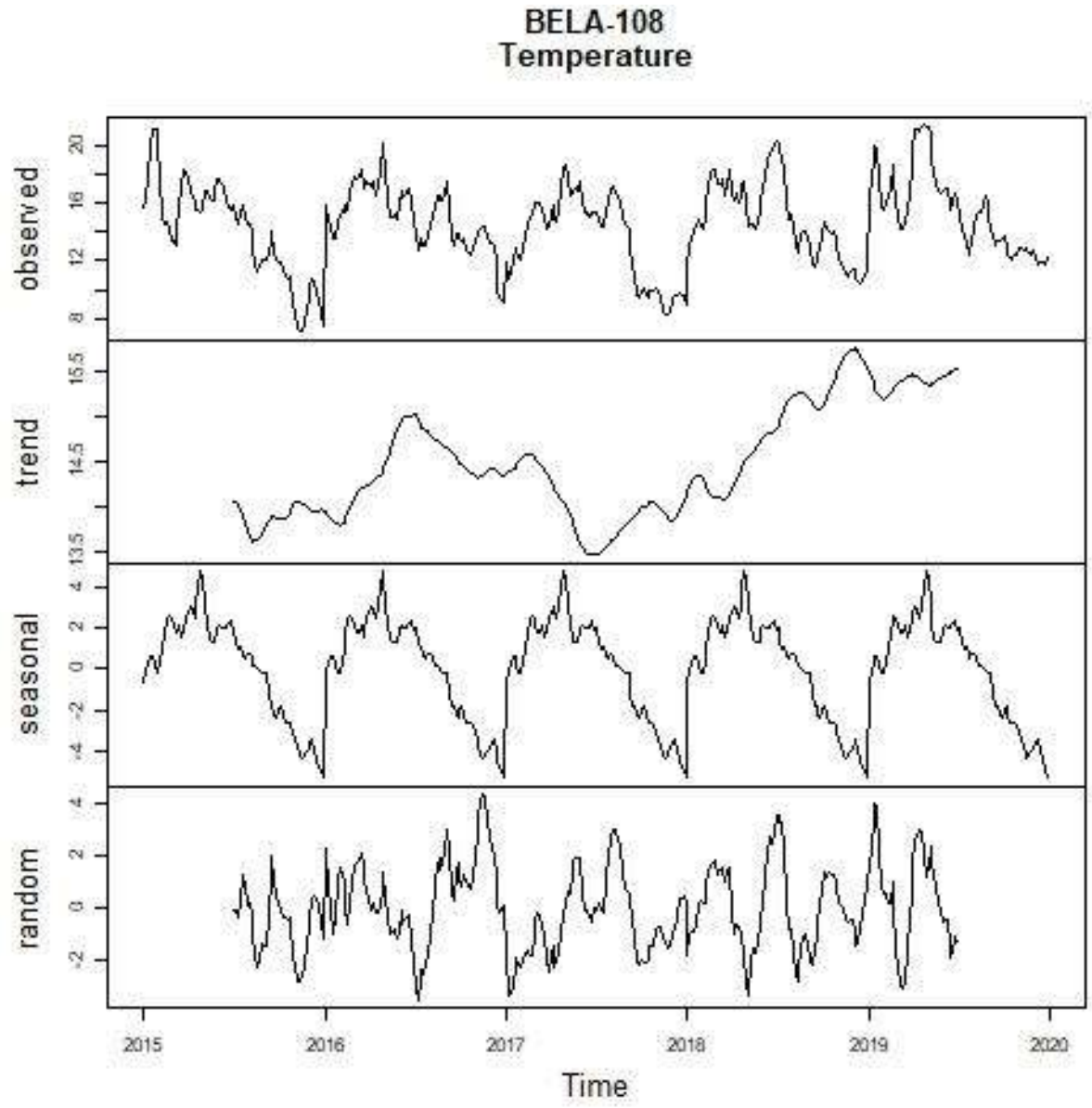


Figure A.111. Time series decomposition of truncated BELA-108 sonde temperature by year.

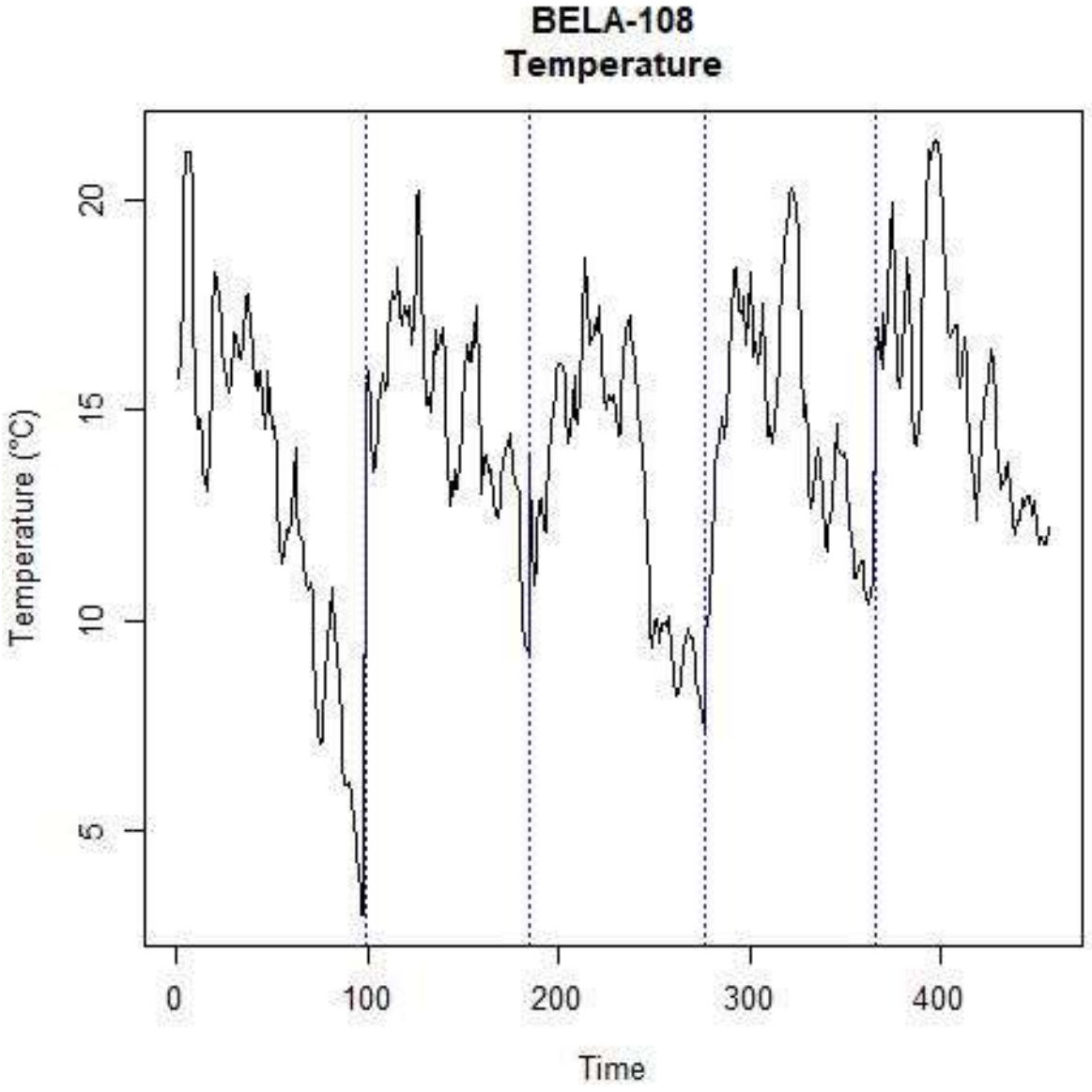


Figure A.112. Time series of BELA-108 sonde temperature by time point with vertical lines for additive outliers.

Table A.120. Trend modeling results for daily sonde temperature data at BELA-108.

			Trend			ARMA order		Ljung-Box Test	
Logged	**Method**	**Intercept**	**Coefficient**	**SE**	**p-value**	**AR**	**MA**	**Statistic**	**p-value**
FALSE	complete	0.4526	1.1537	0.1785	< 0.0001	0	4	322.43	< 0.0001
FALSE	completeAO	NA	1.2405	0.0802	< 0.0001	1	3	3.05	0.3846

			Trend			ARMA order		Ljung-Box Test	
Logged	**Method**	**Intercept**	**Coefficient**	**SE**	**p-value**	**AR**	**MA**	**Statistic**	**p-value**
FALSE	trunc	NA	1.2011	0.0163	< 0.0001	0	1	1973.50	< 0.0001
FALSE	truncSA	11.9555	0.2222	0.1324	0.0934	4	1	113.98	0.0061
TRUE	complete	1.2416	0.1154	0.0182	< 0.0001	0	5	168.08	< 0.0001
TRUE	completeAO	1.7108	0.0761	0.0157	< 0.0001	0	5	219.49	< 0.0001
TRUE	trunc	1.7163	0.0785	0.0147	< 0.0001	0	5	340.57	< 0.0001
TRUE	truncSA	2.4797	0.0154	0.0113	0.1746	4	3	99.66	0.0423

Table A.121. Top covariate models for daily sonde temperature data at BELA-108.

Model	**AICc**	**ΔAICc**	**Ljung-Box Test p-value**
Wind Speed + Relative Humidity + Year + Month	628.74	0.00	0.0641
Year + Month	641.33	12.60	0.3196
Wind Speed + Year + Month	643.34	14.60	0.2125
Daily Precipitation + Year + Month	643.37	14.64	0.2106
Wind Speed + Daily Precipitation + Year + Month	645.37	16.63	0.1217
Relative Humidity + Month	663.59	34.85	0.1466
Wind Speed + Relative Humidity + Month	667.22	38.49	0.1492
Wind Speed + Month	678.92	50.19	0.2575
Daily Precipitation + Month	678.93	50.20	0.2639
Wind Speed + Daily Precipitation + Month	681.00	52.26	0.1636

Table A.122. Coefficients and variance components estimates for the top covariate model for daily sonde temperature data at BELA-108.

Parameter	**Coefficient**	**SE**	**p-value**
ar1	0.95	0.02	< 0.0001
ma1	0.53	0.06	< 0.0001
ma2	0.09	0.06	0.1534
Wind Speed	0.00	0.01	0.5727
Relative Humidity	-0.01	0.00	< 0.0001
Year	2.42	0.13	< 0.0001
Month	-1.48	0.11	< 0.0001

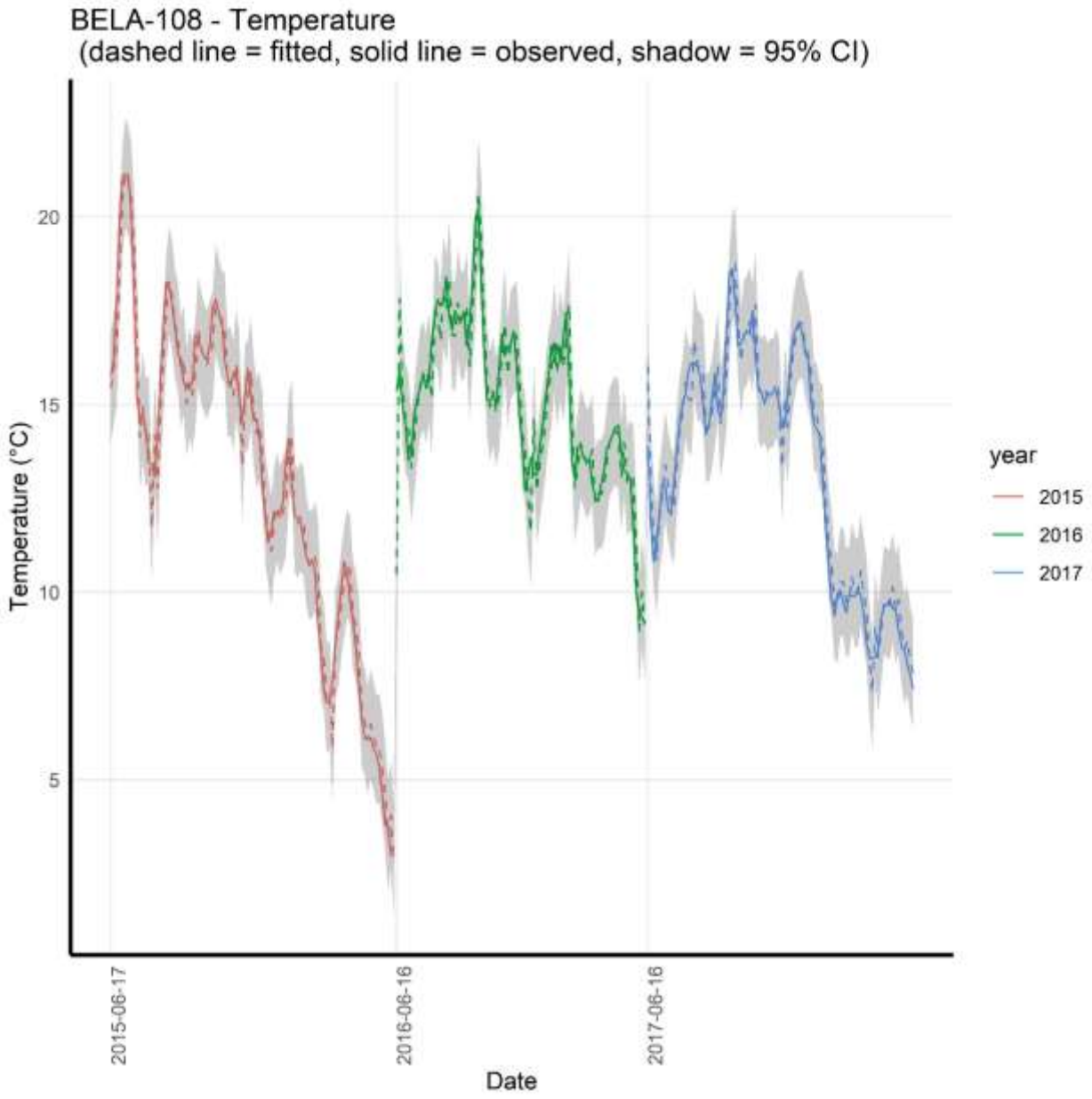


Figure A.113. Model predictions of BELA-108 sonde temperature by date.

DENA-018

Data

For DENA-018, temperature was recorded from 2009 through 2019. However, 2013 was missing from the dataset, so analysis addressed the years 2014-2019. Over this period, there were 696 records of temperature. Data were recorded from May to September, except in 2019, when the record began in June. Truncated to the 99 days that were sampled every year, the dataset had 594 observations.

Model Selection

For ARIMA models fitting all possible covariate combinations at lake DENA-018 with temperature as the response variable, AICc-based model selection resulted in ARIMA(1,0,1) with wind speed, air temperature, and month as the main covariates in the best model. No trend model of daily data exhibited stationarity. The truncated and seasonally adjusted models of weekly means demonstrated stationary residuals and positive trend estimates, but of very different magnitudes.

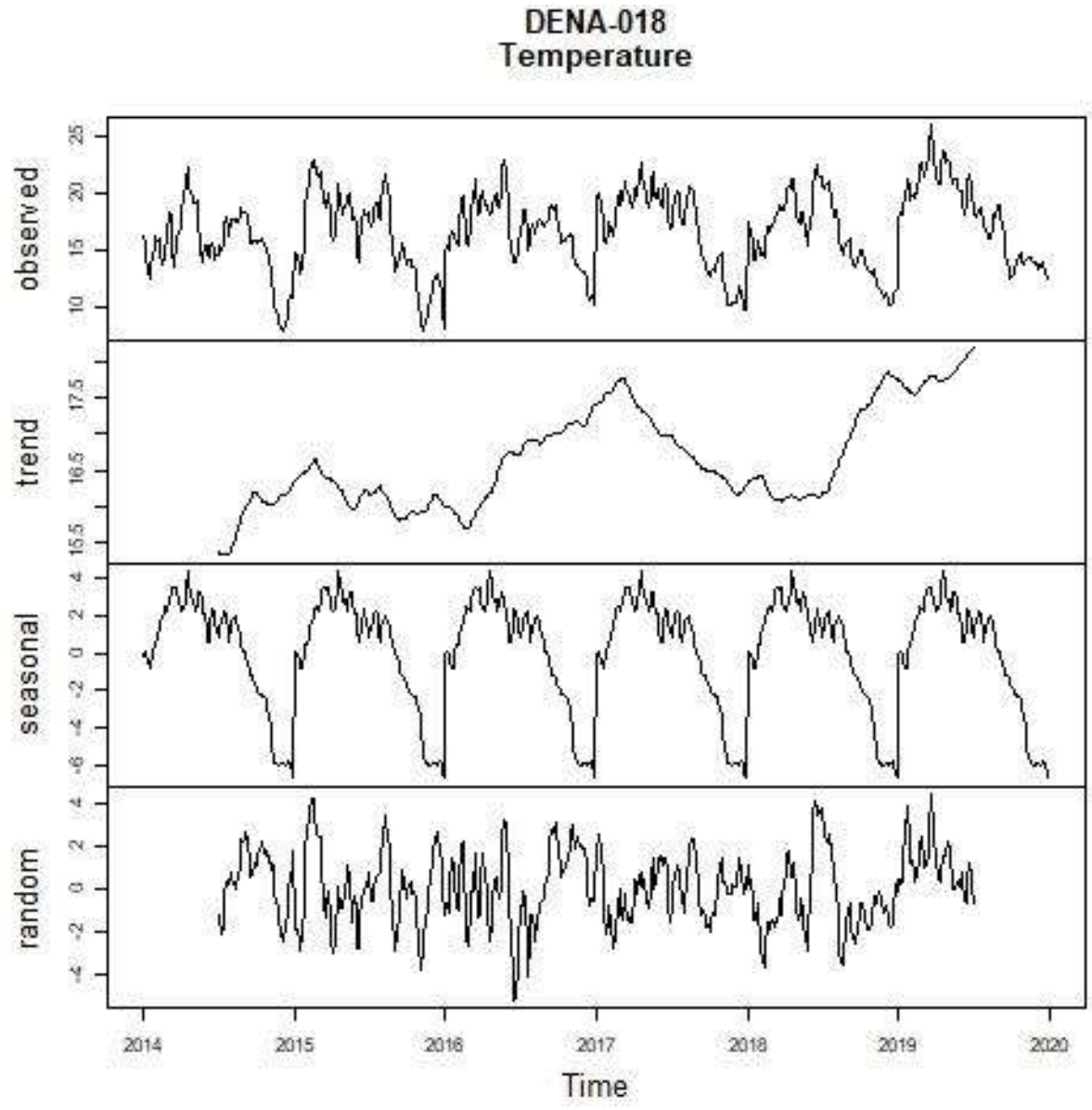


Figure A.114. Time series decomposition of truncated DENA-018 sonde temperature by year.

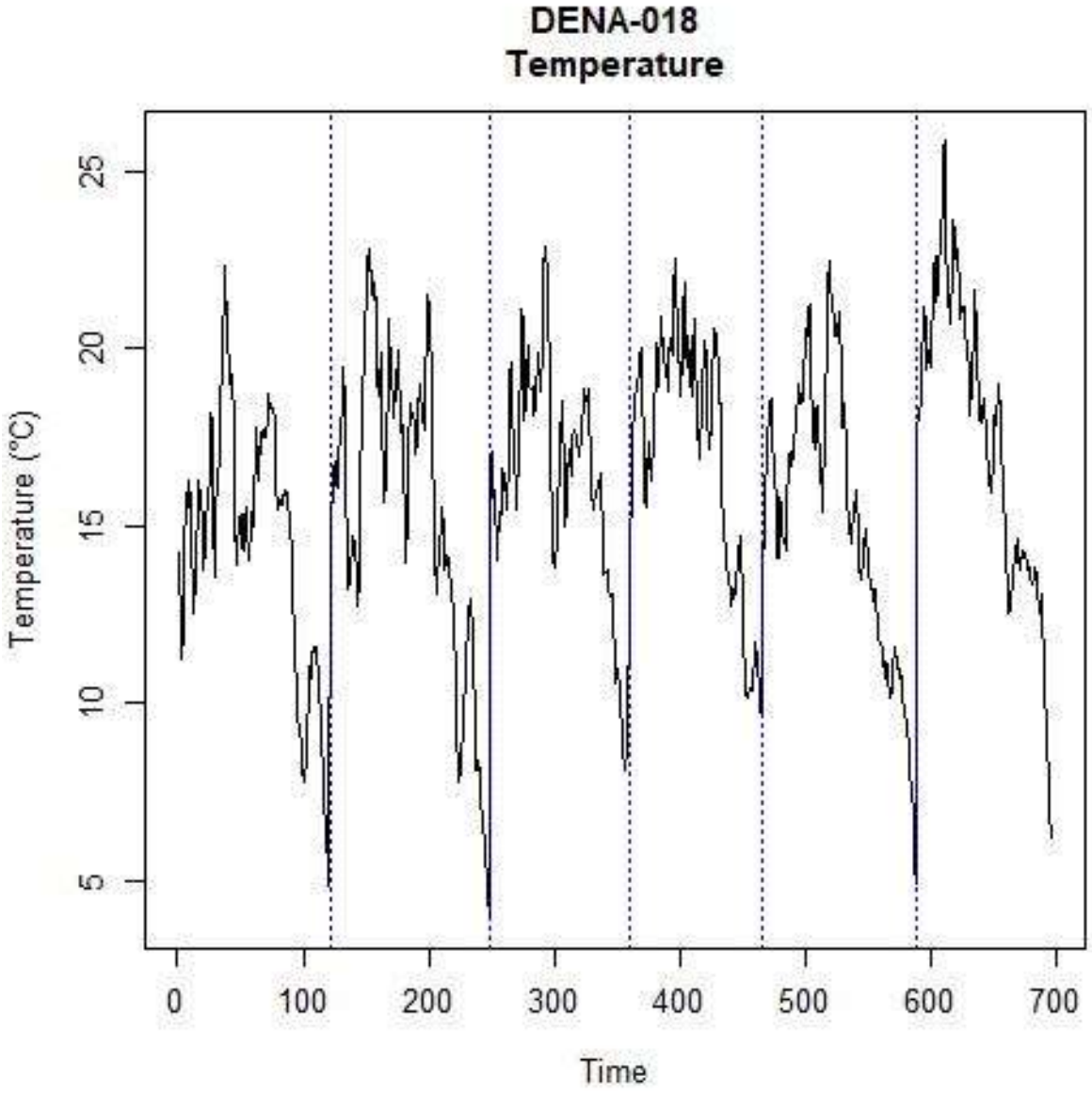


Figure A.115. Time series of DENA-018 sonde temperature by time point with vertical lines for additive outliers.

Table A.123. Trend modeling results for daily sonde temperature data at DENA-018.

			Trend			ARMA order		Ljung-Box Test	
Logged	**Method**	**Intercept**	**Coefficient**	**SE**	**p-value**	**AR**	**MA**	**Statistic**	**p-value**
FALSE	complete	NA	1.1006	0.0188	< 0.0001	0	5	311.19	< 0.0001
FALSE	completeAO	6.5650	0.6442	0.1517	< 0.0001	0	5	365.85	< 0.0001

			Trend			ARMA order		Ljung-Box Test	
Logged	**Method**	**Intercept**	**Coefficient**	**SE**	**p-value**	**AR**	**MA**	**Statistic**	**p-value**
FALSE	trunc	1.8890	1.0137	0.1565	< 0.0001	0	5	1016.42	< 0.0001
FALSE	truncSA	11.5913	0.3468	0.1265	0.0061	1	2	194.23	< 0.0001
TRUE	complete	1.6526	0.0745	0.0127	< 0.0001	0	5	232.65	< 0.0001
TRUE	completeAO	2.3152	0.0288	0.0063	< 0.0001	0	0	2949.58	< 0.0001
TRUE	trunc	1.7889	0.0687	0.0105	< 0.0001	0	5	1034.03	< 0.0001
TRUE	truncSA	2.4712	0.0218	0.0081	0.0072	1	2	198.75	< 0.0001

Table A.124. Trend modeling results for weekly sonde temperature data at DENA-018.

			Trend			ARMA order		Ljung-Box Test	
Logged	**Method**	**Intercept**	**Coefficient**	**SE**	**p-value**	**AR**	**MA**	**Statistic**	**p-value**
FALSE	complete	9.6149	0.8036	0.3469	0.0205	0	2	32.47	< 0.0001
FALSE	completeAO	NA	2.0320	0.1936	< 0.0001	1	1	11.64	0.0087
FALSE	trunc	NA	1.9868	0.3309	< 0.0001	1	0	11.75	0.5480
FALSE	truncSA	13.6713	0.3976	0.1290	0.0021	1	0	8.79	0.7206
TRUE	complete	2.2664	0.0587	0.0281	0.0367	0	2	20.56	0.0022
TRUE	completeAO	2.0730	0.0804	0.0492	0.1019	1	1	13.09	0.0044
TRUE	trunc	2.5144	0.0381	0.0212	0.0717	1	0	29.00	0.0066
TRUE	truncSA	2.6114	0.0241	0.0075	0.0013	0	2	8.06	0.7082

Table A.125. Top covariate models for daily sonde temperature data at DENA-018.

Model	**AICc**	**ΔAICc**	**Ljung-Box Test p-value**
Air Temperature + Wind Speed + Daily Precipitation	1673.66	0.00	0.5856
Air Temperature + Wind Speed	1675.34	1.68	0.6462
Air Temperature	1754.95	81.29	0.7864
Air Temperature + Daily Precipitation	1756.88	83.22	0.6846
Wind Speed + Daily Precipitation + Month	1838.98	165.32	0.0592
Wind Speed + Month	1839.72	166.06	0.0598
Daily Precipitation + Month	1854.10	180.43	0.0952
Wind Speed + Solar Radiation	2069.79	396.13	0.2928
Wind Speed + Solar Radiation + Daily Precipitation	2070.50	396.84	0.1679
Wind Speed + Relative Humidity	2083.92	410.25	0.3563

Table A.126. Coefficients and variance components estimates for the top covariate model for daily sonde temperature data at DENA-018.

Parameter	Coefficient	SE	p-value
ar1	0.93	0.02	< 0.0001
ma1	0.09	0.04	0.0306
intercept	10.60	0.51	< 0.0001
Air Temperature	0.41	0.02	< 0.0001
Wind Speed	-0.53	0.06	< 0.0001

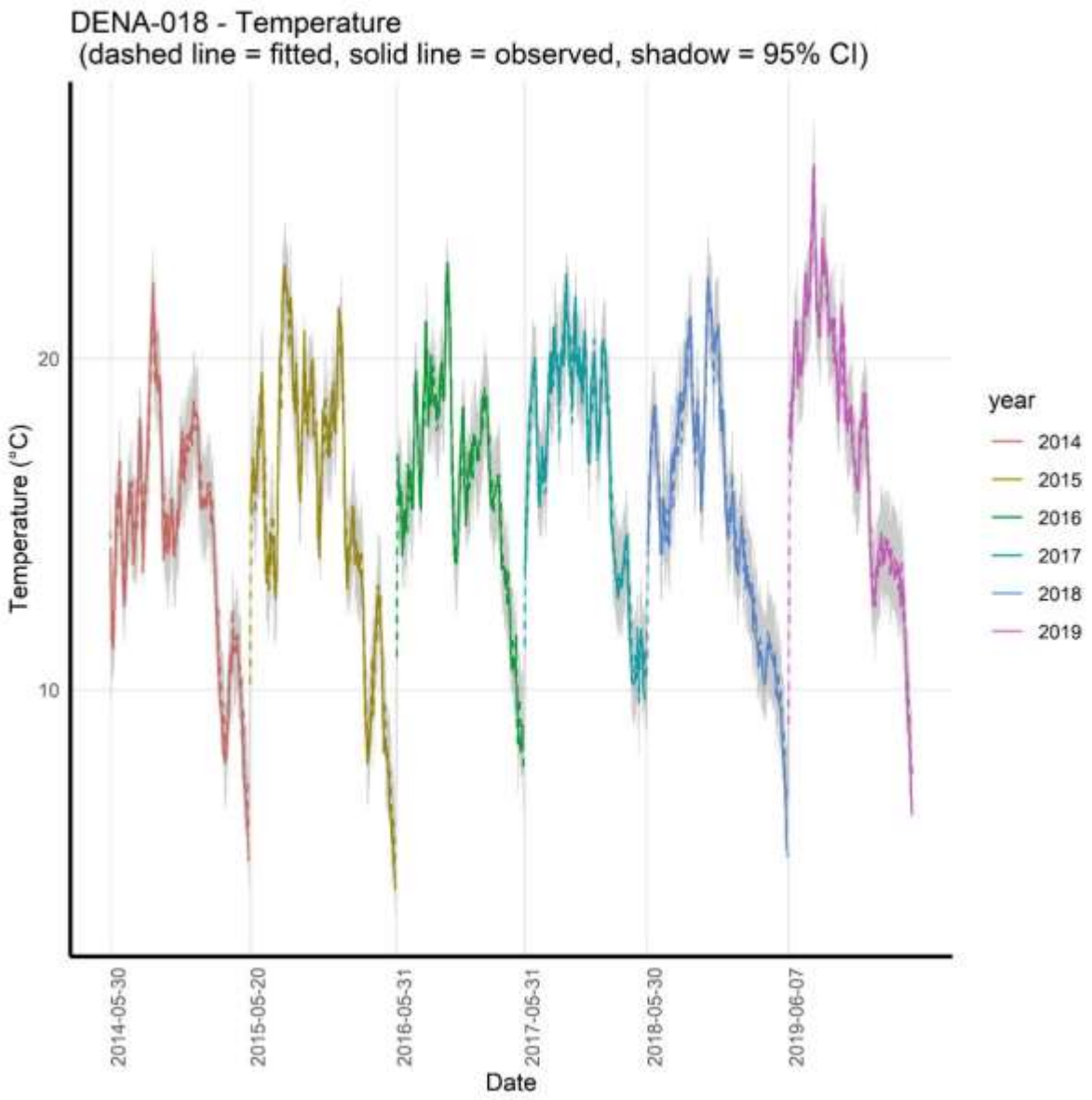


Figure A.116. Model predictions of DENA-018 sonde temperature by date.

DENA-023

Data

For DENA-023, temperature was recorded from 2011 through 2019. Over this period, there were 1017 records of temperature. Data were recorded from a variable start date in May or June to September or November, except in 2019, when the record ended in July. Truncated to the 45 days that were sampled every year, the dataset had 405 observations.

Model Selection

For ARIMA models fitting all possible covariate combinations at lake DENA-023 with temperature as the response variable, AICc-based model selection resulted in ARIMA(2,0,0) with air temperature and wind speed as the main covariates in the best model. All truncated analyses, whether logged or seasonally adjusted, resulted in stationary ARIMA(1,0,2) trend models.

An alternate analysis excluded the short 2019 season and had 972 records. After truncation to the common set of 95 days per year, the dataset had 760 records. No acceptable trend model was found with these longer season lengths, possibly due to the shorter monitoring period examined.

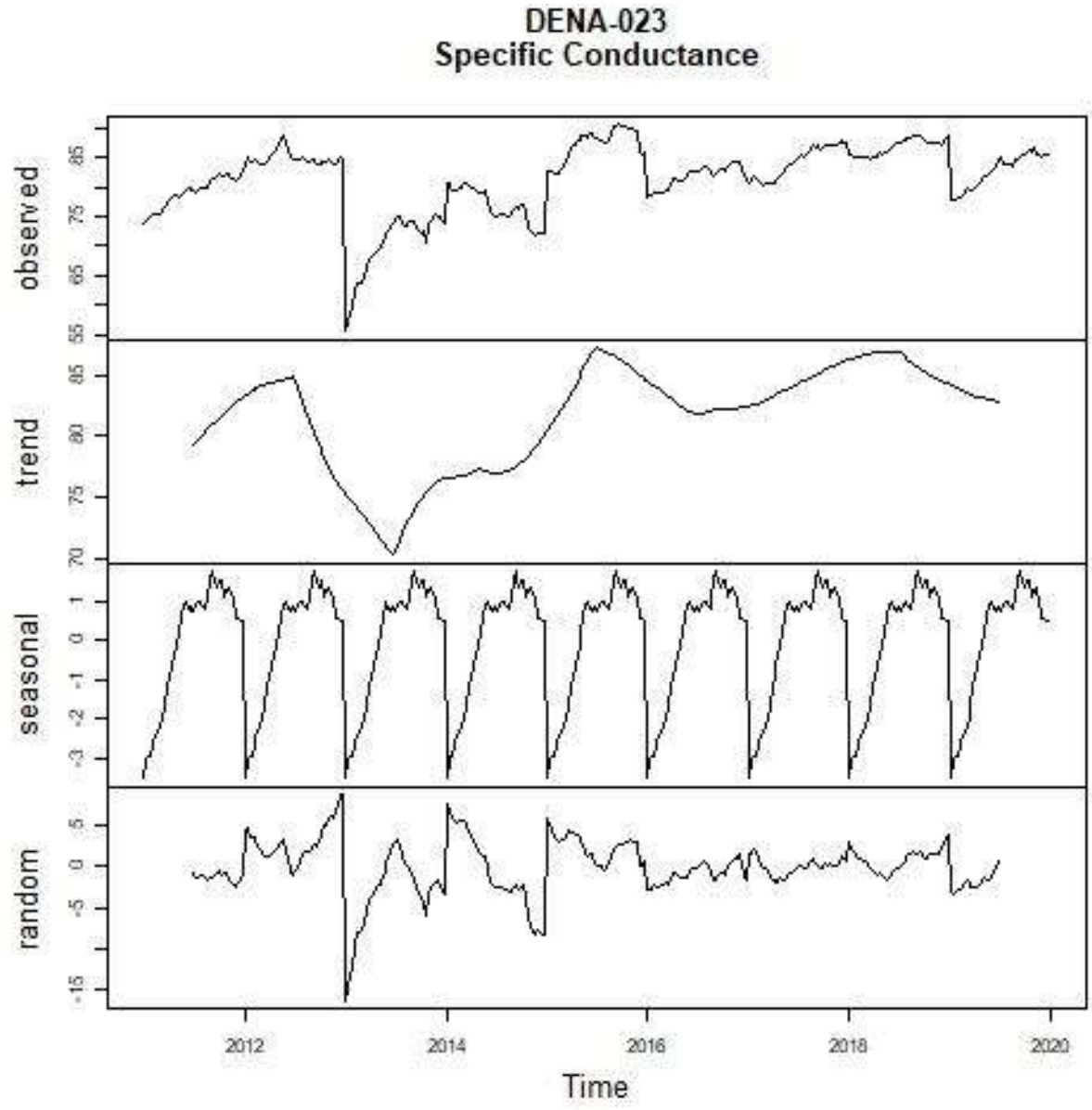


Figure A.117. Time series decomposition of truncated DENA-023 sonde temperature by year.

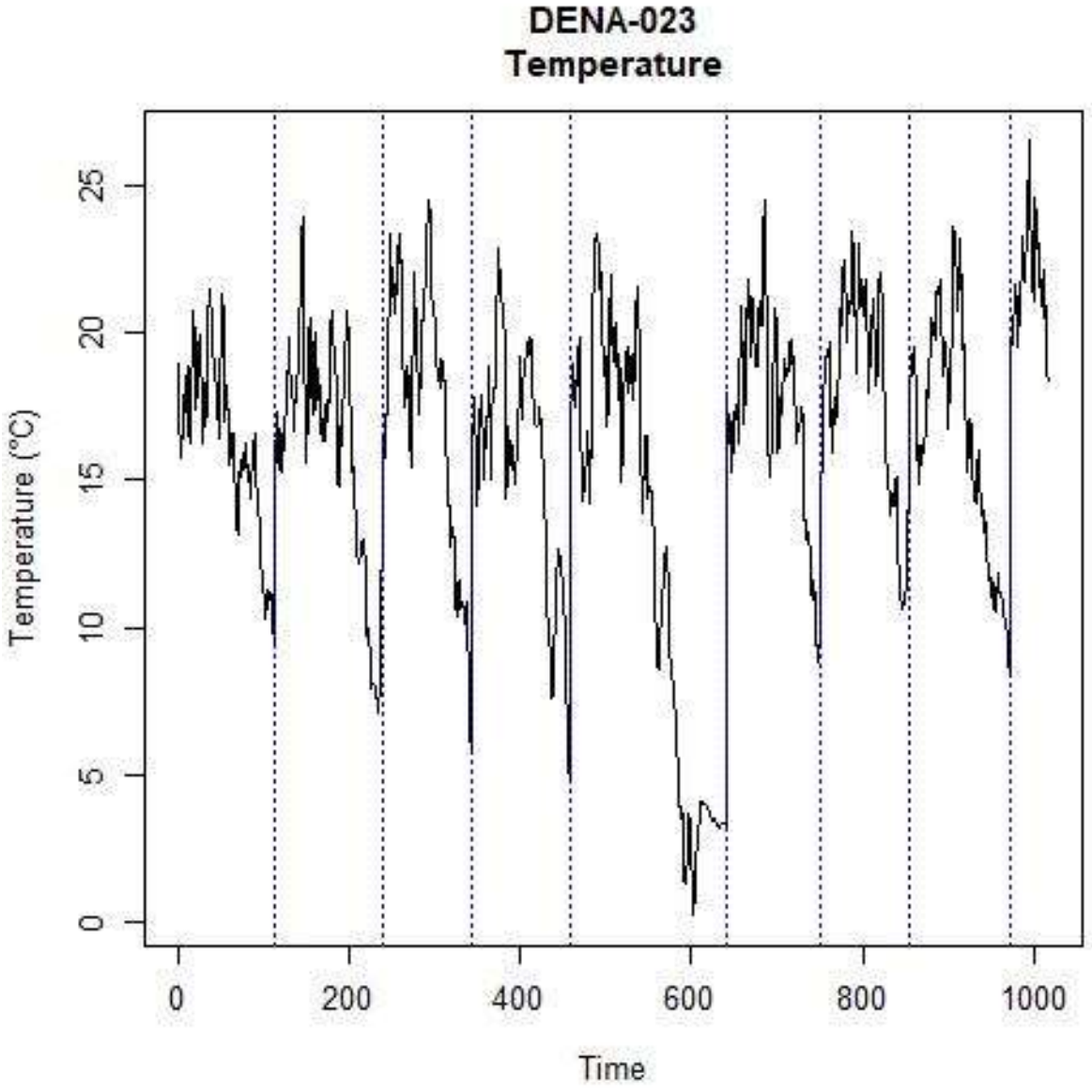


Figure A.118: Time series of LAKE sonde temperature by time point with vertical lines for additive outliers.

Table A.127. Trend modeling results for daily sonde temperature data at DENA-023.

			Trend			ARMA order		Ljung-Box Test	
Logged	**Method**	**Intercept**	**Coefficient**	**SE**	**p-value**	**AR**	**MA**	**Statistic**	**p-value**
FALSE	complete	6.4864	0.7578	0.1182	< 0.0001	0	5	737.10	< 0.0001
FALSE	completeAO	10.7199	0.4225	0.1095	0.0001	0	5	1139.69	< 0.0001

			Trend			ARMA order		Ljung-Box Test	
Logged	**Method**	**Intercept**	**Coefficient**	**SE**	**p-value**	**AR**	**MA**	**Statistic**	**p-value**
FALSE	trunc	17.6210	0.1242	0.1239	0.3161	1	2	69.14	0.6984
FALSE	truncSA	16.0439	0.2469	0.0917	0.0071	1	2	77.23	0.4390
TRUE	complete	1.9189	0.0612	0.0120	< 0.0001	0	5	717.22	< 0.0001
TRUE	completeAO	2.3266	0.0289	0.0112	0.0096	0	5	1143.89	< 0.0001
TRUE	trunc	2.8630	0.0067	0.0063	0.2898	1	2	73.74	0.5521
TRUE	truncSA	2.7872	0.0126	0.0047	0.0074	1	2	85.25	0.2191

Table A.128. Top covariate models for daily sonde temperature data at DENA-023.

Model	**AICc**	**ΔAICc**	**Ljung-Box Test p-value**
Air temperature + Wind Speed	2359.29	0.00	0.2535
Air temperature + Wind Speed + Daily precipitation	2361.20	1.91	0.1571
Air temperature + daily precipitation	2443.95	84.66	0.4273
Air temperature	2444.59	85.30	0.5357
Wind Speed + Daily precipitation + Month	2679.76	320.47	0.4340
Wind Speed + Month	2684.67	325.38	0.5259
Daily precipitation + Month	2699.33	340.04	0.6413
Wind Speed + Solar Radiation	3009.25	649.96	0.1611
Wind Speed + Solar Radiation + Daily precipitation	3010.09	650.80	0.0898
Solar Radiation	3031.33	672.04	0.1965

Table A.129. Coefficients and variance components estimates for the top covariate model for daily sonde temperature data at DENA-023.

Parameter	**Coefficient**	**SE**	**p-value**
ar1	1.17	0.03	< 0.0001
ar2	-0.21	0.03	< 0.0001
intercept	12.02	0.64	< 0.0001
Air Temperature	0.35	0.01	< 0.0001
Wind Speed	-0.40	0.04	< 0.0001

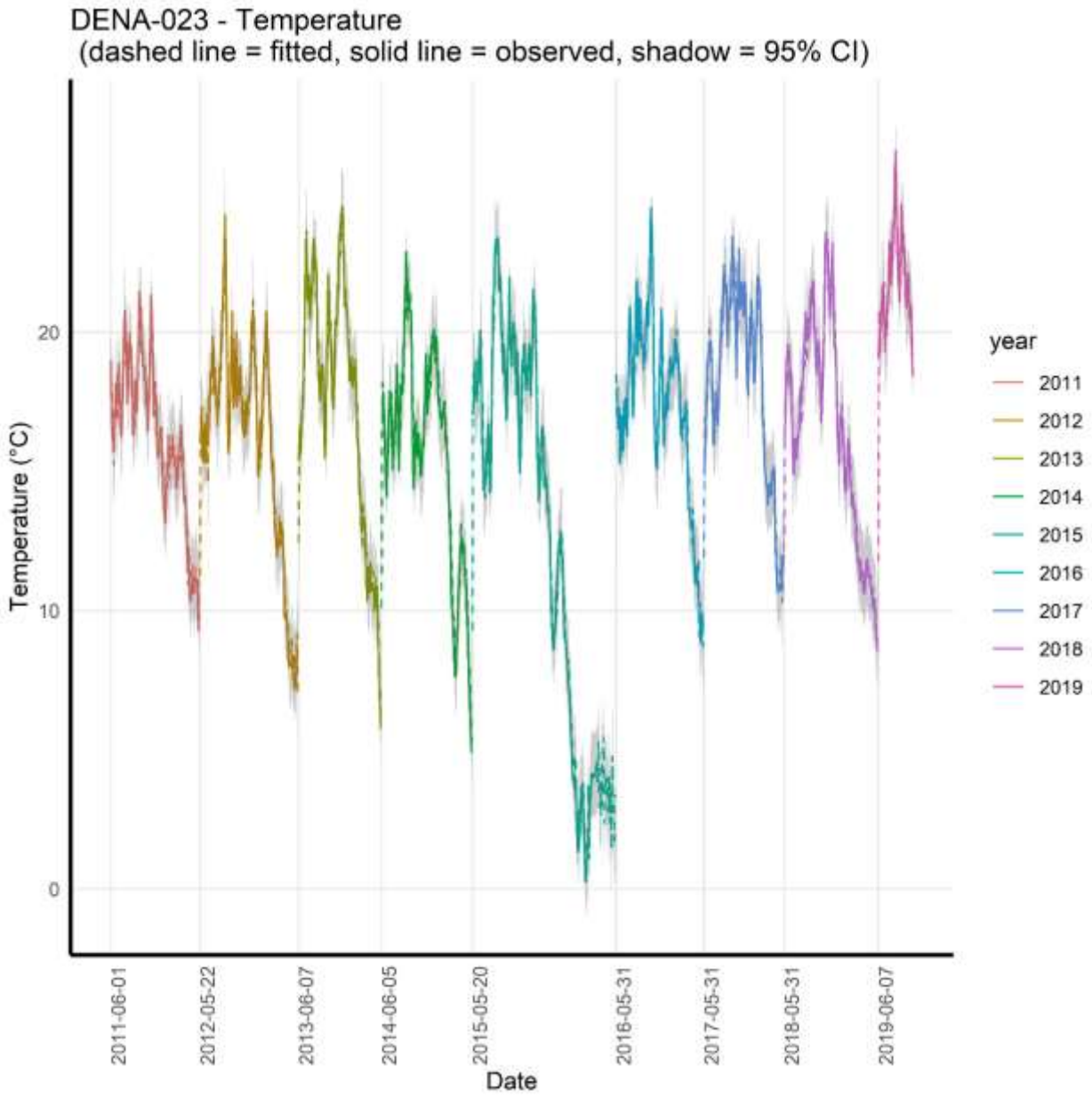


Figure A.119. Model predictions of DENA-023 sonde temperature by date.

KOVA-085

Data

For the KOVA-085 lake, temperature was recorded from 2010 through 2018. Over this period, there were 801 records of temperature. Data were recorded from June to September, except in 2013 and 2014, when the record began in July. Truncated to the 66 days that were sampled every year, the dataset had 594 observations.

Model Selection

For ARIMA models fitting all possible covariate combinations at lake KOVA-085 with temperature as the response variable, AICc-based model selection resulted in ARIMA(2,0,1) with air temperature and wind speed as the main covariates in the best model. The only trend models in the analysis with stationary residuals were the truncated, seasonally adjusted models. This model, an ARIMA(4,0,2), did not detect a significant annual trend in temperature.

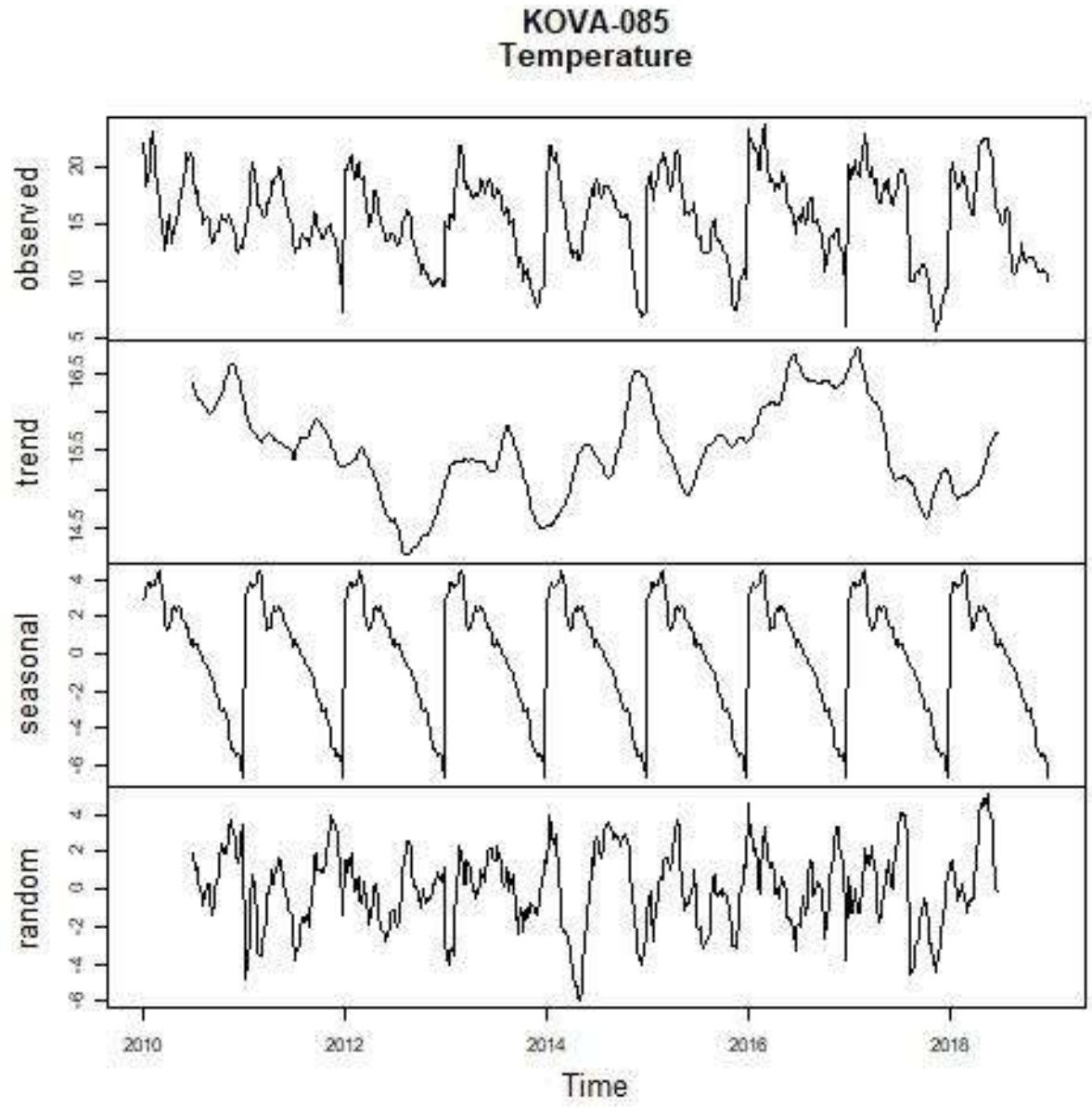


Figure A.120. Time series decomposition of truncated KOVA-085 sonde temperature by year.

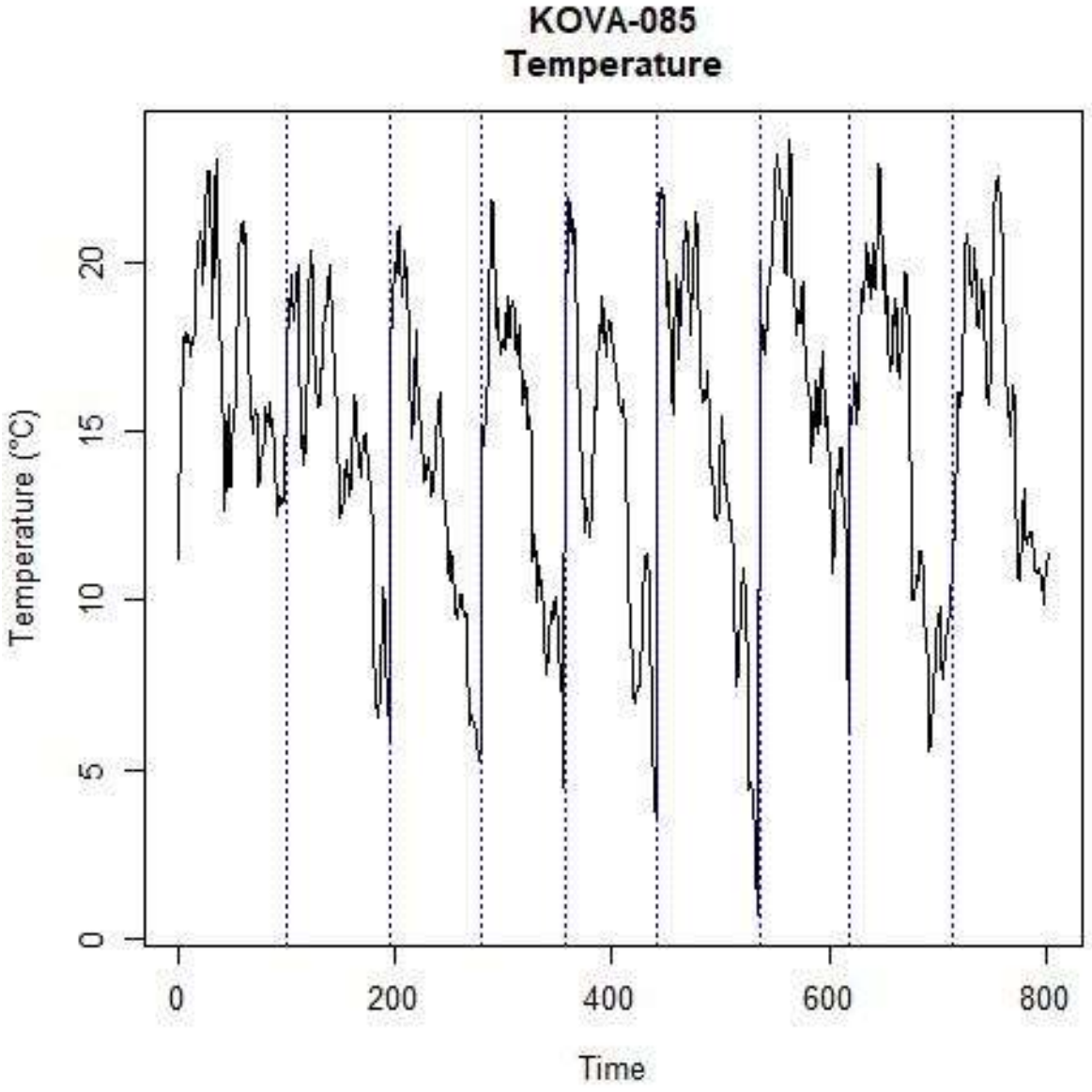


Figure A.121. Time series of KOVA-085 sonde temperature by time point with vertical lines for additive outliers.

Table A.130. Trend modeling results for daily sonde temperature data at KOVA-085.

			Trend			ARMA order		Ljung-Box Test	
Logged	**Method**	**Intercept**	**Coefficient**	**SE**	**p-value**	**AR**	**MA**	**Statistic**	**p-value**
FALSE	complete	10.7433	0.3944	0.1123	0.0004	0	5	312.28	< 0.0001
FALSE	completeAO	12.8070	0.2017	0.1024	0.0490	0	5	442.72	< 0.0001

			Trend			ARMA order		Ljung-Box Test	
Logged	**Method**	**Intercept**	**Coefficient**	**SE**	**p-value**	**AR**	**MA**	**Statistic**	**p-value**
FALSE	trunc	13.1523	0.2241	0.1194	0.0606	0	4	391.75	< 0.0001
FALSE	truncSA	15.6620	-0.0075	0.1076	0.9446	4	2	92.22	0.9022
TRUE	complete	2.3582	0.0269	0.0106	0.0111	0	5	149.01	< 0.0001
TRUE	completeAO	2.6692	-0.0015	0.0053	0.7743	0	0	3112.67	< 0.0001
TRUE	trunc	2.6673	0.0039	0.0057	0.4988	0	2	1959.96	< 0.0001
TRUE	truncSA	2.7506	-0.0036	0.0049	0.4652	2	2	95.64	0.8800

Table A.131. Top covariate models for daily sonde temperature data at KOVA-085.

Model	**AICc**	**ΔAICc**	**Ljung-Box Test p-value**
Air Temperature + Wind Speed	2335.65	0.00	0.3214
Air Temperature + Wind Speed + Daily Precipitation	2336.41	0.76	0.2046
Air Temperature	2343.48	7.83	0.5603
Air Temperature + Daily Precipitation	2346.50	10.85	0.4877
Relative Humidity + Month	2459.65	124.00	0.9368
Wind Speed + Relative Humidity + Month	2461.30	125.64	0.8493
Wind Speed + Month	2464.25	128.59	0.9393
Daily Precipitation + Month	2464.58	128.93	0.9480
Wind Speed + Daily Precipitation + Month	2466.06	130.41	0.8698
Wind Speed + Solar Radiation	2797.38	461.73	0.4249

Table A.132. Coefficients and variance components estimates for the top covariate model for daily sonde temperature data at KOVA-085

Parameter	**Coefficient**	**SE**	**p-value**
ar1	1.92	0.02	< 0.0001
ar2	-0.93	0.02	< 0.0001
ma1	-0.98	0.01	< 0.0001
intercept	9.59	0.30	< 0.0001
Air Temperature	0.43	0.02	< 0.0001
Wind Speed	-0.03	0.04	0.5337

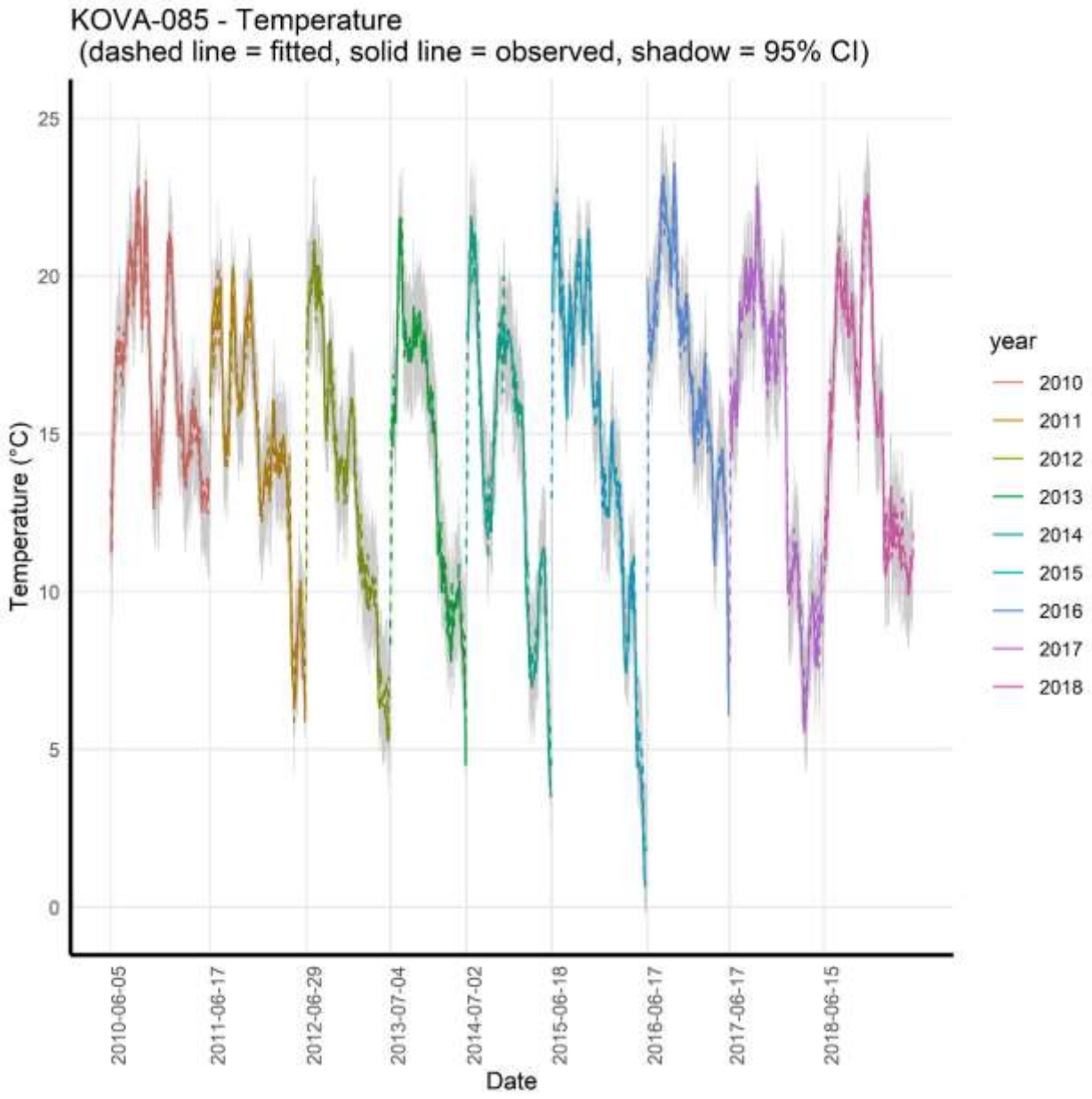


Figure A.122. Model predictions of KOVA-085 sonde temperature by date.

KOVA-086

Data

For KOVA-086, temperature was recorded from 2009 through 2019. However, no data were collected in 2010, so the analysis addressed 2011 through 2019. Over this period, there were 783 records of temperature. Data were recorded from June to September, except in 2013 and 2014, when the record began in July. Truncated to the 59 days that were sampled every year, the dataset had 531 observations.

Model Selection

For ARIMA models fitting all possible covariate combinations at lake KOVA-086 with temperature as the response variable, AICc-based model selection resulted in ARIMA(2,0,0) with wind speed and month as the main covariates in the best model, but no annual trend. The only trend model with stationary residuals was the truncated, seasonally adjusted model for untransformed data. This model, an ARIMA(2,0,0), had a positive annual trend term, but the trend was not significant.

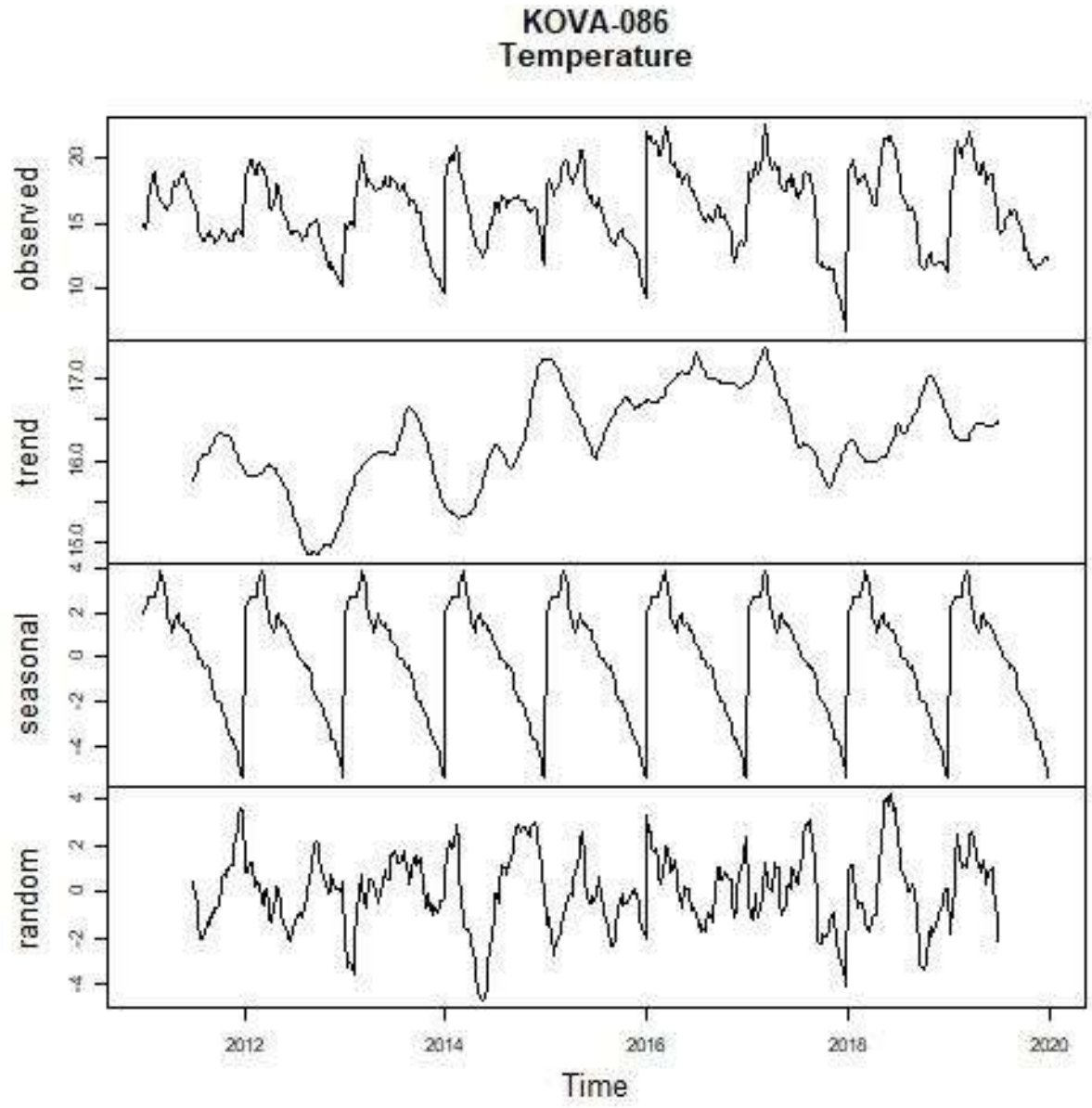


Figure A.123. Time series decomposition of truncated KOVA-086 sonde temperature by year.

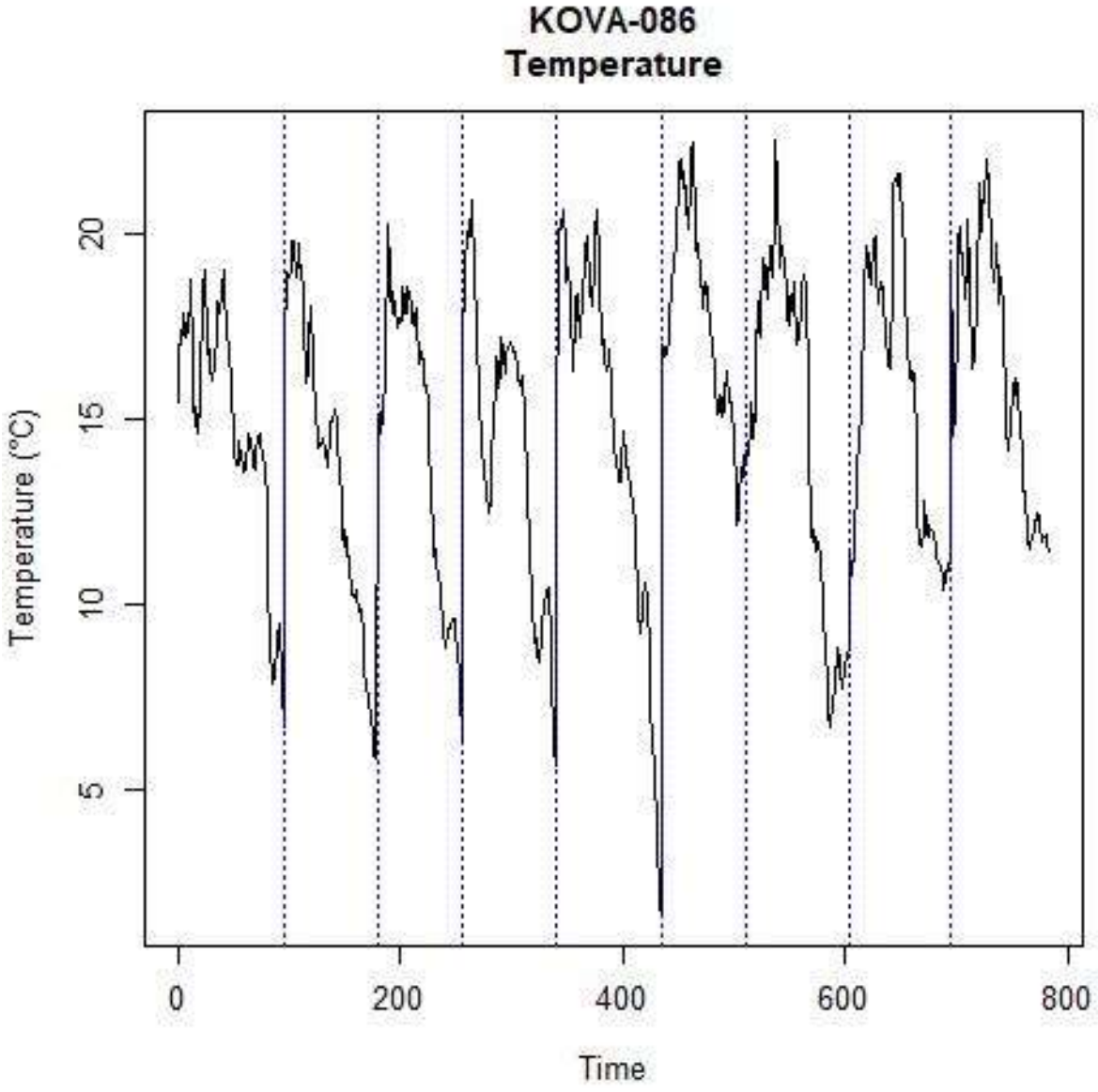


Figure A.124. Time series of KOVA-086 sonde temperature by time point with vertical lines for additive outliers.

Table A.133. Trend modeling results for daily sonde temperature data at KOVA-086.

			Trend			ARMA order		Ljung-Box Test	
Logged	**Method**	**Intercept**	**Coefficient**	**SE**	**p-value**	**AR**	**MA**	**Statistic**	**p-value**
FALSE	complete	7.6728	0.6116	0.0994	< 0.0001	0	5	424.05	< 0.0001
FALSE	completeAO	11.9806	0.2536	0.0539	< 0.0001	0	0	4723.08	< 0.0001

			Trend			ARMA order		Ljung-Box Test	
Logged	**Method**	**Intercept**	**Coefficient**	**SE**	**p-value**	**AR**	**MA**	**Statistic**	**p-value**
FALSE	trunc	11.4756	0.3913	0.1077	0.0003	0	5	259.50	< 0.0001
FALSE	truncSA	14.7521	0.1194	0.0940	0.2038	2	0	126.12	0.0529
TRUE	complete	2.1544	0.0425	0.0085	< 0.0001	0	5	250.31	< 0.0001
TRUE	completeAO	2.4474	0.0181	0.0044	< 0.0001	0	0	3918.33	< 0.0001
TRUE	trunc	2.5503	0.0179	0.0064	0.0052	0	4	321.20	< 0.0001
TRUE	truncSA	2.6890	0.0065	0.0064	0.3086	2	0	143.19	0.0045

Table A.134. Top covariate models for daily sonde temperature data at KOVA-086.

Model	**AICc**	**ΔAICc**	**Ljung-Box Test p-value**
Wind Speed + Month	1959.89	0.00	0.7120
Daily Precipitation + Month	1960.22	0.32	0.7027
Wind Speed + Daily Precipitation + Month	1961.92	2.03	0.5721
Air Temperature	1994.87	34.98	0.2354
Air Temperature + Daily Precipitation	1995.26	35.36	0.1574
Air Temperature + Wind Speed	1995.63	35.74	0.1386
Air Temperature + Wind Speed + Daily Precipitation	1995.71	35.82	0.0830
Solar Radiation	2344.79	384.89	0.1002
Wind Speed + Solar Radiation	2346.77	386.88	0.0561
Relative Humidity	2380.58	420.69	0.3511

Table A.135. Coefficients and variance components estimates for the top covariate model for daily sonde temperature data at KOVA-086.

Parameter	**Coefficient**	**SE**	**p-value**
ar1	1.16	0.03	< 0.0001
ar2	-0.22	0.03	< 0.0001
intercept	32.84	0.87	< 0.0001
Wind Speed	-0.02	0.03	0.5600
Month	-2.35	0.09	< 0.0001

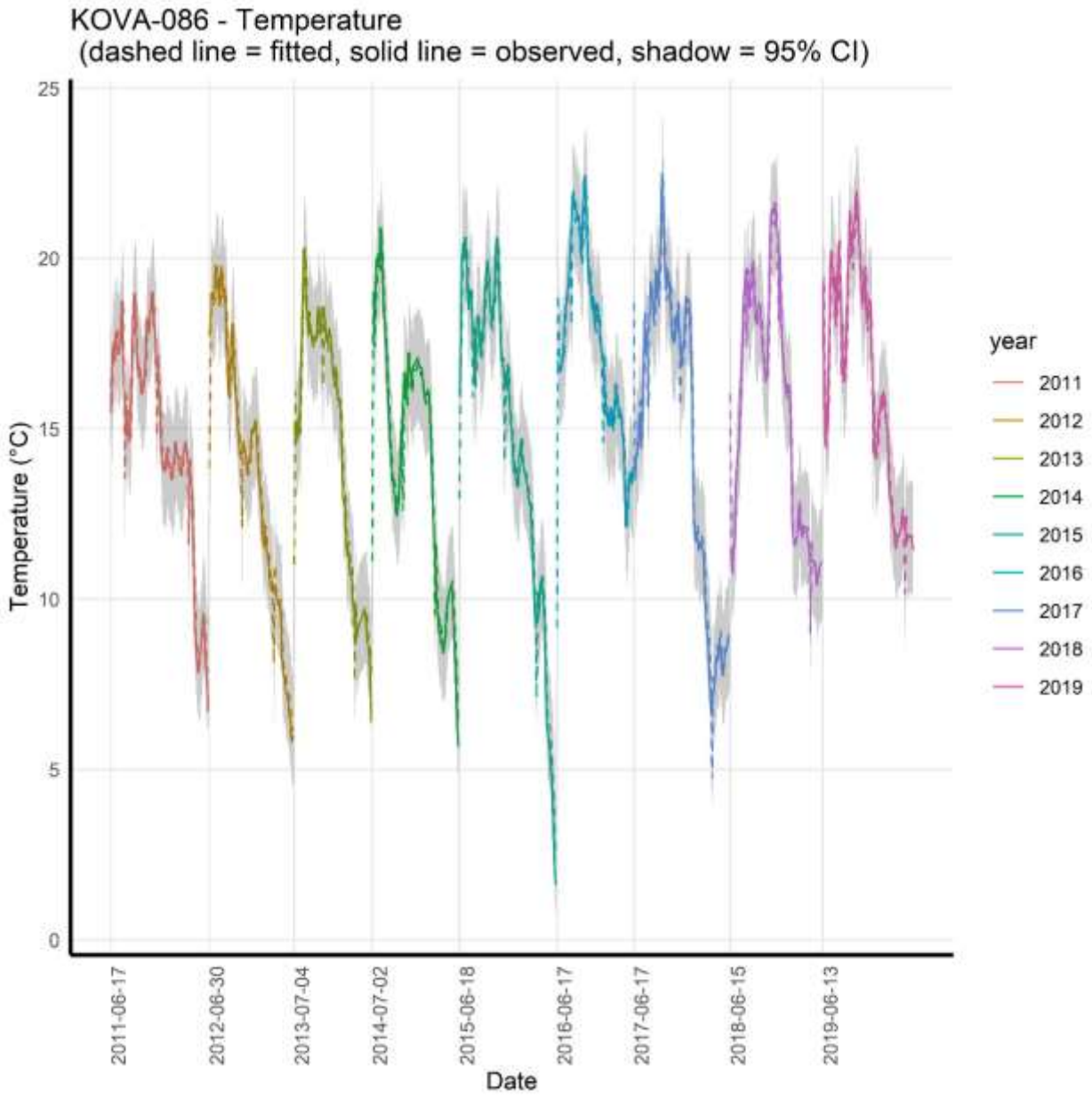


Figure A.125. Model predictions of KOVA-086 sonde temperature by date.

NOAT-052

Data

For the NOAT-052 lake, temperature was recorded from 2015 through 2019. Over this period, there were 723 records of temperature. Data were recorded from June to September, except in 2015-16, when the record was continuous. Truncated to the 85 days that were sampled every year, the dataset had 425 observations.

Model Selection

For ARIMA models fitting all possible covariate combinations at lake NOAT-052 with temperature as the response variable, no stationary models were identified. A seasonally adjusted ARIMA (2,0,2) model using the log-transformed and truncated dataset detected no significant annual trend in temperature. The covariate model was based on weekly mean temperature and contained fixed effects for solar radiation and year. This model indicated a positive association with solar radiation and a significant annual trend that lies in contrast to the trend estimate from the daily data that was not significantly different from zero.

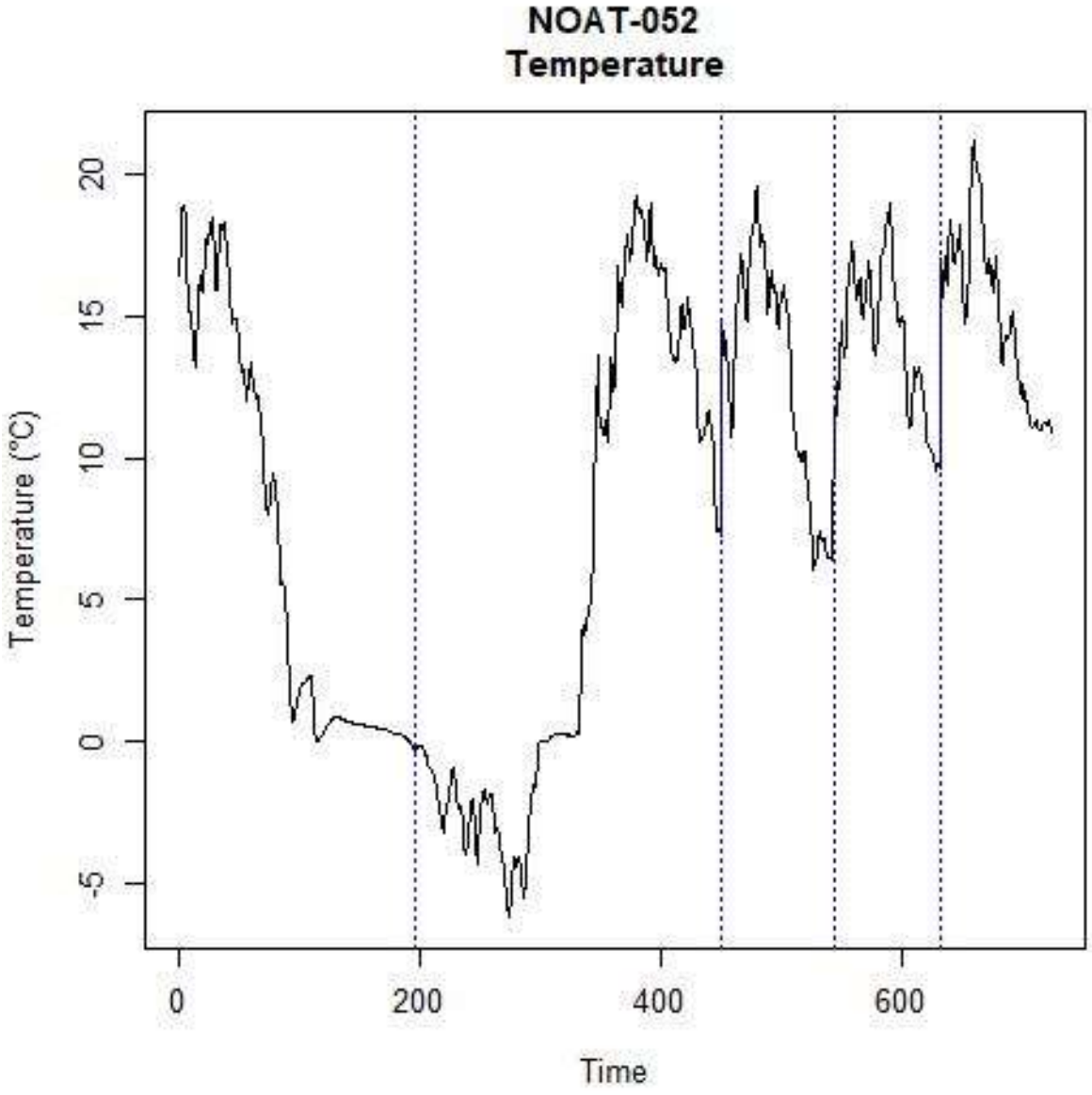


Figure A.126. Time series decomposition of truncated NOAT-052 sonde temperature by year.

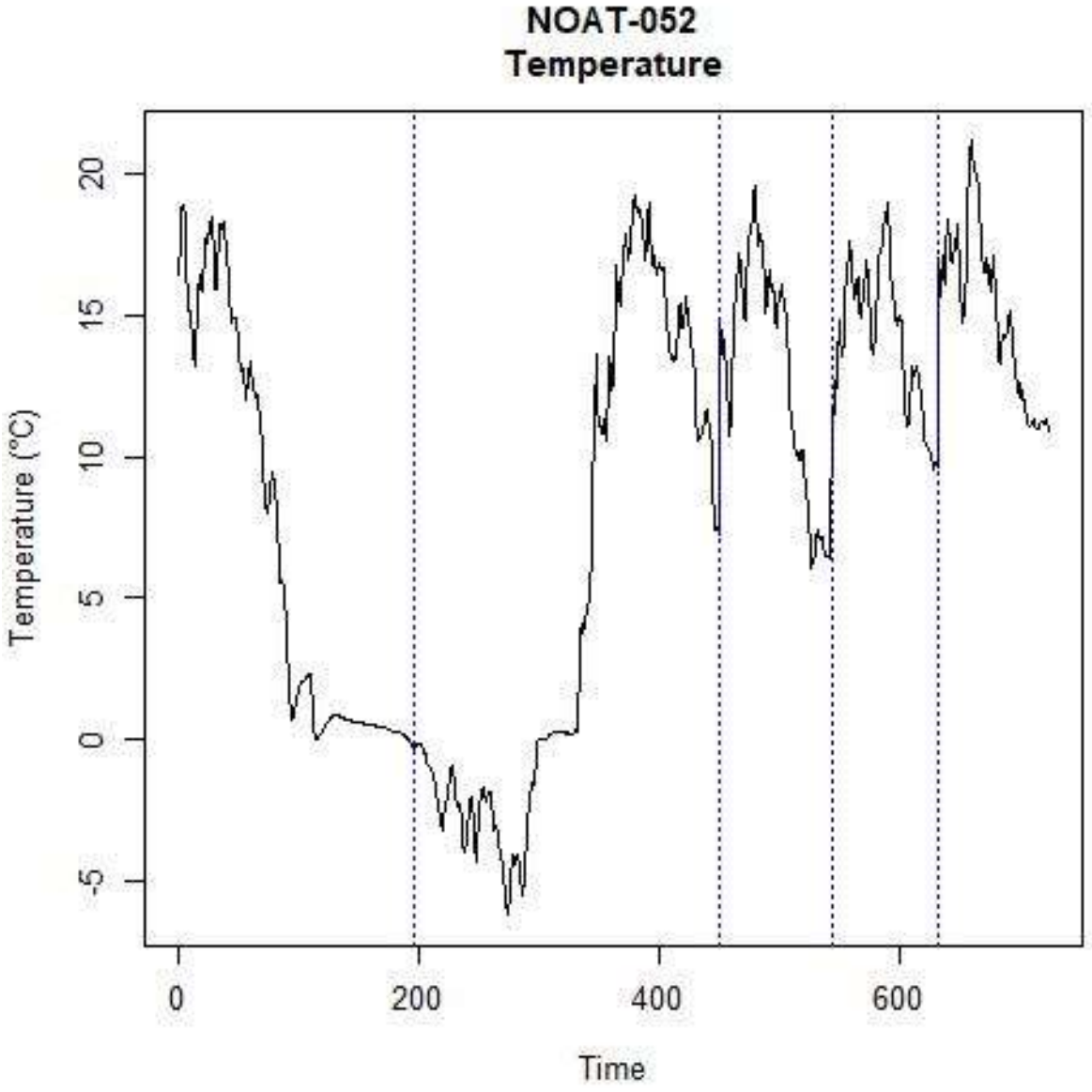


Figure A.127. Time series of NOAT-052 sonde temperature by time point with vertical lines for additive outliers.

Table A.136. Trend modeling results for daily sonde temperature data at NOAT-052.

			Trend			ARMA order		Ljung-Box Test	
Logged	**Method**	**Intercept**	**Coefficient**	**SE**	**p-value**	**AR**	**MA**	**Statistic**	**p-value**
FALSE	complete	-44.9007	3.7142	0.2100	< 0.0001	0	5	1572.50	< 0.0001
FALSE	completeAO	-29.4254	2.6451	0.1880	< 0.0001	0	1	6120.36	< 0.0001

			Trend			ARMA order		Ljung-Box Test	
Logged	**Method**	**Intercept**	**Coefficient**	**SE**	**p-value**	**AR**	**MA**	**Statistic**	**p-value**
FALSE	trunc	NA	0.9547	0.0195	< 0.0001	0	5	706.46	< 0.0001
FALSE	truncSA	12.7018	0.1081	0.1338	0.4194	4	0	84.04	0.3279
TRUE	complete	-1.5496	0.2887	0.0170	< 0.0001	2	1	30.37	< 0.0001
TRUE	completeAO	-1.3283	0.2689	0.0354	< 0.0001	1	2	39.16	< 0.0001
TRUE	trunc	0.9167	0.1140	0.0214	< 0.0001	0	5	703.28	< 0.0001
TRUE	truncSA	2.4750	0.0107	0.0122	0.3788	2	2	82.51	0.3713

Table A.137. Top covariate models for weekly sonde temperature means at NOAT-052.

Model	**AICc**	**ΔAICc**	**Ljung-Box Test p-value**
Solar Radiation + year	411.85	0.00	0.0799
Wind Speed + Solar Radiation	420.79	8.94	0.0547
Air temperature + Month	423.03	11.18	0.0981
Solar Radiation + Month	424.54	12.69	0.0784
Air temperature + daily precipitation + Month	424.77	12.92	0.0566
Solar Radiation	425.22	13.37	0.0801
Air temperature	428.18	16.33	0.1589
Air temperature + daily precipitation	430.07	18.23	0.0897
year + Month	435.03	23.18	0.0866
Daily precipitation + year	435.35	23.51	0.0560

Table A.138. Coefficients and variance components estimates for the top covariate model for daily sonde temperature data at NOAT-052.

Parameter	**Coefficient**	**SE**	**p-value**
ar1	1.78	0.13	< 0.0001
ar2	-0.80	0.13	< 0.0001
ma1	-0.60	0.17	0.0006
Solar Radiation	0.01	0.00	< 0.0001
Year	3.31	0.70	< 0.0001

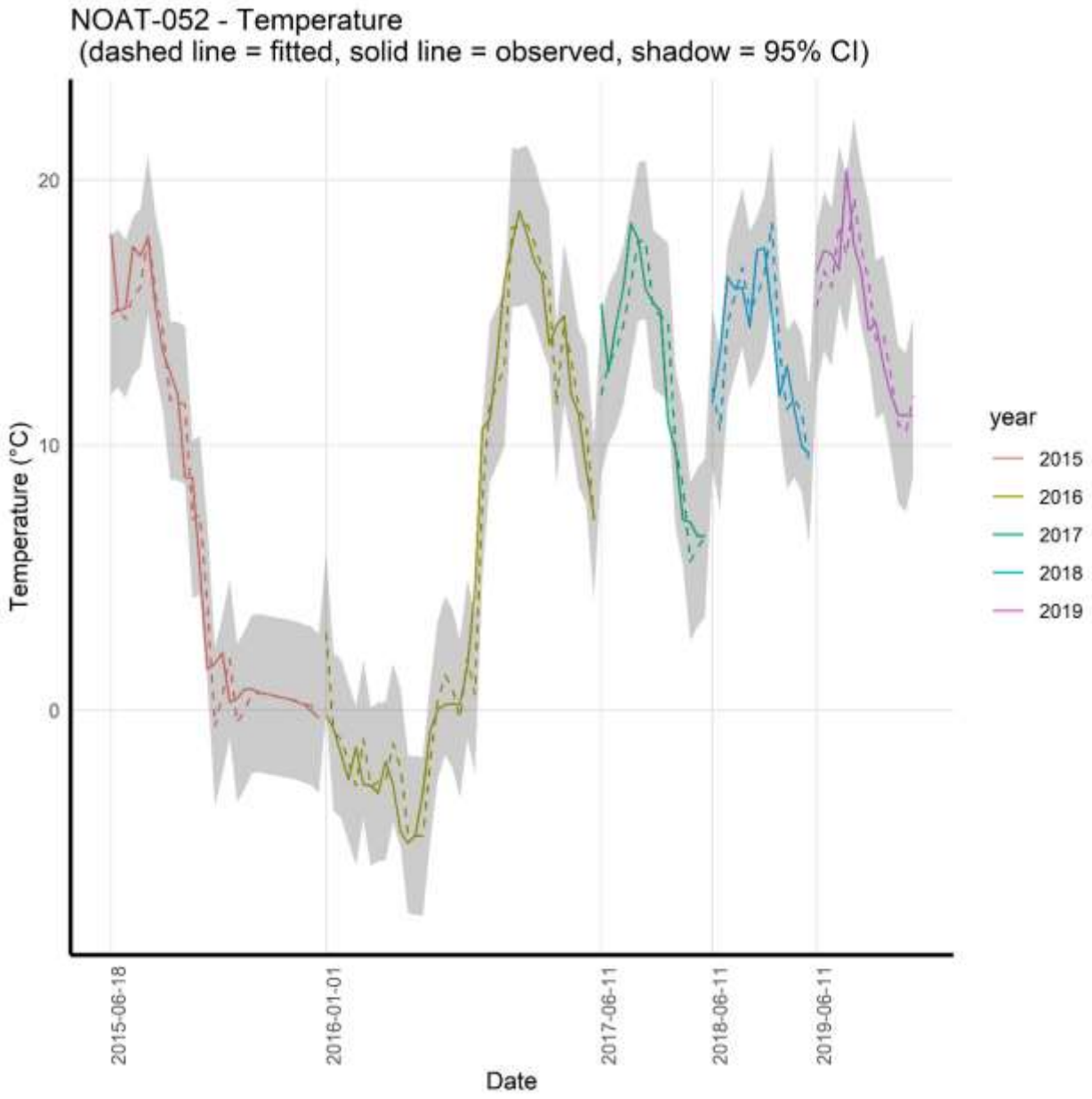


Figure A.128. Model predictions of NOAT-052 sonde temperature by week.

NOAT-107

Data

For NOAT-107, temperature was recorded from 2014 through 2018. Over this period, there were 385 records of temperature. Data were recorded from a variable start date in June or July to August or September. Truncated to the 35 days that were sampled every year, the dataset had 175 observations.

Model Selection

For ARIMA models fitting all possible covariate combinations at lake NOAT-107 with temperature as the response variable, model selection based on AICc and parsimony chose an ARIMA(1,0,2) with air temperature and year as the main covariates as the best model. The model detected a significant positive trend in temperature over years. Trend models for the truncated and seasonally adjusted models both obtained stationary residuals, but the former indicated a significant increasing trend while the latter suggested that the trend was not significantly different from zero. The trend component in the top covariate model also indicated a significant increasing trend, but the magnitude of the trend is smaller and the estimate is more precise.

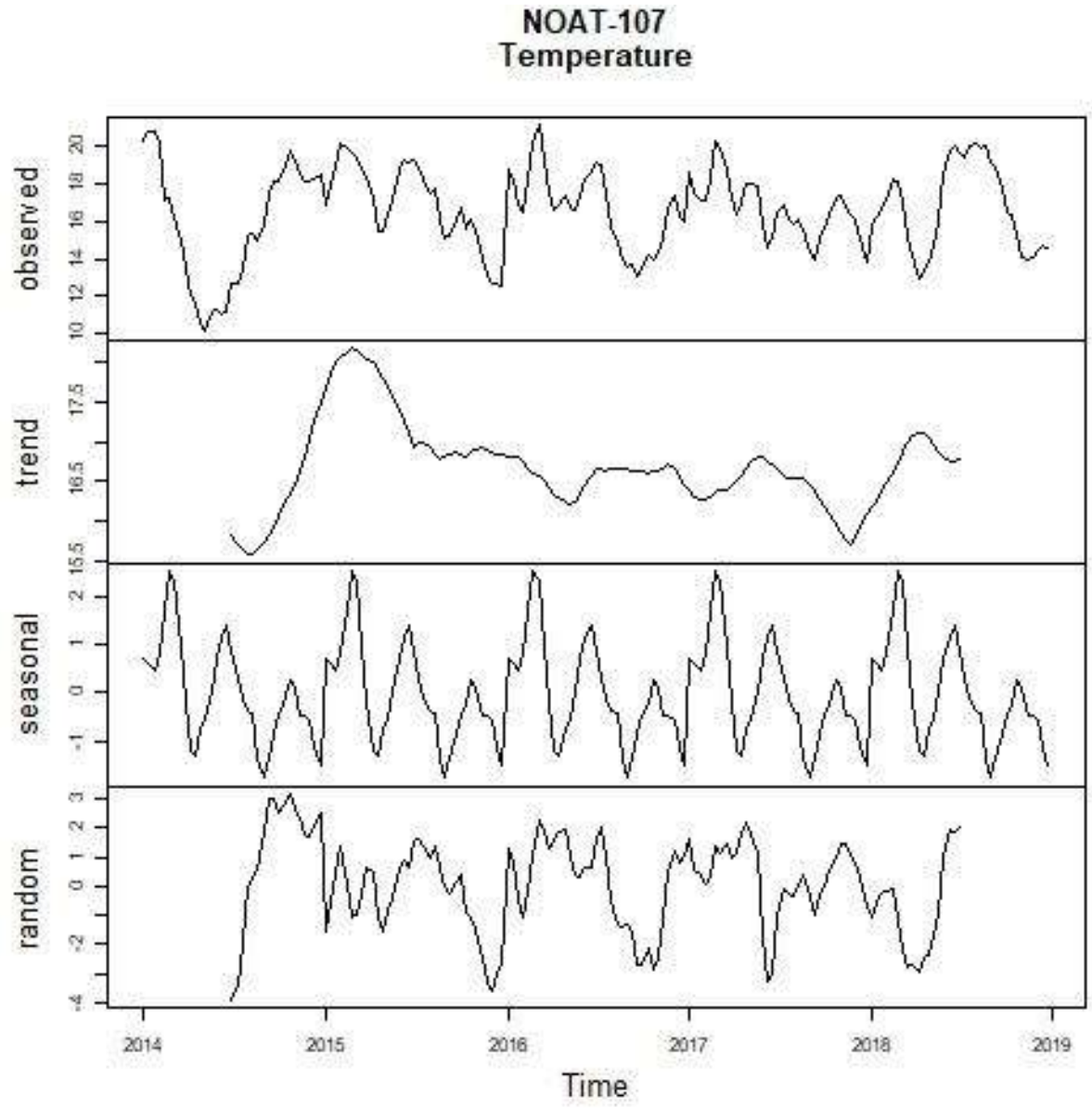


Figure A.129. Time series decomposition of truncated NOAT-107 sonde temperature by year.

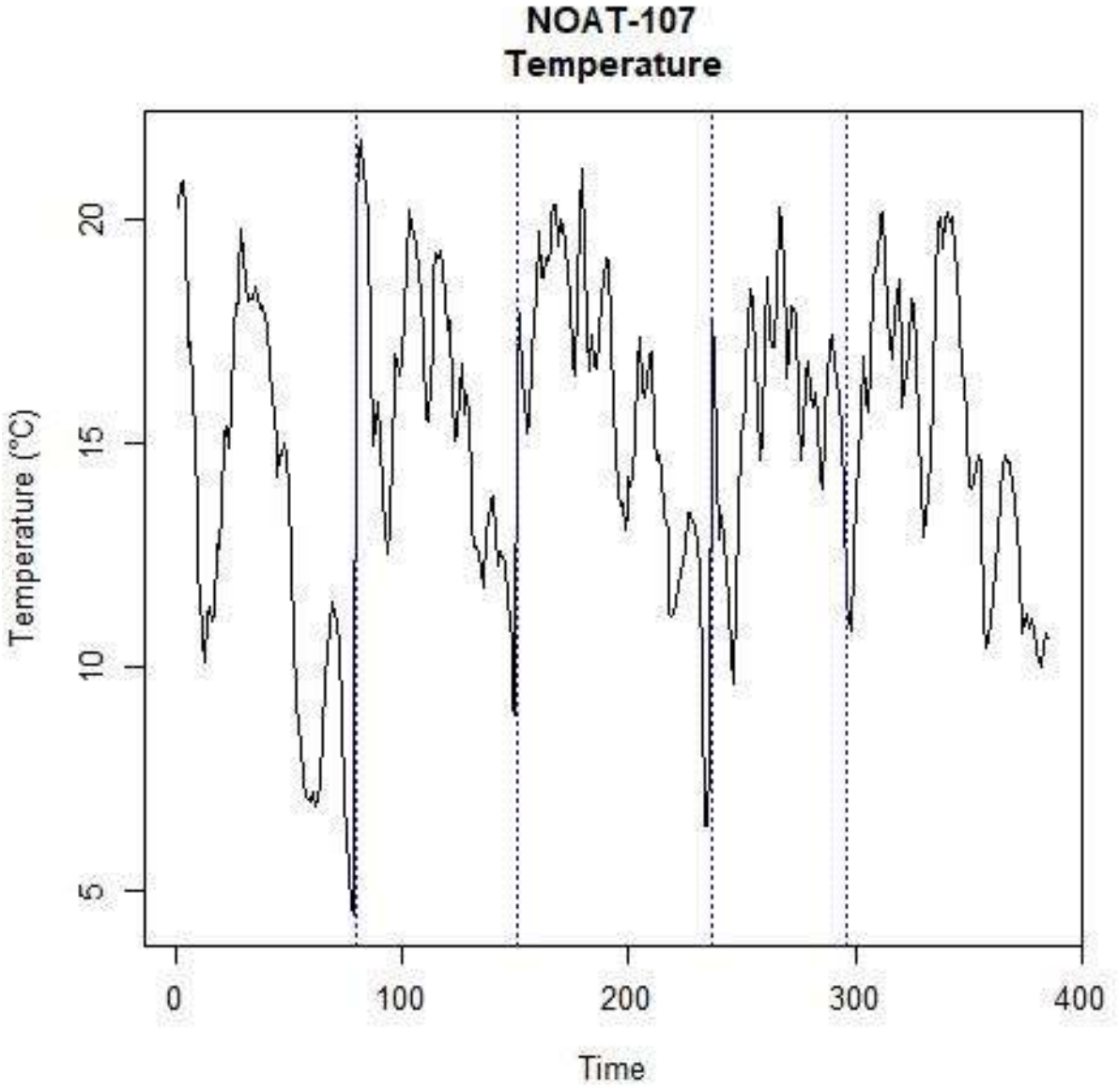


Figure A.130. Time series of NOAT-107 sonde temperature by time point with vertical lines for additive outliers.

Table A.139. Trend modeling results for daily sonde temperature data at NOAT-107.

			Trend			ARMA order		Ljung-Box Test	
Logged	**Method**	**Intercept**	**Coefficient**	**SE**	**p-value**	**AR**	**MA**	**Statistic**	**p-value**
FALSE	complete	NA	1.1216	0.0644	< 0.0001	1	2	2.76	0.8388
FALSE	completeAO	4.6748	0.7368	0.2285	0.0013	0	5	86.92	< 0.0001

			Trend			ARMA order		Ljung-Box Test	
Logged	Method	Intercept	Coefficient	SE	p-value	AR	MA	Statistic	p-value
FALSE	trunc	-13.5904	2.1636	0.5120	< 0.0001	4	1	19.84	0.7990
FALSE	truncSA	15.8087	0.0578	0.2706	0.8308	2	0	33.62	0.3415
TRUE	complete	0.2003	0.1557	0.0311	< 0.0001	0	5	43.03	< 0.0001
TRUE	completeAO	0.8552	0.1086	0.0273	< 0.0001	0	5	63.36	< 0.0001
TRUE	trunc	0.7324	0.1477	0.0285	< 0.0001	3	0	20.89	0.8630
TRUE	truncSA	2.7287	0.0051	0.0176	0.7720	2	0	36.69	0.2217

Table A.140. Top covariate models for daily sonde temperature data at NOAT-107.

Model	AICc	ΔAICc	Ljung-Box Test p-value
Air Temperature + Year	1022.82	0.00	0.3975
Air Temperature + Daily Precipitation + Year	1023.41	0.58	0.2681
Air Temperature + Wind Speed + Year	1024.75	1.93	0.2894
Air Temperature + Wind Speed + Daily Precipitation + Year	1025.15	2.32	0.1765
Air Temperature	1047.85	25.02	0.5339
Air Temperature + Daily Precipitation	1048.04	25.22	0.4319
Air Temperature + Wind Speed + Daily Precipitation	1049.75	26.93	0.3383
Air Temperature + Wind Speed	1049.77	26.94	0.4325
Relative Humidity + Year + Month	1110.22	87.40	0.0517
Wind Speed + Relative Humidity + Year + Month	1111.14	88.32	0.0531

Table A.141. Coefficients and variance components estimates for the top covariate model for daily sonde temperature data at NOAT-107.

Parameter	Coefficient	SE	p-value
ar1	0.89	0.03	< 0.0001
ma1	0.29	0.06	< 0.0001
ma2	0.13	0.06	0.0194
Air Temperature	0.30	0.02	< 0.0001
Year	0.84	0.05	< 0.0001

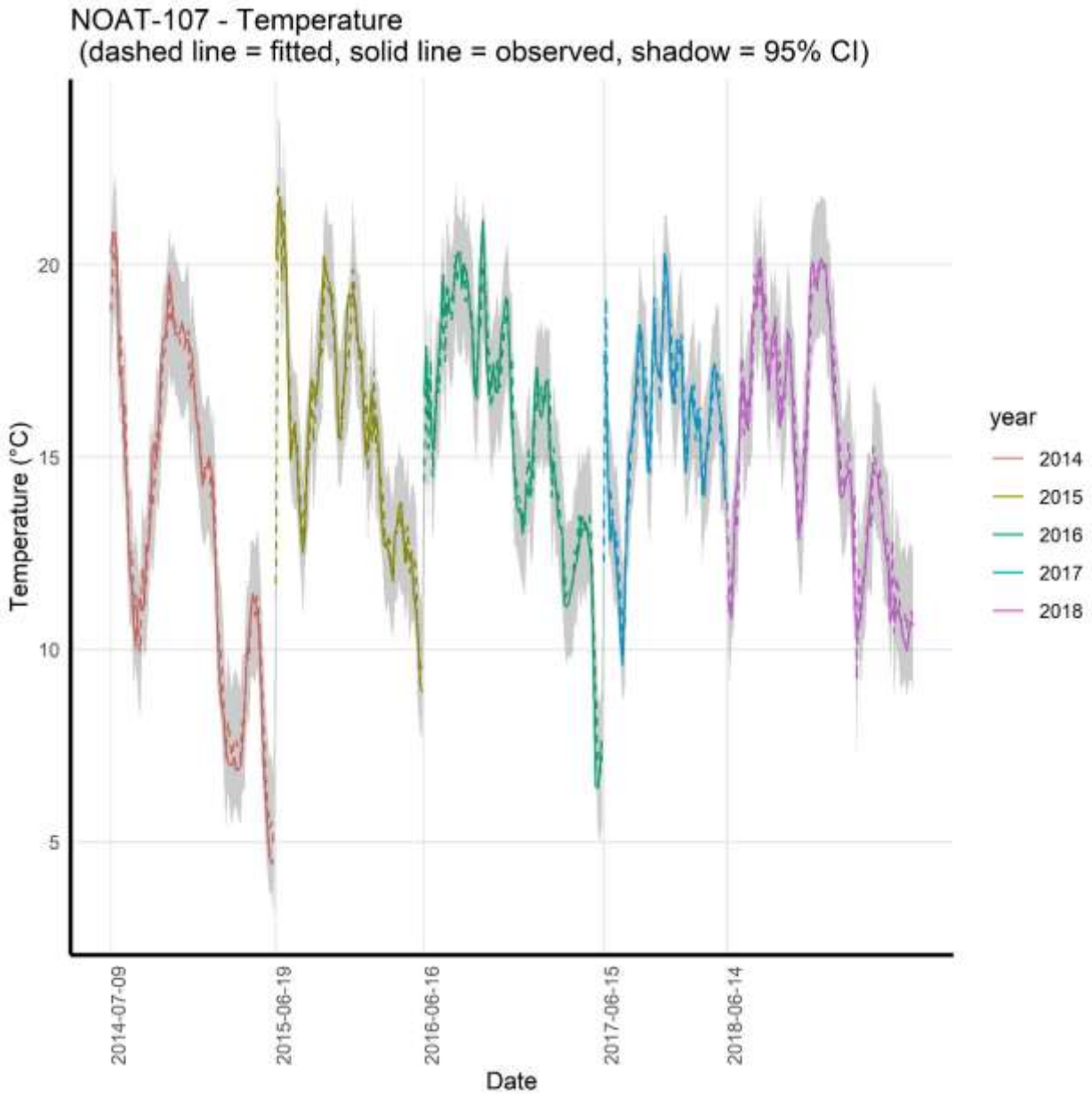


Figure A.131. Model predictions of NOAT-107 sonde temperature by date.

WRST-005

Data

For the WRST-005 lake, temperature was recorded from 2010 through 2019. Over this period, there were 1074 records of temperature. Data were recorded from a variable start date in June or July to September. Truncated to the 74 days that were sampled every year, the dataset had 740 observations.

Model Selection

For ARIMA models fitting all possible covariate combinations at lake WRST-005 with temperature as the response variable, model selection based on AICc and parsimony chose an ARIMA(1,0,1) with air temperature as the main covariate as the top model. The only trend models with stationary residuals were the seasonally adjusted models. The final model used untransformed data and a ARIMA(2,0,1) structure with the truncated dataset, which indicated a marginally significant increase in temperature over years.

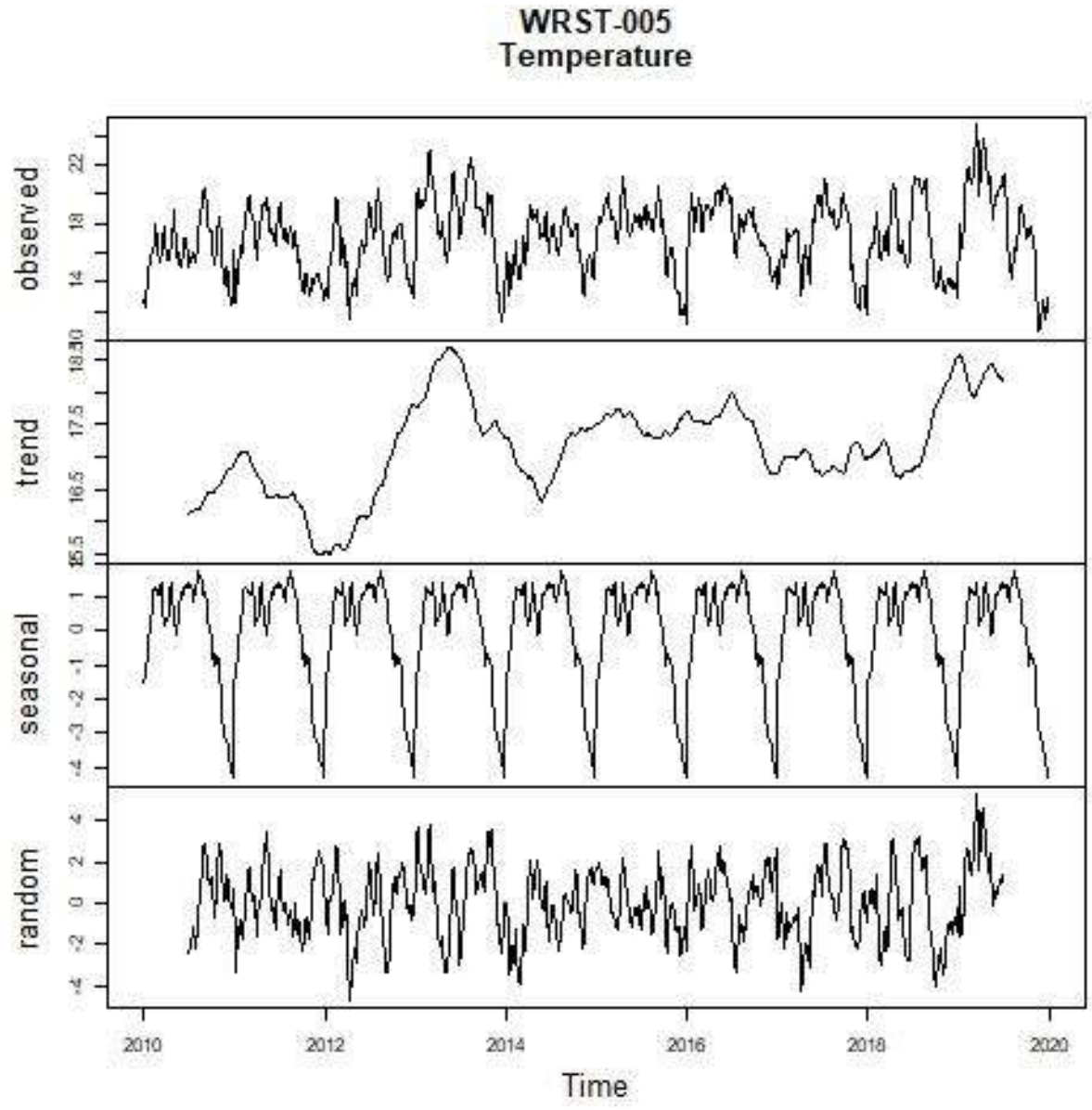


Figure A.132. Time series decomposition of truncated WRST-005 sonde temperature by year.

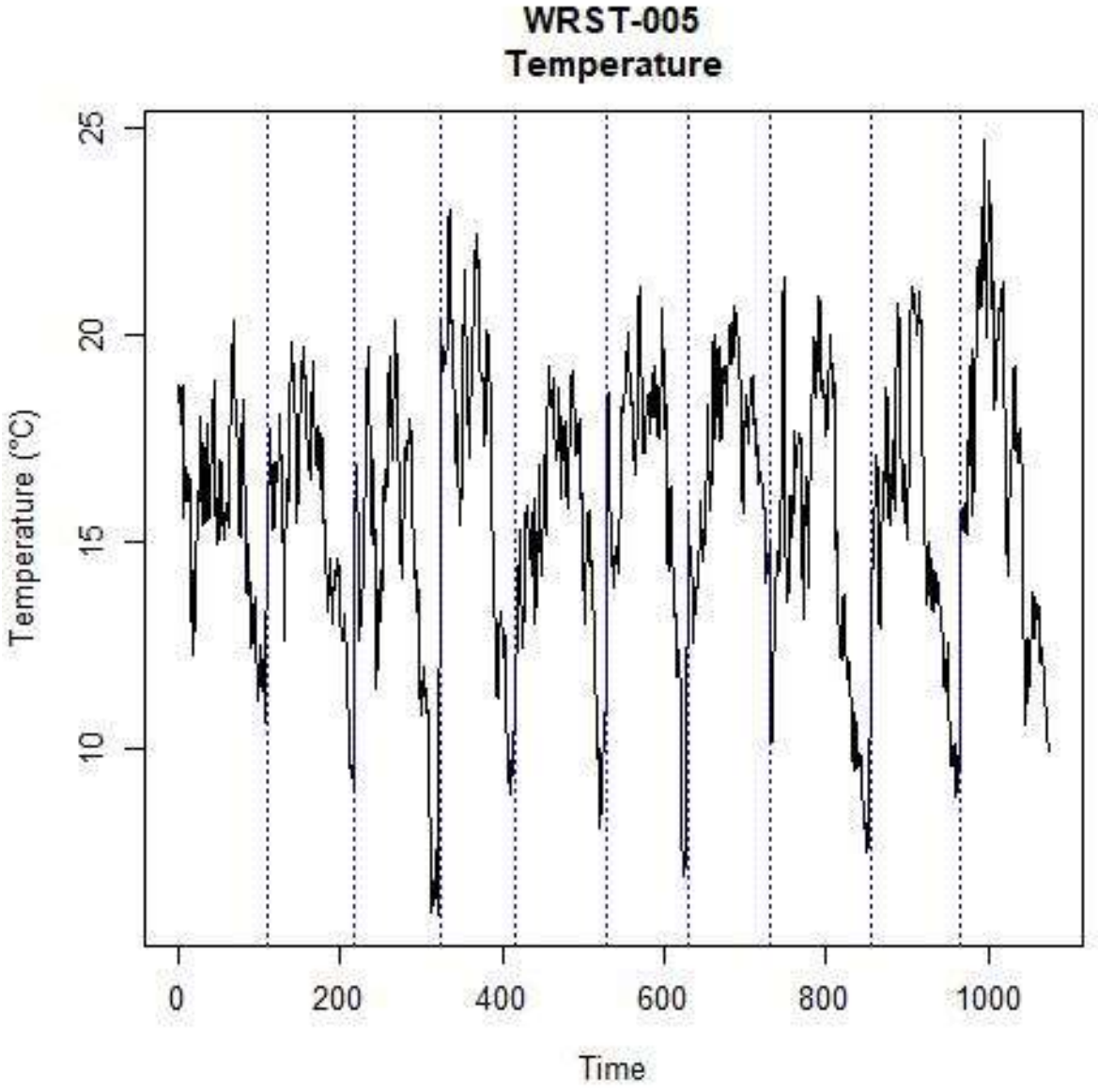


Figure A.133. Time series of WRST-005 sonde temperature by time point with vertical lines for additive outliers.

Table A.142. Trend modeling results for daily sonde temperature data at WRST-005.

			Trend			ARMA order		Ljung-Box Test	
Logged	**Method**	**Intercept**	**Coefficient**	**SE**	**p-value**	**AR**	**MA**	**Statistic**	**p-value**
FALSE	complete	13.2008	0.2026	0.0643	0.0016	0	5	376.57	< 0.0001
FALSE	completeAO	14.3807	0.1073	0.0624	0.0857	0	5	545.57	< 0.0001

			Trend			ARMA order		Ljung-Box Test	
Logged	**Method**	**Intercept**	**Coefficient**	**SE**	**p-value**	**AR**	**MA**	**Statistic**	**p-value**
FALSE	trunc	14.9669	0.1683	0.0401	< 0.0001	0	1	2094.03	< 0.0001
FALSE	truncSA	15.3177	0.1394	0.0731	0.0566	2	1	156.73	0.2043
TRUE	complete	2.5528	0.0142	0.0046	0.0021	0	5	375.92	< 0.0001
TRUE	completeAO	2.6426	0.0069	0.0044	0.1163	0	5	558.11	< 0.0001
TRUE	trunc	2.6497	0.0141	0.0039	0.0003	0	5	325.09	< 0.0001
TRUE	truncSA	2.7309	0.0076	0.0043	0.0786	2	1	168.13	0.0741

Table A.143. Top covariate models for daily sonde temperature data at WRST-005.

Model	**AICc**	**ΔAICc**	**Ljung-Box Test p-value**
Air Temperature	2660.23	0.00	0.6919
Air Temperature + Wind Speed	2660.38	0.15	0.5712
Air Temperature + Daily Precipitation	2662.05	1.82	0.5677
Air Temperature + Wind Speed + Daily Precipitation	2662.19	1.96	0.4293
Daily Precipitation + Month	2761.75	101.52	0.0879
Year + Month	2784.74	124.51	0.0950
Wind Speed + Month	2784.75	124.52	0.0949
Solar Radiation	2895.52	235.29	0.2177
Wind Speed + Solar Radiation	2897.27	237.04	0.1348
Relative Humidity	2915.24	255.00	0.2701

Table A.144. Coefficients and variance components estimates for the top covariate model for daily sonde temperature data at WRST-005.

Parameter	**Coefficient**	**SE**	**p-value**
ar1	0.92	0.01	< 0.0001
ma1	0.23	0.03	< 0.0001
intercept	12.48	0.43	< 0.0001
Air Temperature	0.25	0.01	< 0.0001

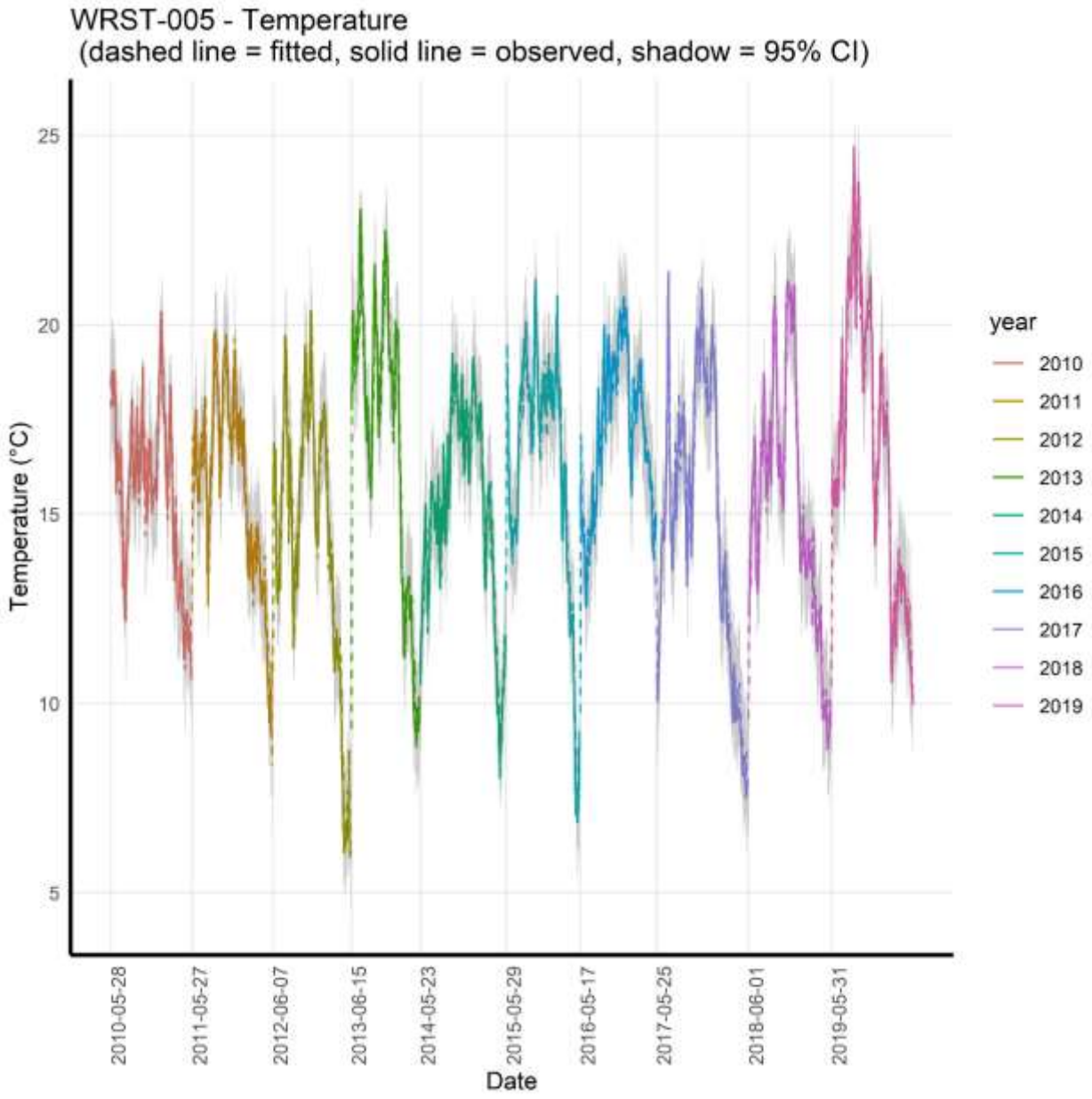


Figure A.134. Model predictions of WRST-005 sonde temperature by date.

WRST-016

Data

For the WRST-016 lake, temperature was recorded from 2009 through 2019. Over this period, there were 1073 records of temperature. Data were recorded from a variable start date in June or July to either August or September. Truncated to the 45 days that were sampled every year, the dataset had 495 observations.

Model Selection

For ARIMA models fitting all possible covariate combinations at lake WRST-016 with temperature as the response variable, model selection based on AICc and parsimony chose an ARIMA(5,0,0) with air temperature and year as the main covariates as the best model. Temperature increased significantly with year.

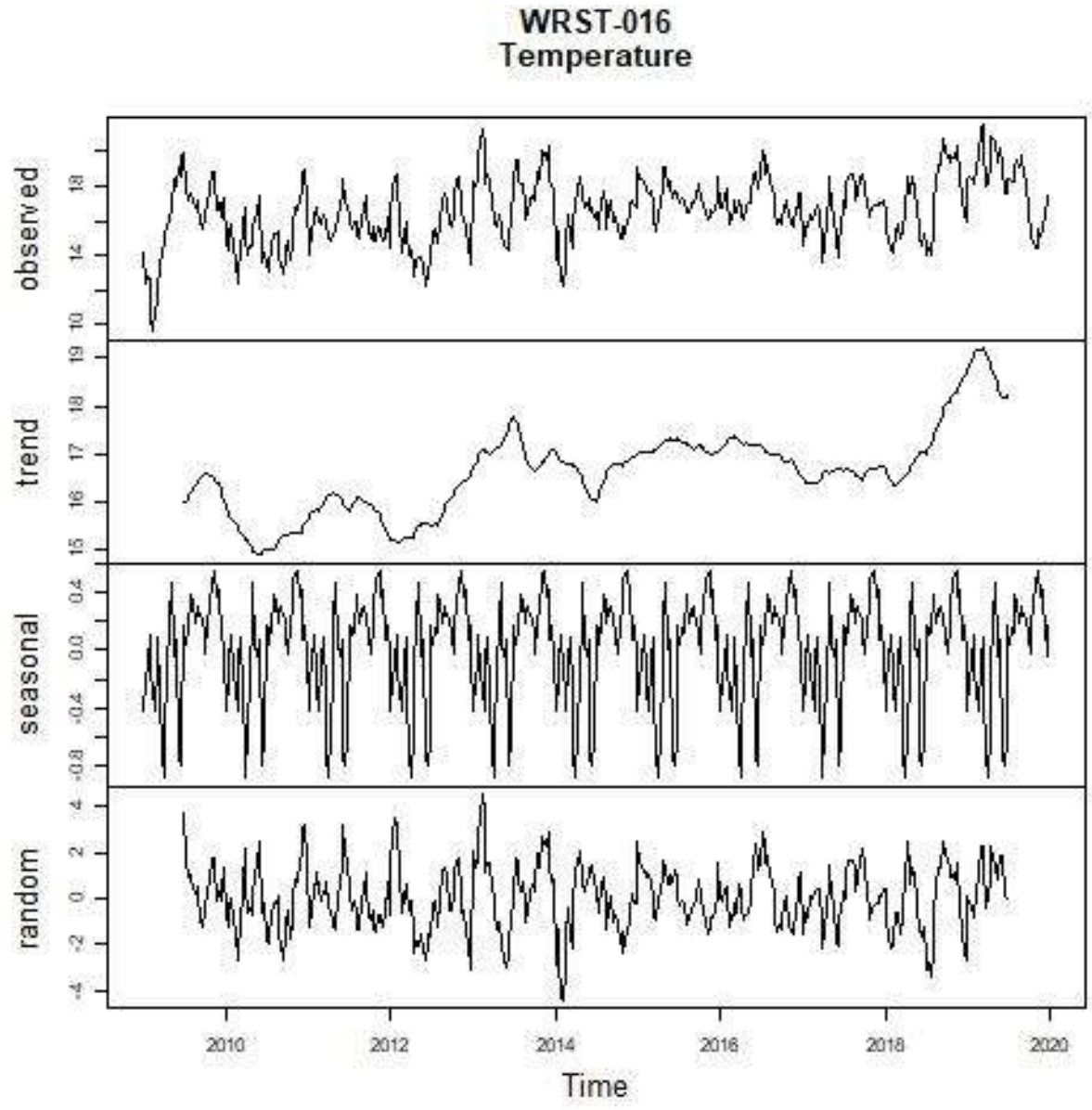


Figure A.135. Time series decomposition of truncated WRST-016 sonde temperature by year.

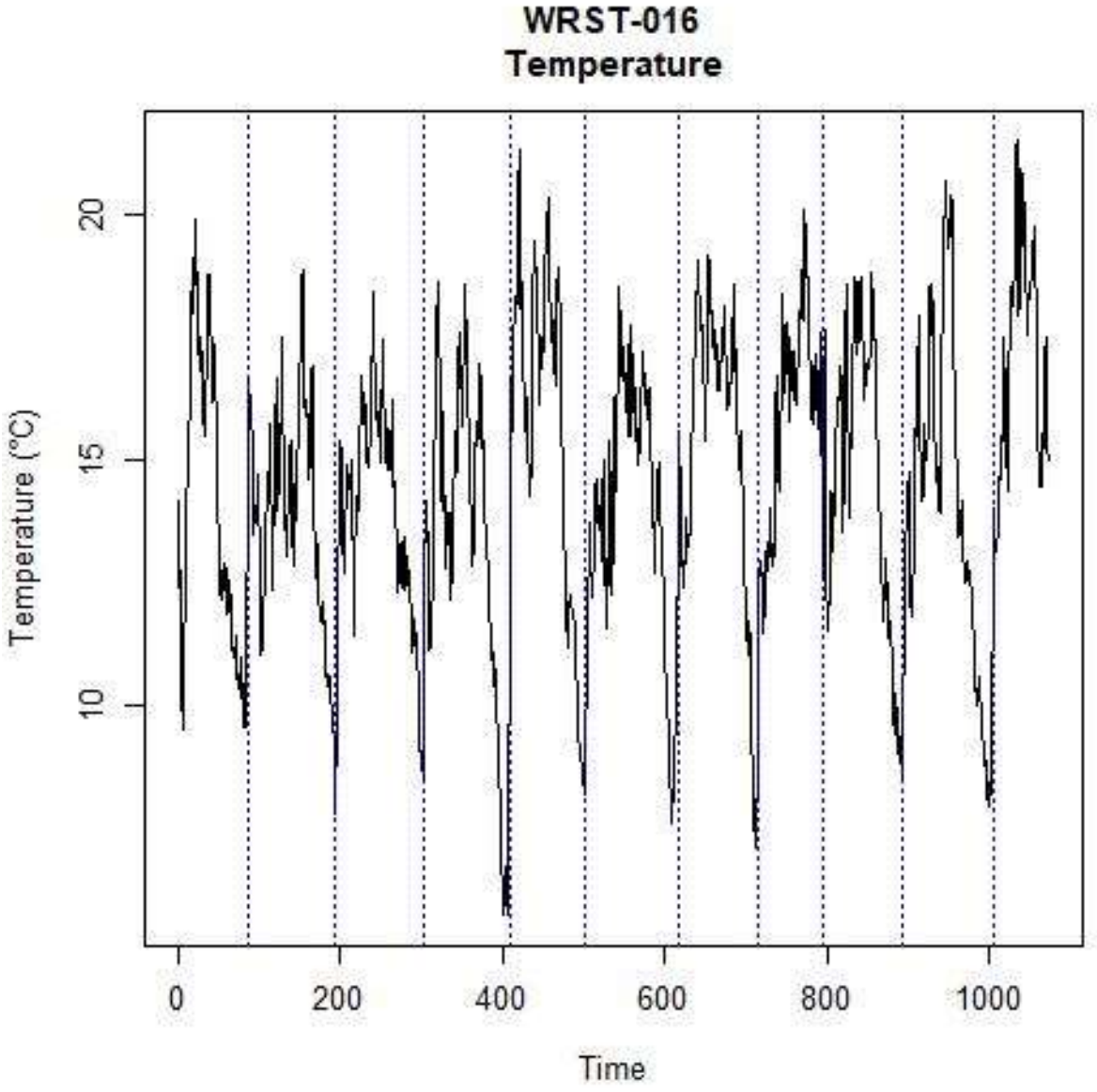


Figure A.136. Time series of WRST-016 sonde temperature by time point with vertical lines for additive outliers.

Table A.145. Trend modeling results for daily sonde temperature data at WRST-016.

			Trend			ARMA order		Ljung-Box Test	
Logged	**Method**	**Intercept**	**Coefficient**	**SE**	**p-value**	**AR**	**MA**	**Statistic**	**p-value**
FALSE	complete	-3.9033	1.5564	0.3946	< 0.0001	2	1	14.41	0.0132
FALSE	completeAO	12.1923	0.1995	0.0513	0.0001	0	5	595.86	< 0.0001

			Trend			ARMA order		Ljung-Box Test	
Logged	Method	Intercept	Coefficient	SE	p-value	AR	MA	Statistic	p-value
FALSE	trunc	14.3041	0.1898	0.0635	0.0028	1	2	67.42	0.8928
FALSE	truncSA	14.0360	0.2151	0.0568	0.0002	2	2	95.88	0.1769
TRUE	complete	2.4489	0.0174	0.0039	< 0.0001	0	5	445.86	< 0.0001
TRUE	completeAO	2.4849	0.0143	0.0039	0.0002	0	5	606.14	< 0.0001
TRUE	trunc	2.6622	0.0116	0.0041	0.0042	1	1	68.09	0.8966
TRUE	truncSA	2.6442	0.0133	0.0034	0.0001	3	2	93.27	0.2067

Table A.146. Top covariate models for daily sonde temperature data at WRST-016.

Model	AICc	ΔAICc	Ljung-Box Test p-value
Air Temperature + Year	2458.08	0.00	0.0758
Air Temperature + Wind Speed + Year	2459.59	1.51	0.0539
Air Temperature	2475.42	17.34	0.3748
Air Temperature + Daily Precipitation	2476.22	18.14	0.2508
Air Temperature + Wind Speed	2476.50	18.43	0.2595
Air Temperature + Wind Speed + Daily Precipitation	2477.32	19.25	0.1545
Wind Speed + Solar Radiation	2597.78	139.70	0.0922
Solar Radiation	2600.88	142.80	0.1420
Relative Humidity	2625.61	167.53	0.2068
Year + Month	2625.69	167.61	0.0501

Table A.147. Coefficients and variance components estimates for the top covariate model for daily sonde temperature data at WRST-016.

Parameter	Coefficient	SE	p-value
ar1	1.13	0.03	< 0.0001
ar2	-0.21	0.05	< 0.0001
ar3	0.00	0.05	0.9549
ar4	0.06	0.05	0.1732
ar5	0.00	0.03	0.9389
intercept	-4.71	4.25	0.2676
Air Temperature	0.17	0.01	< 0.0001
Year	1.44	0.33	< 0.0001

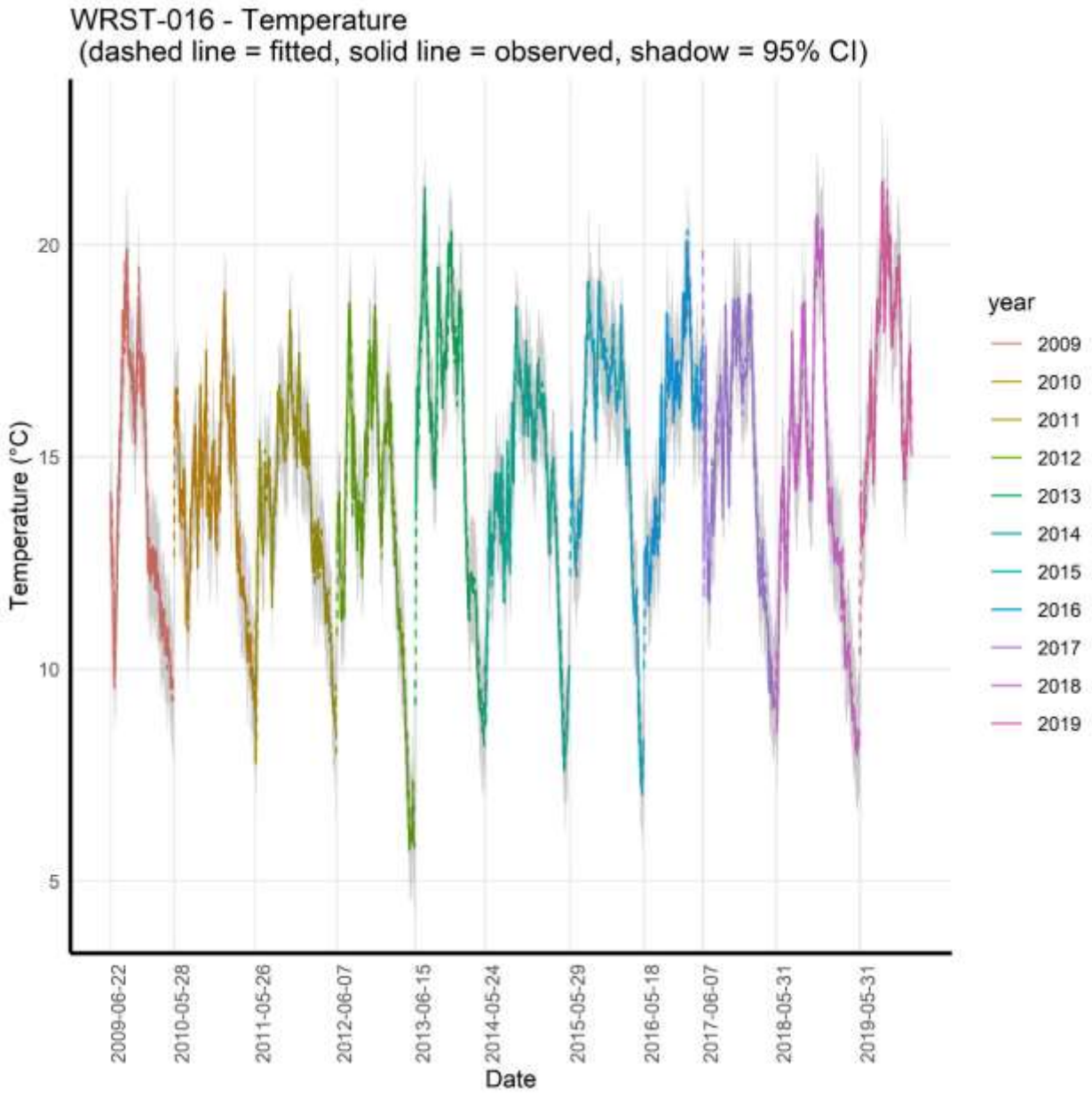


Figure A.137. Model predictions of WRST-016 sonde temperature by date.

YUCH-004

Data

For YUCH-004, temperature was recorded from 2009 through 2019. Over this period, there were 1246 records of temperature. Data were recorded from a variable start date in June or July to September. Truncated to the 98 days that were sampled every year, the dataset had 1078 observations. Covariate coverage was poor in 2019, restricting covariate modeling to 2009-2018 with 1117 records.

Model Selection

For ARIMA models fitting all possible covariate combinations at lake YUCH-004 with temperature as the response variable, model selection based on AICc and parsimony chose an ARIMA(4,0,2) with air temperature as the main covariate as the best model. The top trend model was a seasonally adjusted ARIMA(3,0,0) using the truncated dataset. Temperature had no significant trend over years.

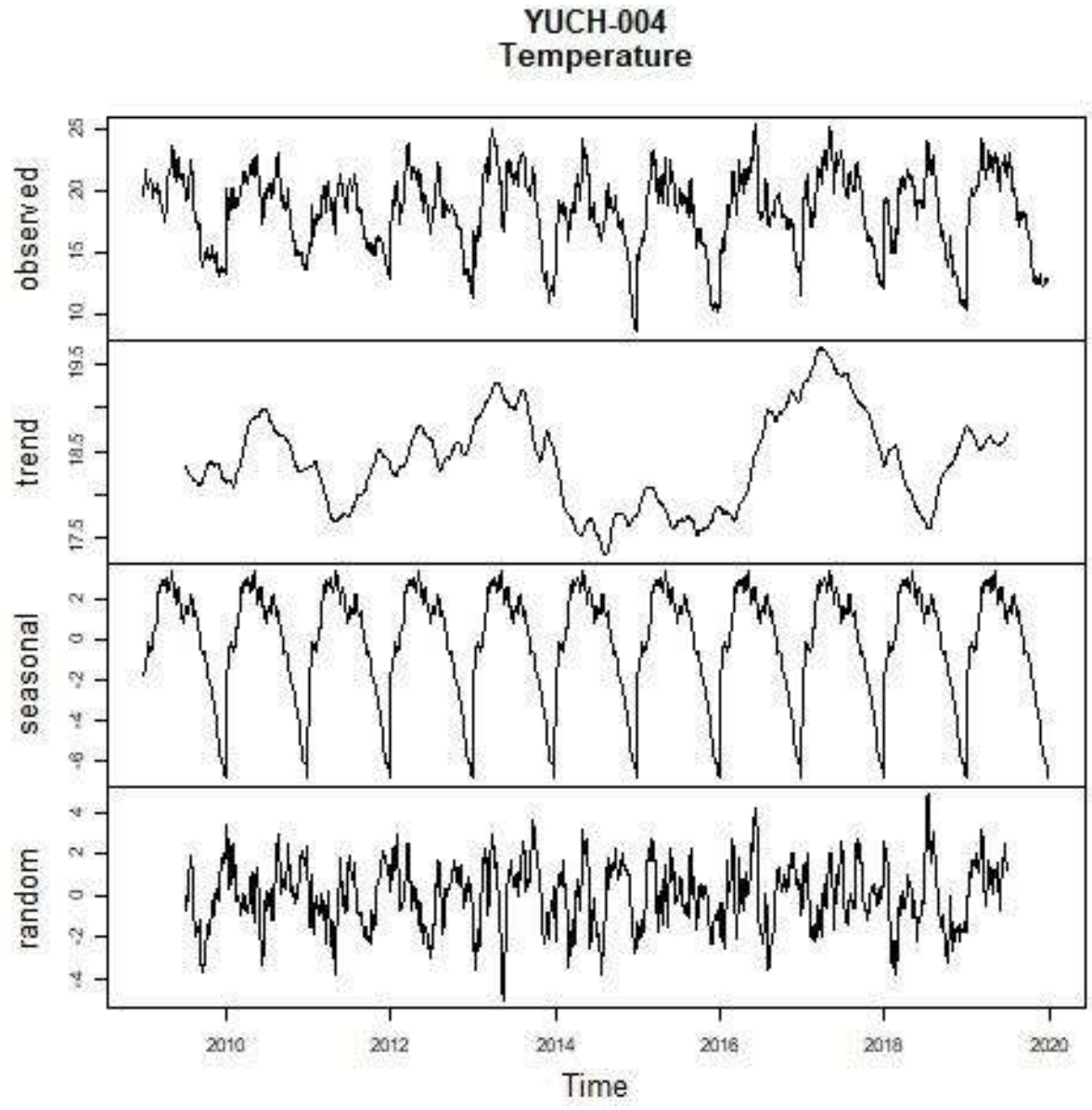


Figure A.138. Time series decomposition of truncated YUCH-004 sonde temperature by year.

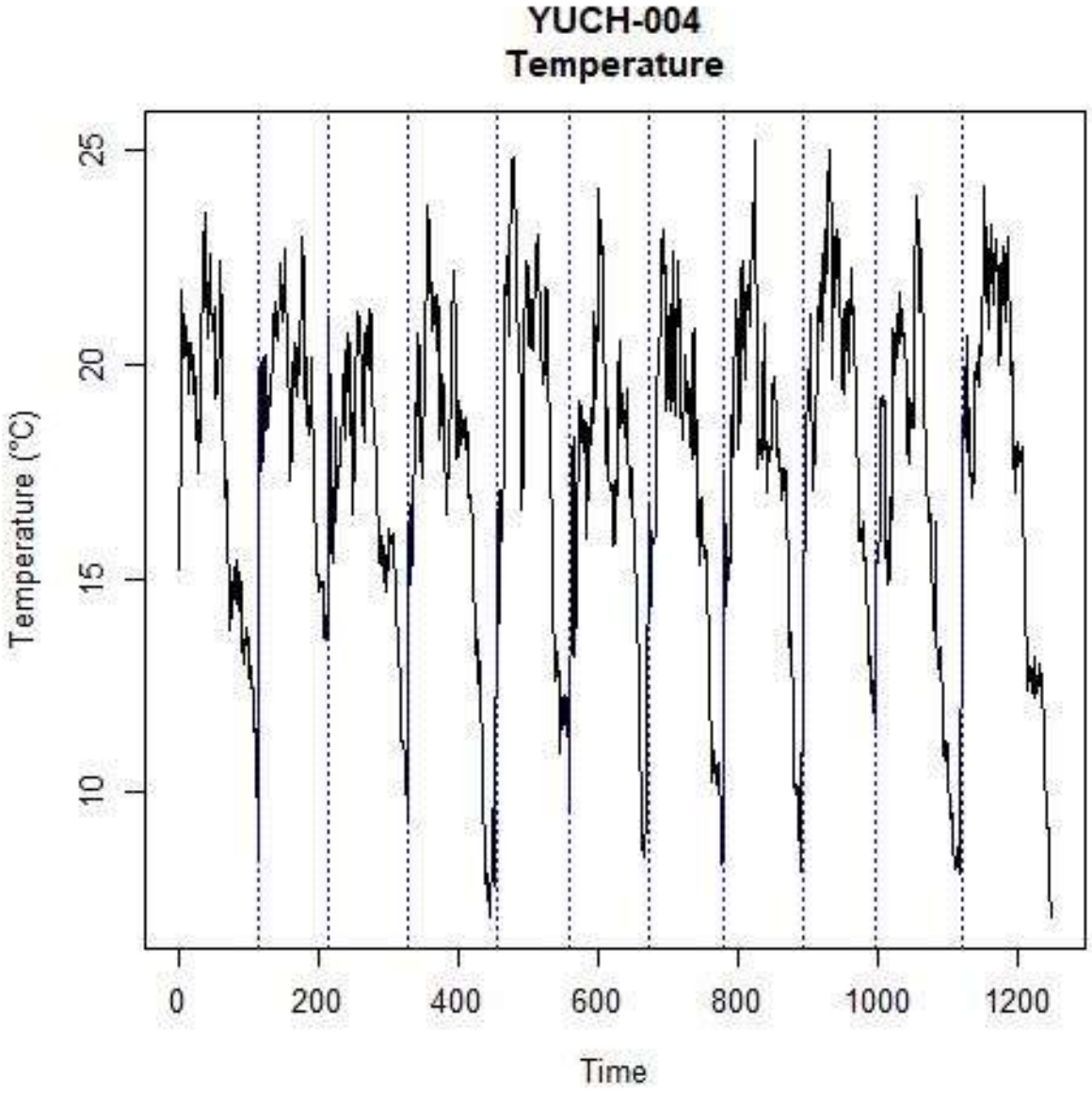


Figure A.139. Time series of YUCH-004 sonde temperature by time point with vertical lines for additive outliers.

Table A.148. Trend modeling results for daily sonde temperature data at YUCH-004.

			Trend			ARMA order		Ljung-Box Test	
Logged	**Method**	**Intercept**	**Coefficient**	**SE**	**p-value**	**AR**	**MA**	**Statistic**	**p-value**
FALSE	complete	15.7873	0.1721	0.0616	0.0052	0	5	758.86	< 0.0001
FALSE	completeAO	17.1251	0.0369	0.0587	0.5296	0	5	1125.47	< 0.0001

			Trend			ARMA order		Ljung-Box Test	
Logged	**Method**	**Intercept**	**Coefficient**	**SE**	**p-value**	**AR**	**MA**	**Statistic**	**p-value**
FALSE	trunc	17.5623	0.0831	0.0488	0.0884	0	3	4113.36	< 0.0001
FALSE	truncSA	18.4247	-0.0017	0.0569	0.9768	3	0	210.03	0.1643
TRUE	complete	2.7219	0.0111	0.0041	0.0067	0	5	734.88	< 0.0001
TRUE	completeAO	2.8089	0.0023	0.0038	0.5541	0	5	1144.39	< 0.0001
TRUE	trunc	2.8115	0.0083	0.0036	0.0215	0	5	1790.34	< 0.0001
TRUE	truncSA	2.9061	-0.0009	0.0034	0.7796	3	0	200.10	0.3112

Table A.149. Top covariate models for daily sonde temperature data at YUCH-004.

Model	**AICc**	**ΔAICc**	**Ljung-Box Test p-value**
Air Temperature + Wind Speed	2670.15	0.00	0.0568
Air Temperature	2670.81	0.66	0.0674
Wind Speed + Daily Precipitation + Month	2671.61	1.46	0.0696
Air Temperature + Daily Precipitation	2672.46	2.31	0.0572
Daily Precipitation + Month	2677.65	7.51	0.0873
Solar Radiation + Daily Precipitation	2840.06	169.92	0.0779
Wind Speed + Solar Radiation + Daily Precipitation	2865.29	195.14	0.0680

Table A.150. Coefficients and variance components estimates for the top covariate model for daily sonde temperature data at YUCH-004.

Parameter	**Coefficient**	**SE**	**p-value**
ar1	0.35	0.32	0.2708
ar2	0.61	0.19	0.0018
ar3	-0.12	0.30	0.6820
ar4	0.11	0.06	0.0935
ma1	0.81	0.32	0.0107
ma2	0.04	0.31	0.8847
intercept	14.77	0.68	< 0.0001
Air Temperature	0.20	0.01	< 0.0001

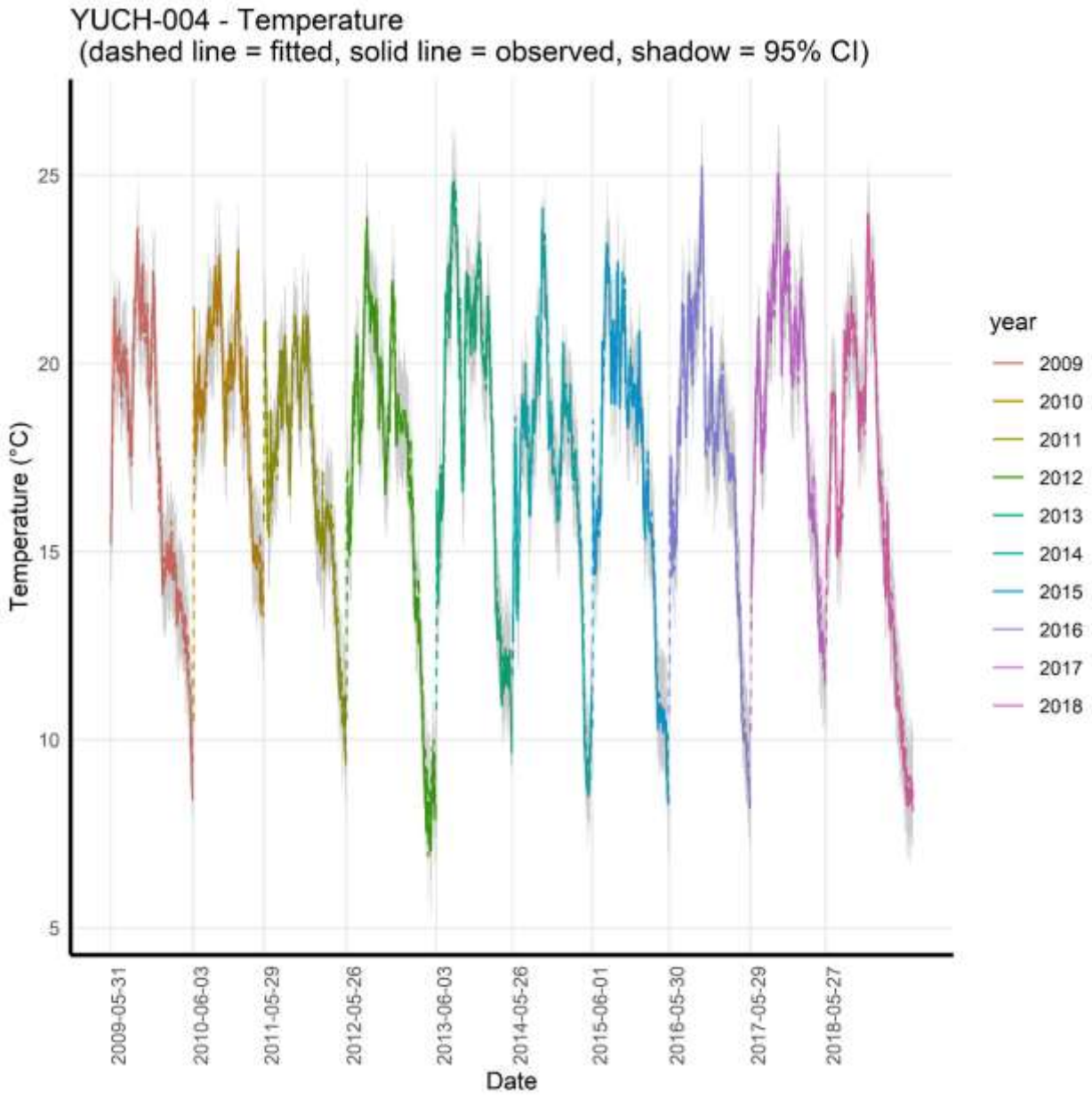


Figure A.140. Model predictions of YUCH-004 sonde temperature by date.

YUCH-005

Data

For the YUCH-005 lake, temperature was recorded from 2009 through 2019. Data from mid-summer 2013 were missing, however, so analysis was restricted to 2014-2019. Over this period, there were 690 records of temperature. Data were recorded from May to September. Truncated to the 99 days that were sampled every year, the dataset had 594 observations. Covariate coverage was poor in 2019, restricting covariate modeling to 2009-2018 with 563 records.

Model Selection

For ARIMA models fitting all possible covariate combinations at lake YUCH-005 with temperature as the response variable, model selection based on AICc and parsimony chose an ARIMA(1,0,2) with wind speed and month as the main covariates as the best model. The best trend model was a seasonally adjusted ARIMA(2,0,3) using the truncated dataset. The model included a statistically significant positive trend in temperature over years.

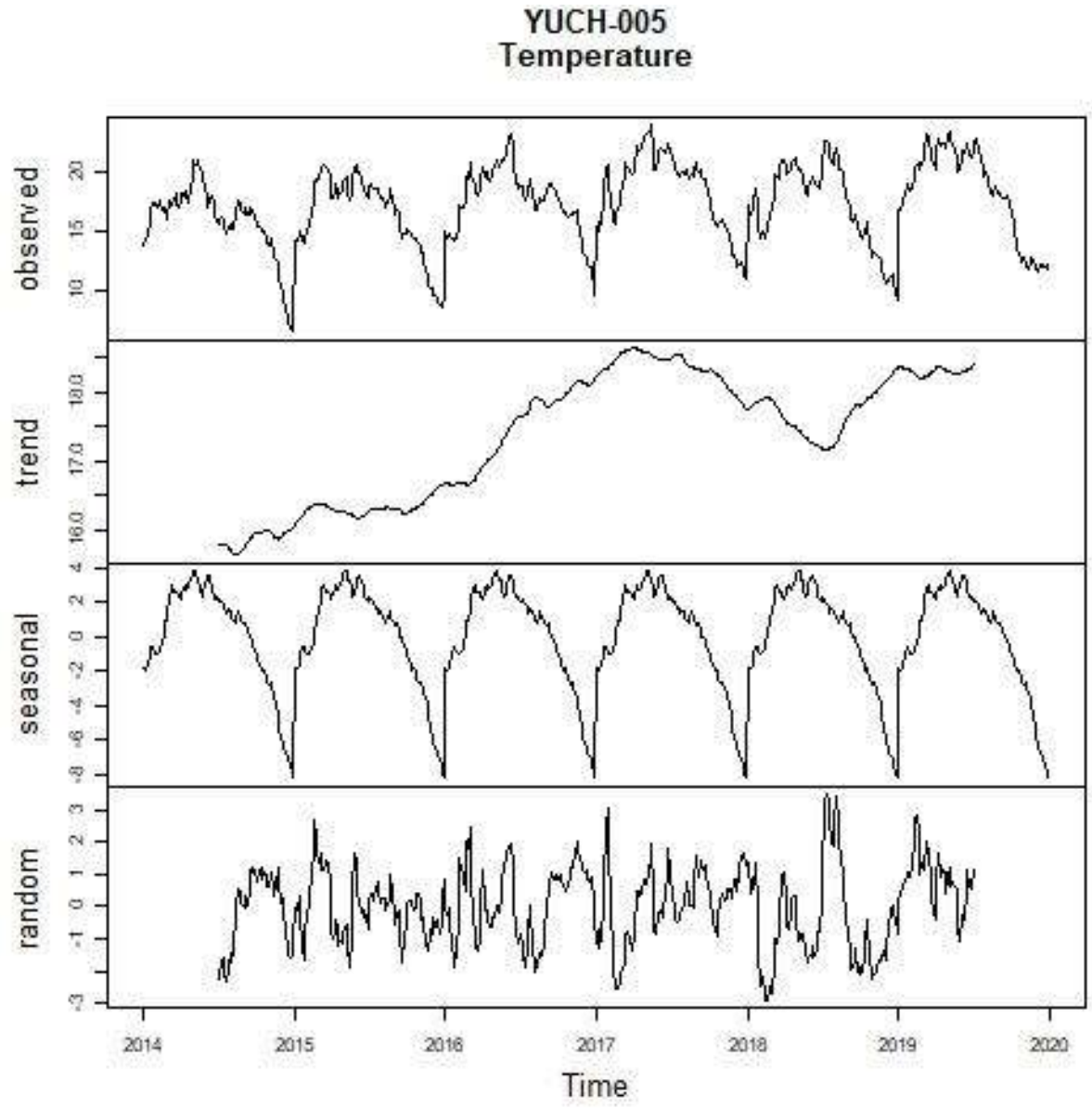


Figure A.141. Time series decomposition of truncated YUCH-005 sonde temperature by year.

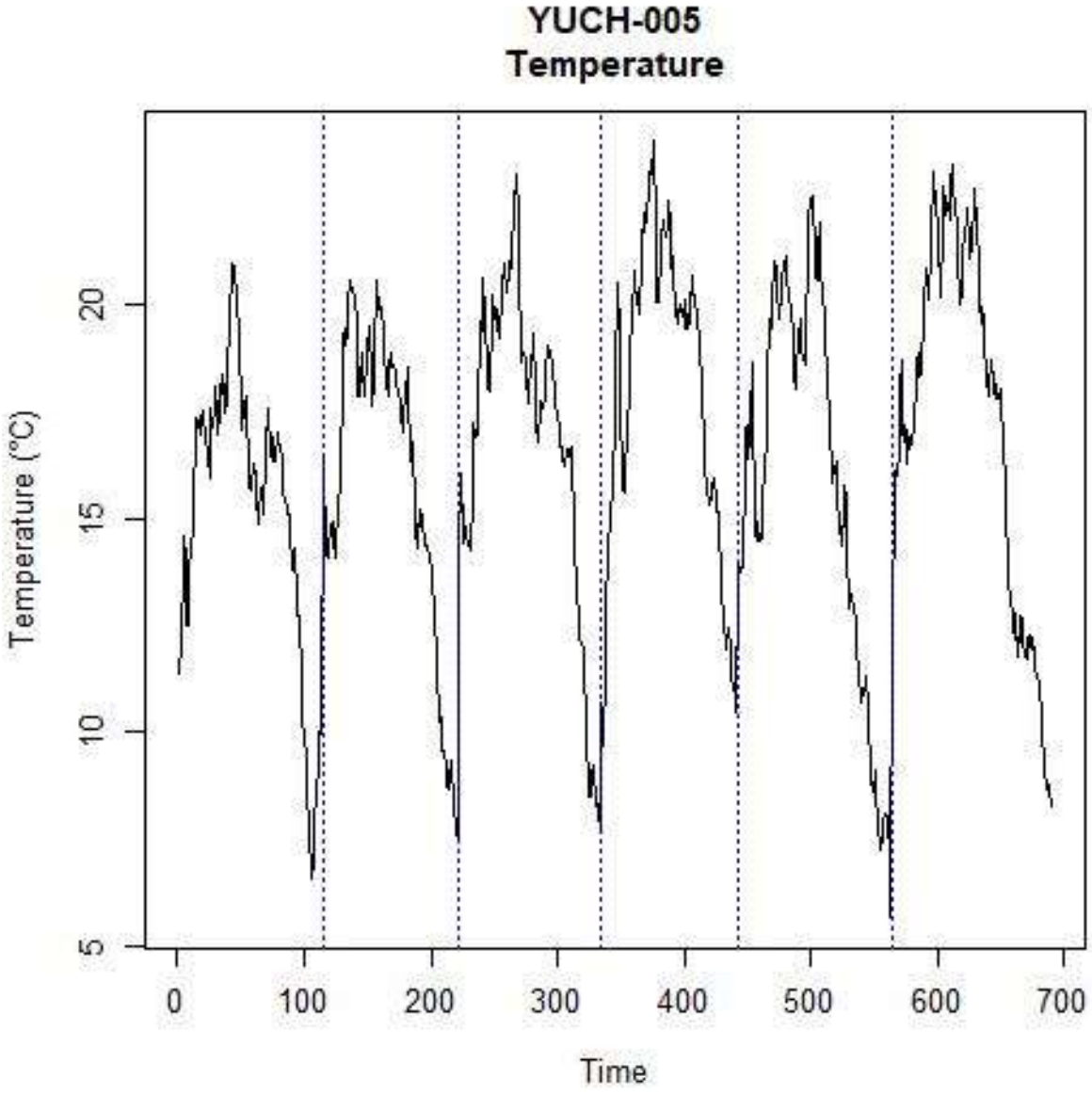


Figure A.142. Time series of YUCH-005 sonde temperature by time point with vertical lines for additive outliers.

Table A.151. Trend modeling results for daily sonde temperature data at YUCH-005.

			Trend			ARMA order		Ljung-Box Test	
Logged	**Method**	**Intercept**	**Coefficient**	**SE**	**p-value**	**AR**	**MA**	**Statistic**	**p-value**
FALSE	complete	NA	1.3002	0.0203	< 0.0001	0	5	788.14	< 0.0001
FALSE	completeAO	9.7245	0.5311	0.1361	< 0.0001	0	5	891.51	< 0.0001

			Trend			ARMA order		Ljung-Box Test	
Logged	**Method**	**Intercept**	**Coefficient**	**SE**	**p-value**	**AR**	**MA**	**Statistic**	**p-value**
FALSE	trunc	3.0945	1.1339	0.1459	< 0.0001	0	5	2007.23	< 0.0001
FALSE	truncSA	12.6001	0.3769	0.1080	0.0005	2	3	111.21	0.5034
TRUE	complete	1.8411	0.0733	0.0112	< 0.0001	0	5	601.24	< 0.0001
TRUE	completeAO	2.2870	0.0377	0.0098	0.0001	0	5	795.82	< 0.0001
TRUE	trunc	1.9014	0.0740	0.0100	< 0.0001	0	5	1624.73	< 0.0001
TRUE	truncSA	2.5506	0.0224	0.0070	0.0013	2	3	98.89	0.8073

Table A.152. Top covariate models for daily sonde temperature data at YUCH-005.

Model	**AICc**	**ΔAICc**	**Ljung-Box Test p-value**
Wind Speed + Month	1055.16	0.00	0.1587
Daily Precipitation + Month	1057.10	1.94	0.1910
Wind Speed + Daily Precipitation + Month	1057.20	2.05	0.0860
Wind Speed + Solar Radiation	1211.61	156.45	0.0569
Wind Speed	1236.49	181.33	0.0779
Intercept Only	1242.03	186.87	0.0988
Daily Precipitation	1243.94	188.78	0.0879

Table A.153. Coefficients and variance components estimates for the top covariate model for daily sonde temperature data at YUCH-005.

Parameter	**Coefficient**	**SE**	**p-value**
ar1	0.97	0.01	< 0.0001
ma1	0.42	0.04	< 0.0001
ma2	0.18	0.05	< 0.0001
intercept	22.25	1.36	< 0.0001
Wind Speed	0.05	0.03	0.1604
Month	-0.95	0.06	< 0.0001

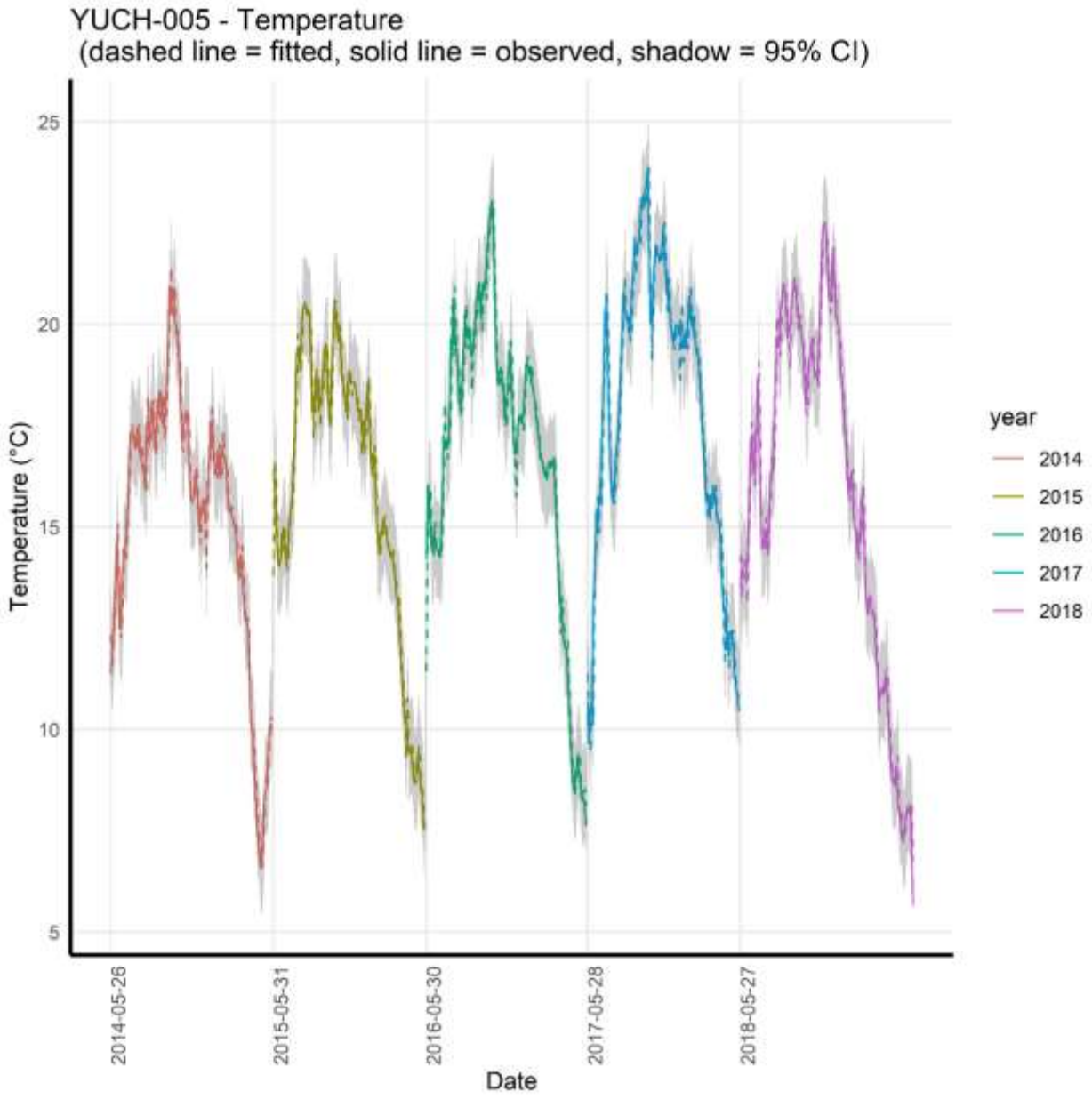


Figure A.143. Model predictions of YUCH-005 sonde temperature by date.

Sediment Temperature

BELA-088

Data

For the BELA-088 lake, sediment temperature was recorded in two continuous periods. The first began July 2012, and ended in September 2015. The second began in June 2016, and ended in September 2019. These two sampling periods comprise 2347 records of sediment temperature. Truncated to the 55 days that were sampled every year, the dataset had 440 observations. For log-transformed analyses, the data were first shifted to eliminate negative values. Covariate coverage was satisfactory over the duration of data collection and no further truncation was required for analysis.

Model Selection

For ARIMA models fitting all possible covariate combinations at lake BELA-088 with sediment temperature as the response variable, AICc-based model selection resulted in ARIMA(2,0,2) with air temperature as the main covariate in the best model. The best trend model was a seasonally adjusted ARIMA(2,0,1) using the truncated dataset. No significant trend in sediment temperature was detected.

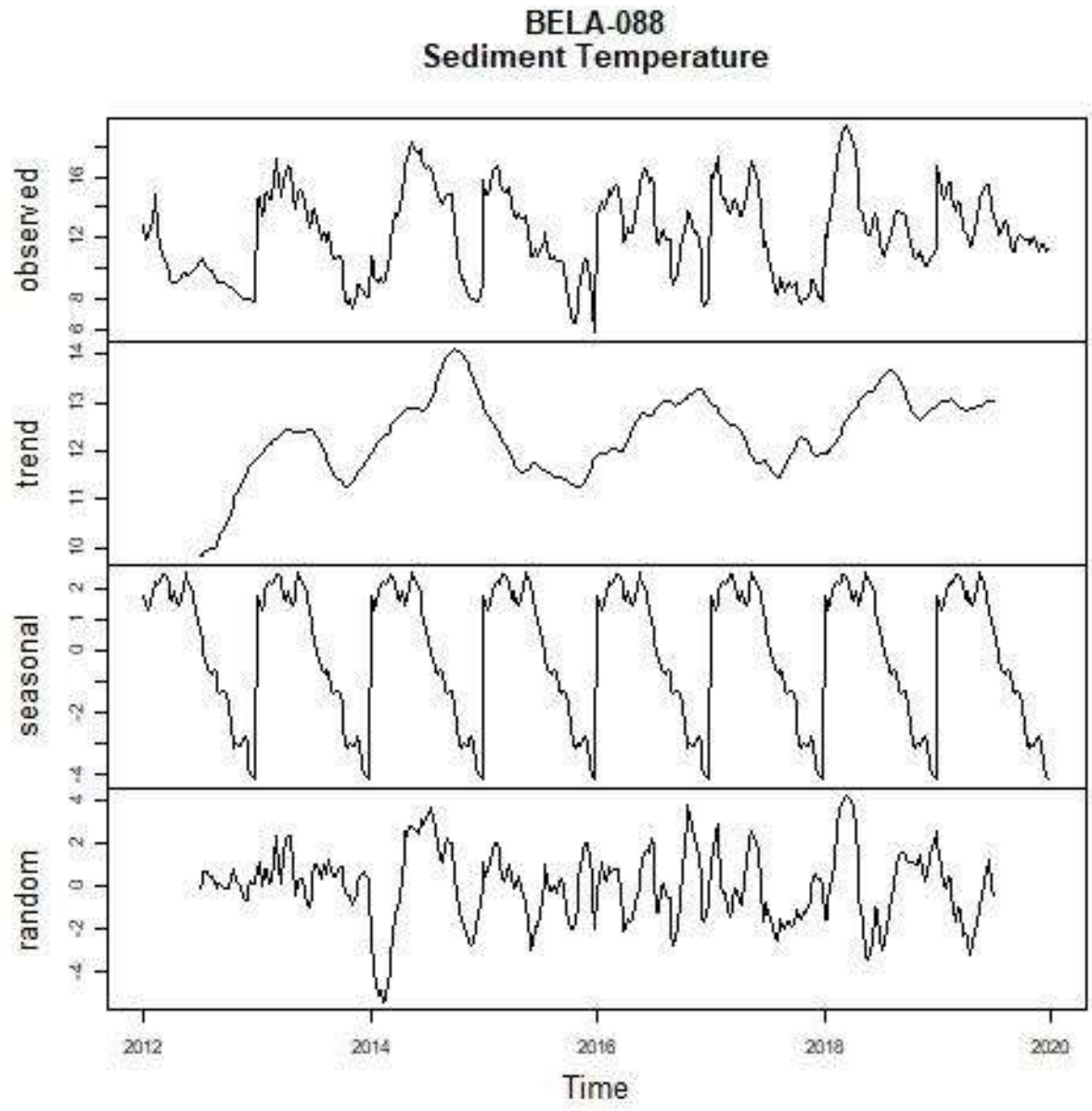


Figure A. 144. Time series decomposition of truncated BELA-088 sediment temperature by year.

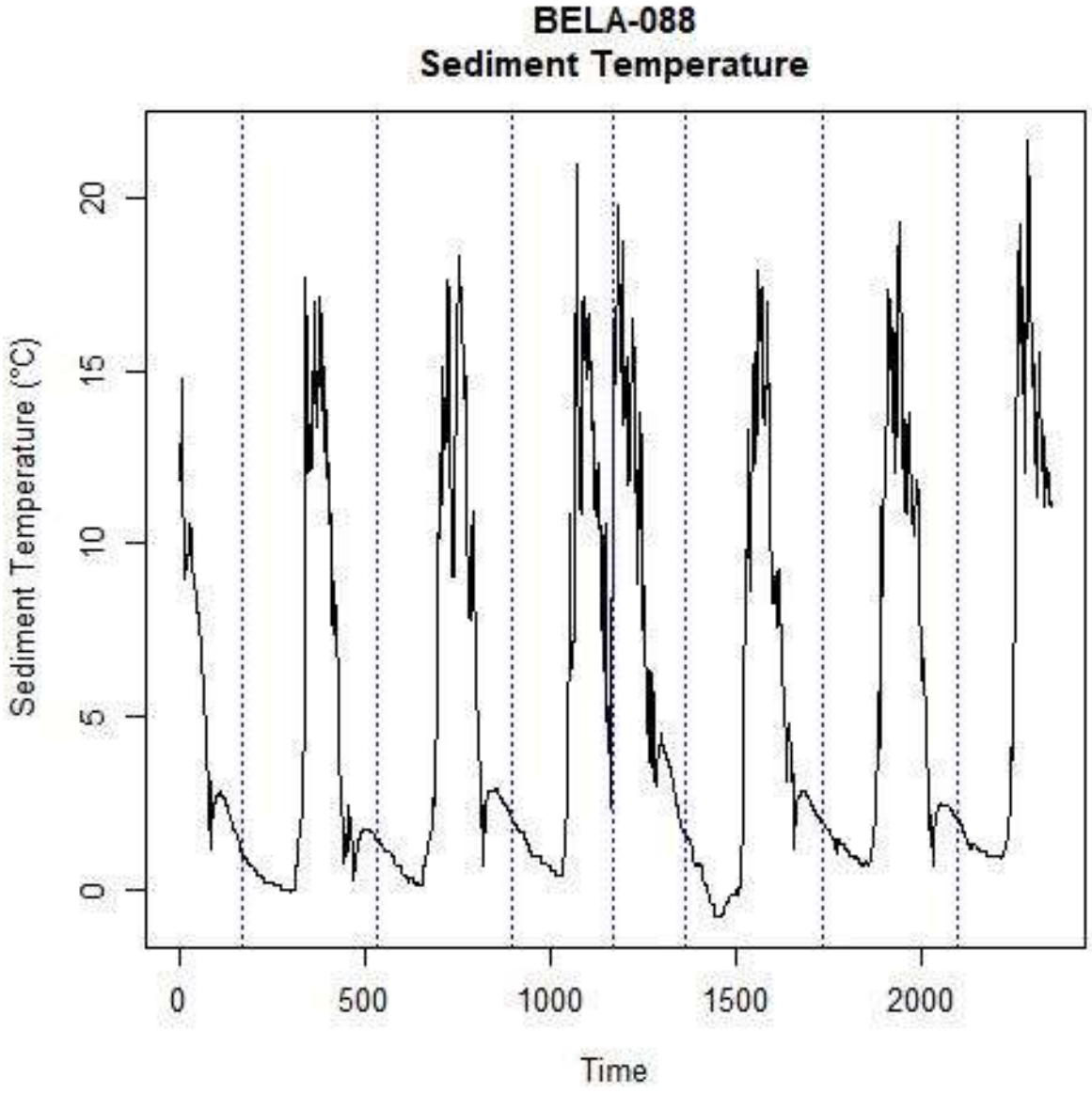


Figure A. 145: Time series of BELA-088 sediment temperature by time point with vertical lines for additive outliers.

Table A.154. Trend modeling results for daily sediment temperature data at BELA-088.

			Trend			ARMA order		Ljung-Box Test	
Logged	**Method**	**Intercept**	**Coefficient**	**SE**	**p-value**	**AR**	**MA**	**Statistic**	**p-value**
FALSE	complete	-10.1937	1.4658	0.1663	< 0.0001	2	1	24.98	0.0001
FALSE	completeAO	2.9035	0.2218	0.0527	< 0.0001	0	1	24675.09	< 0.0001

			Trend			ARMA order		Ljung-Box Test	
Logged	**Method**	**Intercept**	**Coefficient**	**SE**	**p-value**	**AR**	**MA**	**Statistic**	**p-value**
FALSE	trunc	8.2990	0.3687	0.0720	< 0.0001	0	1	1669.35	< 0.0001
FALSE	truncSA	10.2470	0.1936	0.1276	0.1292	2	1	89.96	0.2818
TRUE	complete	1.1701	0.0449	0.0091	< 0.0001	0	5	6074.41	< 0.0001
TRUE	completeAO	1.3295	0.0299	0.0096	0.0018	0	5	10251.09	< 0.0001
TRUE	trunc	2.0871	0.0361	0.0069	< 0.0001	0	1	1553.51	< 0.0001
TRUE	truncSA	2.2741	0.0197	0.0106	0.0627	2	0	91.96	0.2589

Table A.155. Top covariate models for daily sediment temperature data at BELA-088.

Model	**AICc**	**ΔAICc**	**Ljung-Box Test p-value**
Air Temperature	3472.46	0.00	0.0841
Relative Humidity	3508.92	36.46	0.0588
Intercept Only	3519.16	46.70	0.1551
Daily Precipitation	3520.80	48.34	0.0915
Wind Speed	3521.07	48.61	0.0923

Table A.156. Coefficients and variance components estimates for the top covariate model for daily sediment temperature data at BELA-088.

Parameter	**Coefficient**	**SE**	**p-value**
ar1	0.92	0.12	< 0.0001
ar2	0.07	0.11	0.5395
ma1	0.60	0.11	< 0.0001
ma2	0.22	0.05	< 0.0001
intercept	5.41	1.39	< 0.0001
Air Temperature	0.02	0.00	< 0.0001

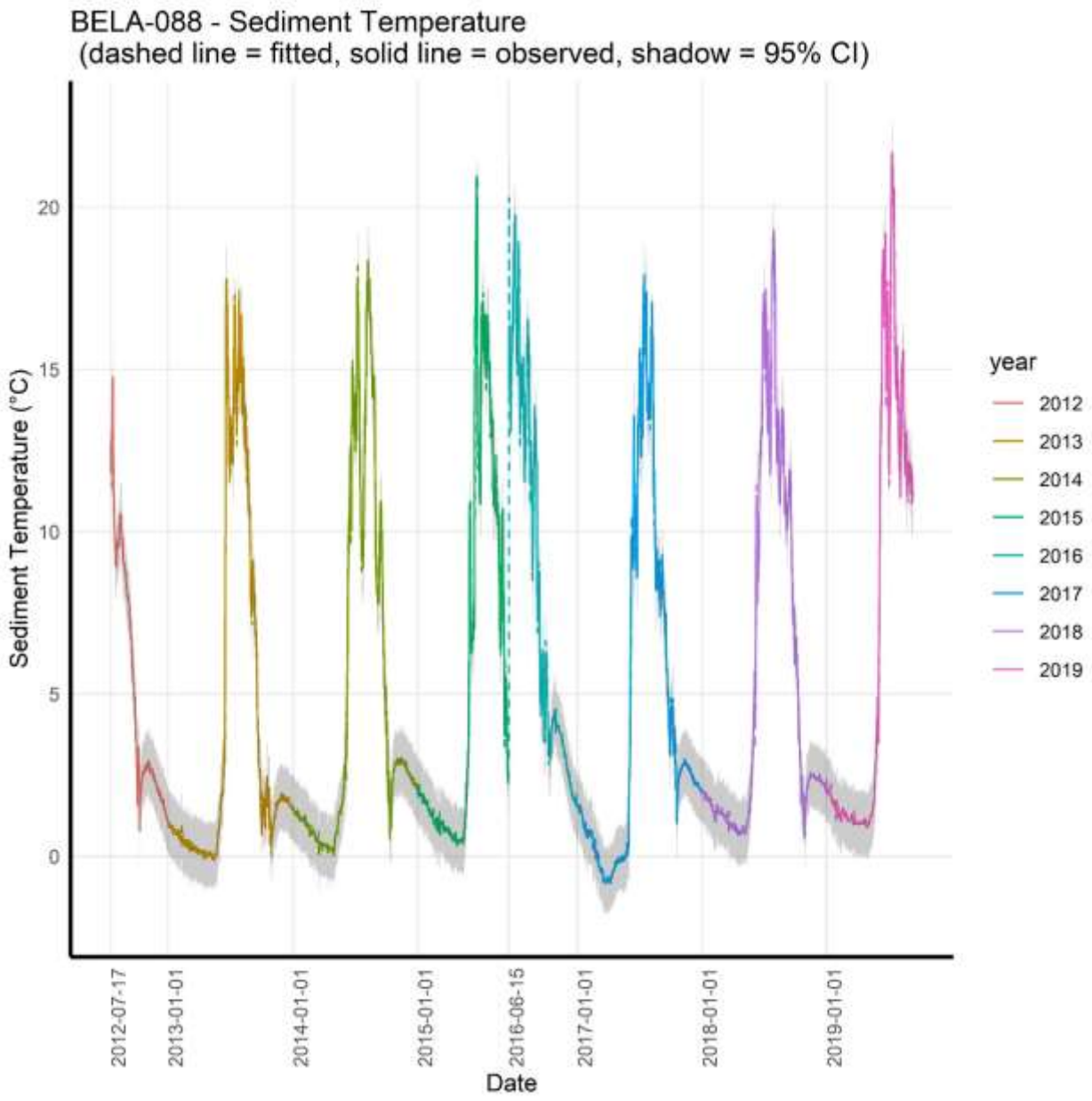


Figure A.146. Model predictions of BELA-088 sediment temperature by date.

BELA-108

Data

For the BELA-108 lake, sediment temperature was recorded from June 2015 through September 2019. Over this period, there were 1549 records of sediment temperature. Truncated to the 88 days that were sampled every year, the dataset had 440 observations. For log-transformed analyses, the data were first shifted to eliminate negative values. Covariate coverage was satisfactory over the duration of data collection and no further truncation was required for analysis. However, a continuous missing period during the summer of 2018 for wind speed and solar radiation was long enough that imputation did not reproduce seasonal mean values. The covariate analysis was therefore restricted to the period 2015-2017. No covariate models with the full dataset over this period exhibited stationarity, so the truncated dataset was used.

Model Selection

A stationary trend model with an ARIMA(3,0,0) was obtained using the seasonally adjusted truncated dataset. No significant trend in sediment temperature was detected. Weekly means were used to evaluate covariate relationships at lake BELA-108 where air temperature was found to be positively associated with sediment temperature.

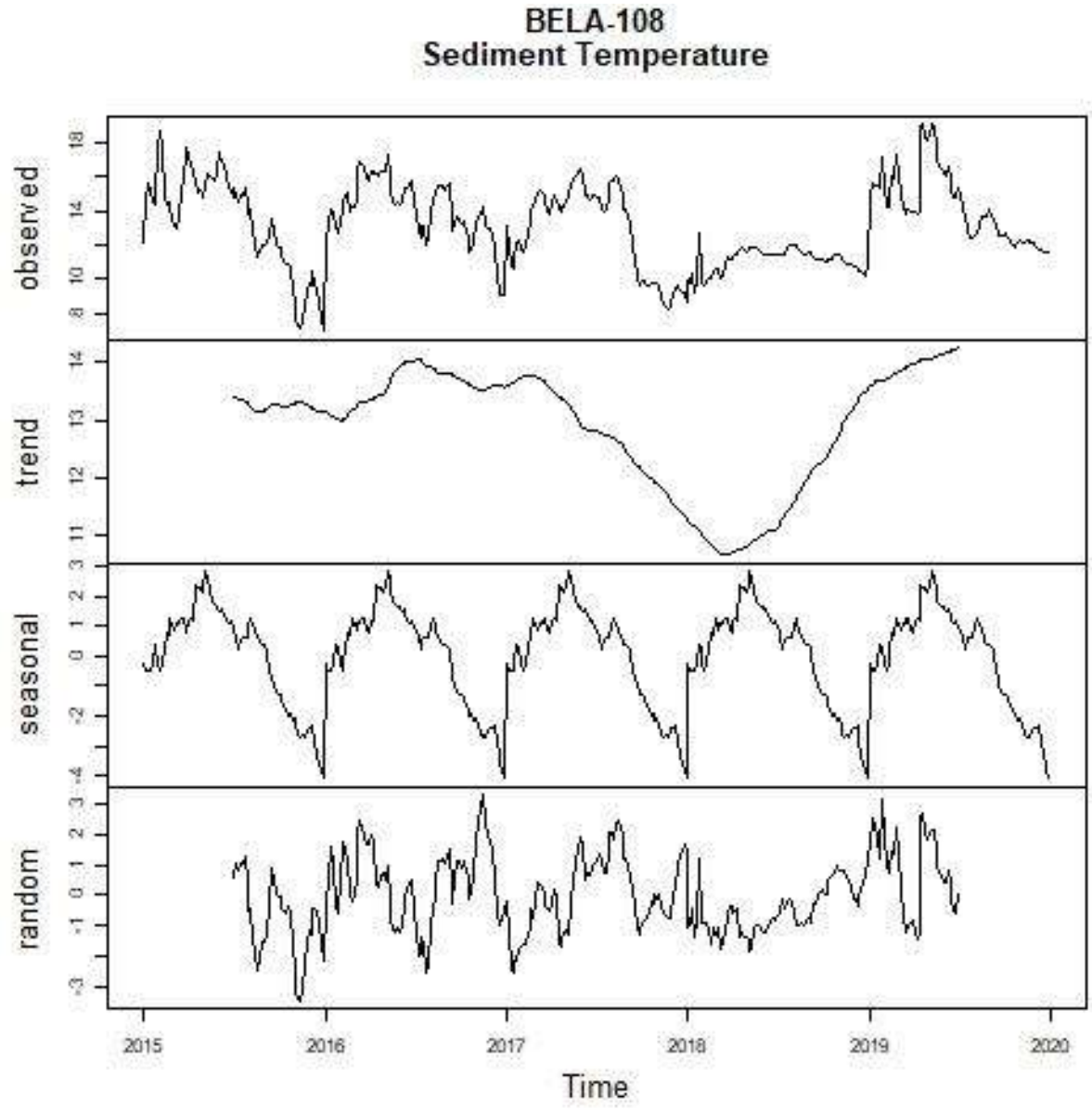


Figure A.147. Time series decomposition of truncated BELA-108 sediment temperature by year.

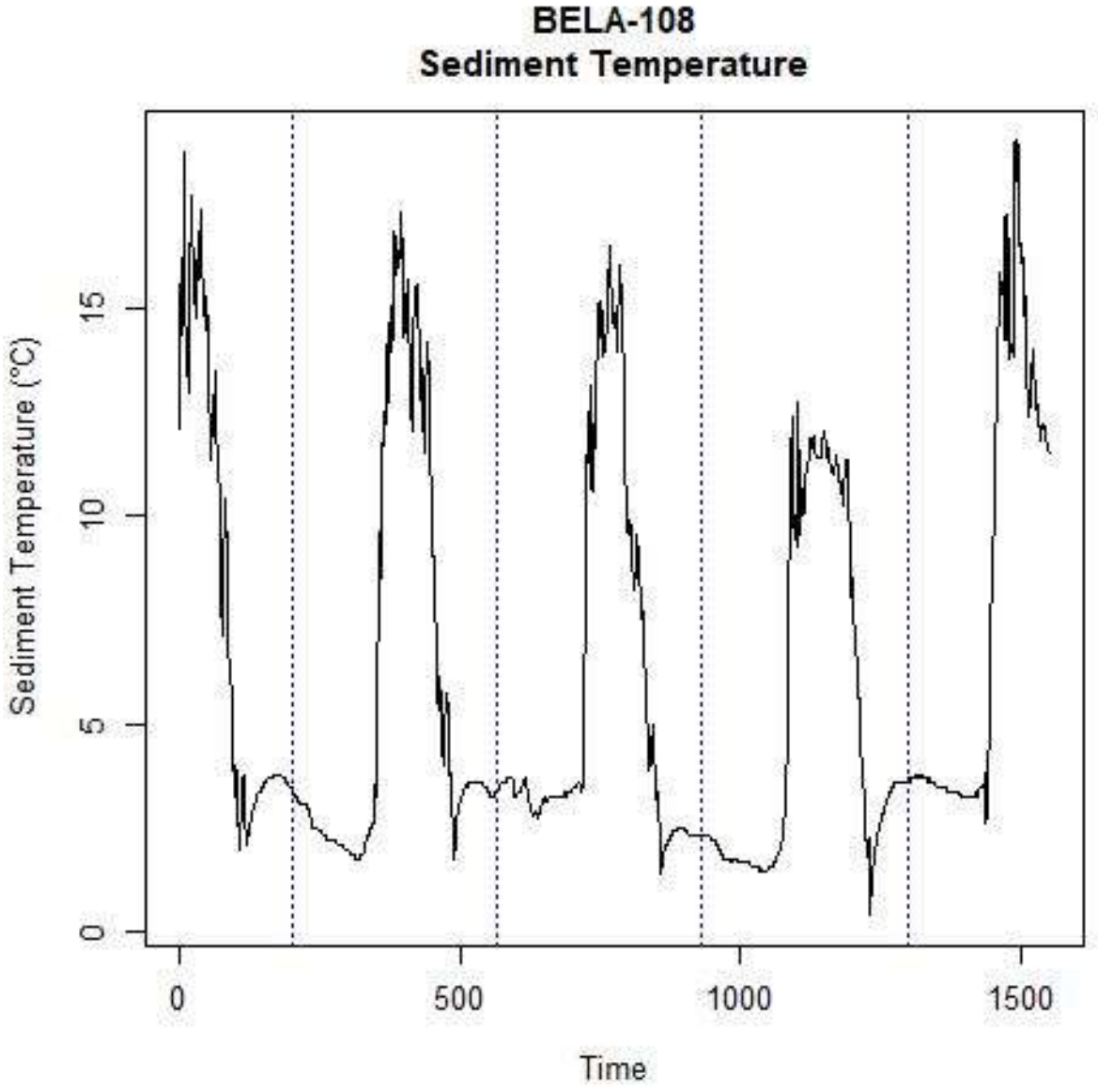


Figure A.148. Time series of BELA-108 sediment temperature by time point with vertical lines for additive outliers.

Table A.157. Trend modeling results for daily sediment temperature data at BELA-108.

			Trend			ARMA order		Ljung-Box Test	
Logged	**Method**	**Intercept**	**Coefficient**	**SE**	**p-value**	**AR**	**MA**	**Statistic**	**p-value**
FALSE	complete	6.6832	-0.0335	0.1145	0.7695	0	5	3314.29	< 0.0001
FALSE	completeAO	6.8465	-0.0471	0.1315	0.7201	0	5	4617.91	< 0.0001

			Trend			ARMA order		Ljung-Box Test	
Logged	**Method**	**Intercept**	**Coefficient**	**SE**	**p-value**	**AR**	**MA**	**Statistic**	**p-value**
FALSE	trunc	11.7493	0.1218	0.1124	0.2786	0	2	1577.22	< 0.0001
FALSE	truncSA	13.3096	-0.0130	0.1988	0.9479	3	0	79.43	0.5907
TRUE	complete	1.7476	-0.0042	0.0142	0.7663	0	5	3995.27	< 0.0001
TRUE	completeAO	1.8080	-0.0092	0.0171	0.5883	0	5	5525.87	< 0.0001
TRUE	trunc	2.0402	0.0437	0.0137	0.0014	0	5	410.22	< 0.0001
TRUE	truncSA	2.5454	0.0013	0.0158	0.9347	3	0	70.15	0.8417

Table A.158. Top covariate models for weekly sediment temperature data at BELA-108.

Model	**AICc**	**ΔAICc**	**Ljung-Box Test p-value**
Air temperature	680.97	0.00	0.0660
Air temperature + Wind Speed	682.48	1.51	0.0653
Air temperature + daily precipitation	682.79	1.82	0.0670
Air temperature + Month	682.80	1.83	0.0730
Air temperature + year	683.09	2.12	0.0631
Air temperature + Relative Humidity	683.13	2.16	0.0633
Air temperature + Wind Speed + daily precipitation + Month	685.99	5.02	0.0514
Intercept only	687.67	6.70	0.0514
Solar Radiation + Month	689.04	8.07	0.0514

Table A.159. Coefficients and variance components estimates for the top covariate model for weekly sediment temperature data at BELA-108.

Parameter	**Coefficient**	**SE**	**p-value**
ar1	1.33	0.30	< 0.0001
ar2	0.14	0.53	0.7937
ar3	-0.51	0.25	0.0393
ma1	-0.10	0.30	0.7480
ma2	-0.53	0.17	0.0018
intercept	6.21	0.64	< 0.0001
Air temperature	0.04	0.01	0.0027

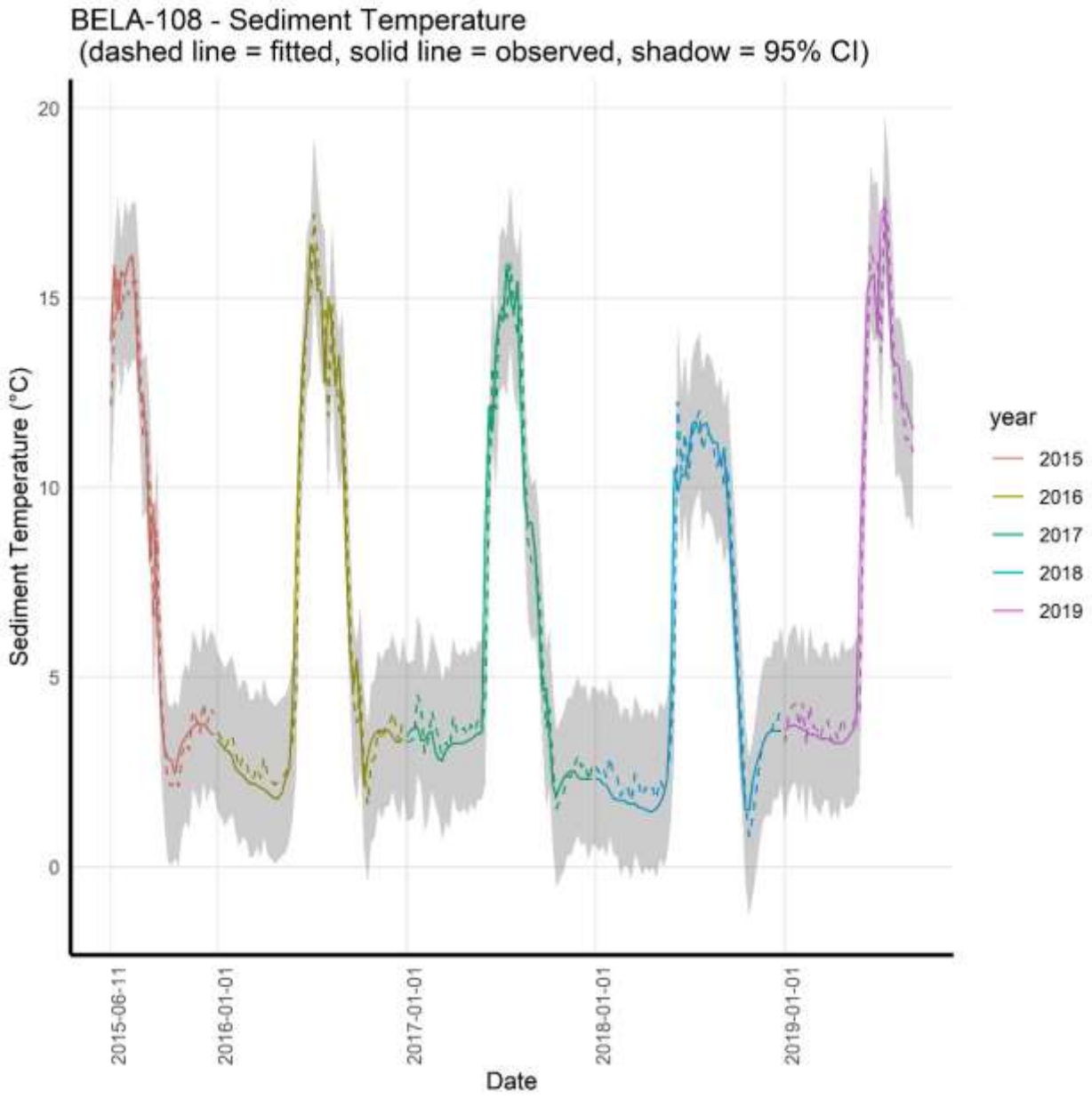


Figure A.149. Model predictions of BELA-108 sediment temperature by week.

DENA-018

Data

For the DENA-018 lake, sediment temperature was recorded from June 2007 to September 2008, then from May 2009 to June 2019. However, 2019 was removed from the analysis to ensure a summer record in every year. Over this period, there were 3951 records of sediment temperature. Truncated to the 79 days that were sampled every year, the dataset had 948 observations. For log-transformed analyses, the data were first shifted to eliminate negative values. Covariate coverage was satisfactory over the duration of data collection and no further truncation was required for analysis.

Model Selection

For ARIMA models fitting all possible covariate combinations at lake DENA-018 with sediment temperature as the response variable, AICc-based model selection resulted in ARIMA(2,0,2) with air temperature as the main covariate in the top model. The best trend model was an ARIMA(2,0,0) using the seasonally adjusted truncated dataset. No significant trend in sediment temperature was detected.

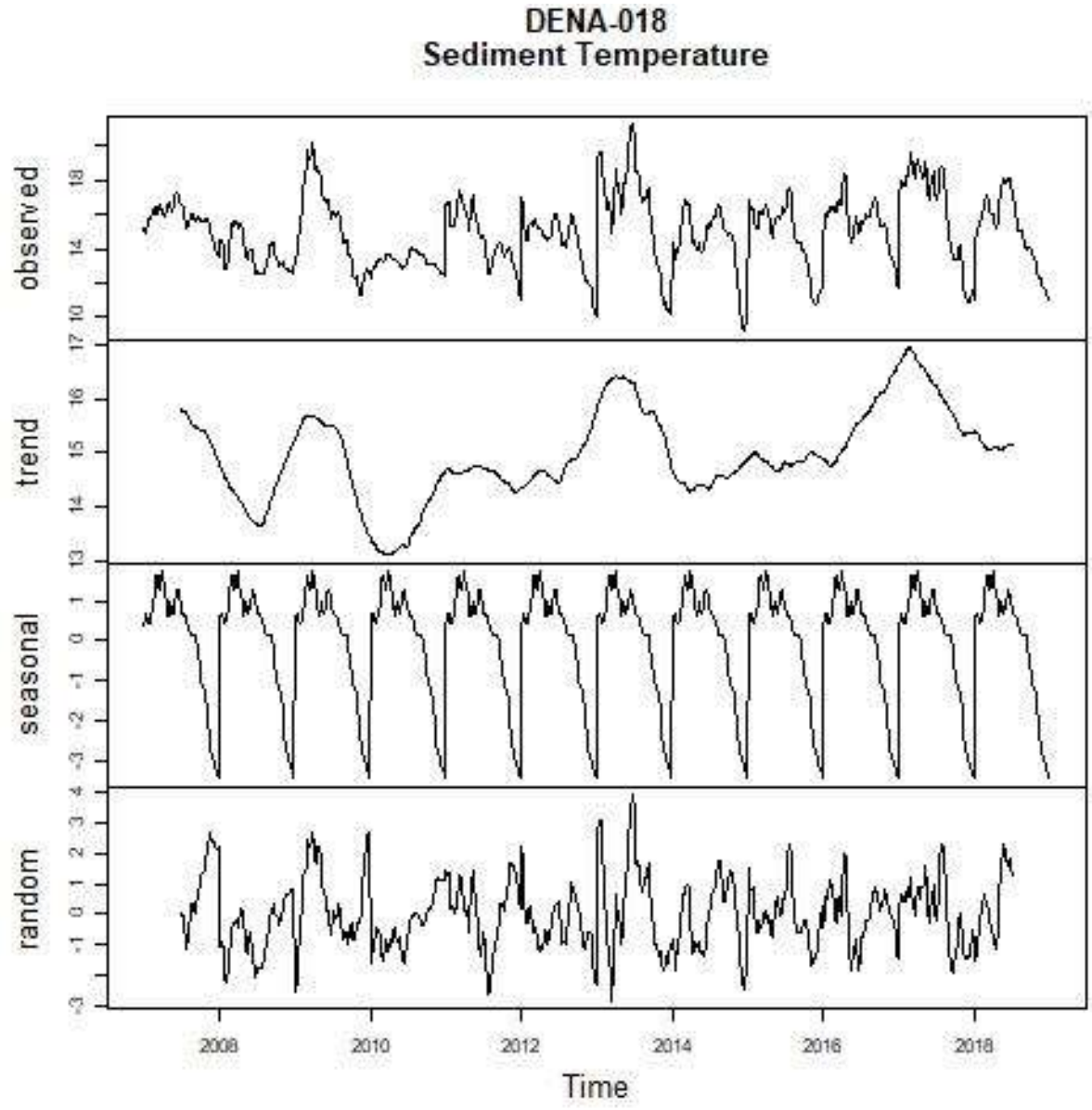


Figure A.150. Time series decomposition of truncated DENA-018 sediment temperature by year.

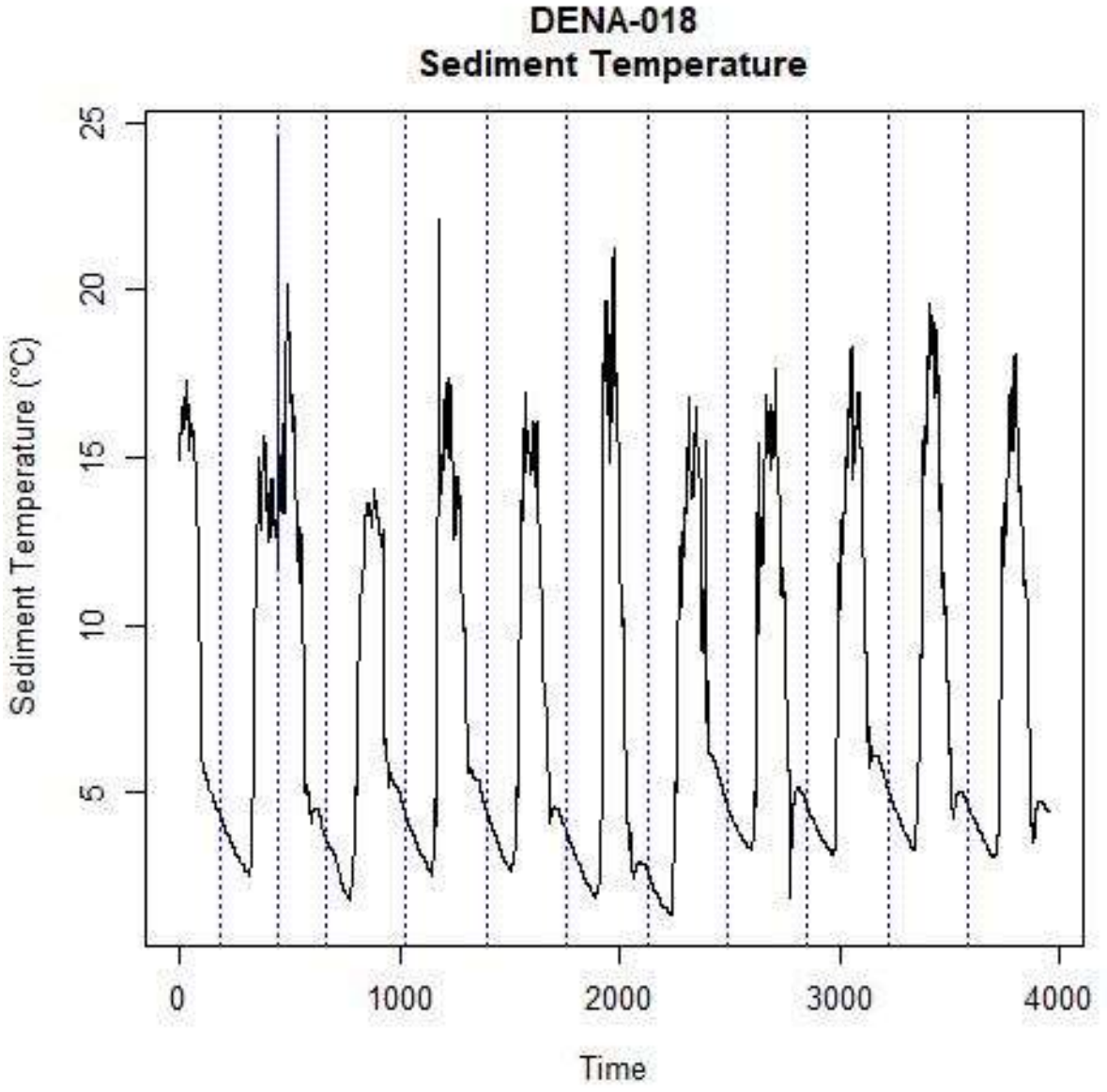


Figure A.151. Time series of DENA-018 sediment temperature by time point with vertical lines for additive outliers.

Table A.160. Trend modeling results for daily sediment temperature data at DENA-018.

			Trend			ARMA order		Ljung-Box Test	
Logged	**Method**	**Intercept**	**Coefficient**	**SE**	**p-value**	**AR**	**MA**	**Statistic**	**p-value**
FALSE	complete	7.9311	-0.0194	0.0347	0.5753	0	5	8877.94	< 0.0001
FALSE	completeAO	8.3131	-0.0547	0.0343	0.1106	0	5	19490.90	< 0.0001

			Trend			ARMA order		Ljung-Box Test	
Logged	Method	Intercept	Coefficient	SE	p-value	AR	MA	Statistic	p-value
FALSE	trunc	14.0249	0.0932	0.0278	0.0008	0	2	5370.09	< 0.0001
FALSE	truncSA	14.3819	0.0567	0.0562	0.3132	2	0	168.87	0.1951
TRUE	complete	1.1343	0.0548	0.0117	< 0.0001	3	1	7.96	0.0932
TRUE	completeAO	1.2606	0.0437	0.0167	0.0090	3	4	12.54	0.0058
TRUE	trunc	2.6582	0.0038	0.0015	0.0110	0	0	10415.50	< 0.0001
TRUE	truncSA	2.6591	0.0036	0.0038	0.3478	2	0	200.70	0.0068

Table A.161. Top covariate models for daily sediment temperature data at DENA-018.

Model	AICc	ΔAICc	Ljung-Box Test p-value
Daily Precipitation + Month	1130.33	0.00	0.5405
Wind Speed + Daily Precipitation + Month	1131.46	1.13	0.3727
Wind Speed + Month	1137.63	7.29	0.4467
Wind Speed + Relative Humidity + Month	1139.13	8.79	0.3308
Relative Humidity + Month	1139.46	9.12	0.4959
Air Temperature + Wind Speed + Daily Precipitation	1518.91	388.58	0.3296
Air Temperature + Daily Precipitation	1521.04	390.70	0.3823
Air Temperature + Wind Speed	1526.06	395.72	0.5712
Air Temperature	1530.83	400.49	0.5983
Wind Speed + Relative Humidity	1632.28	501.94	0.8212

Table A.162. Coefficients and variance components estimates for the top covariate model for daily sediment temperature data at DENA-018.

Parameter	Coefficient	SE	p-value
ar1	1.28	0.03	< 0.0001
ar2	-0.33	0.03	< 0.0001
intercept	22.24	0.42	< 0.0001
Daily Precipitation	0.11	0.04	0.0020
Month	-0.97	0.04	< 0.0001

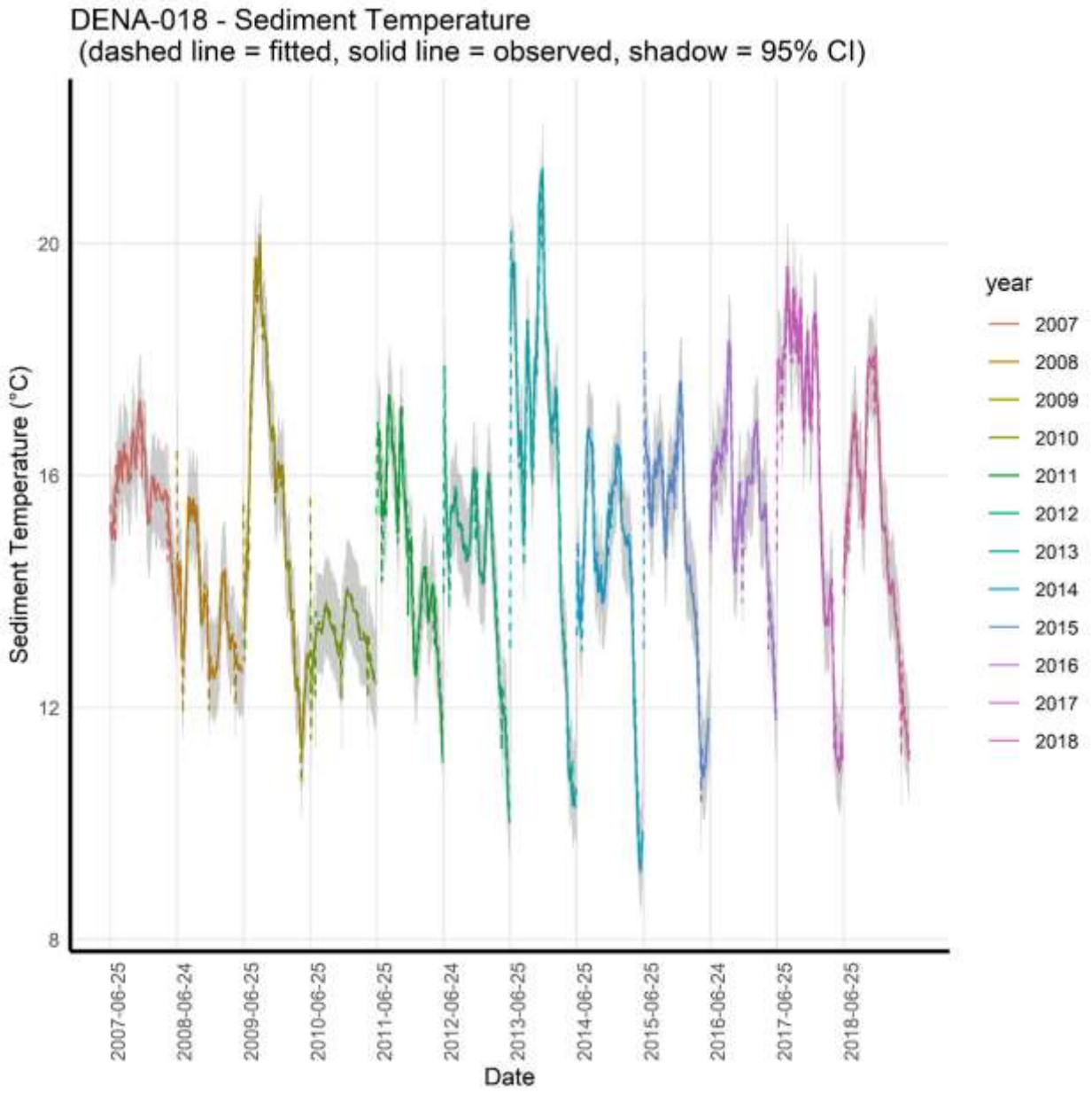


Figure A.152. Model predictions of DENA-018 sediment temperature by date.

DENA-023

Data

For the DENA-023 lake, sediment temperature was recorded from 2007 to 2019. However, only 2009 to 2017 included summer, which was a key season for other lakes in the analysis. Over this period, there were 3027 records of sediment temperature. Truncated to the 105 days that were sampled every year, the dataset had 945 observations.

Model Selection

For ARIMA models fitting all possible covariate combinations at lake DENA-023 with sediment temperature as the response variable, AICc-based model selection resulted in ARIMA(2,0,0) with daily precipitation and year as the main covariates in the best model. The model detected a significant positive trend in sediment temperature over years. The covariate model indicated an annual trend an order of magnitude higher than that estimated from the trend model.

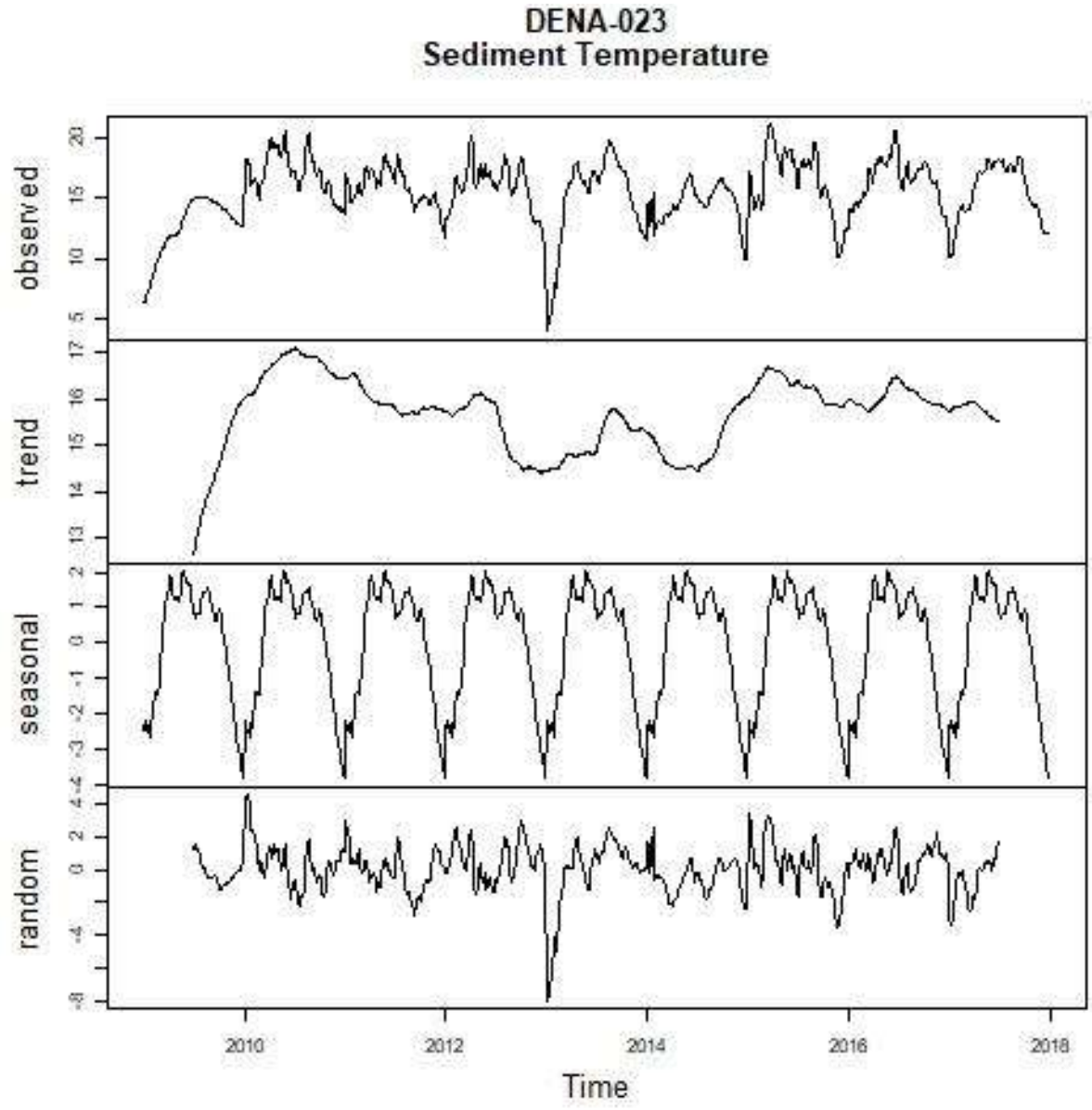


Figure A.153. Time series decomposition of truncated DENA-023 sediment temperature by year.

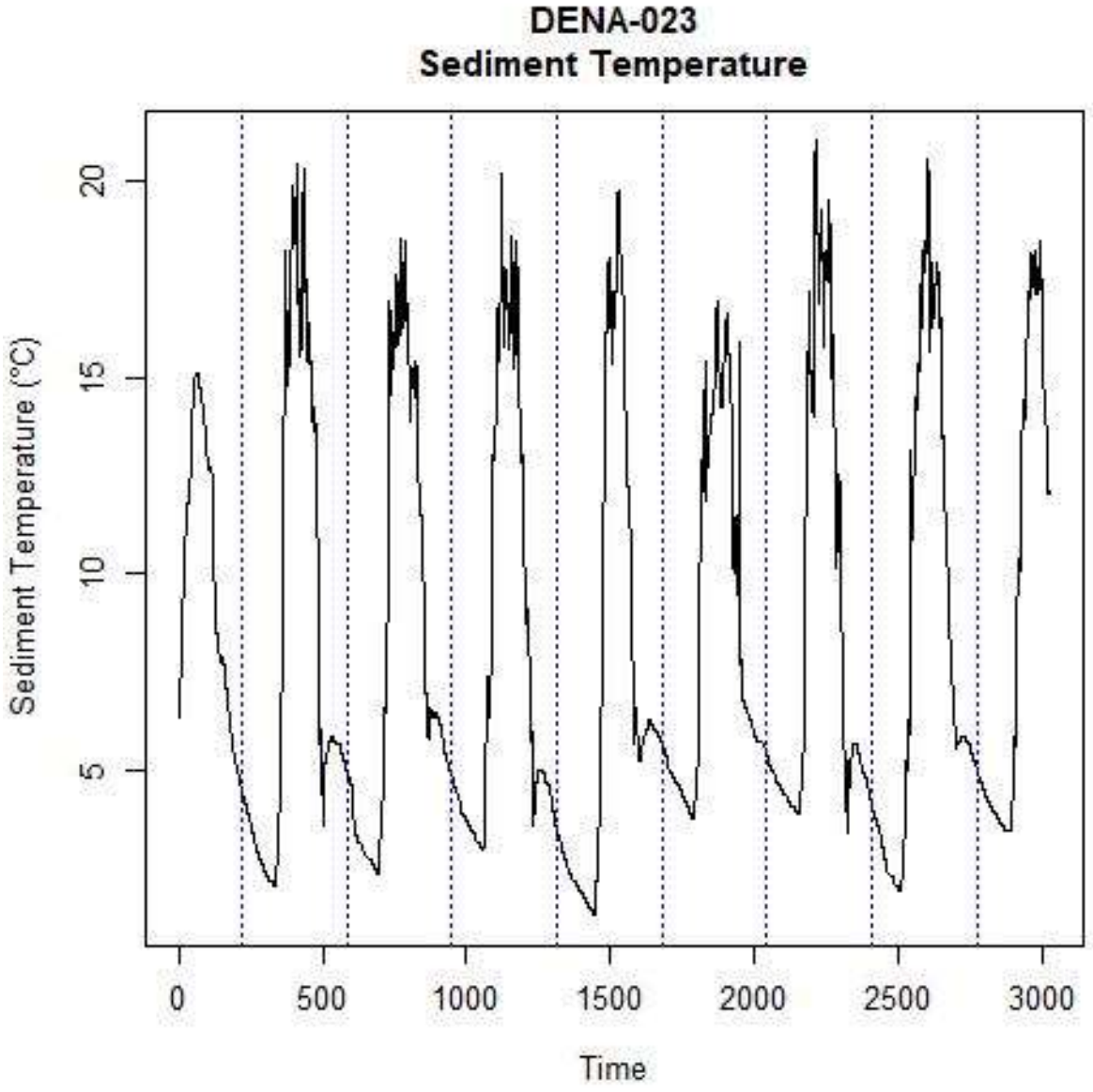


Figure A.154. Time series of DENA-023 sediment temperature by time point with vertical lines for additive outliers.

Table A.163. Trend modeling results for daily sediment temperature data at DENA-023.

			Trend			ARMA order		Ljung-Box Test	
Logged	**Method**	**Intercept**	**Coefficient**	**SE**	**p-value**	**AR**	**MA**	**Statistic**	**p-value**
FALSE	complete	8.4781	-0.0064	0.0516	0.9018	0	5	7938.50	< 0.0001
FALSE	completeAO	8.4760	-0.0064	0.0540	0.9052	0	5	13981.02	< 0.0001

			Trend			ARMA order		Ljung-Box Test	
Logged	**Method**	**Intercept**	**Coefficient**	**SE**	**p-value**	**AR**	**MA**	**Statistic**	**p-value**
FALSE	trunc	NA	1.2826	0.1036	< 0.0001	1	2	169.35	0.7890
FALSE	truncSA	13.9933	0.1263	0.1088	0.2457	2	0	180.17	0.5865
TRUE	complete	1.9344	-0.0019	0.0105	0.8536	3	1	45.50	< 0.0001
TRUE	completeAO	2.0120	-0.0089	0.0162	0.5829	3	1	51.88	< 0.0001
TRUE	trunc	2.5685	0.0136	0.0042	0.0014	0	5	1171.09	< 0.0001
TRUE	truncSA	2.5846	0.0117	0.0091	0.1987	2	1	127.81	0.9994

Table A.164. Top covariate models for daily sediment temperature data at DENA-023.

Model	**AICc**	**ΔAICc**	**Ljung-Box Test p-value**
Daily Precipitation + Year + Month	1428.96	0.00	0.3126
Daily Precipitation + Year	1429.46	0.50	0.5128
Air Temperature + Daily Precipitation + Year	1431.47	2.52	0.3859
Daily Precipitation + Month	1434.07	5.11	0.3934
Wind Speed + Daily Precipitation + Month	1434.08	5.12	0.2757
Solar Radiation + Year	1437.06	8.10	0.3133
Air Temperature + Year	1438.82	9.86	0.4476
Relative Humidity + Year	1439.09	10.13	0.4427
Year + Month	1440.36	11.40	0.2316
Wind Speed + Month	1441.33	12.37	0.3900

Table A.165. Coefficients and variance components estimates for the top covariate model for daily sediment temperature data at DENA-023.

Parameter	**Coefficient**	**SE**	**p-value**
ar1	1.32	0.03	< 0.0001
ar2	-0.34	0.03	< 0.0001
Daily Precipitation	0.14	0.04	0.0018
Year	1.29	0.10	< 0.0001

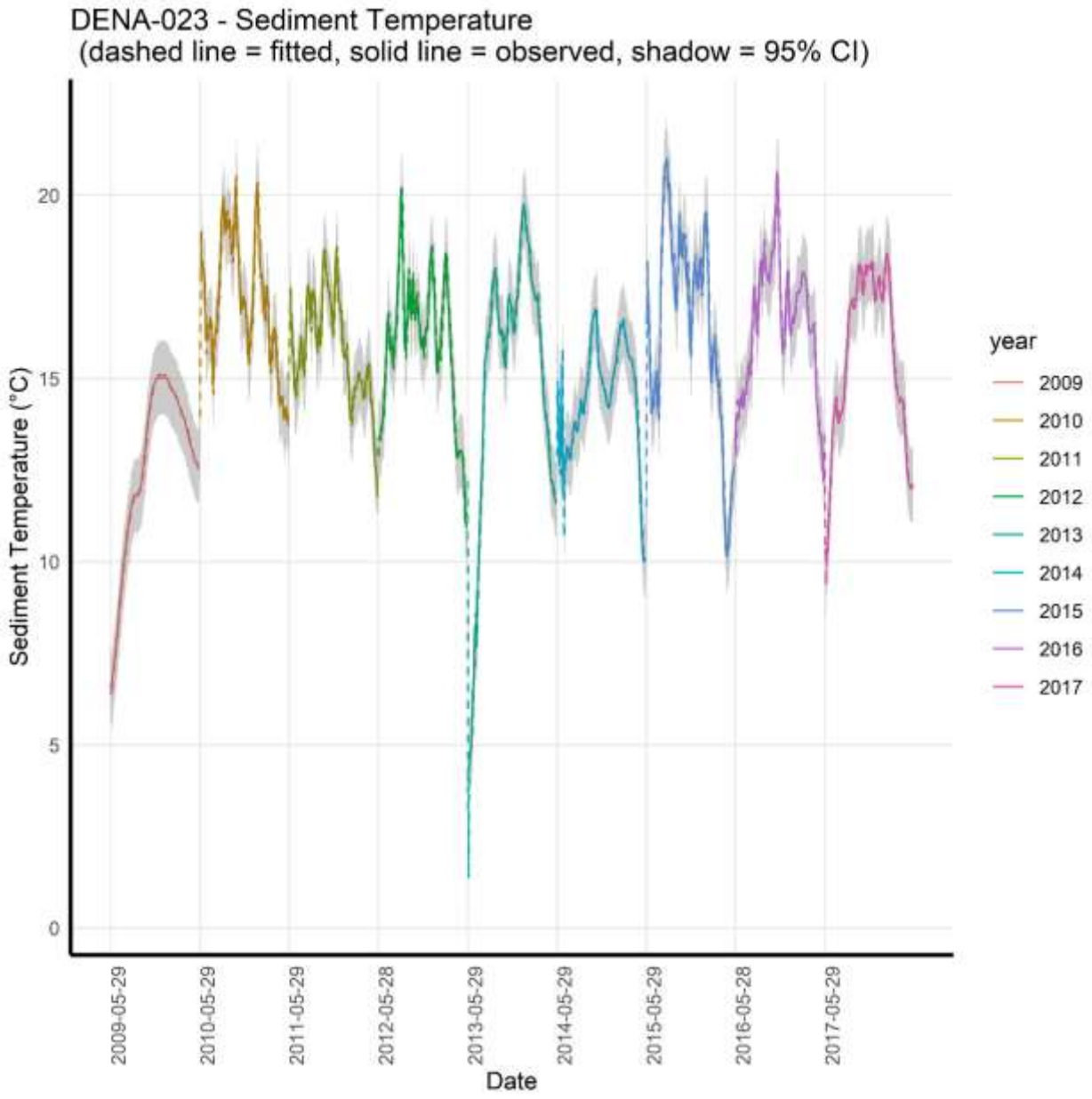


Figure A.155. Model predictions of DENA-023 sediment temperature by date.

KOVA-085

Data

For the KOVA-085 lake, sediment temperature was recorded from 2010-2019. However, 2019 data were excluded because they did not include summer. Over the remaining period, there were 2684 records of sediment temperature. Truncated to the 88 days that were sampled every year, the dataset had 792 observations. Covariate models did not exhibit stationarity with the full dataset, so the truncated dataset was used for covariate model selection. Covariate coverage was amenable to imputation for further modeling.

Model Selection

For ARIMA models fitting all possible covariate combinations at lake KOVA-085 with sediment temperature as the response variable, AICc-based model selection resulted in ARIMA(1,0,3) with wind speed and month as the main covariates in the best model, but no annual trend term. The best trend model was an ARIMA(2,0,0) using a truncated and seasonally adjusted dataset. The model did not detect a significant trend in sediment temperature over years.

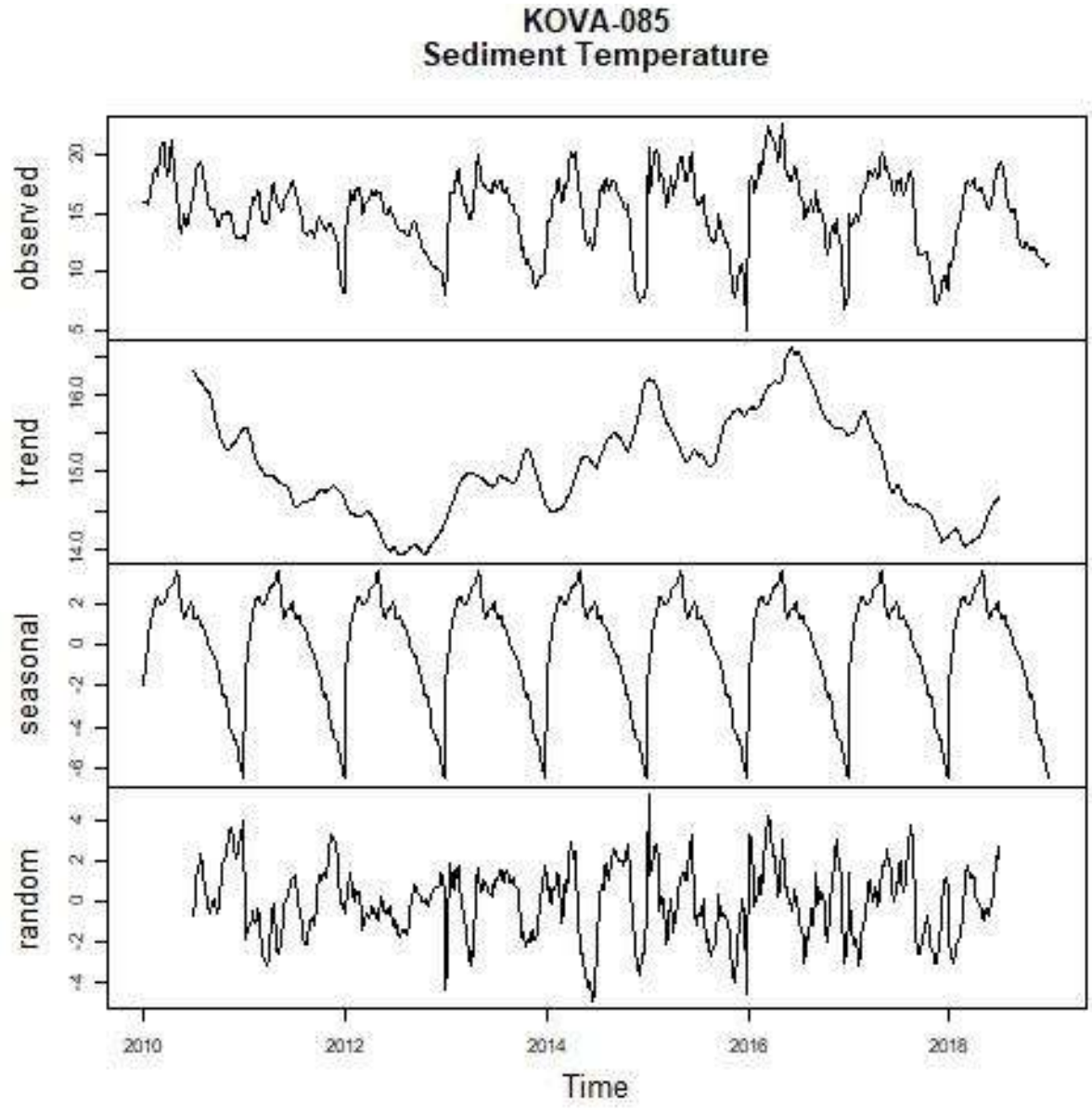


Figure A.156. Time series decomposition of truncated KOVA-085 sediment temperature by year.

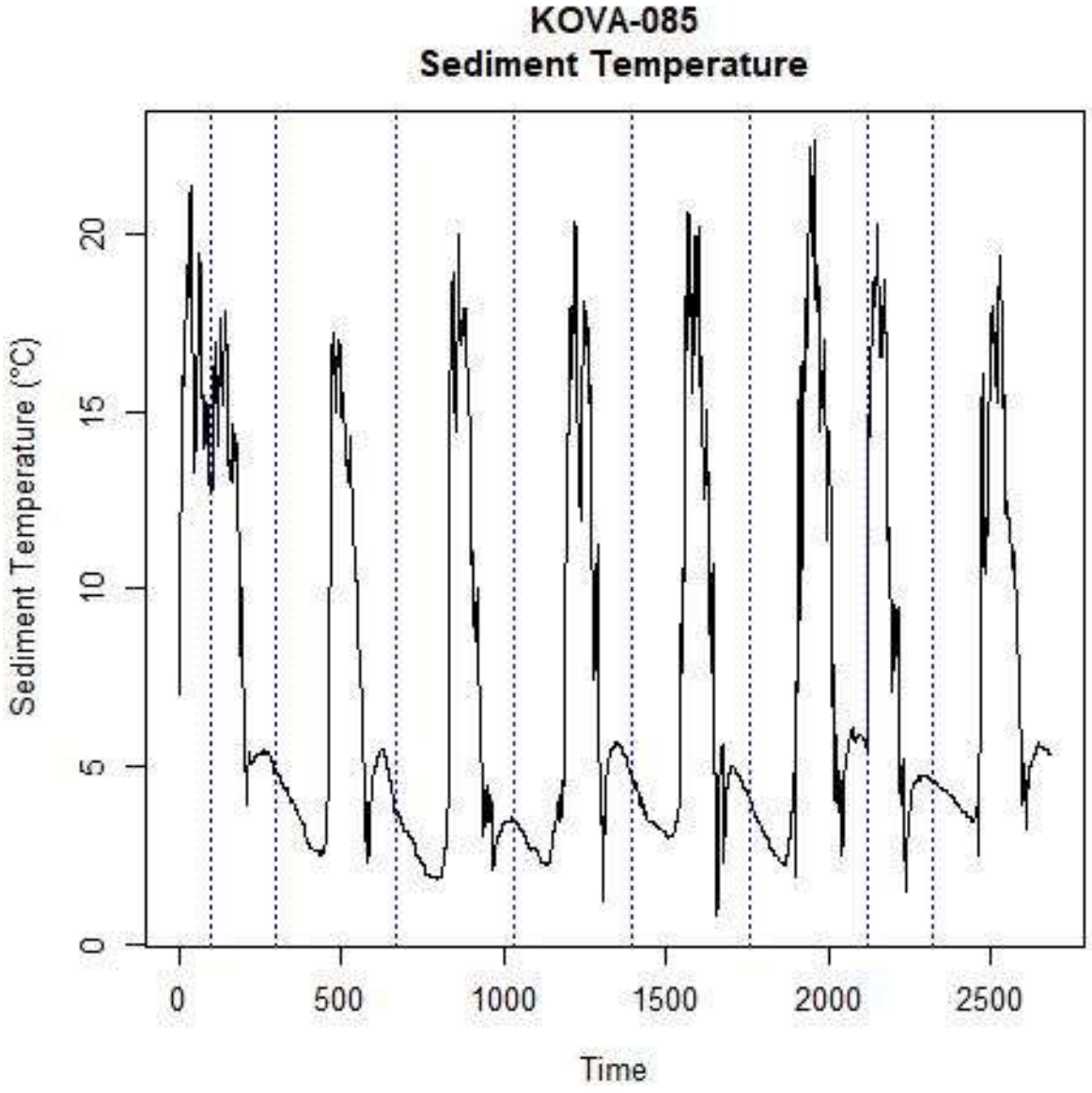


Figure A.157. Time series of KOVA-085 sediment temperature by time point with vertical lines for additive outliers.

Table A.166. Trend modeling results for daily sediment temperature data at KOVA-085.

			Trend			ARMA order		Ljung-Box Test	
Logged	**Method**	**Intercept**	**Coefficient**	**SE**	**p-value**	**AR**	**MA**	**Statistic**	**p-value**
FALSE	complete	7.8505	-0.0236	0.0603	0.6959	0	5	6044.17	< 0.0001
FALSE	completeAO	9.1445	-0.1376	0.0623	0.0273	0	5	10566.95	< 0.0001

			Trend			ARMA order		Ljung-Box Test	
Logged	**Method**	**Intercept**	**Coefficient**	**SE**	**p-value**	**AR**	**MA**	**Statistic**	**p-value**
FALSE	trunc	14.2566	0.0816	0.0748	0.2752	0	4	1547.96	< 0.0001
FALSE	truncSA	15.2505	-0.0082	0.0883	0.9264	2	0	145.90	0.6670
TRUE	complete	1.7530	0.0026	0.0076	0.7355	0	5	5785.81	< 0.0001
TRUE	completeAO	0.5900	0.1044	0.0319	0.0010	3	2	20.60	0.0001
TRUE	trunc	2.7084	-0.0013	0.0045	0.7684	0	2	3212.23	< 0.0001
TRUE	truncSA	2.7212	-0.0025	0.0065	0.6995	1	1	101.22	0.9997

Table A.167. Top covariate models for daily sediment temperature data at KOVA-085.

Model	**AICc**	**ΔAICc**	**Ljung-Box Test p-value**
Wind Speed + Month	1764.42	0.00	0.2693
Wind Speed + Daily Precipitation + Month	1766.03	1.61	0.1356
Daily Precipitation + Month	1777.68	13.26	0.2445
Air Temperature + Wind Speed	1826.60	62.18	0.2933
Air Temperature + Wind Speed + Daily Precipitation	1828.66	64.24	0.2406
Air Temperature	1833.17	68.75	0.3806
Air Temperature + Daily Precipitation	1835.22	70.80	0.3054
Solar Radiation	1929.25	164.83	0.4144
Wind Speed + Relative Humidity	1931.30	166.88	0.1207
Wind Speed + Relative Humidity + Daily Precipitation	1933.00	168.58	0.0702

Table A.168. Coefficients and variance components estimates for the top covariate model for daily sediment temperature data at KOVA-085.

Parameter	**Coefficient**	**SE**	**p-value**
ar1	0.92	0.02	< 0.0001
ma1	0.38	0.04	< 0.0001
ma2	0.10	0.04	0.0164
ma3	0.07	0.04	0.0722
intercept	22.39	0.72	< 0.0001
Wind Speed	0.10	0.03	0.0002
Month	-1.01	0.07	<0.0001

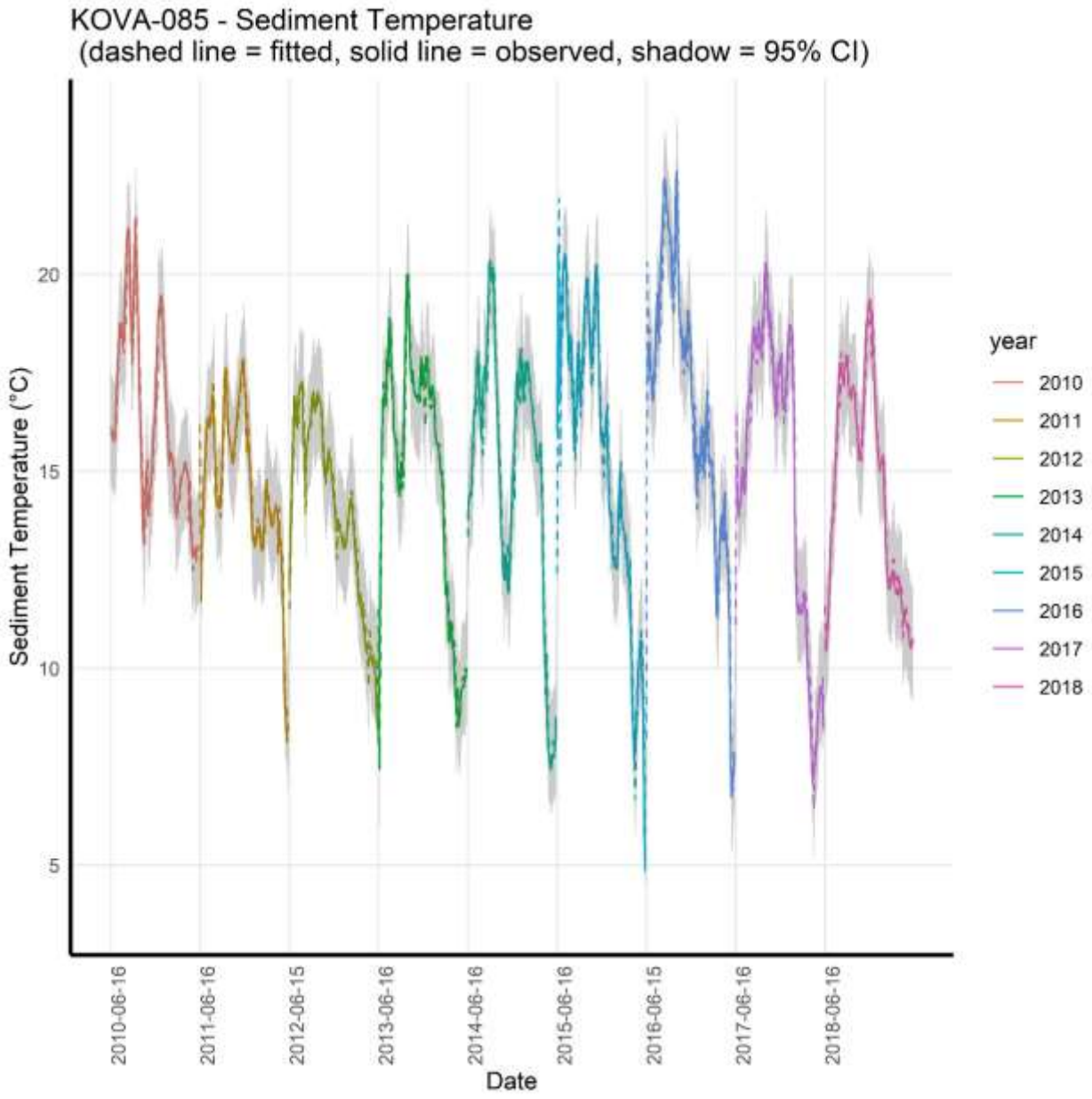


Figure A.158. Model predictions of KOVA-085 sediment temperature by date.

KOVA-086

Data

For KOVA-086, sediment temperature was recorded from 2009-2020. However, 2020 data were excluded because they only included January. Over the remaining period, there were 3434 records of sediment temperature. The months with data varied over the dataset. Truncated to the 58 days that were sampled every year, the dataset had 638 observations. Acceptable covariate models were not identified with the full dataset, so the truncated dataset was used for covariate model selection. When aggregated to weekly means, the sediment temperature dataset contained 501 observations. When truncating to the subset of nine common weeks sampled in every year, the number of observations was reduced to 99.

Model Selection

For ARIMA models fitting all possible covariate combinations at lake KOVA-086 with sediment temperature as the response variable, AICc-based model selection resulted in ARIMA(2,0,3) with air temperature, wind speed, and relative humidity as the main covariates in the top model, but no annual trend term. No trend model of daily data exhibited stationary residuals.

When fitting trend models to the weekly sediment temperature data the truncated and truncated seasonally adjusted datasets yielded stationary residuals for both the logged and unlogged data. None of these four models included a trend coefficient that was significantly greater than zero, thus there is no evidence for a trend in sediment temperature at lake KOVA-086.

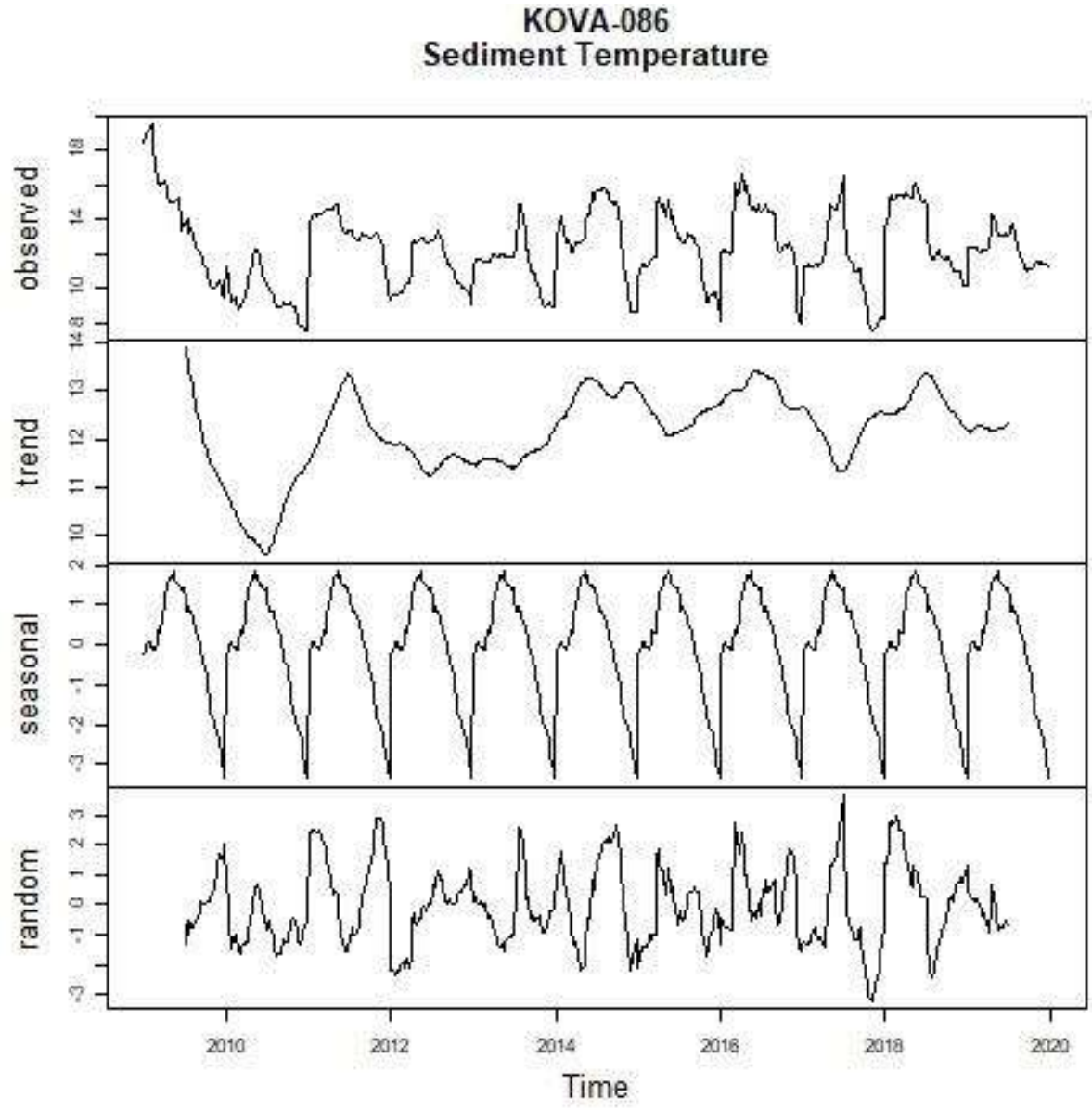


Figure A.159. Time series decomposition of truncated KOVA-086 sediment temperature by year.

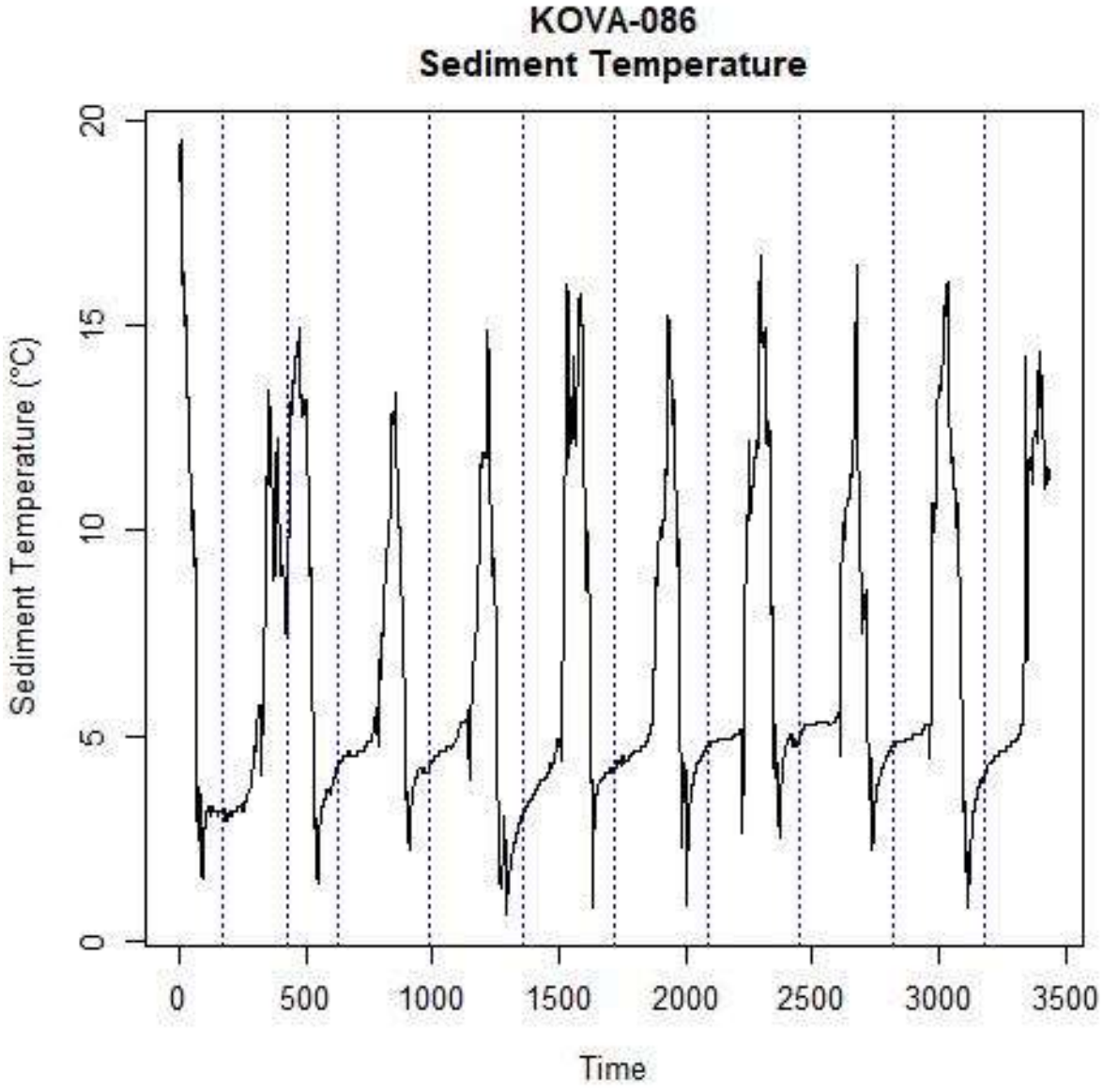


Figure A.160. Time series of KOVA-086 sediment temperature by time point with vertical lines for additive outliers.

Table A.169. Trend modeling results for daily sediment temperature data at KOVA-086.

			Trend			ARMA order		Ljung-Box Test	
Logged	**Method**	**Intercept**	**Coefficient**	**SE**	**p-value**	**AR**	**MA**	**Statistic**	**p-value**
FALSE	complete	5.7531	0.0649	0.0297	0.0290	0	5	7208.85	< 0.0001
FALSE	completeAO	NA	0.5015	0.0507	< 0.0001	5	4	14.89	0.0019

			Trend			ARMA order		Ljung-Box Test	
Logged	Method	Intercept	Coefficient	SE	p-value	AR	MA	Statistic	p-value
FALSE	trunc	12.0157	0.0312	0.0368	0.3967	0	1	4461.64	< 0.0001
FALSE	truncSA	12.2641	0.0157	0.0825	0.8487	2	2	163.10	0.0008
TRUE	complete	1.4753	0.0219	0.0150	0.1437	2	5	31.18	< 0.0001
TRUE	completeAO	1.4842	0.0214	0.0230	0.3521	4	5	43.13	< 0.0001
TRUE	trunc	2.3646	0.0125	0.0056	0.0248	0	5	819.11	< 0.0001
TRUE	truncSA	2.4686	0.0030	0.0064	0.6338	2	2	157.36	0.0021

Table A.170. Trend modeling results for weekly sediment temperature data at KOVA-086.

			Trend			ARMA order		Ljung-Box Test	
Logged	Method	Intercept	Coefficient	SE	p-value	AR	MA	Statistic	p-value
FALSE	complete	6.1440	0.0484	0.0535	0.3662	5	3	20.38	0.0001
FALSE	completeAO	6.3989	0.0263	0.1429	0.8541	4	1	27.67	< 0.0001
FALSE	trunc	11.8894	0.1004	0.1680	0.5501	2	0	10.07	0.6098
FALSE	truncSA	11.7451	0.0744	0.0530	0.1601	2	0	17.25	0.1405
TRUE	complete	1.6855	0.0153	0.0297	0.6055	1	1	24.30	0.0005
TRUE	completeAO	1.6887	0.0151	0.0356	0.6714	1	1	40.06	< 0.0001
TRUE	trunc	2.4438	0.0109	0.0142	0.4454	2	0	10.55	0.5682
TRUE	truncSA	2.4381	0.0081	0.0053	0.1241	2	0	13.32	0.4237

Table A.171. Top covariate models for daily sediment temperature data at KOVA-086.

Model	AICc	ΔAICc	Ljung-Box Test p-value
Air Temperature + Wind Speed + Relative Humidity + Daily Precipitation	1029.16	0.00	0.0623
Air Temperature + Wind Speed + Relative Humidity	1029.26	0.10	0.0628
Air Temperature + Wind Speed	1041.04	11.88	0.0651
Air Temperature + Wind Speed + Daily Precipitation	1042.54	13.38	0.0525
Air Temperature + Relative Humidity	1044.29	15.13	0.1107
Air Temperature + Relative Humidity + Daily Precipitation	1045.00	15.85	0.1086
Air Temperature	1054.93	25.78	0.3462
Air Temperature + Daily Precipitation	1056.75	27.59	0.1105
Wind Speed + Solar Radiation	1115.40	86.24	0.0521
Wind Speed	1117.96	88.80	0.2067

Table A.172. Coefficients and variance components estimates for the top covariate model for daily sediment temperature data at KOVA-086.

Parameter	Coefficient	SE	p-value
ar1	1.91	0.05	< 0.0001
ar2	-0.92	0.04	< 0.0001
ma1	-0.76	0.06	< 0.0001
ma2	-0.06	0.05	0.2696
ma3	-0.08	0.05	0.0885
intercept	10.32	0.36	< 0.0001
Air Temperature	0.10	0.01	< 0.0001
Wind Speed	0.09	0.02	< 0.0001
Relative Humidity	0.01	0.00	0.0002

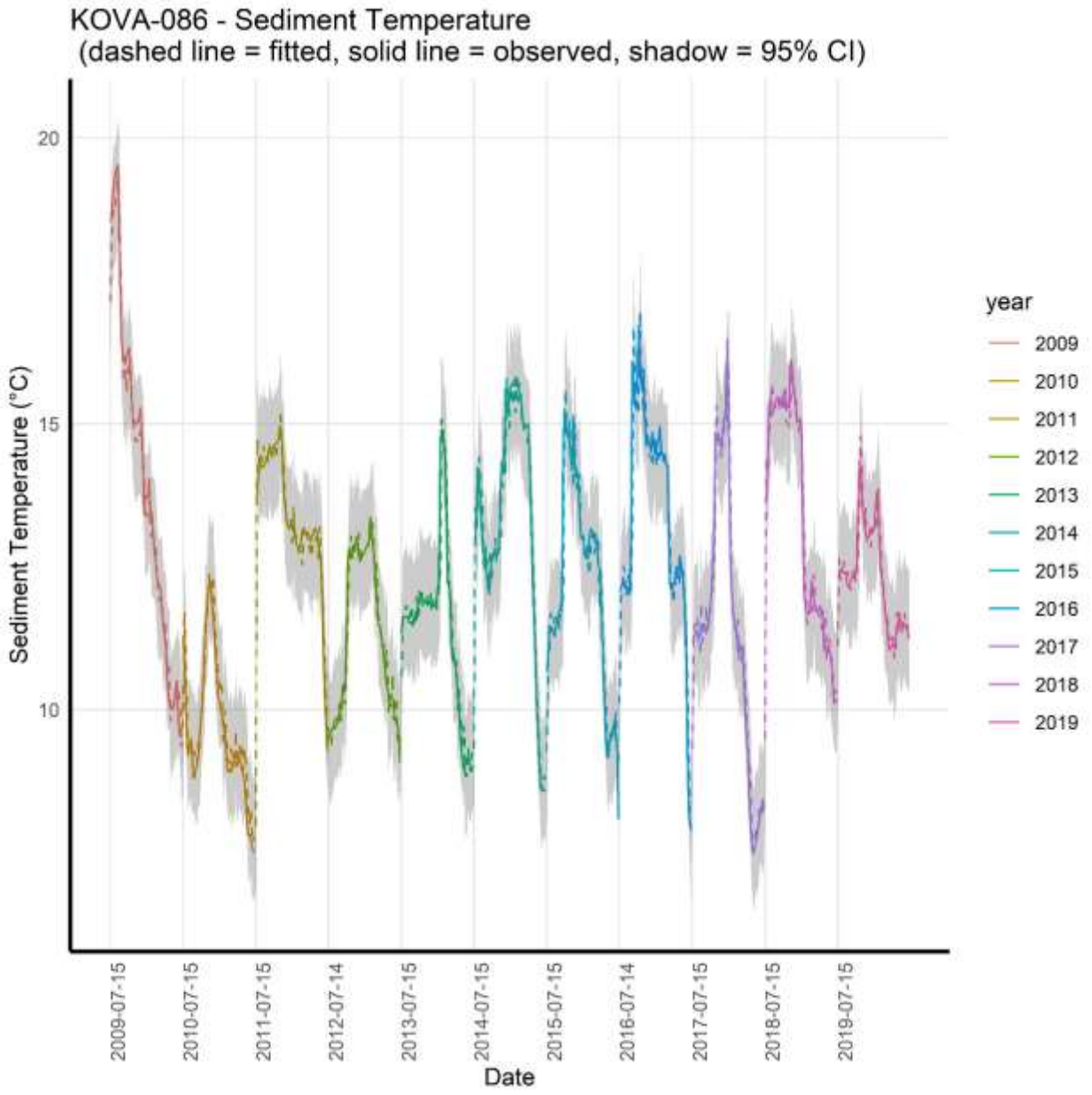


Figure A.161. Model predictions of KOVA-086 sediment temperature by date.

NOAT-052

Data

For the NOAT-052 lake, sediment temperature was recorded from 2015-2019. Over this period, there were 1272 records of sediment temperature. The complete dataset addressed two continuous periods, the first from June 2015 to September 2016, and the second from June 2017 to September 2019. Truncated to the 87 days that were sampled every year, the dataset had 435 observations.

Model Selection

For ARIMA models fitting all possible covariate combinations at lake NOAT-052 with sediment temperature as the response variable, AICc-based model selection resulted in ARIMA(1,0,2) with air temperature and month as the main covariates in the best model, but no annual trend term. The best trend model was an ARIMA(2,0,2) using the truncated dataset, which detected a significant negative trend in sediment temperature.

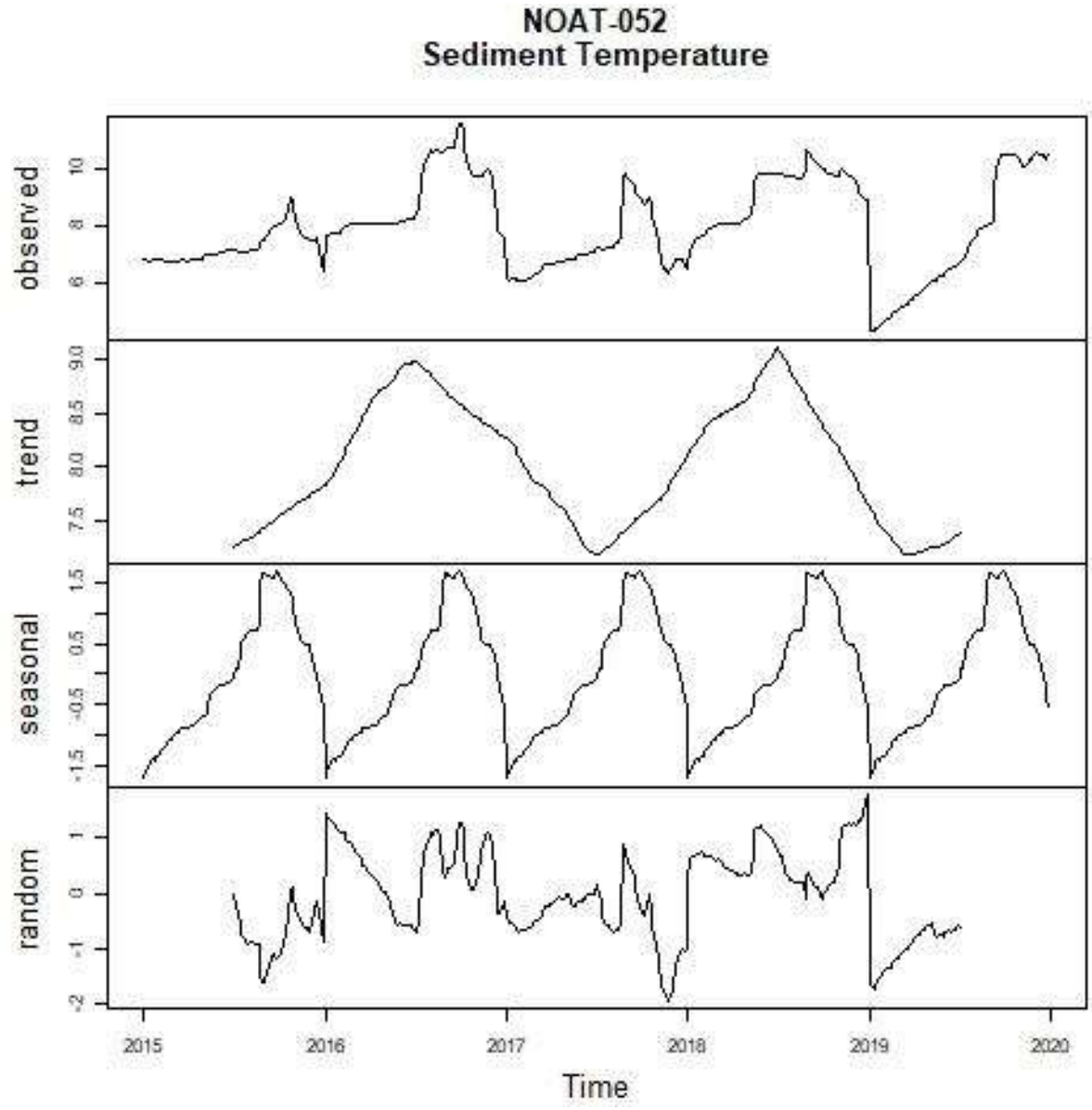


Figure A.162. Time series decomposition of truncated NOAT-052 sediment temperature by year.

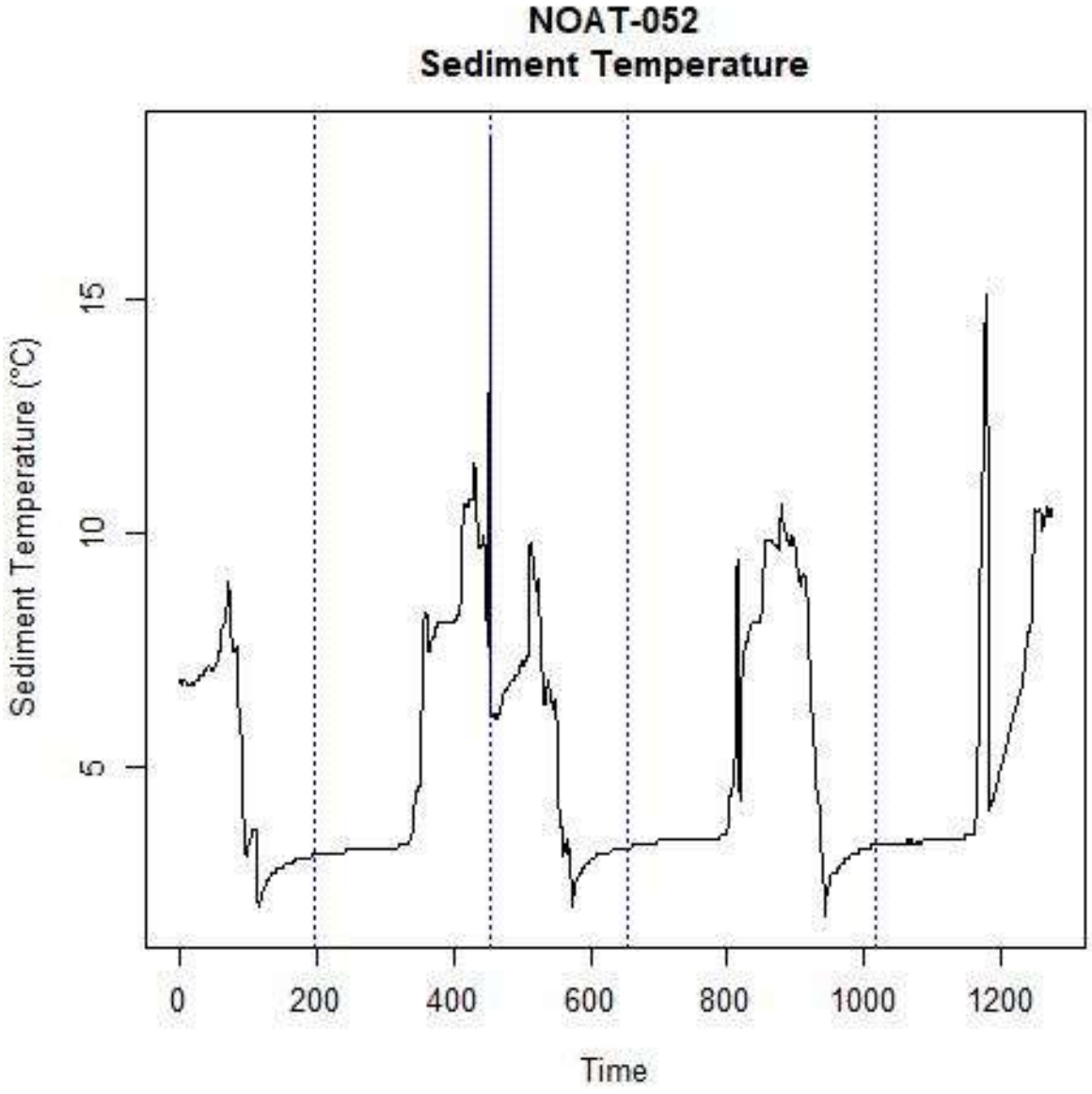


Figure A.163. Time series of NOAT-052 sediment temperature by time point with vertical lines for additive outliers.

Table A.173. Trend modeling results for daily sediment temperature data at NOAT-052.

			Trend			ARMA order		Ljung-Box Test	
Logged	**Method**	**Intercept**	**Coefficient**	**SE**	**p-value**	**AR**	**MA**	**Statistic**	**p-value**
FALSE	complete	0.8789	0.2848	0.0850	0.0008	0	5	1418.25	< 0.0001
FALSE	completeAO	-16.8711	1.4602	0.2898	< 0.0001	1	1	7.98	0.0465

			Trend			ARMA order		Ljung-Box Test	
Logged	**Method**	**Intercept**	**Coefficient**	**SE**	**p-value**	**AR**	**MA**	**Statistic**	**p-value**
FALSE	trunc	25.2099	-1.1118	0.1392	< 0.0001	2	2	66.79	0.8721
FALSE	truncSA	7.8392	0.0246	0.1202	0.8381	2	0	96.03	0.1554
TRUE	complete	0.7502	0.0519	0.0130	< 0.0001	0	5	2134.67	< 0.0001
TRUE	completeAO	NA	0.1086	0.0119	< 0.0001	1	3	5.89	0.1169
TRUE	trunc	2.5540	-0.0329	0.0106	0.0019	0	5	893.58	< 0.0001
TRUE	truncSA	2.0528	0.0020	0.0169	0.9036	1	1	81.25	0.5337

Table A.174. Top covariate models for daily sediment temperature data at NOAT-052.

Model	**AICc**	**ΔAICc**	**Ljung-Box Test p-value**
Air Temperature + Month	1810.81	0.00	0.5515
Air Temperature + Relative Humidity + Month	1812.23	1.42	0.3697
Air Temperature + Daily Precipitation + Month	1812.76	1.96	0.3837
Solar Radiation + Month	1813.80	2.99	0.5181
Relative Humidity + Month	1814.50	3.69	0.5302
Wind Speed + Month	1815.11	4.30	0.5569
Daily Precipitation + Month	1815.38	4.58	0.5538
Wind Speed + Solar Radiation + Month	1815.41	4.61	0.3565
Solar Radiation + Daily Precipitation + Month	1815.50	4.69	0.3458
Wind Speed + Solar Radiation + Daily Precipitation + Month	1817.05	6.24	0.3282

Table A.175. Coefficients and variance components estimates for the top covariate model for daily sediment temperature data at NOAT-052.

Parameter	**Coefficient**	**SE**	**p-value**
ar1	0.98	0.01	< 0.0001
ma1	0.10	0.03	0.0003
ma2	-0.14	0.03	< 0.0001
intercept	5.82	0.80	< 0.0001
Air Temperature	0.01	0.00	0.0319
Month	-0.08	0.02	0.0016

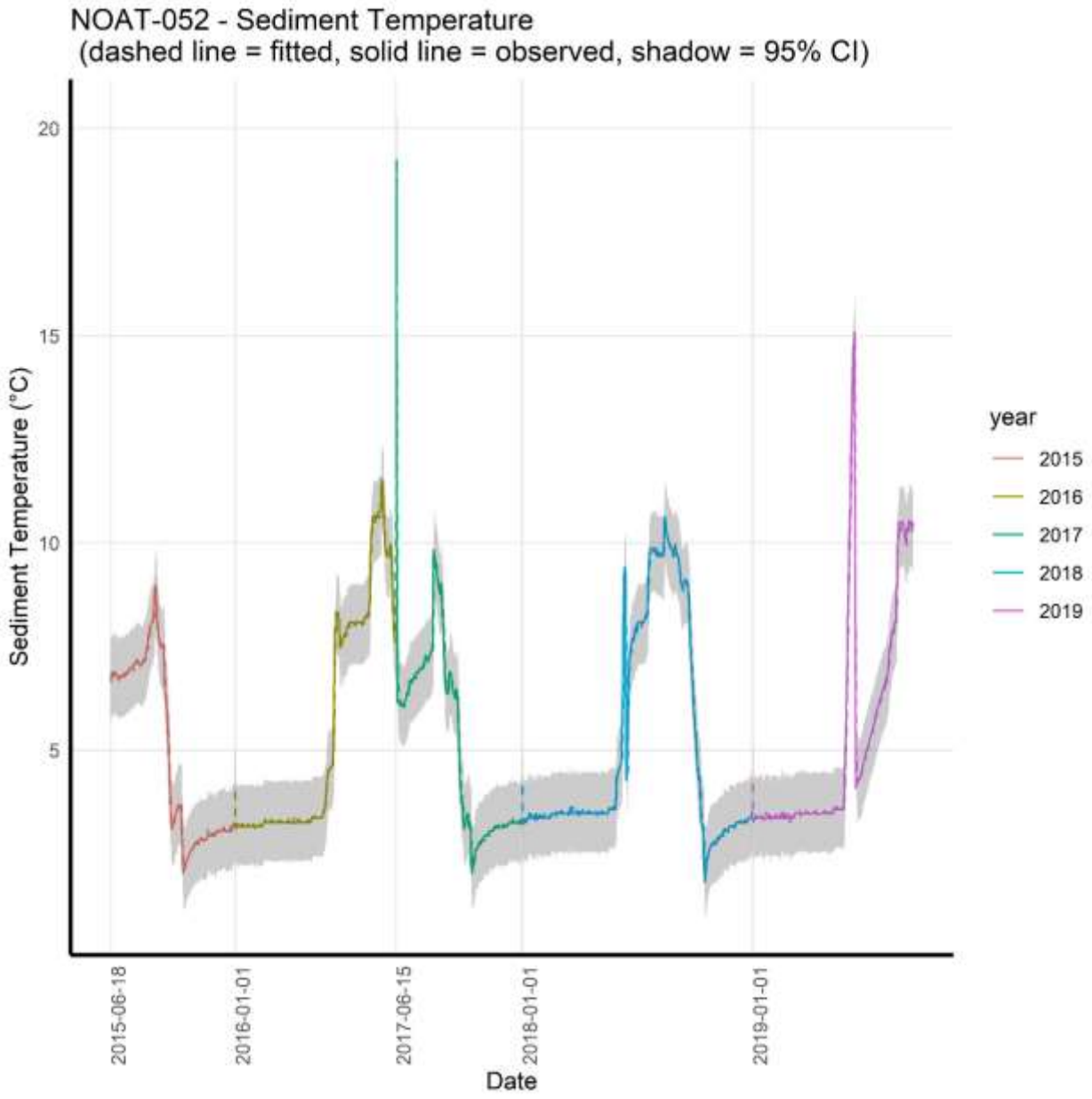


Figure A.164. Model predictions of NOAT-052 sediment temperature by date.

NOAT-107

Data

For the NOAT-107 lake, sediment temperature was recorded from 2014-2018. However, no data were recorded in 2016, so the analysis only included 2017 and 2018. Over this period, 365 records of sediment temperature were observed. Being a single year, further truncation was not productive. Covariate coverage was adequate for modeling.

Model Selection

For ARIMA models fitting all possible covariate combinations at lake NOAT-107 with sediment temperature as the response variable, AICc-based model selection resulted in ARIMA(1,0,2) with air temperature and wind speed as the main covariates in the best model, but no annual trend term was possible due to the short duration of the dataset. No trend model with stationary residuals was obtained.

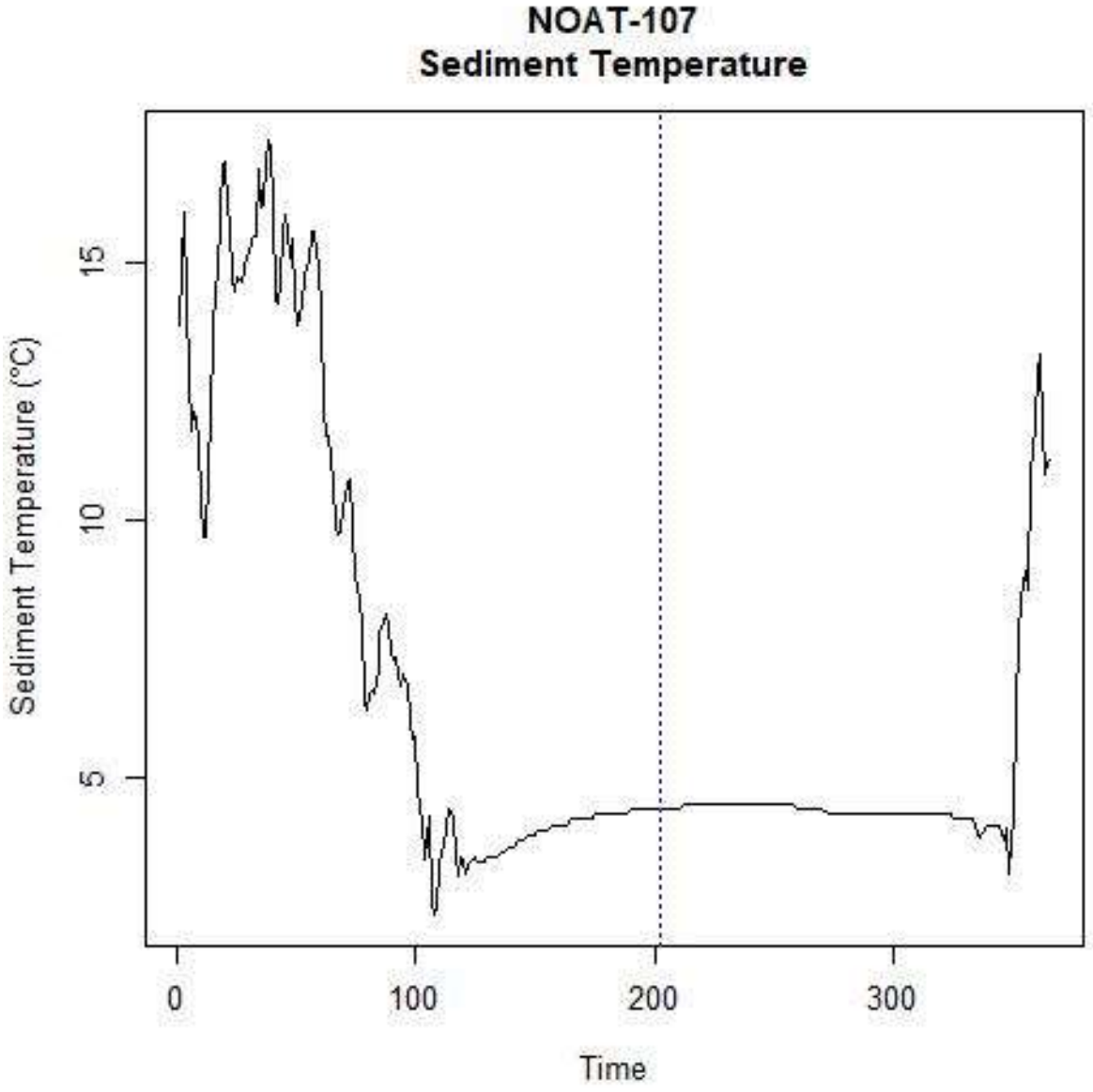


Figure A.165. Time series of NOAT-107 sediment temperature by time point with vertical lines for additive outliers.

Table A.176. Trend modeling results for daily sediment temperature data at NOAT-107.

			Trend			ARMA order		Ljung-Box Test	
Logged	**Method**	**Intercept**	**Coefficient**	**SE**	**p-value**	**AR**	**MA**	**Statistic**	**p-value**
FALSE	complete	8.6951	-0.0078	0.3675	0.9831	4	3	21.36	< 0.0001
FALSE	completeAO	8.9468	-0.0283	0.6632	0.9660	4	3	21.53	< 0.0001

			Trend			ARMA order		Ljung-Box Test	
Logged	**Method**	**Intercept**	**Coefficient**	**SE**	**p-value**	**AR**	**MA**	**Statistic**	**p-value**
TRUE	complete	2.0150	-0.0019	0.0548	0.9729	2	0	16.66	0.0106
TRUE	completeAO	NA	0.1182	0.0213	< 0.0001	2	0	16.58	0.0109

Table A.177. Top covariate models for daily sediment temperature data at NOAT-107.

Model	**AICc**	**ΔAICc**	**Ljung-Box Test p-value**
Air temperature + Wind Speed	379.97	0	0.0885

Table A.178. Coefficients and variance components estimates for the top covariate model for daily sediment temperature data at NOAT-107.

Parameter	**Coefficient**	**SE**	**p-value**
ar1	-0.19	0.34	0.5764
ar2	0.48	0.26	0.0628
ar3	0.31	0.31	0.3045
ar4	0.36	0.27	0.1880
ma1	1.68	0.34	< 0.0001
ma2	1.38	0.55	0.0112
ma3	0.84	0.46	0.0662
ma4	0.20	0.21	0.3371
ma5	-0.11	0.09	0.2254
intercept	8.06	2.46	0.0010
Air Temperature	0.01	0.01	0.1623
Wind Speed	0.00	0.01	0.6736

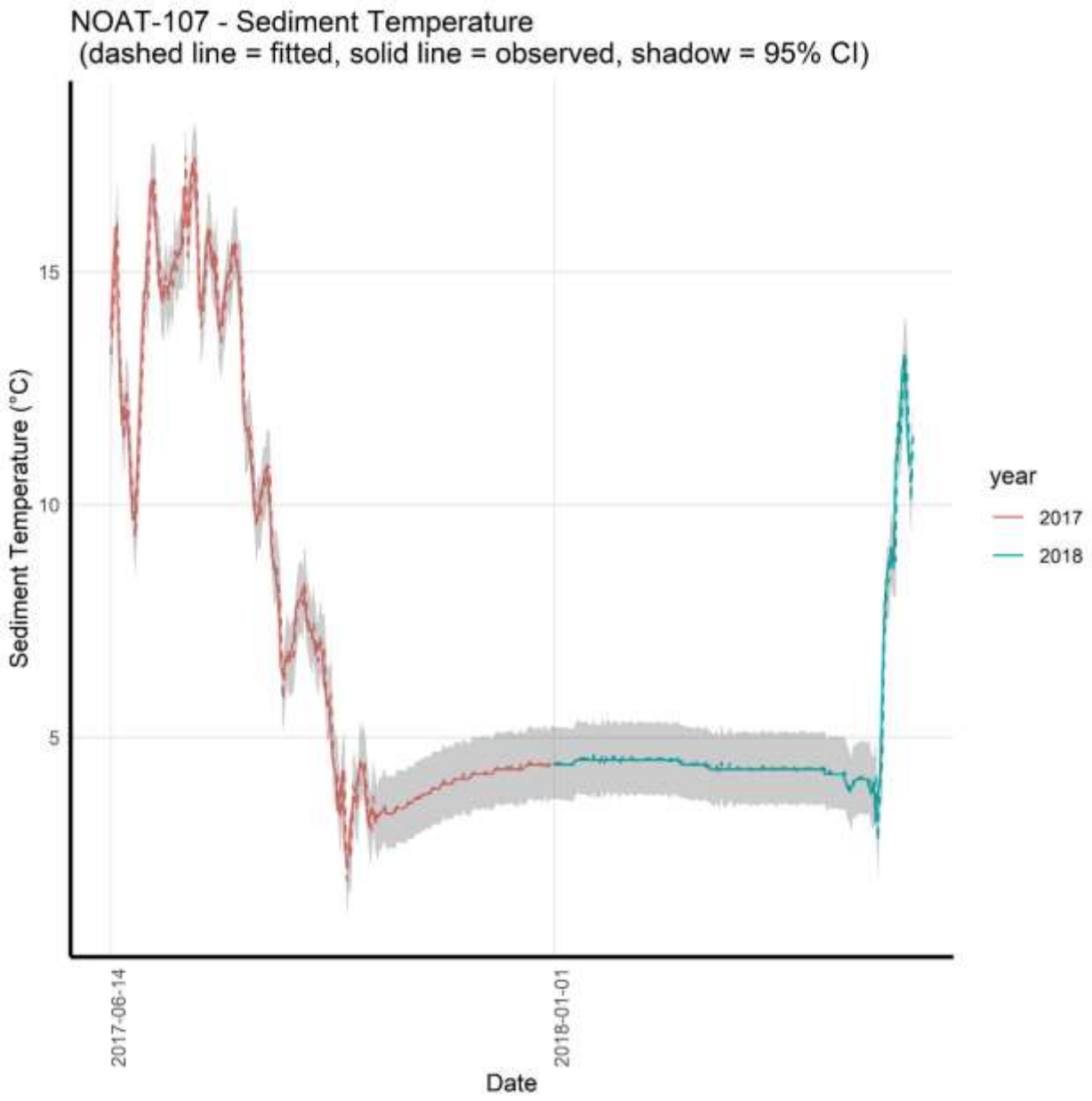


Figure A.166. Model predictions of NOAT-107 sediment temperature by date.

WRST-005

Data

For the WRST-005 lake, sediment temperature was recorded from 2010 to 2018. Over this period, there were 2428 records of sediment temperature. Data were collected for the full year in most years, but started in May in 2010, 2015, and 2017 and ended in September in 2014 and 2018. The record of sediment temperature ends in May of 2018. Truncation to a common set of days sampled in every year required the exclusion of 2018. Truncation left 110 days per year and 880 days overall in the dataset. Covariate coverage was poor in parts of 2015, 2016, and 2018. Restricting covariate analysis to the years 2010 to 2014 produced no stationary models. However, using the truncated dataset (2010-2017), which only included days between May and September, avoided the seasons with low data coverage and allowed successful covariate analysis with no further truncation.

Model Selection

For ARIMA models fitting all possible covariate combinations at lake WRST-005 with sediment temperature as the response variable, AICc-based model selection resulted in ARIMA(2,0,0) with wind speed and solar radiation as the main covariates in the best model, but no annual trend term. The best trend model was an ARIMA(2,0,1) using the truncated dataset. The model detected a significant positive trend in sediment temperature over time.

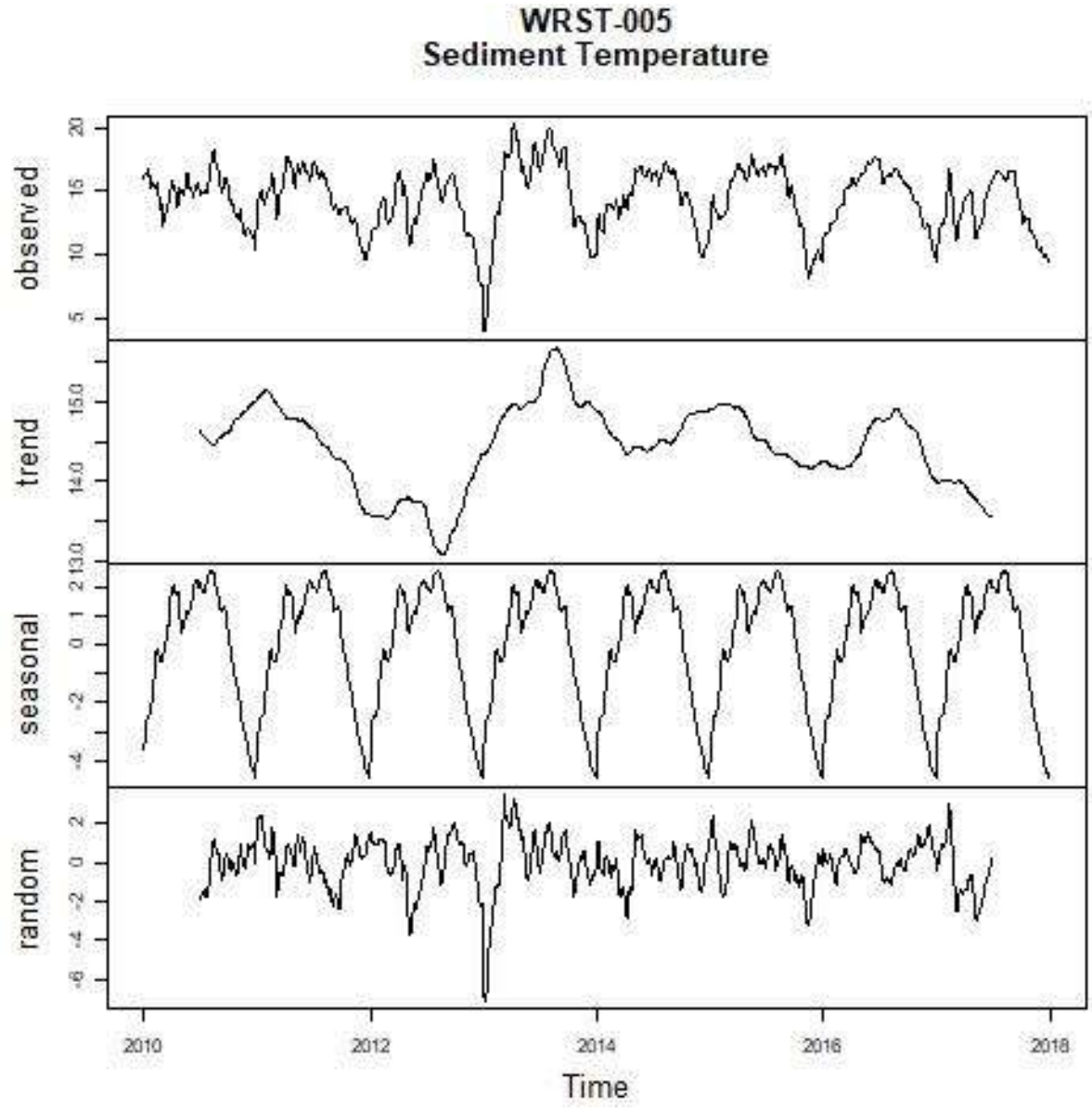


Figure A.167. Time series decomposition of truncated WRST-005 sediment temperature by year.

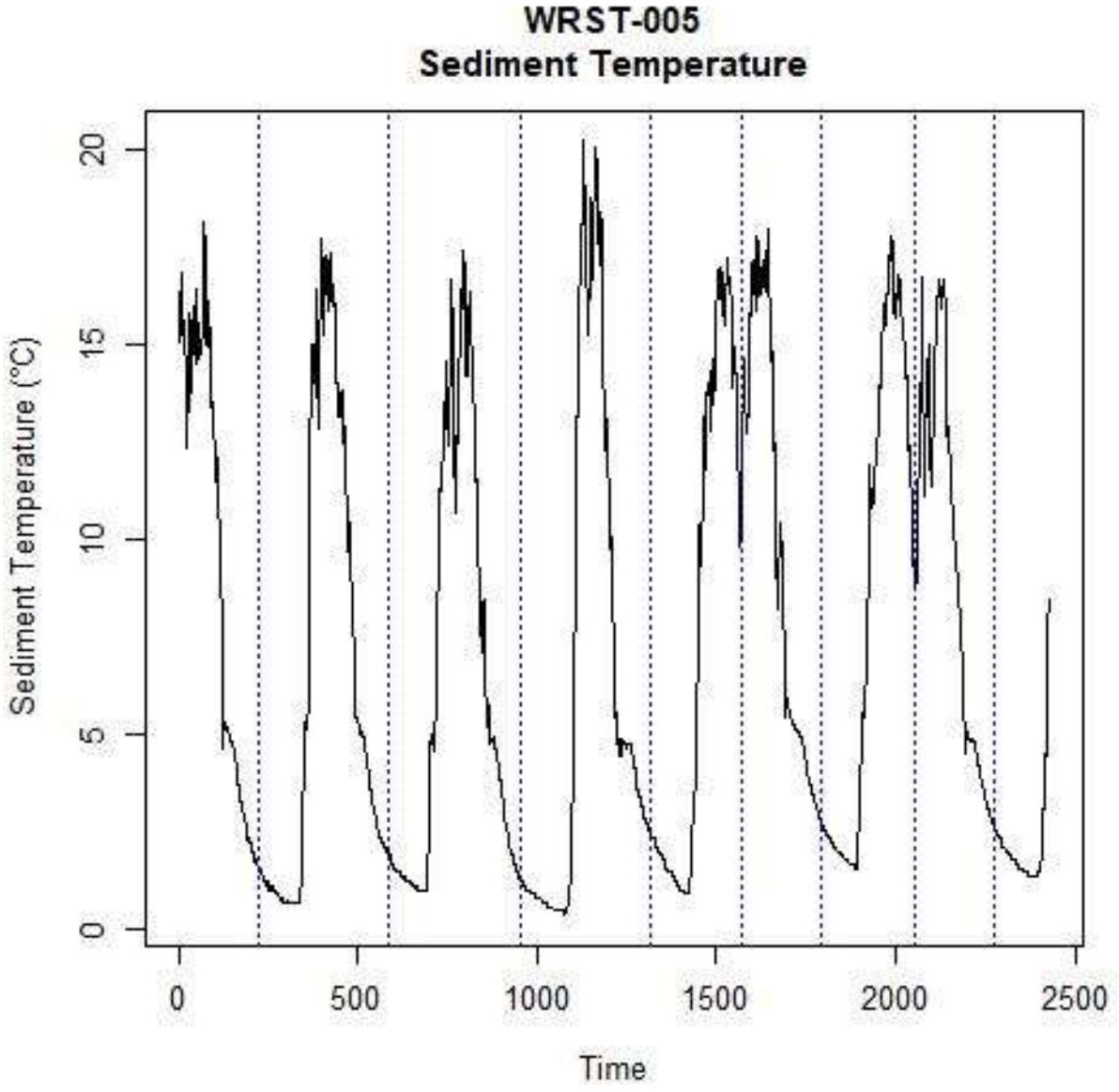


Figure A.168. Time series of WRST-005 sediment temperature by time point with vertical lines for additive outliers.

Table A.179. Trend modeling results for daily sediment temperature data at WRST-005.

			Trend			ARMA order		Ljung-Box Test	
Logged	**Method**	**Intercept**	**Coefficient**	**SE**	**p-value**	**AR**	**MA**	**Statistic**	**p-value**
FALSE	complete	6.8549	0.0345	0.0520	0.5067	0	5	8297.88	< 0.0001
FALSE	completeAO	7.6660	-0.0361	0.0626	0.5640	0	5	14431.43	< 0.0001

			Trend			ARMA order		Ljung-Box Test	
Logged	Method	Intercept	Coefficient	SE	p-value	AR	MA	Statistic	p-value
FALSE	trunc	5.1212	0.7942	0.1457	< 0.0001	2	1	187.45	0.1846
FALSE	truncSA	15.1597	-0.0613	0.0772	0.4271	2	0	174.87	0.4248
TRUE	complete	1.3536	0.0126	0.0103	0.2239	2	3	7.33	0.0622
TRUE	completeAO	1.4092	0.0091	0.0185	0.6222	3	3	20.36	0.0001
TRUE	trunc	2.4306	0.0186	0.0118	0.1149	2	0	174.46	0.4333
TRUE	truncSA	2.7193	-0.0057	0.0067	0.3983	2	0	147.66	0.9105

Table A.180. Top covariate models for daily sediment temperature data at WRST-005.

Model	AICc	ΔAICc	Ljung-Box Test p-value
Wind Speed + Solar Radiation	925.68	0.00	0.2523
Solar Radiation	930.69	5.01	0.3057
Wind Speed + Month	930.74	5.06	0.0507
Daily Precipitation	951.47	25.79	0.1284
Wind Speed + Daily Precipitation	951.60	25.92	0.0811
Air Temperature + Daily Precipitation	952.04	26.36	0.0817
Relative Humidity	954.68	29.00	0.1687
Air Temperature + Wind Speed	959.08	33.40	0.0931
Air Temperature	959.76	34.08	0.1399
Intercept Only	961.86	36.18	0.2079

Table A.181. Coefficients and variance components estimates for the top covariate model for daily sediment temperature data at WRST-005.

Parameter	Coefficient	SE	p-value
ar1	1.47	0.03	< 0.0001
ar2	-0.50	0.03	< 0.0001
intercept	14.48	0.58	< 0.0001
Wind Speed	0.07	0.03	0.0079
Solar Radiation	0.00	0.00	< 0.0001

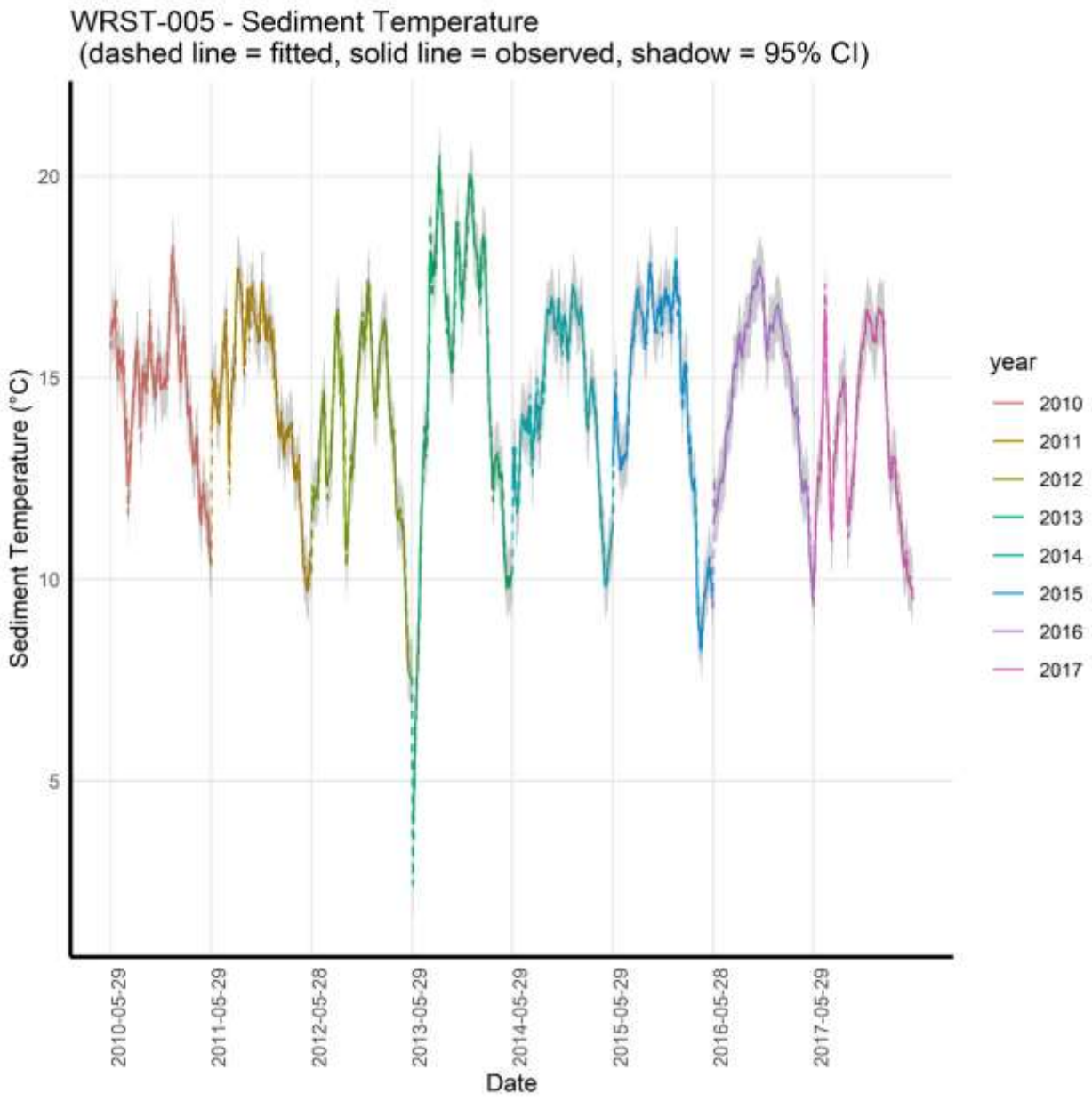


Figure A.169. Model predictions of WRST-005 sediment temperature by date.

WRST-016

Data

For the WRST-016 lake, sediment temperature was recorded from 2010 to 2018. Over this period, there were 2428 records of sediment temperature. Data were collected for the full year in most years, but started in May in 2010, 2015, and 2017 and ended in September in 2014 and 2018. The record of sediment temperature ends in May of 2018. Truncation to a common set of days sampled in every year required the exclusion of 2018. Truncation left 110 days per year and 880 days overall in the dataset. Covariate coverage was poor in parts of 2015, 2016, and 2018. Restricting covariate analysis to the years 2010 to 2014 produced no stationary models. However, using the truncated dataset (2010-2017), which only included days between May and September, avoided the seasons with low data coverage and allowed successful covariate analysis with no further truncation.

When aggregated to weekly mean values, the sediment temperature dataset contained 493 observations. When truncating to the subset of 13 common weeks sampled in every year the number of observations was reduced to 130.

Model Selection

For ARIMA models fitting all possible covariate combinations at lake WRST-016 with sediment temperature as the response variable, AICc-based model selection resulted in ARIMA(1,0,0) with relative humidity and month as the main covariates in the best model, but no annual trend term. No trend model of daily data exhibited stationarity.

When fitting trend models to the weekly sediment temperature data the truncated and truncated seasonally adjusted datasets yielded stationary residuals for both the logged and unlogged data. Of these four models, three included a positive trend coefficient that was significantly greater than zero, providing evidence for an increasing trend in sediment temperature at lake WRST-016. It should however be noted that this trend may be driven by the 2019 sediment temperature data which do not follow the consistent annual warming and cooling trend observed in the previous years. The data from 2019 should be inspected closely to ensure they are accurate.

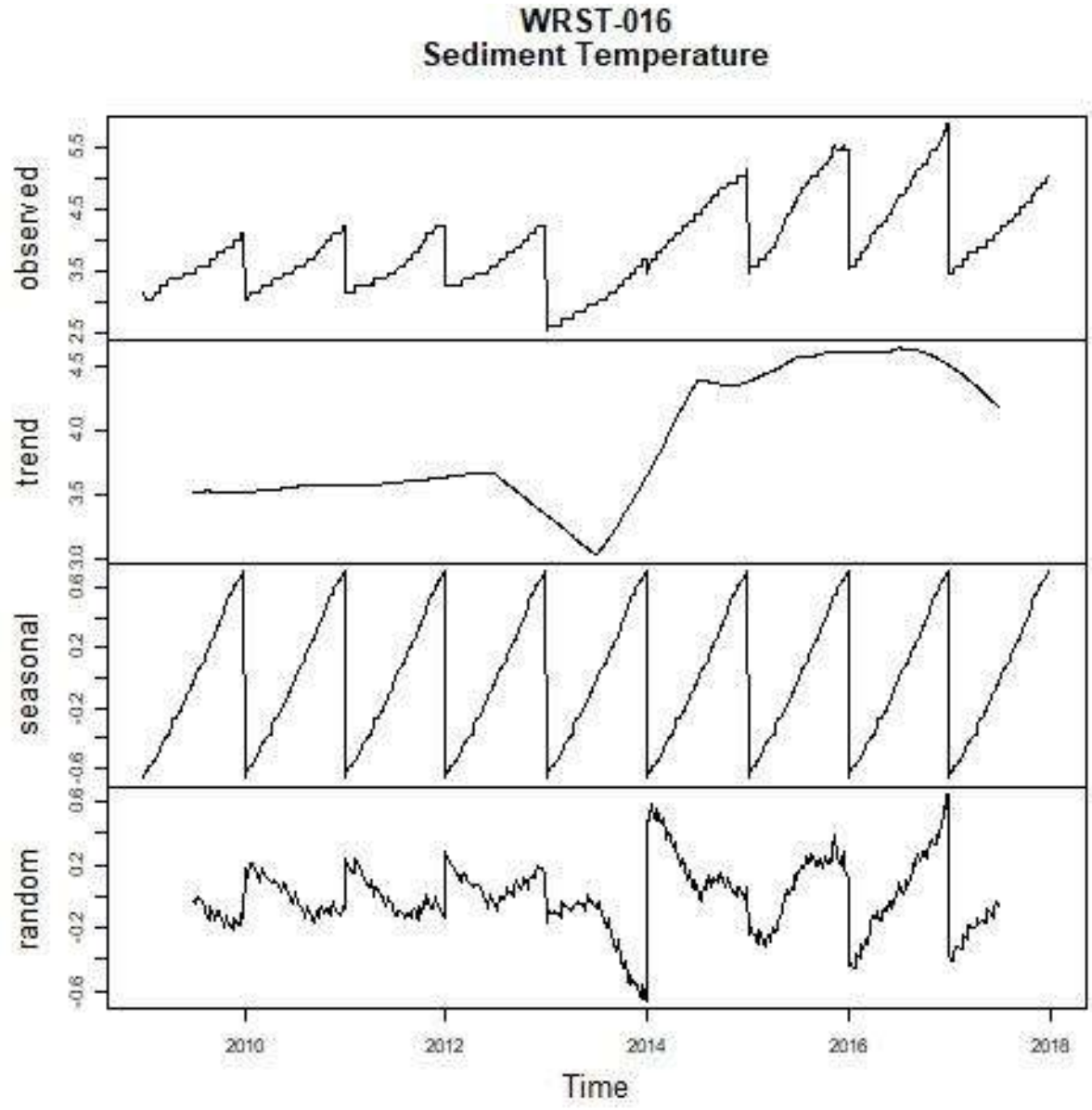


Figure A.170. Time series decomposition of truncated WRST-016 sediment temperature by year.

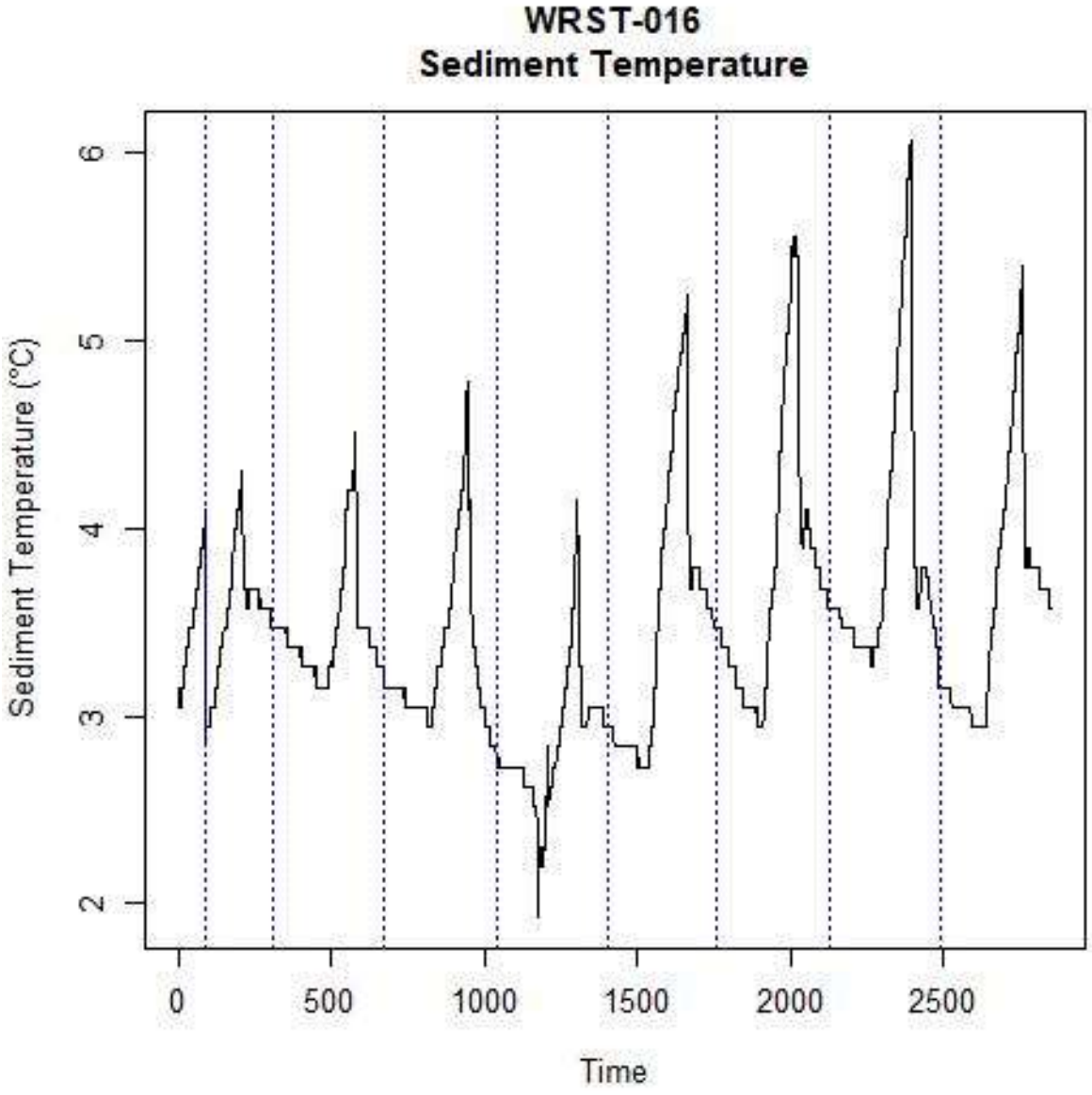


Figure A.171. Time series of WRST-016 sediment temperature by time point with vertical lines for additive outliers.

Table A.182. Trend modeling results for daily sediment temperature data at WRST-016.

			Trend			ARMA order		Ljung-Box Test	
Logged	**Method**	**Intercept**	**Coefficient**	**SE**	**p-value**	**AR**	**MA**	**Statistic**	**p-value**
FALSE	complete	3.0998	0.0336	0.0066	< 0.0001	0	5	6999.17	< 0.0001
FALSE	completeAO	2.8706	0.0535	0.0051	< 0.0001	0	1	33306.22	< 0.0001

			Trend			ARMA order		Ljung-Box Test	
Logged	**Method**	**Intercept**	**Coefficient**	**SE**	**p-value**	**AR**	**MA**	**Statistic**	**p-value**
FALSE	trunc	2.9784	0.0847	0.0151	< 0.0001	0	5	1604.01	< 0.0001
FALSE	truncSA	2.4543	0.1323	0.0086	< 0.0001	0	5	2837.42	< 0.0001
TRUE	complete	1.1320	0.0089	0.0018	< 0.0001	0	5	6657.37	< 0.0001
TRUE	completeAO	1.0981	0.0118	0.0018	< 0.0001	0	5	11941.25	< 0.0001
TRUE	trunc	0.9795	0.0335	0.0023	< 0.0001	0	1	7861.95	< 0.0001
TRUE	truncSA	0.9954	0.0321	0.0021	< 0.0001	0	5	3377.76	< 0.0001

Table A.183. Trend modeling results for weekly sediment temperature data at WRST-016.

			Trend			ARMA order		Ljung-Box Test	
Logged	**Method**	**Intercept**	**Coefficient**	**SE**	**p-value**	**AR**	**MA**	**Statistic**	**p-value**
FALSE	complete	4.3147	-0.0419	0.1078	0.6975	1	1	19.32	0.0037
FALSE	completeAO	3.6703	0.0693	0.1480	0.6393	1	1	30.21	< 0.0001
FALSE	trunc	NA	0.9490	0.1842	< 0.0001	1	0	12.77	0.9568
FALSE	truncSA	NA	0.8182	0.1537	< 0.0001	1	0	13.57	0.9558
TRUE	complete	1.4029	-0.0158	0.0211	0.4551	1	1	17.04	0.0091
TRUE	completeAO	1.2527	0.0111	0.0257	0.6659	1	1	22.92	< 0.0001
TRUE	trunc	1.2328	0.0660	0.0412	0.1094	1	0	12.28	0.9513
TRUE	truncSA	1.0642	0.0956	0.0210	< 0.0001	1	0	6.25	0.9998

Table A.184. Top covariate models for daily sediment temperature data at WRST-016.

Model	**AICc**	**ΔAICc**	**Ljung-Box Test p-value**
Relative Humidity + Month	-1353.59	0.00	0.2523
Wind Speed + Month	-1352.11	1.48	0.2546
Daily Precipitation + Month	-1351.92	1.68	0.2453
Wind Speed + Daily Precipitation + Month	-1350.16	3.43	0.1632
Air Temperature + Daily Precipitation	-758.69	594.90	0.4705
Air Temperature + Wind Speed + Daily Precipitation	-757.10	596.49	0.3425
Air Temperature	-755.88	597.71	0.6620
Air Temperature + Wind Speed	-754.38	599.21	0.5349
Relative Humidity	-680.49	673.10	0.9968
Wind Speed	-679.98	673.62	0.9982

Table A.185. Coefficients and variance components estimates for the top covariate model for daily sediment temperature data at WRST-016.

Parameter	Coefficient	SE	p-value
ar1	0.98	0.01	< 0.0001
intercept	1.38	0.23	< 0.0001
Relative Humidity	0.00	0.00	0.1881
Month	0.34	0.01	< 0.0001

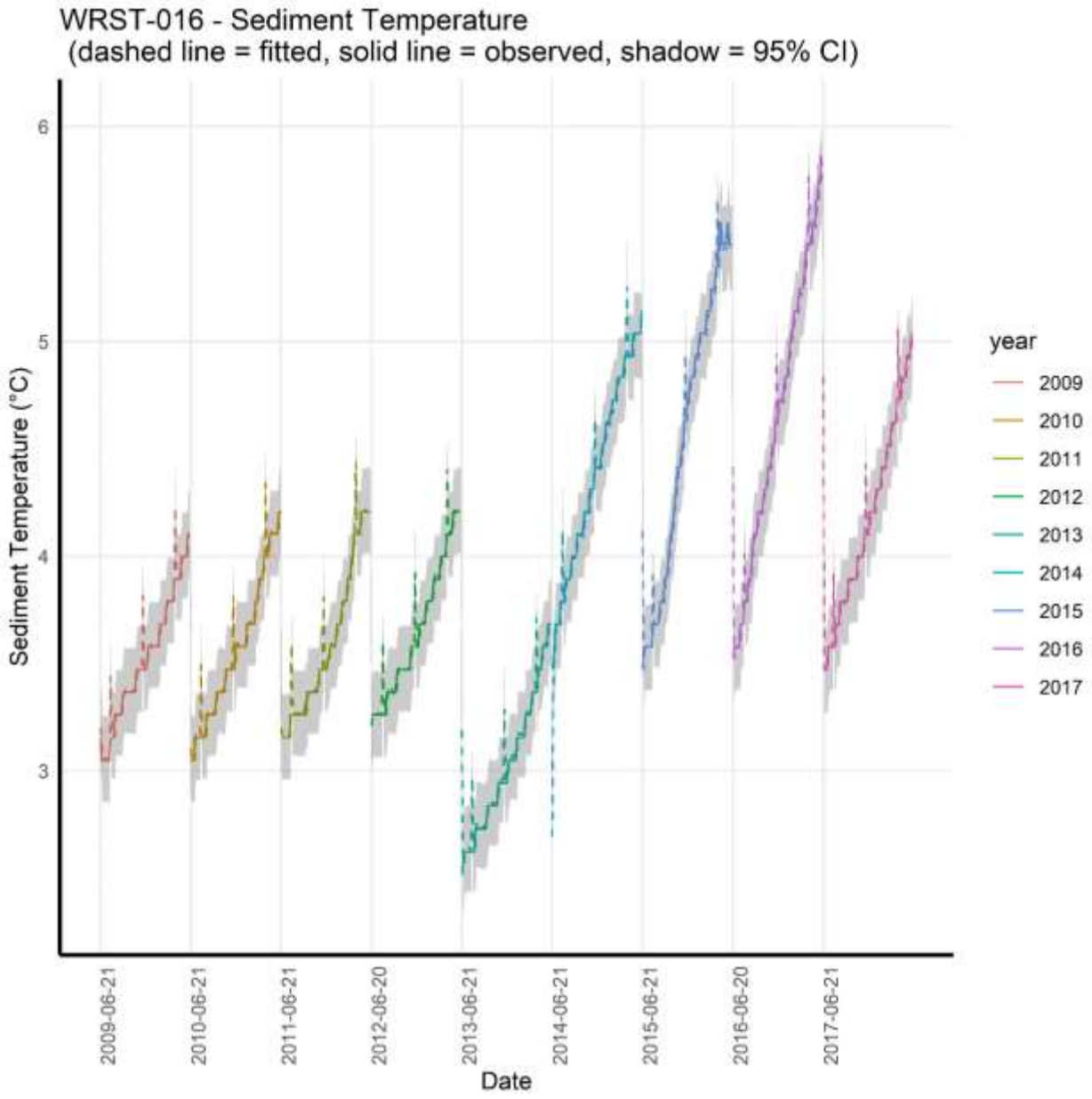


Figure A.172. Model predictions of WRST-016 sediment temperature by date.

YUCH-004

Data

For the YUCH-004 lake, sediment temperature was recorded from September 2010 to September 2019. Over this period, there were 3402 records of sediment temperature. Truncation to a common set of 116 days sampled in every year left 1160 days overall in the dataset. Covariate coverage was poor in 2019, so covariate modeling addressed 2010-2018. Covariate analysis with the complete record over this period produced no stationary models, so the truncated dataset was used.

Model Selection

For ARIMA models fitting all possible covariate combinations at lake YUCH-004 with sediment temperature as the response variable, AICc-based model selection resulted in ARIMA(1,0,0) with wind speed and month as the main covariates in the best model, but no annual trend term. The best trend model was ARIMA(2,0,1) with the seasonally adjusted and truncated dataset. No significant trend in sediment temperature was detected.

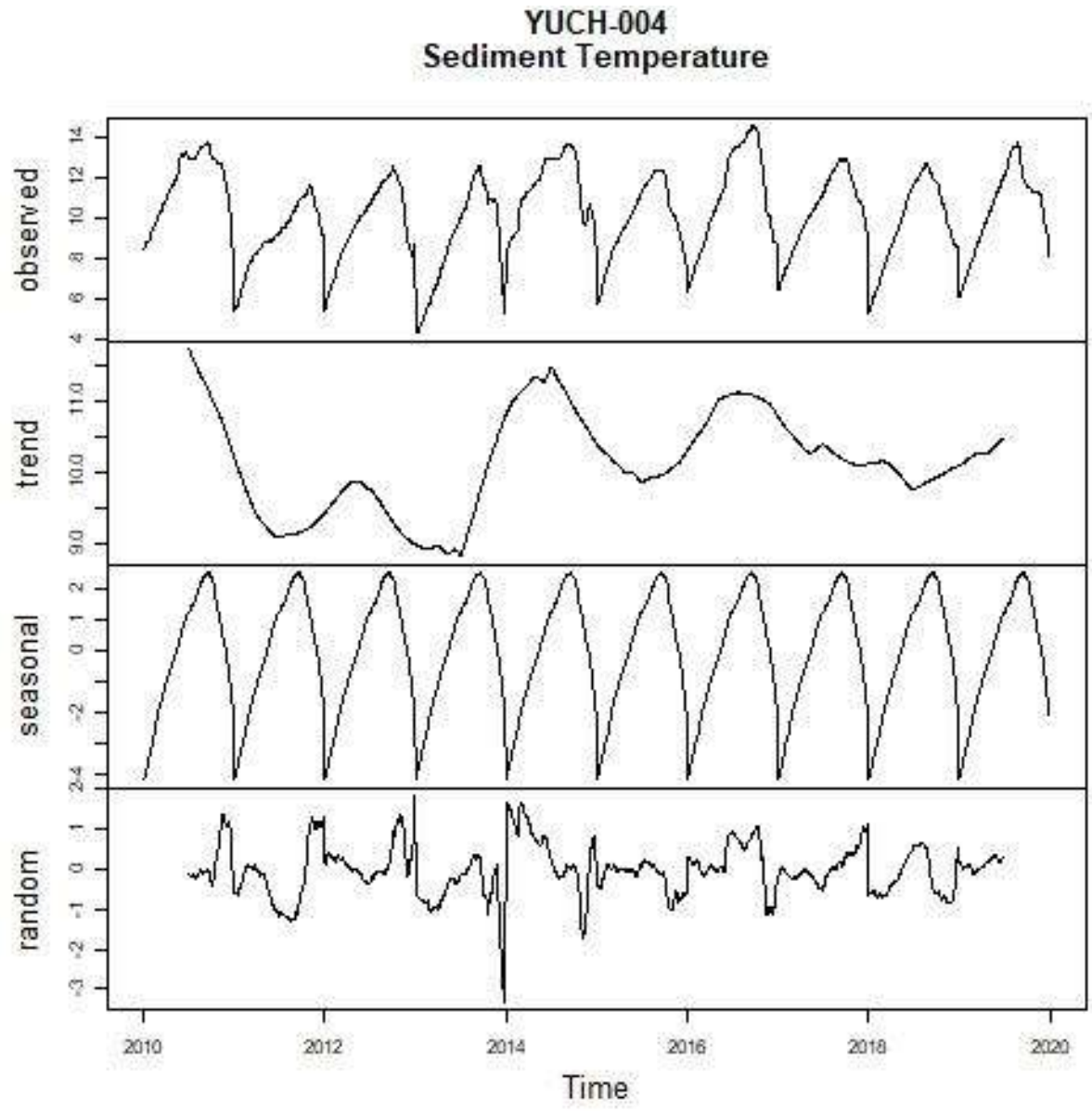


Figure A.173. Time series decomposition of truncated YUCH-004 sediment temperature by year.

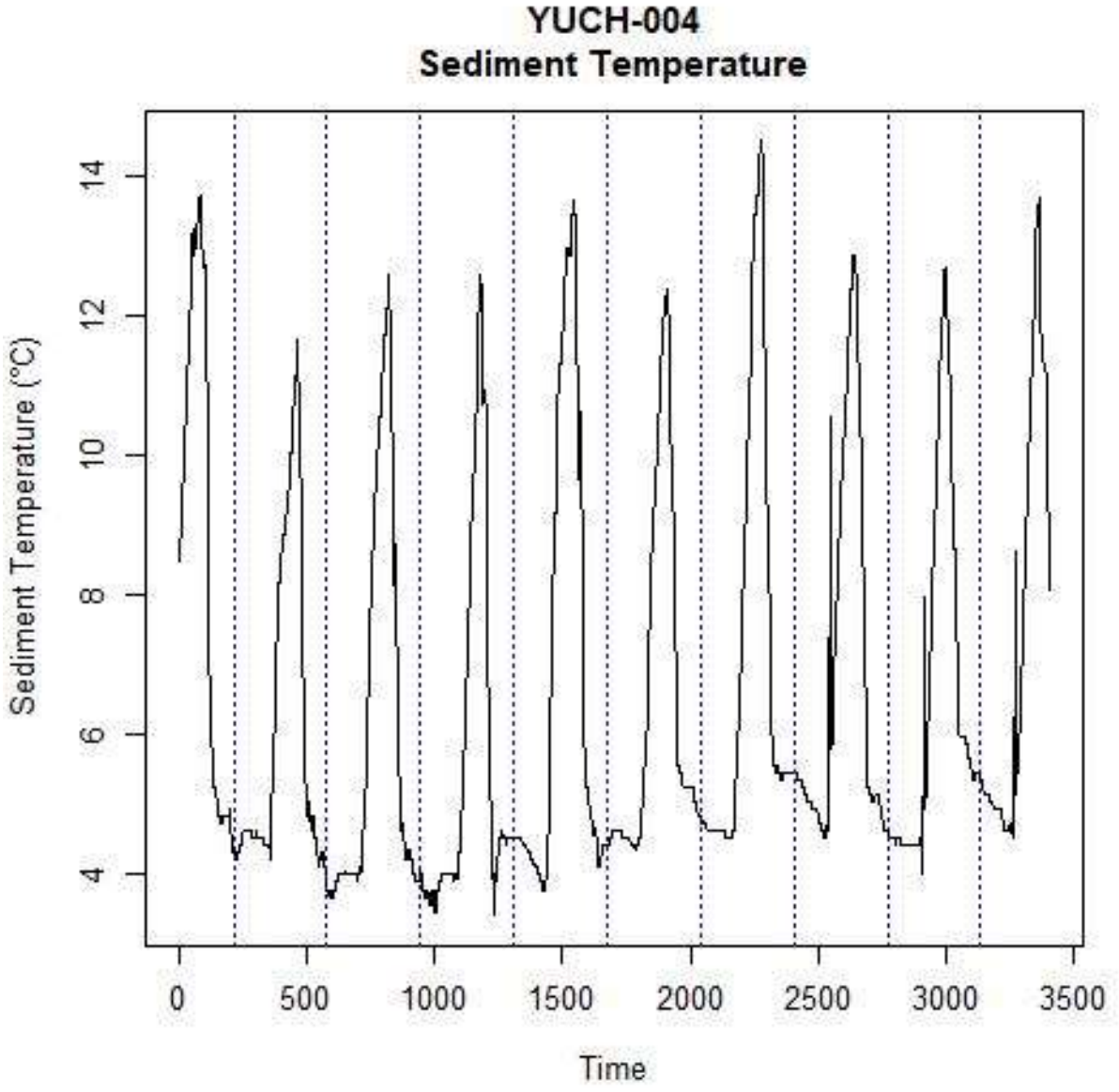


Figure A.174. Time series of YUCH-004 sediment temperature by time point with vertical lines for additive outliers.

Table A.186. Trend modeling results for daily sediment temperature data at YUCH-004.

			Trend			ARMA order		Ljung-Box Test	
Logged	**Method**	**Intercept**	**Coefficient**	**SE**	**p-value**	**AR**	**MA**	**Statistic**	**p-value**
FALSE	complete	6.7253	-0.0074	0.0307	0.8102	2	2	54.40	< 0.0001
FALSE	completeAO	6.9840	-0.0326	0.0607	0.5907	2	2	68.91	< 0.0001

			Trend			ARMA order		Ljung-Box Test	
Logged	Method	Intercept	Coefficient	SE	p-value	AR	MA	Statistic	p-value
FALSE	trunc	11.3051	-0.1004	0.0303	0.0009	0	4	16798.37	< 0.0001
FALSE	truncSA	10.3991	-0.0100	0.0538	0.8522	2	1	238.54	0.2865
TRUE	complete	1.7261	0.0078	0.0029	0.0061	0	5	10874.28	< 0.0001
TRUE	completeAO	1.8730	-0.0062	0.0085	0.4674	2	2	127.93	< 0.0001
TRUE	trunc	2.4090	-0.0097	0.0037	0.0082	0	4	8462.64	< 0.0001
TRUE	truncSA	2.3260	-0.0017	0.0067	0.8012	1	2	234.17	0.3578

Table A.187. Top covariate models for daily sediment temperature data at YUCH-004.

Model	AICc	ΔAICc	Ljung-Box Test p-value
Wind Speed + Month	-8.03	0.00	0.2975
Daily Precipitation + Month	-7.45	0.58	0.3034
Wind Speed + Daily Precipitation + Month	-6.00	2.03	0.1765
Air Temperature	224.81	232.84	0.1106
Air Temperature + Daily Precipitation	226.40	234.43	0.0703
Air Temperature + Wind Speed	226.76	234.79	0.0675
Air Temperature + Wind Speed + Daily Precipitation	228.35	236.38	0.0644
Wind Speed + Relative Humidity	272.53	280.56	0.0704
Relative Humidity	273.22	281.25	0.0747
Solar Radiation	276.43	284.46	0.1224

Table A.188. Coefficients and variance components estimates for the top covariate model for daily sediment temperature data at YUCH-004.

Parameter	Coefficient	SE	p-value
ar1	1.88	0.04	< 0.0001
ar2	-0.89	0.04	< 0.0001
ma1	-0.72	0.06	< 0.0001
intercept	6.67	0.42	< 0.0001
Wind Speed	0.01	0.01	0.4465
Month	0.47	0.02	< 0.0001

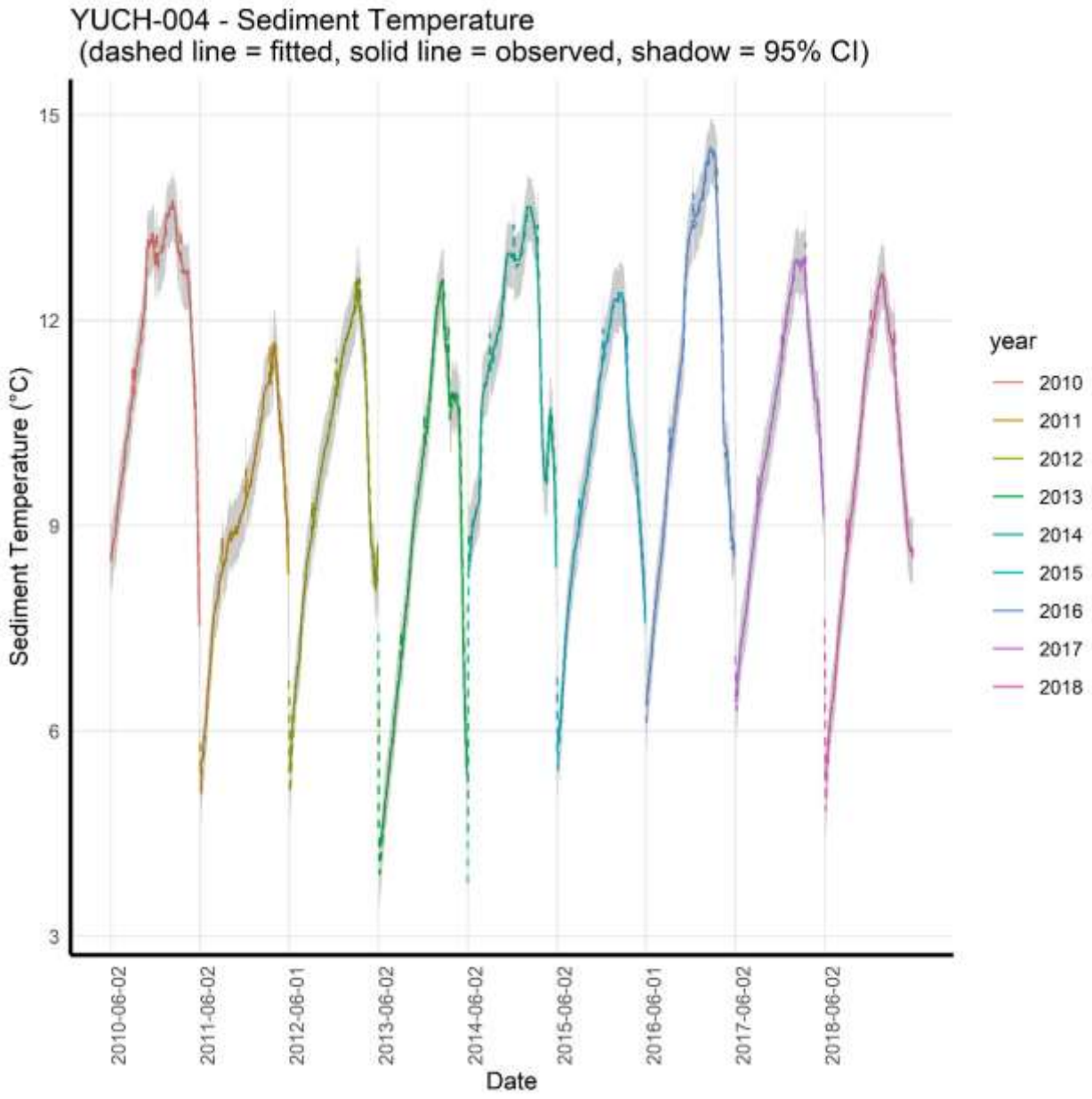


Figure A.175. Model predictions of YUCH-004 sediment temperature by date.

YUCH-005

Data

For the YUCH-005 lake, sediment temperature was recorded from May 2009 to September 2019. However, all of summer 2018 was missing, so analysis was restricted to the 2097 records between 2009 and 2017. There were nine missing days in 2013 and one in 2017, forcing truncation to a common set of 101 days from June to September, leaving 909 records. Covariate analysis utilized this truncated dataset. When aggregated to weekly means, the sediment temperature dataset contained 526 observations. Truncating to the subset of 30 common weeks sampled in every year the number of observations reduced the number of records to 270.

Model Selection

For ARIMA models fitting all possible covariate combinations at lake YUCH-005 with sediment temperature as the response variable, AICc-based model selection resulted in ARIMA(1,0,0) with solar radiation as the main covariate in the best model, but no annual trend term. No trend model of the daily data exhibited stationarity.

When fitting trend models to the weekly sediment temperature data all methods (complete, additive outliers, truncated, and truncated seasonally adjusted) yielded stationary residuals for both the logged and unlogged data. Of these eight models, only one included a trend coefficient that was significantly less than zero, thus there is little evidence for a decreasing trend in sediment temperature at lake YUCH-005.

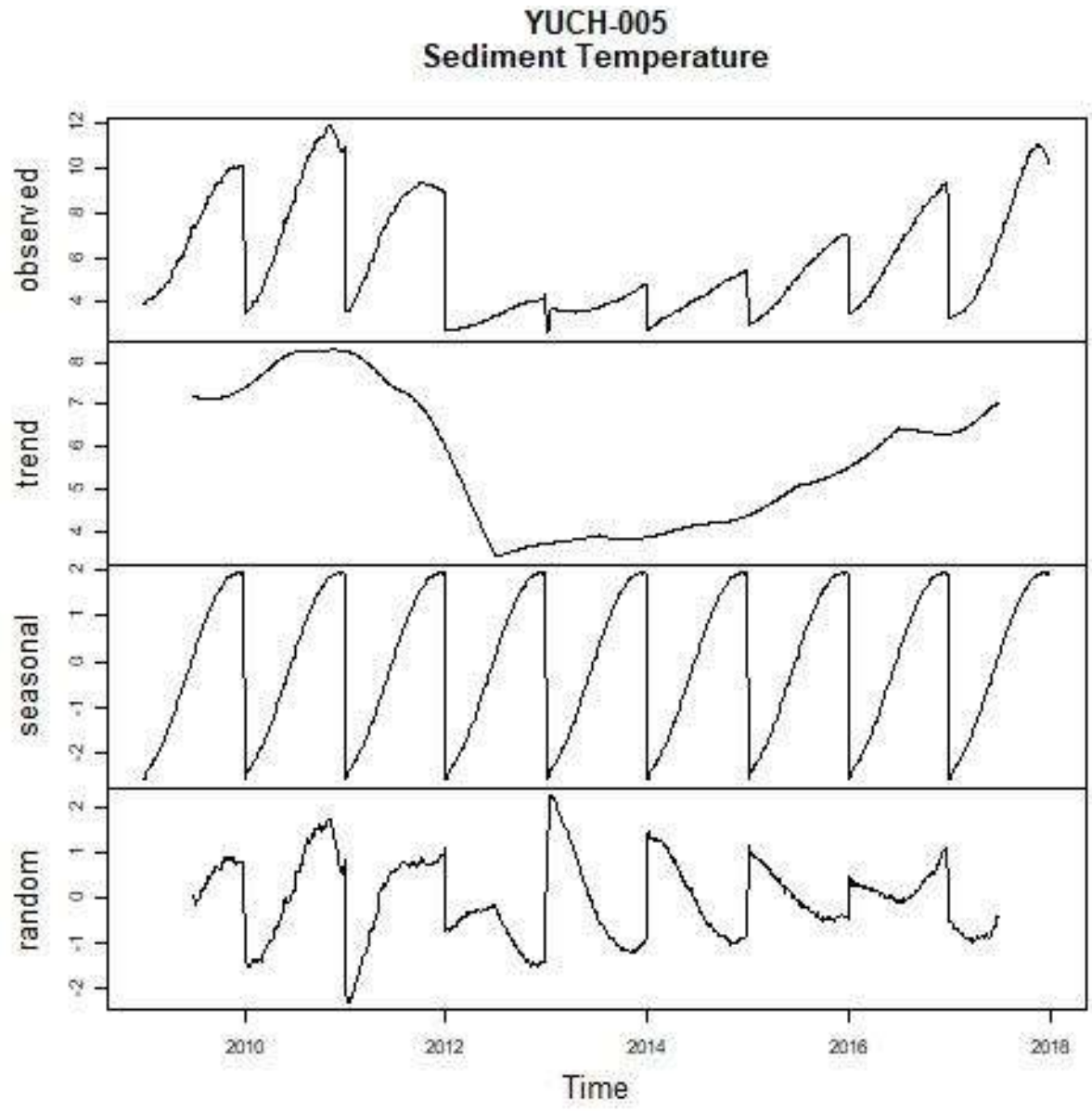


Figure A.176. Time series decomposition of truncated YUCH-005 sediment temperature by year.

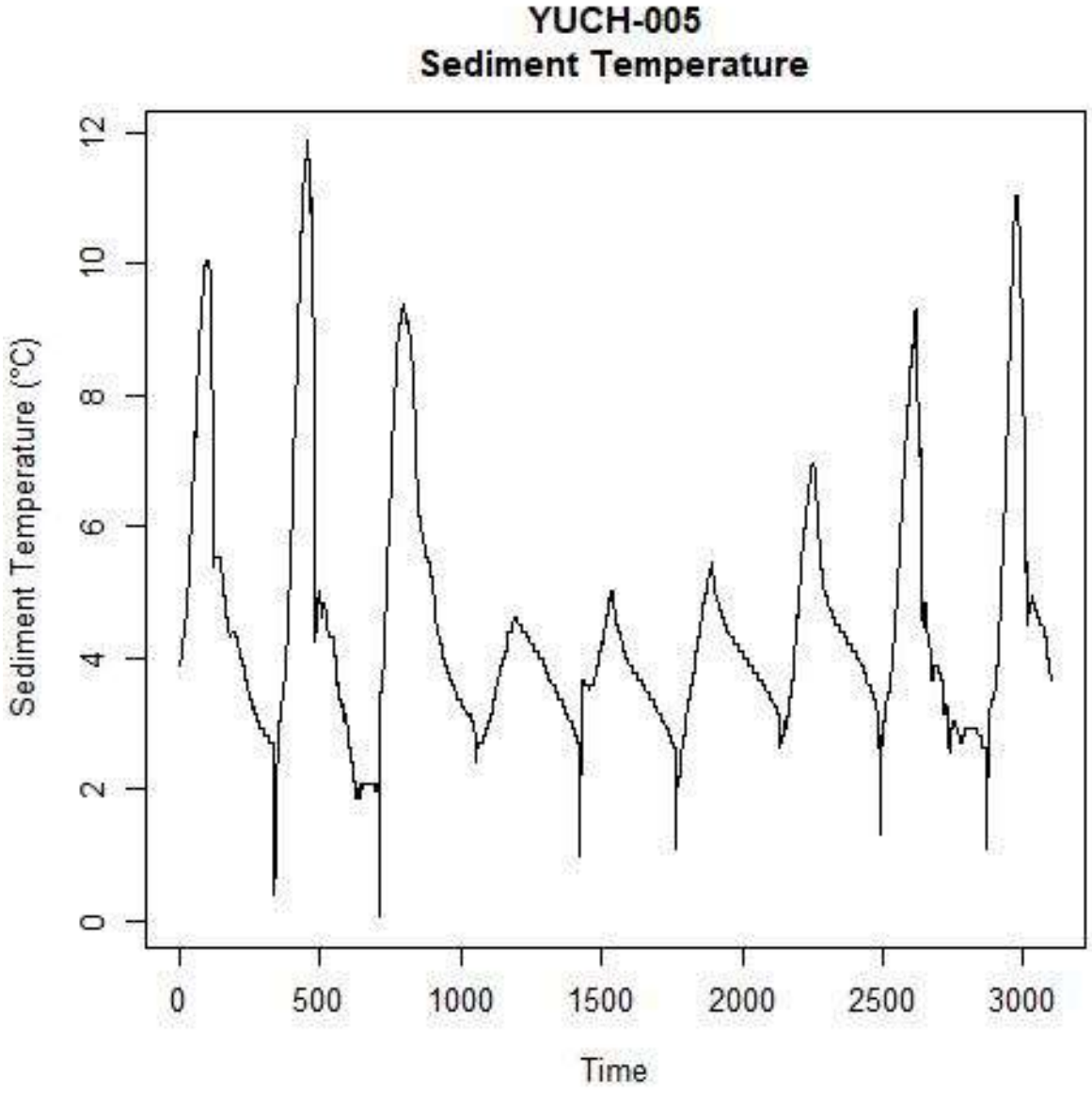


Figure A.177. Time series of YUCH-005 sediment temperature by time point with vertical lines for additive outliers.

Table A.189. Trend modeling results for daily sediment temperature data at YUCH-005.

			Trend			ARMA order		Ljung-Box Test	
Logged	**Method**	**Intercept**	**Coefficient**	**SE**	**p-value**	**AR**	**MA**	**Statistic**	**p-value**
FALSE	complete	4.8587	-0.0391	0.0399	0.3276	2	2	14.69	0.0054
FALSE	completeAO	5.3894	-0.0967	0.0186	< 0.0001	0	5	14834.17	< 0.0001

			Trend			ARMA order		Ljung-Box Test	
Logged	Method	Intercept	Coefficient	SE	p-value	AR	MA	Statistic	p-value
FALSE	trunc	9.7049	-0.4262	0.0544	< 0.0001	0	5	4030.41	< 0.0001
FALSE	truncSA	6.0666	-0.0067	0.0702	0.9238	2	3	269.29	< 0.0001
TRUE	complete	1.5551	-0.0141	0.0221	0.5228	5	0	26.58	< 0.0001
TRUE	completeAO	1.5548	-0.0141	0.0262	0.5909	5	0	33.54	< 0.0001
TRUE	trunc	2.3084	-0.0694	0.0093	< 0.0001	0	5	3919.07	< 0.0001
TRUE	truncSA	1.8660	-0.0202	0.0050	< 0.0001	0	5	11335.64	< 0.0001

Table A.190. Trend modeling results for weekly sediment temperature data at YUCH-005.

			Trend			ARMA order		Ljung-Box Test	
Logged	Method	Intercept	Coefficient	SE	p-value	AR	MA	Statistic	p-value
FALSE	complete	4.5855	-0.0305	0.0679	0.6533	2	1	1.75	0.8823
FALSE	completeAO	4.6015	-0.0337	0.0750	0.6533	2	1	4.85	0.1829
FALSE	trunc	7.2877	-0.4689	0.1749	0.0073	2	1	55.65	0.1558
FALSE	truncSA	5.6253	-0.0766	0.0716	0.2847	2	1	47.12	0.4677
TRUE	complete	1.4130	-0.0024	0.0081	0.7692	2	2	1.89	0.7567
TRUE	completeAO	1.4131	-0.0023	0.0082	0.7764	2	2	5.32	0.1495
TRUE	trunc	2.0174	-0.0961	0.0796	0.2274	2	1	47.40	0.4152
TRUE	truncSA	1.6887	-0.0188	0.0131	0.1499	2	1	42.66	0.6529

Table A.191. Top covariate models for daily sediment temperature data at YUCH-005.

Model	AICc	ΔAICc	Ljung-Box Test p-value
Solar Radiation	1172.49	0.00	0.7675
Wind Speed + Solar Radiation	1172.81	0.32	0.6849
Solar Radiation + Daily Precipitation	1174.39	1.90	0.6614
Wind Speed + Solar Radiation + Daily Precipitation	1178.72	6.23	0.2650
Relative Humidity	1179.47	6.97	0.9960
Air Temperature + Wind Speed	1179.62	7.13	0.9876
Relative Humidity + Daily Precipitation	1181.49	9.00	0.9844
Air Temperature + Wind Speed + Daily Precipitation	1181.59	9.09	0.9523
Air Temperature	1181.76	9.27	0.7933
Wind Speed + Relative Humidity	1182.50	10.00	0.6880

Table A.192. Coefficients and variance components estimates for the top covariate model for daily sediment temperature data at YUCH-005.

Parameter	Coefficient	SE	p-value
ar1	0.98	0.01	< 0.0001
intercept	6.26	0.89	< 0.0001
Solar Radiation	0.00	0.00	< 0.0001

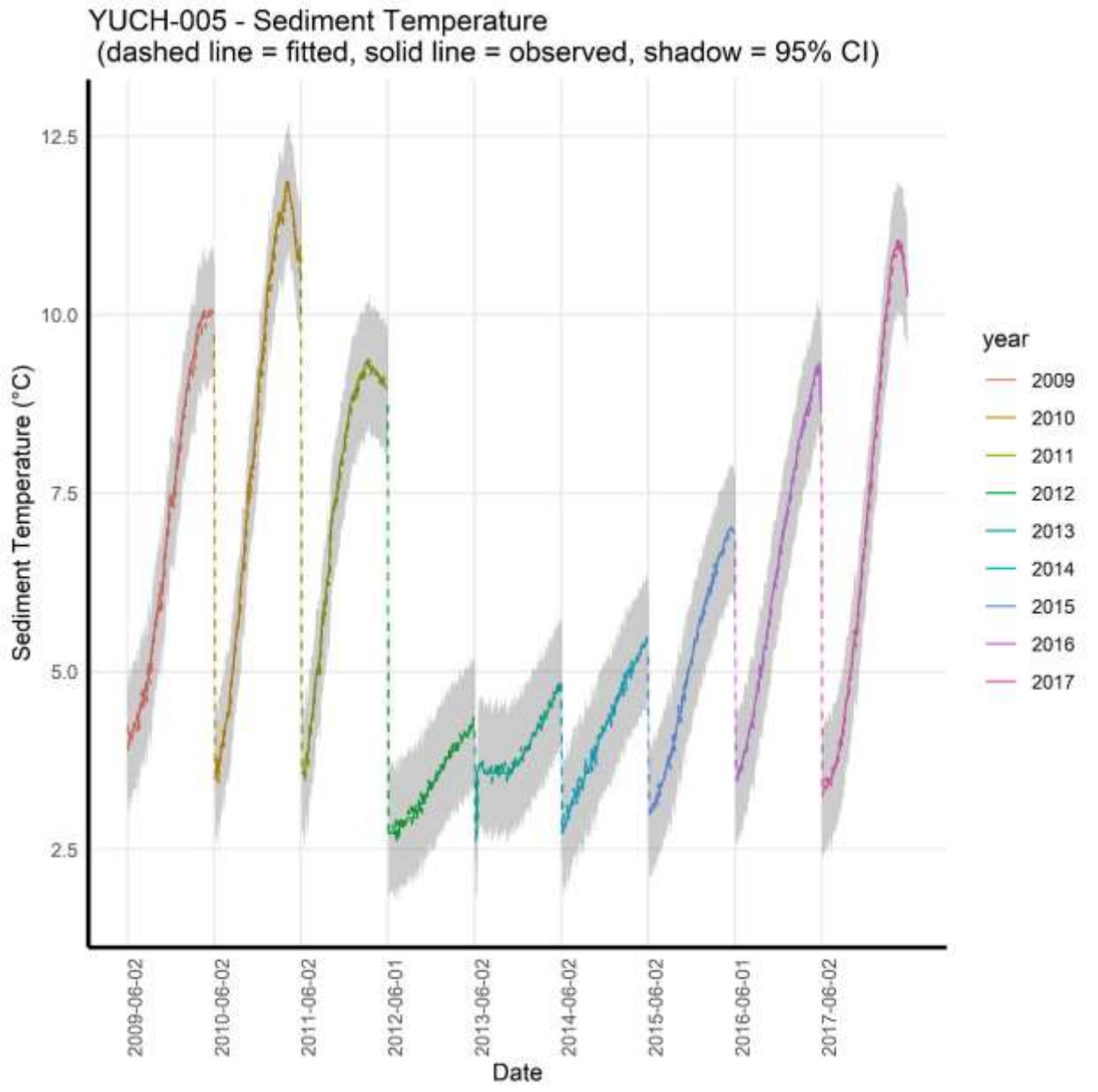


Figure A.178. Model predictions of YUCH-005 sediment temperature by date.

Water Temperature

Water temperature is collected with a thermistor chain at multiple depths, and temperatures collected at different depths one the same day are highly correlated. In this section, trend is assessed at a single depth on the assumption that trends are similar for water temperatures collected at the remaining depths. The depth used for the trend and covariate analyses is selected as the depth at which water temperature is measured consistently across all years. The analysis scripts provide code to impute water temperature values for years with missing depths.

BELA-088

Data

For BELA-088, water temperature was recorded from 2012-2019. Because data were not collected in 2013, the analysis focused on years 2014 through 2019. Water temperature was recorded at depths 0.25, 0.50, and 1.00 m, but no measurements were made at 0.25 m in 2018 or at 0.50 m in 2016. Data were collected during the months June through September and infrequently between October and December, though these later months were excluded from the analysis as data were sparse. A water depth of 1 m was selected for this analysis as no water temperature observations were missing at this depth. There were 1629 water temperature observations included in the analysis when considering all dates and depths. When restricting to water temperature measurements collected at 1.00 m depth, the data set contained 543 observations. When truncating to the set of 72 common dates, the number of observations were reduced to 432. Data for covariates were sufficiently complete such that none of the covariates nor model years were omitted from the model selection process. When aggregating water temperature data to weekly mean values the number of observations was reduced to 294 observations. When truncated the weekly data to the common set of 9 weeks sampled in every year the number of observation was further reduced to 63.

Model Selection

For BELA-088, none of the eight trend models fit to the daily water temperature data yielded stationary residuals, so trend was assessed with weekly water temperature data. The truncated and truncated seasonally adjusted models for unlogged and logged data yielded stationary residuals. The p-values for the two-sided trend tests for the four models with stationary residuals ranged from 0.0201 to 0.0517, providing weak evidence of a positive trend in water temperature over the monitoring period. For ARIMA models fitting all possible covariate combinations at lake BELA-088, AICc-based model selection yielded a final model with a ARIMA(2,0,0) structure and fixed effects for relative humidity and month, and the effects of both covariates were negatively associated with water temperature.

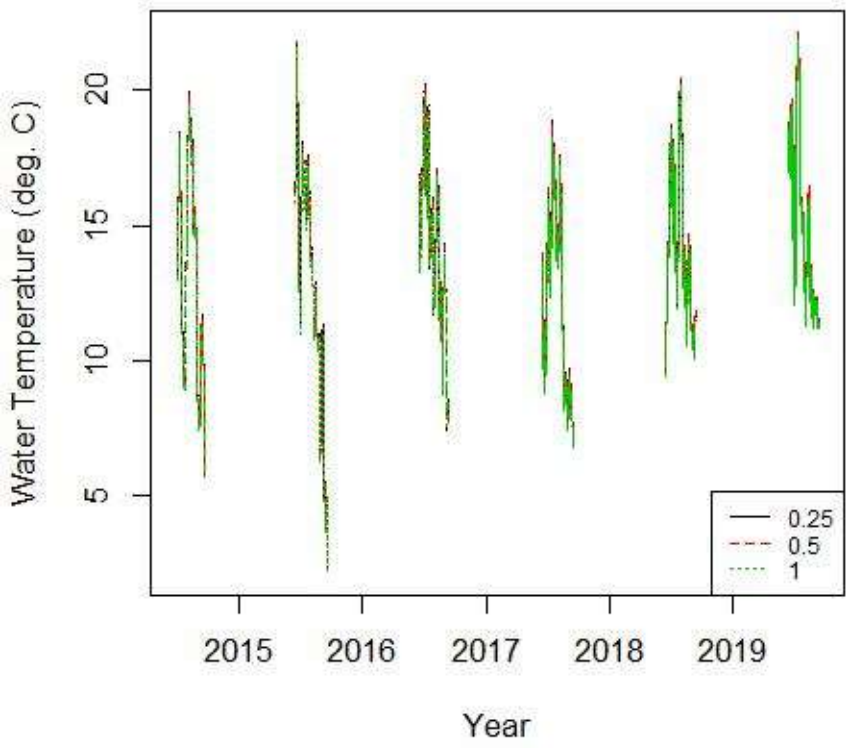


Figure A.179. BELA-088 water temperature by depth and year.

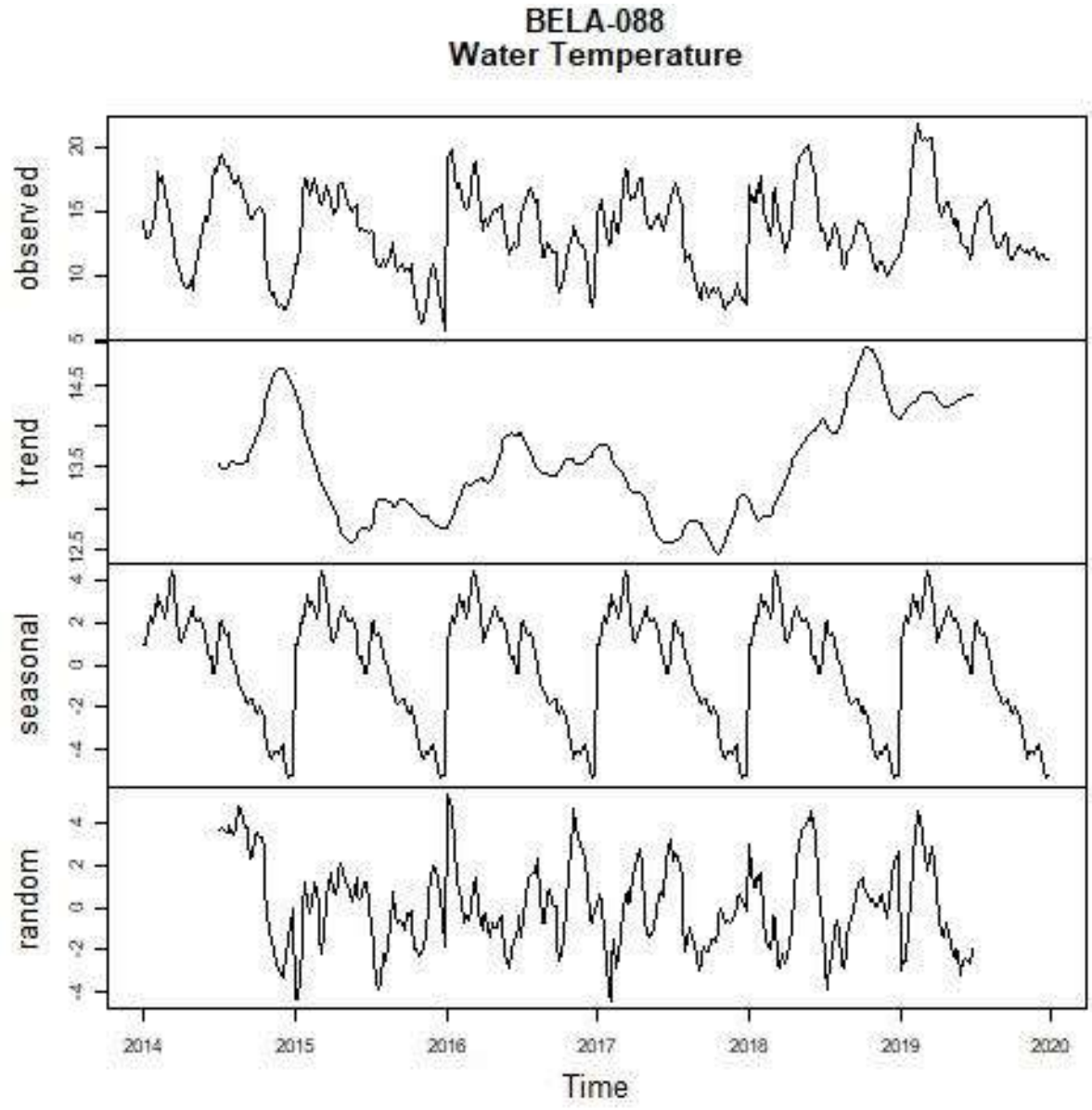


Figure A.180. Time series decomposition of truncated BELA-088 water temperature measured at 1 m depth by year.

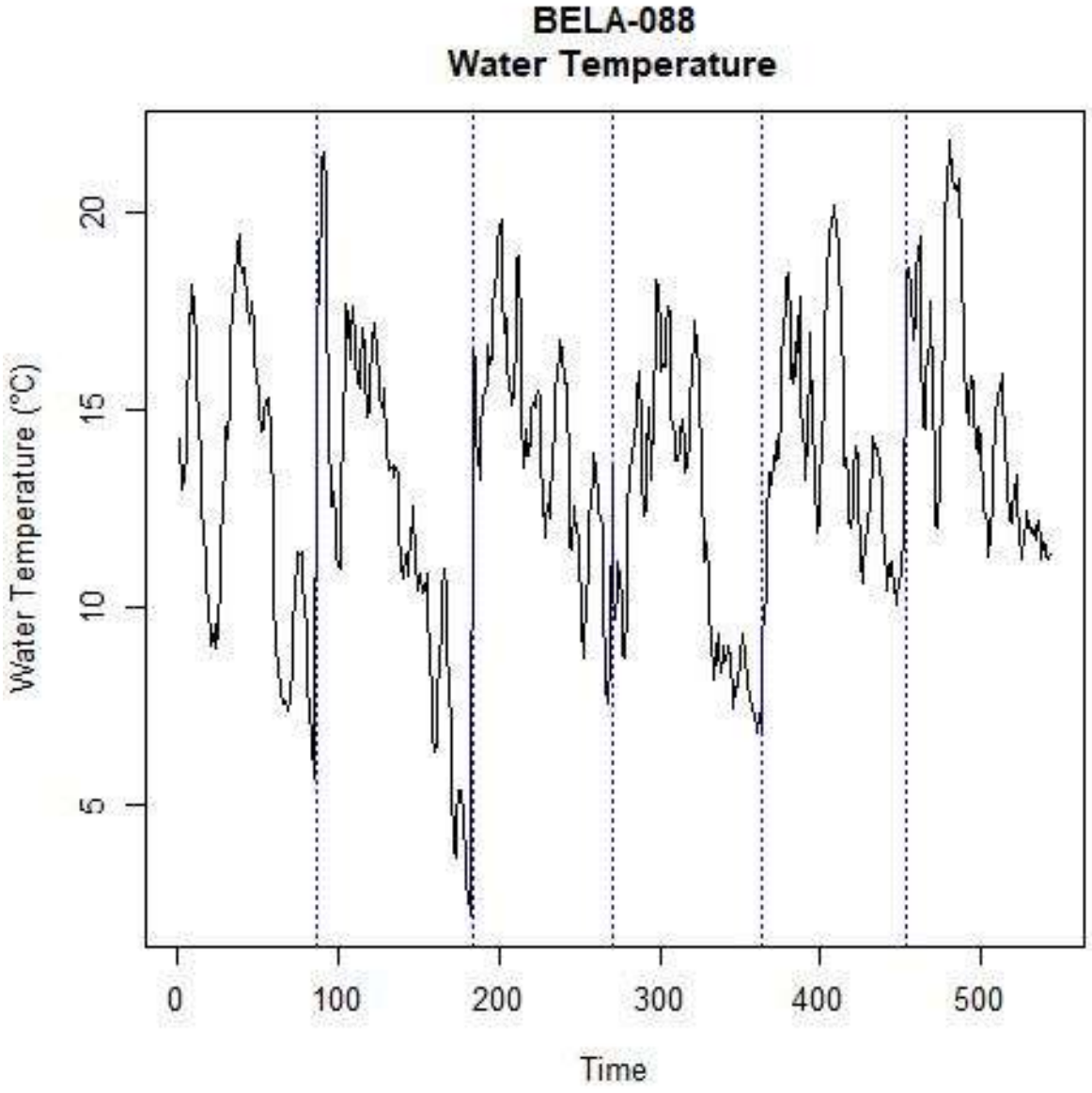


Figure A.181. Time series of BELA-088 water temperature measured at 1 m depth by time point with vertical lines for additive outliers.

Table A.193. Trend modeling results for daily water temperature data measured at 1 m depth at BELA-088.

			Trend			ARMA order		Ljung-Box Test	
Logged	**Method**	**Intercept**	**Coefficient**	**SE**	**p-value**	**AR**	**MA**	**Statistic**	**p-value**
FALSE	complete	0.5112	1.1159	0.1843	< 0.0001	0	5	157.71	< 0.0001
FALSE	completeAO	6.0387	0.6331	0.1603	< 0.0001	0	5	171.86	< 0.0001

			Trend			ARMA order		Ljung-Box Test	
Logged	Method	Intercept	Coefficient	SE	p-value	AR	MA	Statistic	p-value
FALSE	trunc	10.9799	0.2262	0.1099	0.0395	0	1	1356.78	< 0.0001
FALSE	truncSA	11.6754	0.1660	0.1868	0.3743	2	0	136.20	0.0002
TRUE	complete	1.4365	0.0964	0.0166	< 0.0001	0	5	135.79	< 0.0001
TRUE	completeAO	1.7918	0.0653	0.0147	< 0.0001	0	5	162.65	< 0.0001
TRUE	trunc	1.9896	0.0511	0.0149	0.0006	0	5	177.90	< 0.0001
TRUE	truncSA	2.3912	0.0164	0.0148	0.2679	2	0	130.65	0.0005

Table A.194. Trend modeling results for weekly water temperature data measured at 1 m depth at BELA-088.

			Trend			ARMA order		Ljung-Box Test	
Logged	Method	Intercept	Coefficient	SE	p-value	AR	MA	Statistic	p-value
FALSE	complete	7.8276	1.2019	0.5366	0.0251	1	0	13.98	0.0516
FALSE	completeAO	9.1837	0.8026	0.3095	0.0095	1	1	19.99	0.0002
FALSE	trunc	10.1164	0.6620	0.3402	0.0517	1	0	5.33	0.8048
FALSE	truncSA	11.1420	0.4022	0.1863	0.0308	1	0	8.04	0.6248
TRUE	complete	2.0309	0.1075	0.0295	0.0003	0	2	14.87	0.0213
TRUE	completeAO	1.9814	0.1121	0.0398	0.0049	1	1	11.98	0.0075
TRUE	trunc	2.2823	0.0586	0.0293	0.0456	1	0	5.85	0.7548
TRUE	truncSA	2.3766	0.0348	0.0150	0.0201	1	0	5.07	0.8866

Table A.195. Top covariate models for daily water temperature data at BELA-088.

Model	AICc	ΔAICc	Ljung-Box Test p-value
Relative Humidity + Month	1005.39	0.00	0.1973
Wind Speed + Relative Humidity + Month	1006.98	1.58	0.1343
Wind Speed + Month	1027.37	21.98	0.2144
Daily Precipitation + Month	1027.75	22.35	0.2006
Wind Speed + Daily Precipitation + Month	1029.45	24.05	0.1314
Air Temperature + Wind Speed	1079.92	74.53	0.2636
Air Temperature + Wind Speed + Daily Precipitation	1081.89	76.50	0.1692
Air Temperature	1082.05	76.66	0.4198
Air Temperature + Daily Precipitation	1083.81	78.42	0.3039
Wind Speed + Solar Radiation	1156.56	151.17	0.2272

Table A.196. Coefficients and variance components estimates for the top covariate model for daily water temperature data measured at 1 m depth at BELA-088.

Parameter	Coefficient	SE	p-value
Ar1	1.32	0.05	< 0.0001
Ar2	-0.41	0.05	< 0.0001
Intercept	32.30	1.29	< 0.0001
Relative Humidity	-0.02	0.00	< 0.0001
Month	-2.34	0.15	< 0.0001

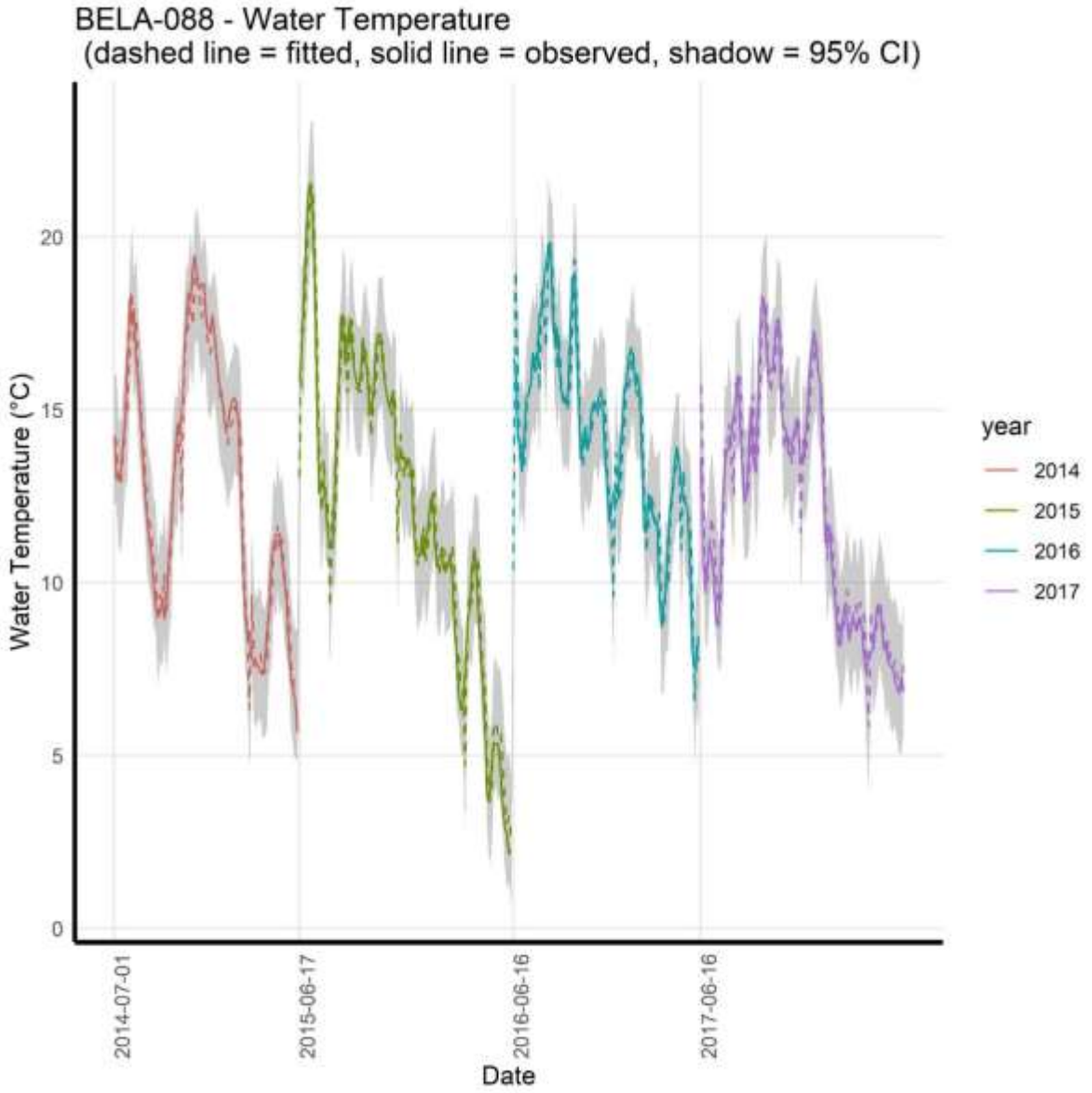


Figure A.182. Model predictions of BELA-088 water temperature measured at 1 m depth by date.

BELA-108

Data

For BELA-108, water temperature was recorded from 2015-2019. Water temperature was recorded at depths 0.25, 0.50, 1.00, 1.50, 2.00, and 3.00 m, but no measurements were made at 0.25 m in 2018, at 0.50 m in 2019, or at 1.00 m in 2016. Data were collected during the months June through September, but infrequently in October, so these measurements were excluded from the analysis. A water depth of 1.5 m was selected for this analysis as no water temperature observations were missing at this depth. A total of 2473 water temperature observations were collected across all depths. Reducing to water temperature measurements collected at 1.50 m depth, the data set contained 543 observations. When truncating to the set of 86 common dates, the number of observations were reduced to 430. Covariate data for air temperature and relative humidity were missing for 2018, so the covariate analysis included only the 276 observations recorded in years 2015-2017.

Model Selection

For BELA-108, none of the eight trend models fit to the daily water temperature data yielded stationary residuals, but the top covariate model contained a trend term and exhibited stationary residuals so this model was used to assess trend. Note that the years examined for the covariate analysis excluded 2018 and 2019. The trend in water temperature was positive for the years 2015 through 2017, and the effects of relative humidity and month were negatively associated with water temperature collected at 1.50 m depth.

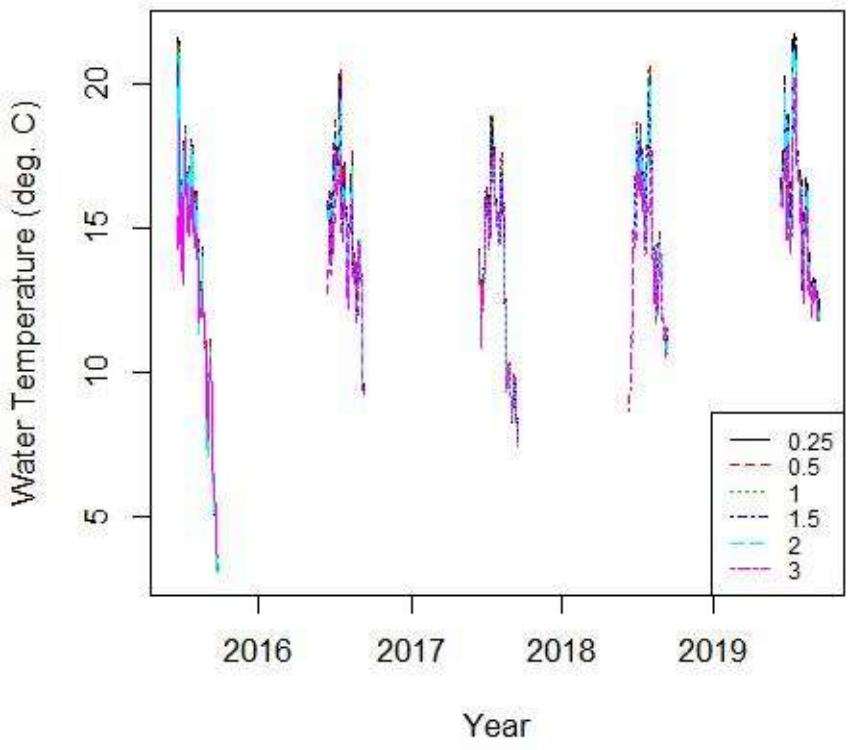


Figure A.183. BELA-108 water temperature by depth and year.

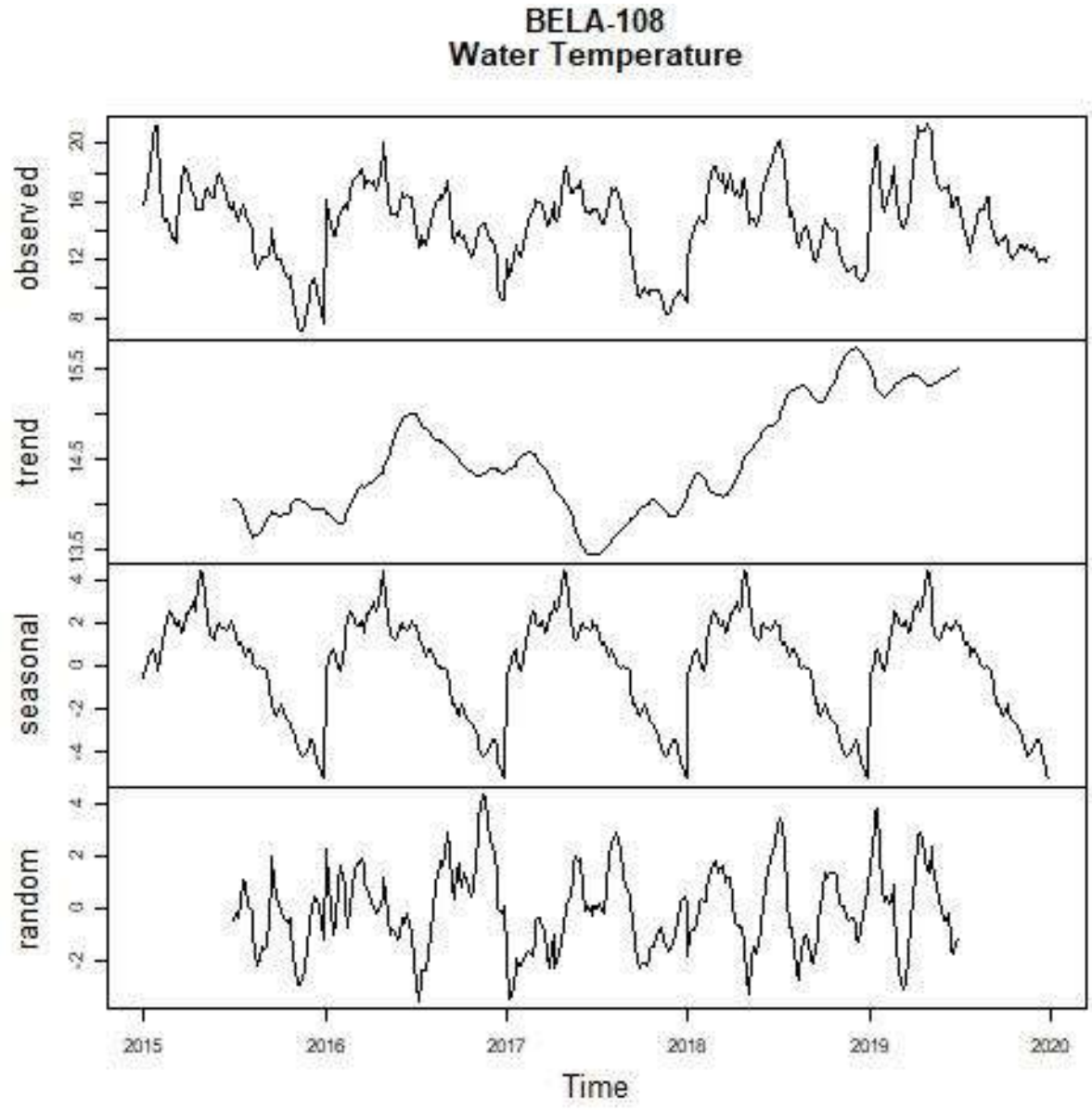


Figure A.184. Time series decomposition of truncated BELA-108 water temperature measured at 1.5 m depth by year.

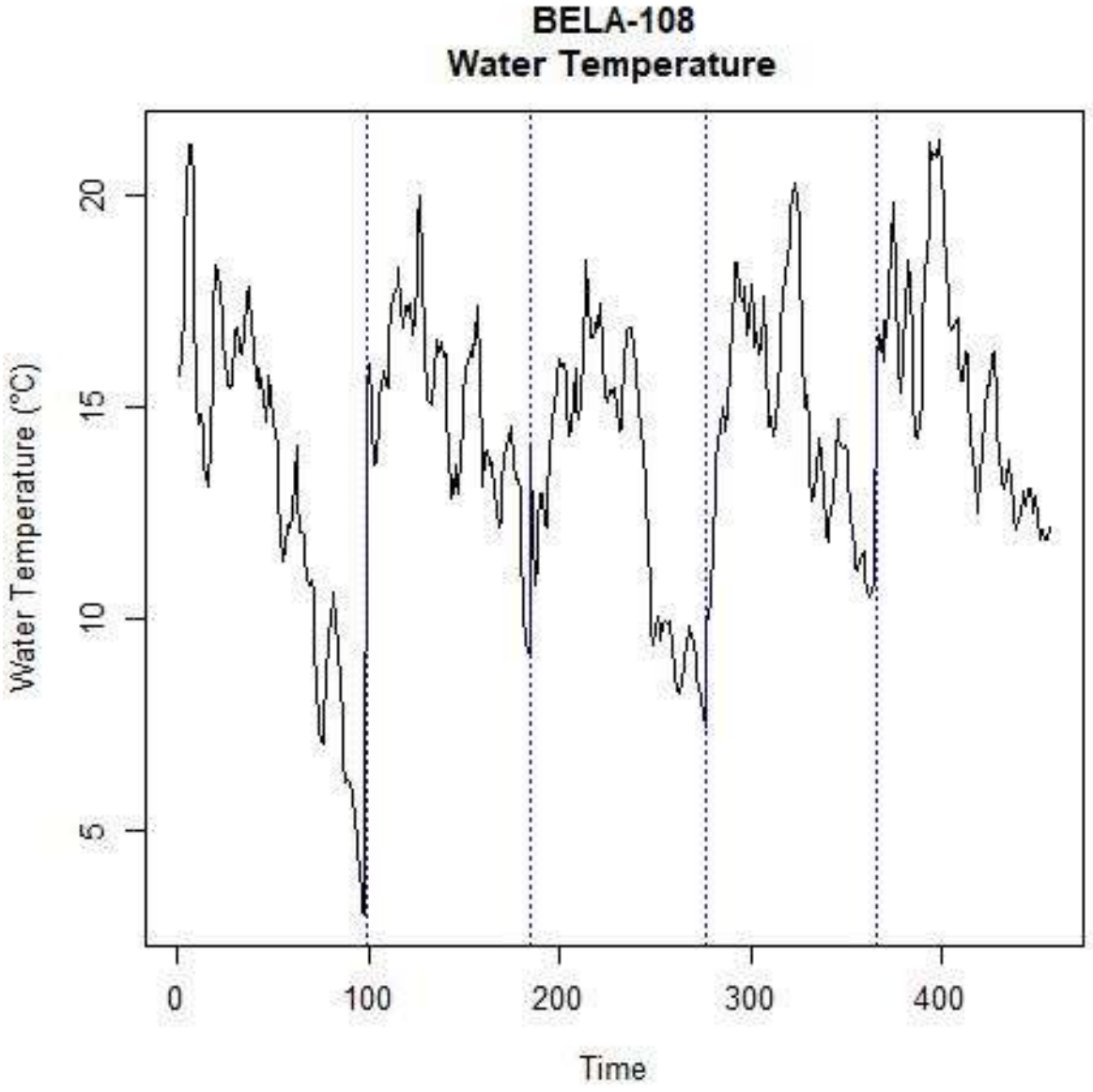


Figure A.185. Time series of BELA-108 water temperature measured at 1.5 m depth by time point with vertical lines for additive outliers.

Table A.197. Trend modeling results for daily water temperature data measured at 1.5 m depth at BELA-108.

			Trend			ARMA order		Ljung-Box Test	
Logged	**Method**	**Intercept**	**Coefficient**	**SE**	**p-value**	**AR**	**MA**	**Statistic**	**p-value**
FALSE	complete	NA	1.1936	0.0228	< 0.0001	0	5	201.80	< 0.0001
FALSE	completeAO	4.6799	0.7981	0.1781	< 0.0001	0	5	253.91	< 0.0001

			Trend			ARMA order		Ljung-Box Test	
Logged	**Method**	**Intercept**	**Coefficient**	**SE**	**p-value**	**AR**	**MA**	**Statistic**	**p-value**
FALSE	trunc	10.7219	0.3217	0.1041	0.0020	0	0	3029.34	< 0.0001
FALSE	truncSA	12.0055	0.2169	0.1292	0.0933	4	3	112.83	0.0049
TRUE	complete	1.2360	0.1159	0.0181	< 0.0001	0	5	169.23	< 0.0001
TRUE	completeAO	1.6882	0.0780	0.0156	< 0.0001	0	5	218.65	< 0.0001
TRUE	trunc	2.3219	0.0281	0.0077	0.0003	0	1	3784.92	< 0.0001
TRUE	truncSA	2.4659	0.0164	0.0105	0.1192	3	3	107.65	0.0147

Table A.198. Top covariate models for daily water temperature data recorded at 1.5 m depth at BELA-088.

Model	**AICc**	**ΔAICc**	**Ljung-Box Test p-value**
Relative Humidity + Year + Month	621.23	0.00	0.2895
Year + Month	624.55	3.32	0.3063
Daily Precipitation + Year + Month	628.27	7.04	0.1357
Relative Humidity + Month	659.07	37.84	0.1669
Daily Precipitation + Month	664.24	43.01	0.2376
Air Temperature	753.26	132.03	0.5747
Air Temperature + Daily Precipitation	755.19	133.96	0.4452
Relative Humidity	799.70	178.47	0.7175
Intercept Only	801.83	180.61	0.8748
Daily Precipitation	803.88	182.65	0.7915

Table A.199. Coefficients and variance components estimates for the top covariate model for daily water temperature data measured at 1.5 m depth at BELA-108.

Parameter	**Coefficient**	**SE**	**p-value**
ar1	0.93	0.03	< 0.0001
ma1	0.55	0.07	< 0.0001
ma2	0.15	0.08	0.0645
ma3	0.10	0.07	0.1218
Relative Humidity	-0.01	0.00	0.0164
Year	2.37	0.12	< 0.0001
Month	-1.49	0.11	< 0.0001

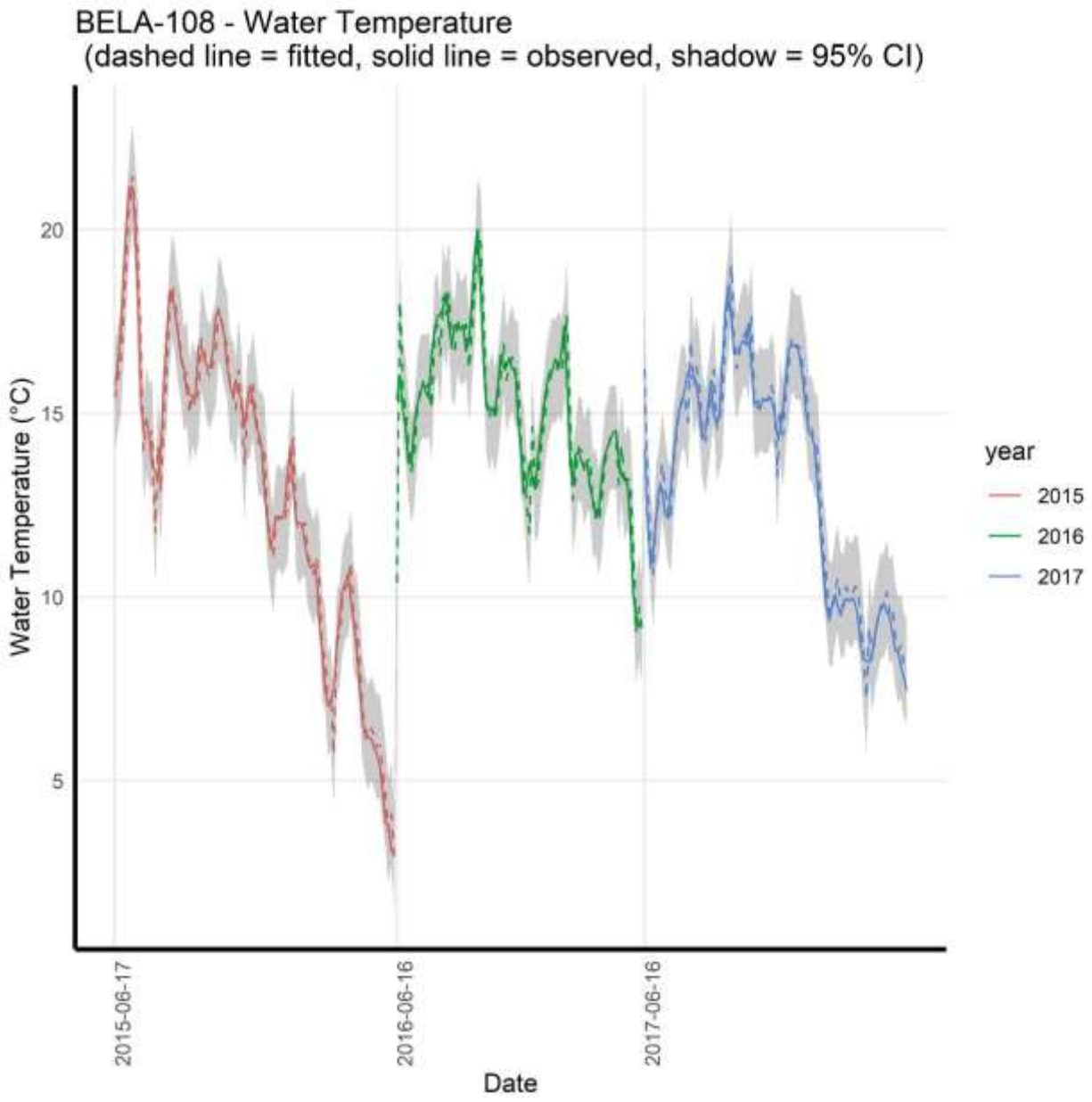


Figure A.186. Model predictions of BELA-108 water temperature measured at 1.5 m depth by week.

DENA-018

Data

For DENA-018, water temperature was recorded from 2010-2019. Because data were not collected in 2013, the analysis focused on years 2014 through 2019. Water temperature was recorded at depths 0.25, 0.50, 1.00, and 1.50 m, but water temperature was only measured at a depth of 1.50 m in 2010 and 2011, so this depth was not included in the analysis. No measurements were made at 0.50 m in 2018. Data were collected during the months of May through September, but infrequently in October, so this month was excluded from the analysis. A water depth of 1 m was selected for this analysis as no water temperature observations were missing at this depth. There were 1967 water temperature observations included in the analysis when considering surveys conducted between May and September at depths of 0.25, 0.50, and 1.00 m. When restricting to water temperature measurements collected at 1.00 m depth, the data set contained 697 observations. When truncating to the set of 99 common dates, the number of observations were reduced to 594. Data for covariates were sufficiently complete such that none of the covariates nor model years were omitted from the model selection process. When aggregating water temperature data to weekly mean values the number of observations was reduced to 243 observations. When truncated the weekly data to the common set of 14 weeks sampled in every year the number of observations was further reduced to 70.

Model Selection

For DENA-018, none of the eight trend models fit to the daily water temperature data yielded stationary residuals, so trend was assessed with weekly water temperature data. The truncated and truncated seasonally adjusted models for unlogged and logged data as well as the additive outlier model for logged data yielded stationary residuals. The trends differed substantially between the truncated and seasonally adjusted models, but both models for both types of transformations provided evidence of a positive trend in water temperature over the monitoring period. For ARIMA models fitting all possible covariate combinations at lake DENA-018, AICc-based model selection yielded a final model with a ARIMA(4,0,3) structure and fixed effects for wind speed and solar radiation. Wind speed was negatively associated with water temperature, while increasing solar radiation was associated with increasing water temperature.

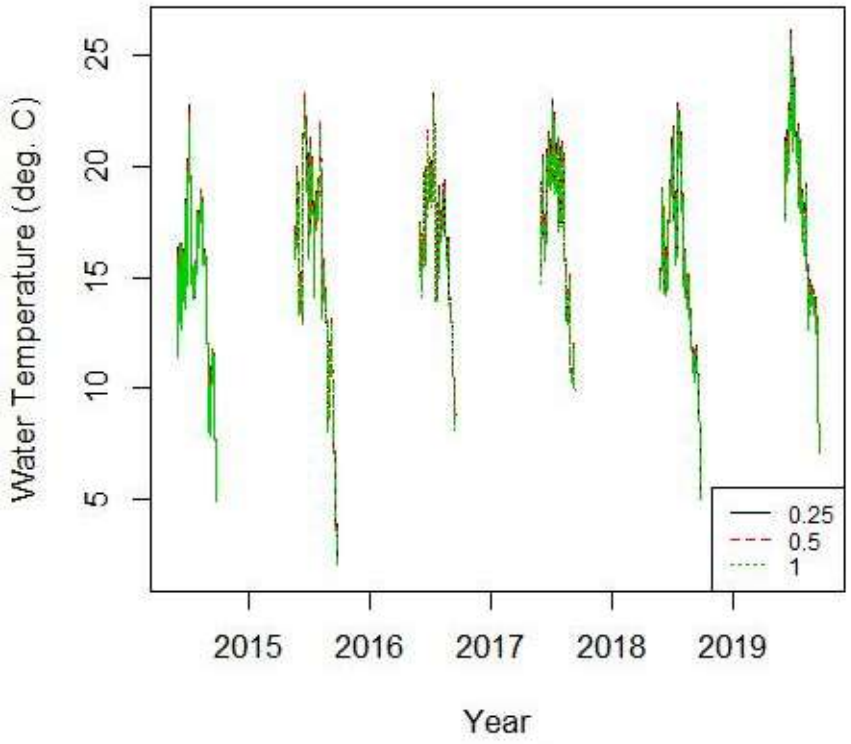


Figure A.187. DENA-018 water temperature by depth and year.

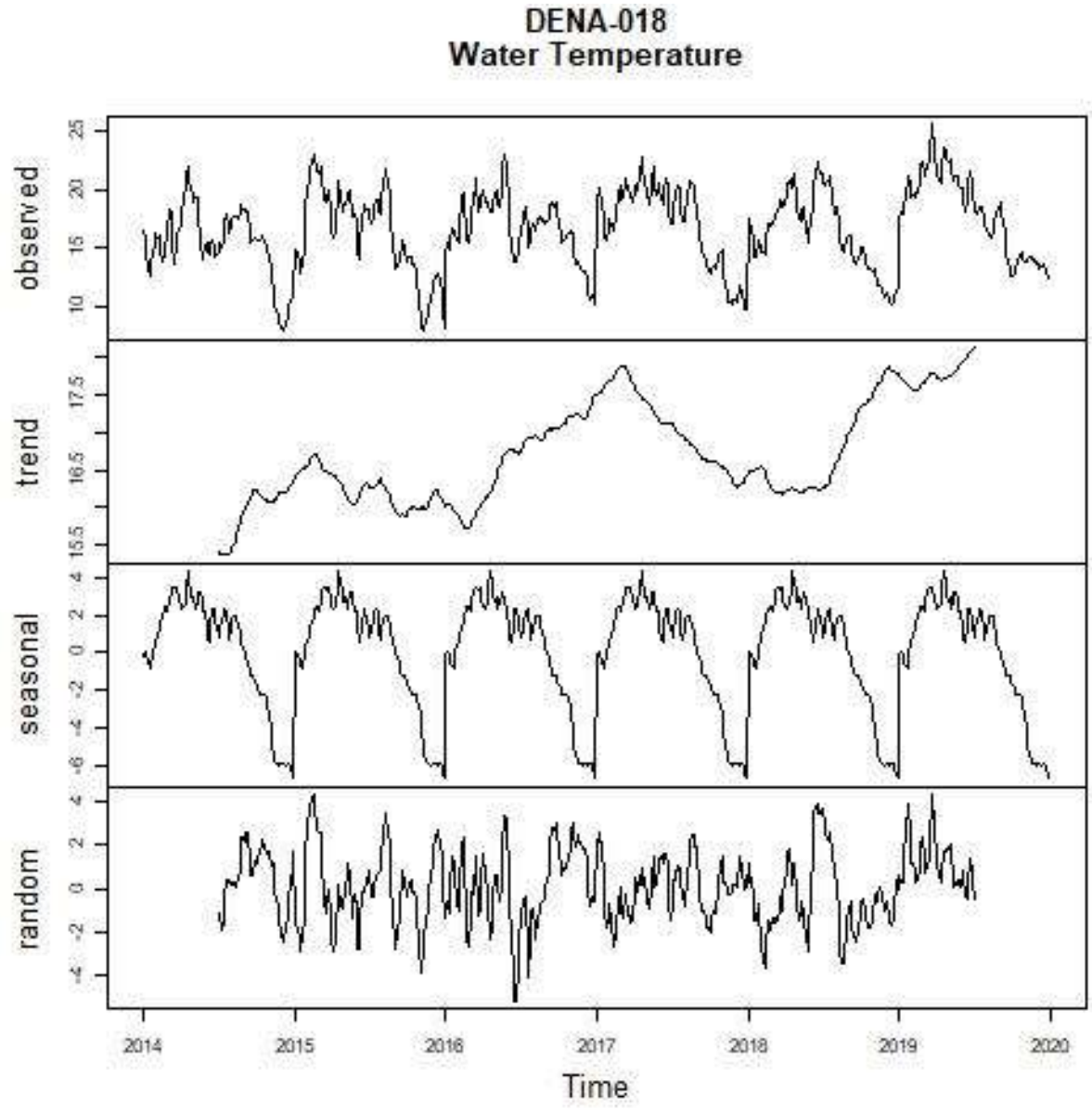


Figure A.188. Time series decomposition of truncated DENA-018 water temperature measured at 1 m depth by year.

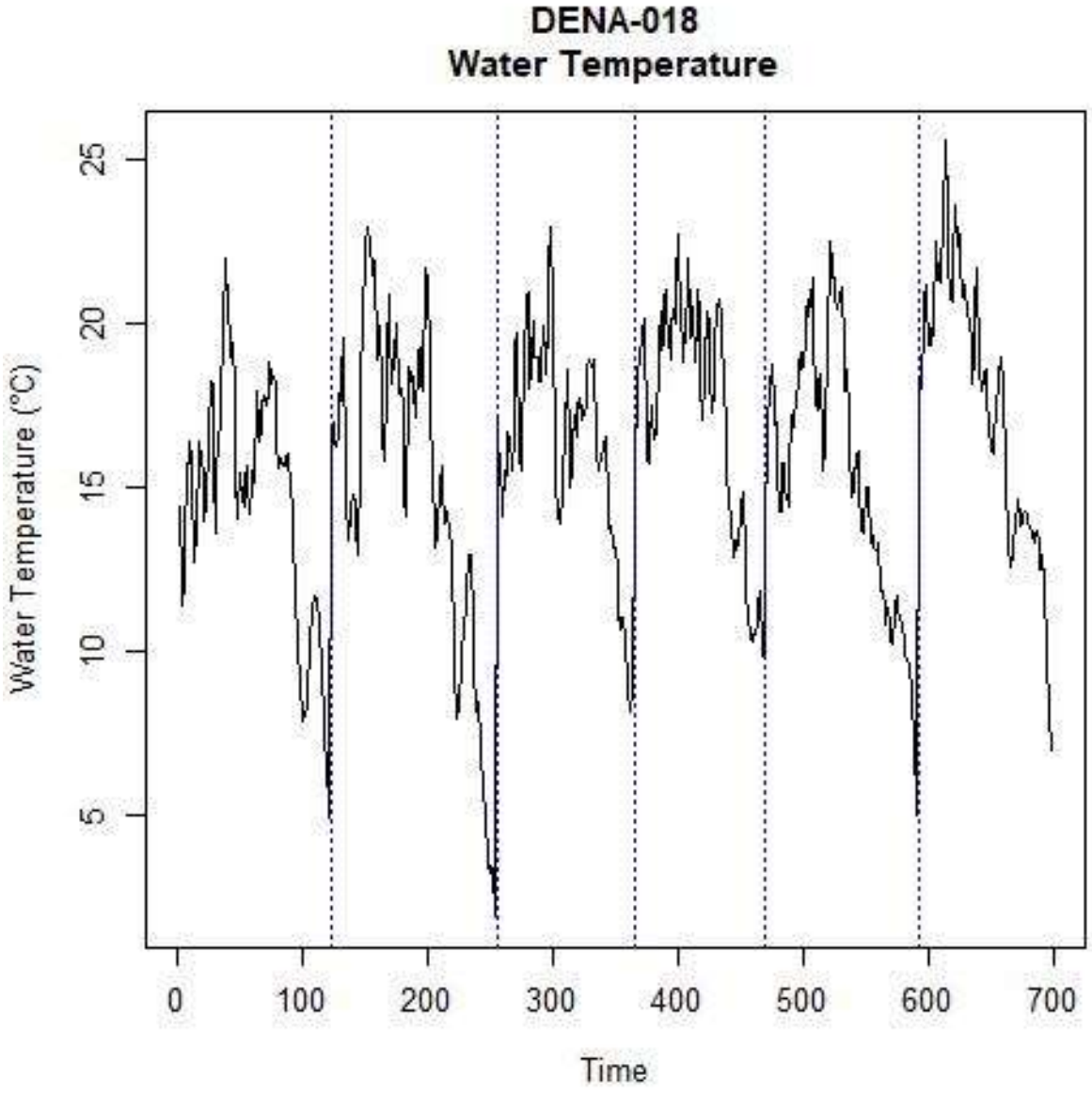


Figure A.189. Time series of DENA-018 water temperature measured at 1 m depth by time point with vertical lines for additive outliers.

Table A.200. Trend modeling results for daily water temperature data measured at 1 m depth at DENA-018.

			Trend			ARMA order		Ljung-Box Test	
Logged	**Method**	**Intercept**	**Coefficient**	**SE**	**p-value**	**AR**	**MA**	**Statistic**	**p-value**
FALSE	complete	NA	1.0995	0.0190	< 0.0001	0	5	339.26	< 0.0001
FALSE	completeAO	5.4196	0.7214	0.1545	< 0.0001	0	5	417.29	< 0.0001

			Trend			ARMA order		Ljung-Box Test	
Logged	**Method**	**Intercept**	**Coefficient**	**SE**	**p-value**	**AR**	**MA**	**Statistic**	**p-value**
FALSE	trunc	2.3164	0.9879	0.1556	< 0.0001	0	5	1020.59	< 0.0001
FALSE	truncSA	11.8268	0.3341	0.1234	0.0068	1	2	180.21	< 0.0001
TRUE	complete	1.6179	0.0764	0.0134	< 0.0001	0	5	241.32	< 0.0001
TRUE	completeAO	1.8894	0.0573	0.0128	< 0.0001	0	5	316.38	< 0.0001
TRUE	trunc	1.8160	0.0671	0.0104	< 0.0001	0	5	1044.13	< 0.0001
TRUE	truncSA	2.4860	0.0210	0.0079	0.0076	1	2	191.76	< 0.0001

Table A.201. Trend modeling results for weekly water temperature means measured at 1 m depth at DENA-018.

			Trend			ARMA order		Ljung-Box Test	
Logged	**Method**	**Intercept**	**Coefficient**	**SE**	**p-value**	**AR**	**MA**	**Statistic**	**p-value**
FALSE	complete	9.9995	0.8557	0.4671	0.0670	0	2	29.71	< 0.0001
FALSE	completeAO	10.8770	0.6976	0.5154	0.1759	0	3	26.10	< 0.0001
FALSE	trunc	NA	2.2710	0.3361	< 0.0001	1	0	4.73	0.9082
FALSE	truncSA	14.3250	0.3677	0.1436	0.0104	1	0	5.33	0.8681
TRUE	complete	2.2577	0.0674	0.0378	0.0747	0	2	16.91	0.0096
TRUE	completeAO	1.8941	0.1156	0.1425	0.4174	1	2	5.69	0.1276
TRUE	trunc	-0.2893	0.4291	0.0987	< 0.0001	1	0	7.86	0.5480
TRUE	truncSA	2.6502	0.0224	0.0081	0.0057	0	1	4.41	0.9272

Table A.202. Top covariate models for daily water temperature data measured at 1 m depth at DENA 018.

Model	**AICc**	**ΔAICc**	**Ljung-Box Test p-value**
Wind Speed + Solar Radiation	4461.52	0.00	0.0622
Solar Radiation	4494.23	32.71	0.1301
Solar Radiation + Daily Precipitation	4496.25	34.73	0.0692
Wind Speed + Relative Humidity	4498.89	37.37	0.1205
Relative Humidity	4568.43	106.91	0.0936
Wind Speed + Daily Precipitation	4711.98	250.46	0.1701
Wind Speed	4722.89	261.37	0.2250
Daily Precipitation	4745.58	284.05	0.2020
Intercept Only	4764.54	303.01	0.2233

Model	AICc	ΔAICc	Ljung-Box Test p-value
Wind Speed + Solar Radiation	4461.52	0.00	0.0622

Table A.203. Coefficients and variance components estimates for the top covariate model for daily water temperature data measured at 1 m depth at DENA-018.

Parameter	Coefficient	SE	p-value
ar1	1.00	0.09	< 0.0001
ar2	-0.16	0.10	0.1216
ar3	0.52	0.10	< 0.0001
ar4	-0.38	0.08	< 0.0001
ma1	-0.12	0.09	0.1963
ma2	0.14	0.08	0.0564
ma3	-0.16	0.09	0.0645
intercept	15.13	0.76	< 0.0001
Wind Speed	-0.29	0.05	< 0.0001
Solar Radiation	0.01	0.00	< 0.0001

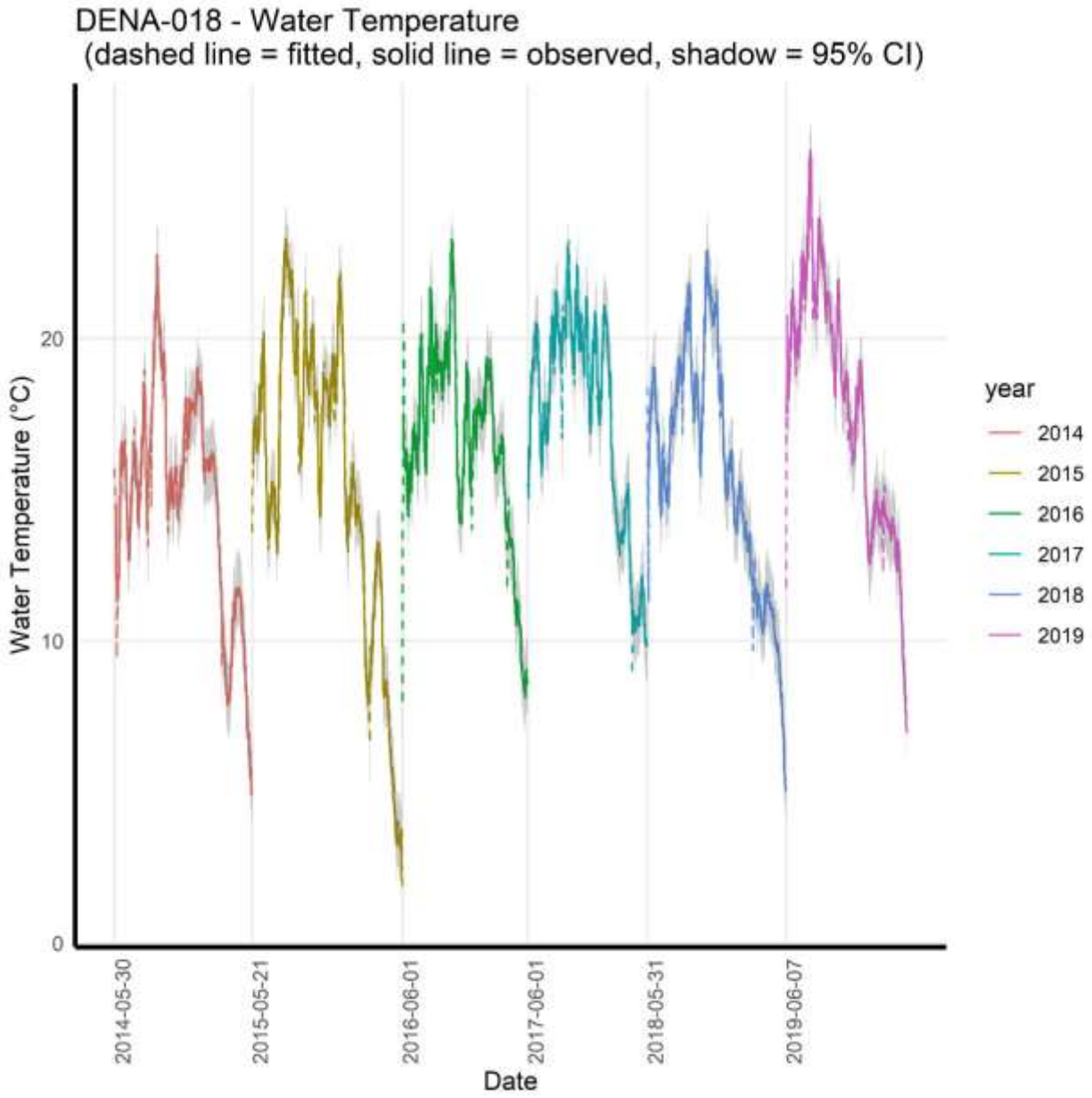


Figure A.190. Model predictions of DENA-018 water temperature measured at 1 m depth by date.

DENA-023

Data

For DENA-023, water temperature was recorded from 2009-2019. Water temperature was recorded at depths 0.25, 0.50, and 1.00 m for all years except 2015 and 2019 for which data at depth 0.25 m was missing. For years 2009-2011, water temperature was also recorded at a depth of 1.5 m, but these data were excluded from the analysis. Data were collected during the months May through September and infrequently between October and December, though these later months were excluded from the analysis as data were sparse. A water depth of 1 m was selected for this analysis as no water temperature observations were missing at this depth. There were 1235 water temperature observations included in the analysis when considering all dates, and the when truncating to the set of 89 common dates the number of observations were reduced to 979. Data for covariates were sufficiently complete that none of the covariates nor model years were omitted from the model selection process. When aggregating water temperature data to weekly mean values the number of observations was reduced to 187 observations. When truncated the weekly data to the common set of 14 weeks sampled in every year the number of observation was further reduced to 154.

Model Selection

For DENA-023, none of the eight trend models fit to the daily water temperature data yielded stationary residuals, and the residuals for the top covariate contained many large positive outliers. When fit to weekly water temperature data, the truncated and truncated seasonally adjusted models for unlogged data yielded stationary residuals, as well as the truncated seasonally adjusted model for logged water temperatures. None of these three models included a trend coefficient that was significantly different than zero, thus there is no evidence for a trend in water temperature at lake DENA-023. For ARIMA models fitting all possible covariate combinations at lake DENA-023, AICc-based model selection yielded a final model with an ARIMA(1,0,0) structure and fixed effects for air temperature and daily precipitation. Air temperature and daily precipitation are both estimated to have a positive effect on water temperature.

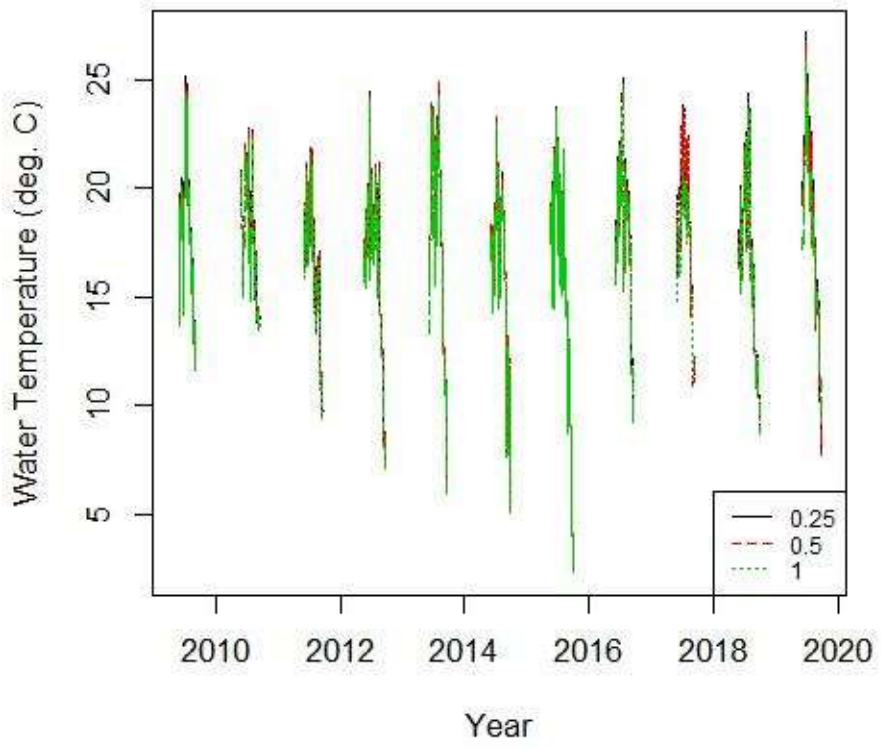


Figure A.191. DENA-023 water temperature by depth and year.

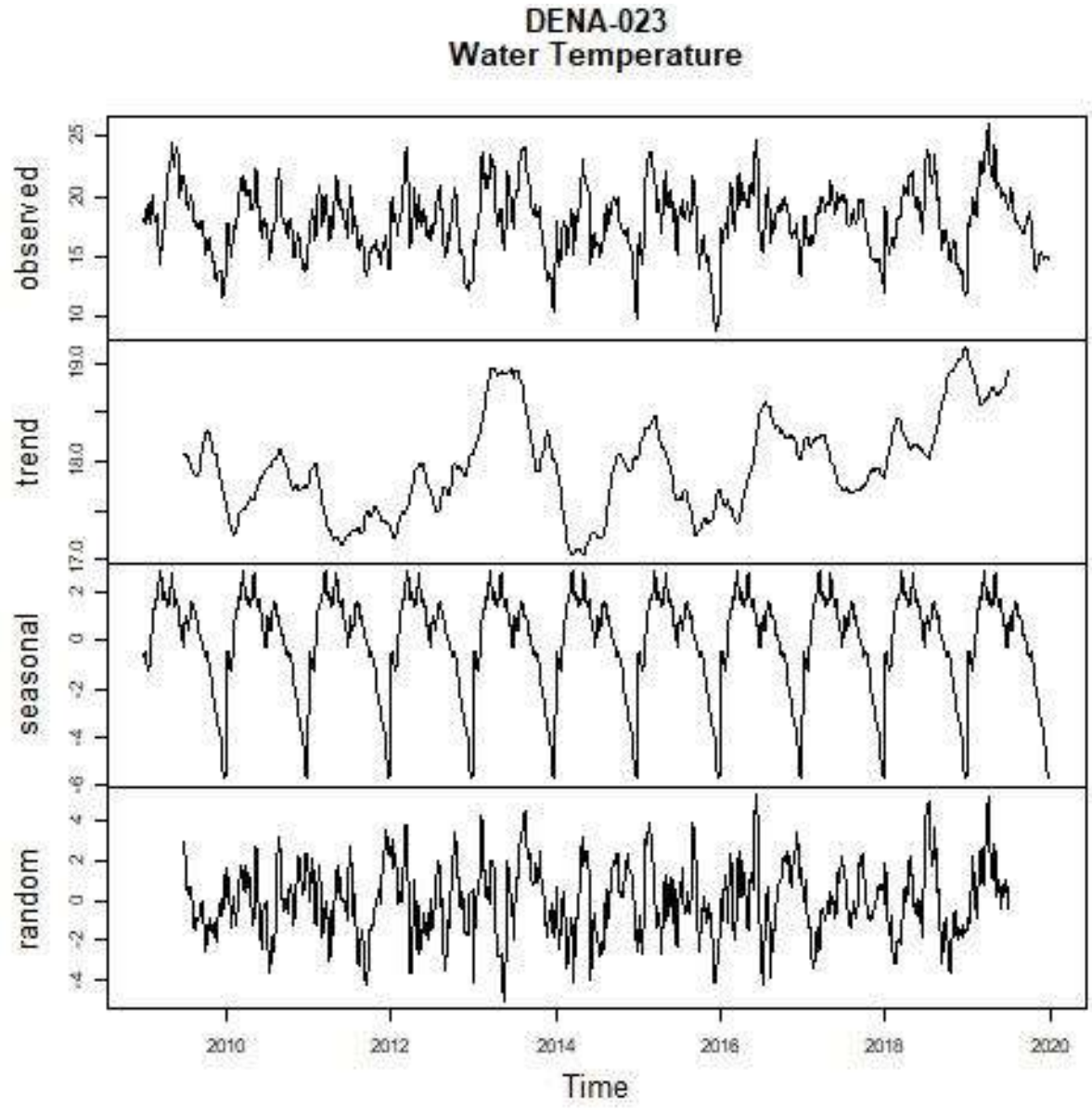


Figure A.192. Time series decomposition of truncated DENA-023 water temperature measured at 1 m depth by year.

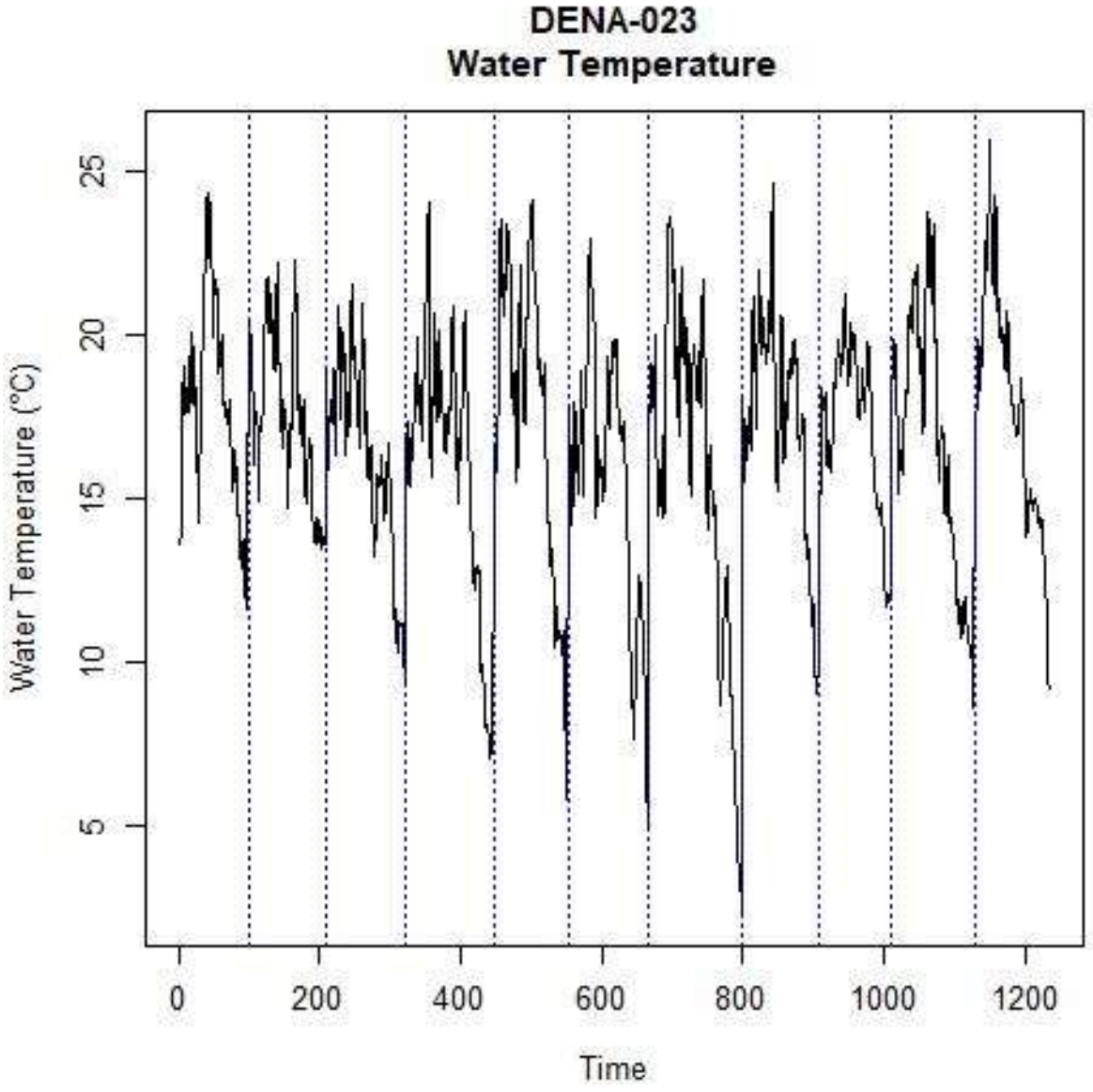


Figure A.193. Time series of DENA-023 water temperature measured at 1 m depth by time point with vertical lines for additive outliers.

Table A.204. Trend modeling results for daily water temperature data measured at 1 m depth at DENA-023.

			Trend			ARMA order		Ljung-Box Test	
Logged	**Method**	**Intercept**	**Coefficient**	**SE**	**p-value**	**AR**	**MA**	**Statistic**	**p-value**
FALSE	complete	14.5323	0.1913	0.0632	0.0025	0	5	542.69	< 0.0001
FALSE	completeAO	15.8858	0.0759	0.0604	0.2085	0	5	791.00	< 0.0001

			Trend			ARMA order		Ljung-Box Test	
Logged	Method	Intercept	Coefficient	SE	p-value	AR	MA	Statistic	p-value
FALSE	trunc	17.0728	0.0785	0.0358	0.0285	0	1	4327.71	< 0.0001
FALSE	truncSA	17.2940	0.0591	0.0570	0.2999	1	2	243.11	0.0004
TRUE	complete	2.6591	0.0110	0.0046	0.0181	0	5	435.41	< 0.0001
TRUE	completeAO	2.7271	0.0051	0.0045	0.2559	0	5	672.04	< 0.0001
TRUE	trunc	2.8286	0.0040	0.0018	0.0269	0	1	7838.24	< 0.0001
TRUE	truncSA	2.8392	0.0032	0.0032	0.3123	1	2	240.29	0.0005

Table A.205. Trend modeling results for weekly water temperature data measured at 1 m depth at DENA-023.

			Trend			ARMA order		Ljung-Box Test	
Logged	Method	Intercept	Coefficient	SE	p-value	AR	MA	Statistic	p-value
FALSE	complete	12.0489	0.3715	0.3199	0.2455	2	0	14.25	0.0270
FALSE	completeAO	16.5872	-0.0175	0.0647	0.7861	4	1	39.03	< 0.0001
FALSE	trunc	16.8055	0.0734	0.1188	0.5364	0	1	28.34	0.2031
FALSE	truncSA	16.5507	0.0705	0.0506	0.1629	2	0	24.25	0.3900
TRUE	complete	2.7948	-0.0017	0.0052	0.7529	2	2	11.22	0.0242
TRUE	completeAO	2.7839	-0.0026	0.0069	0.7100	2	2	41.52	< 0.0001
TRUE	trunc	2.8035	0.0035	0.0042	0.4102	2	1	48.83	0.0008
TRUE	truncSA	2.7894	0.0041	0.0030	0.1704	2	0	25.25	0.2854

Table A.206. Top covariate models for daily water temperature data measured at 1 m depth at DENA-023.

Model	AICc	ΔAICc	Ljung-Box Test p-value
Air Temperature + Wind Speed	3039.44	0.00	0.2650
Air Temperature + Wind Speed + Daily Precipitation	3041.03	1.59	0.1683
Air Temperature	3101.41	61.97	0.4279
Air Temperature + Daily Precipitation	3103.22	63.79	0.3101
Wind Speed + Daily Precipitation + Month	3270.43	230.99	0.0618
Wind Speed + Month	3279.39	239.95	0.1379
Daily Precipitation + Month	3288.00	248.57	0.0931
Wind Speed + Solar Radiation	3624.08	584.65	0.2013
Wind Speed + Solar Radiation + Daily Precipitation	3626.00	586.56	0.1155

Model	AICc	ΔAICc	Ljung-Box Test p-value
Solar Radiation	3640.87	601.43	0.2970

Table A.207. Coefficients and variance components estimates for the top covariate model for daily water temperature data measured at 1 m depth at DENA-023.

Parameter	Coefficient	SE	p-value
ar1	1.07	0.03	< 0.0001
ar2	-0.13	0.03	< 0.0001
intercept	12.21	0.39	< 0.0001
Air Temperature	0.36	0.01	< 0.0001
Wind Speed	-0.33	0.04	< 0.0001

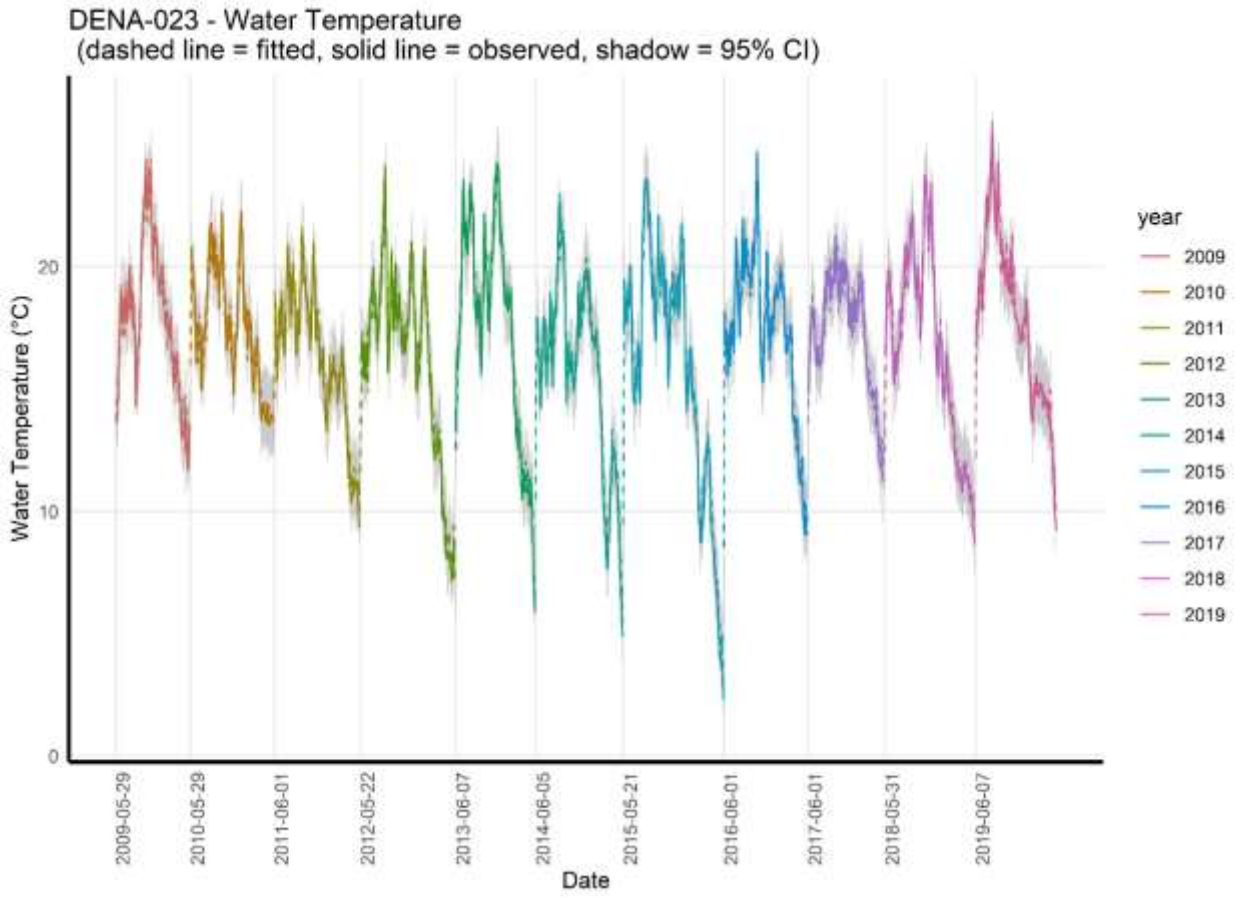


Figure A.194. Model predictions of DENA-023 water temperature measured at 1 m depth by date.

KOVA-085

Data

For KOVA-085, water temperature was recorded from 2010-2019. Water temperature was recorded at depths 0.25, 0.50, 1.00, and 1.50 m for all years except 2019 for which data at depth 0.50 m were missing. For years 2010-2014, water temperature was also recorded at depths 2.0 and 3.0, but these data were excluded from the analysis. Additionally, to reduce autocorrelation we only considered water observations from the depth 1.00 m. In total, 893 water temperature observations were included in the analysis when considering all dates, when truncated data to a common set of 68 dates observed in all years the dataset was reduced to 680 observations. Data for covariates were sufficiently complete that none of the covariates nor model years were omitted from the model selection process.

Model Selection

For KOVA-085, the truncated seasonally adjusted model for logged water temperature data yielded stationary residuals. The trend coefficient for this model was not significantly different from zero indicating there is no evidence for an increasing or decreasing trend in water temperature at KOVA-085. For ARIMA models fitting all possible covariate combinations at lake KOVA-085, AICc-based model selection yielded a final model with an ARIMA(3,0,0) structure and a fixed effect for air temperature. Water temperature was estimated to increase with increasing air temperature.

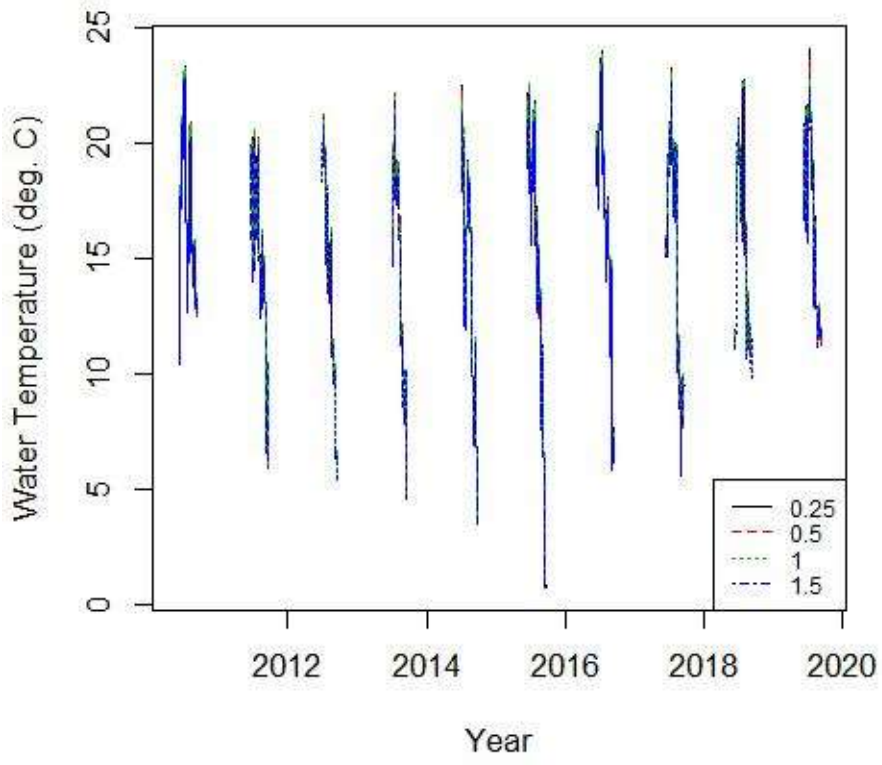


Figure A.195. KOVA-085 water temperature by depth and year.

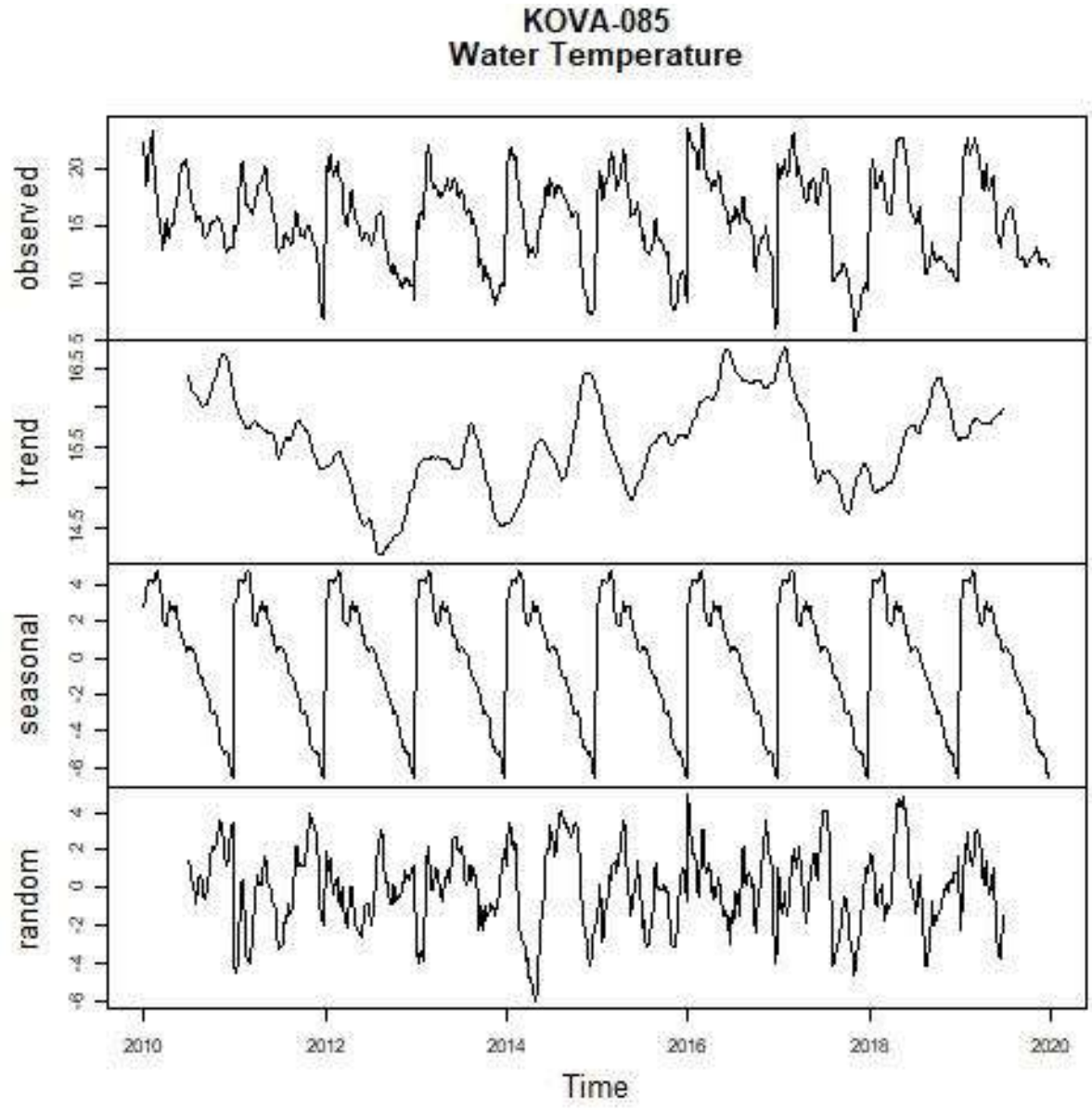


Figure A.196. Time series decomposition of truncated KOVA-085 water temperature measured at 1 m depth by year.

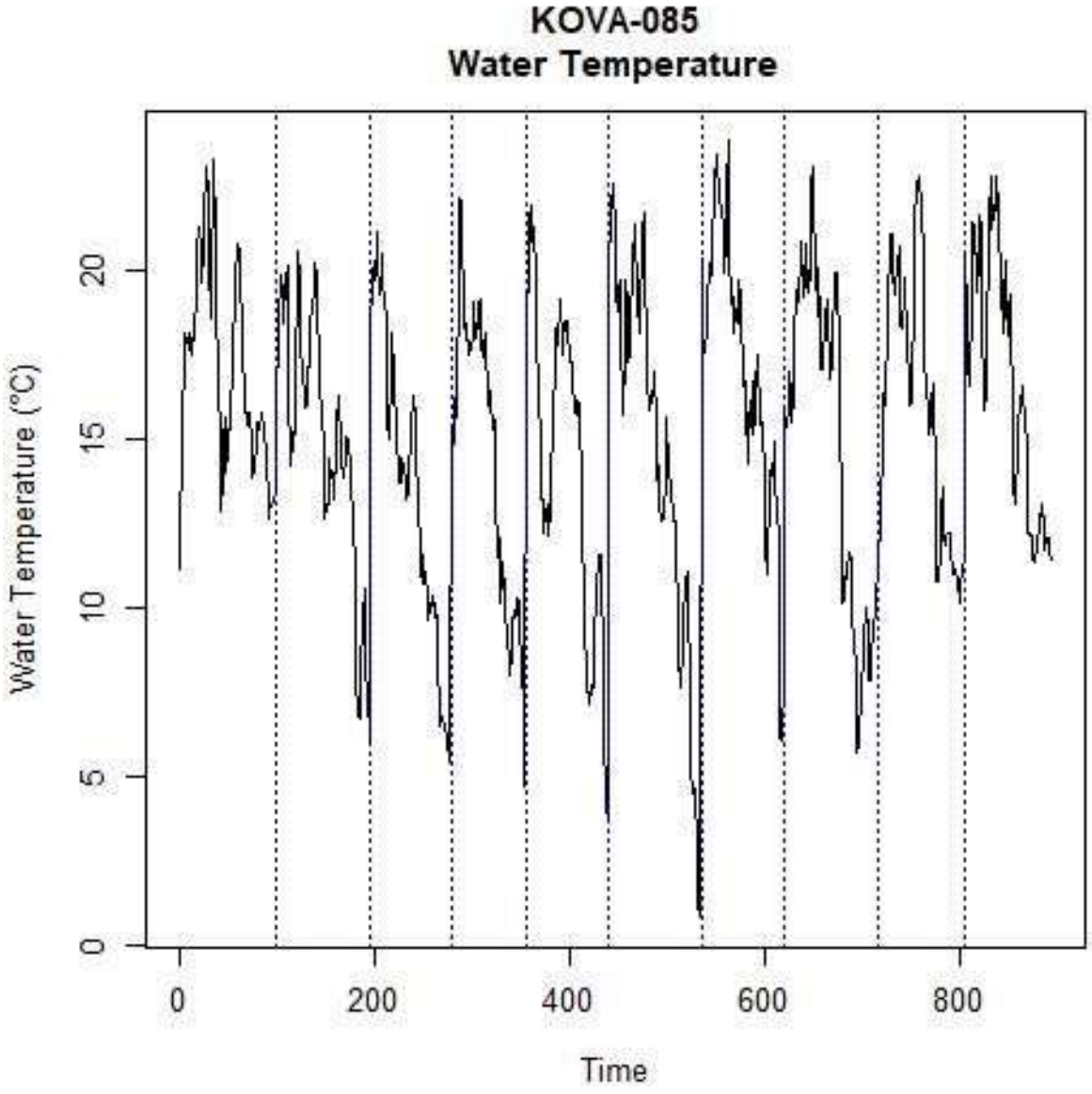


Figure A.197. Time series of KOVA-085 water temperature measured at 1 m depth by time point with vertical lines for additive outliers.

Table A.208. Trend modeling results for daily water temperature data measured at 1 m depth at KOVA-085.

			Trend			ARMA order		Ljung-Box Test	
Logged	**Method**	**Intercept**	**Coefficient**	**SE**	**p-value**	**AR**	**MA**	**Statistic**	**p-value**
FALSE	complete	10.7334	0.4042	0.0953	< 0.0001	0	5	336.45	< 0.0001
FALSE	completeAO	12.5412	0.2421	0.0867	0.0053	0	5	500.74	< 0.0001

			Trend			ARMA order		Ljung-Box Test	
Logged	Method	Intercept	Coefficient	SE	p-value	AR	MA	Statistic	p-value
FALSE	trunc	13.2381	0.2087	0.1019	0.0404	0	4	802.15	< 0.0001
FALSE	truncSA	15.3813	0.0215	0.0863	0.8036	2	0	128.09	0.5800
TRUE	complete	2.3579	0.0278	0.0085	0.0011	0	5	175.44	< 0.0001
TRUE	completeAO	2.4490	0.0194	0.0078	0.0137	0	5	288.51	< 0.0001
TRUE	trunc	2.6181	0.0085	0.0065	0.1957	0	3	1055.17	< 0.0001
TRUE	truncSA	2.7150	-0.0001	0.0062	0.9930	2	0	116.58	0.8282

Table A.209. Top covariate models for daily water temperature data measured at 1 m depth at KOVA-085.

Model	AICc	ΔAICc	Ljung-Box Test p-value
Air Temperature	2604.48	0.00	0.1047
Air Temperature + Wind Speed	2611.35	6.87	0.2777
Air Temperature + Wind Speed + Daily Precipitation	2611.97	7.49	0.1835
Air Temperature + Daily Precipitation	2614.44	9.96	0.1304
Wind Speed + Month	2695.95	91.46	0.7527
Wind Speed + Daily Precipitation + Month	2697.97	93.49	0.7010
Daily Precipitation + Month	2698.74	94.25	0.7433
Wind Speed + Solar Radiation	3084.03	479.55	0.6220
Solar Radiation	3084.15	479.66	0.7563
Solar Radiation + Daily Precipitation	3084.75	480.27	0.6170

Table A.210. Coefficients and variance components estimates for the top covariate model for daily water temperature data measured at 1 m depth at KOVA-085.

Parameter	Coefficient	SE	p-value
ar1	1.99	0.04	< 0.0001
ar2	-1.06	0.07	< 0.0001
ar3	0.07	0.03	0.0593
ma1	-0.98	0.01	< 0.0001
intercept	9.95	0.27	< 0.0001
Air Temperature	0.41	0.02	< 0.0001

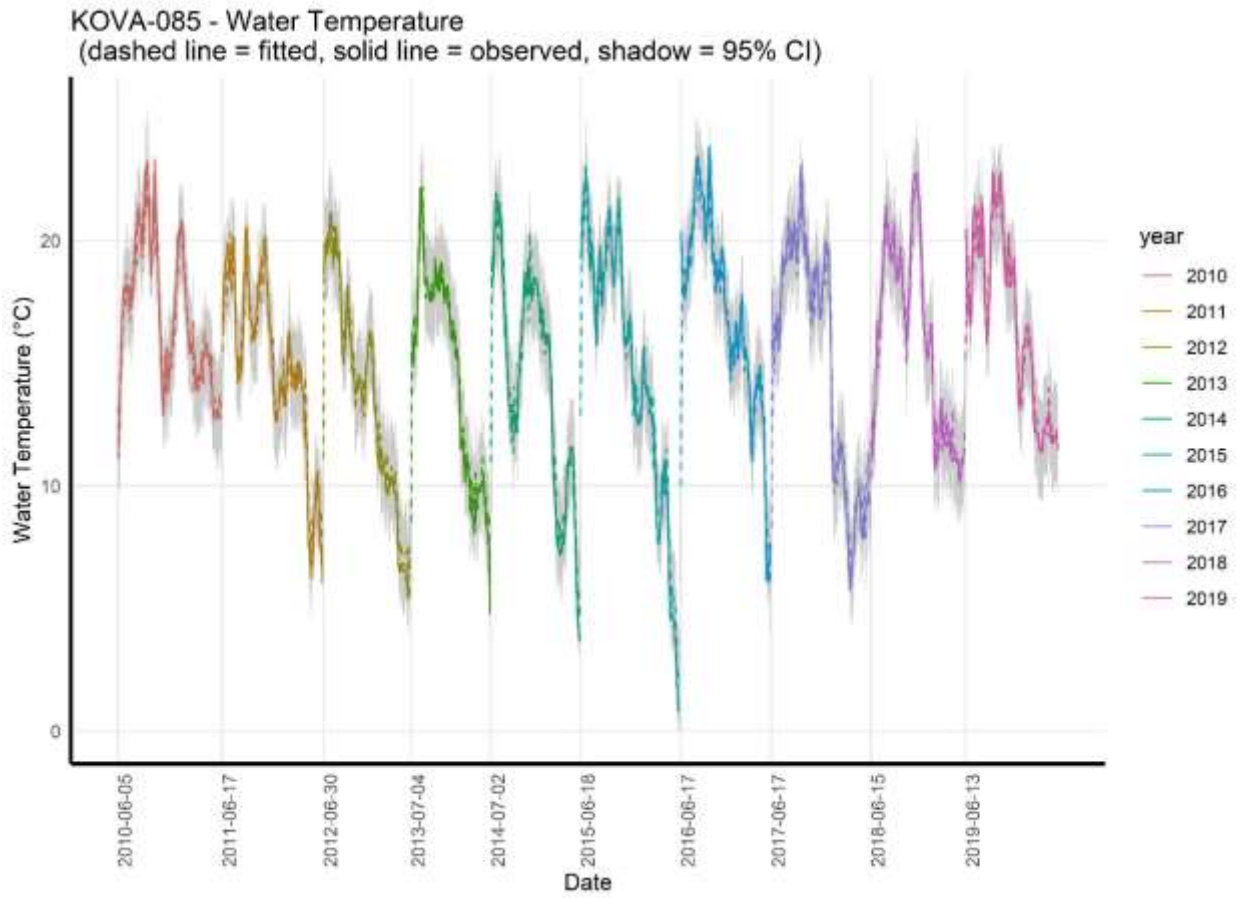


Figure A.198. Model predictions of KOVA-085 water temperature measured at 1 m depth by date.

KOVA-086

Data

For KOVA-086, water temperature was recorded from 2009-2019, however data were absent from year 2010, thus only years 2011-2019 were included in this analysis. Water temperature was recorded from June-September at depths 0.25, 0.50, 1.00, 1.50, 2.00, and 3.00 m. To reduce autocorrelation we only considered water observations from a single depth in this analysis and selected depth 0.25 m as it was the only depth with no missing water temperature data. In total, 794 observations were included in the analysis when considering all dates; when truncating data to the common set of 68 dates visited in every year, the number of observations was reduced to 612. Please note that values of the wind speed covariate are suspiciously low for year 2013, these data should be inspected for accuracy.

Model Selection

For KOVA-086, the truncated seasonally adjusted model for logged water temperature data yielded stationary residuals. The trend coefficients for these models were not significantly different from zero indicating there is no evidence for an increasing or decreasing trend in water temperature at KOVA-086. For ARIMA models fitting all possible covariate combinations at lake KOVA-086, AICc-based model selection yielded a final model with an ARIMA(2,0,1) structure and fixed effects for relative humidity and month. Water temperature was estimated to decrease with increasing relative humidity and increasing month (from June-September).

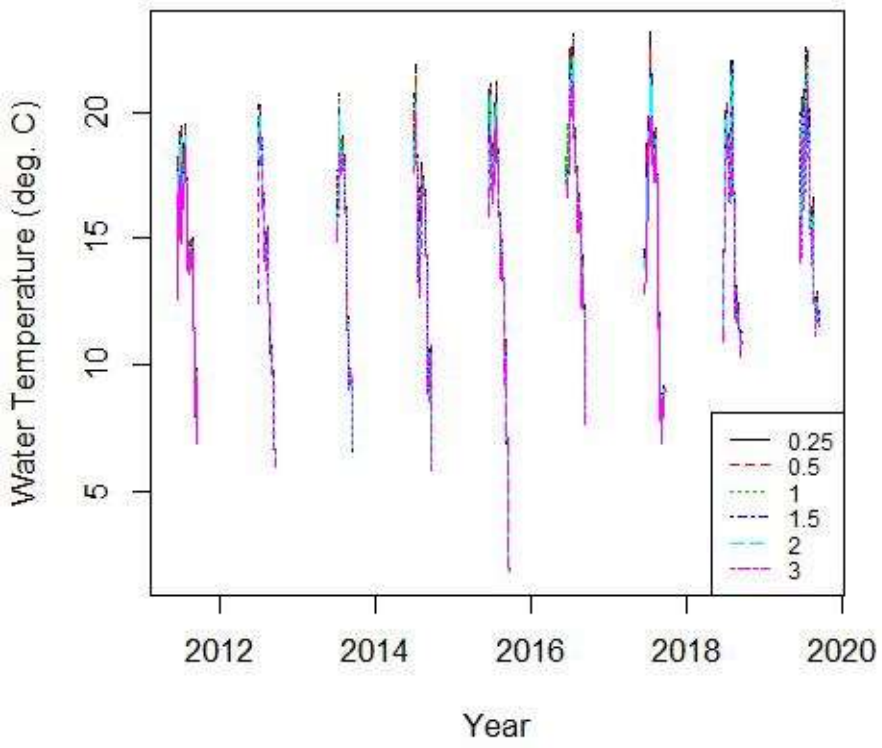


Figure A.199. KOVA-086 water temperature by depth and year.

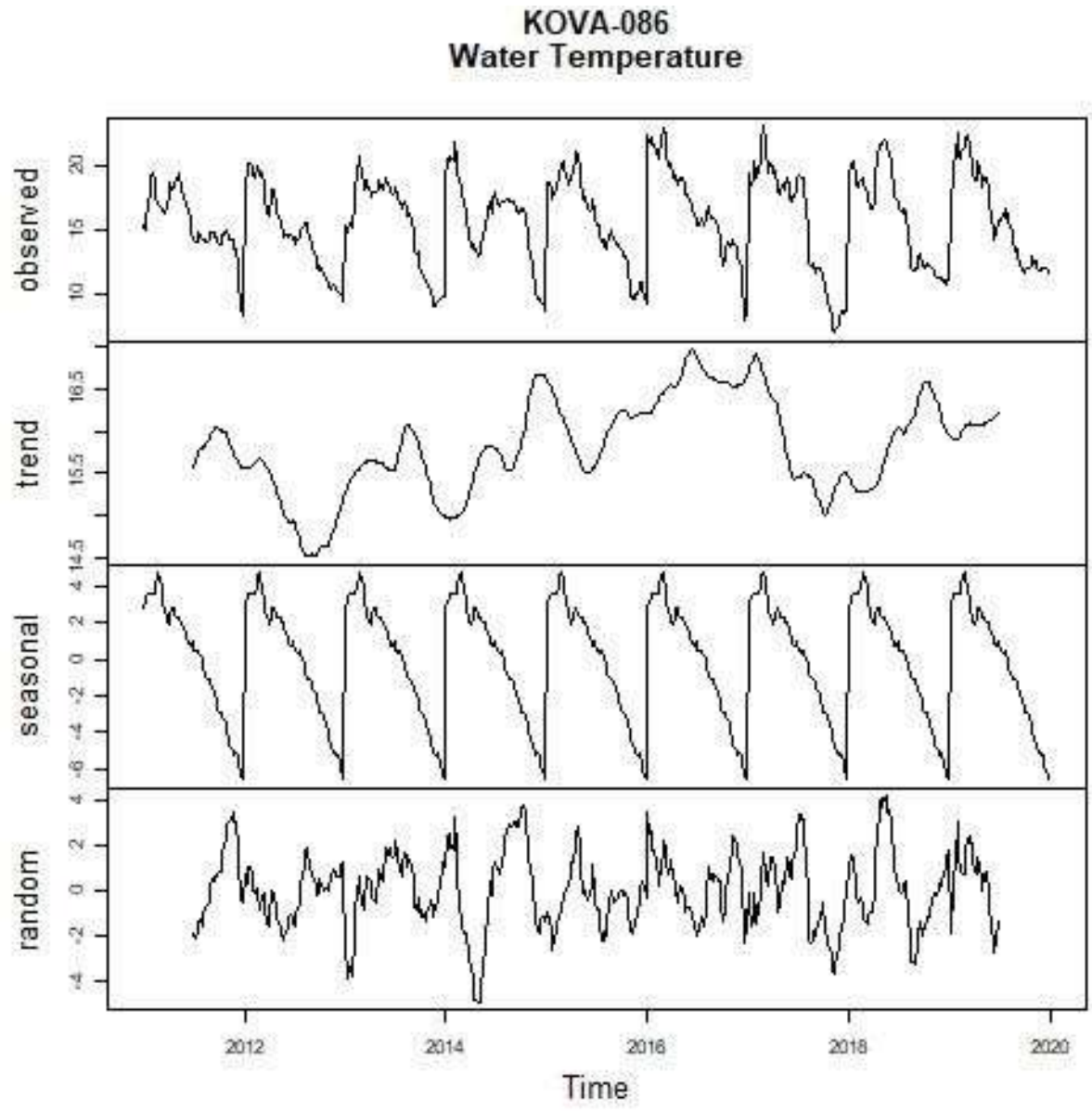


Figure A.200. Time series decomposition of truncated KOVA-086 water temperature measured at 0.25 m depth by year.

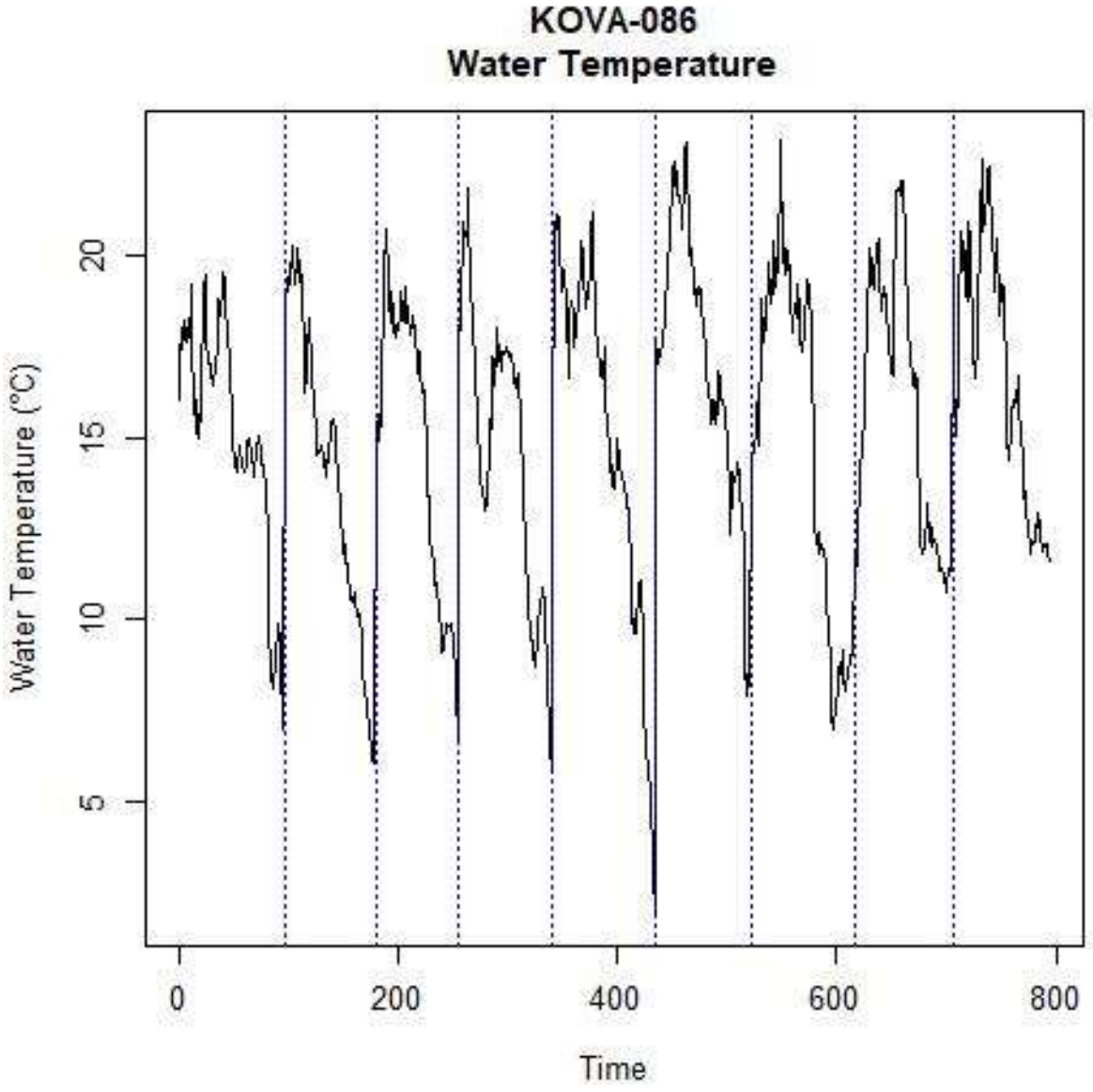


Figure A.201. Time series of KOVA-086 water temperature measured at 0.25 m depth by time point with vertical lines for additive outliers.

Table A.211. Trend modeling results for daily water temperature data measured at 0.25 m depth at KOVA-086.

			Trend			ARMA order		Ljung-Box Test	
Logged	**Method**	**Intercept**	**Coefficient**	**SE**	**p-value**	**AR**	**MA**	**Statistic**	**p-value**
FALSE	complete	7.8403	0.6241	0.1024	< 0.0001	0	5	416.93	< 0.0001
FALSE	completeAO	10.2576	0.4192	0.0921	< 0.0001	0	5	584.89	< 0.0001

			Trend			ARMA order		Ljung-Box Test	
Logged	**Method**	**Intercept**	**Coefficient**	**SE**	**p-value**	**AR**	**MA**	**Statistic**	**p-value**
FALSE	trunc	10.9135	0.4046	0.0970	< 0.0001	0	4	1331.17	< 0.0001
FALSE	truncSA	14.3884	0.1155	0.0934	0.2163	2	0	97.44	0.9164
TRUE	complete	2.1702	0.0429	0.0084	< 0.0001	0	5	254.89	< 0.0001
TRUE	completeAO	2.2958	0.0321	0.0077	< 0.0001	0	5	387.83	< 0.0001
TRUE	trunc	2.3573	0.0310	0.0076	< 0.0001	0	5	988.59	< 0.0001
TRUE	truncSA	2.6593	0.0060	0.0064	0.3473	2	0	102.57	0.8433

Table A.212. Top covariate models for daily water temperature data measured at 0.25 m depth at KOVA 086.

Model	**AICc**	**ΔAICc**	**Ljung-Box Test p-value**
Relative Humidity + Month	2020.54	0.00	0.5126
Wind Speed + Relative Humidity + Month	2021.02	0.48	0.3958
Daily Precipitation + Month	2040.67	20.13	0.5825
Wind Speed + Month	2040.71	20.16	0.5966
Wind Speed + Daily Precipitation + Month	2041.85	21.31	0.4670
Air Temperature	2076.19	55.64	0.4481
Air Temperature + Wind Speed	2076.76	56.22	0.3057
Air Temperature + Daily Precipitation	2077.94	57.39	0.3254
Air Temperature + Wind Speed + Daily Precipitation	2078.37	57.83	0.1975
Solar Radiation	2418.39	397.84	0.0958

Table A.213. Coefficients and variance components estimates for the top covariate model for daily water temperature data measured at 0.25 m depth at KOVA-086.

Parameter	**Coefficient**	**SE**	**p-value**
Ar1	1.40	0.16	< 0.0001
Ar2	-0.44	0.15	0.0036
Ma1	-0.27	0.17	0.1199
Intercept	34.38	0.85	< 0.0001
Relative Humidity	-0.01	0.00	< 0.0001
Month	-2.38	0.09	< 0.0001

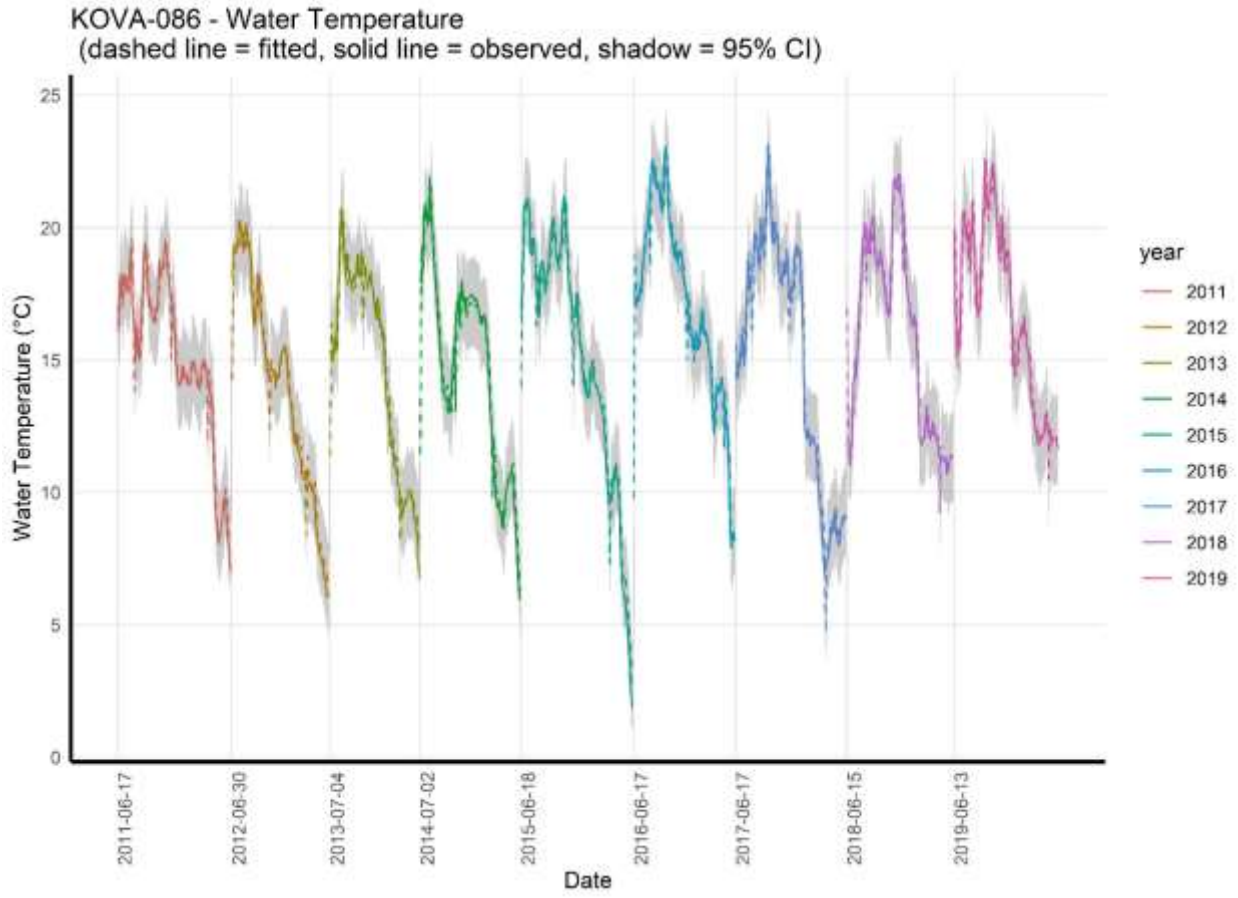


Figure A.202. Model predictions of KOVA-086 water temperature measured at 0.25 m depth by date.

NOAT-052

Data

For NOAT-052, water temperature was recorded from 2015-2019, during the months June-September, at depths 0.25, 0.50, 1.00, 1.50, 2.00, and 3.00 m. To reduce autocorrelation we only considered water observations from a single depth in this analysis and selected depth 1.50 m as it there were no missing water temperature data at this depth. When considering all dates and water temperature observations at depth 1.50 m, 456 observations were included in the analysis. When truncating data to the common set of 85 days visited in every year, the number of observations was reduced to 425. Data for covariates were sufficiently complete that none of the covariates nor model years were omitted from the model selection process.

Model Selection

For NOAT-052, the truncated seasonally adjusted model for logged water temperature data yielded stationary residuals. The trend coefficients for these models were not significantly different from zero indicating there is no evidence for an increasing or decreasing trend in water temperature at NOAT-052. For ARIMA models fitting all possible covariate combinations at lake NOAT-052, AICc-based model selection yielded a final model with an ARIMA(2,0,0) structure and fixed effects for relative humidity and month. Water temperature was estimated to decrease with increasing relative humidity and increasing month (from June-September). When inspecting residuals from this top covariate model we observed that the model appears to over-predict water temperature at low air temperatures and at high wind speeds.

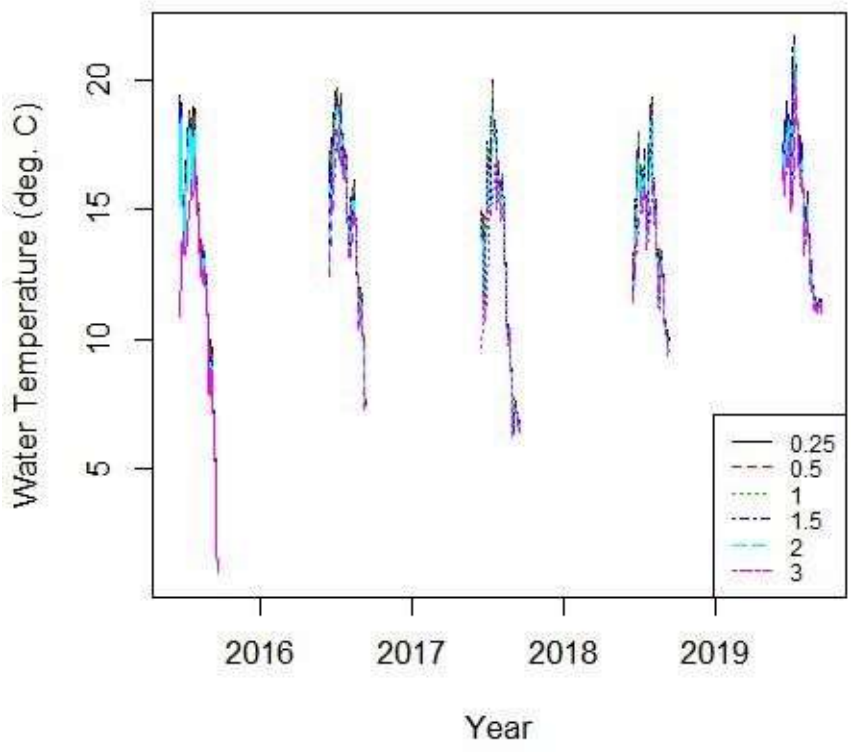


Figure A.203. NOAT-052 water temperature by depth and year.

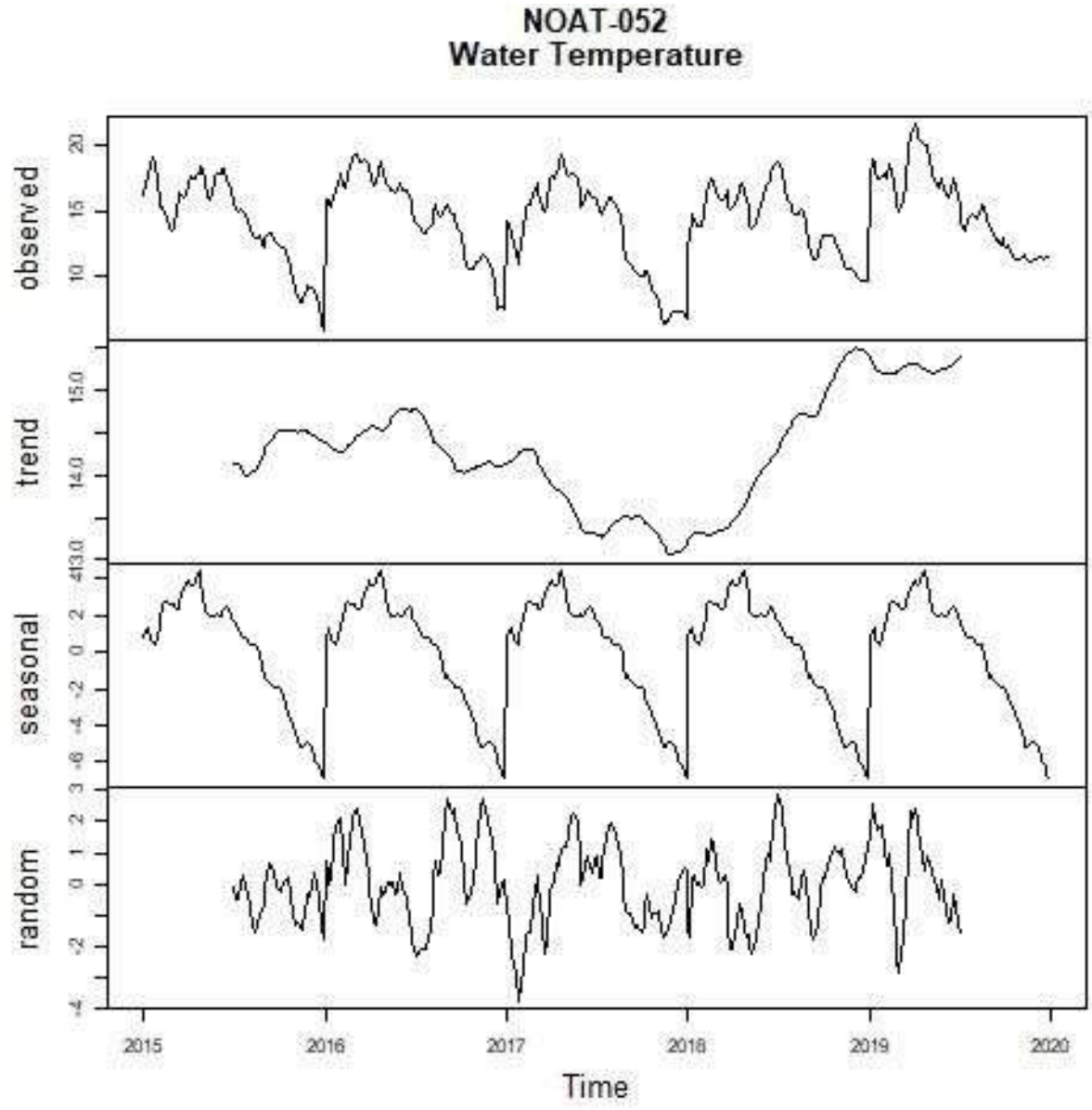


Figure A.204. Time series decomposition of truncated NOAT-052 water temperature measured at 1.5 m depth by year.

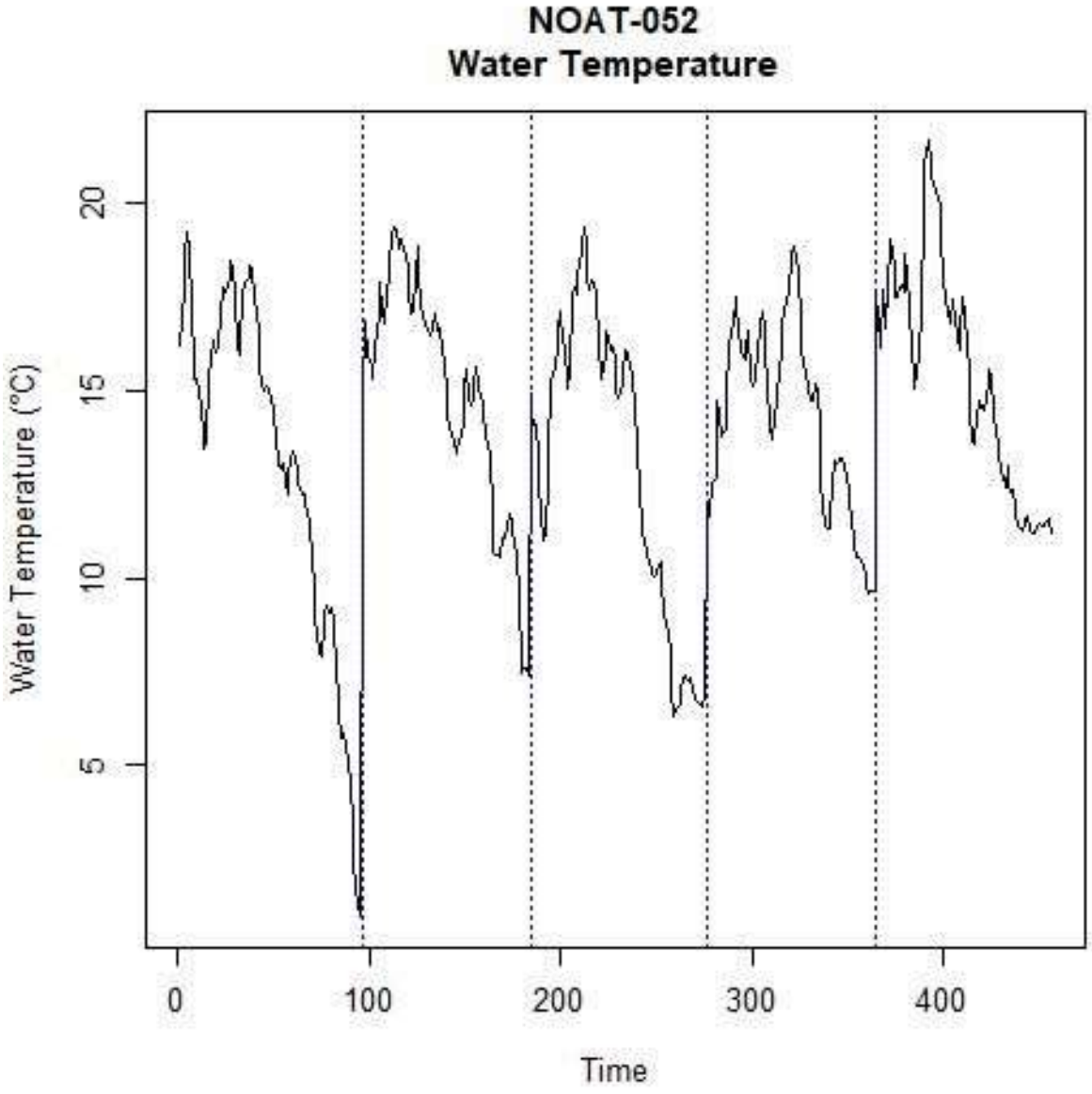


Figure A.205. Time series of NOAT-052 water temperature measured at 1.5 m depth by time point with vertical lines for additive outliers.

Table A.214. Trend modeling results for daily water temperature data measured at 1.5 m depth at NOAT-052.

			Trend			ARMA order		Ljung-Box Test	
Logged	**Method**	**Intercept**	**Coefficient**	**SE**	**p-value**	**AR**	**MA**	**Statistic**	**p-value**
FALSE	complete	-12.6317	1.7810	0.2599	< 0.0001	0	5	358.31	< 0.0001
FALSE	completeAO	7.7200	0.4237	0.1182	0.0003	0	0	2593.04	< 0.0001

			Trend			ARMA order		Ljung-Box Test	
Logged	**Method**	**Intercept**	**Coefficient**	**SE**	**p-value**	**AR**	**MA**	**Statistic**	**p-value**
FALSE	trunc	NA	0.9623	0.0192	< 0.0001	0	5	699.12	< 0.0001
FALSE	truncSA	12.3256	0.1403	0.1355	0.3005	3	3	96.70	0.0640
TRUE	complete	0.6186	0.1319	0.0239	< 0.0001	0	5	138.41	< 0.0001
TRUE	completeAO	1.8593	0.0491	0.0114	< 0.0001	0	0	1900.28	< 0.0001
TRUE	trunc	0.9093	0.1151	0.0210	< 0.0001	0	5	699.75	< 0.0001
TRUE	truncSA	2.4666	0.0119	0.0126	0.3448	2	1	89.99	0.2086

Table A.215. Top covariate models for daily water temperature data measured at 1.5 m depth at NOAT-052.

Model	**AICc**	**ΔAICc**	**Ljung-Box Test p-value**
Relative Humidity + Month	957.40	0.00	0.4611
Daily Precipitation + Month	965.85	8.45	0.5209
Wind Speed + Month	966.84	9.44	0.5130
Wind Speed + Daily Precipitation + Month	967.61	10.21	0.4140
Air Temperature	1155.44	198.04	0.1940
Air Temperature + Daily Precipitation	1156.67	199.27	0.1039
Air Temperature + Wind Speed	1157.37	199.97	0.1134
Air Temperature + Wind Speed + Daily Precipitation	1158.69	201.29	0.0518
Solar Radiation	1235.29	277.89	0.2483
Wind Speed + Solar Radiation	1237.26	279.86	0.1517

Table A.216. Coefficients and variance components estimates for the top covariate model for daily water temperature data measured at 1.5 m depth at NOAT-052.

Parameter	**Coefficient**	**SE**	**p-value**
Ar1	1.27	0.04	< 0.0001
Ar2	-0.32	0.04	< 0.0001
Intercept	28.86	0.93	< 0.0001
Relative Humidity	-0.01	0.00	0.0015
Month	-1.91	0.09	< 0.0001

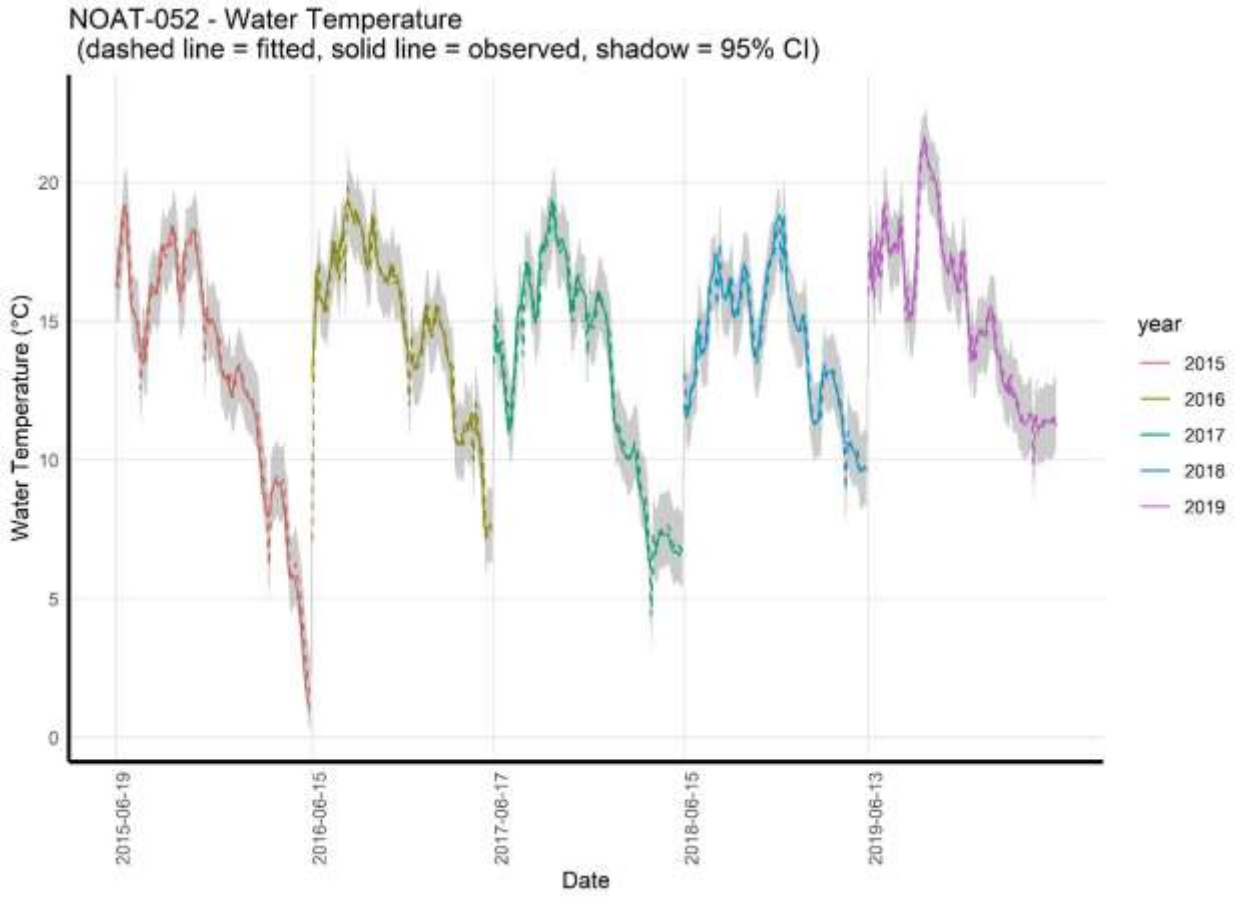


Figure A.206. Model predictions of NOAT-052 water temperature measured at 1.5 m depth by date.

NOAT-107

Data

For NOAT-107, water temperature was recorded from 2014-2019, however no data were recorded in 2016. Therefore, only two consecutive years of data are available for analysis so trend analysis cannot be conducted.

WRST-005

Water temperature data were not collected at WRST-005.

WRST-016

Data

For WRST-016, water temperature was recorded from 2009-2019, during the months May-September, at water depths of 0.25, 0.50, 1.00, 1.50, 2.00, and 3.00 m. To reduce autocorrelation we only considered water observations from a single depth in this analysis and selected depth 1.00 m as it there were no missing water temperature data at this depth. When considering all dates and water temperature observations at depth 1.00 m, 1173 observations were included in the analysis. When truncating the data to a common set of 74 days, the total number of observations was reduced to 814.

When aggregated to mean weekly values the water temperature dataset contained 180 observations. When truncating to the subset of 12 common weeks sampled in every year the number of observations was reduced to 132.

Model Selection

For lake WRST-016, no trend models nor any covariate models yielded stationary residuals when fit to daily water temperature data. However, when fitting trend models to the weekly water temperature data, the complete, truncated, and truncated seasonally adjusted for unlogged and logged data yielded stationary residuals. Of these six models, three included positive trend coefficients that were significantly greater than zero, indicating there is evidence for an increasing trend in water temperature at lake WRST-016. For ARIMA models fitting all possible covariate combinations at lake WRST-016, AICc-based model selection yielded a final model with a ARIMA(4,0,1) structure and a fixed effect for air temperature. Water temperature is estimated to increase with increasing air temperature.

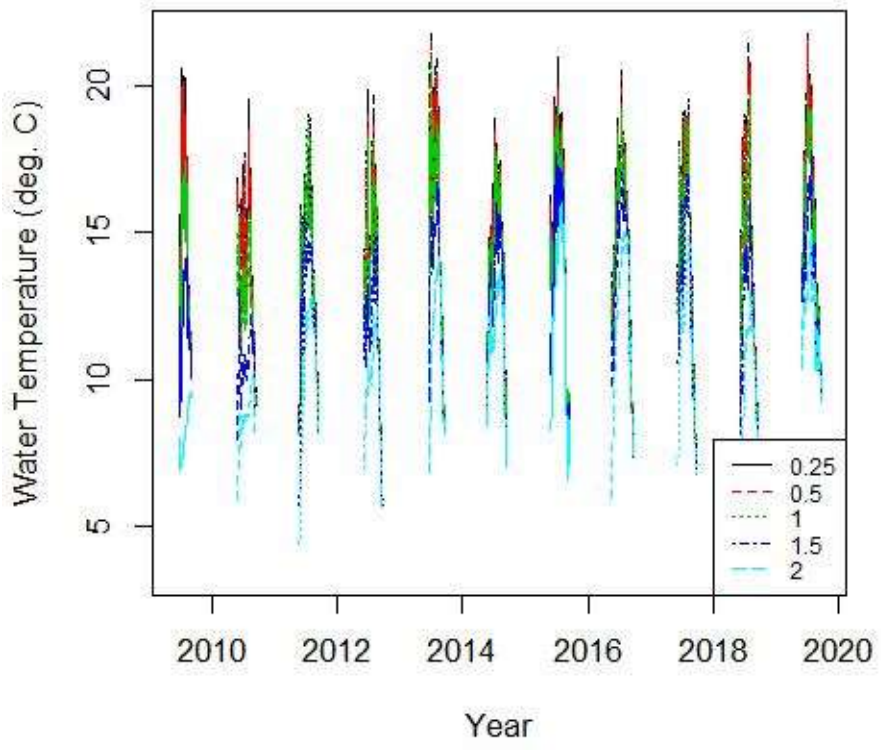


Figure A.207. WRST-016 water temperature by depth and year.

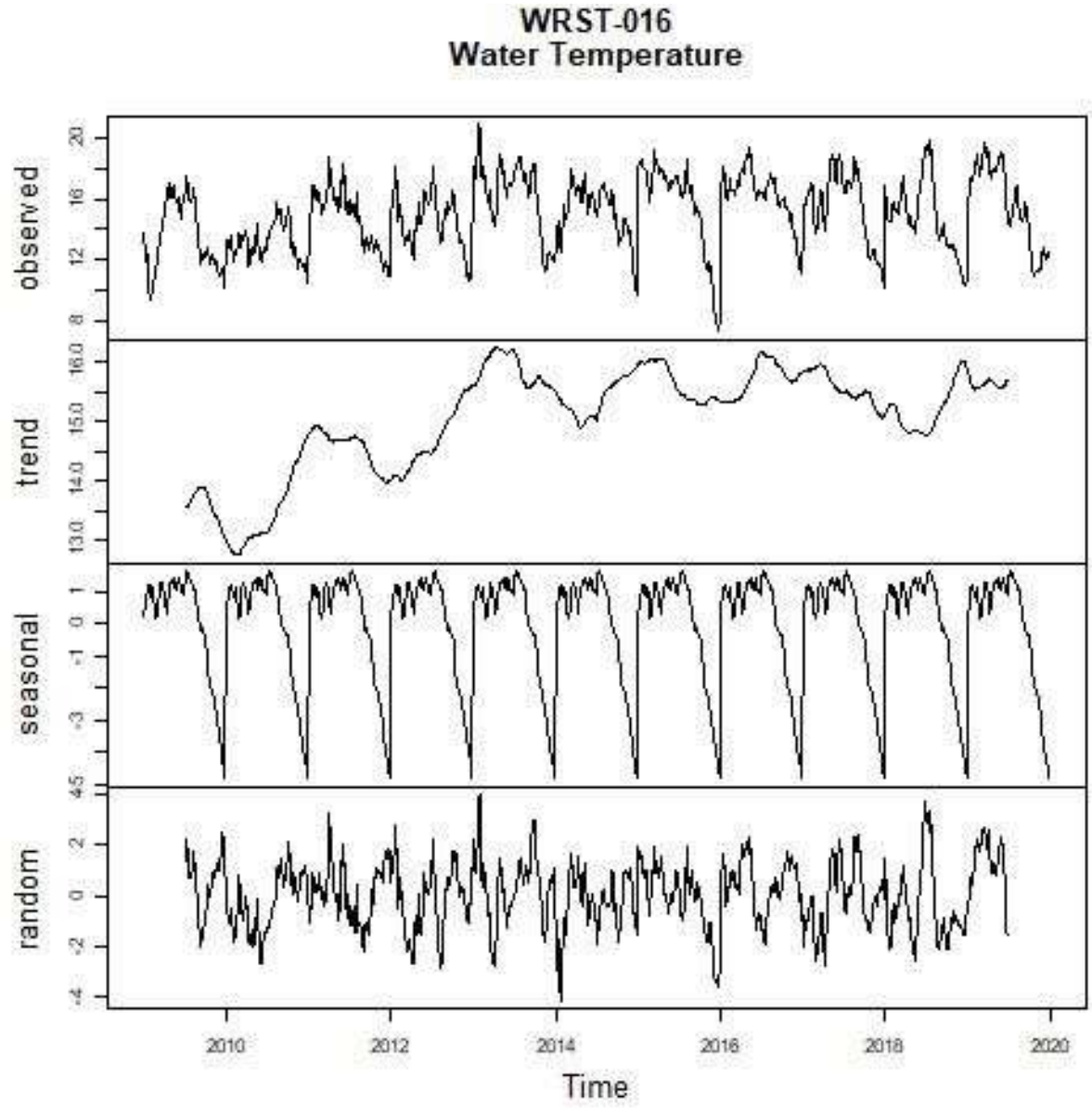


Figure A.208. Time series decomposition of truncated WRST-016 water temperature measured at 1 m depth by year.

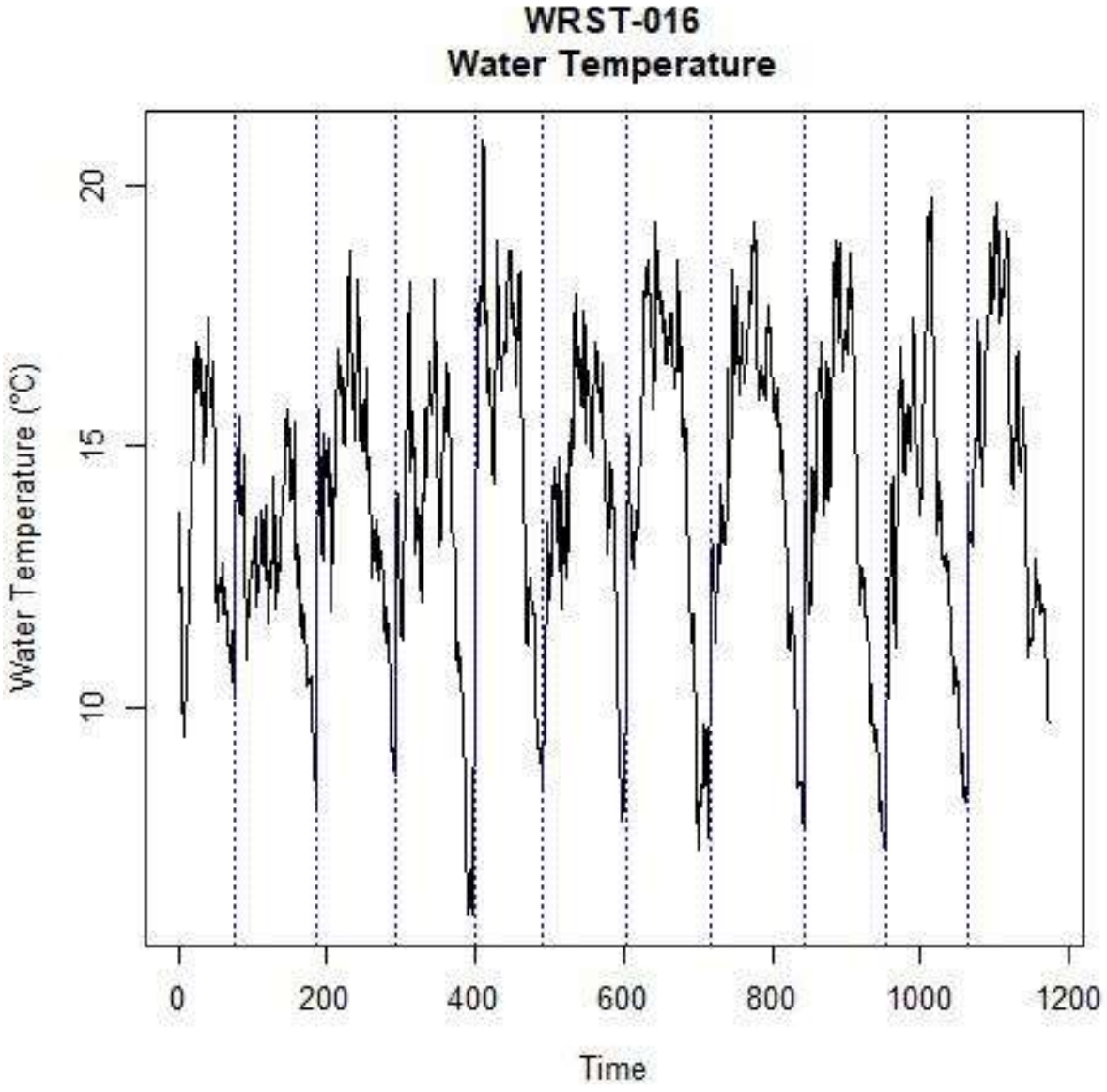


Figure A.209. Time series of WRST-016 water temperature measured at 1 m depth by time point with vertical lines for additive outliers.

Table A.217. Trend modeling results for daily water temperature data measured at 1 m depth at WRST-016.

			Trend			ARMA order		Ljung-Box Test	
Logged	**Method**	**Intercept**	**Coefficient**	**SE**	**p-value**	**AR**	**MA**	**Statistic**	**p-value**
FALSE	complete	11.6963	0.1909	0.0460	< 0.0001	0	5	662.75	< 0.0001
FALSE	completeAO	12.3772	0.1343	0.0456	0.0032	0	5	915.46	< 0.0001

			Trend			ARMA order		Ljung-Box Test	
Logged	Method	Intercept	Coefficient	SE	p-value	AR	MA	Statistic	p-value
FALSE	trunc	11.9748	0.2499	0.0425	< 0.0001	0	3	1299.15	< 0.0001
FALSE	truncSA	12.7220	0.1891	0.0590	0.0014	2	2	209.60	0.0002
TRUE	complete	2.4326	0.0152	0.0036	< 0.0001	0	5	649.80	< 0.0001
TRUE	completeAO	2.4984	0.0097	0.0035	0.0060	0	5	914.59	< 0.0001
TRUE	trunc	2.4437	0.0208	0.0039	< 0.0001	0	5	574.27	< 0.0001
TRUE	truncSA	2.5423	0.0127	0.0040	0.0015	2	2	199.27	0.0011

Table A.218. Trend modeling results for weekly water temperature data measured at 1 m depth at WRST-016.

			Trend			ARMA order		Ljung-Box Test	
Logged	Method	Intercept	Coefficient	SE	p-value	AR	MA	Statistic	p-value
FALSE	complete	12.5542	0.0991	0.0432	0.0218	4	1	4.97	0.1739
FALSE	completeAO	12.6004	0.0914	0.0484	0.0586	2	3	16.71	0.0008
FALSE	trunc	11.4847	0.2272	0.1106	0.0399	0	1	14.79	0.7358
FALSE	truncSA	11.9124	0.2136	0.0335	< 0.0001	0	1	19.20	0.4440
TRUE	complete	2.5396	0.0047	0.0029	0.1085	2	1	4.25	0.5147
TRUE	completeAO	2.5522	0.0031	0.0027	0.2416	4	1	14.89	0.0019
TRUE	trunc	2.4455	0.0159	0.0082	0.0525	2	0	14.75	0.6790
TRUE	truncSA	2.4690	0.0152	0.0024	< 0.0001	0	1	14.28	0.7670

Table A.219. Top covariate models for weekly water temperature means measured at 1 m depth at WRST-016.

Model	AICc	ΔAICc	Ljung-Box Test p-value
Air Temperature + Year	620.19	0.00	0.2914
Air Temperature	620.51	0.32	0.3206
Air Temperature + Daily Precipitation + Year	620.95	0.76	0.1111
Air Temperature + Daily Precipitation	621.13	0.93	0.3099
Air Temperature + Wind Speed + Year	621.49	1.29	0.0690
Air Temperature + Wind Speed	621.56	1.37	0.3226
Air Temperature + Wind Speed + Daily Precipitation	621.62	1.43	0.1103
Air Temperature + Wind Speed + Daily Precipitation + Year	621.76	1.57	0.0982
Year + Month	651.94	31.75	0.0833

Model	AICc	ΔAICc	Ljung-Box Test p-value
Daily Precipitation + Month	656.53	36.34	0.0775

Table A.220. Coefficients and variance components estimates for the top covariate model for weekly mean water temperature measured at 1 m depth at WRST-016.

Parameter	Coefficient	SE	p-value
Ar1	1.52	0.11	< 0.0001
Ar2	-0.65	0.16	< 0.0001
Ar3	0.04	0.14	0.7579
Ar4	-0.09	0.08	0.3065
Ma1	-0.77	0.07	< 0.0001
Intercept	9.14	0.58	< 0.0001
Air Temperature	0.37	0.04	< 0.0001

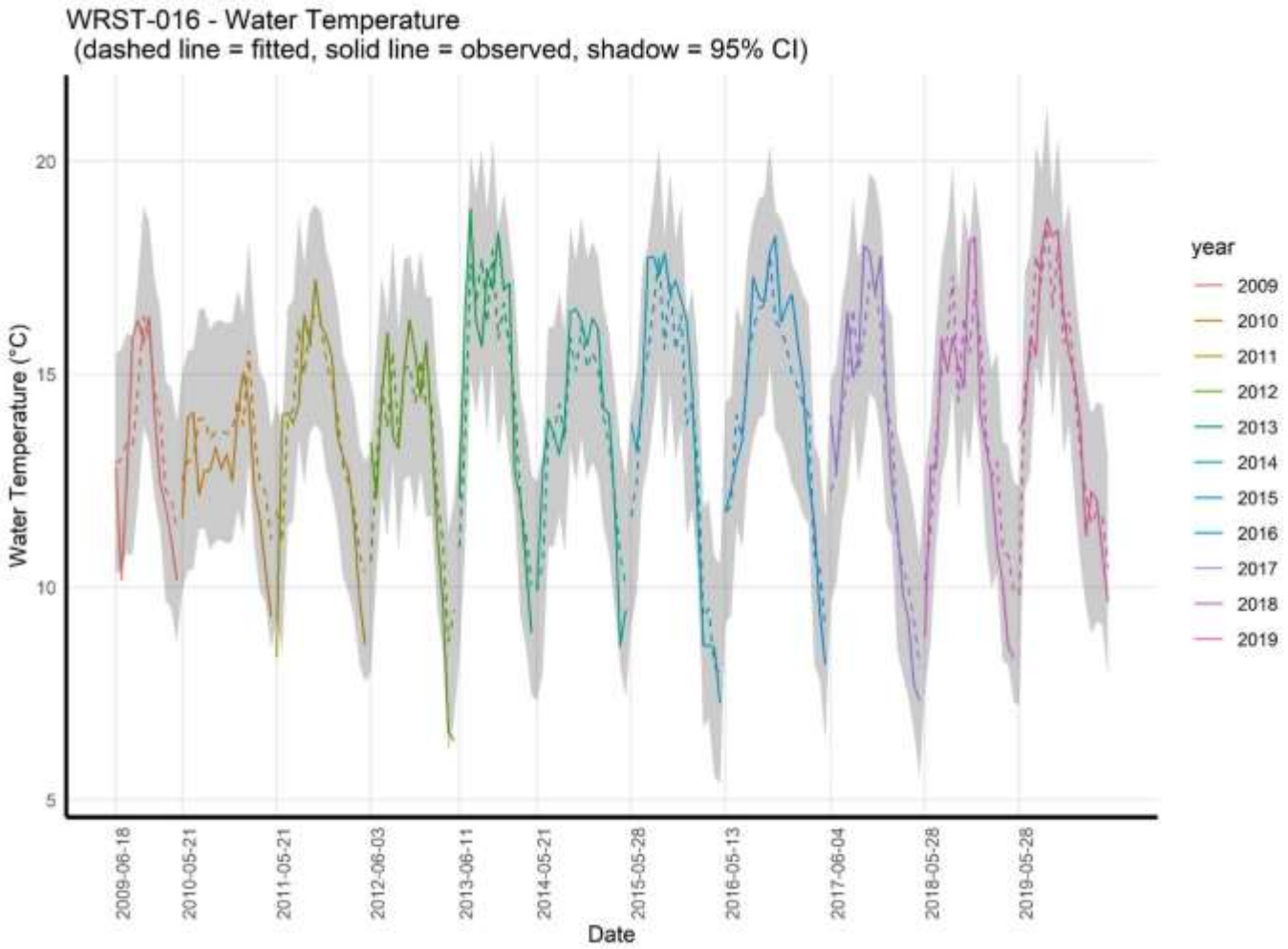


Figure A.210. Model predictions of WRST-016 water temperature measured at 1 m depth by week.

YUCH-004

Data

For YUCH-004, water temperature was recorded from 2005-2019, however data were not available for years 2007-2008 and data were not recorded at a water depth of 3.00 m in 2009, thus we only considered years 2010-2019 in this analysis. During this time span (2010-2019), water temperature was recorded during the months May-October and at water depths 0.25, 0.50, 1.00, 1.50, 2.00, and 3.00 m. To reduce autocorrelation we only considered water observations from a single depth in this analysis and selected depth 1.00 m as it there were no missing water temperature data at this depth. Additionally, we excluded the months May and October from the analyses due to sparse data. The resulting dataset included 1100 water temperature observations. When the data were further truncated to the common set of 98 days visited in every year the number of observations was reduced to 980. Data for covariates were missing in 2019, thus data from this year was removed from the ARIMA covariate models.

When aggregating water temperature to weekly means, the total number of observations was reduced to 174, and when truncating the weekly data to the common set of 14 weeks visiting in every year the number of observations was reduced to 140.

Model Selection

For lake YUCH-004, no trend models nor covariate models yielded stationary residuals when fit to the daily water temperature data. When fit to the weekly water temperature data the truncated seasonally adjusted models of the logged and unlogged water temperature data yielded stationary residuals. Neither of these two models included a trend coefficient that was significantly different from zero, indicating there is no evidence for an increasing or decreasing trend in water temperature at lake YUCH-004. For ARIMA models fitting all possible covariate combinations at lake YUCH-004 only two models yielded stationary residuals and the top-ranked model with the lowest AICc score had an ARIMA(5,0,3) structure and fixed effects for winds speed and month. Water temperature is estimated to increase with speed and decrease with month (June-September). When inspecting residuals from this covariate model it is apparent that the residuals are positively correlated to air temperature and solar radiation.

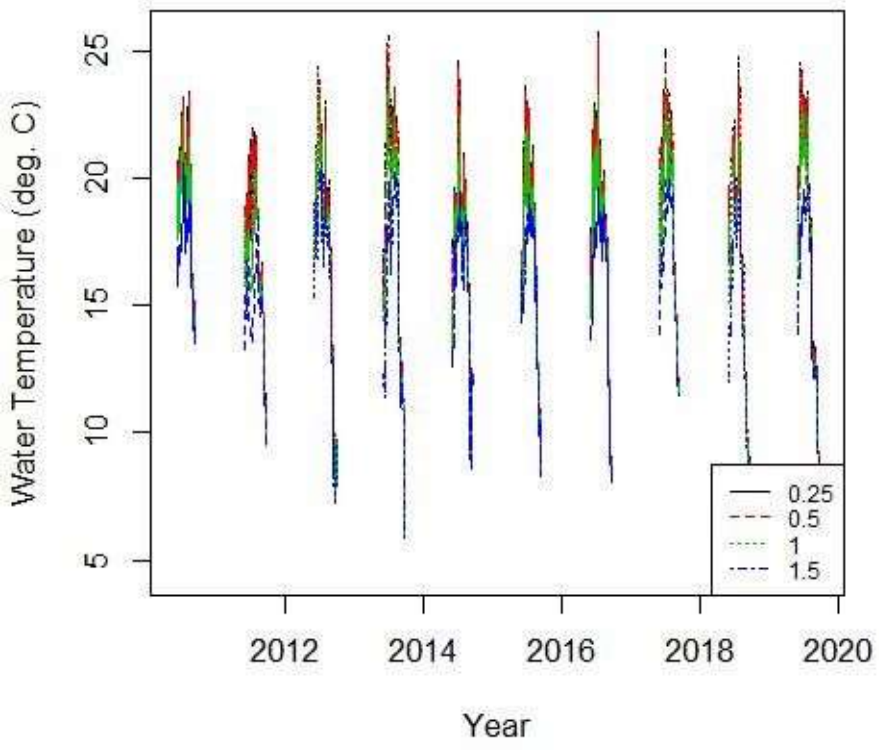


Figure A.211. YUCH-004 water temperature by depth and year.

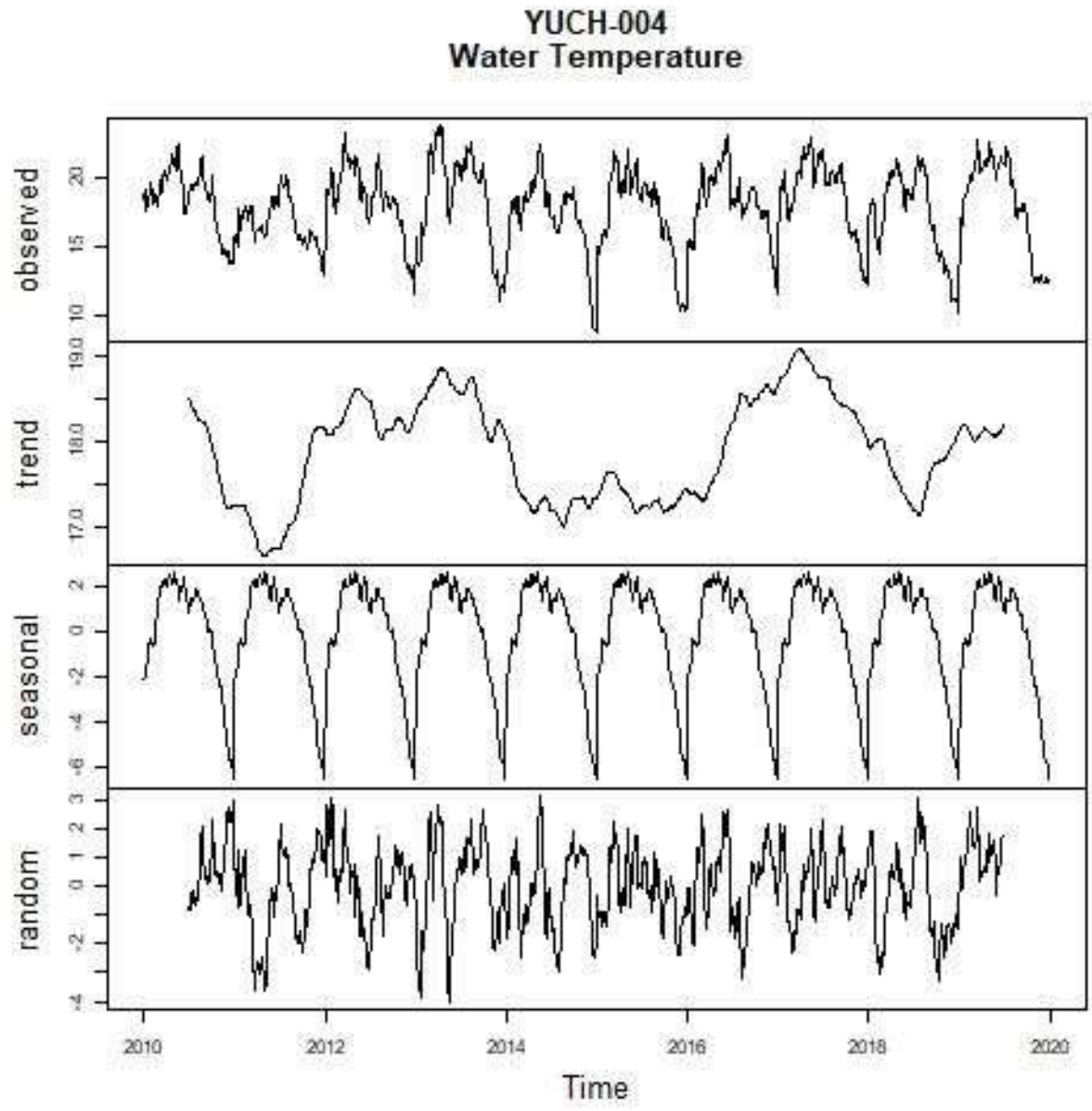


Figure A.212. Time series decomposition of truncated YUCH-004 water temperature measured at 1 m depth by year.

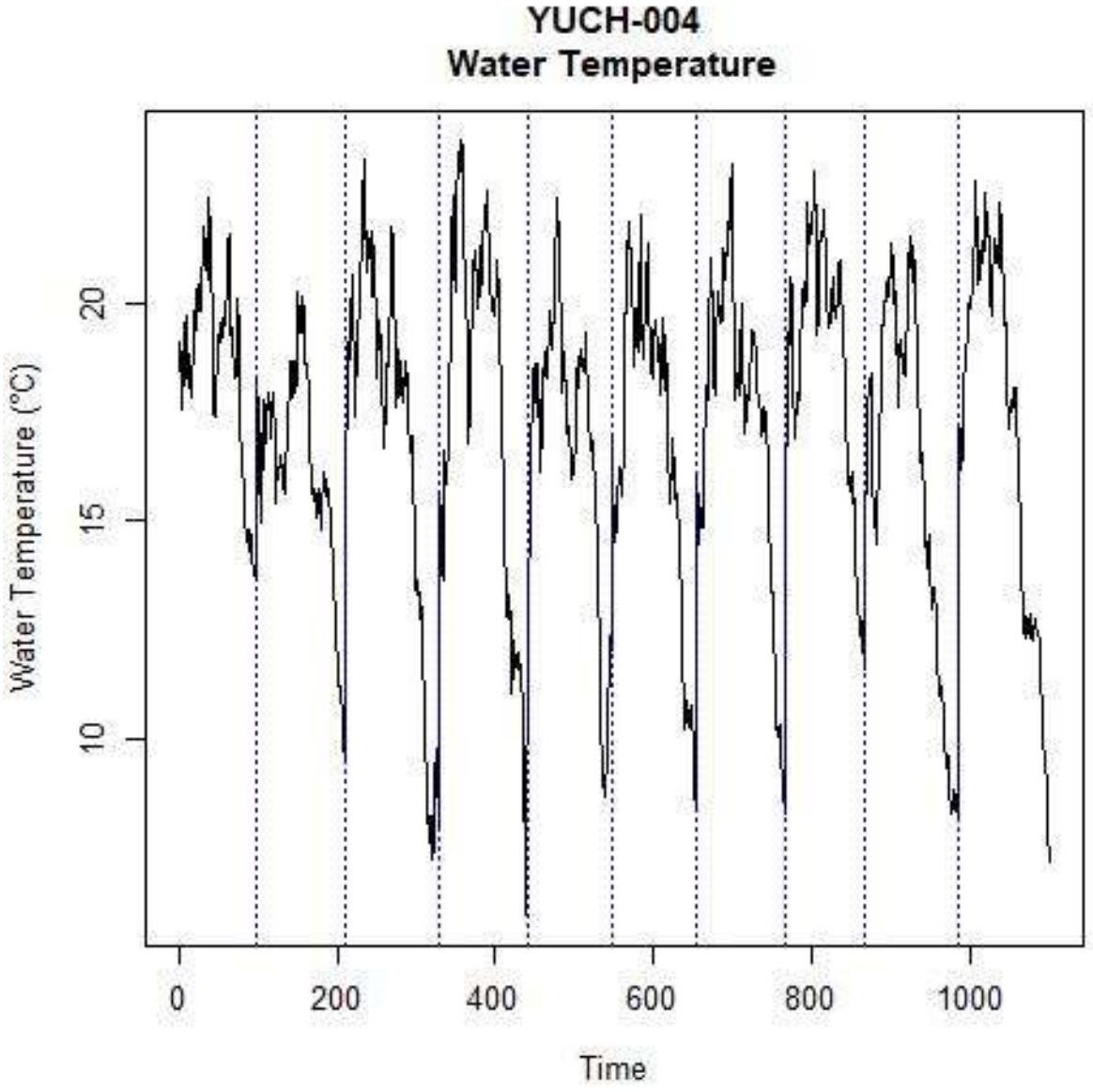


Figure A.213. Time series of YUCH-004 water temperature measured at 1 m depth by time point with vertical lines for additive outliers.

Table A.221. Trend modeling results for daily water temperature data measured at 1 m depth at YUCH-004.

			Trend			ARMA order		Ljung-Box Test	
Logged	**Method**	**Intercept**	**Coefficient**	**SE**	**p-value**	**AR**	**MA**	**Statistic**	**p-value**
FALSE	complete	14.6130	0.2333	0.0686	0.0007	0	5	807.75	< 0.0001
FALSE	completeAO	16.4282	0.0588	0.0633	0.3532	0	5	1213.03	< 0.0001

			Trend			ARMA order		Ljung-Box Test	
Logged	Method	Intercept	Coefficient	SE	p-value	AR	MA	Statistic	p-value
FALSE	trunc	16.3862	0.1489	0.0624	0.0170	0	5	1824.27	< 0.0001
FALSE	truncSA	17.9451	-0.0011	0.0670	0.9872	2	1	231.02	0.0254
TRUE	complete	2.6562	0.0145	0.0048	0.0023	0	5	705.86	< 0.0001
TRUE	completeAO	2.7630	0.0042	0.0043	0.3380	0	5	1120.14	< 0.0001
TRUE	trunc	2.7569	0.0107	0.0035	0.0022	0	5	3150.19	< 0.0001
TRUE	truncSA	2.8815	-0.0009	0.0041	0.8348	1	1	237.21	0.0146

Table A.222. Trend modeling results for weekly water temperature data measured at 1 m depth at YUCH-004.

			Trend			ARMA order		Ljung-Box Test	
Logged	Method	Intercept	Coefficient	SE	p-value	AR	MA	Statistic	p-value
FALSE	complete	17.1506	-0.0375	0.1147	0.7440	0	1	233.73	< 0.0001
FALSE	completeAO	16.9332	-0.0317	0.0512	0.5357	2	2	22.20	< 0.0001
FALSE	trunc	17.4337	0.0540	0.1284	0.6743	0	2	25.02	0.2960
FALSE	truncSA	17.6862	0.0327	0.0505	0.5178	0	2	23.38	0.4390
TRUE	complete	2.7726	0.0013	0.0100	0.8967	0	2	67.37	< 0.0001
TRUE	completeAO	2.8569	-0.0060	0.0068	0.3816	0	0	414.17	< 0.0001
TRUE	trunc	2.8555	0.0029	0.0109	0.7892	1	0	42.57	0.0111
TRUE	truncSA	2.8682	0.0012	0.0029	0.6692	0	2	22.52	0.4892

Table A.223. Top covariate models for mean weekly water temperature data measured at 1 m depth at YUCH-004.

Model	AICc	ΔAICc	Ljung-Box Test p-value
Wind Speed + Month	1943.66	0.00	0.1160
Daily Precipitation	2416.68	473.01	0.0600

Table A.224. Coefficients and variance components estimates for the top covariate model for mean weekly water temperature measured at 1 m depth at YUCH-004.

Parameter	Coefficient	SE	p-value
Ar1	0.85	0.25	0.0007
Ar2	-0.51	0.31	0.0962
Ar3	0.40	0.27	0.1408

Parameter	Coefficient	SE	p-value
Ar4	0.21	0.30	0.4888
Ar5	-0.03	0.09	0.7295
Ma1	0.40	0.25	0.1097
Ma2	0.69	0.24	0.0035
Ma3	0.42	0.25	0.1016
Intercept	28.46	0.77	< 0.0001
Wind Speed	0.08	0.03	0.0091
Month	-1.59	0.06	< 0.0001

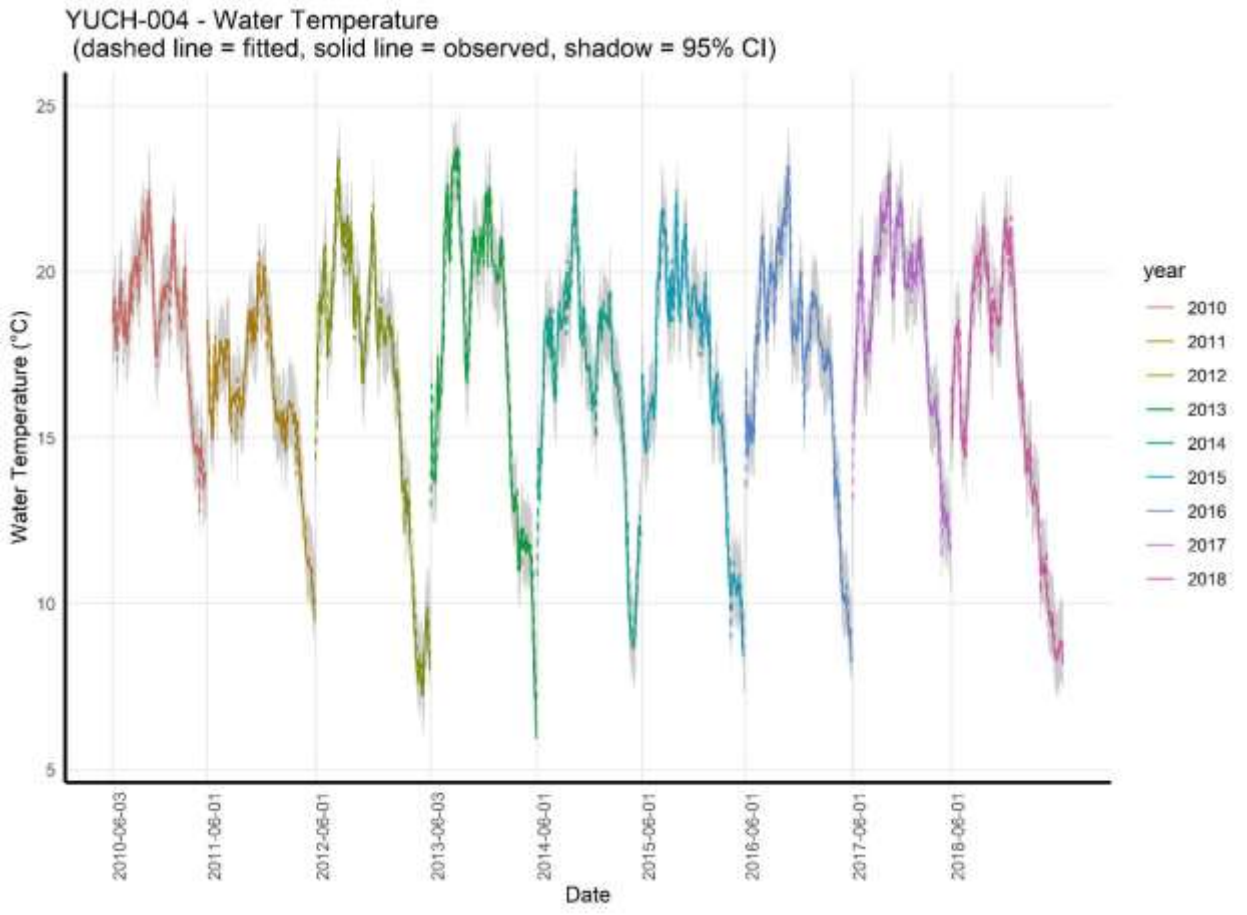


Figure A.214. Model predictions of YUCH-004 water temperature measured at 1 m depth by week.

YUCH-005

Data

For YUCH-005, water temperature was recorded from 2009-2019. Water temperature observations were collected during the months May-September and at water depths 0.25, 0.50, 1.00, 1.50, 2.00, and 3.00 m. To reduce autocorrelation we only considered water observations from a single depth in this analysis and selected depth 1.50 m as it there were no missing water temperature data at this depth. Additionally, we excluded the month October from the analyses due to sparse data. The resulting dataset included 1234 water temperature observations. When the data were further truncated to the common set of 93 days visited in every year the number of observations was reduced to 1023. Covariate data were missing for four of the five covariates in 2019, thus 2019 was excluded from the ARIMA covariate models. Additionally, we noted that solar radiation appears to decline from 2009-2010—the data from these years should be inspected for accuracy.

Model Selection

For lake YUCH-005, three trend models yielded stationary residuals (complete unlogged data, truncated seasonally adjusted logged data, truncated seasonally adjusted unlogged data). Only the model of the complete unlogged data included a trend coefficient significantly different from zero, indicated there is weak evidence for a declining trend in water temperature at lake YUCH-005. For ARIMA models fitting all possible covariate combinations the AICc model selection identified a top model with ARIMA(2,0,2) structure and fixed effects for daily precipitation and year. For this covariate model, water temperature is estimated to decrease with year (2009-2019), whereas the effect of daily precipitation was not significantly greater than zero.

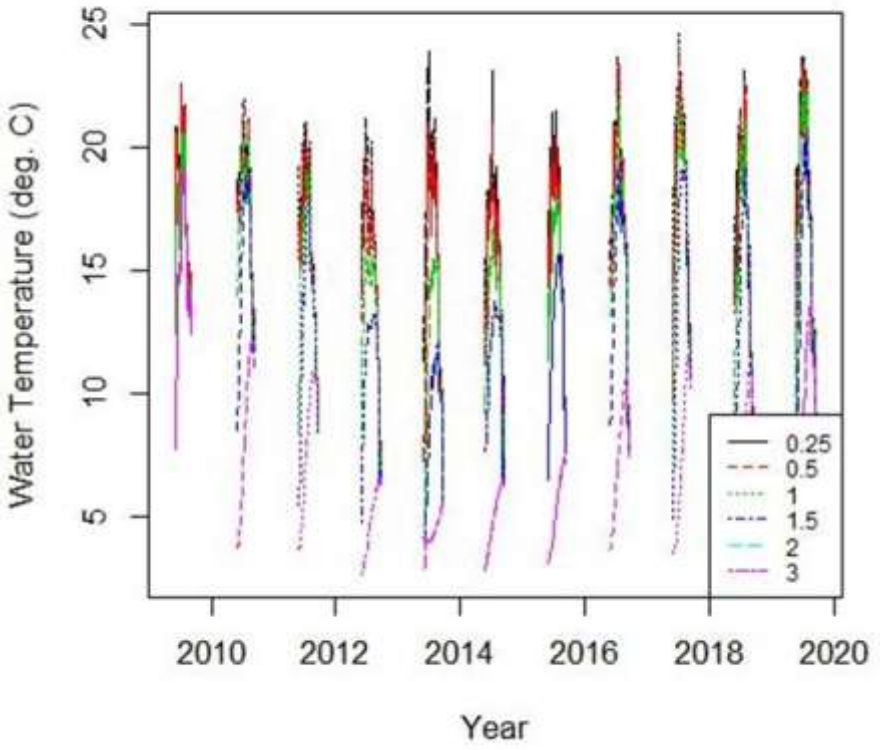


Figure A.215. YUCH-005 water temperature by depth and year.

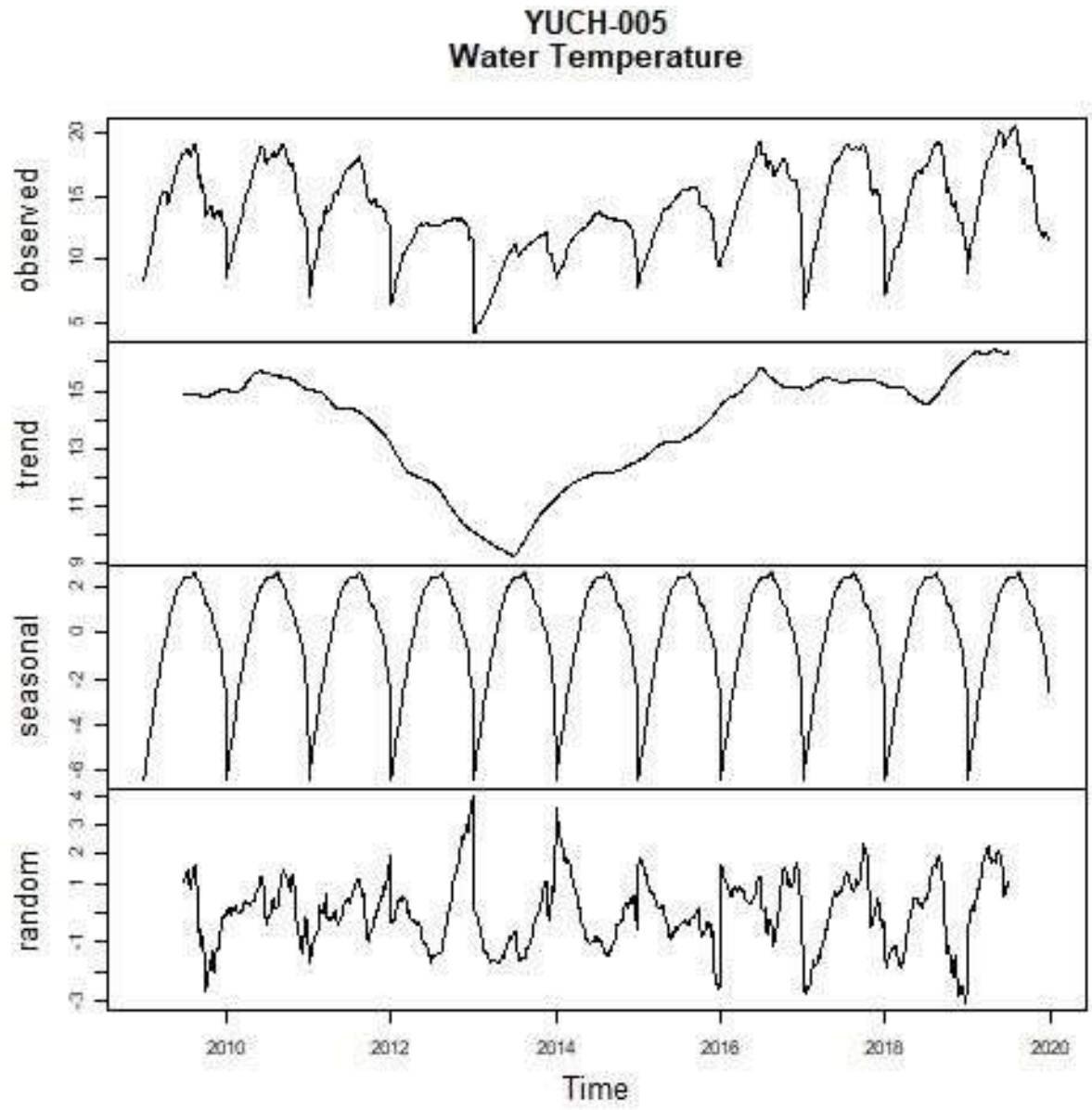


Figure A.216. Time series decomposition of truncated YUCH-005 water temperature measured at 1.5 m depth by year.

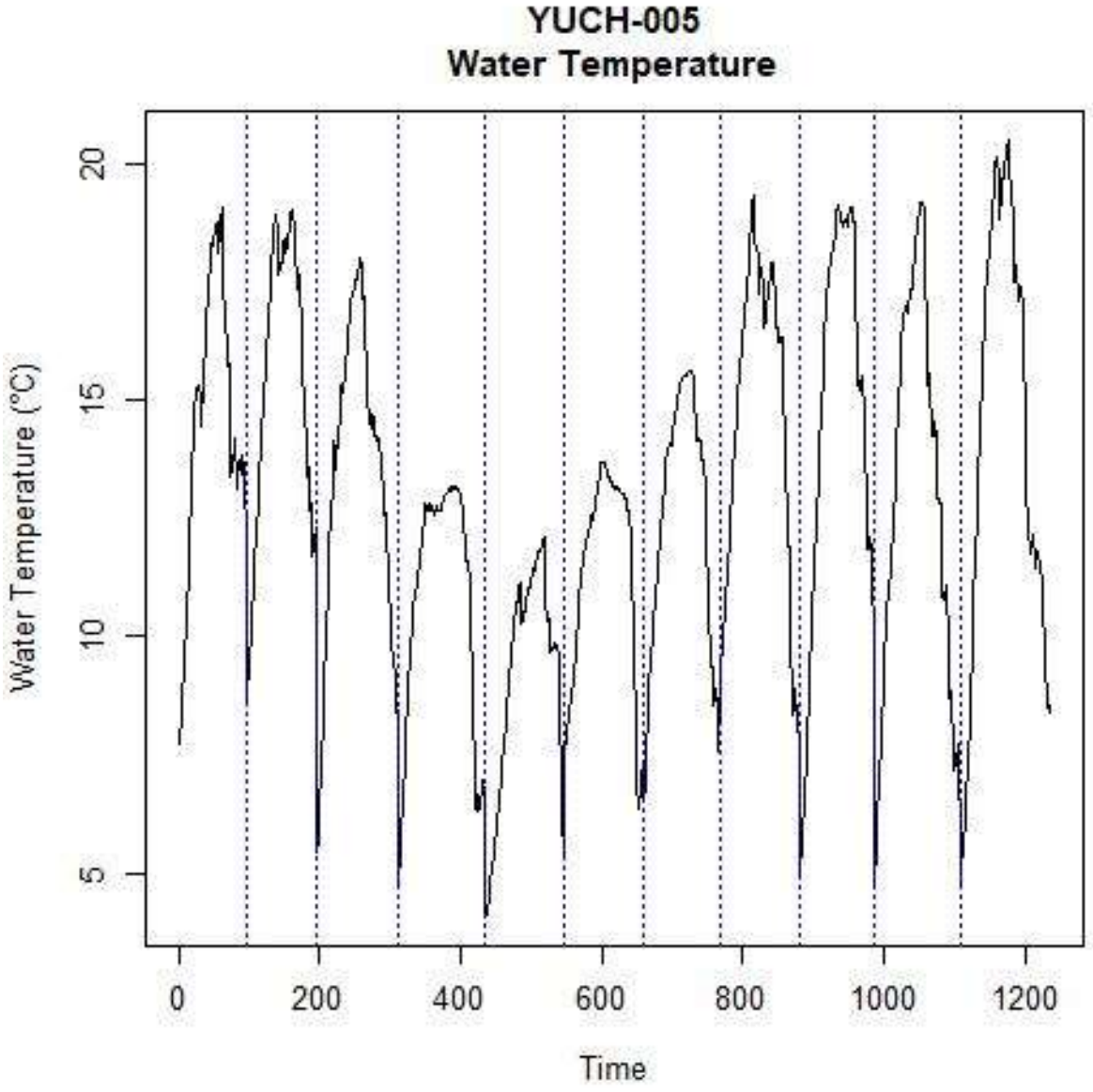


Figure A.217. Time series of YUCH-005 water temperature measured at 1.5 m depth by time point with vertical lines for additive outliers.

Table A.225. Trend modeling results for daily water temperature data measured at 1.5 m depth at YUCH-005.

			Trend			ARMA order		Ljung-Box Test	
Logged	**Method**	**Intercept**	**Coefficient**	**SE**	**p-value**	**AR**	**MA**	**Statistic**	**p-value**
FALSE	complete	37.2627	-2.3868	0.1049	< 0.0001	2	2	5.23	0.2648
FALSE	completeAO	34.6739	-2.1304	0.1455	< 0.0001	2	2	15.15	0.0017

			Trend			ARMA order		Ljung-Box Test	
Logged	**Method**	**Intercept**	**Coefficient**	**SE**	**p-value**	**AR**	**MA**	**Statistic**	**p-value**
FALSE	trunc	14.8994	-0.0975	0.0540	0.0709	0	5	5761.68	< 0.0001
FALSE	truncSA	13.7578	0.0188	0.0892	0.8332	1	2	143.16	0.9826
TRUE	complete	2.6721	-0.0156	0.0046	0.0007	0	5	1713.80	< 0.0001
TRUE	completeAO	2.5724	-0.0057	0.0042	0.1799	0	5	3200.41	< 0.0001
TRUE	trunc	2.6693	-0.0070	0.0046	0.1271	0	5	3995.77	< 0.0001
TRUE	truncSA	2.5833	0.0018	0.0089	0.8390	1	3	102.78	> 0.9999

Table A.226. Top covariate models for daily water temperature data measured at 1.5 m depth at YUCH-005.

Model	**AICc**	**ΔAICc**	**Ljung-Box Test p-value**
Daily Precipitation + Year	821.60	0.00	0.0799
Wind Speed + Year	821.76	0.17	0.0823
Air Temperature + Year	822.02	0.43	0.0790
Relative Humidity + Year	822.08	0.48	0.0785
Year + Month	822.14	0.54	0.0730
Wind Speed + Daily Precipitation + Year	823.11	1.52	0.0805
Relative Humidity + Daily Precipitation + Year	823.54	1.95	0.0780
Daily Precipitation + Year + Month	823.66	2.06	0.0745
Air Temperature + Wind Speed + Year	823.68	2.08	0.0810
Wind Speed + Year + Month	823.85	2.25	0.0755

Table A.227. Coefficients and variance components estimates for the top covariate model for daily water temperature data measured at 1.5 m depth at YUCH-005.

Parameter	**Coefficient**	**SE**	**p-value**
Ar1	1.94	0.02	< 0.0001
Ar2	-0.94	0.02	< 0.0001
Ma1	-0.66	0.04	< 0.0001
Ma2	-0.12	0.03	0.0002
Intercept	37.28	3.77	< 0.0001
Daily Precipitation	0.04	0.05	0.4515
Year	-2.53	0.11	< 0.0001

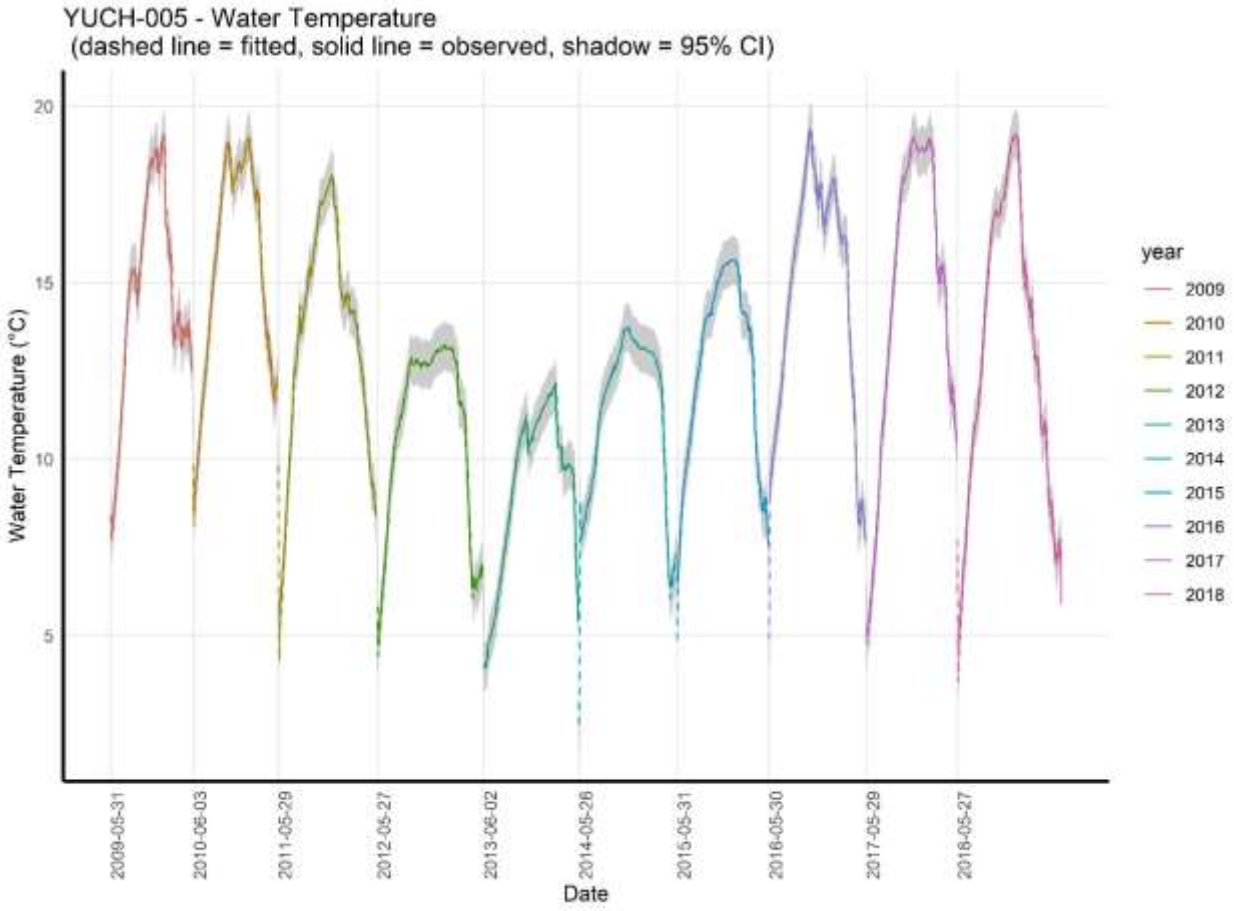


Figure A.218. Model predictions of YUCH-005 water temperature measured at 1.5 m depth by date.

Appendix B: Temperature Correlation Plots by Lake

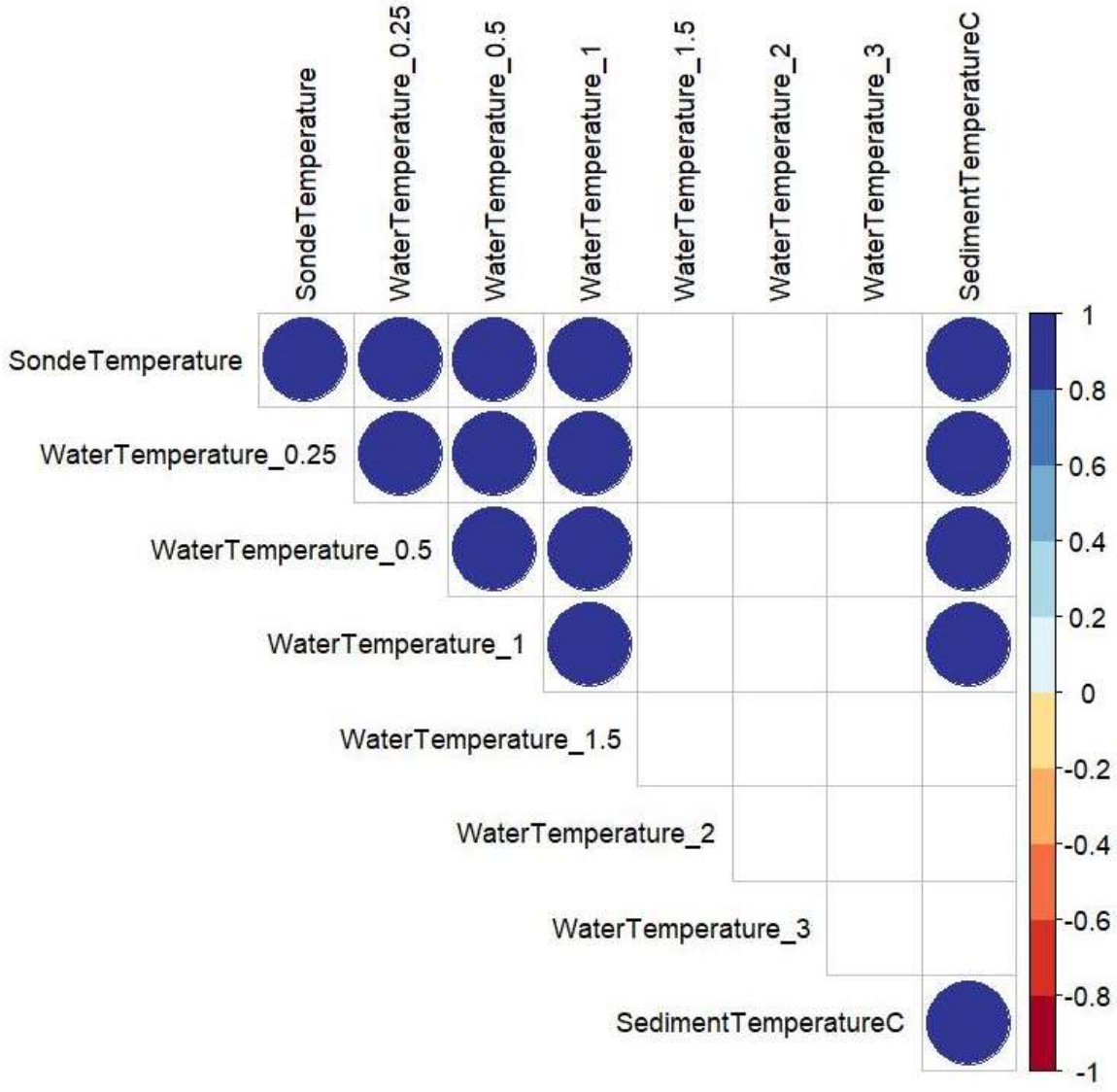


Figure B.1. Correlation among temperature outcomes at BELA-088.

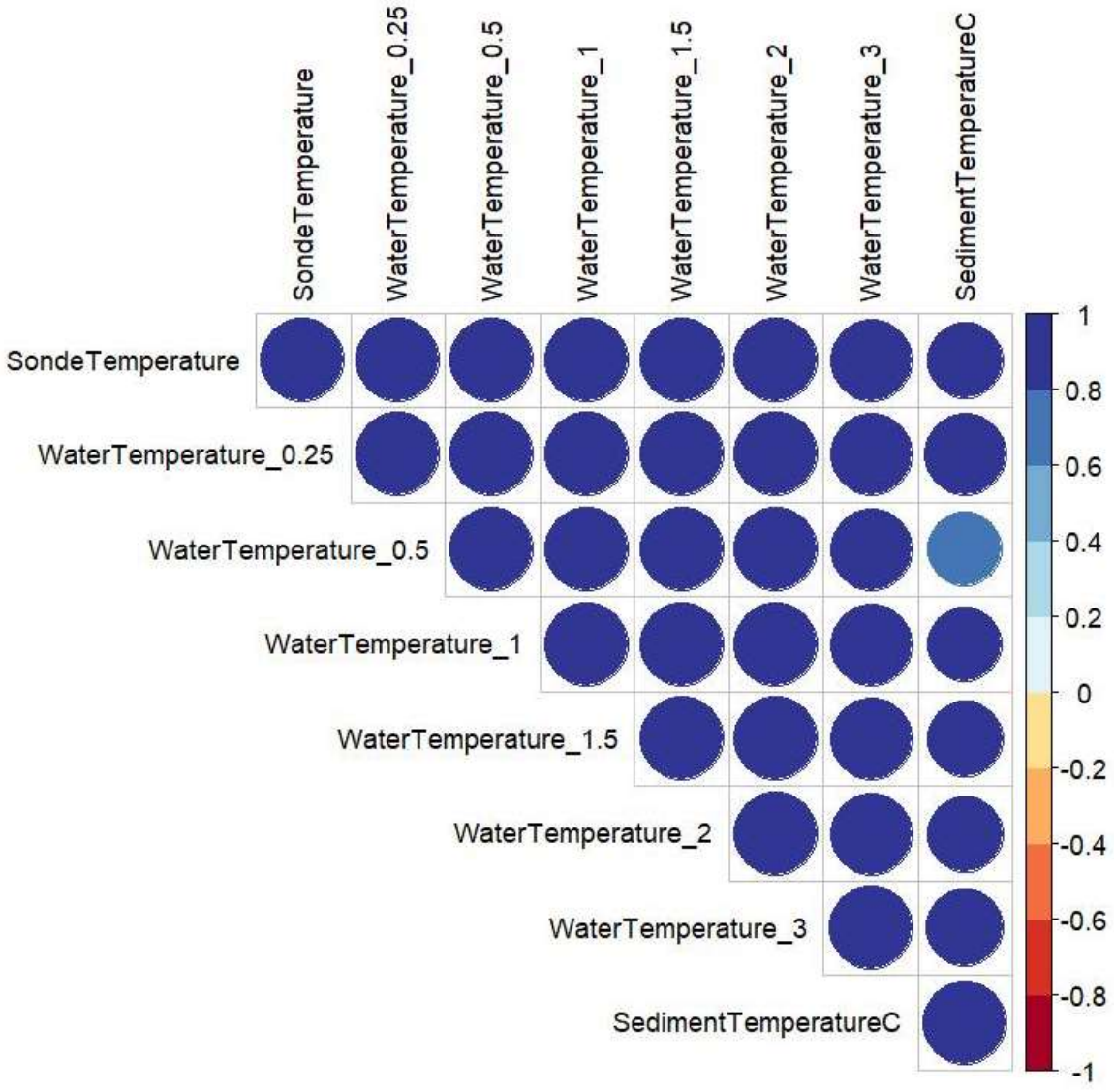


Figure B.2. Correlation among temperature outcomes at BELA-108.

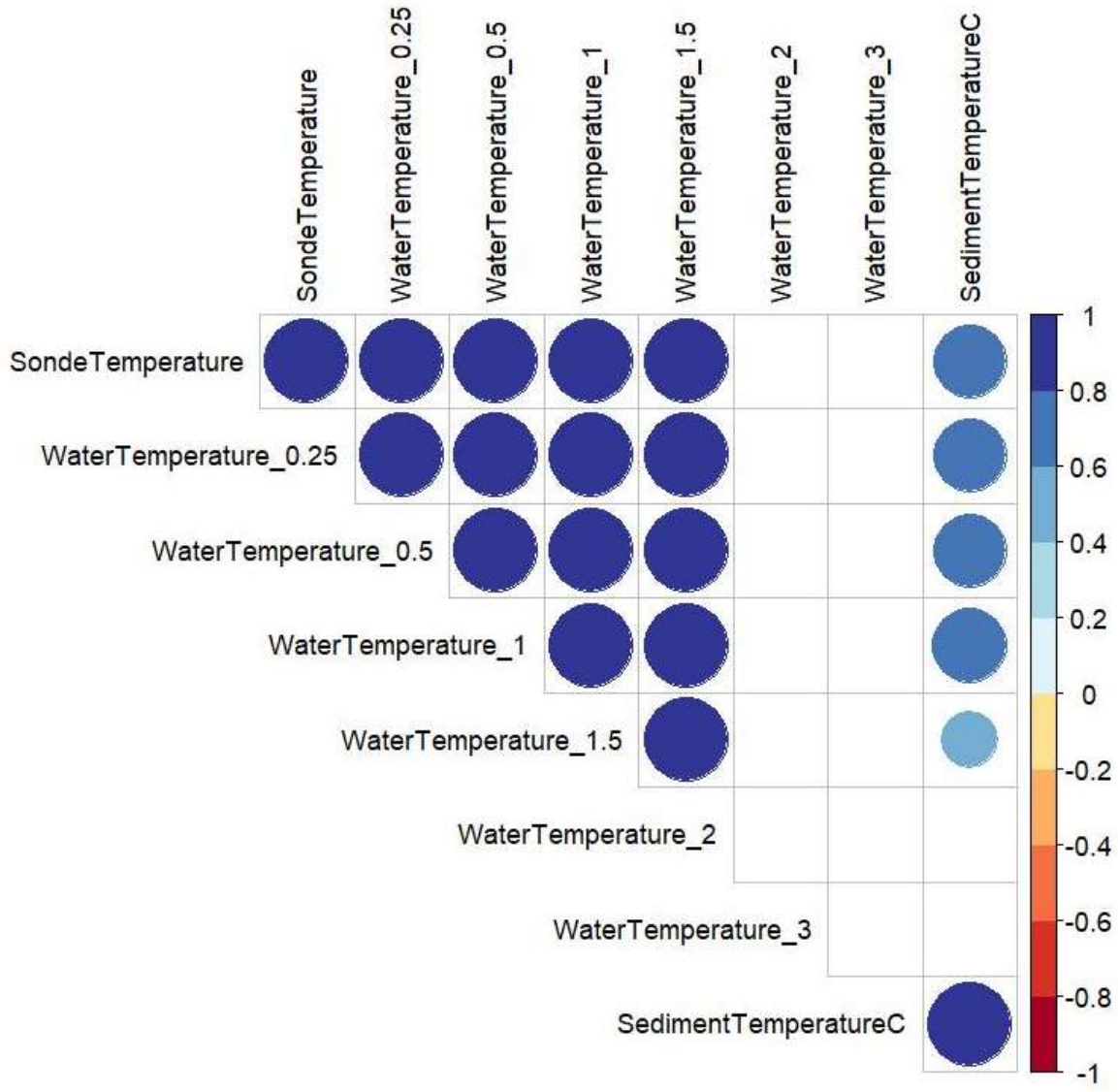


Figure B.3. Correlation among temperature outcomes at DENA-018.

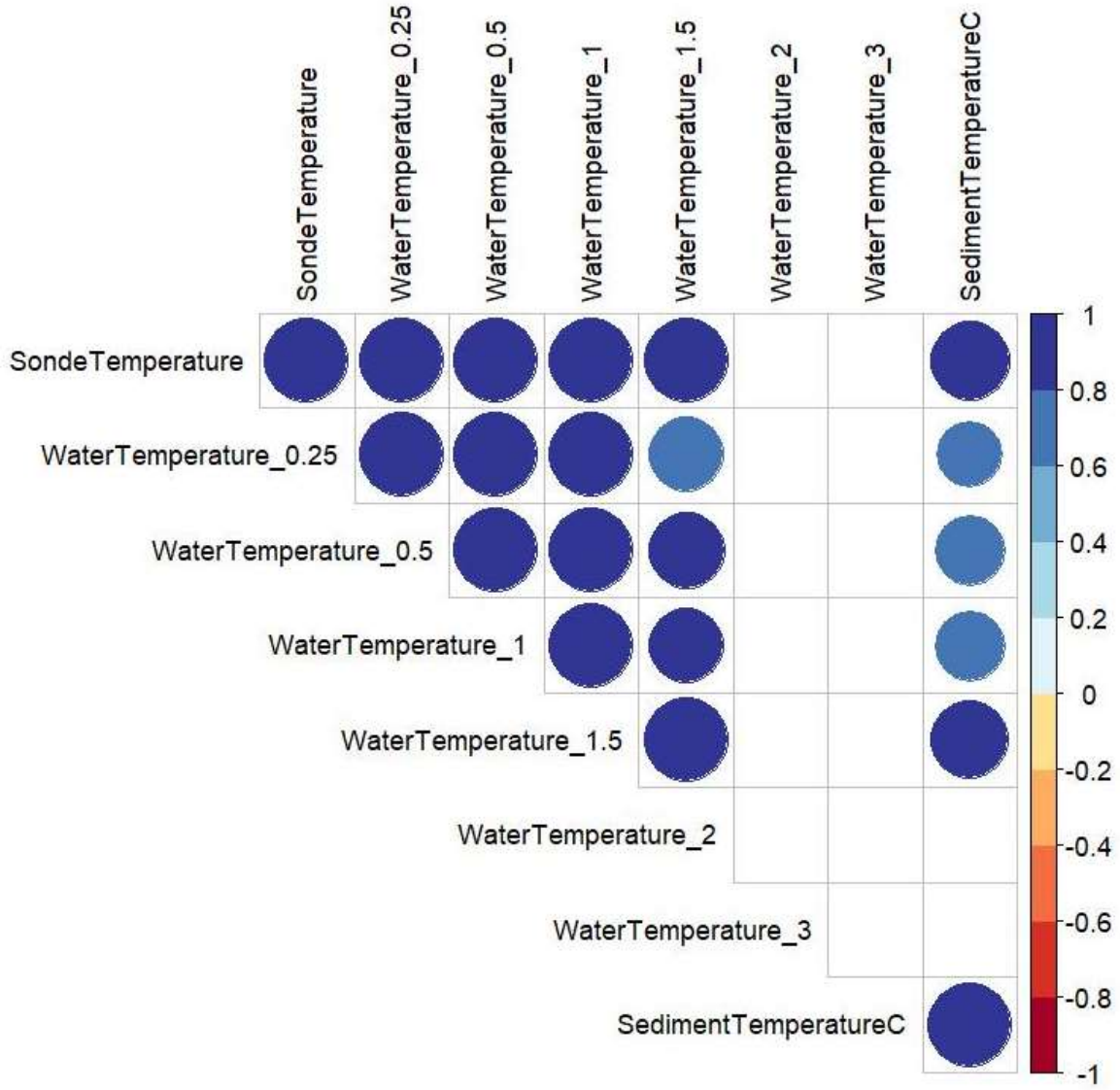


Figure B.4. Correlation among temperature outcomes at DENA-023.

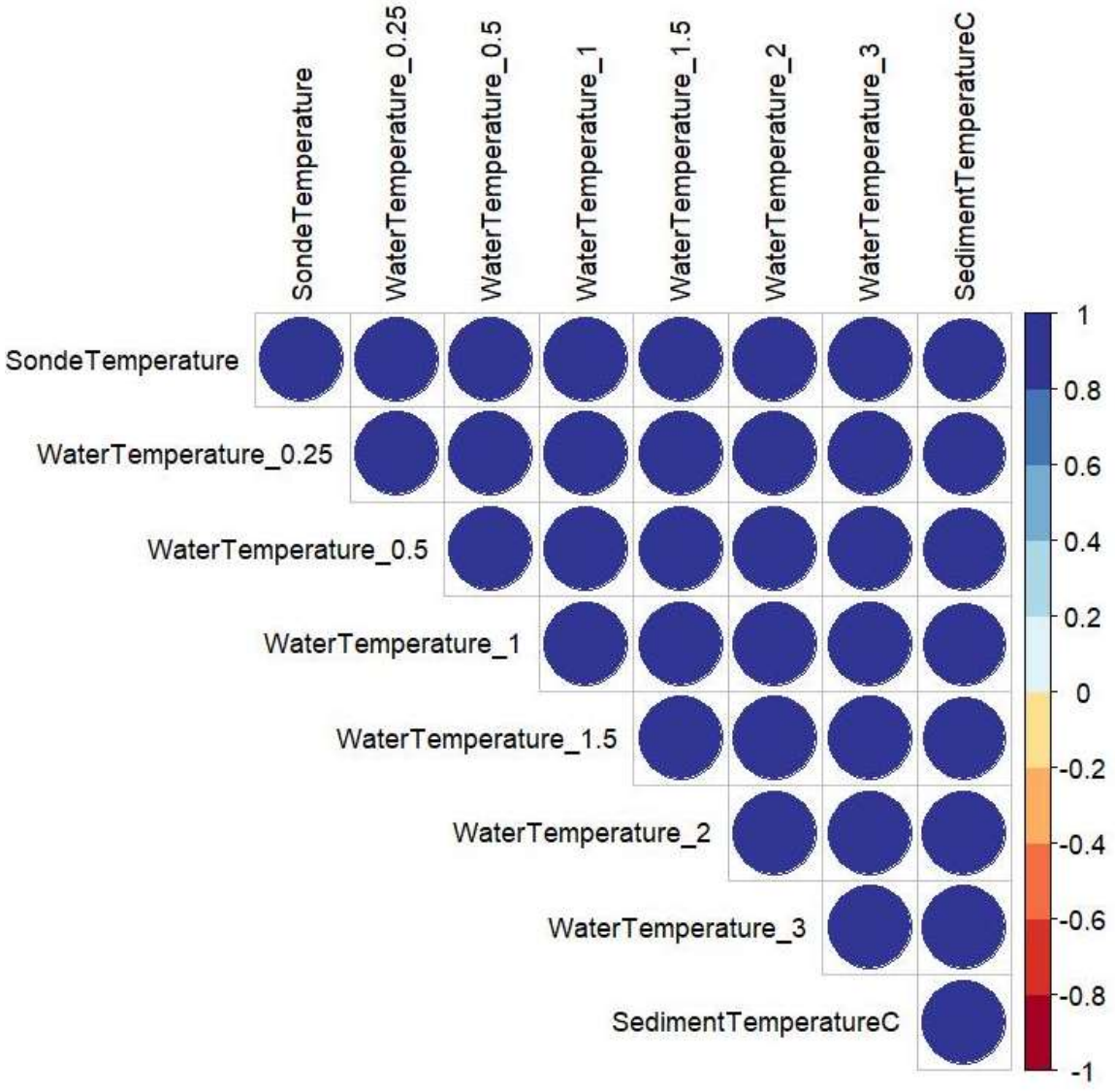


Figure B.5. Correlation among temperature outcomes at KOVA-085.

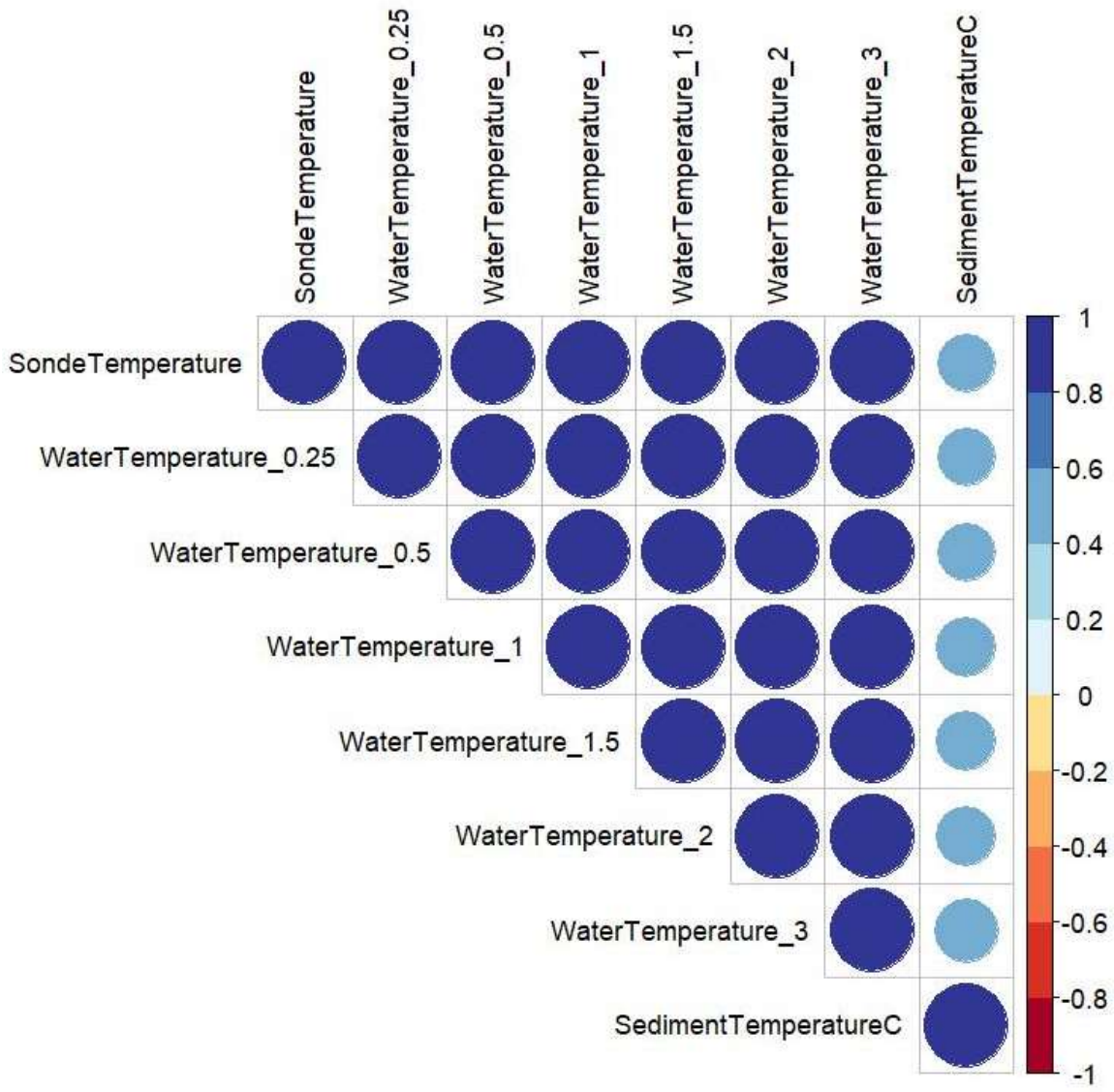


Figure B.6. Correlation among temperature outcomes at KOVA-086.

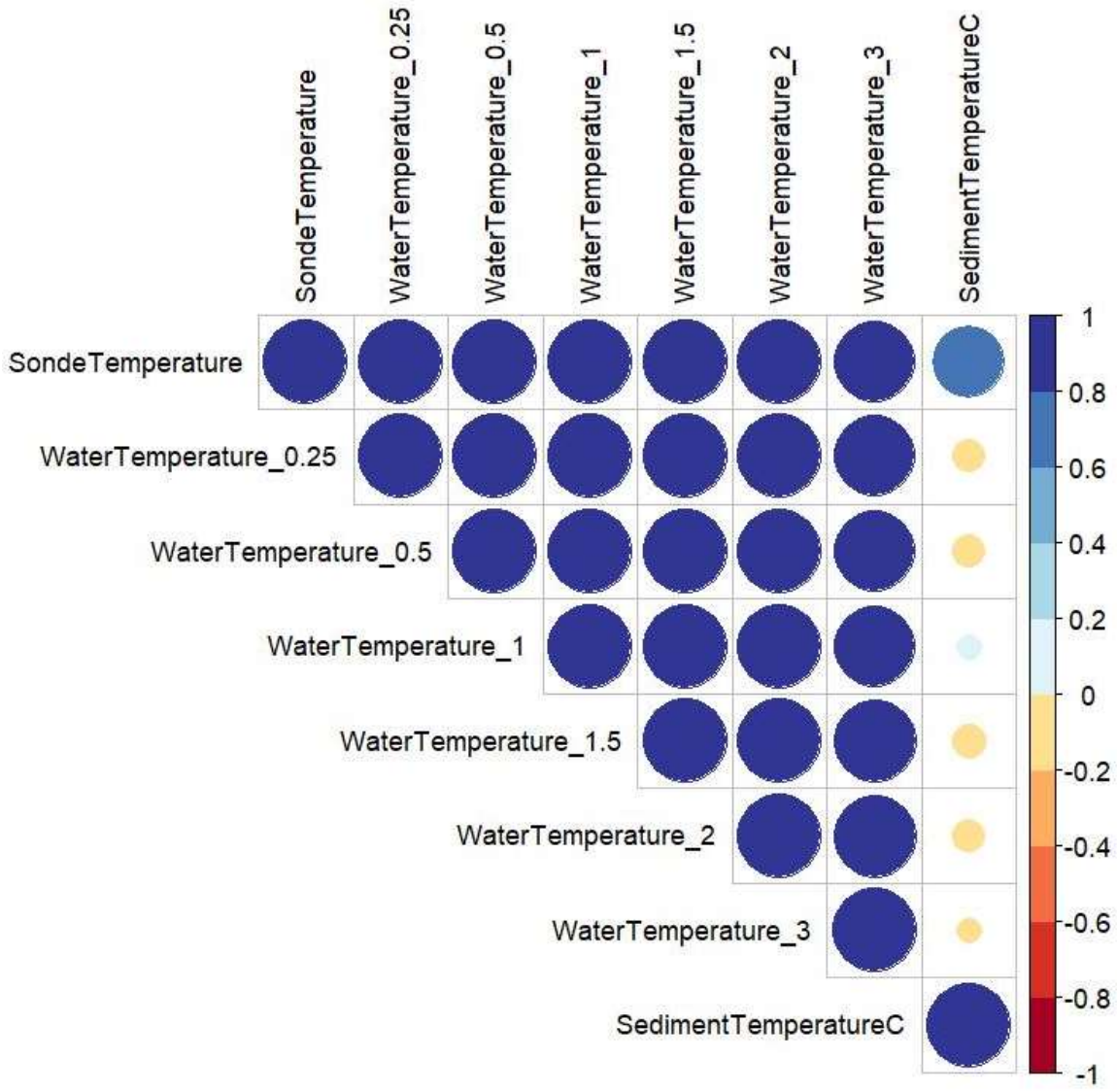


Figure B.7. Correlation among temperature outcomes at NAOT-052.

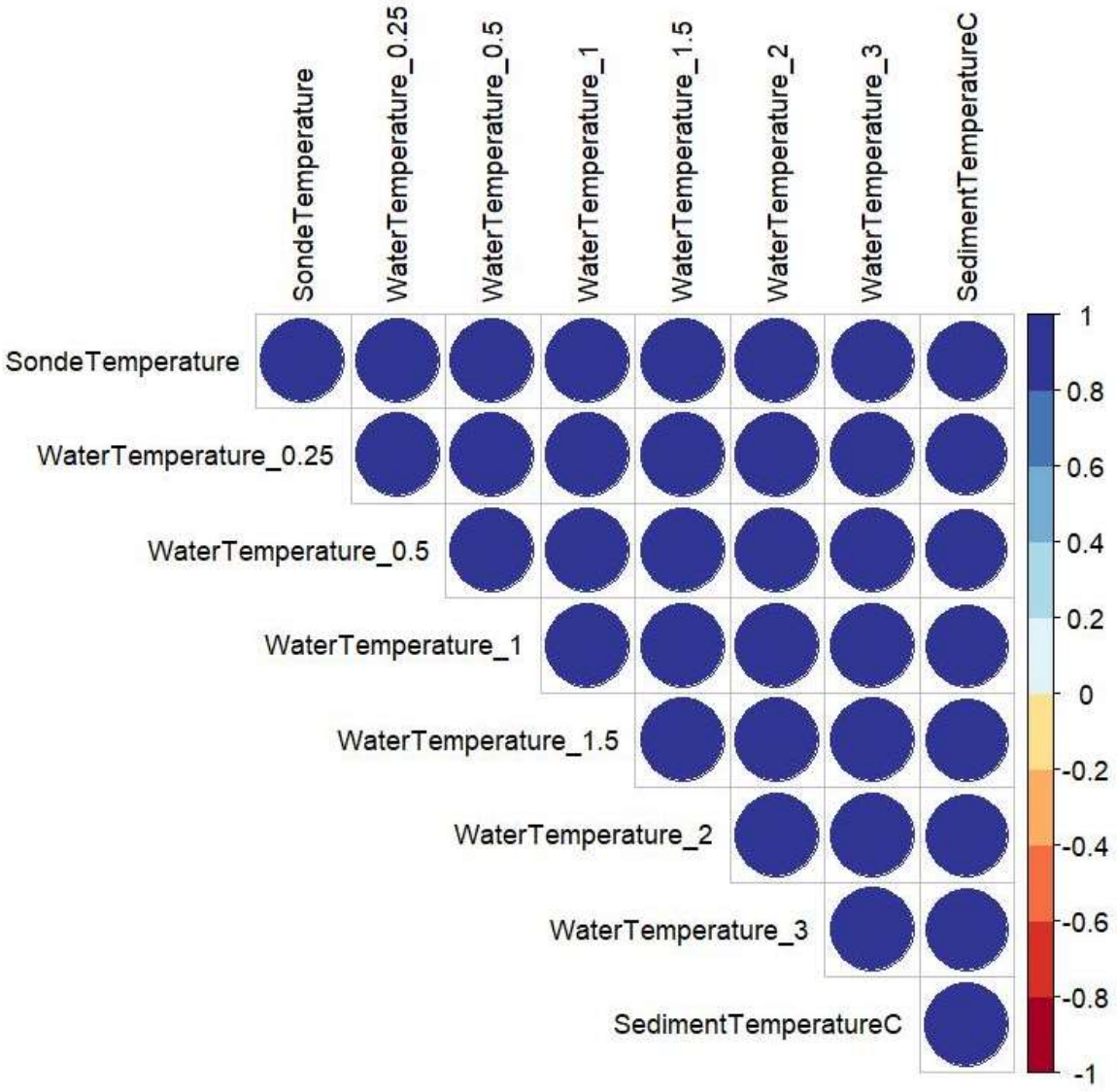


Figure B.8. Correlation among temperature outcomes at NAOT-107.

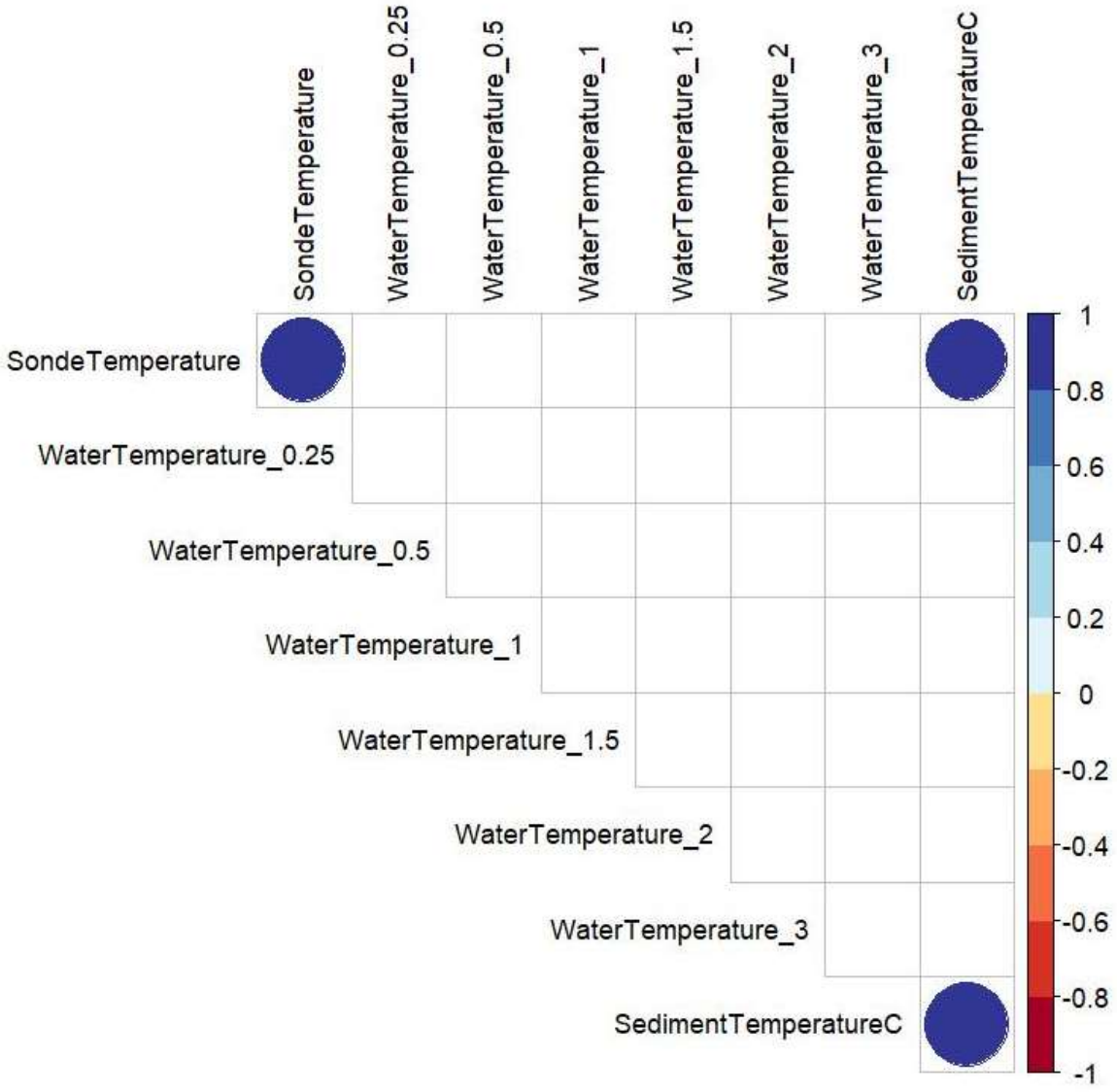


Figure B.9. Correlation among temperature outcomes at WRST-005.

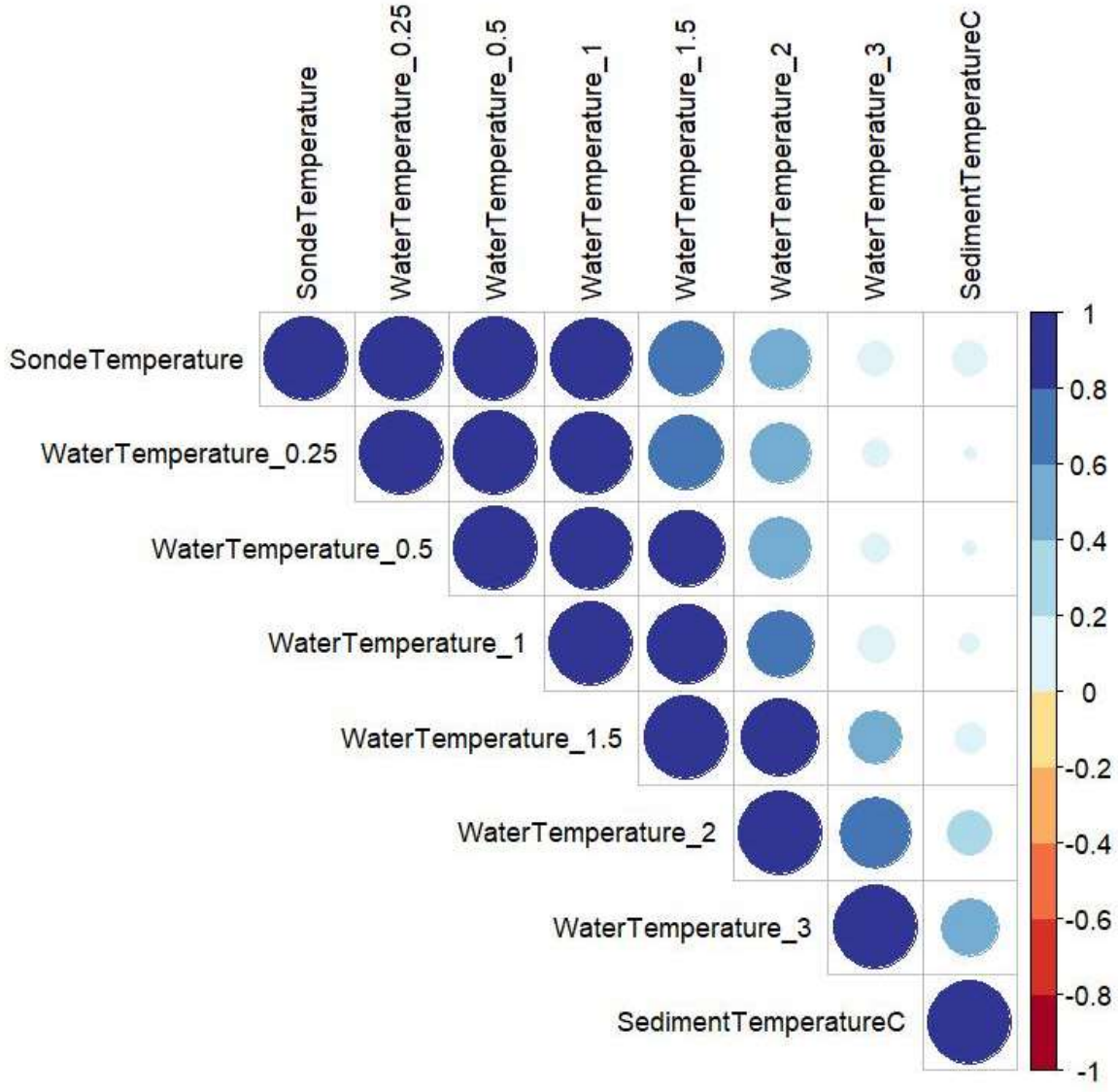


Figure B.10. Correlation among temperature outcomes at WRST-016.

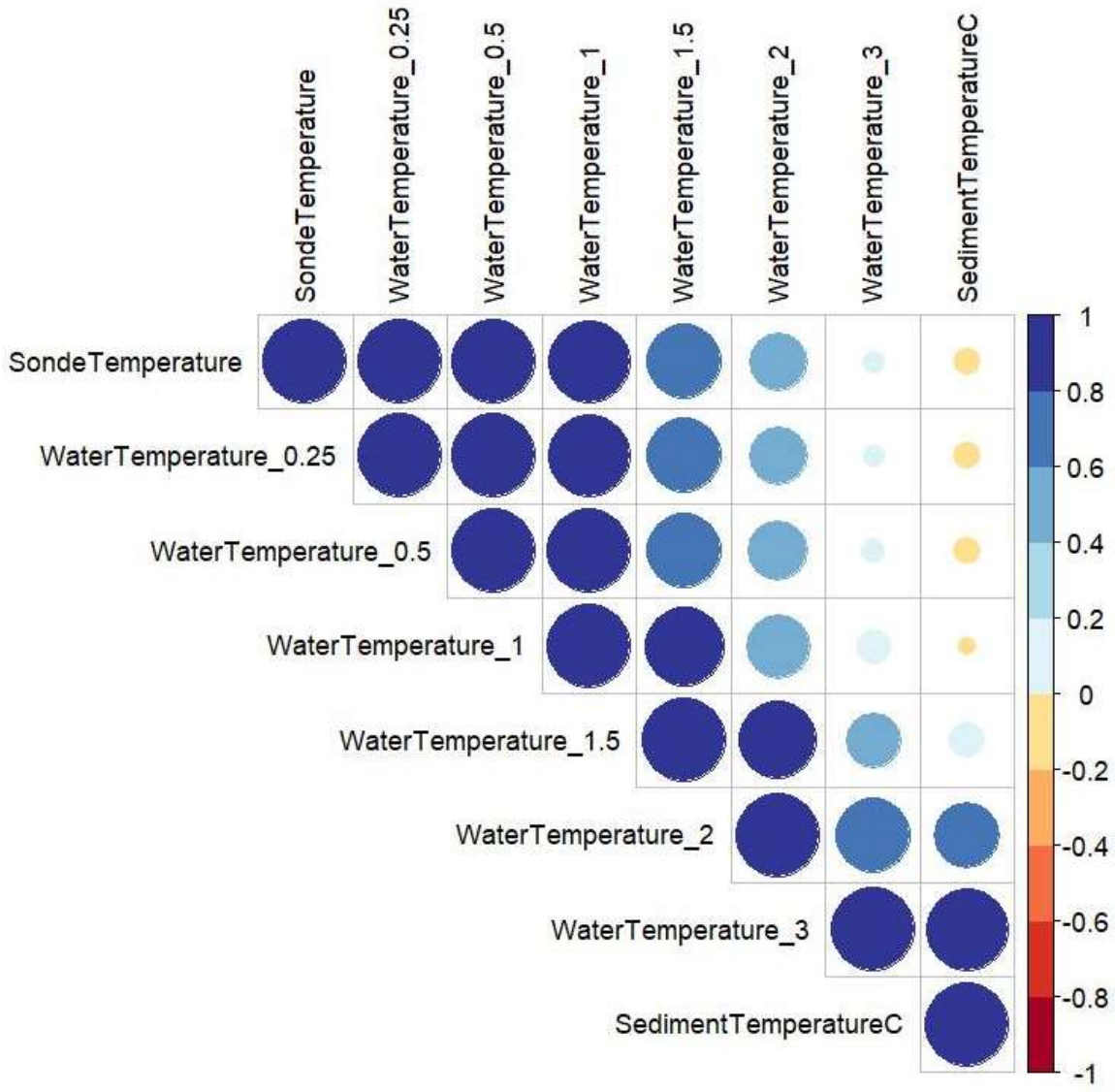


Figure B.11. Correlation among temperature outcomes at YUCH-004.

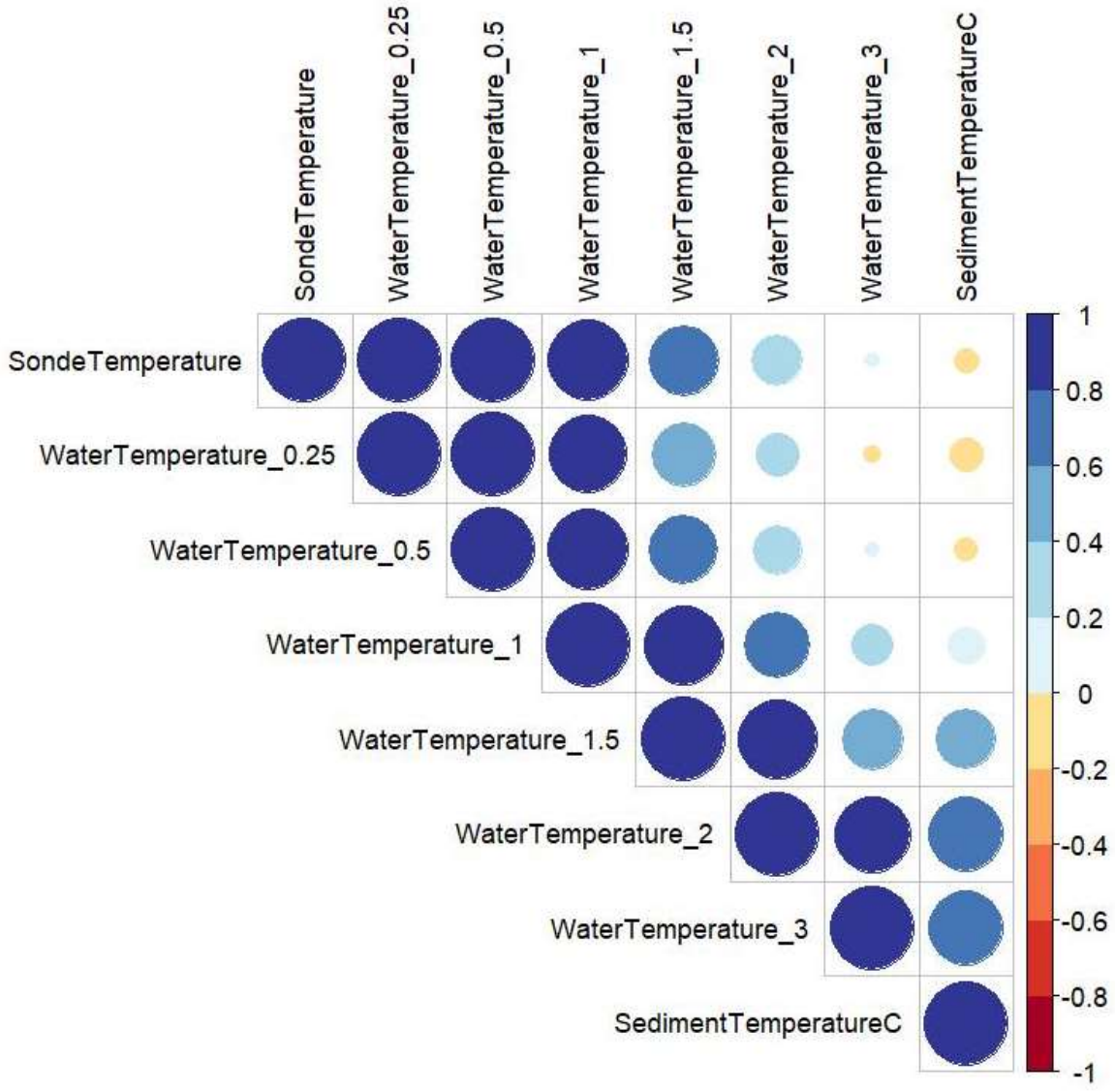


Figure B.12. Correlation among temperature outcomes at YUCH-005.

The Department of the Interior protects and manages the nation’s natural resources and cultural heritage; provides scientific and other information about those resources; and honors its special responsibilities to American Indians, Alaska Natives, and affiliated Island Communities.

National Park Service

U.S. Department of the Interior



Natural Resource Stewardship and Science
1201 Oakridge Drive, Suite 150
Fort Collins, CO 80525